Classical Electromagnetic Theory

A Modern Perspective

MIKE GUIDRY

Contents

Preface *page* xiv

1 Introduction 1
1.1 The Synthesis of Classical Electromagnetism 1
1.2 The Maxwell Equations 2
1.3 Charge Conservation 3
1.4 Maxwell and the Displacement Current 5
1.5 Classical Electromagnetic Forces 6
1.6 Internal Consistency of Electromagnetism 6
1.7 Classical Electromagnetic Solutions 8
1.8 Electromagnetism in Modern Physics 8
1.8.1 Gauge Symmetry 8
1.8.2 Quantization of Electrical Charge 9
1.8.3 Charges of Known Elementary Particles 10
Problems 15

2 Electrostatics in Vacuum 17
2.1 Categories of Electrostatics Problems 17
2.1.1 Summation Problems 17
2.1.2 Boundary Value Problems 18
2.2 Coulomb's Law 20
2.3 The Electric Field 22
2.4 The Principle of Superposition 23
2.5 Gauss's Law 27
2.6 The Scalar Potential 32
2.7 The Electric Field and the Scalar Potential 35
2.8 Work and Energy for Electric Fields 37
2.8.1 The Work Required to Move a Test Charge 37
2.8.2 Energy of a Continuous Charge Distribution 39
2.9 Equipotential Surfaces and Field Lines 40
2.9.1 Equipotential Contours and Vector Fields 40
2.9.2 Electric Field Lines 41
2.9.3 2D Projections of 3D Physics 44
2.10 Superposition of Scalar Potentials 44
2.11 The Poisson and Laplace Equations 46
2.11.1 The Poisson Equation 46

2.11.2 The Laplace Equation 48
2.11.3 Linearity of Laplace and Poisson Equations 48
2.12 Mathematical Classification of PDEs 48
2.13 Key Properties of Elliptic Equations 50
2.13.1 Physical Interpretation: Equilibrium 50
2.13.2 Boundary Value Problems (BVP) 51
2.13.3 Global Dependence (Instantaneous Propagation) 51
2.13.4 Smoothing (Regularity) 51
2.13.5 No Local Extrema 51
Problems 53

3 Electrostatic Boundary Value Problems 57
3.1 Electric Fields and Surface Charge Layers 57
3.2 Properties of Poisson and Laplace Solutions 58
3.2.1 The Laplace Equation in 1D 59
3.2.2 2D and 3D Laplace Equations 60
3.3 Boundary Conditions and Uniqueness 61
3.3.1 Dirichlet and Neumann Boundary Conditions 62
3.3.2 Uniqueness Theorems I and II 64
3.3.3 Uniqueness Theorems by Green's Methods 64
3.3.4 Proof of Uniqueness 66
3.3.5 Summary of Legitimate Boundary Conditions 69
3.3.6 The Helmholz Theorem 69
3.4 Poisson and Laplace Solution Methods 70
3.4.1 Analytical Methods 71
3.4.2 Numerical Methods 72
3.5 Boundary-Value Problems by Green Functions 73
3.6 The Method of Images 76
3.7 Green Function for the Conducting Sphere 80
3.8 Approximate Solutions 83
3.8.1 Spherical Harmonic Expansions of the Potential 84
3.8.2 Multipole Components of the Electric Field 92
3.8.3 Energy of a Charge Distribution in a Field 94
Problems 96

4 Solution of the Poisson and Laplace Equations 99
4.1 Solutions by Separation of Variables 99
4.1.1 Separation of Variables in Cartesian Coordinates 99
4.1.2 Separation of Variables in Spherical Coordinates 106
4.1.3 Separation of Variables in Cylindrical Coordinates 110
4.2 Variational Methods 110
4.3 Solution by Numerical Methods 111
4.3.1 The Finite Difference Method 111
4.3.2 Finite Element Method 112

4.3.3 Boundary Element Method (BEM) 113
4.4 Algorithmic Optimizations 114
4.4.1 Vectorization 114
4.4.2 Parallelization and Domain Decomposition 115
4.4.3 Efficient Grid Points and Integration Steps 117
Problems 118

5 Electrostatics in Conducting Matter 120
5.1 Properties of Conductors 120
5.1.1 Electric Fields Vanish Inside a Conductor 121
5.1.2 Charge Density Is Zero Inside a Conductor 121
5.1.3 Excess Charge Resides on the Surface 122
5.1.4 Any Exterior Electric Field is Normal to the Surface 122
5.1.5 A Conductor is an Equipotential 122
5.1.6 Surface Charge Density and Curvature 123
5.2 Capacitance 124
5.2.1 Parallel Plate Capacitors 124
5.2.2 Energy Stored in a Capacitor 126
Problems 127

6 Electrostatics in Dielectric Matter 130
6.1 Dielectrics 130
6.1.1 Capacitors and Dielectrics 131
6.1.2 Dielectric Constants 132
6.1.3 Bound Charge and Free Charge 133
6.2 Moments of a Molecular Charge Distribution 134
6.2.1 Multipole Expansion of the Potential 134
6.2.2 Dominence of Monopole and Dipole Terms 135
6.3 Induced Dipole Moments 135
6.3.1 Polarization of the Electron Cloud 136
6.3.2 Atomic Polarizabilities 136
6.4 Permanent Dipole Moments of Polar Molecules 137
6.5 Polarization Density 139
6.6 Field Outside Polarized Matter 140
6.7 Field Inside Polarized Matter 142
6.8 The Electric Displacement $\boldsymbol{D}$ 143
6.8.1 Constituitive Relationships 144
6.8.2 Boundary Conditions 145
6.9 Surface and Volume Bound Charges 146
6.10 Average Electric Fields in Matter 149
6.11 Boundary Conditions at Interfaces 150
6.11.1 Differential Form of Maxwell Equations in Medium 151
6.11.2 Integral Form of Maxwell Equations in Medium 151
6.11.3 Matching Conditions at Boundaries 152

6.12 Dielectric Boundary Value Problems 154
6.12.1 Dielectric Ball in External Electric Field 155
6.12.2 A Spherical Dielectric Shell 162
6.12.3 A Vacuum Bubble in a Dielectric Medium 164
Problems 166

7 Steady Currents 170
7.1 Steady-Current Conditions 170
7.2 Vacuum Currents 171
7.2.1 Vacuum Diodes at Low Temperature 172
7.2.2 Vacuum Diodes at Intermediate Temperatures 172
7.2.3 Vacuum Diodes at High (Saturation) Temperature 173
7.2.4 Space Charge and the Child–Langmuir Law 173
7.3 Currents in Matter 174
7.3.1 Ohm's Law 174
7.3.2 The Drude Model of Metallic Conduction 175
Problems 179

8 Magnetostatics in Vacuum 180
8.1 Magnetostatics versus Electrostatics 180
8.2 Magnetic Forces 182
8.3 Work and the Lorentz Force 184
8.4 The Biot–Savart Law 186
8.4.1 Magnetic Flux 188
8.4.2 Application to Long Straight Wires 188
8.5 Differential Form of the Biot–Savart Law 189
8.6 Magnetostatics Using Ampère's Law 191
8.7 Surface Currents and Volume Currents 194
8.8 Vector Potentials and Gauge Invariance 195
8.8.1 Magnetic Fields and the Vector Potential 196
8.8.2 Gauge Transformations 196
8.8.3 The Coulomb Gauge Condition 197
8.9 Magnetic Fields of Localized Currents 197
8.9.1 Multipole Expansion of the Vector Potential 198
8.9.2 Magnetic Dipole Moment of a Current Loop 199
Problems 201

9 Magnetostatics in Matter 206
9.1 Aligning Current Loops in Magnetic Fields 206
9.2 Ampère's Law in Polarized Matter 207
9.2.1 Macroscopic Averaging 208
9.2.2 Auxiliary Field $\boldsymbol{H}$ and Constituitive Relations 209
9.2.3 Magnetic Boundary-Value Conditions 210
9.3 Magnetostatic Boundary-Value Problems 213

9.3.1 Solutions Using a Vector Potential 213
9.3.2 Solutions Using a Magnetic Scalar Potential 214
9.3.3 Solutions for Hard Ferromagnets 214
9.3.4 Example: Uniformly Magnetized Sphere 217
9.3.5 Example: A Shell of Permeable Matter 221
Problems 224

10 Dynamical Charges and Currents 226
10.1 Faraday and the Law of Induction 226
10.2 Mathematical Content of Faraday's Results 227
10.2.1 Quasistatic Approximations 229
10.2.2 Sources of EMF and Special Relativity 231
10.3 Electromagnetic Induction 233
10.3.1 Self-Inductance 233
10.3.2 Mutual Inductance 233
Problems 234

11 Maxwell's Equations 236
11.1 The Not-Quite Maxwell Equations 236
11.1.1 Ampère's Law and the Displacement Current 236
11.1.2 Implications of the Ampère–Maxwell Law 239
11.2 Vector and Scalar Potentials 240
11.3 Exploiting Gauge Symmetry 241
11.3.1 Lorenz Gauge 242
11.3.2 Coulomb Gauge 244
11.4 Retarded Green Function 247
11.4.1 Fourier Transforms 248
11.4.2 Green Functions Using Fourier Transforms 249
11.4.3 Causal Potential Solutions 252
11.4.4 Retarded and Advanced Solutions 253
Problems 254

12 Symmetries and Conservation Laws 255
12.1 Conservation of Charge 255
12.2 Conservation of Energy 255
12.3 Conservation of Momentum 255
12.4 Conservation of Angular Momentum 255
12.5 Noether's Theorem 255

13 Electromagnetic Waves in Vacuum 257
13.1 The Classical Wave Equation 257
13.2 Electromagnetic Waves in Vacuum 260
13.2.1 Wave Equations for the Fields 260
13.2.2 Wave Equations for Potentials 262

13.2.3 Monochromatic Plane-Wave Solutions 262
13.2.4 Energy and Momentum 264
13.3 Polarization of Electromagnetic Waves 266
13.3.1 The Polarization Ellipse 266
13.3.2 Linear (Plane) Polarization 268
13.3.3 Circular Polarization 268
13.3.4 Circular Polarization Basis 269
13.3.5 Helicity and Circular Polarization 270
13.3.6 Measuring Polarization: Stokes Parameters 271
13.3.7 The Poincaré Sphere 272
13.3.8 The Mueller Matrix 273
Problems 275

14 Electromagnetic Waves in Matter 276
14.1 Electromagnetic Waves in Simple Matter 276
14.2 Reflection and Refraction at Interfaces 277
14.2.1 Frequency Matching and Coplanar Vectors 278
14.2.2 Law of Reflection and Snell's Law 279
14.3 The Fresnel Equations 279
14.3.1 Transverse Electric and Magnetic Polarizations 280
14.3.2 Stokes Parameters from Fresnel States 280
14.4 Key Physical Phenomena 281
14.4.1 Brewster's Law and Brewster's Angle 282
14.4.2 Total Internal Reflection 282
14.4.3 Phase Shifts 282
14.5 Transport of Energy 283
14.6 Radiation Pressure 283
14.7 The Faraday Effect 283
14.7.1 The Microscopic Origin 284
14.7.2 Key Characteristics 284
14.8 Magneto-Optic Material 287
14.8.1 Gyroelectric Response 287
14.8.2 Gyromagnetic Response 287
14.9 Polarization of Light by Reflection 288
14.9.1 The Physical Mechanism 288
14.9.2 Brewster's Law 289
14.10 Waveguides 289
14.10.1 General Helmholtz Formulation 290
14.10.2 Decomposing into Transverse Fields 290
14.10.3 Rectangular Metallic Waveguides 291
14.10.4 Cutoff Frequency and Dispersion 291
14.10.5 The Dominant Mode TE_{10} 292
Problems 295

15 Electromagnetic Radiation 297
15.1 Introduction 297
15.2 Time Domain and Frequency Domain 297
15.3 Time Dependent Numerical Methods 297
15.3.1 Finite-Difference Time-Domain Method 299
15.3.2 The Method of Moments 299
15.4 Dipole Radiation 301
15.5 Scattering and Diffraction 301
15.5.1 Introduction 301
15.5.2 Scattering Cross Section 301
15.5.3 Thomson Scattering 301
15.5.4 Rayleigh Scattering 302
15.5.5 Absorption and Dispersion 303
15.6 Radiation from a Single Particle 303
15.6.1 Liénard–Wiechert Potentials 303
15.6.2 Syncrotron Radiation 303

16 Coordinate-Free Representations 305
16.1 Introduction 305
16.2 Electromagnetism's New Clothes 305
16.3 Sets 306
16.3.1 Maps between Sets 306
16.3.2 Differentiation and Continuity of Maps 308
16.4 Vector Spaces and Linear Transformations 309
16.4.1 Vector Spaces 309
16.4.2 Linear Transformations 310
16.5 Differentiable Manifolds 311
16.5.1 Composition of Two Maps 311
16.6 Vectors 312
16.7 One-Forms 312
16.8 Tensors 312
16.9 Differentiation on Manifolds 312
Problems 315

17 Spacetime Tensors 316
17.1 Minkowski Spacetime and Spacetime Tensors 316
17.1.1 Transformations between Inertial Systems 317
17.1.2 Lorentz Transformations 319
17.1.3 Minkowski Space 320
17.2 Symmetry under Coordinate Transformations 321
17.3 Spacetime Tensors and Covariance 321
17.3.1 Spacetime Coordinates 322
17.3.2 Vectors in Non-Euclidean Space 324
17.3.3 Coordinates in Spacetime 324

17.3.4 Coordinate and Non-Coordinate Bases 325
17.3.5 Tensors and Coordinate Transformations 328
17.3.6 Tensors as Linear Maps to Real Numbers 328
17.3.7 Vectors and Dual Vectors 329
17.3.8 Evaluating Components in a Basis 331
17.3.9 Identification of Vectors and Dual Vectors 333
17.3.10 Index-Free versus Component Transformations 334
17.4 Tensors Specified by Transformation Laws 334
17.4.1 Scalar Transformation Law 335
17.4.2 Dual Vector Transformation Law 335
17.4.3 Vector Transformation Law 336
17.4.4 Duality of Vectors and Dual Vectors 336
17.5 Scalar Product of Vectors 337
17.6 Tensors of Higher Rank 337
17.7 The Metric Tensor 338
17.8 Symmetric and Antisymmetric Tensors 339
17.9 Algebraic Tensor Operations 340
17.10 Tensor Calculus on Curved Manifolds 340
17.10.1 Invariant Integration 341
17.10.2 Partial Derivatives 342
17.10.3 Covariant Derivatives 343
17.11 Covariant Equations 346
Problems 347

18 Special Relativity 349
18.1 Maxwell's Equations and Special Relativity 349
18.2 Minkowski Space 349
18.2.1 The Indefinite Metric of Spacetime 350
18.2.2 Scalar Products and the Metric Tensor 350
18.2.3 The Line Element 350
18.2.4 Invariance of the Spacetime Interval 351
18.3 Tensors in Minkowski space 353
18.4 Lorentz Transformations 353
18.4.1 Rotations in Euclidean Space 354
18.4.2 Generalized 4D Minkowski Rotations 354
18.4.3 Lorentz Spatial Rotations 355
18.4.4 Lorentz Boost Transformations 357
18.5 Lightcone Diagrams 359
18.6 The Causal Structure of Spacetime 361
18.7 Lightcones and Lorentz Transformations 362
18.7.1 Lorentz Boosts and the Lightcone 362
18.7.2 Spacelike and Timelike Intervals 364
18.8 Electromagnetism in Special Relativity 365
18.8.1 A Charge Moving Parallel to a Current 365

18.8.2 A Boosted Line Charge 366
18.8.3 A Boosted Point Charge 366
18.9 Lorentz Covariance of Maxwell's Equations 366
18.9.1 Maxwell Equations in Non-Covariant Form 367
18.9.2 Scalar and Vector Potentials 369
18.9.3 Gauge Transformations 369
18.10 Manifestly Covariant Maxwell Equations 371
18.11 Lorentz Transformations on the Field Tensor 374
18.12 Covariance and the Lorentz Force Law 376
Problems 377

19 Geometry and Topology in Electromagnetism 379
19.1 A Brief Introduction to Topology 379
19.2 Differential Forms 379
19.3 Fiber Bundles 379
19.4 Topological Aspects of Electromagnetism 379
19.4.1 The Boundary Operator 379
19.4.2 The Boundary of a Boundary 379
19.4.3 The Exterior Derivative and Duality 380
19.4.4 Maxwell's Equations Using Exterior Calculus 382
19.4.5 Conserved Charges and Fluxes 384
19.4.6 The Exterior Calculus 385
19.4.7 Maxwell's Equations from the Exterior Calculus 389
19.4.8 Topology and the Aharonov–Bohm Effect 390
19.5 Covariant Derivatives 391
19.6 Differential Forms 391
Problems 392

20 Action Formulation of Classical Electromagnetism 393
20.1 The Principle of Least Action 393
20.2 The Action Principle For Fields 393
20.3 A Lagrangian Formulation of Electromagnetism 393
20.3.1 Principle of Extremal Proper Time 393
20.3.2 Construction of Classical Fields 394
20.3.3 Lagrangian Densities for Photons and Charged Fields 396

21 Electromagnetism as an Abelian Gauge Field Theory 400
21.1 Symmetry and Gauge Invariance 400
21.2 The Minimal Coupling Prescription 400
21.3 Gauge Invariance and the Photon Mass 404
21.4 Conserved Currents and Charges 405
21.4.1 Noether's Theorem 405
21.4.2 Conservation of Energy and Momentum 405
21.4.3 Internal Noether Currents and Charges 406

21.5 The Aharonov–Bohm Effect 408
21.5.1 Experimental Setup 408
21.5.2 Analysis of Magnetic Fields 409
21.5.3 Phase of the Electron Wavefunction 410
21.5.4 Topological Origin 410
21.6 Primacy of the Potentials 410
Problems 412

Appendix A Mathematics Review 413
A.1 Vectors and other Tensors 413
A.2 Vector Algebra 415
A.3 Useful Vector Identities 417
A.4 Vector Calculus 417
A.4.1 First Derivatives 417
A.4.2 Directional Derivative and Normal Derivative 419
A.4.3 Second Derivatives 420
A.4.4 Integrals 421
A.5 Fundamental Theorems 422
A.5.1 Fundamental Theorem of Gradients 422
A.5.2 Fundamental Theorem of Divergences 422
A.5.3 Fundamental Theorem of Curls 423
A.6 Laws, Theorems, and Definitions 423
A.7 Curvilinear Coordinate Systems 425
A.7.1 Spherical Coordinates 425
A.7.2 Cylindrical Coordinates 426
A.8 Taylor Series Expansion 427
A.9 Binomial Expansion 427
A.10 Miscellaneous Equations 427
A.11 Integration by Parts 428
A.12 The Dirac Delta Function 428

Appendix B Electromagnetic Units 431

Appendix C The Faraday Tensor 433

Appendix D The Exterior Calculus 436

Appendix E Solutions and Visualization with Computers 441

Appendix F Iterative PDE Solvers 444

Appendix G GenAI: Tutor, Assistant, and Problem Solver 450

Appendix H Using NotebookLM 458

References 461
Index 464

Preface

The material presented in these pages is based on a graduate-level introduction to classical electromagnetism (E&M) that I sometimes teach at the University of Tennessee. It is written approximately at the level of existing graduate texts such as Jackson [41], Zangwill [77], Garg [31], Chaichian et al [23], or Wald [74]. It is suitable for a graduate course in classical electrodynamics and assumes the reader to have a basic familiarity with the mathematical material summarized in Appendix A, which would typically be covered in an advanced undergraduate electromagnetism course (the material in the book by Griffiths [33] is representative). Because the proper theory of microscopic matter is quantum mechanics, our discussions of electromagnetism in matter will necessarily touch on some quantum concepts and theory, but these instances should be accessible to a reader with an undergraduate knowledge of quantum theory. Some background in solving problems using a computer is desirable, but is not essential, since the optional numerical problems that are offered are themselves tutorials in solving problems with *Python* that assume a minimal background in computing.

"Modern" E&M: The adjective "Modern" appearing in the subtitle of this book is often encountered as a general-purpose marketing ploy, but what does it mean here? In many respects this book is a traditional approach to advanced classical E&M, but the subtitle alludes to five broad themes that have been adopted in this book that set it apart in various ways from many earlier treatments.

1. An overall emphasis on *classical electromagnetism as a field theory that is precursor to modern quantum field theories* such as the Standard Model of elementary particle physics.
2. An emphasis on *generative artificial intelligence* (*GenAI*) as a potentially transformative learning and research tool for the study of physics in general, and classical electromagnetism in particular.
3. The systematic inclusion of examples and problems that require students to *program computer solutions and associated graphics*, in addition to traditional problems emphasizing analytical solutions, with particular emphasis placed on *using GenAI as computational tutor to assist in writing, debugging, and understanding the functionality of the code*.
4. An introduction to *geometrical and topological aspects of electromagnetism* expressed in the modern mathematical language of *differential forms* and *fiber bundles*, but always with translation to standard vector calculus notation.
5. A treatment of special relativity, and the Maxwell equations expressed in manifestly

Lorentz covariant form, that is *grounded in the geometry of spacetime*, expressed through differential geometry and tensor calculus.

By bridging the gaps among traditional analytical methods, modern topological and geometrical concepts, and numerical computational tools, and by leveraging the power of generative AI for learning and coding, this book offers a comprehensive framework for understanding how electromagnetic fields govern the microscopic and macroscopic world. Let us now elaborate on these themes.

Prototypical Classical Field Theory: Classical electromagnetism is the inspiration and often the logical starting point for modern quantum field theories (QFT) such as the *Standard Model* of elementary particle physics.

A typical methodology for quantum field theories is to construct the Lagrangian, action, and equations of motion for the appropriate *classical fields*, and then to quantize by

1. imposing *canonical commutation/anticommutation constraints* on the field operators,
2. or by invoking *path integral quantization methods* based on the classical action.

Hence, classical electromagnetic fields are the starting point to develop quantum electrodynamics (QED), which then serves as the prototype for a general quantum theory of gauge fields (the Standard Model).

Thus, a graduate-level presentation of classical electromagnetism should teach the basics of electromagnetism at an advanced level, but should do so in a context that acknowledges this historical role: classical E&M begets classical field theory which in turn begets quantum field theory,

$$Classical\ E\&M \longrightarrow Classical\ field\ theory \longrightarrow Quantum\ field\ theory,$$

which, in the guise of the Standard Model (with its known flaws), is the most successful description ever produced of the subatomic world. Accordingly, this book emphasizes classical E&M as a *prototypical classical field theory*, and where appropriate points out connections to the development of modern (relativistic and nonrelativistic) quantum field theory. This has been woven into the general discussion, but also the last several chapters are devoted specifically to a more formal exposition of classical electromagnetic field theory based on the action principle that is couched in the language of modern field theory. It should be noted that two recent presentations, Tong [71] and Wald [74], have been motivated by similar considerations to take related approaches in describing classical electromagnetism.

Leveraging Generative AI: *Artificial intelligence (AI)* is presently surrounded by an enormous bubble of hype, but that should not blind us to the very real potential of *generative*

*AI (*GenAI*)* implementing *Large Language Models (LLMs)*, which are described in Box 0.1, for both research and teaching. If you doubt this, invite Google *Gemini* 3 to your class as a student and give it the tests from your most recent semester of teaching by pasting the questions into the *Gemini* 3 chat input field, and grade the responses. Do not be surprised if Gemini sets the curve for the entire class![1]

For this reason, many educators—even tech-forward ones—view *GenAI* primarily as a threat enabling unprecedented cheating by the (human) students. But by giving in to this fear without a fight we are forfeiting the truly revolutionary potential of this new technology to transform both learning and research in a positive way. The potential downsides are quite real and we must proceed with due caution, chanting "*Question and Verify*" as our mantra. But we have no choice other than to embrace these powerful and rapidly evolving new tools, and to teach our students how to use them creatively, efficiently, and ethically, in both the classroom and the laboratory. Otherwise, we are sending our students to the metaphorial gunfight armed only with the equivalent of a slide rule and a table of logarithms.

Accordingly, I have incorporated a substantial (but mostly optional) AI presence in the support material for this book, primarily in systematic learning resources tailored specifically for each chapter with the aid of *GenAI* and made available on the Web, and in a subset of problems at the ends of each chapter that require the use of *GenAI*. One can use other AI resources, but for the presentation, problems, solutions, and support material associated with this book I assume the use of Google *Gemini* 3 in league with Google *NotebookLM*. The former is a remarkably capable *GenAI* (with a cool sidekick *Nano Banana* to generate images), and the latter is a sophisticated and AI-savvy management and content generation tool that interfaces smoothly with *Gemini* and allows creation of AI projects centered on specific topics defined by the user and employing AI training resources controlled by the user. *Gemini* and *NotebookLM* were chosen for the following reasons:

1. I have found this combination to be extremely powerful, efficient, and reliable when tested in a variety of both pedagogical and research applications.
2. *Gemini*, *Nano Banana*, and *NotebookLM* are easy to use and are free of charge (and free of ads) at the entry level.[2]
3. *NotebookLM* + *Gemini* supports collaboration in a manner similar to that for Google

[1] In 2025, I gave the midterm test for an undergraduate senior-level Astronomy 411 class ("Stars and Stellar Processes") to *Gemini* 3 and graded the response; it got 100% of the questions right (correct final answers and also valid intermediate reasoning). That test was not particularly hard, but each of the five questions required a mathematical solution of a problem, and some required detailed technical understanding of intermediate-level stellar physics (for example, of how to calculate thermonuclear reaction rates in a star, given some rate data and initial conditions). That exercise taught me two things: (1) If you give an unsupervised test—even a hard one—in advanced undergraduate or graduate classes, modern GenAIs are probably capable of solving most or all of the test. (2) This is a remarkable capability that we have to harness, and teach our students to harness, in both the classroom and the laboratory.

[2] The standard versions of *Gemini* and *NotebookLM* (which are free to use, ad-free, and easily accessible through a web browser or phone app) are adequate for most moderately sophisticated tasks but the subscription "Pro" tiers convey additional benefits such as permitting larger and more complex projects with more generous limits on the maximum number of content-generation requests allowed per day. As of this writing, a subscription to the Pro versions of *Gemini* and *NotebookLM* costs ∼$20 per month. The applica-

Box 0.1 Generative Artificial Intelligence and Large Language Models

Large Language Models (LLMs) are a specialized type of artificial intelligence (AI) trained on large sets of data to understand and generate human-like language. *Generative AI (GenAI)* aims to create new, original content (text, images, video, audio, music, software, ...) by learning patterns from existing data, often with an LLM as their language engine.

AI in Generative Form

Unlike traditional AI, which typically classifies or predicts based on fixed rules, generative AI produces novel output resembling work created by a human.

> For example, the same prompt given twice in succession to a *GenAI* will typically return similar but not exactly the same responses, as would be expected of a human expert responding extemporaneously at two different times to the same complex query.

The ability of LLMs to give human-like responses arises because they *predict statistically the most likely words in a correct response* rather than retrieving static, verified, and tabulated facts.

AI Hallucinations

This signature feature underlying the success of *GenAI* also is the source of its most glaring shortcoming,

> *AI hallucination* is where an AI model produces confident-sounding, plausible, but false, nonsensical, or fabricated information that is grounded neither in reality nor in its training data.

This spontaneous invention of bogus facts, citations, events, and so on can lead to convincingly stated but erroneous output ranging from minor inaccuracies to misinformation that could be harmful or even deadly if applied literally (for example, a confidently stated but erroneous list of edible mushrooms), especially if the AI is given vague prompts and/or is trained on limited or biased data. (A list of some famous AI hallucinations may be found at the link [1].)

Docs, but for a collaborative project rather than for a single document. This has obvious benefits within a research group, but also enables innovative collaborative assignments in the classroom.

tions discussed in this book are well within the capabilities of the free versions of the software, but note that the Pro tier may be available to qualifying students free of charge or at a discount.

4. In principle, the methodology employed by *NotebookLM* of grounding generated material in user-delimited sources rather than just in their general training greatly reduces the likelihood of *AI hallucinations*,[3] and the systematic referencing of sources that is enabled by *NotebookLM* facilitates greatly implementation of the *Question and Verify* mantra.

The generative AI resource material associated with this book may be accessed at

`http://eagle.phys.utk.edu/guidry/541/AI/as.html`

and an overview of how these resources may be integrated with the content of this book is given in Appendix G. It should be emphasized that these AI capabilities represent optional additions to the traditional textbook, and can be omitted completely simply by neglecting the above website supplying AI resources, omitting all problems after the "Numerical and GenAI Problems" subheading in the problem sets at the end of each chapter, and ignoring several appendices.

Systematic Inclusion of Computer Solutions and Graphics: Traditionally, classical E&M textbooks have emphasized problems having (sometimes challenging) analytical solutions, and often have been viewed (sometimes unfairly) as mostly an exercise in advanced mathematical physics. However,

1. real-world physics problems generally are not amenable to analytical solutions that are both comprehensive and accurate, and
2. recent advances in high-performance computation have been nothing short of breathtaking, placing increased emphasis on computational literacy as an essential skill for today's student. [4]

Thus it is incumbent on us, and on the students that we are training, to be conversant with desktop and high-performance computing for both research and teaching. Accordingly I have retained the traditional focus on analytical solution of advanced problems in electromagnetism, but have added various examples and problems exploring electromagnetic phenomena by numerical means. To implement this, I have chosen the computer language *Python*, for reasons given in Appendix E. These computing resources supporting the present book may be accessed at

`http://eagle.phys.utk.edu/guidry/541/cs/cs.html`

[3] This approach is called *Retrieval-Augmented Generation (RAG).* It improves LLMs by giving them access to external, up-to-date information from a knowledge base before they generate a response, making answers more accurate, relevant, and grounded in specific data, rather than just relying on their generic AI training data (which could be biased, out of date, and/or sparse in the specific area being investigated), which increases the likelihood of returning false information or encourages, in the parlance of AI, "hallucination to remain fluent".

[4] As this is written in early 2026, five undergraduate students and one graduate student carrying out research with me are developing improved modeling of thermonuclear and neutrino kinetic networks for simulation of supernova explosions and binary neutron star mergers. This development is being carried out on an *exascale machine* (*Frontier,* at Oak Ridge National Laboratory), which is capable of exceeding 10^{18} FLOPS = 1 exaFLOPS, where exa = 10^{18} and FLOPS = Floating Point Operations Per Second. Even undergraduates are computing at the exascale now!

and an overview of integrating those resources with the text of this book is given in Appendix E. I have also used systematically in examples and problems the capabilities of *Gemini* and *NotebookLM* to show students how to prompt an AI to write basic code for problems in electromagnetism, and how to implement and verify that code and its results. For example, many problems in the book that use *GenAI*-written code require as part of the solution a brief synopsis of how the *GenAI* was prompted, any debugging steps that were required, a description of the code functionality, and a narrative describing how the validity of the code and its solutions were verified. I have followed several guidelines in choosing the numerical exercises to include as problems in the book.

1. Numerical exercises should illustrate aspects of classical electromagnetism that exhibit some combination of
   a. Effects that require going beyond standard analytical solutions; for example, the more realistic fields associated with parallel-plate capacitors having plates of finite extent or solenoids having finite length.
   b. Providing multi-D interactive graphics and motion graphics illustrating important basic principles (even when the solution can be expressed analytically). For example, the 3D animation of the fields associated with a point charge viewed from a reference frame with relative velocity $0 < v < c$ that students are asked to construct in Ch. 18, which illustrates visually the relativistic pancake compression of the electric field in the direction of motion and the spontaneous generation of a transverse magnetic field where there was none before for $v > 0$.[5] This conveys in dramatic visual fashion that in special relativity electric fields and magnetic fields are two sides of the same coin.
2. Students should be exposed to important aspects of computational physics as part of the exercise. For example, Problem 2.15 asks students to use the *GenAI* to solve numerically the 2D Laplace equation on a 100×100 grid with execution timings. In the process of prompting the *GenAI* to write Python code to solve this problem, the student is required to explore (1) setting up and timing the code for the calculation with normal Python loops that solve the problem by Jacobi iteration, (2) accelerating convergence by using Gauss–Seidel and successive over-relaxation (SOR) methods, (3) optimizing by introducing adaptive step size, (4) implementing parallelization (vectorization) of the SOR algorithm using a red–black (checkerboard) algorithm, (5) comparative timing of these different numerical approaches to emphasize the enormous increase in speed that can be realized from choice of algorithm, adaptive integration steps, and implementation of efficient parallelization.[6] In this one problem, students are taught
   1. how to prompt a *GenAI* to write and debug *Python* code for a realistic physics problem (summarized in Appendix E),

[5] See `http://eagle.phys.utk.edu/guidry/541/cs/ch/ch16/relativistic_v13_6.html` for the 3D interactive animation showing the electric and magnetic vector fields at rest, with relative velocities up to $0.95c$ set by a slider, and user ability to zoom and rotate the 3D vector fields, and turn fields on and off to highlight specifics.

[6] In this exercise, it is common for students to see factors of order hundreds increase in speed in going from simple Jacobi iteration to the final optimized and parallelized SOR code.

2. numerical algorithms to solve Poisson or Laplace equations (summarized in Appendix F),
3. speeding code up by choice of algorithm and optimization of integration steps, and
4. implementing parallelization (vectorization).

Unless you can assume that students come to class already proficient in *Python* programming, only *GenAI* provides the possibility of incorporating options of this kind in a standard advanced E&M course without having to expand the required credit hours for the course, or attach an additional programming-experience prerequisite. With the approach advocated here, a tireless virtual assistant is teaching programming to students as an integral part of solving specific physics problems. I consider myself to be a competent programmer, fluent in multiple computer languages. In my experience,[7] the tutoring in computational methods offered by the *GenAI* in developing the *Python* code for individual problems in this book has been exemplary. In the representative example of Problem 2.15 discussed above, each step of the process generated a basic *Python* script, and then adding successive improvements to make the code more efficient or to cure problems that cropped up in the solution was an interplay between suggestions by the student and suggestions by the *GenAI*, with the AI offering clear rationale for each step attempted, and an explanation and suggested correction if a step failed, and usually a concise explanation of *why* the correction should work. In no case did the *GenAI* simply produce a black-box solution. As a consequence, I felt an integral part of coding the problem solution, even though I was not physically writing any lines of code.

Finally, these *GenAI* and numerical computing capabilities represent *optional additions* to the traditional textbook. They can be omitted completely by neglecting the above website supplying numerical computing resources, omitting all problems after the "Numerical and GenAI Problems" subheading in the problem sets at the end of each chapter, and ignoring a few Appendices and Examples.

Geometrical and Topological Aspects of Electromagnetism: The traditional vector calculus approach to classical electromagnetism emphasizes a practical way to deal with vectors and more generally tensors by expanding them in a suitably chosen basis. For solving realistic physics problems this is often the most expeditious approach, and it is used extensively in this book. But vectors and tensors are *geometrical objects* that exist independent of any specific coordinate system, and our utilitarian approach of expanding in a basis obscures the geometrical elegance of these objects.

For two centuries, mathematicians have labored to formulate the equations dear to theoretical physics in a *coordinate-free manner* that is often less practical for solving realistic problems, but is more concise and elegant, and often renders deeper truths more apparent.

[7] I presume that other *GenAI* options may afford similar capabilities, but any specific statements made here about *GenAI* are based only on my experience with *Gemini* and *NotebookLM*.

Some buzzwords associated with this more mathematical approach include vectors, duality, dual vectors, differential forms, exterior derivatives and the exterior calculus, Hodge star operators, covariant derivatives, connections, fiber bundles, ..., most of which are at best vaguely familiar to students of classical electromagnetic physics.

But we can have beauty and efficient solution of problems too! Even if our everyday physics workhorse is expansion in a basis and manipulation of the resulting indices according to the rules governing tensor components, we can still appreciate the more elegant index-free approach as the mathematical foundation of our methods. Accordingly, I have devoted Chapter 16 to a concise introduction to the coordinate-free mathematical approach, and used it in later chapters to introduce topics that are then translated into vector-calculus language.

Topology, once a niche aspect of particular subfields of physics, is arguably now the most consequential idea in all of condensed matter physics and material science. But topology also plays a role in electromagnetic phenomena other than those in topological matter. Thus I include Chapter 19 on topological aspects of electromagnetism, expressed initially in the mathematical language of *differential forms* and *fiber bundles*, but with a clear translation of these concepts into the familiar language of vector calculus.

Special Relativity and the Geometry of Spacetime: The *special theory of relativity* typically appears within the syllabus of an advanced E&M course for several reasons.

1. Historically, the structure and implications Maxwell's equations describing classical electromagnetic theory were a large influence on Einstein in developing the special theory of relativity (and on Lorentz in developing the eponymous transformations laying the mathematical framework for Einstein's theory).
2. Special relativity provides a deep and elegant understanding of the relationship between classical electric and magnetic forces.
3. Electromagnetism specifically for relativistic charged particles is important for certain problems in fields like astrophysics or accelerator physics.

However, the treatment of special relativity in the context of classical E&M is often a specialized one that obscures the mathematical foundations of special relativity (that it is a consequence of geometry described by a spacetime metric), and obscures the historical sequence that Maxwell's equations describing classical electromagnetism led Einstein to special relativity, which led eventually to general relativity,

$$Maxwell's\ equations \longrightarrow Special\ relativity \longrightarrow General\ relativity.$$

As Minkowski taught us, special relativity follows from the geometry of spacetime, which is a flat (no intrinsic curvature), 4D Lorentzian manifold, and is described in terms of *differential geometry* and *spacetime tensors*. I introduce the spacetime tensor formalism in its general form (valid for curved or flat spacetime, though we shall deal only with flat spacetime here), beginning from the mathematician's index-free view of tensors as maps from vectors and dual vectors to the real numbers, and then derive the physicist's pragmatic "index-manipulation of tensors expanded in a basis" approach. I then restrict to flat spacetime to recover the tensor formalism for flat Minkowski space, and discuss the basics of

special relativity in that framework, and the tensor formulation of the Maxwell equations in a manifestly covariant form. This approach anchors the discussion of special relativity and Maxwell equations mathematically, gives a basic introduction to mathematics that students will encounter if they consider more advanced topics such as general relativity, and provides a unified framework to view Maxwell's equations, special relativity, and general relativity in the same covariant notation.

Supplemental Material: As outlined above, free and open websites associated with this book provide extensive tutorial material for application of *GenAI* and Python programming, including production of publication-quality graphics, for problems in classical electromagnetism. In addition, solutions for all problems found at the ends of chapters in the book are contained in the *Instructor Solutions Manual*, which is free of charge but available only to instructors. About half of the problems at the ends of chapters are marked ***, indicating that their solutions may be found in the *Student's Solutions Manual*, which is free of charge and available to everyone.

Finally, let me emphasize that this draft book is a continuously updated work in progress, made available for the benefit of students taking Physics 541 at the University of Tennessee. *Please do not distribute its contents without checking with me first.*

Mike Guidry
Knoxville, Tennessee
May 26, 2026

1 Introduction

The first inkling of the properties that we now attribute to electricity and magnetism traces to the distant past when humans began to realize and remark upon observed physical phenomena such as the behavior of naturally occurring electricity in amber and the properties of naturally occurring magnetism in lodestones. Although these phenomena were known qualitatively to the ancient Greeks, they remained mysterious for centuries and the modern quantitative understanding of electricity and magnetism emerged over a period of only a little over a century, beginning in the late 1700s.

1.1 The Synthesis of Classical Electromagnetism

At the risk of slighting the contributions of many, one could say that the explosion in knowledge of electricity and magnetism beginning in the late 18th century, and the forging of that knowledge over the next century or so into a theoretically and mathematically coherent framework that we now call electromagnetism, can be illustrated by citing a few landmark achievements.

1. *Henry Cavendish* (1731-1810) did pioneering experiments on electrostatics in the early 1770s, including establishing that electrical forces varied as one over the square of the distance. However, his work was not widely published until after Coulomb's publication in 1785.
2. *Charles-Augustin de Coulomb* (1736-1806) published his extensive work on electrostatics beginning in 1785, including the eponymous inverse-square law for electrical interaction between charges.
3. *Hans Christian Ørsted* (1777-1827) discovered the magnetic effect of the electric current, establishing the first connection between electric and magnetic phenomena.
4. *André–Marie Ampère* (1775-1827) extended the work of Ørsted, finding in 1823 the circuit law between electric current passing through a loop and magnetic field around the loop, and establishing the formula describing the interaction of two currents.
5. *Michael Faraday* (1791-1867) did his highly influential work studying time-varying currents and fields in the mid-1800s. He discovered electromagnetic induction in 1831, which proved to be a crucial step in Maxwell's unification of electric and magnetic phenomena into modern electromagnetism.
6. *James Clerk Maxwell* (1831-1879) published his famous 1865 paper (read to the Royal Society in 1864), which unified electricity and magnetism and synthesized in equations a dynamical theory of what could now be termed the *electromagnetic field* [50, 53].

7. *Oliver Heaviside* (1850-1925) reformulated Maxwell's equations in their more modern vector calculus form in the late 1800s.
8. Heinrich Rudolph Herz (1857-1894) produced the transverse electromagnetic waves predicted by Maxwell's theory in the laboratory in 1888, and studied their wave properties (refraction, reflection, ...) This placed Maxwell's theory on firm experimental footing and established experimentally the connection between electromagnetism and optics suggested by Maxwell's theory.
9. *Joseph John Thomson* (1856-1940) discovered the electron in 1897. This was the first step in elaborating how electromagnetic waves interacted with matter at a microscopic level, though a full microscopic theory of atoms and molecules awaited the invention of quantum mechanics in ∼1925-1926. This, for example, allowed the classical Drude model for conduction electrons described in Section 7.3.2 to be constructed, even though there wasn't yet (in the year 1900) a theory of atoms in any modern form.
10. *Albert Einstein* (1879-1955) published his *special theory of relativity* in 1905. It was inspired by Maxwell's theory, since Einstein was strongly motivated by a desire to unify particle motion and electromagnetism, which he realized could be accomplished only if both were described by Lorentz-covariant theories.

One should add to this list the *invention of quantum mechanics* in 1925-1926, which provided a firm basis for describing electromagnetism interacting with matter. But this book is about *classical electromagnetism,* and the quantum revolution that shook the foundations of microscopic physics beginning in 1925 is primarily part of a *quantum theory of electromagnetism*, which merits a separate book and is necessarily beyond our present scope. Nevertheless, we shall often need to allude to the microscopic behavior of atoms and molecules in our discussion of electromagnetism in the presence of matter, which ultimately requires quantum mechanics. Thus, we shall freely invoke quantum mechanics, when needed, but those discussions will tend to be qualitative.

1.2 The Maxwell Equations

By the late 1800s the basics of classical electromagnetic theory could be summarized concisely in the *Maxwell equations,*which may be written in free space and in modern vector calculus notation as

$$\boldsymbol{\nabla}\cdot\boldsymbol{E}=\frac{\rho}{\epsilon_0} \qquad \text{(Gauss's law)}, \tag{1.1a}$$

$$\boldsymbol{\nabla}\times\boldsymbol{E}+\frac{\partial\boldsymbol{B}}{\partial t}=0 \qquad \text{(Faraday's law)}, \tag{1.1b}$$

$$\boldsymbol{\nabla}\cdot\boldsymbol{B}=0 \qquad \text{(No magnetic charges)}, \tag{1.1c}$$

$$\boldsymbol{\nabla}\times\boldsymbol{B}-\frac{1}{c^2}\frac{\partial\boldsymbol{E}}{\partial t}=\mu_0\boldsymbol{J} \qquad \text{(Ampère's law, as modified by Maxwell)}, \tag{1.1d}$$

using modern notation and SI units (see the discussion of units in Section 2.2), where

1. $\boldsymbol{E}$ is the electric field,
2. $\boldsymbol{B}$ is the magnetic field,
3. ρ is the charge density,
4. $\boldsymbol{J}$ the current vector,
5. ϵ_0 is the *permittivity of free space* [defined for SI units in Eq. (2.3)], and
6. μ_0 is the *permeability of free space,* which takes the value

$$\mu_0 = 4\pi \times 10^{-7}\,\mathrm{N\,A^{-2}}, \tag{1.2}$$

when expressed in SI units, where N is newtons and A is amperes.

It should be noted that the SI-system constants ϵ_0 and μ_0 are *not independent* but are constrained by $\mu_0\epsilon_0 = 1/c^2$, where c is the speed of light.[1] Equation (1.1c) is also sometimes referred to as "Gauss's law for magnetism" or "the magnetic Gauss's law", because of its similarity to Eq. (1.1a). Equations (1.1b) and (1.1c) are termed collectively the "inhomogenous Maxwell equations" or the "source-free Maxwell equations", and Equations (1.1a) and (1.1d) are termed collectively the "homogeneous Maxwell equations" or the "sourced Maxwell equations".

Maxwell's original formulation of what we now call the Maxwell equations was in terms of the vector and scalar potentials instead of the electric and magnetic fields (see Sections 2.7 and 8.8 for the relationship between the potentials and the fields), required 20 equations instead of four, and did not use the modern vector calculus notation of Eqs. (1.1), which was invented later by Oliver Heaviside and independently by J. Willard Gibbs.[2] Heaviside reduced Maxwell's 20 equations to the four in Eqs. (1.1), by writing them entirely in terms of the electric and magnetic fields in the new vector calculus notation. Later we will see that in modern mathematical notation it is possible to reduce this further to just two independent equations (see Sections 18.10 and 19.4.4). One cannot overstate the value of compact, concise, and evocative notation in the advancement of mathematical physics, and Ref. [40] may be consulted for the history of this evolution in notation for electromagnetic equations.

The Maxwell equations exhibit a set of symmetries that are summarized in Box 1.1. In Ch. 12 we shall elaborate on the relationship of these symmetries to the conservation laws obeyed by classical electromagnetism.

1.3 Charge Conservation

An important symmetry listed in Box 1.1 is local conservation of charge. The charge density ρ and the current vector $\boldsymbol{J}$ appearing in the Maxwell equations are not independent but are constrained by the *continuity equation,*

$$\frac{\partial \rho}{\partial t} + \boldsymbol{\nabla}\cdot\boldsymbol{J} = 0 \qquad \text{(Continuity equation)}, \tag{1.3}$$

[1] This relationship between ϵ_0 and μ_0 is a consequence of the units chosen for the electric field and magnetic field in the SI system.

[2] Maxwell's original 20 equations are displayed and explained at the website [2].

Box 1.1 Symmetries of the Maxwell Equations

Symmetry plays a fundamental role in physics [38]. The Maxwell equations (1.1) exhibit symmetries that have important implications for electromagnetism.

1. *Space and Time Translations:* Invariance under translations in space and time is associated with conservation of momentum and energy, respectively. Satisfaction of these invariances by the Maxwell equations implies that *energy and momentum can be assigned to the electromagnetic field*.
2. *Rotations:* The formulation of the Maxwell equations as vector equations ensures rotational invariance (isotropy of space), which in turn implies conservation of angular momentum by the electromagnetic field.

The association of invariance under space translations, time translations, and rotations with conservation of linear momentum, energy, and angular momentum, respectively, is a general consequence of Noether's theorem: *For every continuous symmetry of a field theory Lagrangian there is a corresponding conserved quantity.* See Section 16.2 of Ref. [38].

3. *Space Inversion (Parity) P:* In the presence of rotational invariance, parity is equivalent to mirror reflection. Under inversion $\boldsymbol{E} \to -\boldsymbol{E}$, which is the transformation law for a *polar vector* (normal 3-vector), but under inversion $\boldsymbol{B} \to \boldsymbol{B}$, which is the transformation law for a *pseudovector* or *axial vector*.
4. *Time Reversal (T):* A motion picture of electromagnetic events would be consistent with the Maxwell equations if run backward or forward.
5. *Lorentz Covariance:* Electromagnetism isn't Galilean invariant but is Lorentz covariant (it is consistent with special relativity), while Newtonian mechanics is Galilean invariant but not Lorentz invariant (it is inconsistent with special relativity). The Maxwell equations (1.1) are *Lorentz covariant* (their validity is unaltered by Lorentz transformations). However, this isn't clear from the notation because space and time enter on an equal footing in special relativity and the use in Eqs. (1.1) of 3-vectors instead of 4-vectors, and of separate derivatives for space and time, obscures this covariance. Later we will re-write the Maxwell equations in a manifestly Lorentz-covariant form.
6. *Gauge Invariance:* Consistency of the Maxwell equations with Eq. (1.3) requires *charge to be conserved locally,* which implies *local gauge invariance of the electromagnetic field* (see Section 1.3). We shall have much to say about gauge symmetry and its far-reaching implications in later chapters.
7. *Electric and Magnetic Field Asymmetry:* The Maxwell equations exhibit a large *asymmetry* between electric and magnetic fields [most obvious in CGS units; see Appendix B.2]. If a magnetic charge $4\pi\rho_{\rm m}$ were added to the right side of Eq. (B.3c) and a magnetic current $(4\pi/c)\boldsymbol{J}_{\rm m}$ added to the right side of Eq. (B.3b), the Maxwell equations would become symmetric under $\boldsymbol{E} \to \boldsymbol{B}$ and $\boldsymbol{B} \to -\boldsymbol{E}$. However, *no free magnetic charges have ever been observed*.

which ensures *local conservation of charge* by requiring that variation of electrical charge in some arbitrarily small volume V is caused by flow of electrical current through the surface S bounding that volume.[3] The local conservation of charge implied by Eq. (1.3) is not a separate feature, but is implied by the Maxwell equations themselves (see Problem 1.1). As indicated in Box 1.1, this conservation of charge by the equations of electromagnetism is associated with the *gauge symmetry of electromagnetism*, which will enter our later discussion in a number of forms.[4]

1.4 Maxwell and the Displacement Current

A feature of the Maxwell equations with profound implications is that Maxwell realized that the original form of Ampére's law [which lacked the $\partial \boldsymbol{E}/\partial t$ term of Eq. (1.1d)] was *inconsistent with Eq. (1.3)* because it was valid only for *stationary charge densities*. As will be discussed in Section 11.1.1, Maxwell then added the $\partial \boldsymbol{E}/\partial t$ term (which is called the *displacement current*) to Ampère's law in Eq. (1.1d); this brought the full set of equations (1.1) into harmony with Eq. (1.3), and effectively brought together the previously separate subjects of electricity and magnetism. As a result, Eq. (1.1d) is also called the Ampère–Maxwell law. The addition of the displacement current to Eq. (1.1d) has a number of far-reaching implications.

1. We may now speak of the unified subject of *electromagnetism*.
2. The fundamental equations of electromagnetism are now consistent with charge conservation.
3. This modification will lead eventually to the interpretation of electromagnetic waves as light waves.
4. That Maxwell's equations are consistent with the continuity equation and thus conserve charge locally will lead to the idea of classical *electromagnetic gauge invariance*, which will underlie a quantum field theory of electromagnetism (*quantum electrodynamics* or QED).
5. Electromagnetic gauge invariance will eventually be generalized to more complex gauge invariance in the weak and strong interactions, resulting in the quantum field theory that we term the *Standard Model* of elementary particle physics.

We emphasize that the introduction of the displacement current by Maxwell was not in

[3] We shall sometimes use the notation from algebraic topology $S = \partial V$ for the surface S bounding a closed volume V, where in this context ∂ is an operator that returns the surface bounding a closed volume (see the discussion in Section 19.4).

[4] Some authors object to terming gauge invariance a symmetry because some properties of a gauge transformation differ from those of traditional symmetries (for example, see Ref. [71]). We believe it more useful to employ an expansive definition: the essence of a symmetry principle is that some quantity is fundamentally unobservable, and this implies an invariance under a related mathematical transformation [38]. By this criterion gauge invariance qualifies as a symmetry since a gauge transformation does not change the classically observable consequences of the electric and magnetic fields, so we will use "gauge invariance" and "gauge symmetry" interchangeably here.

response to any new experimental results demanding a revision of the theory; Maxwell introduced it to fix what he saw as an inconsistency in the equations thought to describe electricity and magnetism at that time. The rather remarkable consequences of the above list have been confirmed experimentally and are testament to the power of requiring mathematical consistency in physical theories.

1.5 Classical Electromagnetic Forces

The four Maxwell equations of Eqs. (1.1), supplemented by appropriate boundary conditions,[5] may be solved for the fields $\boldsymbol{E}$ and $\boldsymbol{B}$, if the charge density ρ and current $\boldsymbol{J}$ are known. However, these equations make no reference to *forces*, which are often the tangible connection to experimental results in classical physics. This is remedied by introducing the empirically justified *Lorentz force law*,

$$\boldsymbol{F} = q(\boldsymbol{E} + \boldsymbol{v} \times \boldsymbol{B}) \qquad \text{(Lorentz force)}, \tag{1.4}$$

which implies that the electromagnetic force acting on a particle having charge q and velocity $\boldsymbol{v}$ at the point $\boldsymbol{x}$ is determined completely by the instantaneous values of the fields $\boldsymbol{E}$ and $\boldsymbol{B}$ at $\boldsymbol{x}$. Then Newton's second law relating momentum change to force,

$$\frac{d\boldsymbol{p}}{dt} = \boldsymbol{F}, \tag{1.5}$$

allows calculating the complete motion of charges in an classical electromagnetic field.

1.6 Internal Consistency of Electromagnetism

Classical mechanics is internally self-consistent, in the sense that there are phenomena outside its domain (very small requires quantum theory; very fast requires special relativity; very strong gravity requires general relativity), but it gives internally consistent results when restricted to its domain of validity. Classical electromagnetism is different. In Eq. (2.45) we shall show that the energy U of a continuous charge distribution $\rho(\boldsymbol{x})$ is the work W required to assemble it,

$$U = W = \frac{\epsilon_0}{2} \int E^2 d\tau,$$

[5] We will have much more to say about this later but, loosely, physically acceptable boundary conditions in static problems require fields to vanish rapidly enough at infinity, while in dynamical problems fields must represent outgoing solutions so that there is no unphysical flow of energy from infinity into regions of interest.

where $\boldsymbol{E}$ is the electric field associated with $\rho(\boldsymbol{x})$ and the integration is over all of space. But from Eq. (2.9), the electric field of a continuous charge distribution behaves as

$$\boldsymbol{E}(\boldsymbol{x}) = \frac{1}{4\pi\epsilon_0}\int \rho(\boldsymbol{x}')\,\frac{\boldsymbol{x}-\boldsymbol{x}'}{|\boldsymbol{x}-\boldsymbol{x}'|^3}\,d^3x',$$

and U diverges as $|\boldsymbol{x}-\boldsymbol{x}'|^{-4}$ upon approaching a point charge located at $\boldsymbol{x}'$. This *infinite self-energy* of a classical point charge may be viewed as resulting from the charge acting on itself and is clearly unphysical; the first thought is that it must be excluded from the energy of a charge distribution. But further problems arise if one considers *accelerated charges*, which radiate electromagnetic waves and must lose energy; this can be thought of most simply as a radiative damping force acting on the charged particle, which again forces us to think of the charge acting on itself, with the short-range limit diverging.

We conclude that there is no consistent way to deal with such self-energies in classical electromagnetism and the theory is internally inconsistent.[6] However, as a practical matter we may ask at what order of magnitude for distance and time scales does one expect such inconsistencies lead to actual problems? Consider the self-energy of an electron. As far as is known experimentally elementary particle like electrons are point-like, without spatial extent. But if the electron is assumed to have a finite radius $r_{\rm e}$, the electrostatic energy becomes of order $e^2/r_{\rm e}$, where e is the electron charge. The only other energy scale in the problem is the electron restmass energy $m_{\rm e}c^2$, and if we equate these two energy scales and solve for $r_{\rm e}$,

$$r_{\rm e} = \frac{e^2}{mc^2} = 2.82\times10^{-13}\,\text{cm}, \tag{1.6}$$

which is known as the *classical radius of the electron*. (In comparison, the Bohr radius of the hydrogen atom is 0.529×10^{-8} cm.) A corresponding timescale is given by the time for light to travel this distance,

$$\tau_e = \frac{r_{\rm e}}{c} = \frac{e^2}{mc^3} \simeq 10^{-21}\,\text{s}. \tag{1.7}$$

Unless we consider motion of charges that changes over a length scale of order $r_{\rm e}$, or a timescale of order $\tau_{\rm e}$, the infinities associated with self energies are of no practical significance. In fact, one expects quantum effects to become important on a length given by the *Compton wavelength* $r_{\rm C} = \hbar/mc$, which is

$$\frac{r_{\rm C}}{r_{\rm e}} = \frac{\hbar/mc}{e^2/mc^2} = \frac{\hbar c}{e^2} \simeq 137$$

[6] Similar problems with infinities associated with matrix elements evaluated at a point (such as the infinite self-energies of point particles) arise in quantum field theory (QFT). There a scheme called the *renormalization program* has been developed to systematically subtract away the infinities in observable quantities and bury them in quantities that are not observable. Not everyone is comfortable philosophically with the "sweeping under the rug" nature of the quantum renormalization scheme, but it is undeniable that renormalization succeeds in removing infinities from observables, and that the resulting (finite) predictions of quantum field theory are usually in spectacular agreement with experimental observables. Furthermore, there are arguments derived from the Wilson renormalization group formalism that renormalization of physical systems at some physical scale by integrating over quantities at a more microscopic scale is a natural property of all physical systems, not just those described by QFT. However, exploring that would cause us to stray far from the central topic of this book, and must be left for a different conversation.

times larger than the classical electron radius. We conclude that inconsistencies associated with self-energies of charged particles are irrelevant for our discussion.

1.7 Classical Electromagnetic Solutions

Thus the understanding of classical electromagnetism can be summarized in a succinct admonition: to be blunt, "shut up and calculate", or to be less blunt and more precise,

> *Solve Maxwell's equations with appropriate boundary conditions for the electric and magnetic fields, and use those to compute forces and observables.*

While this admonition is not wrong, it risks leaving two things at loose ends.

1. Solution of Maxwell's equations with appropriate boundary conditions can be a demanding task, often requiring considerable mathematical and computational prowess.
2. Although classical electromagnetism itself has changed little since the late 1800s, the context in which we view classical electromagnetism has been altered dramatically by modern advances in quantum field theory (which were often inspired and guided by the theoretical understanding of classical electrodynamics).

The following chapters will address the first point practically, by providing mathematical and computational tools to facilitate solution of Maxwell's equations in various contexts. The rest of the current chapter addresses the second point more philosophically, by setting electromagnetism more broadly in the context of modern theoretical physics.

1.8 Electromagnetism in Modern Physics

Let us make some general remarks about the relationship of classical electromagnetism to modern theoretical physics.

1.8.1 Gauge Symmetry

A remarkable findings of modern physics is that the already beautiful edifice of Maxwell's equations for electromagnetism that we shall elaborate in these lectures hides within it a deceptively powerful symmetry called *(local) gauge invariance*—in essence a symmetry under local phase transformations—that was introduced in Box 1.1 and, with suitable exposition, explains the origin of both classical and quantum theories of electromagnetism. But that is not all! The local gauge symmetry describing electromagnetism can be generalized mathematically into a more powerful theory that can *partially unify* the electromagnetic and weak nuclear forces into a single *electroweak interaction*, and this can be

generalized into the *Standard Model* (of elementary particle physics) that partially unifies the electromagnetic, weak, and strong interactions in a single non-abelian gauge theory.

In quantum field theory local gauge symmetries are generated by a set of quantum operators. If the quantum operators all commute among themselves, the gauge symmetry is said to be *abelian*; if they do not all commute, the gauge symmetry is said to be *non-abelian* (see the discussion of symmetries and group theory in Box 18.1). Because of the constraints arising from non-zero commutators among operators, non-abelian gauge symmetries typically exhibit more complex behavior than abelian gauge symmetries. Electromagnetism corresponds to an abelian local gauge symmetry (with the quantum version known as *quantum electrodynamics or QED*). In Ch. 21 we shall explore in more depth this view of classical electromagnetism as an abelian gauge field theory and its relationship to quantum electrodynamics. The Standard Electroweak Model and its generalization to the Standard Model incorporating the strong interactions (*quantum chromodynamics or QCD*) correspond to more complex non-abelian local gauge symmetries. Non-abelian models of elementary particles are also known as *Yang–Mills field theories*.

1.8.2 Quantization of Electrical Charge

The basic unit of electrical charge is given by the magnitude of the charge on an electron, which is measured to be

$$e \equiv |q_{\rm e}| = 1.60217733 \times 10^{-19}\,{\rm C} \qquad [\text{in SI units}]. \tag{1.8}$$

The charges on protons, and all presently known particles or systems of particles, are found to be *integral multiples of this unit* (with positive or negative signs for non-zero charges). It is known experimentally that the ratios of electrical charges between different particles are integers to one part in 10^{20}. Indeed, the stability of the atomic matter all around us would be compromised by even a tiny difference in the absolute values of the electron and proton charges, so the very existence of the observable Universe is strong evidence for quantization of electrical charge. One argument for why electrical charge is quantized is Dirac's topological argument, as described in Box 1.2.

Since Dirac's topological argument presumes the existice of magnetic monopoles and there is no evidence for the existence of free magnetic charge, we must conclude that there is presently no convincing fundamental explanation for the observed quantization of electrical charge in integer multiples of the electron charge within classical electromagnetism. There are constraints arising from from what are called *anomalies* in relativistic quantum field theory and the phenomenology of the Standard Model of elementary particles physics outlined in Box 1.3 that might provide an explanation, but that is beyond the scope of our discussion of classical electromagnetism. Nevertheless, we know empirically that electrical charge exists and appears to be conserved, so absence of a convincing fundamental explanation for quantization of charge does not preclude developing a theory of classical electromagnetism.

Box 1.2 Dirac Topological Argument for Quantized Electrical Charge

Dirac proposed long ago that if fundamental magnetic charges (magnetic monopoles) existed, there could be a topological reason for electrical charge quantization. However, no reproducible observations of magnetic monopoles have ever been reported, so Dirac's idea remains only conjecture. As we have noted in Box 1.1, if magnetic monopoles did exist the Maxwell equations (1.1) would require modifications that would make them more symmetric with respect to electric and magnetic fields.

Theory and Magnetic Monopoles

Magnetic monopoles are forbidden by the present Maxwell equations (absent the Dirac topological argument), and have never been observed experimentally. But it should be noted that most theories that go beyond the Standard Model such as Grand Unified Theories (GUTs) and String Theory lead naturally to topological excitations having the character of magnetic monopoles, which might have formed in the very early Universe when energy densities were extremely high.

Monopoles and Cosmology

However, such theories have not been confirmed experimentally, and the predictions of *inflationary cosmology* (see Section 21.3 of Ref. [36] for an introduction) suggest that any magnetic monopoles that were formed in the very early Universe would have been diluted to essentially zero density by the exponential expansion of the Universe in the inflationary period.

1.8.3 Charges of Known Elementary Particles

Our modern view is that matter in the Universe consists of the fermions in the Standard Model (of elementary particle physics). The elementary particles of the Standard Model are summarized in Fig. 1.1. In the Standard Model all matter is formed from fermions ($e, \nu_e, u, ...$), while interactions between elementary particles are mediated by the exchange of gauge bosons ($\gamma, G, W^{\pm}, Z^0$), and masses for bare (that is, non-interacting) particles arise from couplings to the Higgs boson H. For reasons that remain elusive, the fermions (matter fields) of the Standard Model may be divided into three generations (or families), I, II, and III, with the fermions of each generation being successively more massive than in the preceding generation, and with many properties repeating themselves in successive generations. To give one example, the muon μ in generation II acts in many respects as if it were a heavier version of the electron e in generation I. Table 1.1 gives Standard Model quark quantum number assignments for the six known quark flavors displayed in Fig. 1.1. As indicated in Table 1.1, the (electrical) charge Q of each quark is given

Box 1.3 **Anomalies, GUTs, and Charge Quantization**

In a quantum gauge field theory, when a symmetry that is obeyed in a classical system is broken by the act of quantizing that system, it is termed an *anomaly*. Anomalies by themselves do not require electric charge to be quantized, but for a gauge theory like the Standard Model of elementary particle physics to be renormalizable and thus self-consistent, any anomalies arising in its quantization must cancel exactly, and that required cancellation effectively imposes quantization of electrical charge in order to reproduce the phenomenology of the Standard Model. In addition, the symmetry requirements in various grand unified theories (GUTs), such as those based on SU(5) or SO(10) symmetries, impose quantization of charge. However, we now know that there is (as yet uncertain) physics beyond the standard model because of observed neutrino flavor oscillations, implying a finite neutrino mass, contrary to the assumption of identically zero neutrino mass in the Standard Model, and GUTs are conjectures that are not yet supported experimentally, so change quantization is suggested by anomaly cancellation in the Standard Model and by some grand unified theories, but cannot yet be taken as proven.

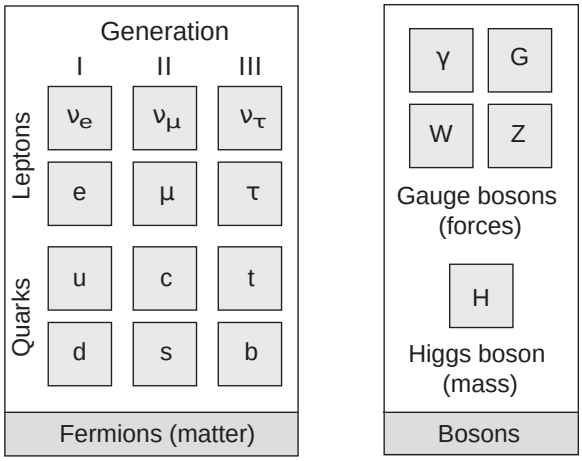

Fig. 1.1 Elementary particles of the Standard Model. Photons are labeled by γ and gluons by G. Elementary particles of half-integer spin that don't undergo strong interactions are called *leptons;* electrons and electron neutrinos are examples. Particles made from quarks, antiquarks, and gluons (and thus that undergo strong interactions) are called *hadrons*; pions (pi mesons) and protons are examples. A subset of hadrons corresponding to more massive particles containing three quarks are called *baryons*; protons and neutrons are examples. The different types of neutrinos $(\nu_e, \nu_\mu, ...)$ and the different types of quarks (u, d, s, ...) are called *flavors*. For simplicity the largely parallel classification of antiparticles has been omitted in this diagram.

Table 1.1 Quantum number assignments for quarks [34]

	Up	Down	Strange	Charm	Bottom	Top
Symbol	u	d	s	c	b	t
Baryon number (B)	$\frac{1}{3}$	$\frac{1}{3}$	$\frac{1}{3}$	$\frac{1}{3}$	$\frac{1}{3}$	$\frac{1}{3}$
Spin	$\frac{1}{2}$	$\frac{1}{2}$	$\frac{1}{2}$	$\frac{1}{2}$	$\frac{1}{2}$	$\frac{1}{2}$
Charge (Q)	$\frac{2}{3}e$	$-\frac{1}{3}e$	$-\frac{1}{3}e$	$\frac{2}{3}e$	$-\frac{1}{3}e$	$\frac{2}{3}e$
Isospin (T)	$\frac{1}{2}$	$\frac{1}{2}$	0	0	0	0
Projection of isospin (T_3)	$\frac{1}{2}$	$-\frac{1}{2}$	0	0	0	0
Strangeness number (S)	0	0	-1	0	0	0
Charm number (c)	0	0	0	1	0	0
Bottom number (b)	0	0	0	0	-1	0
Top number (t)	0	0	0	0	0	1

The additive quantum numbers Q, T_3, S, c, B, b, and t of the corresponding antiquarks are the negative of those for quarks. The charge is given by $Q/e = T_3 + \frac{1}{2}(B + S + c + b + t)$, where e the absolute value of the electron charge.

by

$$Q/e = T_3 + \frac{1}{2}(B + S + c + b + t), \tag{1.9}$$

which leads to third-integer charges for all the quarks (row 4 of Table 1.1).

Example 1.1 From Eq. (1.9) and Table 1.1, the charge of the down quark d is

$$\begin{aligned} Q_d/e &= T_3 + \frac{1}{2}(B + S + c + b + t) \\ &= -\frac{1}{2} + \frac{1}{2}\left(\frac{1}{3} + 0 + 0 + 0 + 0\right) \\ &= -\frac{1}{3}. \end{aligned}$$

This quantization of charge in integer multiples of $\pm\frac{1}{3}$ of the absolute value of the electron charge is characteristic of quarks, as may be seen from Table 1.1.

However, the non-abelian gauge field theory of the strong interactions (quantum chromodynamics) predicts that *quarks are confined and can never appear as free particles,*[7] and

[7] More precisely, the gauge theory of the strong interactions, quantum chromodynamics (QCD), is thought to exhibit *color confinement:* particles carrying the strong-interaction gauge charge (called whimsically "color", with no relationship to the usual meaning of color) are *confined* to the interior of the hadrons such as neutrons and protons, and can never appear as free particles. Finding solutions for the equations of QCD is extremely difficult because it is a strongly interacting, highly non-linear field theory in the limit that would lead to confinement. Thus it is not simple to prove that QCD is color-confining. However, modern large-scale

indeed no free particles with fractional charges have ever been observed reproducibly in experiments.

Example 1.2 A proton has a udu quark structure (two up quarks and one down quark) and charge is an additive quantum number, so the charge of the proton is the sum of the charges of its quarks. From Table 1.1, the charge of a proton is

$$Q_p = 2Q_u + Q_d = \left(\frac{2}{3} + \frac{2}{3} - \frac{1}{3}\right) e = +1e,$$

in terms of the fundamental charge unit e given by Eq. (1.8), while a neutron has a udd quark structure and

$$Q_n = Q_u + 2Q_d = \left(\frac{2}{3} - \frac{1}{3} - \frac{1}{3}\right) e = 0,$$

so neutrons have zero net electrical charge.

Thus both neutrons and protons carry integer charges, even though their constituent quarks have fractional charges.

Modern high energy physics proposes a variety of elementary particles, some of which (various flavors of quarks) have electrical charges that are fractions of the fundamental unit (1.8) set by the charge on the electron. However, the *physically observable particles* entering into classical electromagnetism (and into relativistic quantum field theory) all appear to have electrical charges that are integer multiples of the fundamental charge unit given by Eq. (1.8). Even if one admits quarks (not directly observable because of confinement) to the discussion, the electric charge still appears in quantized form, but in third-integer units.

Hence we shall develop the theory of classical electromagnetism assuming that charged particles carry an electrical charge quantized in integer units of the electron charge, even though we presently have scant fundamental explanation for why this should be so.

Background and Further Reading

The history of classical electromagnetism is summarized in various parts of Jackson [41]. A view of classical electromagnetism with emphasis on the relationship of modern quantum field theory to classical electromagnetism may be found in Wald [74]. Introductions to the Standard Model of elementary particle physics and the origin of the particle and

computer simulations of QCD (a discipline called *lattice gauge theory*) have increasingly converged on the conclusion that QCD exhibits confinement of quarks and gluons because they carry a color charge.

quantum number assignments in Fig. 1.1 and Table 1.1 may be found in many places; for example, in Refs. [34, 38].

Problems

1.1 Prove that Maxwell's equations (1.1) are consistent with the continuity equation (1.3) that ensures local conservation of electrical charge.

1.2 Use Eq. (1.9) and Table 1.1 to confirm that the top quark is expected to carry an electrical charge of $\frac{2}{3}$. Should you worry about seeing a particle with charge $\frac{2}{3}$ in your experimental apparatus? ***

1.3 A family of subatomic particles called the Δ-resonance has four distinct members (Δ^{++}, Δ^{+}, Δ^{0}, Δ^{-}), which have a valence quark stucture (uuu, uud, udd, ddd), respectively, where u is the up quark and d is the down quark, with properties summarized in Table 1.1. Use this table to confirm the electrical charge assignments

$$Q(\Delta^{++}) = +2e \qquad Q(\Delta^{+}) = +1e \qquad Q(\Delta^{0}) = 0\,e \qquad Q(\Delta^{-}) = -1e$$

for these particles. Thus, show that the four members of the Δ-resonance (each of which is observable in high-energy physics experiments) have charges that are integer multiples of e, even though each consists of valence quarks having charges that are fractions of e (not observable because of color confinement for quarks).

1.4 In cylindrical coordinates (ρ, ϕ, z), a long, straight wire of radius R carries a uniform current density $\boldsymbol{J} = J_0\hat{\boldsymbol{z}}$. Inside the wire ($\rho < R$), the magnetic field is given by:

$$\boldsymbol{B} = \frac{\mu_0 J_0 \rho}{2}\hat{\boldsymbol{\phi}}.$$

What is the magnetic field inside the wire, and Calculate the divergence $\boldsymbol{\nabla}\cdot\boldsymbol{B}$ and curl $\boldsymbol{\nabla}\times\boldsymbol{B}$ of this field in cylindrical coordinates and compare with Maxwell's equations.

Numerical and GenAI Problems[8]

1.5 Using *GenAI* as your assistant to write and debug code:

a. Write *Python* code to plot a 2D vector field having components $(u = -y, v = x)$, where (x, y) are the cartesian coordinated for your 2D plot. Plot to the screen, and also output the plot to *EPS*, *PDF*, and *PNG* files.

b. Repeat, but for a streamline plot of the vector field.

In each case document the AI prompts that you used, describe briefly what the code does and what checks you have used to verify the validity of the results, and include representative graphics images. ***

1.6 Using *GenAI* as your assistant to write and debug code:

a. Make a 2D streamline plot of the electric field for an electric dipole charge distribution.

[8] See Appendix E.3 and Appendix G for guidance concerning solving computer problems using *GenAI*.

b. Write *Python* code to make a 2D contour plot of the electric field generated by 3 equal positive charges arranged in a equilateral triangle. Use grayscale and do not fill between the contours.
c. Repeat the previous case for 3 equal positive charges in an equilateral triangle but plot as a 3D surface plot.
d. Turn the 3D surface plot of part (c) into an animation rotating slowly about the z axis.

In each case, document the AI prompts that you used, describe briefly what the code does and what checks you have used to verify the validity of the results, and include representative graphics images.

1.7 Using *GenAI* as your assistant, (a) write *Python* code to calculate and plot in 2D vector plots representative vector fields having (i) zero divergence, (ii) positive divergence, and (iii) negative divergence. Replot case (i) in a streamline plot. (b) Using *GenAI* as your assistant, write python code to plot the vector potential $\boldsymbol{A}$ in a horizontal plane outside a cylindrical solenoid (which you may assume to have infinite length). In each case, save the plots to *PNG*, *EPS*, and *PDF* files.

1.8 Using Example H.1 and Appendix H as guidance, create a *NotebookLM* personal study guide project in which the first source is the text of this book (available from the Web link [3]). Add to that the YouTube playlist on electromagnetism at the Web link [4]. Add to that any additional Web pages or other sources that you have found useful in studying electromagnetism. Use the central Chat panel in *NotebookLM* to explore several topics of your choosing in classical electromagnetism to get a feeling for how the project responds to specific questions. Select 5 topics of interest to you, and generate an infographic (see right Studio panel in the *NotebookLM* project) for each. Finally, using the right Studio panel, generate a podcast for two of those subjects (the "Audio" button in the Studio panel).

2 Electrostatics in Vacuum

The fundamental problem to be solved in electrodynamics is that we have some set of charged particles interacting among themselves, and we wish to compute the electric forces acting among them. The *distribution of charge* may be described either by

1. a discrete list giving the position of each charge at a given time $q_i(\boldsymbol{x}, t)$, or by
2. a continuous charge density described by a function $\rho(\boldsymbol{x}, t)$, in which discrete charges are assumed smeared out into a smooth charge distribution, with the charge at a point $(\boldsymbol{x}, t)$ given by the value of the function $\rho(\boldsymbol{x}, t)$.

A typical problem is illustrated schematically in Fig. 2.1(b), where we have a distribution of n distinct *source charges* q_1, q_2, q_3, ...q_n, and wish to know the net force that the source charges exert on some *test charge* Q. In the most general case both the source charges and test charges may be in motion but we shall begin with basics and consider in this chapter the simplified case of *electrostatics,* where the source charges $q_i(\boldsymbol{x})$ are assumed to be fixed in spatial position [but the test charge $Q(\boldsymbol{x}, t)$ may move].

2.1 Categories of Electrostatics Problems

Problems in electrostatics can be divided schematically into two broad categories according to what information is available and what methods are required to solve the problem using that information [77]:

1. *summation problems,* and
2. *boundary value problems*,

with the distinction between the two lying in how initial conditions and constraints are used, as we shall now describe.

2.1.1 Summation Problems

In a *summation problem*, the location of each charge [or the charge density function $\rho(\boldsymbol{x})$] is specified initially at every point in space at a given time, which reduces the task of solving the electrostatics problem to evaluating a summation for a set of discrete charges, or an integral in the case of a continuous charge distribution. The integrals or summations might be easy or difficult to evaluate, but conceptually a summation problem has a clearly defined solution. Consider the problem solved in Example 2.1.

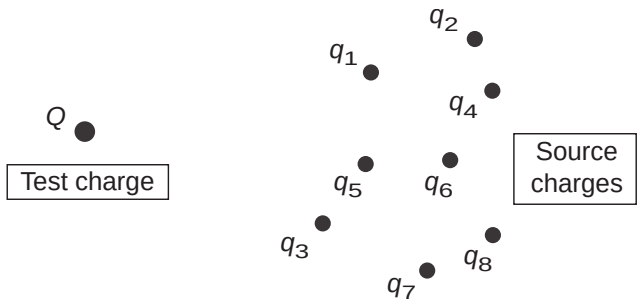

Fig. 2.1 The prototype electrostatics problem: interaction in vacuum of a test charge Q with a set of stationary source charges q_n.

Example 2.1 What is the scalar (electric) potential $\Phi(\boldsymbol{x})$ at the center of a square with sides of length a if identical charges $+q$ are place at the corners of the square?

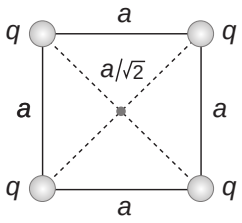

The discrete charges and their locations are given as initial conditions, so we can solve this problem by summation using Coulomb's law and the principle of superposition (Section 2.4). From Eq. (2.30), the scalar potential is defined by

$$\Phi(\boldsymbol{r}) = \frac{1}{4\pi\epsilon_0}\sum_{i=1}^{4}\frac{q_i}{r_i} = 4\times\left(\frac{q}{4\pi\epsilon_0(a/\sqrt{2})}\right) = \frac{\sqrt{2}\,q}{\pi\epsilon_0 a},$$

where Eq. (2.30) gives the form of the contribution from each charge, the superposition principle allows us to sum those contributions independently, and we've used that the distance from each corner to the center is $r_i = a/\sqrt{2}$.

The summation approach may be characterized as *"bottom-up"*, since it solves an electrostatics problem by a direct application of Coulomb's law (Section 2.2) and the superposition principle (Section 2.4) [or equations derived from them like the expression (2.30) for the scalar potential] to an initially specified charge distribution.

2.1.2 Boundary Value Problems

However, in many real-world situations we may not know beforehand where the charges are. If the charge density cannot be specified initially at every point in space, we are deal-

ing with a (typically more challenging) *boundary value problem*. This will be the case if matter is present in any form, because the Coulomb force will cause charge to redistribute itself in the matter until equilibrium is reached.[1] Instead we may know the scalar potential or the electric field on the boundaries of a region. Typically, one then must solve a differential equation [the *Poisson equation* (2.54), if there is charge in the region of interest, or the *Laplace equation* (2.58), if no charges are present], subject to the boundary conditions to determine the scalar potential and electric field everywhere in the interior. Example 2.2 illustrates.

Example 2.2 Consider a parallel plate capacitor with two infinite conducting plates separated by a vertical distance d.

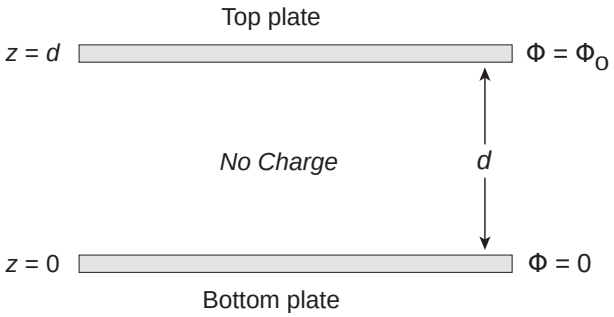

The bottom plate is grounded (held at scalar potential $\Phi = 0$) and the top plate is held at a constant potential $\Phi = \Phi_0 \neq 0$, and we wish to solve for the scalar potential Φ (and thus the electric field) at an arbitrary point between the plates. There is no charge between the capacitor plates so we may obtain a solution by solving the Laplace equation of Eq. (2.58)

$$\nabla^2\Phi = 0 \qquad \nabla^2 = \frac{\partial^2}{\partial x^2} + \frac{\partial^2}{\partial y^2} + \frac{\partial^2}{\partial z^2},$$

subject to the boundary conditions for the potential Φ. Defining a vertical z axis, in 1D the Laplace equation is $d^2\Phi/dz^2 = 0$, which has a solution of the form $\Phi(z) = az + b$, where a and b are constants. Setting $\Phi = 0$ at the lower plate gives $b = 0$ and setting $\Phi = \Phi_0$ at the upper plate gives $a = \Phi_0/d$, and we obtain the solution

$$\Phi(z) = \frac{\Phi_0}{d}\, z,$$

for the scalar potential between the plates as a function of the vertical coordinate z measured from the lower plate. This is a very simple boundary value problem and solving the required differential equation with constraints is not hard. We shall see in subsequent chapters that boundary value problems can much more challenging than this one.

[1] For historical reasons, this charge redistribution is typically called *electrostatic induction* in conductors and *electrostatic polarization* in non-conductors. The underlying physical reasons are similar in the two cases but consequences are different, because charge mobilities are very different in these two environments.

Solutions for boundary value problems are sometimes characterized as *"outside-in"* because the problem is solved by applying boundary conditions, often specified on outer bounding surfaces, to deduce the fields in the interior of the bounding regions.

It is a remarkable fact that electrostatics problems can be *solved uniquely for every spatial point*, even if the initial charge distribution is unknown, provided that one can specify

1. a model of any polarizable matter that is present,
2. a model providing the behavior of the electric field in any matter present, and
3. boundary or matching conditions for the Maxwell equations.

This is a consequence of some *uniqueness theorems* that will be proven in Section 3.3. Of course knowing that any valid solution is unique doesn't guarantee that finding it is easy; but the knowledge that any solution must be unique can be very helpful in devising solution strategies.

The summation ("bottom-up") and boundary value ("outside-in") approaches to solving electrostatics problems are compared and contrasted in Table 2.1. The remainder of this chapter will consider summation problems for electrostatics and will introduce the Poisson and Laplace equations; Chs. 3 and 4 will then address boundary value problems and their solutions in terms of the Poisson and Laplace equations.

2.2 Coulomb's Law

Let us assume initially that the source charges and the test charges in Fig. 2.1(b) are embedded in vacuum, so that it isn't necessary to worry about a polarized medium altering the interactions between charges (that will be the subject of extensive discussion in later

Table 2.1 Summation and boundary value electrostatic methods

Feature	For summation problem	For boundary value problem
Primary input:	The source (charge locations)	Fields on boundaries
Key principle:	Superposition $\Phi = \sum_i \Phi_i$	Uniqueness theorems (Section 3.3)
Primary tool:	Coulomb's law + integration	Laplace or Poisson equations (Section 2.11)
Charges:	$\rho(\boldsymbol{x})$ known everywhere	Initial $\rho(\boldsymbol{x})$ unknown
Moving charges:	Difficult if charges can move	Designed for cases where charges move
Complexity:	Difficult with many particles	Depends on boundary symmetry
Goal:	Field from known source	Field in region constrained by conductors

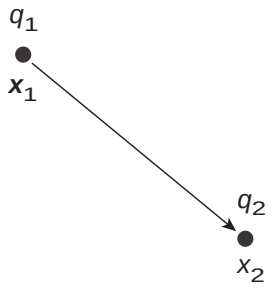

Fig. 2.2 Coulomb interaction between two isolated and stationary test charges.

chapters). Let us now consider a quantitative description of this idealized electrostatics problem, utilizing experimental data, physical intuition, and mathematics for guidance.

Consider first the force acting between two isolated charges at rest with respect to each other, as illustrated in Fig. 2.2. The force exerted on a single charge q_1 located at position $\boldsymbol{x}_1$ by a single charge q_2 located at position $\boldsymbol{x}_2$ may be measured experimentally and is found to be given by *Coulomb's law*,

$$\boldsymbol{F} = kq_1q_2\,\frac{\boldsymbol{x}_1 - \boldsymbol{x}_2}{|\boldsymbol{x}_1 - \boldsymbol{x}_2|^3} \qquad \text{(Coulomb's law)}, \tag{2.1}$$

where the charges q_n are algebraic quantities that may be positive or negative, the force points along the line from q_1 to q_2 and is attractive if the signs of the changes are opposite and repulsive if they are the same. The constant k appearing in Coulomb's law depends on the system of units that is in use. Three common choices are *the SI system*, *Gaussian or electrostatic units*, and *Heaviside–Lorentz* units.

1. In the *SI system* of units,

$$k = \frac{1}{4\pi\epsilon_0}, \tag{2.2}$$

where the constant ϵ_0 is called the *permittivity of free space*. In the SI system the unit of force is the Newton (N), the unit of distance is the meter (m), the unit of charge is the coulomb (C), and

$$\epsilon_0 \simeq 8.85 \times 10^{-12}\,\frac{\mathrm{C}^2}{\mathrm{N\ m}^2} = 8.85 \times 10^{-12}\,\frac{\mathrm{F}}{\mathrm{m}}, \tag{2.3}$$

where the farad (F) is the derived SI unit of electrical capacitance. The constants μ_0, ϵ_0, and the speed of light c that may appear in SI units are related by[2]

$$\mu_0\epsilon_0 = \frac{1}{c^2}. \tag{2.4}$$

[2] The three constants that enter into SI units, the permeability of free space μ_0 defined in Eq. (1.2), the permittivity of free space ϵ_0 defined in Eq. (2.3), and the speed of light c, are related by Eq. (2.4). This has the potentially confusing implication that the form of equations written in SI units can be changed by using $\mu_0\epsilon_0c^2 = 1$ to interchange constants appearing in them. As will be discussed in Section 8.2, SI units also partially obscure that under typical laboratory conditions magnetic phenomena are intrinsically much weaker than electrostatic phenomena, but that the two become comparable in strength if the characteristic speeds of charged particles approach that of light.

Thus Coulomb's law (2.1) written explicitly in SI units is

$$\boldsymbol{F} = \frac{q_1 q_2}{4\pi\epsilon_0} \frac{\boldsymbol{x}_1 - \boldsymbol{x}_2}{|\boldsymbol{x}_1 - \boldsymbol{x}_2|^3} \qquad \text{(Coulomb's law, SI units).} \tag{2.5}$$

The Maxwell equations and the Lorentz force law in SI units are summarized in Appendix B.1. We will use SI units in these lectures by default, specifying explicitly if we choose other units in a few limited situations.

2. In *Gaussian* or *CGS units*, also termed *electrostatic units (esu)*, $k = 1$ and unit charge is chosen such that it exerts a force of one dyne on an equivalent point charge located one centimeter away. In the Gaussian system the unit charge is called a *statcoulomb*. The Maxwell equations and the Lorentz force law are expressed in Gaussian units in Appendix B.2. There are some advantages to Gaussian units and many older books use them, but more modern books tend to use SI units because of the affinity with standardized MKS units for non-electromagnetic quantities.
3. In some disciplines (for example, elementary particle physics) *Heaviside–Lorentz units* may be used, where $k = 1/4\pi$. The Maxwell equations and the Lorentz force law are given in Heaviside–Lorentz units in Appendix B.3.

In some cases one may encounter specialized variations on units where fundamental constants like the speed of light c or Planck's constant $\hbar$ (in quantum problems) are set to one, though that is probably more common in quantum field theory than in classical field theory.

Beginning with the time of Cavendish and Coulomb, the empirical validity of Coulomb's law (2.5) has been tested by a variety of techniques applied over a range of distance scales. As discussed in Box 2.1, well-established experimental limits suggest that for classical electromagnetism we can safely assume the photon to be massless and the deviation from Coulomb's law to be negligible.

2.3 The Electric Field

In experiments on the interaction of charges one typically measures a force, as implied by Eq. (2.1). However, much of the power of theoretical physics derives from abstracting broader implications from measurements. Perhaps no abstraction has been more influential in the development of physics than that of a *field*, which is simply an instance of something that is defined at every point of spacetime. Let us introduce an *electric field* $\boldsymbol{E}$ acting on a test charge q by *defining* the force $\boldsymbol{F}$ acting on the charge to be

$$\boldsymbol{F} = q\boldsymbol{E}. \tag{2.6}$$

Thus an electric field $\boldsymbol{E} = \boldsymbol{F}/q$ may be interpreted as an object that can exert a force per unit test charge for a test charge located at any point in in spacetime. The electric field is a function of position, but *it doesn't depend on whether there is a test charge located at* P. The field exists, independent of whether there is a test charge exists upon which it acts. Since force is a vector and charge is a scalar, the electric field is a *vector field* $\boldsymbol{E}(t, \boldsymbol{x})$ defined at

Box 2.1 Deviations from the Inverse-Square Force Law

As established in the original experiments of Cavendish and Coulomb, the electrostatic force between two charges in vacuum obeys an inverse square law (2.1). Since those days, the precision of testing for possible deviations from the inverse square law has improved substantially. It is common to report possible experimental deviation from the inverse square law in one of two ways.

1. Assume that the electrostatic force has the dependence $F \sim 1/r^{2+\epsilon}$ and report an experimental upperlimit on the value of $|\epsilon|$.
2. Assume that the electrostatic potential has the Yukawa form
$$V \sim r^{-1}e^{-\mu r} = r^{-1}e^{-(m_\gamma c/\hbar)r} \qquad \mu \equiv \frac{m_\gamma c}{\hbar},$$
where m_γ is the photon mass (zero for an inverse-square force). Then deviations from the inverse square law may be reported as limits on μ or m_γ.

The original experiments of Cavendish using concentric spheres in 1772 established an upper limit $|\epsilon| \leq 0.02$.

1. Greatly improved modern determinations based on Gauss's law have pushed this limit to $\epsilon = (2.7 \pm 3.1) \times 10^{-16}$ [76].
2. The best limits on the mass of the photon come from measuring planetary magnetic fields. Such measurements place a limit on the photon mass of $m_\gamma < 4 \times 10^{-51}$ kg [32, 41, 44].

Hence the photon mass can be taken as zero for classical electrodynamics, with no significant deviation from an inverse-square force law.

each point of spacetime $(t, \boldsymbol{x})$, but we ignore time dependence for now. Comparing Eqs. (2.6) and (2.1), the electric field at a point $P(\boldsymbol{x})$ produced by a point charge q_1 at $\boldsymbol{x}_1$ is

$$\boldsymbol{E}(\boldsymbol{x}) = kq_1 \frac{\boldsymbol{x} - \boldsymbol{x}_1}{|\boldsymbol{x} - \boldsymbol{x}_1|^3}, \tag{2.7}$$

as illustrated in Fig. 2.3. In the SI system the unit of charge is the coulomb (C) and the electric field $\boldsymbol{E}$ has units of volts per meter. The importance of the field concept in the development of modern physics is elaborated in Box 2.2.

2.4 The Principle of Superposition

Now let us address the more general case in Fig. 2.1(b) of the interaction of a test charge with a set of n source charges. In principle this could be a quite complicated problem, but it is an experimentally verified fact that

Box 2.2 Significance of Fields in Electromagnetism

Equation (2.6) suggests measuring forces to infer fields, implying that fields are derivative and not fundamental. But modern physics places strong emphasis directly on the fields. Indeed, Maxwell's equations (1.1) are formulated in terms of electric and magnetic fields, which are the central concepts of classical electromagnetism. The importance of fields is most obvious in relativistic quantum field theory (QFT) , which is not our subject here, but the field concept traces historically to the introduction of electric and magnetic fields in classical electromagnetism (largly due to Faraday), which is our subject.

Action at a Distance

Originally it was believed that forces associated with charges, currents, and magnets acted *instantaneously over any distance* (this was termed *action at a distance*).[a] The modern view—shaped by experimental measurement and the development of relativistic QFT—is that fields are every bit as fundamental as particles. In this picture, forces are mediated by fields, and the light speed limit of special relativity means that no signal can transmit a force faster than the speed of light, relegating action at a distance to the dustbin.

Actions Mediated by Fields

For example, if a charge moves the fields associated with the charge change, but the change isn't felt immediately at every point $(\boldsymbol{x}, t)$ of spacetime. Maxwell's equations (1.1) describing electromagnetism require the change to be propagated through changes in two vector fields, the *electric field* $\boldsymbol{E}(\boldsymbol{x}, t)$ and the *magnetic field* $\boldsymbol{B}(\boldsymbol{x}, t)$, defined at each point of spacetime, and those changes can propagate only at a finite speed (less than or equal to the speed of light).

This abstract view was resisted initially because the fields did not describe tangible matter, and many doubted that they could exist in vacuum. Modern physics takes quite a different view. The introduction of electric and magnetic fields allows a simple mathematical description of electromagnetic phenomena, but the fields are *not just mathematical abstractions;* they are *real physical entities* ("as real as a rinoceros" [31]), carrying concrete physical properties such as energy, momentum, and angular momentum. This is most clear in QFT, where these physical attributes become properties of *quanta of the field* (photons) and electromagnetic interactions are viewed as being mediated by exchange of virtual photons. These photons associated with the electromagnetic field have observable consequences: at high enough energy the collision of two photons can produce matter in the form of an electron and positron pair; real as a rinoceros indeed! Relativistic QFT implies that all non-gravitational fundamental interactions (electromagnetic, strong, and weak) are mediated by the gauge bosons of Fig. 1.1, which are the quanta of fields that generalize the gauge symmetry of photons. Such is the rich legacy of classical electromagnetic fields.

[a] Likewise, Newtonian physics assumes gravity to act instantaneously on a distant object. Replacement of Newtonian gravity with general relativity (a field theory consistent with the limiting speed of light) eliminated action at a distance for gravity, just as relativistic QFT eliminated it for electromagnetism.

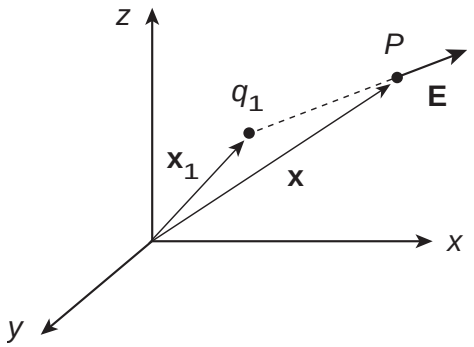

Fig. 2.3 The electric field vector $\boldsymbol{E}$ at a point $P(\boldsymbol{x})$ that is generated by a charge q_1 located at position $\boldsymbol{x}_1$.

1. if the *charged-particle interactions are not too large*, and
2. if *quantum effects can be ignored*,

then the interaction between any two charges is unaffected by the presence of all other charges.[3]

> Thus, the total force acting on the test charge Q in Fig. 2.1(a) can be obtained to excellent approximation by summing the interactions of the charges pairwise, while holding all other charges constant. This is termed the *principle of linear superposition (of forces)*. The ultimate source of this linearity may be traced to the linear dependence of the Maxwell equations (1.1) on the electric field $\boldsymbol{E}$ and magnetic field $\boldsymbol{B}$.

Since the principle of linear superposition applies to the forces computed from Eq. (2.1) it applies also to the electric fields calculated from Eq. (2.7), by virtue of the linear relationship (2.6). Therefore, the electric field acting at position $\boldsymbol{x}$ in Fig. 2.1(a) is given by a vector sum of contributions from all the source charges q_i,

$$\boldsymbol{E}(\boldsymbol{x}) = \frac{1}{4\pi\epsilon_0} \sum_{i=1}^{n} q_i \, \frac{\boldsymbol{x} - \boldsymbol{x}_i}{|\boldsymbol{x} - \boldsymbol{x}_i|^3}, \tag{2.8}$$

where we have used Eq. (2.7) expressed in SI units. In most practical problems we will be able to assume that the charges are sufficiently small and numerous that they can be approximated by a continuous charge density $\rho(\boldsymbol{x}')$, such that the charge contained in a small 3D volume element $d^3x' \equiv dx'dy'dz'$ centered at $\boldsymbol{x}'$ is $\Delta q = \rho(\boldsymbol{x}')\Delta x\,\Delta y\,\Delta z$.

[3] In the presence of strong electric fields such as those generated by powerful lasers, and in various *vacuum polarization phenomena* observed in quantum field theory experiments, this linear superposition principle may fail. However, we shall restrict ourselves to the *classical linear regime*, where such effects may be neglected by hypothesis. It is fortunate for development of electromagnetic theory that the experiments that laid the foundations for the classical theory of electricity and magnetism were all performed under conditions where linear superposition holds very precisely, which greatly expedited their original physical interpretation.

Then the sum over discrete charges in Eq. (2.8) may be replaced by an integral over a continuous charge distribution,

$$\boldsymbol{E}(\boldsymbol{x}) = \frac{1}{4\pi\epsilon_0}\int \rho(\boldsymbol{x}')\,\frac{\boldsymbol{x}-\boldsymbol{x}'}{|\boldsymbol{x}-\boldsymbol{x}'|^3}\,d^3x' = \frac{1}{4\pi\epsilon_0}\int \frac{\rho(\boldsymbol{x}')}{R^2}\,\hat{\boldsymbol{R}}\,d^3x' \tag{2.9}$$

where in the last step a compact notation

$$\boldsymbol{R} \equiv \boldsymbol{x}-\boldsymbol{x}' \qquad R = |\boldsymbol{R}| = |\boldsymbol{x}-\boldsymbol{x}'| \qquad \hat{\boldsymbol{R}} = \frac{\boldsymbol{R}}{|\boldsymbol{R}|} = \frac{\boldsymbol{R}}{R} = \frac{\boldsymbol{x}-\boldsymbol{x}'}{|\boldsymbol{x}-\boldsymbol{x}'|} \tag{2.10}$$

such that

$$\frac{\boldsymbol{x}-\boldsymbol{x}'}{|\boldsymbol{x}-\boldsymbol{x}'|^3} = \frac{1}{|\boldsymbol{x}-\boldsymbol{x}'|^2}\cdot\frac{\boldsymbol{x}-\boldsymbol{x}'}{|\boldsymbol{x}-\boldsymbol{x}'|} = \frac{1}{R^2}\,\hat{\boldsymbol{R}}, \tag{2.11}$$

has been introduced that will prove useful in solving problems. We will generally be working with continuous charge distributions in one, two, or three spatial dimensions.

1. If the charge is spread along a line in 1D with a charge per unit length of λ, then the volume element in Eq. (2.9) becomes a *line charge* $\lambda dl'$, where dl' is an infinitesimal length element.
2. If the charge is spread over an area in 2D with a charge density per unit area of σ, the volume element becomes a *surface charge* $\sigma da'$, where da' is a differential element of area.
3. If the charge is spread over a volume in 3D with charge per unit volume ρ, the volume element is a *volume charge* $\rho d^3x'$, which we sometimes abbreviate as $\rho d\tau'$.

Thus, for continuous charge distributions in three, two, and one dimensions, respectively, the electric field is given explicitly by

$$\boldsymbol{E}(\boldsymbol{x})_{\text{3D}} = \frac{1}{4\pi\epsilon_0}\int \rho(\boldsymbol{x}')\,\frac{\boldsymbol{x}-\boldsymbol{x}'}{|\boldsymbol{x}-\boldsymbol{x}'|^3}\,d^3x' = \frac{1}{4\pi\epsilon_0}\int \frac{\rho(\boldsymbol{x}')}{R^2}\,\hat{\boldsymbol{R}}\,d^3x', \tag{2.12a}$$

$$\boldsymbol{E}(\boldsymbol{x})_{\text{2D}} = \frac{1}{4\pi\epsilon_0}\int \sigma(\boldsymbol{x}')\,\frac{\boldsymbol{x}-\boldsymbol{x}'}{|\boldsymbol{x}-\boldsymbol{x}'|^3}\,da' = \frac{1}{4\pi\epsilon_0}\int \frac{\sigma(\boldsymbol{x}')}{R^2}\,\hat{\boldsymbol{R}}\,da', \tag{2.12b}$$

$$\boldsymbol{E}(\boldsymbol{x})_{\text{1D}} = \frac{1}{4\pi\epsilon_0}\int \lambda(\boldsymbol{x}')\,\frac{\boldsymbol{x}-\boldsymbol{x}'}{|\boldsymbol{x}-\boldsymbol{x}'|^3}\,dl' = \frac{1}{4\pi\epsilon_0}\int \frac{\lambda(\boldsymbol{x}')}{R^2}\,\hat{\boldsymbol{R}}\,dl', \tag{2.12c}$$

in terms of volume densities $\rho(\boldsymbol{x}')$, surface densities $\sigma(\boldsymbol{x}')$, and line densities $\lambda(\boldsymbol{x}')$, respectively.

Example 2.3 Let us determine the electric field produced by a straight line charge with uniform charge density λ. First consider the field produced at the point P of Fig. 2.4 if the line charge is of finite length $2L$. As shown in Problem 2.10, from Eq. (2.12c) the

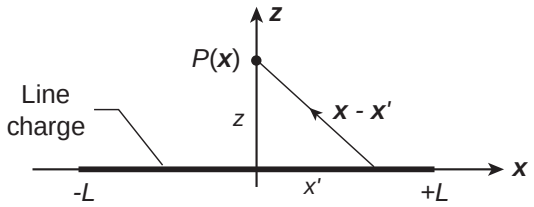

Fig. 2.4 Charged line segment of length $2L$ used to calculate the electric field in Example 2.3.

electric field produced at the point P is

$$\begin{aligned}\boldsymbol{E} &= \frac{1}{4\pi\epsilon_0}\int_{-L}^{+L}\frac{\lambda}{R^2}\hat{\boldsymbol{R}}\,dx' \\ &= \frac{1}{4\pi\epsilon_0}\int_{-L}^{+L}\frac{\lambda}{x^2+z^2}\cdot\frac{z\hat{\boldsymbol{z}}-x\hat{\boldsymbol{x}}}{\sqrt{x^2+z^2}}\,dx \\ &= \frac{1}{2\pi\epsilon_0}\frac{\lambda L}{z(z^2+L^2)^{1/2}}\,\hat{\boldsymbol{z}},\end{aligned} \tag{2.13}$$

where the compact notation of Eq. (2.10) has been used. If we identify this charge segment with a straight wire, the electric field produced by a wire of infinite length along the x axis can be obtained by taking the limit $L \to \infty$ of Eq. (2.13), which gives

$$\boldsymbol{E} = \frac{1}{4\pi\epsilon_0}\frac{2\lambda}{z}\,\hat{\boldsymbol{z}}. \tag{2.14}$$

The electric field is perpendicular to the wire, with magnitude proportional to the inverse of the distance from the wire.

Finally, before leaving this discussion of continuous charge distributions let us note that a discrete set of charges also can be described by a continuous charge distribution $\rho(\boldsymbol{x})$ if the *Dirac delta function* $\delta(\boldsymbol{x}-\boldsymbol{X})$ described in Appendix section A.12 is used to pick out the locations of each of the discrete charges q_i,

$$\rho(\boldsymbol{x}) = \sum_{i=1}^{n} q_1\delta(\boldsymbol{x}-\boldsymbol{X}), \tag{2.15}$$

since substitution of the charge density (2.15) in Eq. (2.9) and integrating using the properties of the delta function is equivalent to the sum over contributions from discrete charges to the electric field in Eq. (2.8).

2.5 Gauss's Law

The electric field for a continuous charge distribution may be calculated from Eq. (2.9). However, evaluating the integral in this equation isn't always the easiest way to solve

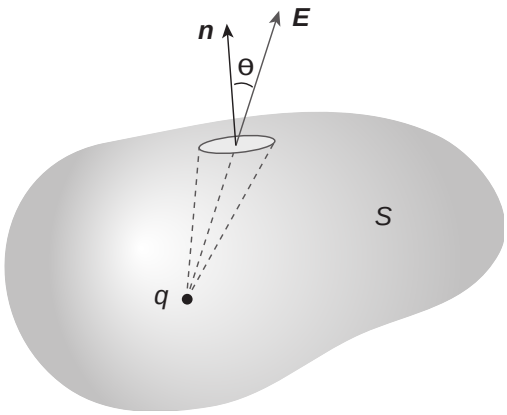

Fig. 2.5 Closed surface S illustrating Gauss's law. The electric field generated by the charge q is $\boldsymbol{E}$, the normal vector to the surface is $\boldsymbol{n}$, and da is an element of surface area.

for the electric field. If a problem has some degree of symmetry, often another integral result called *Gauss's law* can lead to an easier solution. In Fig. 2.5 we indicate a charge q enclosed by a surface S. The normal component of $\boldsymbol{E}$ times a surface area element da is

$$\boldsymbol{E}\cdot\boldsymbol{n}\,da=\frac{q}{4\pi\epsilon_0}\frac{\cos\theta}{r^2}\,da=\frac{q}{4\pi\epsilon_0}\,d\Omega, \tag{2.16}$$

where the last step used $\cos\theta\,da = r^2\,d\Omega$, with $d\Omega$ being the solid angle subtended by da at the position of the charge. If the normal component of $\boldsymbol{E}$ is now integrated over the entire surface S,

$$\oint_S \boldsymbol{E}\cdot\boldsymbol{n}\,da=\begin{cases} q/\epsilon_0 & (\text{for } q \text{ inside } S)\\ 0 & (\text{for } q \text{ outside } S)\end{cases}\qquad (\text{Gauss's law}), \tag{2.17}$$

where $\oint_S \boldsymbol{E}\cdot\boldsymbol{n}\,da$ is called the *(electric) flux* through the surface S. Equation (2.17) is *Gauss's law in integral form* for a single charge. For a set of discrete charges Gauss's law can be generalized to the form,

$$\oint_S \boldsymbol{E}\cdot\boldsymbol{n}\,da=\frac{1}{\epsilon_0}\sum_i q_i, \tag{2.18}$$

where the summation over i is restricted to charges q_i that are *inside the surface* S. If the charge distribution is continuous, Gauss's law takes the form

$$\oint_S \boldsymbol{E}\cdot\boldsymbol{n}\,da=\frac{1}{\epsilon_0}\int_V \rho(\boldsymbol{x})\,d^3x,\qquad (\text{Gauss's law}) \tag{2.19}$$

where the integration is over the volume V contained within the surface S.[4] Gauss's law in the form of Eqs. (2.17)-(2.19) may be viewed as integral formulation of the law of electrostatics. Corresponding differential forms of Gauss's law may be obtained using the *divergence theorem* of Eq. (A.34).

Divergence theorem: For a vector field defined within a volume V that is enclosed by a surface S,

$$\oint_S \boldsymbol{A} \cdot \boldsymbol{n}\, da = \int_V \boldsymbol{\nabla} \cdot \boldsymbol{A}\, d^3x, \tag{2.20}$$

where the left side is the surface integral of the outwardly directed normal component of the vector $\boldsymbol{A}$ and the right side is the volume integral of the divergence of $\boldsymbol{A}$. In essence, the divergence theorem says that the total expansion or contraction of a vector field within the volume is equal to the flux across its boundary. Several mathematical and geometrical conditions for application of the theorem must be satisfied:

1. *Closed surface:* The surface S must be closed and must completely enclose the volume V. The theorem doesn't apply to open surfaces like a hemisphere without a base, unless they are closed by adding another surface.
2. *Piecewise smooth boundary:* The boundary S must be *piecewise smooth*, which means that it can have sharp edges like a cube, but cannot be so irregular that it lacks a well-defined normal almost everywhere.
3. *Continuously differentiable vector field ($\boldsymbol{C}^1$):* The vector field $\boldsymbol{A}$ must have continuous 1st-order partial derivatives throughout the volume V and on the surface S.
4. *Simple solid:* The volume V must be a "simple" solid, though the theorem can be extended to more complex volumes by treating them as the difference of two simple volumes.
5. *Orientation:* The unit normal vector $\hat{\boldsymbol{n}}$ must point *outward* from the volume. If an inward flux is required, the sign of the integral must be adjusted accordingly.

The divergence theorem (2.20) allows Eq. (2.19) to be written in the form

$$\int_V \left(\boldsymbol{\nabla} \cdot \boldsymbol{E} - \frac{\rho}{\epsilon_0} \right) d^3x = 0.$$

[4] Gauss's law (2.19) is a consequence of (1) inverse-square forces between charges, (2) the central nature of the force, and (3) linear superposition of charges. Newtonian gravity obeys similar conditions, so one can construct a Gauss's law for Newtonian gravity, where the gravitational "charge" is mass and mass density replaces charge density. Of course there is only one sign for the gravitational charge in Newtonian gravity, since the gravitational force is always attractive. (In the absence of dark energy, which can effectively turn gravity repulsive on cosmological scales.)

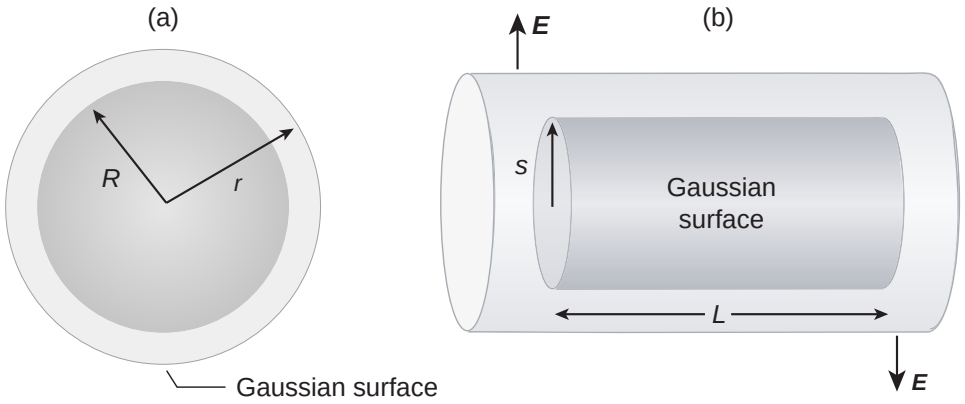

Fig. 2.6 Examples of applying Gauss's law to find the electric field. (a) A ball of uniformly distributed charge with radius R, used in Example 2.4. (b) A cylinder carrying a charge density proportional to the distance s from the cylindrical axis, used in Example 2.5. Gauss's law is often effective for examples like this that have a high degree of symmetry.

But this can be true generally only if the integrand vanishes, giving

$$\boldsymbol{\nabla} \cdot \boldsymbol{E} = \frac{\rho}{\epsilon_0} \qquad \text{(Gauss's law)}, \tag{2.21}$$

which is the *differential form of Gauss's law* (2.19) for continuous charge distributions. Thus, we have now obtained the first of Maxwell's equations (1.1). Before proceeding, let's look at two examples of Gauss's law in action [33].

Example 2.4 Figure 2.6(a) shows a charged solid 2-sphere (a *ball*)[5] of radius R, for which the total charge Q is assumed to be evenly distributed. What is the electric field outside the ball? We may solve this easily using Gauss's law in integral form. Imagine surrounding the charged ball with a 2-sphere of radius $r > R$ (this is called a *Gaussian surface*). Applying Gauss's law (2.18)

$$\oint \boldsymbol{E} \cdot \boldsymbol{n}\, da = \frac{1}{\epsilon_0} Q.$$

Because of the spherical symmetry, $\boldsymbol{E}$ and $\boldsymbol{n}\, da$ point radially outward so that the scalar product is trivial to evaluate:

$$\oint \boldsymbol{E} \cdot \boldsymbol{n}\, da = \oint |\boldsymbol{E}| da,$$

[5] A 2-sphere is hollow when displayed in 3D space, consisting only of the 2D spherical surface. Mathematically, a "solid 2-sphere", which includes the interior of a 2-sphere, is called a *ball* (an *open ball* if the surface points are not included and a *closed ball* if they are).

and the magnitude $|\boldsymbol{E}|$ is constant over the surface by symmetry, so it can be pulled out of the integral,

$$\oint |\boldsymbol{E}| da = |\boldsymbol{E}| \oint da = 4\pi r^2 |\boldsymbol{E}|.$$

Combining the preceding results,

$$4\pi r^2 |\boldsymbol{E}| = \frac{1}{\epsilon_0} Q,$$

or finally,

$$\boldsymbol{E} = \frac{1}{4\pi\epsilon_0} \frac{Q}{r^2} \hat{\boldsymbol{r}},$$

where $\hat{\boldsymbol{r}}$ is a unit vector in the radial direction. Notice the well-known result that the field external to the charge distribution is the same that would have been obtained by putting all charge at the center of the ball.[6]

Example 2.5 Consider Fig. 2.6(b), where a long cylinder carries a charge density proportional to the distance s' from the axis of the cylinder, $\rho = ks'$, where k is a constant. What is the electric field inside the cylinder? Let's draw a Gaussian surface in the form of a cylinder of radius s and length L, as illustrated in Fig. 2.6(b). From Eq. (2.19), Gauss's law for this surface is

$$\oint \boldsymbol{E} \cdot \boldsymbol{n}\, da = \frac{1}{\epsilon_0} Q,$$

where Q is the total charge enclosed by the Gaussian surface, which is given by integrating the charge over the volume within the Gaussian surface using cylindrical coordinates (Appendix A.7.2) with a cylindrical volume element $d\tau = s ds\, d\phi\, dz$

$$\begin{aligned} Q &= \int \rho d\tau \\ &= k \int_0^s s'^2 ds' \int_0^{2\pi} d\phi \int_0^L dz \\ &= 2\pi k L \int_0^s s'^2 ds' \\ &= \frac{2}{3} \pi k L s^3. \end{aligned}$$

By symmetry $\boldsymbol{E}$ must point radially outward from the cylinder's central axis, as indicated in Fig. 2.6(b), so for the curved portion of the Gaussian cylinder

$$\int \boldsymbol{E} \cdot \boldsymbol{n}\, da = \int |\boldsymbol{E}|\, da = |\boldsymbol{E}| \int da = 2\pi s L\, |\boldsymbol{E}|,$$

[6] By similar arguments applied to Newtonian gravity, one finds that for a sphere containing gravitating matter the gravitational field external to the sphere is the same as if all mass were concentrated at the center of the sphere. This similarity is of course because both Newtonian gravity and Coulomb's law correspond to inverse-square forces.

while the two ends contribute zero because $\boldsymbol{E}$ is perpendicular to $\boldsymbol{n}\, da$. Thus, from Gauss's law,

$$2\pi sL\,|\boldsymbol{E}| = \frac{1}{\epsilon_0}\frac{2}{3}\pi kLs^3$$

and the electric field is given by

$$\boldsymbol{E} = \frac{1}{3\epsilon_0} ks^2 \hat{\boldsymbol{s}},$$

where $\hat{\boldsymbol{s}}$ is a unit vector pointing radially from the central axis of the cylinder.

Quite generally, one sees from such examples that using Gauss's theorem to determine the electric field is a useful approach when there is a high degree of symmetry that can be exploited to simplify the evaluation of integrals. Typically, the goal in applying Gauss's law is to simplify the integral on the left side of Eqs. (2.18) or (2.19). Often this can be done if we can choose a gaussian surface such that one or more of the following conditions holds.

1. The electric field is zero over the surface.
2. The electric field is constant over the surface, by symmetry arguments.
3. The integrand $\boldsymbol{E}\cdot\boldsymbol{n}\, da$ reduces to the algebraic product $|\boldsymbol{E}|\, da$ because the vectors $\boldsymbol{E}$ and $\boldsymbol{n}$ are parallel.
4. The integrand $\boldsymbol{E}\cdot\boldsymbol{n}\, da$ is zero because the vectors $\boldsymbol{E}$ and $\boldsymbol{n}$ are orthogonal.

For example, in the problems solved above the third condition was used in Example 2.4 and the third and fourth conditions were used in Example 2.5. If none of these conditions are satisfied, Gauss's law is still valid but there may be easier ways to determine the electric field.

2.6 The Scalar Potential

Consider a line integral between two points $\boldsymbol{A}$ and $\boldsymbol{B}$ in a field generated by a single charge at the origin, as illustrated in Fig. 2.7. In spherical coordinates (Appendix A.7.1) the electric field $\boldsymbol{E}$ and line element $d\boldsymbol{l}$ are

$$\boldsymbol{E} = \frac{1}{4\pi\epsilon_0}\frac{Q}{r^2}\,\hat{\boldsymbol{r}} \qquad d\boldsymbol{l} = dr\,\hat{\boldsymbol{r}} + r\,d\theta\hat{\boldsymbol{\theta}} + r\sin\theta d\phi\,\hat{\boldsymbol{\phi}}, \tag{2.22}$$

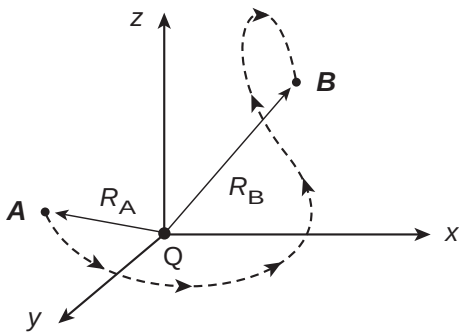

Fig. 2.7 Path for a line integral in an electric field that is generated by a charge Q located at the origin.

where $\hat{\boldsymbol{r}}$, $\hat{\boldsymbol{\theta}}$, and $\hat{\boldsymbol{\phi}}$ are unit vectors. Therefore, the line integral is

$$\begin{aligned}\int_{\boldsymbol{A}}^{\boldsymbol{B}} \boldsymbol{E}\cdot d\boldsymbol{l} &= \frac{1}{4\pi\epsilon_0}\int_{\boldsymbol{A}}^{\boldsymbol{B}} \frac{Q}{r^2}\,dr \\ &= \frac{-Q}{4\pi\epsilon_0 r}\bigg|_{R_A}^{R_B} \\ &= \frac{1}{4\pi\epsilon_0}\left(\frac{Q}{R_A}-\frac{Q}{R_B}\right).\end{aligned} \tag{2.23}$$

The integral around a *closed path* is then zero,

$$\oint \boldsymbol{E}\cdot d\boldsymbol{l} = 0, \tag{2.24}$$

since $R_A = R_B$ in that case. Now we may invoke *Stokes' theorem* [Eq. (A.30)]:

> ***Stokes' theorem:*** If $\boldsymbol{A}$ is a vector field and S is an arbitrary open surface bounded by a closed curve C, then
>
> $$\int_S (\boldsymbol{\nabla}\times\boldsymbol{A})\cdot\boldsymbol{n}\,da = \oint_C \boldsymbol{A}\cdot d\boldsymbol{l} \qquad \text{(Stokes' theorem)}, \tag{2.25}$$
>
> where $\boldsymbol{n}$ is the normal to S, the line element on the curve C is $d\boldsymbol{l}$, and the path in the line integration is traversed in a right-hand screw sense relative to $\boldsymbol{n}$. A geometrical interpretation of Stokes' theorem is given in Box 2.3.

This implies that

$$\int_S (\boldsymbol{\nabla}\times\boldsymbol{E})\cdot\boldsymbol{n}\,da = \oint_P \boldsymbol{E}\cdot d\boldsymbol{l} = 0, \tag{2.26}$$

and since this must be valid for any closed path, the integrand on the left side must vanish,

$$\boldsymbol{\nabla}\times\boldsymbol{E} = 0. \tag{2.27}$$

Box 2.3 **Geometrical Interpretation of Stokes' Theorem**

For a vector field $\boldsymbol{A}$, *Stokes' theorem* relates a surface integral of the curl vector field $\boldsymbol{\nabla} \times \boldsymbol{A}$ to a line integral around the (smooth) boundary of that surface:

$$\oint_C \boldsymbol{A} \cdot d\boldsymbol{r} = \int_S (\boldsymbol{\nabla} \times \boldsymbol{A}) \cdot \boldsymbol{n}\, ds \equiv \int_S (\boldsymbol{\nabla} \times \boldsymbol{A}) \cdot d\boldsymbol{s} \qquad \text{(Stokes' theorem)},$$

where S is the 2D surface enclosed by the 1D boundary C, the outward normal to the surface is $\mathbf{n}$, and the curl $\boldsymbol{\nabla} \times \boldsymbol{A}$ may be expressed explicitly by

$$\boldsymbol{\nabla} \times \boldsymbol{A} = \left(\frac{\partial A_z}{\partial y} - \frac{\partial A_y}{\partial z} \right) \hat{\boldsymbol{x}} + \left(\frac{\partial A_x}{\partial z} - \frac{\partial A_z}{\partial x} \right) \hat{\boldsymbol{y}} + \left(\frac{\partial A_y}{\partial x} - \frac{\partial A_x}{\partial y} \right) \hat{\boldsymbol{z}},$$

in cartesian coordinates. The orientation of the surface $\boldsymbol{n}$ and the direction of the integration path around the boundary curve that are illustrated in the following figure

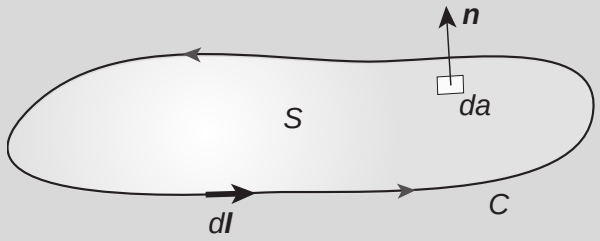

are related by the following *right-hand rule*:

> Point the thumb of your right hand in the direction of a unit normal vector near the edge of the surface S and curl your fingers; the direction that your fingers point indicates the integration direction around C.

The physical content of Stokes' theorem may be understood geometrically if one divides the surface up into plaquettes:

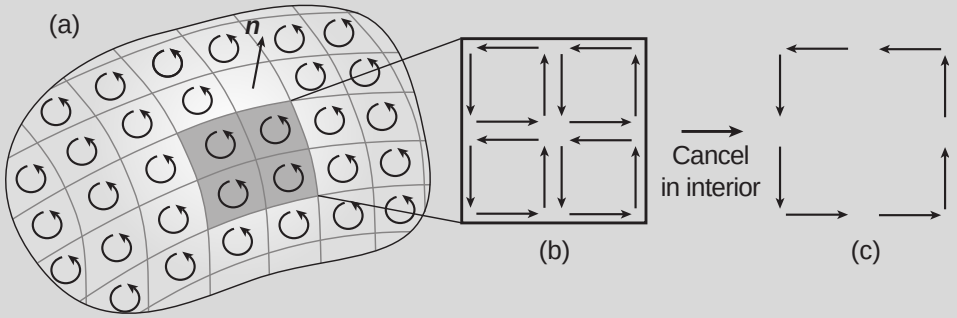

For the darker gray plaquettes in (b) of (a) the circulating currents cancel in the interior, leaving only the contribution from the boundary (c). Generalizing to the whole surface, as plaquette size tends to zero all interior contributions to the surface integral may be expected to cancel, leaving only the boundary contributions.

Thus, we have shown that *the curl of an electric field $\boldsymbol{E}$ is zero.*[7]

Because of Eq. (2.27) and Stokes' theorem, the line integral of the electric field around any closed loop is zero, which implies that the line integral between points $\boldsymbol{A}$ and $\boldsymbol{B}$ in Fig. 2.7 has *the same value for all possible paths.* Thus we can define a function $\Phi(\boldsymbol{x})$ by

$$\Phi(\boldsymbol{x}) = -\int_{\mathcal{O}}^{\boldsymbol{x}} \boldsymbol{E}(\boldsymbol{x}) \cdot d\boldsymbol{l}, \tag{2.28}$$

where $\mathcal{O}$ is a chosen standard reference point. The function $\Phi(\boldsymbol{x})$ is called the *scalar potential* or the *electric potential.* The scalar potential associated with a point charge q at the origin is given by

$$\Phi(\boldsymbol{r}) = \frac{1}{4\pi\epsilon_0}\left(\frac{q}{r}\right), \tag{2.29}$$

where r is the separation between charge and point, and invoking superposition the potential generated by a collection of n charges is

$$\Phi(\boldsymbol{r}) = \frac{1}{4\pi\epsilon_0}\sum_{i=1}^{n}\frac{q_i}{r_i}. \tag{2.30}$$

For a continuous charge distribution in one, two, or three spatial dimensions the potential evaluates to

$$\Phi(\boldsymbol{x}) = \frac{1}{4\pi\epsilon_0}\int \frac{\rho(\boldsymbol{x}')}{|\boldsymbol{x}-\boldsymbol{x}'|}\, d^3x' \qquad \text{(3D volume charge)}, \tag{2.31a}$$

$$\Phi(\boldsymbol{x}) = \frac{1}{4\pi\epsilon_0}\int \frac{\sigma(\boldsymbol{x}')}{|\boldsymbol{x}-\boldsymbol{x}'|}\, da' \qquad \text{(2D surface charge)}, \tag{2.31b}$$

$$\Phi(\boldsymbol{x}) = \frac{1}{4\pi\epsilon_0}\int \frac{\lambda(\boldsymbol{x}')}{|\boldsymbol{x}-\boldsymbol{x}'|}\, dl' \qquad \text{(1D line charge)}, \tag{2.31c}$$

where ρ is a volume charge density, σ is a surface charge density, and λ is a line charge density.

2.7 The Electric Field and the Scalar Potential

The electric field is a special vector field because it has vanishing curl. We shall now use this to reduce finding the electric field, which is inherently a vector problem, to a simpler

[7] Note that this is true for *static electric fields*, but may no longer hold for time-dependent problems. For example, see Eq. (10.11).

scalar problem. The *potential difference* between points $\boldsymbol{A}$ and $\boldsymbol{B}$ in Fig. 2.7 is given by

$$\begin{aligned}\Phi(\mathrm{B}) - \Phi(\mathrm{A}) &= -\int_{\mathcal{O}}^{\boldsymbol{B}} \boldsymbol{E}\cdot d\boldsymbol{l} + \int_{\mathcal{O}}^{\boldsymbol{A}} \boldsymbol{E}\cdot d\boldsymbol{l} \\ &= -\int_{\mathcal{O}}^{\boldsymbol{B}} \boldsymbol{E}\cdot d\boldsymbol{l} - \int_{\boldsymbol{A}}^{\mathcal{O}} \boldsymbol{E}\cdot d\boldsymbol{l} \\ &= -\int_{\boldsymbol{A}}^{\boldsymbol{B}} \boldsymbol{E}\cdot d\boldsymbol{l}. \end{aligned} \tag{2.32}$$

Applying the fundamental theorem for gradients (A.28) to the left side gives,

$$\Phi(\boldsymbol{B}) - \Phi(\boldsymbol{A}) = \int_{\boldsymbol{A}}^{\boldsymbol{B}} (\boldsymbol{\nabla}\Phi)\cdot d\boldsymbol{l}, \tag{2.33}$$

and therefore from Eqs. (2.32) and (2.33),

$$\int_{\boldsymbol{A}}^{\boldsymbol{B}} (\boldsymbol{\nabla}\Phi)\cdot d\boldsymbol{l} = -\int_{\boldsymbol{A}}^{\boldsymbol{B}} \boldsymbol{E}\cdot d\boldsymbol{l}. \tag{2.34}$$

But since Eq. (2.34) must be true for arbitrary points $\boldsymbol{A}$ and $\boldsymbol{B}$, the integrands of the integrals on the two sides of Eq. (2.34) must be equal and we obtain

$$\boldsymbol{E} = -\boldsymbol{\nabla}\Phi, \tag{2.35}$$

which is a differential version of Eq. (2.28).

> The electric field vector $\boldsymbol{E}$ may be obtained by taking minus the gradient of the scalar potential Φ.

In SI units force is measured in newtons and charge in coulombs, so electric fields $\boldsymbol{E}$ have units of newtons per coulomb. Then the potential Φ has units of newton-meters per coulomb, or joules per coulomb, where a joule per coulomb is defined to be a volt.

A major advantage of the potential formulation is that it is usually easier to construct the scalar potential than the electric field, but if one knows the potential Φ, the electric field can be obtained simply by taking the gradient, as in Eq. (2.35). This is perhaps surprising because Φ is a scalar with only *one component*, while $\boldsymbol{E}$ is a vector with *three components*. The source of this seeming miracle is the set of restrictions placed on the components $\boldsymbol{E}$ by the vanishing of the curl in Eq. (2.27), since expansion of $\boldsymbol{\nabla}\times\boldsymbol{E} = 0$ leads to the constraint equations

$$\frac{\partial E_x}{\partial y} = \frac{\partial E_y}{\partial x} \qquad \frac{\partial E_z}{\partial y} = \frac{\partial E_y}{\partial z} \qquad \frac{\partial E_x}{\partial z} = \frac{\partial E_z}{\partial x}, \tag{2.36}$$

as you are asked to show in Problem 2.5.

Changing the arbitrary reference point $\mathcal{O}$ appearing in Eq. (2.28) shifts the potential by a constant amount, implying that there is an essential ambiguity in defining Φ. It follows that the potential itself has no clear physical meaning, but as long as we choose the *same reference $\mathcal{O}$ for all potentials*,

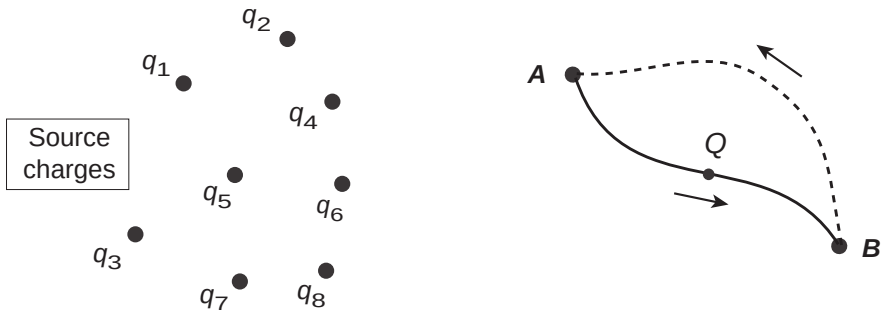

Fig. 2.8 Moving an electrical test charge Q on a path between endpoints $\boldsymbol{A}$ and $\boldsymbol{B}$ in an electric field generated by a static set of source charges. The work done is independent of the path, depending only on the endpoints $\boldsymbol{A}$ and $\boldsymbol{B}$, indicating that the electric field is *conservative*. Alternatively, if the path is closed by the dashed curve from $\boldsymbol{B}$ to $\boldsymbol{A}$, the work done by the electric field over the closed path $\boldsymbol{A}$ to $\boldsymbol{B}$ and back to $\boldsymbol{A}$ is identically zero.

1. *differences between potentials* $(\Phi(\boldsymbol{x}_i) - \Phi(\boldsymbol{x}_j))$ are independent of the reference point $\mathcal{O}$, and
2. *gradients of the potential* $\boldsymbol{\nabla}\Phi$ are unaffected by shifting the reference point a constant amount, since the derivative of a constant is zero.

Thus, potential differences and potential gradients have physical meaning. The selection of the reference point $\mathcal{O}$ for the potential is in principle arbitrary, but the most common choice in electrostatics is to take $\mathcal{O}$ to be an infinite distance away from the (assumed localized) charges, where the potential is taken to drop to zero.[8]

2.8 Work and Energy for Electric Fields

A question of fundamental importance in electrostatics is illustrated in Fig. 2.8: if we have a stationary configuration of source charges and a test charge Q is moved along some path between two points $\boldsymbol{A}$ and $\boldsymbol{B}$, *how much work will be done on the test charge* by the field produced by the source charges?

2.8.1 The Work Required to Move a Test Charge

The electrical force exerted on the charge Q is the product of Q and the electric field $\boldsymbol{E}$ generated by the source charges, $\boldsymbol{F} = Q\boldsymbol{E}$. Thus a minimal force $-Q\boldsymbol{E}$ must be exerted

[8] This prescription requires more thought if a problem hypothesizes a charge distribution that extends to infinity. In that case a different reference point $\mathcal{O}$ must be used. We won't worry about that here, since in real-world problems charge distributions are typically bounded spatially.

at each point to move the charge along the path and the total work W done is given by the line integral

$$W = \int_{\boldsymbol{A}}^{\boldsymbol{B}} \boldsymbol{F} \cdot d\boldsymbol{l} = -Q \int_{\boldsymbol{A}}^{\boldsymbol{B}} \boldsymbol{E} \cdot d\boldsymbol{l} = Q\,[\Phi(\boldsymbol{B}) - \Phi(\boldsymbol{A})], \tag{2.37}$$

where Eq. (2.32) has been used. Because the work was done against an electric field, it is *independent of path.*

Therefore the electrostatic force is *conservative,* meaning that the work depends only on the *difference in potentials between the endpoints of the path* and not on the details of the path followed. An alternative statements is that the work done on a *closed path* in a field is identically zero if the field is conservative.

If we wish to move the charge from an infinite distance away to a point $\boldsymbol{B}$,

$$W = Q\,[\Phi(\boldsymbol{B}) - \Phi(\infty)], \tag{2.38}$$

so the work done in moving a test charge from infinity to a point $\boldsymbol{x} \equiv \boldsymbol{B}$ is

$$W = Q\,\Phi(\boldsymbol{x}), \tag{2.39}$$

if the standard choice is made that the reference point for the potential is $\Phi(\infty) = 0$,

Thus $\Phi(\boldsymbol{x}) = W/Q$ and the scalar potential $\Phi(\boldsymbol{x})$ is the *work per unit charge* required to move a test charge from infinity to the position $\boldsymbol{x}$ in an electric field. It is also the potential energy stored in the fields of the assembled charge configuration that could be released by moving all the assembled charges back to infinity.

Example 2.6 illustrates using Eq. (2.39) to calculate the total work done in assembling a local set of charges.

Example 2.6 Let's use Eq. (2.39) to calculate the total work done in assembling a set of n charges q_i, by bringing them from infinity to their final positions in a local assembly of charges. The first charge costs nothing to move, since there are no assembled charges and no electric field to fight against. Adding each additional charge will require the work specified in Eq. (2.39) summed pairwise over contributions from all charges. Therefore

the total work required to assemble the final distribution of n charges is

$$\begin{aligned} W &= \frac{1}{2}\frac{1}{4\pi\epsilon_0}\sum_{i=1}^{n}\sum_{j\neq i}^{n}\frac{q_i q_j}{r_{ij}} \\ &= \frac{1}{2}\sum_{i=1}^{n} q_i\left(\sum_{j\neq i}^{n}\frac{1}{4\pi\epsilon_0}\frac{q_j}{r_{ij}}\right) \\ &= \frac{1}{2}\sum_{i=1}^{n} q_i\,\Phi(\boldsymbol{r}_i), \end{aligned} \tag{2.40}$$

where r_{ij} is the distance between charges i and j, the restriction $i \neq j$ omits infinite self-energies of a charge interacting with itself (see the discussion in Section 1.6 of infinite self energies of point particles), the initial factor of $\frac{1}{2}$ is to correct for the double counting of pairs in the double summation, and the factor in parentheses on the second line represents the potential $\Phi(\boldsymbol{r}_i)$ at the position $\boldsymbol{r}_i$ of charge q_i generated by all the other charges [see Eq. (2.30)].

Equation (2.40) represents the work required to assemble the n charges into some local configuration. Therefore, Eq. (2.40) also represents a total (potential) energy stored in the electric fields of the final assembly of charges, which could be released by moving all of the charges back to infinity.

2.8.2 Energy of a Continuous Charge Distribution

Previous sections have shown how to calculate the energy of a discrete set of charges. Let's now address determining the energy of a *continuous distribution of charge*. From Eq. (2.40) we infer that assembling a continuous volume charge requires an amount of work

$$W = \frac{1}{2}\int \rho\,\Phi\,d\tau, \tag{2.41}$$

where $d\tau$ is a volume element. This can be rewritten to eliminate the charge density ρ and the scalar potential Φ in favor of the electric field $\boldsymbol{E}$ in the following way. Use Gauss's law $\rho = \epsilon_0 \boldsymbol{\nabla}\cdot\boldsymbol{E}$ from Eq. (2.21) to express ρ in terms of $\boldsymbol{E}$,

$$W = \frac{\epsilon_0}{2}\int (\boldsymbol{\nabla}\cdot\boldsymbol{E})\,\Phi\,d\tau, \tag{2.42}$$

and integrate this by parts (see Appendix A.11) to give

$$W = \frac{\epsilon_0}{2}\left(-\int_V \boldsymbol{E}\cdot(\boldsymbol{\nabla}\Phi)\,d\tau + \oint_S \Phi\boldsymbol{E}\cdot d\boldsymbol{a}\right), \tag{2.43}$$

where $d\boldsymbol{a} \equiv \boldsymbol{n}\,da$. But from Eq. (2.35), $\boldsymbol{\nabla}\Phi = -\boldsymbol{E}$, so

$$W = \frac{\epsilon_0}{2}\left(\int_V E^2\,d\tau + \oint_S \Phi\,\boldsymbol{E}\cdot d\boldsymbol{a},\right) \tag{2.44}$$

where $E \equiv |\boldsymbol{E}|$, and the integration volume V in the first term is large enough to enclose all charge. If we let $V \to \infty$ then the second (surface) term tends to zero relative to the first term, giving

$$W = \frac{\epsilon_0}{2} \int E^2 d\tau, \tag{2.45}$$

where it is understood that the integration is over all space. The use of Eq. (2.45) is illustrated in Example 2.7.

Example 2.7 Let's calculate the energy of a uniformly charged spherical shell of total charge Q and radius R. From the solution of Problem 2.4, inside the sphere $\boldsymbol{E} = 0$ and outside

$$\boldsymbol{E} = \frac{1}{4\pi\epsilon_0} \frac{Q}{r^2} \hat{\boldsymbol{r}} \quad \longrightarrow \quad E^2 = \frac{Q^2}{(4\pi\epsilon_0)^2 r^4},$$

where we work in spherical coordinates. Therefore, from Eq. (2.45),

$$W = \frac{Q^2}{8\pi\epsilon_0} \int_R^\infty \frac{dr}{r^2} = \frac{1}{8\pi\epsilon_0} \frac{Q^2}{R},$$

where all contributions to the energy have come from fields outside the sphere.

2.9 Equipotential Surfaces and Field Lines

The equation $\Phi(\boldsymbol{x}) = \Phi_0$ defines a family of 2D surfaces having constant potential Φ_0 in 3D space that are called *equipotential surfaces*. By virtue of Eq. (2.37), it takes no work to move charges on such equipotential surfaces. It is often useful to visualize the potential in an electrostatics problem by displaying equipotential contours graphically. Likewise, it is useful to visualize the electric field associated with the potential. The potential is a scalar, having one value at a given coordinate. The electric field is a vector field; it can be represented by an arrow at a given point, indicating a magnitude by the length (or color in a color plot) and a direction by an orientation angle for the arrow.

2.9.1 Equipotential Contours and Vector Fields

Figure 2.9 illustrates a 2D projection of equipotential contours (the solid lines) superposed on vectors indicating the magnitude and direction of the corresponding electric field for a static dipole charge configuration (see Box 3.3). Note that in Fig. 2.9 the vectors representing the electric field are generally perpendicular to the potential contours where they cross. We can see that this must be so immediately by considering an equipotential

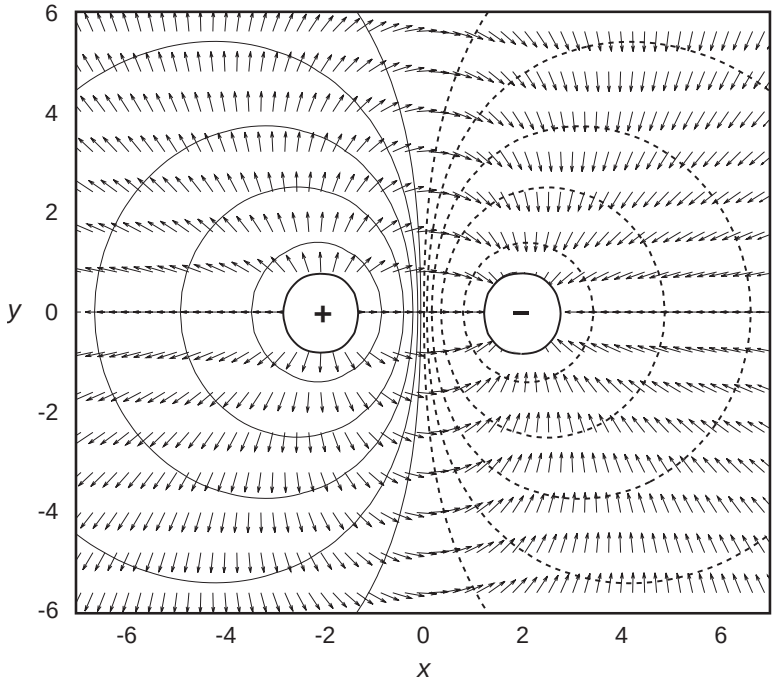

Fig. 2.9 Equipotential contours (solid curves) and the electric vector field (arrows) originating in a dipole charge distribution (see Box 3.3). For clarity, plotting of contours and vectors has been suppressed near the two charges. Notice that the field vectors cross equipotential contours at right angles, and must reverse from outward-going around the positive charge to inward-going around the negative charge. To avoid clutter the equipotentials are not labeled, but they are negative on the right side of the diagram ($x < 0$), as indicated by dashed contours, and positive on the left side $x > 0$, as indicated by solid contours.

contour. From Eq. (2.37), for any path lying entirely on an equipotential surface,

$$\int_{\boldsymbol{x}_1}^{\boldsymbol{x}_2} \boldsymbol{E} \cdot d\boldsymbol{l} = 0, \tag{2.46}$$

which indicates either that $\boldsymbol{E} = 0$ along the entire path, or that the direction of $\boldsymbol{E}$ is orthogonal to the equipotential surface at every point. Thus when any non-vanishing electric field lies on an equipotential surface the field vector must be oriented at right angles to the equipotential surface.

2.9.2 Electric Field Lines

Rather than drawing the full projection in 2D of the vector field, as has been done in Fig. 2.9, it is often useful to construct *electric field lines*, which are continuous curves drawn connecting points corresponding to the same magnitude of the electric field, drawn such that a differential element of arc length on the field line $d\boldsymbol{l}$ points in the direction of $\boldsymbol{E}(\boldsymbol{x})$

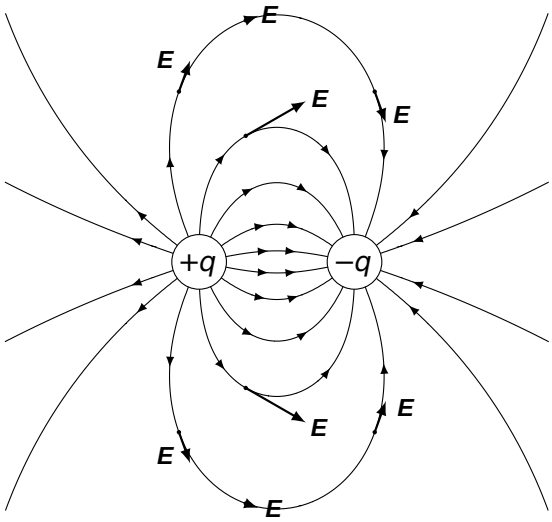

Fig. 2.10 Electric field lines for an electric dipole charge distribution with charges $\pm q$. Notice the convention reflected in the field lines that the electric field points away from positive charges and toward negative charges. Some representative vectors $\boldsymbol{E}$ are shown at several points, with length proportional to the field strength on that curve, and direction tangent to the field line at that point.

at each point; that is

$$d\boldsymbol{l} = \lambda \boldsymbol{E}, \tag{2.47}$$

where λ is a constant. Thus, from the discussion in Section 2.9.1, every electric field line is locally normal to an equipotential surface,[9] except at points where $\boldsymbol{E} = 0$. The differential equations defining the electric field lines correspond to writing out the components of Eq. (2.47); in cartesian coordinates they take the form

$$\frac{dx}{dE_x} = \frac{dy}{dE_y} = \frac{dz}{dE_z} = \lambda. \tag{2.48}$$

An example of electric field lines for an electric dipole charge distribution is given in Fig. 2.10. Each field line connects points having a constant electric field strength, with the direction of $\boldsymbol{E}$ given by the tangent to the curve at that point. Representative electric field vectors are shown at various points. For example, two vectors are drawn on the uppermost lobe, both of the same length since they are on the same field line, but with different directions corresponding to tangents to the field line where they are drawn. Figure 2.11 illustrates plotting electric field lines and electric potential contours on the same graph for an electric dipole. Figure 2.12 displays electric field lines and electric potential contours for a charge distribution consisting of two nearby charges of the same sign.

Notice in these plots that since $\boldsymbol{E}$ has a unique direction at every spatial point, electric field lines cannot cross (except at a null point where the field is tending to zero). The

[9] Notice that this is consistent with the usual geometrical interpretation of the gradient in $\boldsymbol{E} = -\boldsymbol{\nabla}\Phi$ being related to a direction of steepest descent in a potential surface.

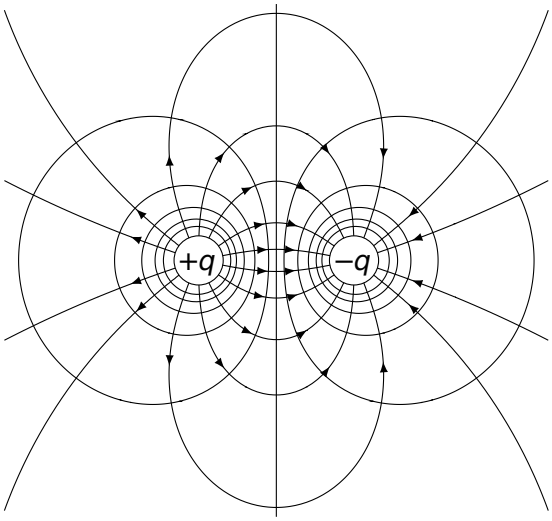

Fig. 2.11 Electric field lines (black with arrows) and equipotential contours (gray, no arrows) for an electric dipole with charges $\pm q$. Notice that the field lines are always locally perpendicular to the potential contours.

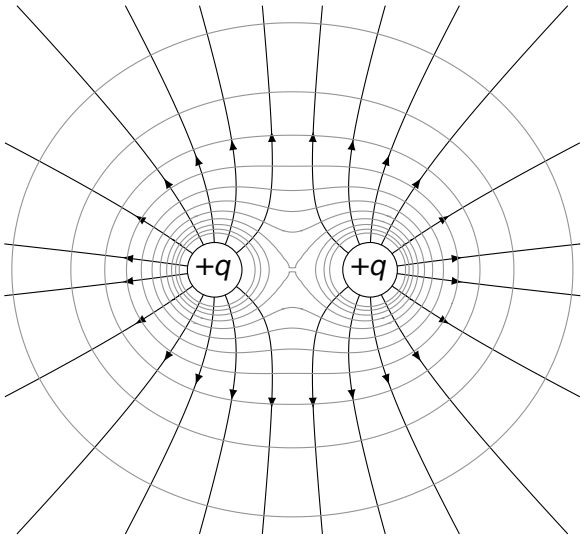

Fig. 2.12 Electric field lines (black with arrows) and equipotential contours (gray, no arrows) for two nearby charges of the same sign $+q$.

number density of field lines passing through a differential element of an equipotential surface is assumed to be proportional to the magnitude of $\boldsymbol{E}$ at that point. This implies that the total number of field lines passing through a surface S is proportional to the electric flux $\mathcal{F}_{\mathrm{E}}$,

$$\mathcal{F}_{\mathrm{E}} = \int_S \hat{\boldsymbol{n}} \cdot \boldsymbol{E} dS. \tag{2.49}$$

As you are asked to show in Problem 2.8, if the surface S is *closed*, charge conservation

demands that the flux through the surface must be proportional to the charge enclosed by the surface,

$$\mathcal{F}_{\mathrm{E}} = \frac{Q_{\mathrm{V}}}{\epsilon_0}, \tag{2.50}$$

which means that the net number of electric field lines crossing S is proportional to the net charge enclosed by S. As a corollary, if no charge is enclosed in the volume V, every field line that enters V must also leave V.

2.9.3 2D Projections of 3D Physics

Two-dimensional representations of (usually 3D) electric fields and potentials can be very useful in visualizing an electrostatics problem, but 2D projections can distort the actual physical situation in a 3D problem. This is particularly true in interpreting the density of field lines as indicating the local strength of the field, since projection from 3D to 2D can give a misleading perception of the actual density of field lines in 3D. On the other hand, more realistic 3D volume rendering is technically more demanding, and may present its own problems of visual interpretation when displayed in static 2D media.

2.10 Superposition of Scalar Potentials

We introduced the principle of linear superposition in Section 2.4 with the hypothesis that the forces acting on a test charge Q are the vector sum of contributions from each source charge q_i,

$$\boldsymbol{F} = \boldsymbol{F}_1 + \boldsymbol{F}_2 + \boldsymbol{F}_3 + \ldots \tag{2.51}$$

and since $\boldsymbol{F} = Q\boldsymbol{E}$, dividing the terms in Eq. (2.51) by Q implies linearity for the electric fields $\boldsymbol{E}$ also,

$$\boldsymbol{E} = \boldsymbol{E}_1 + \boldsymbol{E}_2 + \boldsymbol{E}_3 + \ldots \tag{2.52}$$

Likewise, from the preceding definitions the scalar potential Φ may be expected to obey linear superposition,

$$\Phi = \Phi_1 + \Phi_2 + \Phi_3 + \ldots, \tag{2.53}$$

meaning that the potential at a point $\boldsymbol{x}$ is the sum of the potentials due to all source charges considered separately. However, there is a fundamental difference between linear superposition for potentials and linear superposition for forces and electric fields.

Linear superposition of electrostatic forces and electric fields in Eqs. (2.51) and (2.52) corresponds to *vector sums*, but linear superposition of potentials in Eq. (2.53) entails an ordinary *arithmetic sum* over scalar quantities Φ_i, which is typically easier to deal with than a sum over vectors.

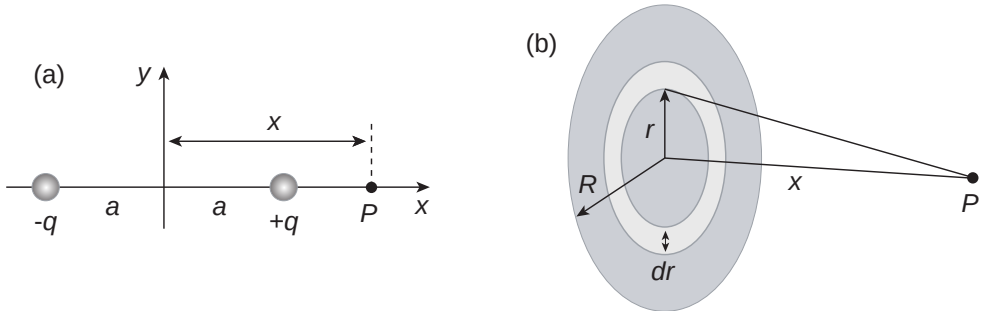

Fig. 2.13 (a) An electric dipole charge configuration used in Example 2.8. (b) Uniformly charged disk of radius R and surface charge density σ used in Example 2.9.

Examples 2.8 and 2.9 illustrate calculating the potential Φ of a charge distribution and then taking its gradient to give the electric field.

Example 2.8 Let's calculate the potential and corresponding electric field for the electric dipole charge configuration displayed in Fig. 2.13(a) at the point P, and also also approximate the result for a very large distance $x \gg a$ along the x axis from the charges. At the point P the potential Φ is the sum of contributions from the two charges,

$$\Phi = \frac{1}{4\pi\epsilon_0}\left(\frac{q}{x-a} + \frac{-q}{x+a}\right) = \frac{1}{2\pi\epsilon_0}\left(\frac{qa}{x^2-a^2}\right).$$

The electric field is then oriented along the x axis with magnitude given by minus the gradient of the potential

$$E_x = -\boldsymbol{\nabla}\Phi = -\frac{d\Phi}{dx} = \frac{1}{\pi\epsilon_0}\left[\frac{aqx}{(x^2-a^2)^2}\right].$$

The scalar potential and electric field may be approximated as

$$\Phi \simeq \frac{1}{2\pi\epsilon_0}\left(\frac{aq}{x^2}\right) \qquad E_x \simeq -\frac{d\Phi}{dx} = \frac{1}{\pi\epsilon_0}\left(\frac{aq}{x^3}\right),$$

if $x \gg a$, so that $x^2 - a^2 \sim x^2$.

Example 2.9 Let's calculate the electric field at the point P along the x axis for the charged disk of radius R and uniform surface charge density σ illustrated in Fig. 2.13(b). For a ring of radius r and width dr the charge element at a distance $(r^2 + x^2)^{1/2}$ from the point P is $dq = (2\pi r dr)\sigma$. Then

$$d\Phi = \frac{1}{2\epsilon_0}\left(\frac{\sigma r dr}{\sqrt{x^2+r^2}}\right)$$

and since the potential obeys the superposition principle the total Φ at the point P is

obtained by integration over the disk,

$$\begin{aligned}\Phi = \int d\Phi &= \int_0^R \frac{1}{2\epsilon_0}\left(\frac{\sigma r dr}{\sqrt{x^2+r^2}}\right) \\ &= \frac{\sigma}{2\epsilon_0}\int_0^R \frac{r\,dr}{\sqrt{x^2+r^2}} \\ &= \frac{\sigma}{2\epsilon_0}\left[\sqrt{x^2+r^2}\right]_0^R \\ &= \frac{\sigma}{2\epsilon_0}\left(\sqrt{x^2+R^2}-x\right).\end{aligned}$$

Then the electric field at P is minus the gradient of the potential,

$$E_x = -\frac{d\Phi}{dx} = \frac{\sigma}{2\epsilon_0}\left(1-\frac{x}{\sqrt{x^2+R^2}}\right),$$

where by symmetry $\boldsymbol{E}$ has only x components.

For relatively simple charge distributions like those in Examples 2.8 and 2.9, the potentials can be worked out easily and then the electric field is determined by taking the gradient of the potential. However, more complex situations may require more powerful and systematic ways to determine potentials. In the next section we show that the problem of finding potentials can be cast in the form of solving a second-order partial differential equation. Although it can become mathematically involved, this approach may be preferred over the ones we have examined so far, particularly for problems with complicated boundary conditions, because it provides a systematic procedure that may be applied to a broad range of complex problems.

2.11 The Poisson and Laplace Equations

We have already found in Eq. (2.27) that the curl $\boldsymbol{\nabla}\times\boldsymbol{E}$ of the electric field vanishes. It is of interest then to ask, what is the divergence $\boldsymbol{\nabla}\cdot\boldsymbol{E}$ of the electric field?

2.11.1 The Poisson Equation

From Eq. (2.35),

$$\boldsymbol{\nabla}\cdot\boldsymbol{E} = \boldsymbol{\nabla}\cdot(-\boldsymbol{\nabla}\Phi) = -\nabla^2\Phi,$$

and comparing this result with Gauss's law (2.21) gives *Poisson's equation,*

$$\nabla^2\Phi = -\frac{\rho}{\epsilon_0} \qquad \text{(Poisson's equation)}, \tag{2.54}$$

where the *Laplacian operator* ∇^2 in cartesian coordinates is given by [see Eq. (A.20)][10]

$$\nabla^2 = \frac{\partial^2}{\partial x^2} + \frac{\partial^2}{\partial y^2} + \frac{\partial^2}{\partial z^2}, \tag{2.55}$$

which operates on a scalar to return a scalar. We will often need the Laplacian operator in other coordinate systems, so let's go ahead and write it in spherical coordinates (r, θ, ϕ),

$$\nabla^2 = \frac{1}{r^2}\frac{\partial}{\partial r}\left(r^2\frac{\partial}{\partial r}\right) + \frac{1}{r^2\sin\theta}\frac{\partial}{\partial\theta}\left(\sin\theta\frac{\partial}{\partial\theta}\right) + \frac{1}{r^2\sin^2\theta}\frac{\partial^2}{\partial\phi^2}, \tag{2.56}$$

[see Eq. (A.51)], and in cylindrical coordinates (ρ, ϕ, z),

$$\nabla^2 = \frac{1}{\rho}\frac{\partial}{\partial\rho}\left(\rho\frac{\partial}{\partial\rho}\right) + \frac{1}{\rho^2}\frac{\partial^2}{\partial\phi^2} + \frac{\partial^2}{\partial z^2}. \tag{2.57}$$

[see Eq. (A.58)].

Example 2.10 Earlier it was asserted that Eq. (2.31a) gives the scalar potential $\Phi(\boldsymbol{x})$ for a 3D continuous charge distribution, which means that $\Phi(\boldsymbol{x})$ should be a solution of the 3D Poisson equation (2.54). Let's check that it is. From Eq. (2.31a),

$$\Phi(\boldsymbol{x}) = \frac{1}{4\pi\epsilon_0}\int\frac{\rho(\boldsymbol{x}')}{|\boldsymbol{x}-\boldsymbol{x}'|}\,d^3x',$$

and applying the Laplacian operator to both sides of this equation gives

$$\nabla^2\Phi(\boldsymbol{x}) = \frac{1}{4\pi\epsilon_0}\int\rho(\boldsymbol{x}')\nabla^2\left(\frac{1}{|\boldsymbol{x}-\boldsymbol{x}'|}\right)d^3x'.$$

Evaluating the right side is potentially tricky as the integrand is singular as $\boldsymbol{x}' \to \boldsymbol{x}$, but this may be handled simply using that from Eq. (A.76) the Laplacian of $|\boldsymbol{x}-\boldsymbol{x}'|^{-1}$ is proportional to a Dirac delta function.

$$\nabla^2\left(\frac{1}{|\boldsymbol{x}-\boldsymbol{x}'|}\right) = -4\pi\delta(\boldsymbol{x}-\boldsymbol{x}'),$$

giving immediately

$$\nabla^2\Phi(\boldsymbol{x}) = -\frac{1}{\epsilon_0}\int\rho(\boldsymbol{x}')\,\delta(\boldsymbol{x}-\boldsymbol{x}')\,d^3x' = -\frac{\rho(\boldsymbol{x})}{\epsilon_0},$$

which is Poisson's equation (2.54). Thus Eq. (2.31a) is indeed a solution of the 3D Poisson equation.

A more involved solution for Example 2.10 that doesn't invoke the Dirac δ-function may be found in Ch. 1 of Jackson [41].

[10] Some author use the symbol Δ instead of ∇^2 for the Laplacian operator. The Poisson and Laplace equations are partial differential equations (PDEs), which are typically more difficult to deal with than ordinary differential equations (ODEs). We shall address methods of solution for the Poisson and Laplace equations shortly.

2.11.2 The Laplace Equation

For regions where there is no charge density $\rho = 0$ and Poisson's equation reduces to *Laplace's equation,*

$$\nabla^2 \Phi = 0 \qquad \text{(Laplace's equation).} \tag{2.58}$$

By construction, solving Poisson's equation (or Laplace's equation if $\rho = 0$) is equivalent physically to solving for the potential Φ using Eq. (2.28), and once Φ has been determined by either means the electric field can be calculated from Eq. (2.35).

2.11.3 Linearity of Laplace and Poisson Equations

An important property of Laplace's equation (2.58) and Poisson's equation (2.54) is that they are *linear,* in two related senses. if each of a set of potentials $\{\Phi_1, \Phi_2, \Phi_3, \dots, \Phi_n\}$ is a solution, then a linear combination of them,

$$\Phi \equiv a_1 \Phi_1 + a_2 \Phi_2 + a_3 \Phi_3, + \dots + \Phi_n,$$

with arbitrary constants a_i is also a solution.

2.12 Mathematical Classification of PDEs

A second-order linear PDE in two variables (x, y) can be written in the general form

$$A\frac{\partial^2 u}{\partial x^2} + 2B\frac{\partial^2 u}{\partial x \partial y} + C\frac{\partial^2 u}{\partial y^2} + D\frac{\partial u}{\partial x} + E\frac{\partial u}{\partial y} + Fu = G, \tag{2.59}$$

and the *discriminant* D is defined by the value of the constants (A, B, C) multiplying the second-derivative terms in Eq. (2.59),

$$D \equiv B^2 - AC. \tag{2.60}$$

Second-order PDEs having the canonical form (2.59) can be classified mathematically into three general classes according to the value of the *discriminant* D, as may be seen in Table 2.2 and Fig. 2.14.

1. *Elliptic PDEs* have $D < 0$.[11] They are characterized smooth solutions that usually do

[11] This condition implies that the eigenvalues of the coefficient matrix of the second-order terms are positive or negative definite, meaning that they all possess the same sign.

Table 2.2 Comparison of PDE types

Type	D	Physical archetype	Characteristics
Elliptic	< 0	Equilibrium / Steady state	Boundary values, global dependence, smooth
Parabolic	$= 0$	Diffusion / Heat flow	Initial values, smoothing, time-evolution
Hyperbolic	> 0	Waves / Propagation	Initial values, finite speed, shocks preserved

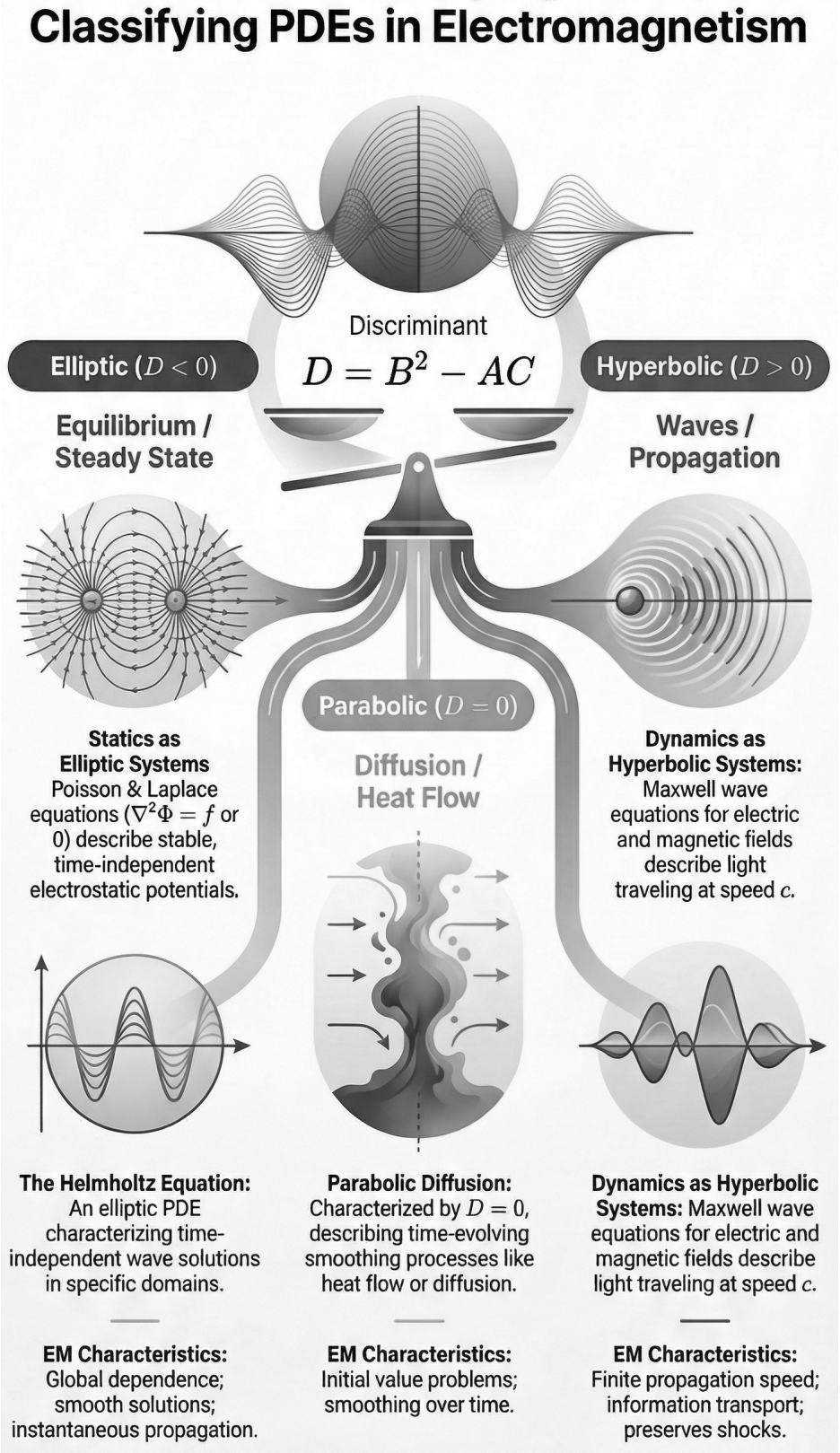

Fig. 2.14 Mathematical and physical classification of second-order, linear partial differential equations (PDEs) in two spatial dimensions.

not depend on time, and describe phenomena like electrostatic potentials in vacuum, steady-state heat flow, and irrotational fluid flow.

2. *Parabolic PDEs* have $D = 0$ and often describe time-evolving phenomena like diffusion and heat flow. For example, how temperature u distributes itself over a metal rod as time t evolves is described by the parabolic equation

$$\frac{\partial u}{\partial t} - \alpha \nabla^2 u = 0.$$

For parabolic PDEs, information travels forward in time, smoothing out as it evolves.

3. *Hyperbolic PDEs* have $D > 0$, and are often associated with waves and propagation of waves. Unlike parabolic equations, hyperbolic equations correspond to a finite propagation speed (speed of light or speed of sound, for example) that transports information rather than smoothing it out. A characteristic hyperbolic PDE is the wave equation

$$\frac{\partial^2 u}{\partial t^2} - c^2 \nabla^2 u = 0,$$

where c is the wave propagation speed.

By these criteria, there are three differential equations of importance in describing classical electromagnetism that can be classified as elliptic, two of which we have already met:

1. The *Laplace equation*, which takes the schematic form $\nabla^2 u = 0$,
2. the *Poisson equation*, which takes the schematic form $\nabla^2 u = f$, where f is called the source term, and
3. the *Helmholtz equation*, which takes the schematic form $\nabla^2 u + k^2 u = 0$, and characterizes time-independent wave equations.

Thus the Laplace and Poisson PDEs that we have been discussing in this chapter are *elliptical differential equations*. Let's examine in more depth the physical interpretation of elliptic differential equations and some of their key properties.

2.13 Key Properties of Elliptic Equations

As illustrated in Table 2.2, while classes of 2nd-order PDEs can be distinguished mathematically by evaluating the discriminant D, they also can be distinguished physically by the kinds of systems that they describe, and by the corresponding physical characteristics of their solutions.

2.13.1 Physical Interpretation: Equilibrium

Elliptic partial differential equations typically describe physical systems that have settled into a stable equilibrium or a steady state. There is no concept of time evolution and for elliptic PDEs a change of any point instantaneously affects all other points in the domain (the solution has the character of a stable snapshot).

2.13.2 Boundary Value Problems (BVP)

Unlike hyperbolic or parabolic equations, which evolve in time from an initial state (*initial value problems*), elliptic equations are solved on a fixed domain Ω subject to boundary conditions on the *entire closed boundary* $\partial\Omega$.[12] As we shall see for Poisson and Laplace equation problems in the next chapter,

1. *Dirichlet boundary conditions:* value specified ($u = g$ on $\partial\Omega$), and
2. *Neumann boundary conditions:* derivative specified ($\partial u/\partial n = h$ on $\partial\Omega$),

are the most common classes of boundary conditions for elliptic problems.

2.13.3 Global Dependence (Instantaneous Propagation)

Information in an elliptic problem propagates instantly across the entire domain. A perturbation in the boundary condition or source term at *any* single point affects the solution at *every* point in the domain immediately. This contrasts with hyperbolic equations, which have finite propagation speeds leading to well defined "domains of dependence" (for example, cosmological horizons defined by the finite speed of propagation for light waves).

2.13.4 Smoothing (Regularity)

Solutions to elliptic equations are typically very smooth (C^∞ or analytic) in the interior of the domain, even if the boundary conditions or source terms are discontinuous. The second-derivative Laplacian operator inherently "irons out" irregularities [29].

2.13.5 No Local Extrema

For elliptic equations like the Laplace equation the solution cannot have a local maximum or minimum in the interior of the domain: extremal values of the solution can occur only on the boundary. Physically, this corresponds to the intuition that in a steady-state heat distribution without internal heat sources, one expects the hottest and coldest points to be at the edges [69].

[12] We shall sometimes employ a notation common in differential geometry and algebraic topology where the symbol ∂ denotes an operator giving the boundary of a closed volume: $S = \partial\Omega$ means "the boundary S of the closed volume Ω". For example, the surface of a spherical ball (a filled sphere) is the sphere S^2. In this notation, the "boundary of a boundary" is denoted by $d^2 = \partial\partial = \partial^2$. Although "the boundary of a boundary equals zero" ($\partial^2 = 0$) may seem like a Zen koan, it is a result of fundamental importance in both differential geometry and algebraic topology, and is the mathematical underpinning for many important results in physics. This is because it represents the mathematical connection between local calculations and global structure.

Background and Further Reading

Introductions to the material of this chapter may be found in Corson and Lorrain [25], Griffiths [33], Kamberaj [43], Lorrain and Corson [49], and Purcell and Morin [62]. More advanced treatments may be found in Jackson [41], Garg [31], Chaichian et al [23], Zangwill [77], and Wald [74]. For classification of differential equations, see Evans [29] and Strauss [69].

Problems

2.1 Find the electric field produced by an infinite plane that carries a uniform surface charge density σ.

2.2 Two infinite parallel planes have equal but opposite charge densities $\pm\sigma$.

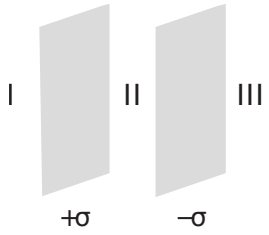

Find the electric fields in regions I, II, and III.

2.3 Prove that an isolated good conductor in electrostatic equilibrium (no net motion of charge carriers) has the following properties.

1. The interior electric field is zero.
2. Any excess charge resides on the surface.
3. The electric field just outside a charged conductor is perpendicular to the surface with a magnitude σ/ϵ_0, where σ is the surface charge density at that point.
4. If the conductor is of irregular shape, the surface charge density σ is greatest where the surface has the largest local curvature (smallest radius of curvature).

Hint: Gauss's law will be extremely useful. ***

2.4 A thin spherical shell of radius a has a total charge of Q distributed uniformly over its surface, as illustrated in the following figure.

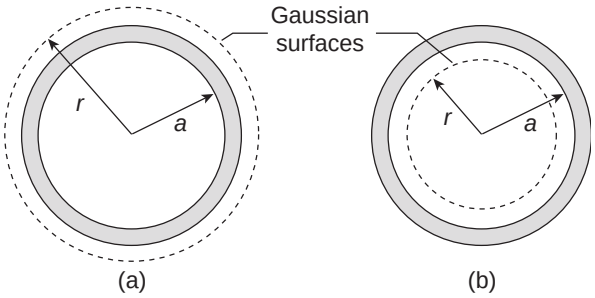

Find the electric field inside and outside the spherical shell using the Gaussian surfaces indicated by dashed circles.

2.5 (a) Use Stokes' theorem to prove that an electric field is conservative by examining the work done on a test charge moved over a closed path. (b) Prove that the components of an electric field $\boldsymbol{E}$ satisfy the constraints imposed by Eq. (2.36).

2.6 Two charge distributions $\rho_{\mathrm{A}}(\boldsymbol{x})$ and $\rho_{\mathrm{B}}(\boldsymbol{x})$ are related by a change of scale: $\rho_{\mathrm{B}}(\alpha\boldsymbol{x}) = \rho_{\mathrm{A}}(\boldsymbol{x})$, where α is a constant. What is the relationship of the scalar potentials and the electric fields for these two charge distributions?

2.7 Consider a 1D line segment of length $2L$, shown in the following figure,

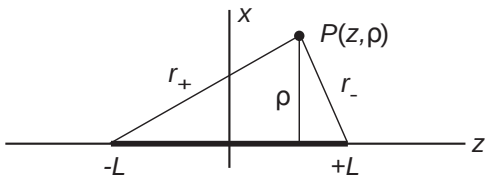

which carries a uniform charge density per unit length of λ. What is the electric potential at an arbitrary point $P(z, \rho)$? ***

2.8 Use Gauss's law to show that if an equipotential contour corresponds to a closed surface S, the electric flux (2.49) through the surface must satisfy $\mathcal{F}_{\rm E} = Q_{\rm V}/\epsilon_0$, where $Q_{\rm V}$ is the charge contained within the volume V bounded by the surface S.

2.9 A uniform electric field $\boldsymbol{E}$ of strength $4 \times 10^4\,{\rm V\,m^{-1}}$ is directed along the positive x-axis. A proton ($Q = 1.6 \times 10^{-19}\,{\rm C}$) is released from rest at point A and is found to undergo a displacement of $d = 0.5\,{\rm m}$ in the direction of $\boldsymbol{E}$ to point B. (a) What is the difference in electrical potential between points A and B? (b) How much does the potential energy of the proton change over this displacement?

2.10 Consider the electric dipole configuration

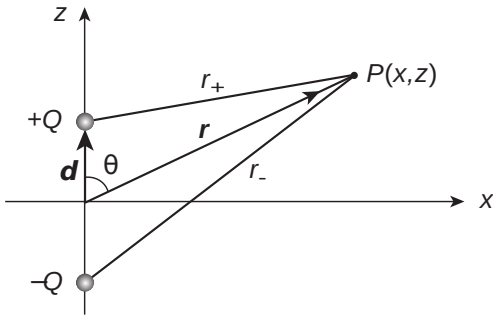

where the distance to the point $P(x, z)$ is much larger than the separation of the two charges. What is the electric potential Φ and what are the components of the electric field E_x and E_z evaluated at $P(x, z)$, expressed as functions of the distance $r = |\boldsymbol{r}|$ and the angle θ?

2.11 (a) Show that the general formula for the electric field produced by an infinite line charge of uniform density λ at a perpendicular distance z from the line charge is

$$E = \frac{\lambda}{2\pi\epsilon_0 z}\,\hat{\boldsymbol{z}},$$

by finding the electric field at the point P in the following figure,

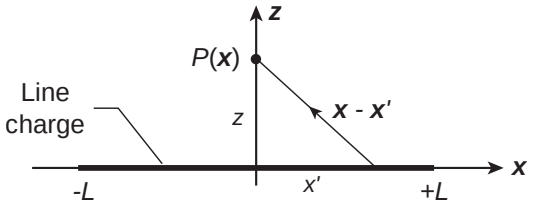

produced by a line charge λ of length $2L$, and then taking the limit $L \to \infty$. (b) Show that in the limit $z \gg L$, the electric field looks like that of a point charge of magnitude $2\lambda L$. ***

2.12 Consider a sphere of radius R centered at the origin of a spherical coordinate system with a non-uniform electric field given by $\boldsymbol{E} = kr^2\hat{\boldsymbol{r}}$, where k is a constant and r is the radial coordinate. Use the divergence theorem to find the total charge Q within the sphere.

Numerical and GenAI Problems

2.13 (a) Using *GenAI*, construct *Python* code to calculate the electrical potential $\Phi(x, y)$ and electric field $\boldsymbol{E}(x, y)$ for n test charges distributed arbitrarily in a 2D plane, where the location (x, y) and charge q of each test charge is specified by an external data file read by the *Python* code. Plot the corresponding potential in a 3D surface plot using *Python* and plot the electric field as a 2D vector plot and the potential contours in *gnuplot*, using *GenAI* to suggest the *gnuplot* script.

(b) Prompt the *GenAI* to write a *Bash* shell script [13] to automate running the *Python* code and then plotting the output in *gnuplot*. *Note:* A *Bash* shell script should run automatically under Linux in a terminal window, but see Ref. [5] for (easily implemented) changes that may be required for the shell script to run in a terminal window on a Windows or Macintosh computer.

(c) Use the *GenAI* to construct a concise user's manual so that you have documented reusable code that can be applied generally for such an electrostatics problem by an arbitrary user. ***

2.14 Guided by Example H.1 and Appendix H, create a *NotebookLM* project "*Python* for Advanced E&M". Use a Web search (regular or AI-enhanced, like *Gemini* in the Chrome browser) to add 5 or more sources to your project (the left **Sources** pane). Use "Search the web for new sources" to add at least 5-10 additional sources. Once *NotebookLM* has processed all added sources, use the central **Chat** panel to learn more about how *Python* can be used to solve complex E&M problems (*NotebookLM* will suggest some possible queries, and you can make up your own). Once you have explored some with Chat, try creating some output based on your project using the buttons at the top of the right **Studio** panel. Provide at least four examples (some initial ones to try are discussed in Appendix H.3).

2.15 Use *GenAI* to implement and debug *Python* code using *Successive Over-Relaxation (SOR)* to speed up convergence for a solution of the 2D Laplace equation on a 100×100 grid. (See Appendix F for an overview of these methods.) Use the *GenAI* to set up timing and compare speed both with normal loops and with vectorization

[13] A shell script is essentially a "to-do list" for your computer. Instead of typing commands one by one into the terminal, you bundle them into a text file that the system executes in sequence. There are various "shells" on computers, but the most common in a Linux environment is the *Bash* shell. See Ref. [5] for how to run Bash shell scripts on MacOS or Windows machines. Note that "*Bash*" should be capitalized when used as a proper name, but should always be lower case "*bash*" when used as part of a computer command.

[*Red–Black (Checkerboard) ordering*; see Section F.3], so that timing can be compared among these methods with and without vectorization. Use `matplotlib` to plot the resulting solution as a 2D heatmap and as a 3D wireframe plot. Describe briefly the *GenAI* prompts that you used to obtain the desired results, and the methods that you used to verify that the code produced by the *GenAI* is giving legitimate answers and not hallucinations. ***

2.16 Using *GenAI*, write *Python* code to display a contour plot and surface plot of the scalar potential around a finite line charge. Comment on the features and associated physics.

3 Electrostatic Boundary Value Problems

In Ch. 2 we introduced the Poisson equation (2.54), with solutions corresponding to scalar potentials $\Phi(\boldsymbol{x})$ in the presence of a charge density, and the Laplace equation (2.58), with solutions corresponding to scalar potentials $\Phi(\boldsymbol{x})$ in regions having no charge density, with the electric field then obtained by taking a gradient of the potential. Those solutions result from solving the corresponding partial differential equations subject to boundary conditions, which can be a highly nontrivial undertaking. This chapter addresses the nature of the solutions of the Poisson and Laplace equations, and some means of obtaining those solutions without necessarily solving the differential equations directly. However, many problems are sufficiently complicated that the simplest approach is to grasp the nettle and solve the partial differential equations analytically or numerically. We shall consider such direct solutions in Ch. 4.

3.1 Electric Fields and Surface Charge Layers

An important property of electric fields is their behavior at boundaries in a system. Let us now demonstrate that an electric field necessarily exhibits a discontinuity if a surface charge layer is crossed. Consider Fig. 3.1, which shows a small piece of a surface having a surface charge density σ. We place a very thin rectangular Gaussian box of height ϵ that extends vertically just below and just above the surface. From Gauss's law,

$$\oint_S \boldsymbol{E} \cdot d\boldsymbol{a} = \frac{}{\epsilon_0} = \frac{\sigma A}{\epsilon_0},$$

where $Q = \sigma A$ is the enclosed charge and $d\mathbf{a} = \boldsymbol{n}a$. In the limit that $\epsilon \to 0$ the sides of the box contribute no flux. The electric fields arising from the surface charge are perpen-

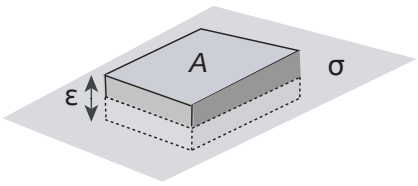

Fig. 3.1 Discontinuous normal of $\boldsymbol{E}$ at surface of a conductor. The surface charge density is σ and the rectangular Gaussian surface has a top area of A and height of ϵ.

dicular to the local plane and parallel to $\boldsymbol{n}$, so

$$\oint_S \boldsymbol{E} \cdot d\boldsymbol{a} = E \int da = EA$$

and therefore

$$\boldsymbol{E} = \frac{\sigma}{2\epsilon_0}\hat{\boldsymbol{n}}, \tag{3.1}$$

where $\hat{\boldsymbol{n}}$ is a unit vector perpendicular to the surface and pointing away from it in Fig. 3.1. Then the difference between electric fields above and below the plane is

$$\boldsymbol{E}_{\text{above}} - \boldsymbol{E}_{\text{below}} = \frac{\sigma}{\epsilon_0}\hat{\boldsymbol{n}}, \tag{3.2}$$

An electric field is necessarily discontinuous at a boundary charge layer: it points in the same direction on either side of the boundary, but its magnitude changes by σ/ϵ_0 when the boundary is crossed.

On the other hand, the *scalar potential is continuous across the boundary*, since if $\boldsymbol{A}$ is a point just below the surface and $\boldsymbol{B}$ is a point just above it,

$$\Phi_{\text{above}} - \Phi_{\text{below}} = -\int_{\boldsymbol{A}}^{\boldsymbol{B}} \boldsymbol{E} \cdot d\boldsymbol{l}, \tag{3.3}$$

which tends to zero as the distance between $\boldsymbol{A}$ and $\boldsymbol{B}$ is decreased. Since $\boldsymbol{\nabla}\Phi = -\boldsymbol{E}$, the scalar potential is continuous but $\boldsymbol{\nabla}\Phi$ inherits the discontinuity in $\boldsymbol{E}$ at the boundary,

$$\boldsymbol{\nabla}\Phi_{\text{above}} - \boldsymbol{\nabla}\Phi_{\text{below}} = -\frac{\sigma}{\epsilon_0}\hat{\boldsymbol{n}}. \tag{3.4}$$

This can also be rewritten as

$$\frac{\partial\Phi_{\text{above}}}{\partial n} - \frac{\partial\Phi_{\text{below}}}{\partial n} = -\frac{\sigma}{\epsilon_0} \qquad \frac{\partial\Phi}{\partial n} = \boldsymbol{\nabla}\Phi \cdot \hat{\boldsymbol{n}}, \tag{3.5}$$

where $\partial\Phi/\partial n$ is the *normal derivative* (directional derivative evaluated in a direction perpendicular to the surface). These boundary conditions are valid only just above and just below the surface, so the above equations are valid only in the limit that the surface in Fig. 3.1 is approached very closely from the top or bottom.

3.2 Properties of Poisson and Laplace Solutions

Since the Poisson or Laplace equations with appropriate boundary conditions can be difficult to solve, it is useful to catalog those features of the solutions that are generic. Let us consider 1D equations first before tackling 2D and 3D versions.

3.2.1 The Laplace Equation in 1D

Laplace's equation in one dimension is a function of a single variable x,

$$\nabla^2\Phi = 0 \quad \longrightarrow \quad \frac{\partial^2\Phi}{\partial x^2} = 0 \quad \longrightarrow \quad \frac{d^2\Phi}{dx^2} = 0, \tag{3.6}$$

where the last step indicates explicitly that the usual partial differential equation (PDE) reduces to an ordinary differential equation (ODE) if there is only one variable. The ODE (3.6) has a general solution

$$\Phi(x) = ax + b, \tag{3.7}$$

which graphs as a straight line parameterized by the constants a and b (two parameters are required because it is a solution to a second-order ordinary differential equation). The values of the parameters are determined by imposing boundary conditions. Two boundary conditions are required, since there are two undetermined parameters. In this example, the boundary conditions could consist of specifying $\Phi(x)$ at two different values of x. The boundary conditions in actual applications reflect the detailed physics of the system being modeled by Eq. (3.6), and can be considerably more involved than this simple example. This solution of the 1D Laplace equation has two unique features (which will carry over in suitable form to 2D and 3D).

1. A solution $\Phi(x)$ is an *average of* $\Phi(x-c)$ *and* $\Phi(x+c)$,

$$\Phi(x) = \frac{1}{2}\left[\Phi(x+c) + \Phi(x-c)\right], \tag{3.8}$$

   for arbitrary values of c.
2. There can be *no local maxima or minima for the solution* as a function of the parameter x, which is a corollary of the first point.

This latter point is sometimes referred to as *Earnshaw's theorem,* which may be interpreted as the mean value theorem applied to electrostatics.[1] An alternative statement of Point 2 is that the average of the scalar potential Φ over any sphere that lies entirely in a charge-free region is equal to the value of the potential at the center of the sphere (see Problem 4.2 in this regard).

Point 2 in the above list implies that maxima or minima of a one-dimensional Laplace solution can occur only at the endpoints of the domain, since if there were a local maximum or minimum of Φ at some value of x that is not an endpoint it necessarily could not be the average of points on either side of it, contradicting the requirement of Eq. (3.8).

[1] *Mean Value Theorem (MVT):* For a continuous and differentiable function, the average rate of change over a closed interval is equal to the instantaneous rate of change at some point in the interval. An illustrative example of applying the MVT concerns detection of automobile speeds with police radar. Suppose the speed limit on a long stretch of road to be 60 miles per hour (MPH). A car is measured by radar at Point A to have a speed of 55 MPH, and a half hour later and 40 miles down the road at Point B the same car is measured to have a speed of 58 MPH. For both local measurements at A and B the car was traveling below the speed limit of 60 MPH, but globally the average speed between A and B was $40\,\text{miles}/0.5\,\text{hours} = 80\,\text{MPH}$. By the MVT, it is necessarily true that at some point between A and B the car had a speed of exactly 80 MPH, which exceeds the speed limit by 20 MPH.

Illustrations of this absence of local maxima or minima will be given later in Figs. 4.4 and 4.6 for 2D Laplace solutions.

One immediate implication of Earnshaw's theorem is that no configuration consisting solely of electrical charges can be held in equilibrium by purely electrostatic forces, because there can be no local minima in energy (which varies as the square of the electric field).

3.2.2 2D and 3D Laplace Equations

Let us now move to 2D and 3D versions of Laplace's equation, where it is necessary to solve partial differential equations that take the form

$$\frac{\partial^2\Phi}{\partial x^2}+\frac{\partial^2\Phi}{\partial y^2}=0 \qquad \frac{\partial^2\Phi}{\partial x^2}+\frac{\partial^2\Phi}{\partial y^2}+\frac{\partial^2\Phi}{\partial z^2}=0, \tag{3.9}$$

in cartesian coordinates. This introduces a higher level of difficulty than for the 1D case because solution of PDE's with boundary conditions are typically more complex than solution of ODEs with boundary conditions. We will illustrate for 3D. The solutions of the Laplace and Poisson equations have two unique features that generalize those found in 1D.

1. The solution $\Phi(\boldsymbol{x})$ at a point $\boldsymbol{x}$ is an average of values over a sphere centered at $\boldsymbol{x}$.

$$\Phi(\boldsymbol{x})=\frac{1}{4\pi R^2}\oint \Phi\, da, \tag{3.10}$$

   where the integral is over the surface of a sphere of radius R centered at $\boldsymbol{x}$.
2. Because of Point 1, the solution cannot have local minima or maxima, so extrema can occur only on the boundaries.

(See illustrations of Point 2 in Figs. 4.4 and 4.6.)

Example 3.1 Let's check Point 1 for a single point charge Q outside a sphere that is a distance r from the center of the sphere, as illustrated in Fig. 3.2. From this figure the law of cosines gives for the distance d from the charge Q to the patch da,

$$d^2=r^2+R^2-2rR\cos\theta.$$

At a single point on the surface of the sphere the potential is (see Fig. 3.2),

$$\Phi=\frac{1}{4\pi\epsilon_0}\frac{Q}{d}=\frac{1}{4\pi\epsilon_0}\frac{Q}{\sqrt{r^2+R^2-2rR\cos\theta}},$$

and from Eq. (3.10) the average over the sphere is

$$\begin{aligned}\Phi_{\text{avg}} &= \frac{1}{4\pi R^2}\frac{Q}{4\pi\epsilon_0}\int (r^2+R^2-2rR\cos\theta)^{-1/2}R^2\sin\theta\,d\theta\,d\phi \\ &= \frac{Q}{4\pi\epsilon_0}\frac{1}{2rR}\,(r^2+R^2-2rR\cos\theta)^{1/2}\Big|_0^{\pi} \\ &= \frac{Q}{4\pi\epsilon_0}\frac{1}{2rR}[(r+R)-(r-R)] = \frac{1}{4\pi\epsilon_0}\frac{q}{r},\end{aligned}$$

which is the potential that would be produced by placing Q at the center of the sphere [see Eq. (2.29)].

3.3 Boundary Conditions and Uniqueness

Use of the Poisson or Laplace equations to determine the potential Φ requires the solution of partial differential equations with boundary conditions. A simple example of such a problem is illustrated in Fig. 3.3, where the task is to solve for the scalar potential in some volume V bounded by a surface S with parts held at constant potentials. For partial differential equations it is often not immediately obvious what constitutes appropriate boundary conditions (meaning that they allow a solution and that it is physically well-behaved). The proof that a given set of boundary conditions fits the bill is called a *uniqueness theorem.*

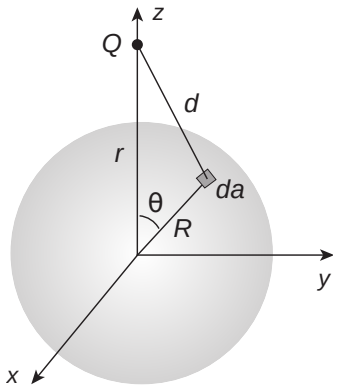

Fig. 3.2 Averaging Φ over a sphere of radius R with a single point charge q lying on the z-axis, external to the sphere and a distance r from its center (used in Example 3.1).

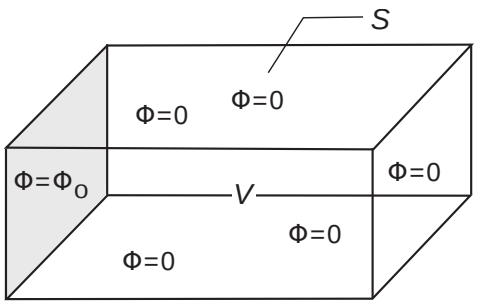

Fig. 3.3 Generic example of an electrostatics problem formulated in a 3D volume V that is bounded by a 2D surface S. In this case the (finite) volume V is surrounded by a rectangular conducting box S with boundary conditions corresponding to five of the six conducting box faces held at zero potential, $\Phi = 0$, and one face at a finite potential, $\Phi = \Phi_0$. Since the potential is being specified on the bounding surface S, this is an example of Dirichlet boundary conditions. The problem would typically be to solve for the electrostatic potential $\Phi(x, y, z)$ in the volume V, subject to the boundary conditions on S. If the charge density $\rho(x, y, z)$ is zero in the volume V, this would correspond to solving the Laplace equation, subject to the boundary conditions.

3.3.1 Dirichlet and Neumann Boundary Conditions

Two categories of boundary conditions are most common in electrostatics problems.[2]

1. *Dirichlet boundary conditions* correspond to specification of the scalar potential at every point on a closed surface. Although not stated at the time, Example 2.2 was an example that employed Dirichlet boundary conditions.
2. *Neumann boundary conditions* correspond to specification of the electric field at every point on the surface, which is equivalent to specifying the normal derivative of the potential or the surface charge density, everywhere the surface.

Example 3.2 and Example 3.3 illustrate these two types of boundary conditions.

[2] From a laboratory perspective, the Dirichlet criteria are typically the simplest and most natural way to set boundary conditions. For example, in the lab one often has conductors connected to batteries, which maintains a fixed finite potential on the conductor, or connected to ground, which corresponds effectively to maintaining $\Phi = 0$. But there may be other situations in which we do not know the potential on the boundaries, but we do know the total charge on each bounding surface. Then Neumann boundary conditions become more natural. Practically, Neumann boundary conditions are seldom natural when only perfect conductors and dielectric matter are present; they can arise in applications such as the theory of waveguides (see Section 14.10.3), or when steady currents flow through an ohmic medium (one that obeys Ohm's law; see Section 7.3.1) [77]. Hence we shall emphasize Dirichlet boundary conditions when examples are needed in our discussion. As will be mentioned later, in principle mixed conditions can result if Dirichlet constraints are applied to parts of a boundary and Neumann constraints to other parts, but that is often mathematically complex and we will consider only one example of such a case, in Box 3.1.

Example 3.2 A typical Dirichlet boundary condition in electrostatics specifies the value of the electrostatic potential $\Phi(\boldsymbol{x})$ on a boundary surface ∂V that encloses a volume V. A simple example is the slot geometry in the following diagram,

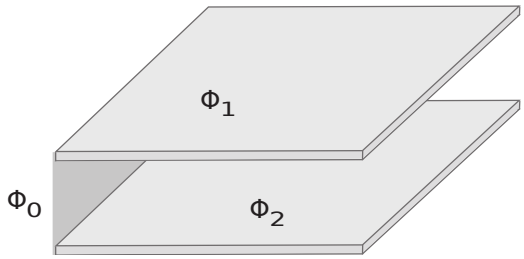

where the two horizontal electrodes and the backplane (insulated from the two horizontal electrodes) are held at constant potentials Φ_1, Φ_2, and Φ_0, respectivley, and there is no free charge in the region between the electrodes. Then the potential inside the slot must satisfy Laplace's equation, $\nabla^2\Phi = 0$ with the potentials Φ_1, Φ_2, and Φ_0 held constant at particular values, which corresponds to *Dirichlet boundary conditions*.

Example 3.3 In electrostatics, Neumann boundary conditions involve specifying the normal derivative of the potential, which is equivalent to specifying the component of the electric field perpendicular to the boundary. Imagine two infinite conducting plates located at $z = 0$ and $z = d$. Instead of being told the voltage on the plates (a Dirichlet boundary condition), you are told that a constant electric field $\boldsymbol{E}$ exists in the gap,

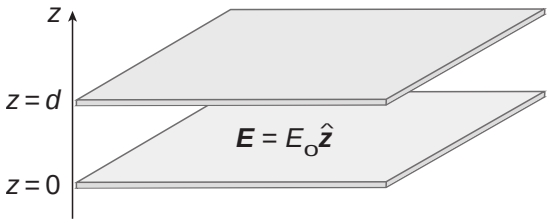

which is a *Neumann boundary condition*.[3] In the vacuum between the plates, if there is no free charge the electrostatic potential Φ satisfies Laplace's equation: $\nabla^2\Phi = 0$. Since $\boldsymbol{E} = \boldsymbol{\nabla}\Phi$, specifying the electric field at the boundary surfaces $z = 0$ and $z = d$ means

$$\frac{\partial\Phi}{\partial z} = -E_z.$$

For a 1D problem where the field is uniform and points in the z-direction, $\boldsymbol{E} = E_0\hat{\boldsymbol{z}}$, the boundary conditions at the surfaces are:

- at the bottom surface ($z = 0$): $\left.\dfrac{\partial\Phi}{\partial n}\right|_{z=0} = -E_0$,
- at the top surface ($z = d$): $\left.\dfrac{\partial\Phi}{\partial n}\right|_{z=d} = -E_0$.

[3] See Box 3.1 for a solution of this problem with mixed boundary conditions: Dirichlet on one plate and Neumann on the other.

Integrating the condition $\dfrac{d\Phi}{dz} = -E_0$ then gives for the potential

$$\Phi(z) = -E_0 z + C,$$

where C is a constant. Unlike Dirichlet conditions (where the potential is specified), Neumann conditions define only the *gradient of the potential*, and the solution contains an arbitrary integration constant C. Physically, this is because only a difference in potential results in a measureable electric field, so adding a constant to Φ has no effect on $\boldsymbol{E}$.

3.3.2 Uniqueness Theorems I and II

The Dirichlet and Neumann boundary condition imply two uniqueness theorems.

> ***Uniqueness Theorem I:*** The solution of Poisson's or Laplace's equations in some volume V is uniquely determined if Φ is specified everywhere on the boundary surface S of the volume V.

The simplest way to set boundary conditions is to specify the value of the scalar field Φ on all surfaces surrounding the region (which corresponds to Dirichlet boundary conditions). Then the first uniqueness theorem applies. However, in some situations we may not know the potential at the boundaries but we do know the total charge on conducting surfaces. This permits formulation of a second uniqueness theorem.

> ***Uniqueness Theorem II:*** If a volume V is surrounded by conductors of having charge densities ρ, the electric field is uniquely determined if the total charge on each conductor is specified.

Thus the second uniqueness theorem is appropriate for Neumann boundary conditions. Let us now turn to proof and a deeper look at these uniqueness theorems.

3.3.3 Uniqueness Theorems by Green's Methods

From a formal point of view, the solution of the Laplace or Poisson equation in a volume V bounded by a surface S with either Dirichlet or Neumann boundary conditions on S (for example, Fig. 3.3) can be obtained using *Green function methods* [41]. These may be derived beginning with the divergence theorem,

$$\oint_S \boldsymbol{A} \cdot \boldsymbol{n}\, da = \int_V \boldsymbol{\nabla} \cdot \boldsymbol{A}\, d^3x \qquad \text{(Divergence theorem)}, \tag{3.11}$$

which is valid for any well-behaved vector field $\boldsymbol{A}$ in a volume V bounded by the closed surface S. Let $\boldsymbol{A} = \phi\boldsymbol{\nabla}\psi$ where ϕ and ψ are arbitrary scalar fields. Then

$$\boldsymbol{\nabla}\cdot(\phi\boldsymbol{\nabla}\psi) = \phi\nabla^2\psi + \boldsymbol{\nabla}\phi\cdot\boldsymbol{\nabla}\psi, \tag{3.12}$$

$$\phi\boldsymbol{\nabla}\psi\cdot\boldsymbol{n} = \phi\frac{\partial\psi}{\partial n}, \tag{3.13}$$

where $\partial/\partial n$ is the normal derivative at the surface, directed from inside to outside the volume V. Substitution of Eqs. (3.12) and (3.13) into the divergence theorem (3.11) then gives *Green's first identity*

$$\int_V (\phi\nabla^2\psi + \boldsymbol{\nabla}\phi\cdot\boldsymbol{\nabla}\psi)\,d^3x = \oint_S \frac{\partial\psi}{\partial n}\,da \qquad \text{(Green's first identity).} \tag{3.14}$$

If we then subtract from Eq. (3.14) the same expression but with ϕ and ψ interchanged, the $\boldsymbol{\nabla}\phi\cdot\boldsymbol{\nabla}\psi$ terms cancel, giving *Green's theorem* (also termed *Green's second identity*)

$$\int_V (\phi\nabla^2\psi - \psi\nabla^2\phi)\,d^3x = \oint_S \left[\phi\frac{\partial\psi}{\partial n} - \psi\frac{\partial\phi}{\partial n}\right] da \qquad \text{(Green's theorem).} \tag{3.15}$$

Let us now choose a particular function for ψ,

$$\psi \equiv \frac{1}{R} = \frac{1}{\boldsymbol{x}-\boldsymbol{x}'},$$

where $\boldsymbol{x}$ is the observation point and $\boldsymbol{x}'$ is an integration variable, set ϕ equal to the scalar potential $\phi = \Phi$, use Poisson's equation

$$\nabla^2\Phi = -\frac{\rho}{\epsilon_0}$$

and use that from Eq. (A.76) the Laplacian operating on $R^{-1} = |\boldsymbol{x}-\boldsymbol{x}'|^{-1}$ is proportional to a Dirac delta function,

$$\nabla^2\left(\frac{1}{R}\right) = 4\pi\delta(\boldsymbol{x}-\boldsymbol{x}'),$$

so that Eq. (3.15) becomes

$$-4\pi\int_V \left[\Phi(\boldsymbol{x}')\delta(\boldsymbol{x}-\boldsymbol{x}') + \frac{1}{\epsilon_0 R}\,\rho(\boldsymbol{x}')\right] d^3x' = \oint_S \left[\Phi\frac{\partial}{\partial n'}\left(\frac{1}{R}\right) - \frac{1}{R}\frac{\partial\Phi}{\partial n'}\right] da'.$$

Then, if $\boldsymbol{x}$ lies within the volume V, this becomes

$$\Phi(\boldsymbol{x}) = \frac{1}{4\pi\epsilon_0}\int_V \frac{\rho(\boldsymbol{x}')}{R}\,d^3x' + \frac{1}{4\pi}\oint_S \left[\frac{1}{R}\frac{\partial\Phi}{\partial n'} - \Phi\frac{\partial}{\partial n'}\left(\frac{1}{R}\right)\right] da'. \tag{3.16}$$

Notice two important implications of this result.

1. If the surface S lies at infinity and the electric field on S falls off faster than R^{-1}, the surface term in Eq. (3.16) vanishes and we recover

   $$\Phi(\boldsymbol{x}) = \frac{1}{4\pi\epsilon_0}\int \frac{\rho(\boldsymbol{x}')}{|\boldsymbol{x}-\boldsymbol{x}'|}\,d^3x',$$

   which is the usual result of Eq. (2.31a),

2. In the second (surface) term *both* the the scalar potential Φ and the normal derivative of the scalar potential $\partial\Phi/\partial n'$ appear.
   - The first is associated with *Dirichlet boundary conditions* and
   - the second with *Neumann boundary conditions.*

This implies that Eq. (3.16) is *overdetermined*, because it isn't legitimate to impose both types of boundary conditions on the same closed surface.[4] Since it is overdetermined, Eq. (3.16) is *not a valid solution.* In Section 3.5 we shall address how to correct this deficiency.

3.3.4 Proof of Uniqueness

Let us now demonstrate explicitly that the use of either (but not both) Dirichlet or Neumann boundary conditions defines a unique potential problem, following the presentation in Jackson [41]. Assume the contrary proposition that the solution is *not unique* and that there are two potentials, Φ_1 and Φ_2 that satisfy the Laplace equation with the same boundary conditions. Let the difference between the two hypothesized solutions be defined by $U = \Phi_2 - \Phi_1$. Then by Laplace

$$\nabla^2 U = \nabla^2\Phi_2 - \nabla^2\Phi_1 = 0$$

inside the volume V, while on the boundary S either

1. $U = 0$ (Dirichlet boundary conditions) or
2. $\partial U/\partial n = 0$ (Neumann boundary conditions).

Setting $\phi = \psi = U$ and applying Green's first identity (3.14) gives

$$\int_V (U\nabla^2 U + \boldsymbol{\nabla} U \cdot \boldsymbol{\nabla} U)\, d^3x = \oint_S U \frac{\partial U}{\partial n}\, da. \tag{3.17}$$

For either Dirichlet or Neumann of boundary conditions the surface integral on the right vanishes, as does the first term in the volume integral on the left, and this reduces to

$$\int_V |\boldsymbol{\nabla} U|^2\, d^3x = 0, \tag{3.18}$$

which implies that U is constant inside V, since $\boldsymbol{\nabla} U = 0$. For Dirichlet boundary conditions $U = 0$ on S (the two purported solutions must be equal on the boundary since they are assumed to have the same boundary conditions). Furthermore, solutions of the Laplace or Poisson equation must have any extrema on the boundaries (see Sections 3.2.1 and 3.2.2), so since $U = 0$ on the boundary, U is also zero inside V, implying that $\Phi_1 = \Phi_2$ and the solution is unique. Likewise, for Neumann boundary conditions the solution is unique, up to an arbitrary additive constant. For simplicity this uniqueness proof was for the Laplace equation, but a similar proof of uniqueness follows for the Poisson equation (see Problem 3.9).

[4] Mathematically, an overdetermined system has more equation constraints than unknowns. Such a system is typically *inconsistent* (no set of values for parameters satisfies all equations), and *contradictory* (its equations can be manipulated to obtain different logically incompatible results).

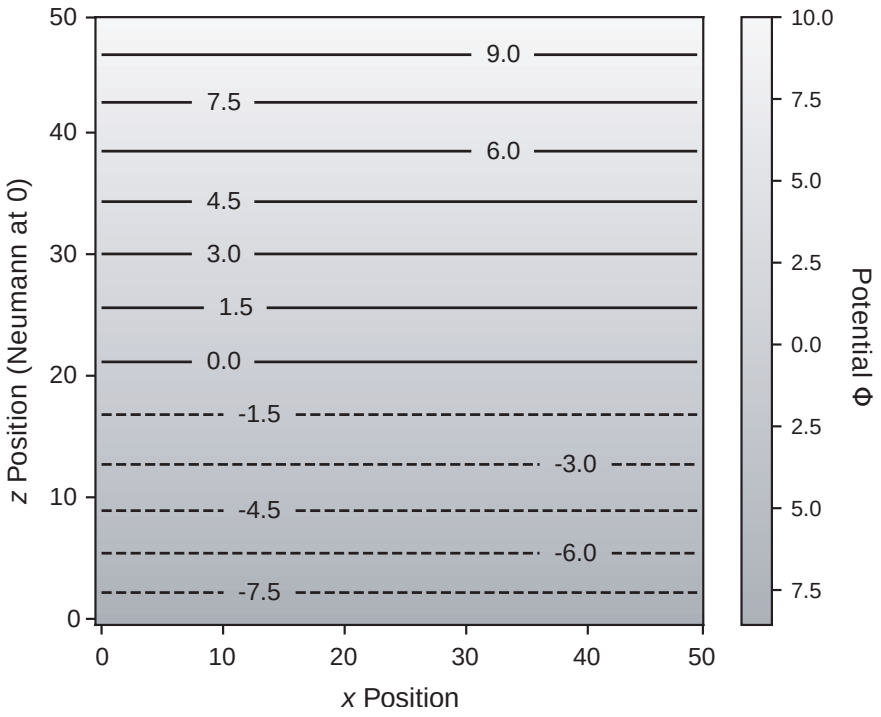

Fig. 3.4 Potential $\Phi(z)$ for the capacitor that is discussed in Box 3.1, subject to mixed Dirichlet–Neumann boundary conditions. Grayscale indicates the potential and the horizontal lines are potential contours, with solid lines for positive values of Φ and dashed lines for negative values.

Thus we have shown that for either Dirichlet or Neumann boundary conditions the *solution of the Laplace equation is unique.*

By similar proofs the solution is unique if the closed surface S has mixed boundary conditions (part with Dirichlet boundary and part with Neumann boundary conditions).

Although non-overlapping mixed boundary conditions are legitimate, they can be difficult to deal with relative to problems with a single type of boundary condition. An example of solving a problem using mixed boundary conditions may be found in Section 3.13 of Ref. [41] and we give a simple example in Box 3.1 of specifying Dirichlet boundary conditions on one of two bounding surfaces and Neumann boundary conditions on the other. This is a legitimate solution, since at no point on the bounding surfaces are both Dirichlet and Neumann conditions applied. However, since Dirichlet and Neumann boundary conditions each define a unique solution, imposing both Dirichlet and Neumann conditions on the same boundary surface will overdetermine the system and no reliable solution will exist.

Box 3.1 Mixed Boundary Conditions for a Parallel-Plate Capacitor

Consider a volume Ω bounded by two parallel conducting plates, S_1 and S_2. We seek the electrostatic potential $\Phi(\boldsymbol{z})$ satisfying Laplace's equation: $\nabla^2\Phi = 0$ in Ω. In Example 3.3 we solved this problem with Neumann boundary conditions. In this example we illustrate a solution for mixed boundary conditions.

Mixed Boundary Conditions

Applying Dirichlet conditions to one plate and Neumann conditions to the other constitutes a valid *mixed boundary value problem*, since the two types of boundary conditions are on different surfaces and do not overlap.

1. *Dirichlet boundary condition on S_1 (fixed potential):* The potential on S_1 is constrained to a specific value Φ_0, by grounding or connecting to a voltage source,
$$\Phi(\boldsymbol{x})\big|_{S_1} = \Phi_0.$$
2. *Neumann boundary condition on S_2 (fixed flux):* The normal derivative on S_2 is constrained, which physically corresponds to fixing the electric field or the surface charge density σ (for example, an isolated or current-injected plate),
$$\left.\frac{\partial\Phi}{\partial n}\right|_{S_2} = \nabla\Phi\cdot\hat{\boldsymbol{n}} = -\boldsymbol{E}\cdot\hat{\boldsymbol{n}} = -\frac{\sigma}{\epsilon_0}.$$

These boundary conditions are illustrated in the following figure,

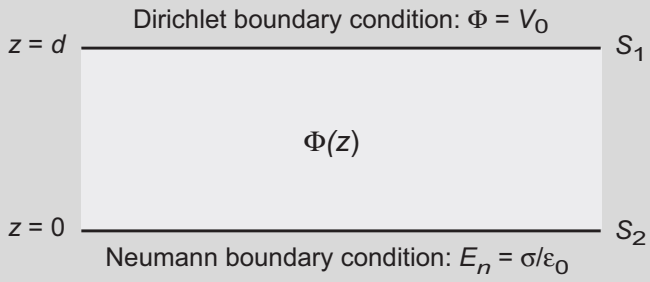

where $E_n = E\cdot\hat{\boldsymbol{n}}$ is the normal component of the electric field evaluated at S_2.

Solution of the Laplace Equation

As shown in Problem 3.14, the Laplace equation with these boundary conditions has the unique solution
$$\Phi(z) = -\frac{\sigma}{\epsilon_0}z,$$
which is plotted in Fig. 3.4. The potential at the Neumann boundary ($z = 0$) is not arbitrary as it would be for pure Neumann boundary conditions (which gives the solution up to an arbitrary additive constant, as found in Example 3.3); it is determined by the field required to satisfy the flux condition.

3.3.5 Summary of Legitimate Boundary Conditions

Let us summarize some general statements about Dirichlet and Neumann boundary conditions in electrostatics problems gleaned from the preceding discussion.

1. One can specify either Dirichlet or Neumann constraints at each point on a boundary, *but not both.*
2. It is legitimate to specify parts of a boundary using Dirichlet conditions and other parts using Neumann conditions (as long as Dirichlet and Neumann conditions don't overlap on any part of the boundary).
3. The uniqueness property means that a solution obtained by any method—even guessing—is the correct (unique) solution, if it satisfies the equations and implements the correct boundary conditions.

Much of the uniqueness for solutions of the Poisson and Laplace equations is a consequence of the *Helmholtz Theorem,* which is described in Section 3.3.6.

3.3.6 The Helmholz Theorem

Let $\boldsymbol{F}(\boldsymbol{r})$ be any continuous vector field with continuous first partial derivatives. Then $\boldsymbol{F}(\boldsymbol{r})$ can be uniquely expressed in terms of the negative gradient of a scalar potential $\Phi(\boldsymbol{r})$ and the curl of a vector potential $\boldsymbol{A}(\boldsymbol{r})$,

$$\boldsymbol{F}(\boldsymbol{r}) = -\boldsymbol{\nabla}\Phi(\boldsymbol{r}) + \boldsymbol{\nabla} \times \boldsymbol{A}(\boldsymbol{r}).$$

This can also be written as the *Helmholtz decomposition*,

$$\boldsymbol{F}(\boldsymbol{r}) = \boldsymbol{F}_{\mathrm{L}}(\boldsymbol{r}) + \boldsymbol{F}_{\mathrm{T}}(\boldsymbol{r}),$$

where L denotes a *longitudinal component* and T a *transverse component* of a vector field. The theorem is sometimes paraphrased as a uniqueness statement:

> ***Uniqueness of Vector Fields:*** A vector field with its curl and divergence specified everywhere is uniquely determined, provided that the sources vanish at infinity, and that the field vanishes at infinity at least as fast as r^{-2}.
>
> *EXAMPLE:* It isn't a coincidence that the Maxwell equations (1.1) in the absence of a magnetic field $\boldsymbol{B}$ satisfy the electrostatic equations
>
> $$\boldsymbol{\nabla} \times \boldsymbol{E}(\boldsymbol{x}) = 0 \qquad \boldsymbol{\nabla} \cdot \boldsymbol{E}(\boldsymbol{x}) = \frac{\rho(\boldsymbol{x})}{\epsilon_0},$$
>
> which ensures by the Helmholtz theorem that the electric field $\boldsymbol{E}(\boldsymbol{x})$ is uniquely defined at all points because its curl and divergence are defined everywhere.

We will have more to say about this in later discussion of gauge invariance and transverse and longitudinal components of the electromagnetic field.

Table 3.1 Common methods of solving Poisson and Laplace equations

Method	Type	Basic idea	Comments/Examples
Separation of variables	Analytical	Reduce a PDE to a set of ODEs	Often gives orthogonal basis like Legendre polynomials
Green function methods	Analytical	Transform differential equation into integral equation using impulse response of operators	Powerful for formal proofs where Green function is known or can be constructed by eigenvalue expansion
Method of images	Analytical	Specialized method for high symmetry and some boundary potentials	Point charge near grounded conducting sphere by placing image charge inside sphere
Conformal mapping	Analytical	Maps complex geometry to simpler geometry, solves there, maps back	Specialized method: only for 2D Laplace solutions
Finite Difference Method (FDM)	Numerical	Discretizes domain into grid; approximates the Laplacian by Taylor series	Reduces PDE to large set of (often sparse) linear algebraic equations
Relaxation: Jacobi and Gauss–Seidel iteration	Numerical	Iterative algorithms used to solve linear systems generated by FDM	Iterate through grid; update each point based on its neighbors; not very parallel
Relaxation: Successive Over-Relaxation (SOR)	Numerical	Accelerates iteration convergence by update extrapolation	Easy to implement in loop or array operations; fast and easy to parallelize
Finite Element Method (FEM)	Numerical	Divide domain into small elements; approximates solution as sum of local basis functions	More robust than FDM for irregular geometry; PDE $\rightarrow$ integral equation that minimizes energy functional
Spectral methods	Numerical	Approximates solution as a sum of global basis functions like Chebyshev polynomials or a Fourier series	Converges exponentially for smooth functions; very efficient for Fast Fourier Transforms (FFT) and periodic boundary conditions

3.4 Poisson and Laplace Solution Methods

Various methods have been developed to solve the inhomogeneous Poisson equation,

$$\nabla^2\Phi = -\frac{\rho}{\epsilon_0} \qquad \text{(Poisson equation)}, \tag{3.19}$$

and its homogeneous counterpart, the Laplace equation

$$\nabla^2\Phi = 0 \qquad \text{(Laplace equation)}, \tag{3.20}$$

subject to boundary conditions. These are summarized in Table 3.1, and will be discussed in more depth in the remainder of this chapter and in Ch. 4. We first consider analytic methods and then will consider numerical methods.

3.4.1 Analytical Methods

Analytical approaches are most effective when the boundary geometry aligns with a separable coordinate system or possesses high symmetry.

Separation of Variables: This method assumes the solution can be written as a product of functions, each depending on a single coordinate. For example, in spherical coordinates (r, θ, ϕ):

$$\Phi(r, \theta, \phi) = \frac{U(r)}{r} P(\theta) Q(\phi). \tag{3.21}$$

Substitution into the Laplacian reduces the partial differential equation (PDE) to a set of ordinary differential equations linked by separation constants that can be determined by imposing boundary conditions, as we shall show for various examples in Ch. 4. The general solution is constructed as a linear combination of orthogonal basis functions, such as Legendre polynomials $P_l(\cos\theta)$, spherical harmonics $Y_{lm}(\theta, \phi)$, or Bessel functions $J_\nu(x)$ [41]. Coefficients are determined by exploiting the orthogonality of these basis functions over the boundary surface.

Method of Green functions: This approach transforms the differential equation into an integral equation using the impulse response of the operator. The Green function $G(\boldsymbol{x}, \boldsymbol{x}')$ is defined by:

$$\nabla^2 G(\boldsymbol{x}, \boldsymbol{x}') = -\delta(\boldsymbol{x} - \boldsymbol{x}'). \tag{3.22}$$

For Dirichlet boundary conditions, the potential $\Phi(\boldsymbol{x})$ is given by:

$$\Phi(\boldsymbol{x}) = \frac{1}{\epsilon_0} \int_V \rho(\boldsymbol{x}') G(\boldsymbol{x}, \boldsymbol{x}') d^3 r' + \oint_S \Phi(\boldsymbol{x}') \frac{\partial G}{\partial n'} da'. \tag{3.23}$$

This method is powerful for formal proofs and geometries where G can be constructed via eigenfunction expansion [17]. We shall expand on the use of this method in Section 3.5 below.

Method of Images: This is a heuristic technique for problems with high symmetry (for example, planes or spheres) and specific classes of boundary potentials (typically grounded conductors). It replaces boundary conditions with fictitious "image charges" placed outside the region of interest to mimic the potential at the boundary. We shall discuss such methods in Section 3.6.

Conformal Mapping: This method utilizes complex analysis and is restricted to 2D Laplace problems. It is based on the following approach:

1. *Analytic Functions:* Any analytic function $f(z) = u + iv$ satisfies the Cauchy-Riemann equations, implying $\nabla^2 u = 0$ and $\nabla^2 v = 0$.

2. *Mapping:* A complex geometry in the z-plane is mapped to a simpler geometry (e.g., upper half-plane) in the w-plane to solve the potential.

Since this is a rather specialized method confined to solving the Laplace problem in 2D, we shall not discuss it further, but the interested reader may consult the treatise by Morse and Feshback [55].

3.4.2 Numerical Methods

Numerical approaches are essential for arbitrary geometries where the analytical solutions discussed above cannot be applied easily. Some numerical approaches for the static problems being emphasized in these chapters are summarized here, with further elaboration in Section 4.3 and in Appendix F. Then in Section 15.3 we will extend the discussion of numerical methods to solving time dependent electromagnetic problems.

Finite Difference Method (FDM): The finite difference method discretizes the domain into a grid (lattice) and approximates derivatives on the lattice using Taylor-series expansions. In 2D Cartesian coordinates with grid spacing h, the discrete Laplacian at point (i, j) is often approximated by the *5-point stencil* [5]

$$\nabla^2 \Phi_{i,j} \approx \frac{\Phi_{i+1,j} + \Phi_{i-1,j} + \Phi_{i,j+1} + \Phi_{i,j-1} - 4\Phi_{i,j}}{h^2}. \tag{3.24}$$

This reduces solving the PDE to solving a sparse system of linear algebraic equations $A\boldsymbol{x} = \boldsymbol{b}$, which can often be solved efficiently by iterative algorithms.

Relaxation Methods: These are iterative algorithms used to solve the linear systems generated by the finite difference method described above [61]. We shall use two such algorithms in problem solutions:

1. *Jacobi and Gauss–Seidel:* Iterate through the grid, updating points based on neighbors. Gauss–Seidel uses the most recently updated values (see Appendix F.1).
2. *Successive Over-Relaxation (SOR):* Accelerates convergence of the iteration by extrapolating the update,

$$\Phi_{\text{new}} = \omega\, \Phi_{\text{calculated}} + (1 - \omega)\Phi_{\text{old}}. \tag{3.25}$$

   with a *relaxation parameter* ω ($1 < \omega < 2$), with ω chosen to optimize convergence rate for a given problem.

Finite Element Method (FEM): FEM divides the domain into smaller elements (e.g., triangles, tetrahedra). As discussed in Appendix F.5, it solves the Weak Form (variational

[5] In the context of finite difference methods, a *stencil* is a geometrical pattern of points used to approximate a derivative at a specific location on the lattice. It can be thought of as a template placed at a point (i, j) on the grid that specifies which neighboring points to include, and the weight coefficient to multiply each neighboring point by, to approximate a derivative at the point (i, j). A common choice is the 5-point stencil in Eq. (3.24), for which the *Center* is the point (i, j) where the derivative is to be evaluated, the *Neighbors* are the four immediate neighbors to that point, *Top:* $(i, j + 1)$, *Bottom:* $(i, j - 1)$, *Left:* $(i - 1, j)$, and *Right:* $(i + 1, j)$, and the Weights are -4 for the *Center* and $+1$ for each *Neighbor*.

formulation) of the PDE by minimizing an energy functional using local basis functions on each element.

Spectral Methods: Approximates the solution as a sum of global basis functions (e.g., Fourier series, Chebyshev polynomials). These methods offer exponential convergence (spectral accuracy) for smooth functions and often utilize Fast Fourier Transforms (FFT) for efficiency.

Let us now look at several of these solution methods in more depth, in the rest of this chapter, and in Ch. 4.

3.5 Boundary-Value Problems by Green Functions

In obtaining the result of Eq. (3.16) (recall: it is *not a valid solution* because the boundary conditions are overdetermined) we chose the function ψ to be $1/|\boldsymbol{x}-\boldsymbol{x}'|$, which satisfies

$$\boldsymbol{\nabla}'^2\left(\frac{1}{|\boldsymbol{x}-\boldsymbol{x}'|}\right) = -4\pi\delta^3(\boldsymbol{x}-\boldsymbol{x}'), \tag{3.26}$$

where $\boldsymbol{\nabla}'^2$ is the Laplace operator acting on $\boldsymbol{x}'$ rather than $\boldsymbol{x}$. The function $1/|\boldsymbol{x}-\boldsymbol{x}'|$ is a specific example of a class of functions called *Green functions*[6] that satisfy Eq. (3.26). A Green function is a solution to an inhomogeneous differential equation with a δ-function source term.[7] It provides a convenient method for solving more complicated inhomogenous differential equations through superposition, because general solutions for inhomogeneous differential equations can be approximated by a superposition of δ-functions evaluated at different spacetime points. See the example of computing a Green function for a driven harmonic oscillator in Box 3.2, and the evaluation of the retarded Green function for electromagnetic wave propagation in Section 11.4.

Generally a Green function $G(\boldsymbol{x},\boldsymbol{x}')$ satisfies

$$\boldsymbol{\nabla}'^2 G(\boldsymbol{x},\boldsymbol{x}') = -4\pi\delta(\boldsymbol{x}-\boldsymbol{x}') \tag{3.27}$$

[6] Perhaps more common in the English literature is the possessive "Green's function" rather than the attributive "Green function", but "Green function" is more in keeping with a modern trend of moving from possessive to adjectival naming (for example, "Bessel function" rather than "Bessel's function"). However, both "Green function" and "Green's function" are viewed as acceptable usage. In quantum field theory the Green function is often called the "propagator" or the "correlation function", which sidesteps the possessive/attributive issue.

[7] *Inhomogeneous (or non-homogeneous) differential equations* contain a non-zero function of the independent variable (often called *source terms*), as opposed to *homogeneous differential equations,* which have no source term. Thus, the Laplace equation is the homogeneous form of the inhomogeneous Poisson equation, which has a source term $-\rho(\boldsymbol{x})/\epsilon_0$. Green functions are applied to classical electromagnetism in the present discussion; they also find extensive use in other areas of mathematical physics such as quantum field theory (QFT). In classical electromagnetism, the Green function is primarily used as an impulse response to solve inhomogeneous differential equations subject to boundary conditions [41]. However, in QFT, a Green function (often referred to as the propagator in that context) expresses the quantum probability amplitude for a particle to travel between two points in spacetime [59]. Classical functions are determined strictly by boundary values, but a QFT Green function must also satisfy causality conditions, such as the Feynman propagator which accounts for time-ordering of operators (since in QFT operators at different times might not commute) [75].

Box 3.2 Green Function for a Driven Harmonic Oscillator

Before diving into Green functions applied to electromagnetism, it is useful to apply the method to the simpler problem of a 1D driven harmonic oscillator,

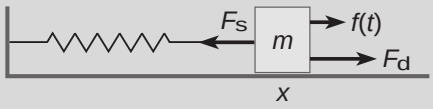

For driving force $f(t)$, spring force $F_s = -m\omega_0^2 x$, and drag force $F_d = -2m\gamma\dot{x}$,

$$\left(\frac{d^2}{dt^2} + 2\gamma\frac{d}{dt} + \omega_0^2\right) x(t) = \frac{f(t)}{m} \qquad \text{(Equation of motion).}$$

First consider

$$\left(\frac{\partial^2}{\partial t^2} + 2\gamma\frac{\partial}{\partial t} + \omega_0^2\right) G(t,t') = \delta(t-t'),$$

where $G(t,t')$ is a Green function that describes an oscillator subject to a δ-function driving force. The solution of this equation is (see Problem 3.8),

$$x(t) = \int_{-\infty}^{\infty} G(t,t')\frac{f(t')}{m}\,dt',$$

The Green function method assumes that $f(t)$ can be expressed as a superposition of δ-function pulses centered at different times. One approach is Fourier transforms (Section 11.4). The Fourier transform of $G(t,t')$ is

$$G(\omega,t') = \int_{-\infty}^{\infty} e^{i\omega t} G(t,t')\,dt.$$

Applying the Fourier transform to both sides of the Green function equation,

$$(-\omega^2 - 2i\gamma\omega + \omega_0^2)\,G(\omega,t') = \int_{-\infty}^{\infty} e^{i\omega t}\delta(t-t')\,dt = e^{i\omega t'}$$

and thus,

$$G(\omega,t') = -\frac{e^{i\omega t'}}{\omega^2 + 2i\gamma\omega - \omega_0^2}.$$

The inverse transform is

$$G(t,t') = \int_{-\infty}^{\infty}\frac{d\omega}{2\pi}e^{-i\omega t}G(\omega,t') = -\int_{-\infty}^{\infty}\frac{d\omega}{2\pi}\frac{e^{-i\omega(t-t')}}{(\omega-\omega_+)(\omega-\omega_-)},$$

where $\omega_\pm = -i\gamma \pm (\omega_0^2 - \gamma^2)^{1/2}$. There are two poles in the negative complex plane. An integration contour may be closed in the upper half-plane for $t < t'$ (enclose no poles) and the lower half-plane for $t > t$ (enclose both poles),

$$G(t,t') = \Theta(t-t')e^{-\gamma(t-t')} \times \begin{cases} (\omega_0^2-\gamma^2)^{-1/2}\sin\left[(\omega_0^2-\gamma^2)^{1/2}(t-t')\right] & (\gamma < \omega_0), \\ (\gamma^2-\omega_0^2)^{-1/2}\sinh\left[(\gamma^2-\omega_0^2)^{1/2}(t-t')\right] & (\gamma > \omega_0), \end{cases}$$

where Θ is the unit step function.

where we define

$$G(\boldsymbol{x},\boldsymbol{x}') = \frac{1}{|\boldsymbol{x}-\boldsymbol{x}'|} + F(\boldsymbol{x},\boldsymbol{x}'), \tag{3.28}$$

where $F(\boldsymbol{x},\boldsymbol{x}')$ satisfies the Laplace equation inside the volume V,

$$\boldsymbol{\nabla}'^2 F(\boldsymbol{x},\boldsymbol{x}') = 0. \tag{3.29}$$

The first term on the right side of Eq. (3.28) is the simplest Green function and is called the Green function of free space (physically it gives the response at a point $\boldsymbol{x}$ to a unit charge placed at $\boldsymbol{x}'$),

$$G_0(\boldsymbol{x},\boldsymbol{x}') = \frac{1}{|\boldsymbol{x}-\boldsymbol{x}'|}. \tag{3.30}$$

Recall that Eq. (3.16) was derived by substituting $G_0(\boldsymbol{x},\boldsymbol{x}')$ into Green's theorem (3.15), but we concluded that Eq. (3.16) is *not a valid solution* because it mixes Dirichlet and Neumann boundary terms in the surface integral. The additional term $F(\boldsymbol{x},\boldsymbol{x}')$ in the generalized Green function (3.28) raises the possibility that if we substitute Eq. (3.28) into Green's theorem, the function $F(\boldsymbol{x},\boldsymbol{x}')$ can be chosen to eliminate from the resulting surface integral either the Dirichlet or the Neumann terms, thus leaving a result with consistent boundary conditions.

Indeed, substitution of $\phi = \Phi$ and $\psi = G(\boldsymbol{x},\boldsymbol{x}')$ into Green's theorem (3.15) and use of Eq. (3.27) generalizes Eq. (3.16) to

$$\begin{aligned}\Phi(\boldsymbol{x}) = {} & \frac{1}{4\pi\epsilon_0}\int_V \rho(\boldsymbol{x}')G(\boldsymbol{x},\boldsymbol{x}')d^3x' \\ & + \frac{1}{4\pi}\oint_S \left[G(\boldsymbol{x},\boldsymbol{x}')\frac{\partial\Phi}{\partial n'} - \Phi(\boldsymbol{x}')\frac{\partial G(\boldsymbol{x},\boldsymbol{x}')}{\partial n'}\right] da'.\end{aligned} \tag{3.31}$$

Now the freedom to choose $F(\boldsymbol{x},\boldsymbol{x}')$ in the definition (3.28) of the Green function means that we can make the surface integral in Eq. (3.31) depend on a specific type of boundary condition.

1. If *Dirichlet boundary conditions* are desired, we may require that

$$G(\boldsymbol{x},\boldsymbol{x}') = 0 \qquad \text{(Dirichlet)} \tag{3.32}$$

for $\boldsymbol{x}'$ on S. Then the first term in the surface integral of Eq. (3.31) vanishes and the *solution with Dirichlet boundary conditions* is

$$\Phi(\boldsymbol{x}) = \frac{1}{4\pi\epsilon_0}\int_V \rho(\boldsymbol{x}')G(\boldsymbol{x},\boldsymbol{x}')d^3x' - \frac{1}{4\pi}\oint_S \left[\Phi(\boldsymbol{x}')\frac{\partial G(\boldsymbol{x},\boldsymbol{x}')}{\partial n'}\right] da'. \tag{3.33}$$

2. If instead *Neumann boundary conditions* are desired, the obvious choice $\partial G(\boldsymbol{x},\boldsymbol{x}')/\partial n' = 0$ for $\boldsymbol{x}'$ on S makes the second term in the surface integral of Eq. (3.31) vanish. But application of Gauss's theorem to Eq. (3.27) indicates that

$$\oint_S \frac{\partial G}{\partial n'}\, da' = -4\pi,$$

implying that the simplest allowable boundary condition is

$$\frac{\partial G(\boldsymbol{x},\boldsymbol{x}')}{\partial n'} = -\frac{4\pi}{\Sigma} \qquad \text{(Neumann)}, \tag{3.34}$$

for $\boldsymbol{x}'$ on S, where Σ is the total area of the bounding surface S.[8] Then the *solution with Neumann boundary conditions* is

$$\Phi(\boldsymbol{x}) = \langle\Phi\rangle_S + \frac{1}{4\pi\epsilon_0}\int_V \rho(\boldsymbol{x}')G(\boldsymbol{x},\boldsymbol{x}')d^3x' + \frac{1}{4\pi}\oint_S \frac{\partial\Phi}{\partial n'}\,G\,da', \tag{3.35}$$

where $\langle\Phi\rangle_S$ is the average of the potential over the entire surface.

Thus, we have shown formally in Eqs. (3.32) and (3.34) how to determine the scalar potential by imposing consistent boundary conditions in an electrostatic boundary-value problem.

The Green functions $G(\boldsymbol{x},\boldsymbol{x}')$ satisfy the rather simple boundary conditions (3.32) or (3.34). Nevertheless, they may be difficult to determine in many cases because of the dependence on the shape of the surface S. Figure 3.5 outlines the use of Green functions to solve the Poisson equation.

3.6 The Method of Images

Various tricks and clever algorithms have been devised to find solutions for the Poisson or Laplace equations without actually solving the differential equations themselves. These methods are generally applicable when certain special features are present in a problem, and can often lead to much easier solutions than solving the relevant differential equation with boundary conditions. One such approach is the *method of images*, where the actual Poisson or Laplace problem is replaced with a different one (the *analog problem*) that is easier to solve, but that is tailored to have boundary conditions equivalent to those of the actual problem. Then, since

1. the analog problem has *the same boundary conditions* and
2. is a *solution of the Laplace or Poisson equation*,

just as the actual problem, *Uniqueness Theorem I or II* given in Section 3.3 guarantees that the solution of the analog problem is also the (unique) solution of the original problem.

Let us illustrate this approach by solving a simple electrostatics problem using the image method. In Fig. 3.6(a) we consider a charge q placed at a distance d above an infinite conducting plane that is grounded (held at the potential $\Phi = 0$). What is the potential

[8] A typical Neumann problem has a volume V bounded by two surfaces, one closed and finite, and the other at infinity [41]. Thus the surface area Σ is infinite, the term $\langle\Phi\rangle_S$ in Eq. (3.35) vanishes, and the right side of the boundary condition (3.34) is zero. Then both the Dirichlet boundary condition Eq. (3.32) and and the Neumann boundary condition Eq. (3.34) become *homogeneous* (zeros on the right side of the equations).

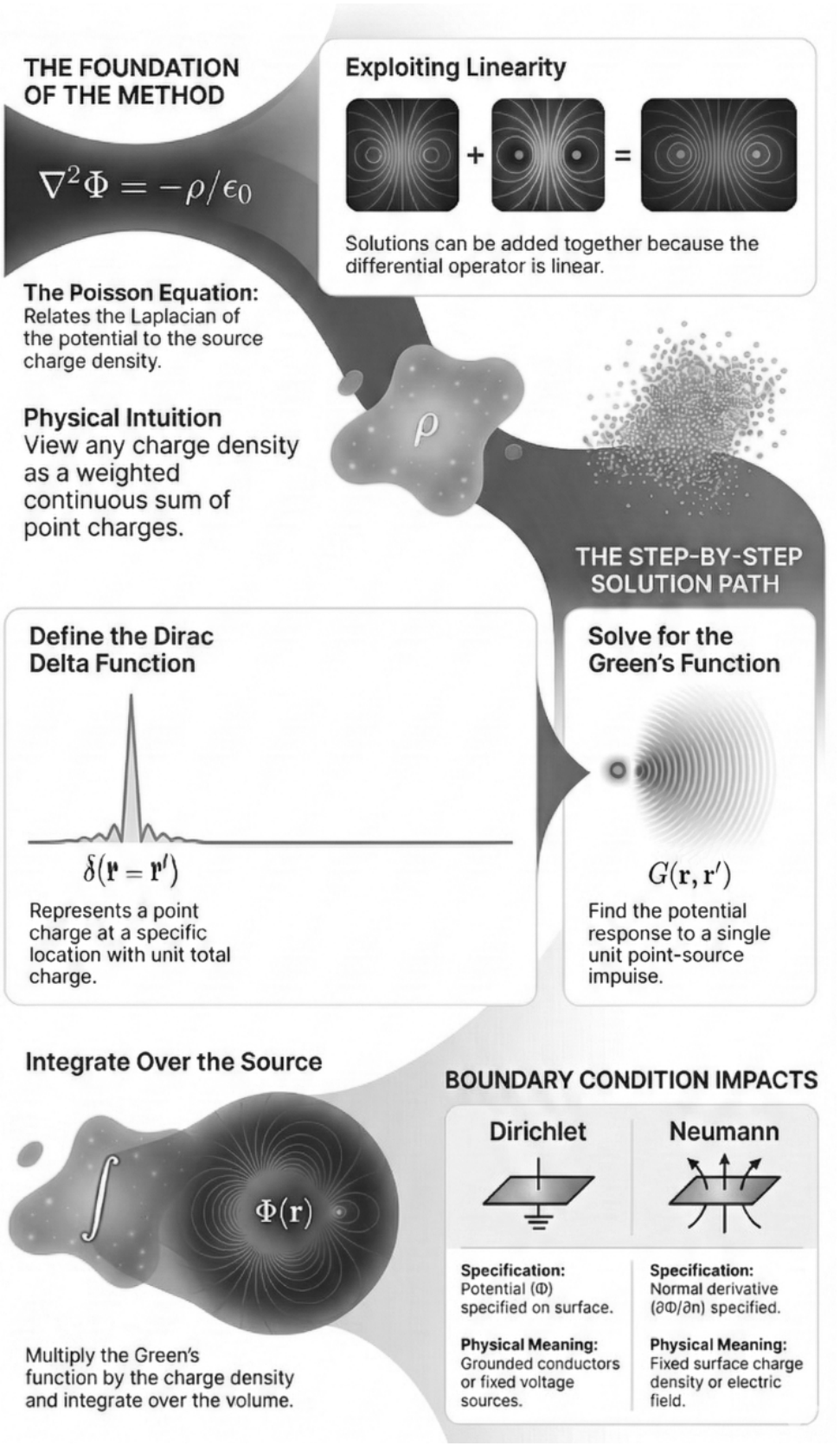

Fig. 3.5 An overview of solving the Poisson equation $\nabla^2\Phi = -\rho/\epsilon_0$ using the method of Green functions. [*Produced by NotebookLM; will be redrawn for resolution and font size.*]

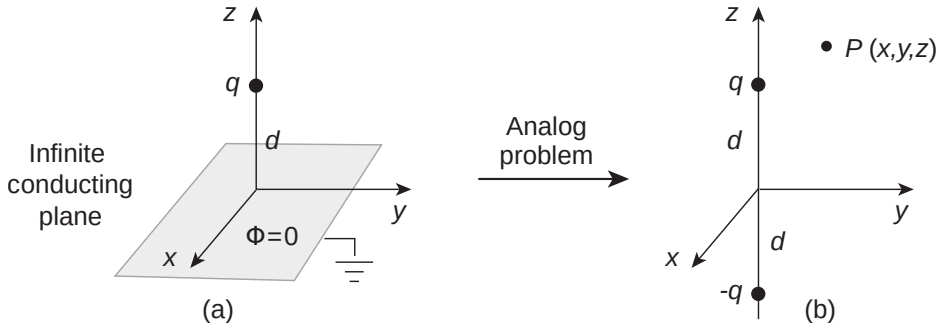

Fig. 3.6 (a) Charge q a distance d above an infinite, grounded, conducting plane at zero potential. (b) An analogous image-charge configuration with the charge $-q$ on the negative z axis, and no infinite conducting plane.

in the region $z > 0$? The presence of the charge will polarize the conducting plane, so the potential will have a part associated with the charge q and a part generated by the polarized infinite conducting plane. How can the field in the region above the conducting plane be determined when the distribution of the polarized charge isn't known beforehand? One way is to solve Poisson's equation for $z > 0$ with the boundary conditions,

1. $\Phi = 0$ at $z = 0$, since the conducting plane is grounded, and
2. $\Phi \to 0$ at very large distances from the charge.

But before rushing off to try to solve the Poisson equation with these boundary conditions, recall Uniqueness Theorem I from Section 3.3, which indicates that there can be *only one independent solution of the Poisson equation* with precisely these boundary conditions. Thus, if we can find such a solution by any means (including guessing!), it must be correct.

This motivates us to consider the completely different *analog problem* illustrated in Fig. 3.6(b). This analog problem

1. has the original charge q at a distance d above the origin, but
2. also has an additional charge $-q$ at a distance d below the origin (this is called an *image charge*), and
3. the conducting plane of the original problem has been removed.

The problem in Fig. 3.6(b) is simple compared with that of Fig. 3.6(a) and can be solved easily using Coulomb's law. For an arbitrary point $P(x, y, z)$ at $z > 0$, the distances from P to the two charges are, respectively,

$$r_+ = \sqrt{x^2 + y^2 + (z-d)^2} \qquad r_- = \sqrt{x^2 + y^2 + (z+d)^2},$$

and the potential at the point $P(x, y, z)$ generated by the two charges is

$$\begin{aligned}\Phi(x,y,z) &= \frac{1}{4\pi\epsilon_0}\left(\frac{q}{r_+} - \frac{q}{r_-}\right) \\ &= \frac{1}{4\pi\epsilon_0}\left(\frac{q}{\sqrt{x^2+y^2+(z-d)^2}} - \frac{q}{\sqrt{x^2+y^2+(z+d)^2}}\right). \end{aligned} \tag{3.36}$$

Now we notice that the *boundary conditions are the same for the two problems:* in the analog problem there is a single charge q in the region $z > 0$ (which is where we seek a solution), and from Eq. (3.36),

1. the potential Φ is equal to zero in the $x - y$ plane, and
2. at large distances from the charges, $\Phi \to 0$,

which are precisely the boundary conditions for the original problem in Fig. 3.6(a). To be sure there is an extra charge $-q$ in the $z < 0$ region for the analog problem, but that is irrelevant because we *restricted the solution to the region* $z > 0$ in the original problem. Thus, we conclude from Uniqueness Theorem I that the solution of our original problem in Fig. 3.6(a) is given by Eq. (3.36), which is the solution of the much simpler analog problem shown in Fig. 3.6(b). This approach can be a powerful one, but it is useful only if we can conjure a solvable analog problem that has the same boundary conditions as the original problem.

In using the method of images the *image charges must be placed in a region that is not in the domain of the original problem.* In this example we accomplished that by putting the image charge in the region $z < 0$, but required a solution only for $z > 0$.

Now that the potential has been found in Eq. (3.36) for the upper half plane we can go further and determine the induced charge in the conducting plane caused by the positive charge at $z = d$. From Eq. (3.5) for the effect of charge layers, keeping only the contribution from above the layer,

$$\sigma = -\epsilon_0 \frac{\partial \Phi}{\partial n}. \tag{3.37}$$

The normal derivative of Φ at the surface is in the z direction, so

$$\sigma = -\epsilon_0 \frac{\partial \Phi}{\partial z}\Big|_{z=0}. \tag{3.38}$$

The derivative may be evaluated from Eq. (3.36) as,

$$\begin{aligned}
\frac{\partial \Phi}{\partial z}\Big|_{z=0} &= \frac{1}{4\pi\epsilon_0}\left(\frac{-q(z-d)}{[x^2+y^2+(z-d)^2]^{3/2}} + \frac{q(z+d)}{[x^2+y^2+(z+d)^2]^{3/2}}\right)\Bigg|_{z=0}, \\
&= \frac{1}{4\pi\epsilon_0}\left(\frac{qd}{[x^2+y^2+d^2]^{3/2}} + \frac{qd}{[x^2+y^2+d^2]^{3/2}}\right) \\
&= \frac{1}{2\pi\epsilon_0}\frac{qd}{[x^2+y^2+d^2]^{3/2}},
\end{aligned}$$

and from Eq. (3.38)

$$\sigma = -\epsilon_0 \frac{\partial \Phi}{\partial n}\Big|_{z=0} = -\frac{qd}{2\pi[x^2+y^2+d^2]^{3/2}}. \tag{3.39}$$

The total induced charge Q then follows by integration. Using polar coordinates (r, ϕ) with $r^2 = x^2 + y^2$ and $da = r\, dr\, d\phi$,

$$Q = \int_0^{2\pi} \int_0^{\infty} \frac{-qd}{2\pi[x^2 + y^2 + d^2]^{3/2}}\, r\, dr\, d\phi = \left. \frac{qd}{\sqrt{r^2 + d^2}} \right|_0^{\infty} = -q. \tag{3.40}$$

So the total induced charge in the infinite sheet has the same magnitude as the polarizing charge q, but with the opposite sign.

Let us also calculate the force $\boldsymbol{F}$ on q produced by the induced charge on the grounded conducting plate. This force must be the same as the force in the analog problem between the charges q and $-q$ separated by a distance $2d$, because the charge q cannot tell whether it is seeing a point charge at a distance $2d$ or a grounded conducting plane at a distance d. Thus from the analog problem Coulomb's law gives for the force between the charge q and the conducting plane,

$$\boldsymbol{F} = -\frac{1}{4\pi\epsilon_0} \frac{q^2}{(2d)^2}\, \hat{\boldsymbol{z}}, \tag{3.41}$$

where $\hat{\boldsymbol{z}}$ is a unit vector in the z direction. It will generally be the case that in a simple image charge problem such as that in Fig. 3.6, the force between a point charge and the conductor is given by the force between the charge and fictitious image charge.

3.7 Green Function for the Conducting Sphere

As discussed in Section 3.5, solution of the Laplace or Poisson equations in a finite volume V with either Dirichlet or Neumann boundary conditions on the bounding surface S of V can be obtained using Green functions. For example, Eq. (3.33) solves for the potential Φ in terms of a Green function with Dirichlet boundary conditions and Eq. (3.35) solves for the potential in terms of a Green function with Neumann boundary conditions. However, choosing an appropriate Green function for a given problem can be difficult.

The physical meaning of $F(\boldsymbol{x}, \boldsymbol{x}')$ in Eq. (3.29) is that it is a *solution of the Laplace equation inside the volume V*, so it represents the *potential due to charges external to V*. It may be thought of as resulting from an external distribution of charges chosen to satisfy the Dirichlet boundary conditions (3.32) or the Neumann boundary conditions (3.34). But this arrangement of charges to satisfy boundary conditions suggests a connection to the method of images described in Section 3.6. As discussed by Jackson (see Section 1.10 of Ref. [41]):

> Determining the proper $F(\boldsymbol{x}, \boldsymbol{x}')$ in Eq. (3.28) to satisfy the boundary conditions (3.32) or (3.34) is physically equivalent to using the method of images. Thus for image problems the potential due to a unit source and its image charge that satisfy homogeneous boundary conditions is just the Green function of Eq. (3.33) for Dirichlet boundary conditions, or Eq. (3.35) for Neumann boundary conditions.

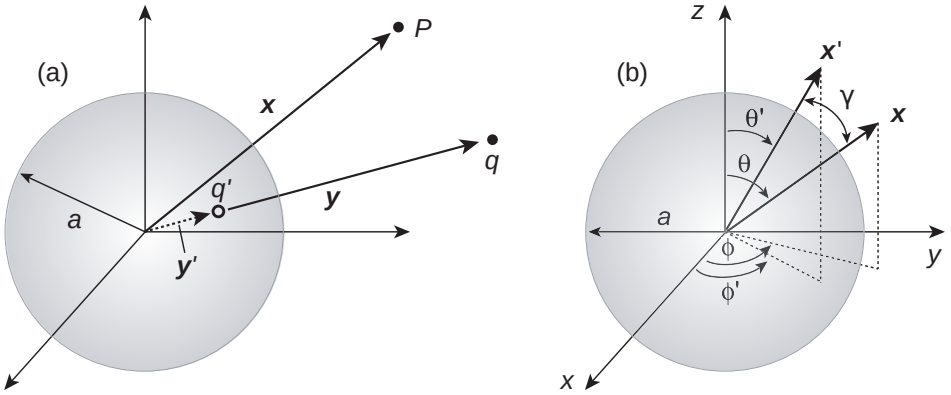

Fig. 3.7 (a) Geometry of image charge method for a charge q indicated by a solid dot outside a conducting sphere, with an image charge q' indicated by an open dot inside the sphere. (b) Coordinates associated with the Green function $G(\boldsymbol{x}, \boldsymbol{x}')$ for a conducting sphere.

As an example, consider the problem of a charge outside a conducting sphere that is solved by the image method in Problem 3.1 and is illustrated in Fig. 3.7(a). In the Green function $G(\boldsymbol{x}, \boldsymbol{x}')$, our usual convention is that the variable $\boldsymbol{x}'$ refers to the location of the unit source and the variable $\boldsymbol{x}$ is the point P at which the potential is being evaluated. These coordinates and a sphere of radius a are illustrated in Fig. 3.7(b). For Dirichlet boundary conditions on the sphere of radius a, the Green function defined by Eq. (3.27),

$$\boldsymbol{\nabla}'^2 G(\boldsymbol{x}, \boldsymbol{x}') = -4\pi\delta(\boldsymbol{x} - \boldsymbol{x}'),$$

for a unit source and its image, the scalar potential is given by [see Fig. 3.7(a)]

$$\Phi(\boldsymbol{x}) = \frac{1}{4\pi\epsilon_0}\left(\frac{q}{|\boldsymbol{x} - \boldsymbol{y}|} + \frac{q'}{|\boldsymbol{x} - \boldsymbol{y}'|}\right), \tag{3.42}$$

with q' and $\boldsymbol{y}'$ chosen such that the potential vanishes on the surface of the sphere in Fig. 3.7(a) ($|\boldsymbol{x}| = a$), which requires that

$$q' = -\frac{a}{y}q \qquad y' = \frac{a^2}{y}. \tag{3.43}$$

Using (3.43), replacing q by $4\pi\epsilon_0$ (to give unit source charge), and replacing y with x' in Eq. (3.42), the required Green function is then

$$G(\boldsymbol{x}, \boldsymbol{x}') = \frac{1}{|\boldsymbol{x} - \boldsymbol{x}'|} - \frac{a}{x'\,|\boldsymbol{x} - (a^2/x'^2)\boldsymbol{x}'|}, \tag{3.44}$$

which can be expressed in spherical coordinates as [41]

$$G(\boldsymbol{x}, \boldsymbol{x}') = \frac{1}{(x^2 + x'^2 - 2xx'\cos\gamma)^{1/2}} - \frac{1}{(x^2x'^2/a^2 + a^2 - 2xx'\cos\gamma)^{1/2}}, \tag{3.45}$$

where γ is the angle between $\boldsymbol{x}$ and $\boldsymbol{x}'$ that is illustrated in Fig. 3.7(b). From Eq. (3.45) it is clear that

1. $G(\boldsymbol{x}, \boldsymbol{x}')$ is symmetric in $\boldsymbol{x}$ and $\boldsymbol{x}$, as it should be,[9] and
2. $G(\boldsymbol{x}, \boldsymbol{x}') = 0$ if either $\boldsymbol{x}$ or $\boldsymbol{x}'$ approaches the spherical radius a, as required by the Dirichlet boundary condition (3.32).

For the solution (3.33), of the Poisson equation with Dirichlet boundary conditions,

$$\Phi(\boldsymbol{x}) = \frac{1}{4\pi\epsilon_0}\int_V \rho(\boldsymbol{x}')G(\boldsymbol{x}, \boldsymbol{x}')d^3x' - \frac{1}{4\pi}\oint_S \left[\Phi(\boldsymbol{x}')\frac{\partial G(\boldsymbol{x}, \boldsymbol{x}')}{\partial n'}\right] da',$$

the second term requires the normal derivative $\partial G/\partial n'$. Recall our standard convention that $\boldsymbol{n}'$ is the unit normal vector *outward from the volume of interest.* Thus, for the solution *outside the sphere* in Fig. 3.7(a), it is inward along $\boldsymbol{x}'$, toward the origin and

$$\left.\frac{\partial G}{\partial n'}\right|_{x'=a} = -\frac{x^2 - a^2}{a(x^2 + a^2 - 2ax\cos\gamma)^{3/2}}. \tag{3.46}$$

Therefore, from Eq. (3.33) quoted above, if there is no charge distribution $\rho(\boldsymbol{x}')$ in the problem, the solution *outside the conducting sphere* of the Laplace equation with the potential specified on its surface (Dirichlet boundary conditions) is

$$\Phi(\boldsymbol{x}) = \frac{1}{4\pi}\int \Phi(a, \theta', \phi')\frac{a(x^2 - a^2)}{(x^2 + a^2 - 2ax\cos\gamma)^{3/2}}\, d\Omega' \qquad \text{(Exterior)}, \tag{3.47}$$

where $d\Omega'$ is the element of solid angle at the point (a, θ', ϕ'), and

$$\cos\gamma = \cos\theta\cos\theta' + \sin\theta\sin\theta'\cos(\phi - \phi'). \tag{3.48}$$

For the solution *interior to the sphere* the only thing that changes is that the normal derivative is radially outward, so the sign on the right side of Eq. (3.46) changes. Thus the interior solution is

$$\Phi(\boldsymbol{x}) = \frac{1}{4\pi}\int \Phi(a, \theta', \phi')\frac{a(a^2 - x^2)}{(x^2 + a^2 - 2ax\cos\gamma)^{3/2}}\, d\Omega' \qquad \text{(Interior)}. \tag{3.49}$$

If there is a charge distribution $\rho(\boldsymbol{x}')$, then one must add to Eqs. (3.47) and (3.49) the first term of Eq. (3.33) with the associated Green function (3.45).

Example 3.4 Let's illustrate use of the exterior solution (3.47) by considering a conducting sphere of radius a, divided into two hemispherical shells separated by an insulating ring, as illustrated in Fig. 3.8. From Eq. (3.47) the solution for $\Phi(x, \theta, \phi)$ is

$$\Phi(x, \theta, \phi) = \frac{V}{4\pi}\int_0^{2\pi} d\phi' \left(\int_0^1 d(\cos\theta') - \int_{-1}^0 d(\cos\theta')\right)\frac{a(x^2 - a^2)}{(x^2 + a^2 - 2ax\cos\gamma)^{3/2}}.$$

By a change of variables in the second integral

$$\theta' \to \pi - \theta' \qquad \phi' \to \phi' + \pi,$$

[9] For Dirichlet boundary conditions, the Green function $G(\boldsymbol{x}, \boldsymbol{x}')$ viewed as a function of one of its variables represents a potential produced by a unit point source. Then symmetry in $\boldsymbol{x}$ and $\boldsymbol{x}'$ implies physical interchangeability of source point and observation point.

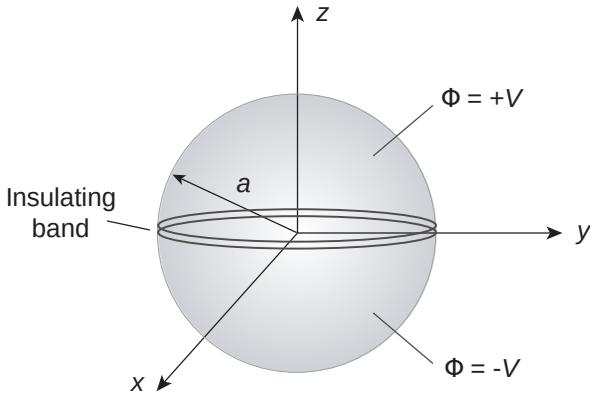

Fig. 3.8 Two hemispheres of radius a separated by an insulating band lying in the $z = 0$ plane, with the upper hemisphere held at potential $+V$ and the lower hemisphere held at potential $-V$. Used in Example 3.4.

this can be put in the form

$$\Phi(x,\theta,\phi) = \frac{Va(x^2-a^2)}{4\pi}\int_0^{2\pi} d\phi' \times \int_0^1 d(\cos\theta')\left[(a^2+x^2-2ax\,\cos\gamma)^{-3/2} - (a^2+x^2+2ax\,\cos\gamma)^{-3/2}\right]. \quad (3.50)$$

Because of the complicated dependence among the angles in Eq. (3.48) this cannot be integrated easily in closed form. If one restricts to the positive z axis the integrals can be done, with the result [41]

$$\Phi(z) = V\left[1 - \frac{z^2-a^2}{z\sqrt{z^2+a^2}}\right] \qquad \text{(Valid on positive } z\text{-axis)}, \quad (3.51)$$

which correctly reduces to $\Phi = V$ at $z = a$. Of potentially more use is to expand the denominator of Eq. (3.50) in a power series and integrate term by term, which yields

$$\Phi(x,\theta,\phi) = \frac{3Va^2}{2x^2}\left[\cos\theta - \frac{7a^2}{12x^2}\left(\frac{5}{2}\cos^2\theta - \frac{3}{2}\cos\theta\right) + \cdots\right]. \quad (3.52)$$

This expansion has been shown to converge rapidly for large x/a, and agrees with the special solution (3.51) for $\cos\theta = 1$ [41].

3.8 Approximate Solutions

In a complicated electrostatics problem it may be sufficient to approximate the solution, as we have done in Eq. (3.52). Often this approximation takes the form of an expansion in some naturally small parameter, with the first few terms of the expansion giving sufficient accuracy for the problem at hand.

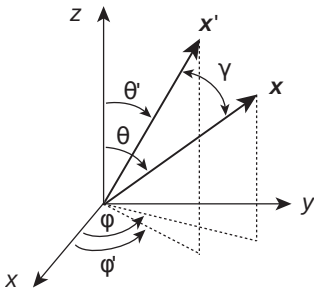

Fig. 3.9 Geometry for the Legendre polynomials and the spherical harmonics in Eqs. (3.54)-(3.57).

3.8.1 Spherical Harmonic Expansions of the Potential

The 3D volume charge density $\rho(\boldsymbol{x})$ appearing in the expression Eq. (2.31a) for the scalar potential,

$$\Phi(\boldsymbol{x}) = \frac{1}{4\pi\epsilon_0}\int \frac{\rho(\boldsymbol{x}')}{|\boldsymbol{x}-\boldsymbol{x}'|}\, d^3x', \tag{3.53}$$

describes a distribution of charge localized in some finite volume V. In many situations we are interested in the potential $\Phi(\boldsymbol{x})$ resulting from this localized charge at distances sufficiently far away that $|\boldsymbol{x}| \gg |\boldsymbol{x}'|$ may be assumed, which suggests a series expansion of $1/|\boldsymbol{x}-\boldsymbol{x}'|$. Two types of expansions are commonly employed:

1. a Taylor series expansion in the cartesian coordinates $(x, y.z)$, or
2. an expansion in terms of spherical harmonics, associated Legendre polynomials, or Legendre polynomials that depends on the spherical coordinates (r, θ, ϕ).

We will discuss here the multipole expansion in terms of Legendre polynomials or spherical harmonics. For a potential due to a unit point charge at $\boldsymbol{x}'$, we may expand $|\boldsymbol{x}-\boldsymbol{x}'|^{-1}$ as

$$\frac{1}{|\boldsymbol{x}-\boldsymbol{x}'|} = \sum_{l=0}^{\infty} \frac{r_<^l}{r_>^{l+1}}\, P_l(\cos\theta), \tag{3.54}$$

where $P_l(\cos\theta)$ is a Legendre polynomial [solution (4.36) of the Legendre equation (4.35)], $r_<$ is the smaller and $r_>$ the larger of $|\boldsymbol{x}|$ and $|\boldsymbol{x}'|$,[10] and θ is the angle between $\boldsymbol{x}$ and $\boldsymbol{x}'$ (see Fig. 3.9). Equation (3.54) is termed a *multipole expansion*. In this expression

- the $l = 0$ term is called the *monopole term*,
- the $l = 1$ term is called the *dipole term*,
- the $l = 2$ term is called the *quadrupole term*, and so on.

The reason for this terminology is suggested by the point-charge distributions discussed in Box 3.3. Comparison of these expressions with the terms in Eq. (3.54) using $r_> = r$ and

[10] The factor $r_<^l/r_>^{l+1}$ in Eq. (3.54) allows the expansion to be made in terms of either r/r' or r'/r, whichever is smaller.

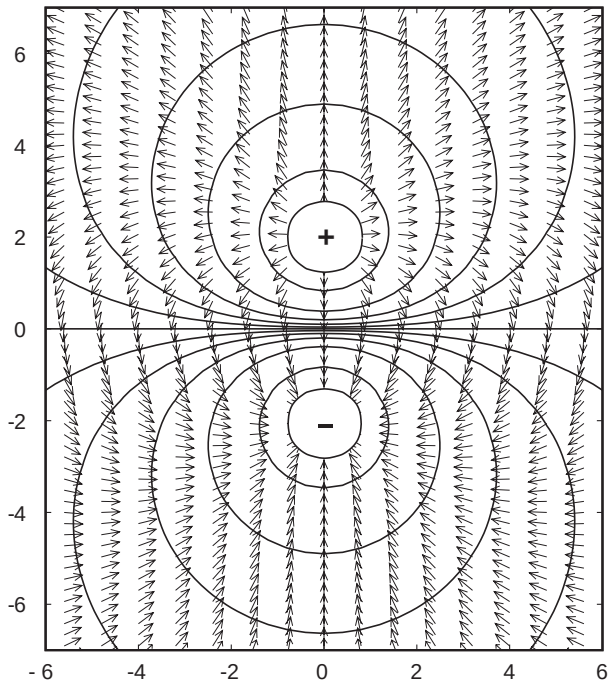

Fig. 3.10 Equipotential contours (curves) and the electric vector field (arrows) for the dipole charge distribution discussed in Box 3.3. For clarity, plotting of field lines and vectors has been suppressed very near the charges.

$r_< = d$ (since $r \gg d$) suggests why Eq. (3.54) is called a multipole expansion: the $l = 1$ term is of the dipole form $P_1(\cos\theta)/r^2$ and the $l = 2$ term is of the quadrupole form $P_2(\cos\theta)/r^3$. (And the $l = 0$ term is $1/r$, which is termed the monopole term.)

Equation (3.54) can be expressed in terms of spherical harmonics using the *spherical harmonic addition theorem*

$$P_l(\cos\gamma) = \frac{4\pi}{2l+1} \sum_{m=-l}^{l} Y^*_{lm}(\theta', \phi')\, Y_{lm}(\theta, \phi), \tag{3.55}$$

where $P_l(\cos\theta)$ is a Legendre polynomial, $Y_{lm}(\theta, \phi)$ is a spherical harmonic, $\boldsymbol{x}$ has the spherical coordinates (r, θ, ϕ), $\boldsymbol{x}'$ has the spherical coordinates (r', θ', ϕ'), and the angle γ between the vectors $\boldsymbol{x}$ and $\boldsymbol{x}'$ is given by

$$\cos\gamma = \cos\theta\cos\theta' + \sin\theta\sin\theta'\cos(\phi - \phi'). \tag{3.56}$$

Then the expansion (3.54) of the potential at $\boldsymbol{x}$ due to a unit charge at $\boldsymbol{x}'$ can be expressed as

$$\frac{1}{|\boldsymbol{x} - \boldsymbol{x}'|} = 4\pi \sum_{l=0}^{\infty} \sum_{m=-l}^{l} \frac{1}{2l+1} \frac{r_<^l}{r_>^{l+1}}\, Y^*_{lm}(\theta', \phi') Y_{lm}(\theta, \phi), \tag{3.57}$$

where angles are defined in Fig. 3.9. This expression gives the potential completely factorized in the coordinates $\boldsymbol{x}$ and $\boldsymbol{x}'$.

Box 3.3 **Multipole moments**

What are the electric potential generated at the point P by the following static charge distributions?

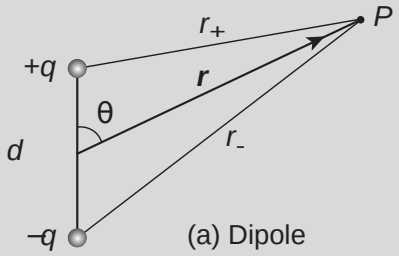

(a) Dipole

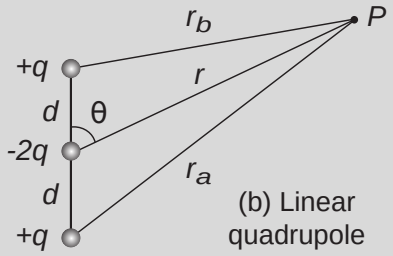

(b) Linear quadrupole

(a) Dipole Potential

For the dipole at P in Fig. (a), the potential is given by

$$\Phi = \frac{q}{4\pi\epsilon_0}\left(\frac{1}{r_+} - \frac{1}{r_-}\right),$$

and from the law of cosines (A.63), the distances are

$$r_\pm^2 = r^2 + \left(\frac{d}{2}\right)^2 \mp rd\cos\theta = r^2\left(1 \mp \frac{d}{r}\cos\theta + \frac{d^2}{4r^2}\right) \simeq r^2\left(1 \mp \frac{d}{r}\cos\theta\right),$$

where $r = |\boldsymbol{r}|$ and the term $d^2/4r^2$ was dropped, since we assume that $r \gg d$. Thus,

$$\frac{1}{r_\pm} \simeq \frac{1}{r}\left(1 \mp \frac{d}{r}\cos\theta\right)^{-1/2} \simeq \frac{1}{r}\left(1 \pm \frac{d}{2r}\cos\theta\right),$$

where a binomial expansion was used in the last step. Therefore,

$$\Phi_{\text{dipole}} = \frac{q}{4\pi\epsilon_0}\left(\frac{1}{r_+} - \frac{1}{r_-}\right) = \frac{q}{4\pi\epsilon_0}\frac{d\cos\theta}{r^2} = \left(\frac{qd}{4\pi\epsilon_0}\right)\frac{P_1(\cos\theta)}{r^2} \qquad (r \gg d).$$

Hence the electric dipole potential is proportional to the Legendre polynomial $P_1(\cos\theta)$, and falls off at large distance as $1/r^2$. The potential contours and electric field vectors for a dipole are illustrated in Fig. 3.10.

(b) Quadrupole Potential

Carrying out a similar analysis for the linear quadrupole in Fig. (b) above (see Problem 3.3), the potential is given by

$$\Phi_{\text{quadrupole}} = \left(\frac{2Qd^2}{4\pi\epsilon_0}\right)\frac{P_2(\cos\theta)}{r^3} \qquad (r \gg d),$$

which is proportional to the Legendre polynomial $P_2(\cos\theta)$ and varies as the cube of the inverse distance.

If the localized distribution of charge $\rho(\boldsymbol{x}')$ in Eq. (3.53) is assumed to vanish outside of a small sphere of radius R centered on the origin, the potential generated by that charge outside the radius R can be expanded in spherical harmonics as

$$\Phi(\boldsymbol{x}) = \frac{1}{4\pi\epsilon_0} \sum_{l=0}^{\infty} \sum_{m=-l}^{l} \frac{4\pi}{2l+1}\, q_{lm} \frac{Y_{lm}(\theta,\phi)}{r^{l+1}} \tag{3.58}$$

The expansion coefficients q_{lm} are given by

$$q_{lm} = \int Y^*_{lm}(\theta',\phi')(r')^l \rho(\boldsymbol{x}') d^3x' \tag{3.59}$$

and are called *multipole moments*. Spherical harmonics are related to associated Legendre polynomials $P_l^m(\cos\theta)$ by

$$Y_{lm}(\theta,\phi) = (-1)^m \sqrt{\frac{2l+1}{4\pi}\,\frac{(l-m)!}{(l+m)!}}\, P_l^m(\cos\theta) e^{im\phi}. \tag{3.60}$$

They behave under complex conjugation as

$$Y^*_{lm}(\theta,\phi) = (-1)^m\, Y_{l-m}(\theta,\phi), \tag{3.61}$$

and obey the *orthogonality condition*

$$\int_0^{2\pi} d\phi \int_0^{\pi} Y^*_{l'm'}(\theta,\phi) Y_{lm}(\theta,\phi) \sin\theta d\theta = \delta_{l'l}\delta_{m'm}, \tag{3.62}$$

and the *completeness relation*

$$\sum_{l=0}^{\infty} \sum_{m=-l}^{l} Y^*_{lm}(\theta',\phi') Y_{lm}(\theta,\phi) = \delta(\phi-\phi')\,\delta(\cos\theta - \cos\theta'). \tag{3.63}$$

The utility of a multipole expansion like Eqs. (3.58) or (3.54) is that the terms in the expansion of the source-charge distribution fall off with distance r as $r^{-(l+1)}$, often justifying an approximation that retains only the first few terms in the multipole expansion.

If we define

1. a total charge Q (monopole moment),
2. the electric dipole moment vector $\boldsymbol{p}$ by

$$\boldsymbol{p} \equiv \int \boldsymbol{x}' \rho(\boldsymbol{x}') d^3x', \tag{3.64}$$

3. and the *traceless quadrupole moment tensor* Q_{ij} by[11]

$$Q_{ij} \equiv \int (3x'_i x'_j - r'^2 \delta_{ij})\, \rho(\boldsymbol{x}') d^3x', \tag{3.65}$$

where $r'^2 \equiv |\boldsymbol{x}'|^2$,

the spherical multipole moments in Eq. (3.59) may be expressed in cartesian coordinates as [41]

$$q_{00} = \frac{1}{\sqrt{4\pi}} \int \rho(\boldsymbol{x}')\, d^3x' = \frac{1}{\sqrt{4\pi}}\, Q, \tag{3.66a}$$

$$q_{11} = -\sqrt{\frac{3}{8\pi}} \int (x' - iy')\, \rho(\boldsymbol{x}')\, d^3x' = -\sqrt{\frac{3}{8\pi}}\, (p_x - ip_y), \tag{3.66b}$$

$$q_{10} = \sqrt{\frac{3}{4\pi}} \int z'\, \rho(\boldsymbol{x}') d^3x' = \sqrt{\frac{3}{4\pi}}\, p_z, \tag{3.66c}$$

$$q_{22} = \frac{1}{4}\sqrt{\frac{15}{2\pi}} \int (x' - iy')^2\, \rho(\boldsymbol{x}')\, d^3x' = \frac{1}{12}\sqrt{\frac{15}{2\pi}}\, (Q_{11} - 2iQ_{12} - Q_{22}), \tag{3.66d}$$

$$q_{21} = -\sqrt{\frac{15}{8\pi}} \int z'(x' - iy')\, \rho(\boldsymbol{x}')\, d^3x' = -\frac{1}{3}\sqrt{\frac{15}{8\pi}}\, (Q_{13} - iQ_{23}), \tag{3.66e}$$

$$q_{20} = \frac{1}{2}\sqrt{\frac{5}{4\pi}} \int (3z'^2 - r'^2)\, \rho(\boldsymbol{x}')\, d^3x' = \frac{1}{2}\sqrt{\frac{5}{4\pi}}\, Q_{33}, \tag{3.66f}$$

where corresponding moments with $m < 0$ may be obtained using $q_{l-m} = (-1)^m q^*_{lm}$. An expansion of $\Phi(\boldsymbol{x})$ in cartesian coordinates may be obtained by a direct Taylor series expansion of $1/|\boldsymbol{x} - \boldsymbol{x}'|$ (see Appendix A.8). The result

$$\Phi(\boldsymbol{x}) = \frac{1}{4\pi\epsilon_0} \left[\frac{Q}{r} + \frac{\boldsymbol{p}\cdot\boldsymbol{x}}{r^3} + \frac{1}{2}\sum_{i,j} Q_{ij}\, \frac{x_i x_j}{r^5} + \cdots \right]. \tag{3.67}$$

is quoted without proof.[12]

The spherical multipole moments like Eq. (3.59) and the corresponding cartesian multipole moments like Eq. (3.64) generally have different numbers of components for a given multipole order. For multipole order l there are $(l+1)(l+2)/2$ cartesian components

[11] With this definition Q_{ij} is traceless (see Problem 3.6). A quadrupole moment definition without the tracelessness property

$$Q_{ij} = \frac{1}{2} \int \rho(\vec{x}') x'_i x'_j\, \mathrm{d}^3x',$$

is also sometimes encountered. (The traceless form arises naturally in a spherical harmonic multipole expansion; the other form arises in a different multipole expansion.) The quadrupole moment is a rank-2 tensor, which can be expressed as a 3×3 matrix, implying nine components. However, it is symmetric in its indices, which reduces the independent components to six, and the traceless constraint reduces the number of independent components further to five.

[12] The mathematical difference between the cartesian multipole expansion and spherical multipole moment expansion is that the former is obtained by expanding $1/|\boldsymbol{x} - \boldsymbol{x}'|$ in a Taylor series (see Appendix A.8), while the latter is obtained by expanding $1/|\boldsymbol{x} - \boldsymbol{x}'|$ in a a binomial series (see Appendix A.9 and Problem 3.2). The spherical moment expansion is favored in problems where angular momentum conservation is important, as is common for atomic or nuclear physics,.

but only $2l+1$ spherical components, which differs for $l > 1$. At a technical level (a consequence of group theory; see Box 21.1) the source of this difference is that the spherical moments are *irreducible representations* of the rotation group (they are said to transform as irreducible *spherical tensors*) while the cartesian moments are *reducible* under rotational transformations. Physically this means that spherical multipole moments define components of definite angular momentum, while cartesian moments are mixtures of components with different angular momenta.

Another technical point is that the coefficients in a multipole moment expansion may depend on choice of origin for the coefficients. In general it can be shown that the value of q_{lm} in Eq. (3.59) for the lowest-order non-vanishing multipole moment of a charge distribution is independent of origin for the coordinates, but higher-order moments will generally depend on the location of the origin for the coordinate system [41].

Example 3.5 Consider a localized charge density

$$\rho(\boldsymbol{r}) = \frac{1}{64\pi} r^2 e^{-r} \sin^2\theta.$$

Let's make a multipole expansion of the potential associated with this charge density and determine all the non-vanishing multipole moments. The charge distribution is axially symmetric, so only Y_{lm} with $m = 0$ are non-zero. From Eq. (3.59), the moments may be written

$$\begin{aligned}
q_{lm} &= \int Y_{l0}^*(\theta,\phi) r^l \rho(\boldsymbol{x}) d^3x \\
&= \int Y_{l0}^*(\theta,\phi) r^l \rho(r,\theta) r^2 dr\, d\phi\, d(\cos\theta) \\
&= 2\pi\sqrt{\frac{2l+1}{4\pi}} \int P_l(\cos\theta) r^l \rho(r,\theta) r^2 dr\, d(\cos\theta) \\
&= \frac{2\pi}{64\pi}\sqrt{\frac{2l+1}{4\pi}} \int_0^\infty r^{l+4} e^{-r} dr \int_{-1}^{+1} P_l(\cos\theta) \sin^2\theta d(\cos\theta) \\
&= \frac{2\pi}{64\pi}\frac{2}{3}\sqrt{\frac{2l+1}{4\pi}} \int_0^\infty r^{l+4} e^{-r} dr \int_{-1}^{+1} P_l(\cos\theta) \left[P_0(\cos\theta) - P_2(\cos\theta)\right] d(\cos\theta) \\
&= \frac{1}{48}\sqrt{\frac{2l+1}{4\pi}}\, \Gamma(l+5) \left(2\delta_{l0} - \frac{2}{5}\delta_{l2}\right).
\end{aligned}$$

where we have used in the third line,

$$Y_{l0}(\theta,\phi) = \sqrt{\frac{2l+1}{4\pi}} P_l(\cos\theta)$$

used in the fifth line,

$$\sin^2\theta = 1 - \cos^2\theta = \frac{2}{3}\left[P_0(\cos\theta) - P_2(\cos\theta)\right]$$

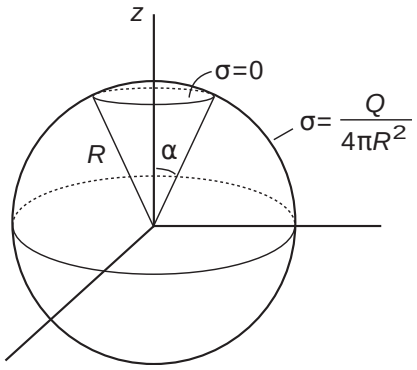

Fig. 3.11 Figure for Example 3.6: a spherical surface has a uniform surface charge of density $\sigma = Q/4\pi R^2$, except for a spherical cap at the north pole defined by a cone with opening $\theta = \alpha$ where $\sigma = 0$.

and used in the last step

$$\int_{-1}^{+1} P_m(x)P_n(x)dx = \frac{2}{2n+1}\,\delta_{mn},$$

and evaluated the radial integral using the tabulated definite integral

$$\int_0^\infty r^{n-1}e^{-(a+1)r}dr = \frac{\Gamma(n)}{(a+1)^n}.$$

Thus the multipole moments are

$$q_{lm} = \frac{1}{48}\sqrt{\frac{2l+1}{4\pi}}\,\Gamma(l+5)\left(2\delta_{l0} - \frac{2}{5}\delta_{l2}\right),$$

and the delta functions allow reading off the only non-vanishing multipole moments as

$$q_{00} = \sqrt{\frac{1}{4\pi}}\,Q \qquad q_{20} = -6\sqrt{\frac{5}{4\pi}}\,Q_{33},$$

where the values were taken from Eq. (3.66).

Example 3.6 A spherical surface of radius R has a uniform surface charge of density $\sigma = Q/4\pi R^2$, except for a spherical cap at the north pole defined by a cone with opening $\theta = \alpha$ where $\sigma = 0$, as illustrated in Fig. 3.11. Use the jump condition at a charge layer of Eq. (3.2) for the electric field to show that the potential inside the spherical surface can be expressed as

$$\Phi = \frac{Q}{8\pi\epsilon_0}\sum_{l=0}^{\infty}\frac{1}{2l+1}\left[P_{l+1}(\cos\alpha) - P_{l-1}(\cos\alpha)\right]\frac{r^l}{R^{l+1}}\,P_l(\cos\theta) \qquad \text{(Inside)}.$$

What is the potential outside the sphere? The surface charge density specifies a jump condition on the normal component of the electric field (see Section 3.1),

$$E_r^{\text{out}}|_{r=R} = E_r^{\text{in}}|_{r=R} + \frac{\sigma}{\epsilon_0},$$

which allows us to solve for the potential $\Phi(r,\theta)$. Because of the axial symmetry about the z axis we may expand the potential in Legendre polynomials according to Eqs. (3.53) and (3.54),

$$\Phi_{\text{in}} = \sum_{l=0}^{\infty} A_l \left(\frac{r}{R}\right)^l P_l(\cos\theta) \qquad \Phi_{\text{out}} = \sum_{l=0}^{\infty} A_l \left(\frac{R}{r}\right)^l P_l(\cos\theta),$$

where the expansion coefficients A_l are the same for Φ_{in} and Φ_{out} because we require Φ to be continuous at the surface $r = R$. The radial components of the interior and exterior electric fields follow from $E_r = -\partial\Phi/\partial r$,

$$E_r^{\text{in}} = -\sum_{l=0}^{\infty} \frac{lA_l}{R} \left(\frac{r}{R}\right)^{l-1} P_l(\cos\theta),$$

$$E_r^{\text{out}} = \sum_{l=0}^{\infty} \frac{(l+1)A_l}{R} \left(\frac{R}{r}\right)^{l+2} P_l(\cos\theta).$$

Substituting this into the jump condition given above for E_r leads to

$$\sigma(\cos\theta) = \epsilon_0 \left[E_r^{\text{out}} - E_r^{\text{in}}\right]_{r=R} = \sum_{l=0}^{\infty} \frac{(2l+1)\epsilon_0 A_l}{R} P_l(\cos\theta).$$

Now multiply both sides by $P_k(\cos\theta)$, integrate over $d(\cos\theta)$, and use

$$\int_{-1}^{+1} P_n(x)P_m(x)dx = \frac{2}{2n+1}\,\delta_{nm}$$

to give

$$\frac{(2l+1)\epsilon_0 A_l}{R} = \frac{2l+1}{2} \int_{-1}^{+1} \sigma(\cos\theta)P_l(\cos\theta)d(\cos\theta),$$

which implies that

$$A_l = \frac{R}{2\epsilon_0} \int_{-1}^{+1} \sigma(\cos\theta)P_l(\cos\theta)d(\cos\theta).$$

Then using that the surface is covered uniformly with charge except within the cone,

$$\sigma(\cos\theta) = \begin{cases} \dfrac{Q}{4\pi R^2} & (\cos\theta < \cos\alpha), \\ 0 & (\cos\theta > \cos\alpha), \end{cases}$$

leads to

$$A_l = \frac{Q}{8\pi\epsilon_0 R} \int_{-1}^{\cos\alpha} P_l(\cos\theta)d(\cos\theta).$$

This can be integrated by using [17]

$$P_l(x) = \frac{1}{2l+1}\left[P'_{l+1}(x) - P'_{l-1}(x)\right]$$

(where the primes indicate derivatives), which gives

$$\begin{aligned}
A_l &= \frac{Q}{8\pi\epsilon_0 R}\int_{-1}^{\cos\alpha} P_l(\cos\theta)d(\cos\theta) \\
&= \frac{Q}{8\pi\epsilon_0 R}\frac{1}{2l+1}\int_{-1}^{\cos\alpha}\left[\frac{dP_{l+1}(\cos\theta)}{d(\cos\theta)} - \frac{dP_{l-1}(\cos\theta)}{d(\cos\theta)}\right]d(\cos\theta) \\
&= \frac{Q}{8\pi\epsilon_0 R}\frac{1}{2l+1}\int_{-1}^{\cos\alpha}\left[dP_{l+1}(\cos\theta) - dP_{l-1}(\cos\theta)\right] \\
&= \frac{Q}{8\pi\epsilon_0 R}\frac{1}{2l+1}\left[P_{l+1}(\cos\theta) - P_{l-1}(\cos\theta)\right]_{-1}^{\cos\alpha} \\
&= \frac{Q}{8\pi\epsilon_0 R}\frac{1}{2l+1}\left[P_{l+1}(\cos\alpha) - P_{l-1}(\cos\alpha)\right],
\end{aligned}$$

where in the last step $P_l(-1) = (-1)^l$ was used. Substituting in the original expansions gives

$$\begin{aligned}
\Phi_{\text{in}} &= \sum_{l=0}^{\infty} A_l \left(\frac{r}{R}\right)^l P_l(\cos\theta) \\
&= \frac{Q}{8\pi\epsilon_0}\sum_{l=0}^{\infty}\frac{1}{2l+1}\left[P_{l+1}(\cos\alpha) - P_{l-1}(\cos\alpha)\right]\frac{r^l}{R^{l+1}}P_l(\cos\theta) \quad \text{(Inside)},
\end{aligned}$$

for the interior solution, and

$$\begin{aligned}
\Phi_{\text{out}} &= \sum_{l=0}^{\infty} A_l \left(\frac{R}{r}\right)^l P_l(\cos\theta) \\
&= \frac{Q}{8\pi\epsilon_0}\sum_{l=0}^{\infty}\frac{1}{2l+1}\left[P_{l+1}(\cos\alpha) - P_{l-1}(\cos\alpha)\right]\frac{R^{l-1}}{r^l}P_l(\cos\theta) \quad \text{(Outside)},
\end{aligned}$$

for the exterior solution,

The preceding example illustrates many techniques that can be used in solving electrostatic problems by means of multipole expansions.

3.8.2 Multipole Components of the Electric Field

We have expanded the potential in multipole moments, so the corresponding electric fields can be expanded in a similar way. It is often useful to express the components of the electric field $\boldsymbol{E} = -\boldsymbol{\nabla}\Phi$ in spherical coordinates. For a term in Eq. (3.58) with definite angular momentum labeled by (l, m), the spherical electric field components (E_r, E_θ, E_ϕ)

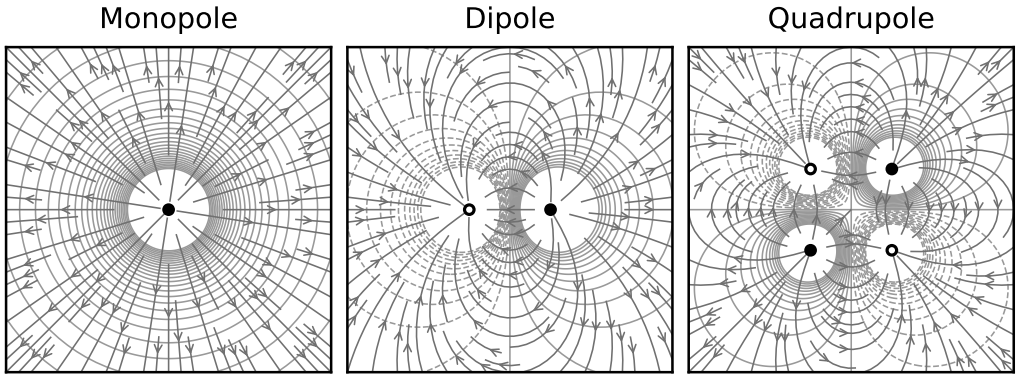

Fig. 3.12 Monopole, dipole, and quadrupole moments for potentials and electric fields (see Problem 3.15). Unit positive charges are solid black circles, unit negative charges are open circles, equipotential contours are lighter-gray curves (solid for positive values and dashed for negative values of the potential), and electric field lines are darker gray curves with arrows indicating direction of the local electric field. Plotting of potential contours has been suppressed near each charge since the potential tends to infinity at the charge. [*NOTE: Contours and field lines suffer from the common default Python problem of not being plotted continuously. Need to fix this for this plot.*]

are given by [41]

$$E_r = \frac{l+1}{(2l+1)\epsilon_0}\, q_{lm}\, \frac{1}{r^{l+2}}\, Y_{lm}(\theta,\phi), \tag{3.68a}$$

$$E_\theta = -\frac{1}{(2l+1)\epsilon_0}\, q_{lm}\, \frac{1}{r^{l+2}} \frac{\partial}{\partial\theta}\, Y_{lm}(\theta,\phi), \tag{3.68b}$$

$$E_\phi = \frac{1}{(2l+1)\epsilon_0}\, q_{lm}\, \frac{1}{r^{l+2}} \frac{im}{\sin\theta}\, Y_{lm}(\theta,\phi), \tag{3.68c}$$

with the multipole moments q_{lm} defined in Eq. (3.66).

Example 3.7 For an electric dipole $\boldsymbol{p}$ that is oriented along the z axis, one finds

$$E_r = \frac{2p\cos\theta}{4\pi\epsilon_0 r^3} \qquad E_\theta = \frac{p\sin\theta}{4\pi\epsilon_0 r^3} \qquad E_\phi = 0,$$

for the electric-field components (3.68).

Figure 3.12 illustrates the potential and electric field for monopole, dipole, and quadrupole moments.

1. *Monopole:* Corresponds to a single point source. Field lines diverge radially to the edge of the plot, while equipotential surfaces form concentric circles.

2. *Dipole:* Two opposite charges create a field where lines curve from the positive source to the negative sink. The equipotentials reflect the combined influence of both charges.
3. *Quadrupole:* Four alternating charges create a more complex, multi-lobed field geometry.

Let us now consider the energy of a localized charge distribution placed in an electric field.

3.8.3 Energy of a Charge Distribution in a Field

If a localized charge distribution $\rho(\boldsymbol{x})$ is subject to an *external potential* $\Phi(\boldsymbol{x})$,[13] the electrostatic energy is

$$W = \int \rho(\boldsymbol{x})\Phi(\boldsymbol{x})d^3x. \tag{3.69}$$

If the potential varies slowly over the extent of $\rho(\boldsymbol{x})$, it can be expanded in a Taylor series,

$$\begin{aligned}\Phi(\boldsymbol{x}) &= \Phi(0) + \boldsymbol{x}\cdot\boldsymbol{\nabla}\Phi(0) + \frac{1}{2}\sum_i\sum_j x_i x_j \frac{\partial^2\Phi}{\partial x_i \partial x_j}(0) + \cdots \\ &= \Phi(0) - \boldsymbol{x}\cdot\boldsymbol{E}(0) - \frac{1}{2}\sum_i\sum_j x_i x_j \frac{\partial E_j}{\partial x_i}(0) + \cdots \\ &= \Phi(0) - \boldsymbol{x}\cdot\boldsymbol{E}(0) - \frac{1}{6}\sum_i\sum_j \left(3x_i x_j - r^2\delta_{ij}\right)\frac{\partial E_j}{\partial x_i}(0) + \cdots,\end{aligned} \tag{3.70}$$

where in line 2 the definition of the electric field $\boldsymbol{E} = -\boldsymbol{\nabla}\Phi$ was used and in the last line $\frac{1}{6}r^2\boldsymbol{\nabla}\cdot\boldsymbol{E}(0)$ was subtracted from the last term since $\boldsymbol{\nabla}\cdot\boldsymbol{E} = 0$ for the external field. Inserting the expansion (3.70) into Eq. (3.69), the energy takes the form

$$W = q\Phi(0) - \boldsymbol{p}\cdot\boldsymbol{E}(0) - \frac{1}{6}\sum_i\sum_j Q_{ij}\frac{\partial E_j}{\partial x_i}(0) + \cdots, \tag{3.71}$$

where q is the total charge, the dipole moment $\boldsymbol{p}$ is defined in Eq. (3.64), and the quadrupole moment Q_{ij} is defined in Eq. (3.65).

Example 3.8 Many atomic nuclei have charge distributions exhibiting a quadrupole deformation. Such nuclei will have a contribution to the energy from the quadrupole term in the expansion (3.71) if they are subject to an external electric field. Such an "external" field can be provided by the electrons of the atom containing the nucleus, or by a crystal lattice in which the nucleus is embedded, and coupling to these external field leads to small energy shifts and breaking of degeneracies for nuclear states that can be detected experimentally. (The energy shifts are small, corresponding typically to radiofrequency wavelengths.) Such methods allow the quadrupole moments of nuclei to be measured,

[13] For example, this could be the charge distribution of an atomic nucleus subject to an external electric field generated by the electrons of that atom, or to the external electric field of another nucleus in a collision between the two nuclei.

which provide important clues to the details of nuclear structure and interactions. In collisions between heavy ions at accelerators, the electric field of one nucleus can cause excited states to be populated in the other nucleus, in a process called *Coulomb excitation*. The study of the rates at which those excited states are populated (for example by detecting the de-excitation by emission of γ-rays) is another way in which nuclear quadrupole deformations can be measured by analyzing their response to an applied electric field.

The expansion (3.71) manifests the characteristic way in which various multipoles of a charge distribution interact with an external electric field:

1. the charge interacts with the potential in the first term,
2. the dipole moment interacts with the electric field in the second term,
3. the quadrupole moment interacts with the gradient of the electric field in the third term, and so on.

Thus multipole expansions serve a pedagogical as well as practical purpose in understanding electrostatic interactions.

Background and Further Reading

An introduction to the material of this chapter may be found in Griffiths [33] or Purcell and Morin [62]. More advanced treatments may be found in Jackson [41], Garg [31], Chaichian et al [23], and Zangwill [77].

Problems

3.1 A charge q is placed outside a grounded ($\Phi = 0$) conducting sphere:

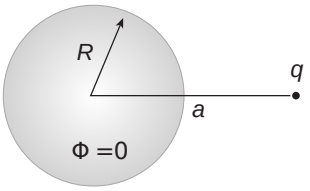

Use the method of images described in Section 3.6 to find the scalar potential Φ outside the sphere, and calculate the force exerted by the sphere on the charge q.

3.2 Assuming that $|\boldsymbol{x}| \gg |\boldsymbol{x}'|$ in the following figure,

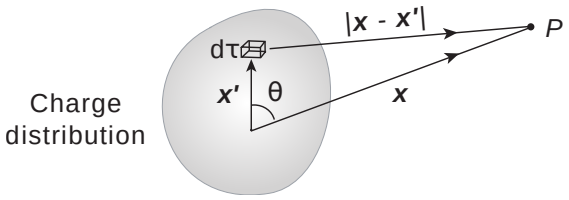

prove that $1/|\boldsymbol{x} - \boldsymbol{x}'|$ can be expanded in the power series

$$\frac{1}{|\boldsymbol{x} - \boldsymbol{x}'|} = \frac{1}{r}\left(1 - \frac{1}{2}\epsilon + \frac{3}{8}\epsilon^2 - \frac{5}{16}\epsilon^3 + \cdots\right),$$

where $r = |\boldsymbol{x}|$ and $r' = |\boldsymbol{x}'|$, and

$$\epsilon \equiv \frac{r'}{r}\left(\frac{r'}{r} - 2\cos\theta\right),$$

and that this is a series expansion in terms of Legendre polynomials that is equivalent to Eq. (3.57). Finally, show that

$$\Phi(\boldsymbol{x}) = \frac{1}{4\pi\epsilon_0}\sum_{l=0}^{\infty} r^{-(l+1)} \int (r')^l P_l(\cos\theta)\rho(\boldsymbol{x}')d^3x'$$

is the scalar potential at the point P.

3.3 The following charge distribution is called a *linear quadrupole*.

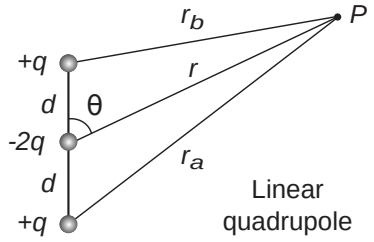

What is the potential generated at the point P assuming that $r \gg d$? ***

3.4 For the charge distribution shown below,

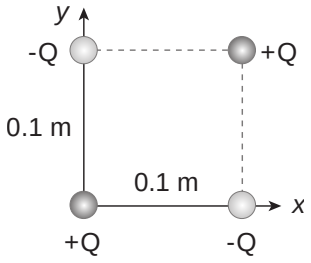

calculate the components of the dipole moment vector $\boldsymbol{p}$ assuming that $|Q| = 3\,\mu$C.

3.5 A point dipole with dipole moment $\boldsymbol{p}$ is located at $\boldsymbol{x}_0$. Show that for calculations of potential Φ or energy density W of a dipole in an external field, the dipole can be described by an effective charge density

$$\rho_{\text{eff}}(\boldsymbol{x}) = -\boldsymbol{p} \cdot \boldsymbol{\nabla}\delta(\boldsymbol{x} - \boldsymbol{x}_0),$$

where $\delta(\boldsymbol{x} - \boldsymbol{x}')$ is the 3D Dirac delta function. *Hint*: See Eq. (A.77).

3.6 The quadrupole moment tensor is given by Eq. (3.65) as

$$Q_{ij} \equiv \int (3x_i' x_j' - r'^2 \delta_{ij})\, \rho(\boldsymbol{x}')\, d^3x',$$

where $r'^2 \equiv |\boldsymbol{x}'|^2$. Evaluate Q_{ij} for a discrete set of N static charges q_i and show that it is traceless.

3.7 For the discrete charge distribution displayed in Problem 3.4, calculate the nine *cartesian components* $Q_{ij} = Q_{xx}, Q_{xy}, \cdots$ of the quadruple moment tensor starting from Eq. (3.65). Assume the origin of the coordinate system to be at the lower left charge and that $|Q| = 3\,\mu$C.

3.8 Prove that in the Green function problem described in Box 3.2,

$$x(t) = \int_{-\infty}^{\infty} dt' G(t, t') \frac{f(t')}{m}$$

is a solution of the equation of motion

$$\left(\frac{d^2}{dt^2} + 2\gamma \frac{d}{dt} + \omega_0^2 \right) x(t) = \frac{f(t)}{m},$$

for a driven mechanical oscillator. ***

3.9 Show that the uniqueness proof for solutions of the Laplace equation given in Section 3.3.4 carries through in similar fashion for the Poisson equation.

3.10 Prove Uniqueness Theorem II given in Section 3.3 by showing that if two different electric fields are assumed to correspond to solutions of the Poisson equation with the same boundary conditions, then the difference between them must be zero. *Hint*: Gauss's law in differential and integral form, general properties of conductors, and some vector calculus voodoo will do the job. ***

3.11 Prove that the Green function associated with the 3D Poisson equation $\nabla^2\psi(\mathbf{r}) = -f(\boldsymbol{x})$ with a generalized source $f(\boldsymbol{x})$ is given by

$$\psi(\boldsymbol{x}) = \int G(\boldsymbol{x},\boldsymbol{x}')f(\boldsymbol{x}')\,d^3r' = \frac{1}{4\pi}\int \frac{f(\boldsymbol{x}')}{|\boldsymbol{x}-\boldsymbol{x}'|}\,d^3x' \quad G(\boldsymbol{x},\boldsymbol{x}') \equiv \frac{1}{4\pi|\boldsymbol{x}-\boldsymbol{x}'|}.$$

Hint: The Green function $G(\boldsymbol{x},\boldsymbol{x}')$ is the potential response to a point source (Dirac delta function) located at $\boldsymbol{x}'$, and the principle of superposition holds for solutions of the linear Poisson equation. ***

3.12 Repeat Problem 3.11 but for the Poisson equation in two spatial dimensions instead of three. Show that the fundamental Green function in that case is given by

$$G(\boldsymbol{x},\boldsymbol{x}') = -\frac{1}{2\pi}\ln\left(|\boldsymbol{x}-\boldsymbol{x}'|\right).$$

Hint: The steps in the solution follow the same logic for those for the solution of Problem 3.11, but the geometry and resulting calculus are different.

3.13 Consider a spherical shell of radius R centered at the origin of a spherical coordinate system, where the surface of the shell carries a non-uniform charge density given by $\sigma(\theta) = \sigma_0\cos\theta$. Find the electrostatic potential $\Phi(\boldsymbol{r})$ everywhere in space by evaluating the direct integral formulation in 2D of Coulomb's law (2.31b). *Hint*: Expand $|\boldsymbol{x}-\boldsymbol{x}'|^{-1}$ in Legendre polynomials.

3.14 Derive a formula for the potential between the plates S_1 and S_2 of the capacitor in Box 3.1 by solving the Laplace equation with mixed Dirichlet and Neumann boundary conditions where plate S_1 is held at fixed potential $\Phi = V_0$ and plate S_2 is held at fixed charge σ such that

$$\frac{\partial\Phi}{\partial n}|_{S_1} = -E_n = -\frac{\sigma}{\epsilon_0}.$$

Hint: The solution is plotted in Fig. 3.4. ***

Numerical and GenAI Problems

3.15 Figure 3.12 is in grayscale for book printing purposes. Command your *GenAI* to write *Python* code to recreate the figure, but now with colors assigned to features like the equipotentials, electric field streamlines, and charges. Be specific in your prompt, specifying details (for example, "figure 4.5 inches wide, green for equipotentials, blue for electric field streamlines, red for positive charges, black for negative charges, a sans serif font in black with sizes no smaller than 8 points, ..."). Such specifications would be important if you were preparing a figure for publication or for use in a presentation.

3.16 Prompt your *GenAI* to solve Problem 3.14 by numerical integration of the Laplace equation using the relaxation method described in Appendix F.4. *Hint*: Use the solution of Problem 3.14 (in the Student Solutions Manual for this book) and Fig. 3.4 to check your results. ***

4 Solution of the Poisson and Laplace Equations

For relatively simple electrostatics problems solutions may be found using Coulomb's law directly, Gauss's law, image methods, and so on, as we have discussed in Chs. 2 and 3. For more complicated problems—particularly those that violate symmetries facilitating Gauss's law or image methods—these methods may be difficult to apply and a more straightforward way to proceed may be to solve the Poisson or Laplace differential equations subject to boundary conditions directly, by either analytical or numerical means. Figures 4.1 and 4.2 summarize some common approaches to solving the Poisson and Laplace equations that will be the subject matter for this chapter.

4.1 Solutions by Separation of Variables

It is more difficult to find systematic solutions for the Poisson and Laplace partial differential equations than for ordinary differential equations. A typical case to be solved is where the potential or the charge density is specified on the boundaries of a region, and we wish to find the potential at arbitrary points in the interior. A standard approach to such a problem is to solve the Laplace or Poisson equation subject to boundary conditions by the *separation of variables method*.

4.1.1 Separation of Variables in Cartesian Coordinates

Let us introduce the separation of variables method using cartesian coordinates. The basic idea is to assume that the solution can be written in the product form

$$\Phi(x, y, z) = X(x)Y(y)Z(z), \tag{4.1}$$

where $X(x)$, $Y(y)$, and $Z(z)$ are functions only of x, y, and z, respectively. Let us illustrate the method by considering the problem corresponding to Fig. 4.3 [25], where it is necessary to solve for the scalar potential Φ subject to boundary conditions given by specifying Φ on three conducting surfaces. The problem is independent of the z direction, and we assume that there is no charge density between the plates. Therefore, we wish to solve the 2D Laplace equation in cartesian coordinates,

$$\frac{\partial^2 \Phi}{\partial x^2} + \frac{\partial^2 \Phi}{\partial y^2} = 0, \tag{4.2}$$

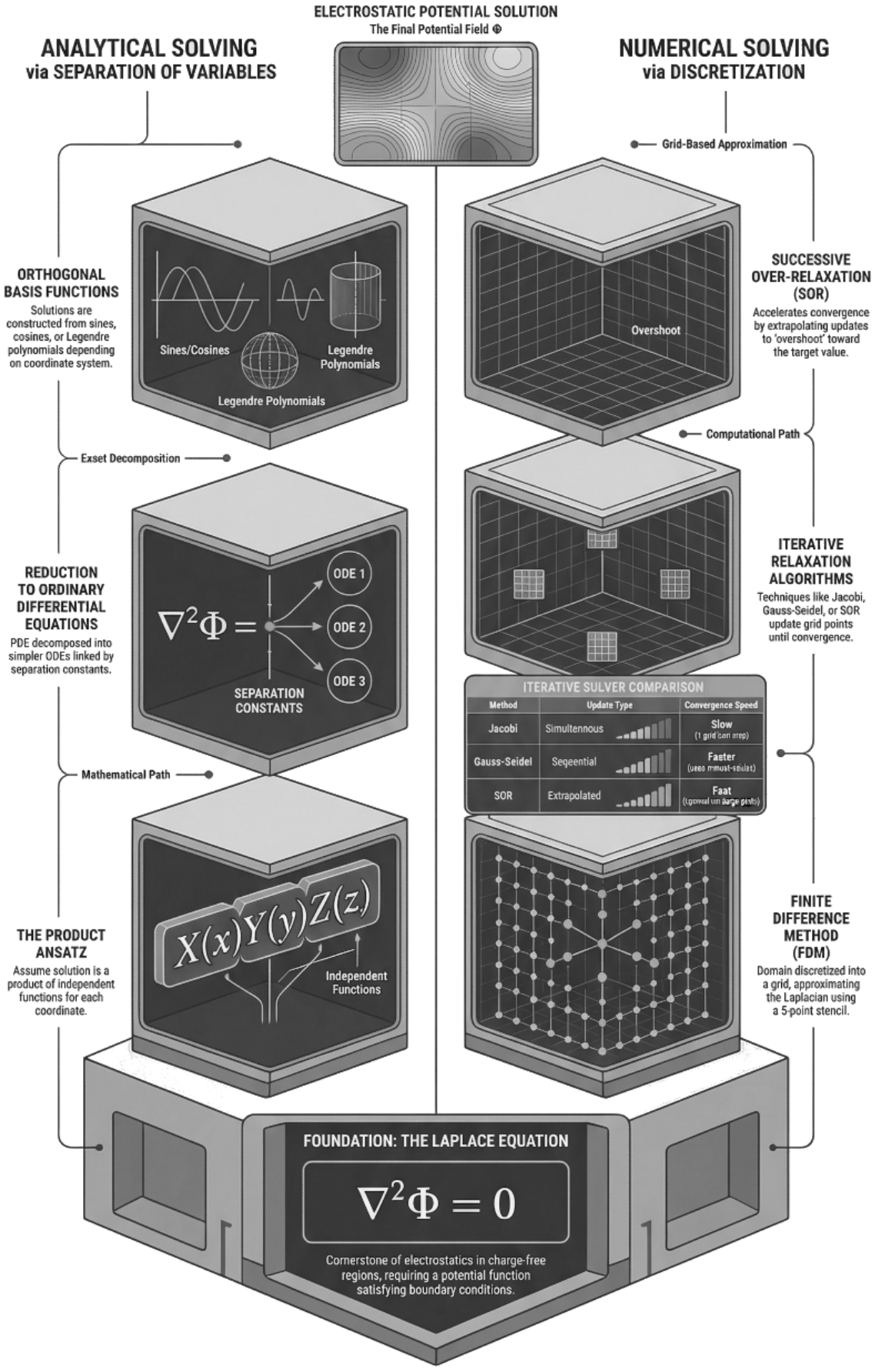

Fig. 4.1 Some standard analytical and numerical methods for solving the Laplace equation.[*Produced by NotebookLM; will be redrawn for resolution and font size.*]

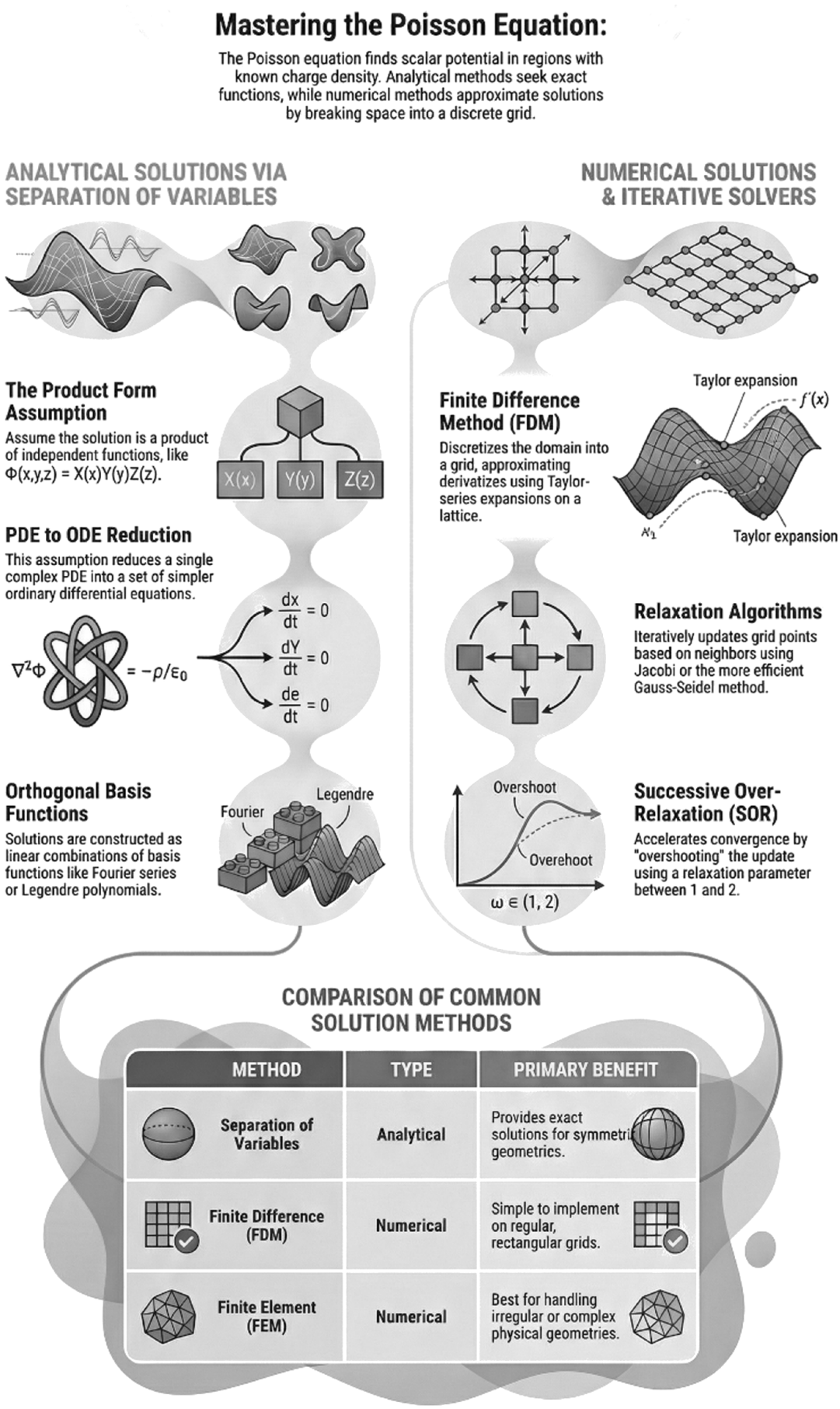

Fig. 4.2 Some common analytical and numerical methods for solving the Poisson equation.

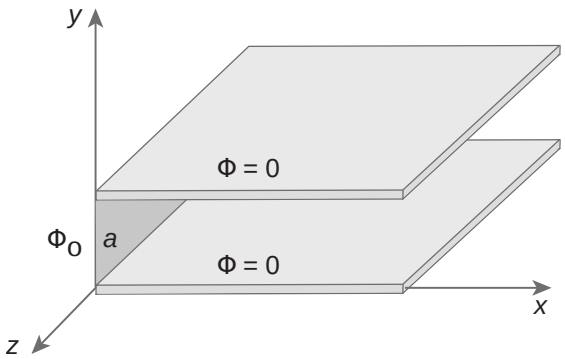

Fig. 4.3 Grounded ($\Phi = 0$) semi-infinite plane-parallel electrodes terminated by a planar electrode at potential Φ_0. The electrodes are assumed to extend infinitely to the right and to be infinite in the direction perpendicular to the page. (Maintaining the difference in potential between the plates at $\Phi = 0$ and $\Phi = \Phi_0$ requires a strip of insulator at the joints.) Adapted from Ref. [25].

subject to the boundary conditions

$$\Phi = 0 \qquad (y = 0,\, y = a), \tag{4.3a}$$

$$\Phi = \Phi_0 \qquad (x = 0), \tag{4.3b}$$

$$\Phi \to 0 \qquad (x \to \infty). \tag{4.3c}$$

Inserting the 2D product function

$$\Phi(x, y) = X(x)Y(y) \tag{4.4}$$

into Eq. (4.2) and dividing through by $\Phi = X(x)Y(y)$ gives

$$\frac{1}{X}\frac{d^2X}{dx^2} + \frac{1}{Y}\frac{d^2Y}{dy^2} = 0, \tag{4.5}$$

where we write the derivatives as ordinary derivatives since $X(x)$ and $Y(y)$ are functions of a single variable. Now the second term of Eq. (4.5) is independent of x and the first term is independent of y, and the two terms must always sum to zero. Thus each term must be equal to a constant C_n,

$$\frac{1}{X}\frac{d^2X}{dx^2} = C_1 \qquad \frac{1}{Y}\frac{d^2Y}{dy^2} = C_2. \tag{4.6}$$

Equation (4.5) then implies that $C_1 + C_2 = 0$, so for later convenience we introduce a new constant k and set $C_1 = k^2$ and $C_2 = -k^2$. Therefore, the problem has been reduced to solving two *ordinary differential equations*

$$\frac{d^2X}{dx^2} - k^2X = 0 \tag{4.7a}$$

$$\frac{d^2Y}{dy^2} + k^2Y = 0. \tag{4.7b}$$

As can be verified by substitution, the second equation (4.7b) has a solution

$$Y = A\sin(ky) + B\cos(ky), \tag{4.8}$$

where A and B are arbitrary constants. We may determine constants by imposing the boundary conditions (4.3). From Eq. (4.3a), $\Phi = 0$ at $y = 0$ requires that $B = 0$, and $\Phi = 0$ at $y = a$ requires that

$$k = \frac{n\pi}{a} \qquad (n = 1, 2, 3, \cdots). \tag{4.9}$$

Therefore,

$$Y = A\sin\left(\frac{n\pi y}{a}\right) \qquad (n = 1, 2, 3, \cdots). \tag{4.10}$$

The equation for X in Eq. (4.7a) now takes the form

$$\frac{d^2X}{dx^2} - \left(\frac{n\pi}{a}\right)^2 X = 0, \tag{4.11}$$

which has a solution

$$X = Ge^{n\pi x/a} + He^{-n\pi x/a}, \tag{4.12}$$

as may be verified by substitution. However, the boundary condition $\Phi \to 0$ as $x \to \infty$ of Eq. (4.3c) can be satisfied only if $G = 0$, so we discard the first term of Eq. (4.12) and insert Eqs. (4.10) and (4.12) into Eq. (4.4) to give

$$\Phi(x, y) = C\sin\left(\frac{n\pi y}{b}\right)e^{-n\pi x/a}, \tag{4.13}$$

with C another arbitrary constant.

The solution (4.13) satisfies the boundary conditions (4.3a) and (4.3c), but does not satisfy the boundary condition (4.3b). However, the Laplace equation is linear, meaning that if $\{\Phi_1, \Phi_2, \Phi_3, \cdots, \Phi_n\}$ satisfy it, then the linear combination

$$\Phi = a_1\Phi_1 + a_2\Phi_2 + a_3\Phi_3 + \cdots + a_n\Phi_n$$

where a_n are arbitrary constants, satisfies it also. Therefore, we take as a better approximation a linear combination of solutions (4.13) in the form

$$\Phi(x, y) = \sum_{n=1}^{\infty} c_n \sin\left(\frac{n\pi y}{a}\right)e^{-n\pi x/a}, \tag{4.14}$$

The boundary condition (4.3b) at $x = 0$ implies that

$$\Phi(0, y) = \Phi_0 = \sum_{n=0}^{\infty} c_n \sin\left(\frac{n\pi y}{a}\right), \tag{4.15}$$

which is a Fourier sine series, so we can exploit the corresponding orthogonality properties to evaluate the coefficients c_n. Specifically, multiply both sides of Eq. (4.15) by $\sin[(pxy)/a]$, where p is an integer, and integrate from $y = 0$ to $y = a$,

$$\int_0^a \Phi_0 \sin\left(\frac{p\pi y}{a}\right)dy = \int_0^a \sum_{n=1}^{\infty} c_n \sin\left(\frac{n\pi y}{a}\right)\sin\left(\frac{p\pi y}{a}\right)dy. \tag{4.16}$$

For the integral on the left side of this equation

$$\int_0^a \Phi_0 \sin\left(\frac{p\pi y}{a}\right) dy = \begin{cases} \dfrac{2a\Phi_0}{p\pi} & (\text{if } p \text{ is odd}), \\ 0 & (\text{if } p \text{ is even}), \end{cases} \tag{4.17}$$

while for the integral on the right side,

$$\int_0^a c_n \sin\left(\frac{n\pi y}{a}\right) \sin\left(\frac{p\pi y}{a}\right) dy = \begin{cases} 0 & (\text{if } p \neq n), \\ \dfrac{a}{2} c_n & (\text{if } p = n), \end{cases} \tag{4.18}$$

Comparing Eqs. (4.17) and (4.18), we conclude that the expansion coefficients are given by

$$c_n = \begin{cases} \dfrac{4\Phi_0}{n\pi} & (\text{if } n \text{ is odd}), \\ 0 & (\text{if } n \text{ is even}), \end{cases} \tag{4.19}$$

and the potential as a function of x and y is

$$\Phi(x,y) = \frac{4\Phi_0}{n\pi} \sum_{n=1,3,5,\cdots}^{\infty} \frac{1}{n} \sin\left(\frac{nxy}{a}\right) e^{-n\pi x/a}. \tag{4.20}$$

This series should converge quickly because of the rapid decrease of the factor $e^{-n\pi x/a}/n$ with n. A convergent power series is a perfectly adequate way to define a solution, but it happens that the series (4.20) can be summed exactly to give the more convenient closed form [33],

$$\Phi(x,y) = \frac{2\Phi_0}{\pi} \tan^{-1}\left(\frac{\sin(\pi y/a)}{\sinh(\pi x/a)}\right), \tag{4.21}$$

This solution is plotted in Fig. 4.4.

Example 4.1 Consider Fig. 4.5, where we wish to calculate the electrostatic potential in the region between the parallel-plane electrodes [25]. There is no z dependence so again let's solve the 2D Laplace equation by separation of variables. This problem has much in common with the example from Fig. 4.3 just worked out, but the boundary conditions are different.

$$\Phi = 0 \qquad (y = 0,\ y = b), \tag{4.22a}$$

$$\Phi = \Phi_1 \qquad (x = 0), \tag{4.22b}$$

$$\Phi = \Phi_2 \qquad (x = a), \tag{4.22c}$$

The most general solution is of the form

$$\Phi(x,y) = \sum_{n=1}^{\infty} \left(A_n e^{-n\pi x/b} + B_n e^{n\pi x/b}\right) \sin\left(\frac{n\pi y}{b}\right), \tag{4.23}$$

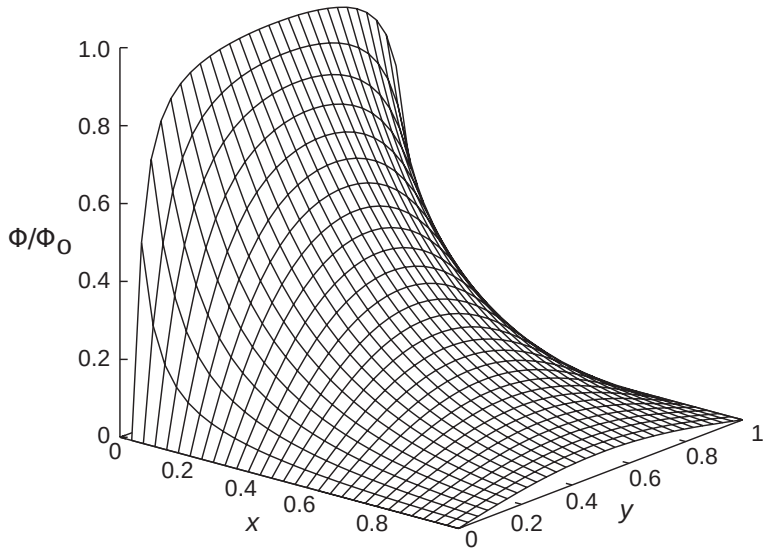

Fig. 4.4 Solution (4.21) of the 2D Laplace equation for the problem in Fig. 4.3, obtained by separation of variables.

where the constants A_n and B_n may be determined using the boundary conditions. As you are asked to show in Problem 4.3, the coefficients A_n and B_n are given by

$$A_n = \frac{4}{n\pi}\left(\frac{\Phi_1 - \Phi_2 e^{-n\pi a/b}}{1 - e^{-2n\pi a/b}}\right) \qquad B_n = \frac{4e^{-n\pi a/b}}{n\pi}\left(\frac{\Phi_2 - \Phi_1 e^{-n\pi a/b}}{1 - e^{-2n\pi a/b}}\right), \tag{4.24}$$

where $n = 1, 3, 5, \cdots$. This gives $\Phi(x, y)$ when inserted in Eq. (4.23). This solution is plotted in Fig. 4.6.

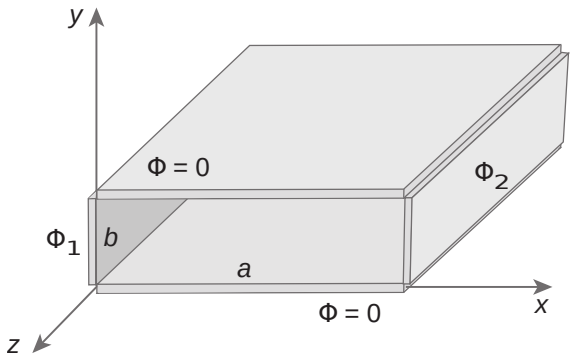

Fig. 4.5 Grounded ($\Phi = 0$) parallel-plane electrodes of width a and separated by a distance b are terminated on two sides with plane electrodes at potentials Φ_1 and Φ_2. The electrodes are assumed to be infinite in the direction perpendicular to the page. Adapted from Ref. [25].

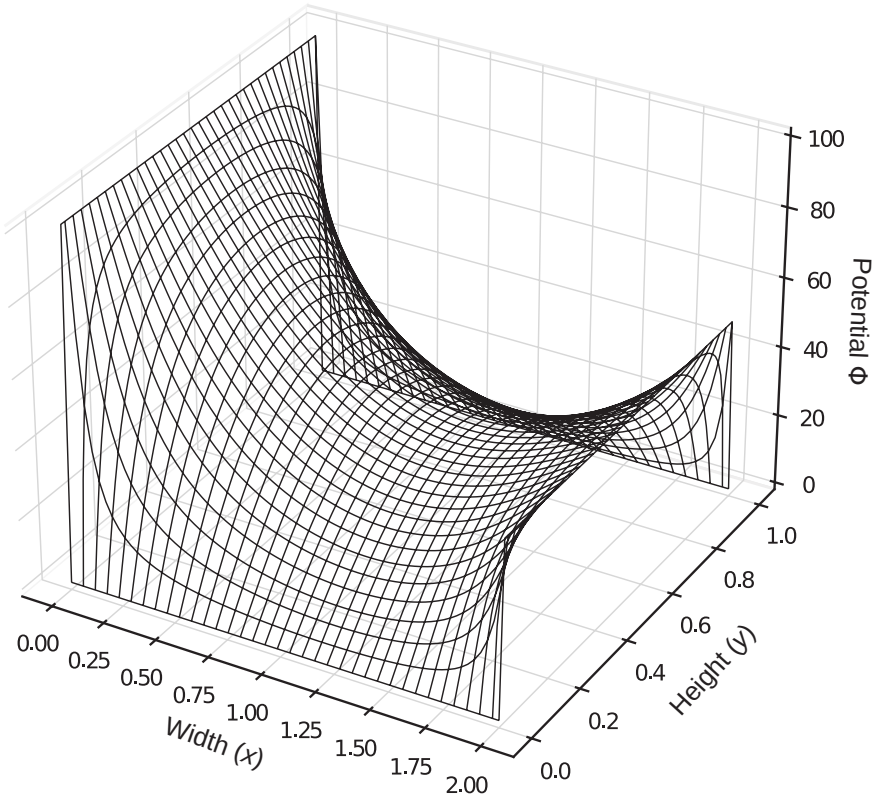

Fig. 4.6 Solution of the 2D Laplace equation for the problem in Example 4.1 and Fig. 4.5. The solution is found by separation of variables in Problem 4.3. This plot was instead made by numerical integration of the Laplace equation corresponding to Problem 4.5.

Notice in Figs. 4.4 and 4.6 the property asserted in Section 3.2.2 that solutions of the Laplace or Poisson equations can have maxima or minima only on the boundaries of the domain, with no local maxima or minima permitted within the volume of the solution.

4.1.2 Separation of Variables in Spherical Coordinates

In the preceding examples of solving the Laplace equation by separation of variables the geometry was rectangular and cartesian coordinates were appropriate. However, for some problems other coordinate systems such as spherical or cylindrical may be more natural. In this section we consider solution of Laplace's equation in spherical coordinates. The Laplace equation in spherical coordinates (r, θ, ϕ) is

$$\frac{1}{r^2}\frac{\partial}{\partial r}\left(r^2\frac{\partial \Phi}{\partial r}\right) + \frac{1}{r^2\sin\theta}\frac{\partial}{\partial \theta}\left(\sin\theta\frac{\partial \Phi}{\partial \theta}\right) + \frac{1}{r^2\sin^2\theta}\frac{\partial^2 \Phi}{\partial \phi^2} = 0, \tag{4.25}$$

To illustrate we will consider problems having axial symmetry (no dependence on ϕ), in which case the Laplacian equation reduces to

$$\frac{\partial}{\partial r}\left(r^2\frac{\partial \Phi}{\partial r}\right) + \frac{1}{\sin\theta}\frac{\partial}{\partial \theta}\left(\sin\theta\frac{\partial \Phi}{\partial \theta}\right) = 0. \tag{4.26}$$

Just as in the cartesian coordinate examples we seek product solutions in which the variables (r, θ) are separated,

$$\Phi(r, \theta) = R(r)\,\Theta(\theta), \tag{4.27}$$

where $R(r)$ is a function only of r and $\Theta(\theta)$ is a function only of θ. Substituting Eq. (4.27) into Eq. (4.26) and dividing through by $R\Theta$ gives,

$$\frac{1}{R}\frac{d}{dr}\left(r^2\frac{dR}{dr}\right) + \frac{1}{\Theta\sin\theta}\frac{d}{d\theta}\left(\sin\theta\frac{d\Theta}{d\theta}\right) = 0, \tag{4.28}$$

where now we use total derivatives rather than partial derivatives since the functions being differentiated are functions of a single variable. By similar logic as in the cartesian case, the second term in Eq. (4.28) is independent of r so the first term must also be independent of r. Thus we write the separated equations as two ordinary differential equations

$$\frac{1}{R}\frac{d}{dr}\left(r^2\frac{dR}{dr}\right) = k \tag{4.29a}$$

$$\frac{1}{\Theta\sin\theta}\frac{d}{d\theta}\left(\sin\theta\frac{d\Theta}{d\theta}\right) = -k \tag{4.29b}$$

where the constants are written as k and $-k$, since the sum of the two equations must be zero.

Consider first the R equation in Eq. (4.29a). Multiplying both sides by R and carrying out the leftmost d/dr operation gives

$$r^2\frac{d^2R}{dr^2} + 2r\,\frac{dR}{dr} - kR = 0, \tag{4.30}$$

which has a solution

$$R = Ar^n + \frac{B}{r^{n+1}}, \tag{4.31}$$

that when inserted in Eq. (4.29a) requires n and k to be related by,

$$n(n+1) = k. \tag{4.32}$$

Now consider the Θ equation (4.29b). Multiplying by $\Theta\sin\theta$ and using Eq. (4.32), it may be written

$$\frac{d}{d\theta}\left(\sin\theta\frac{d\Theta}{d\theta}\right) + n(n+1)\sin\theta\,\Theta = 0 \tag{4.33}$$

It is convenient to change variables by letting $\mu = \cos\theta$. By the chain rule, for any function $f(\mu)$ of μ,

$$\frac{df}{d\theta} = \frac{df}{d\mu}\frac{d\mu}{d\theta} = -\sin\theta\frac{df}{d\mu} = -\sqrt{1-\mu^2}\,\frac{df}{d\mu} \tag{4.34}$$

where we have used $d\mu/d\theta = -\sin\theta$ and $1-\mu^2 = \sin^2\theta$. Then, Eq. (4.33) becomes

$$\frac{d}{d\mu}\left[(1-\mu^2)\frac{d\Theta}{d\mu}\right] + n(n+1)\Theta = 0 \qquad \text{(Legendre's equation).} \tag{4.35}$$

This is called *Legendre's equation* and its solutions are polynomials in $\cos\theta$ called *Legendre*

Table 4.1 Legendre polynomials $P_n(\cos\theta)$

n	$P_n(\cos\theta)$
0	1
1	$\cos\theta$
2	$\frac{1}{2}(3\cos^2\theta - 1)$
3	$\frac{1}{2}(5\cos^3\theta - 3\cos\theta)$
4	$\frac{1}{8}(35\cos^4\theta - 30\cos^2\theta + 3)$
5	$\frac{1}{8}(63\cos^5\theta - 70\cos^3\theta + 15\cos\theta)$

polynomials, designated by $P_n(\cos\theta)$, where n is termed the order of the polynomial. [1] Letting $\cos\theta \equiv x$, normalized Legendre polynomials[2] are typically defined by *Rodrique's formula*

$$P_n(x) = \frac{1}{2^n n!}\frac{d^n}{dx^n}(x^2-1)^n. \tag{4.36}$$

Some low-order Legendre polynomials are tabulated in Table 4.1. A general solution of Laplace's equation in spherical coordinates assuming axial symmetry is then given by

$$\Phi(r,\theta) = \sum_{n=0}^{\infty} A_n r^n P_n(\cos\theta) + \sum_{n=0}^{\infty} B_n r^{-(n+1)} P_n(\cos\theta) \tag{4.37}$$

The Legendre polynomials form a complete set, so arbitrary boundary conditions for problems with axial symmetry can be satisfied using them. Furthermore, they satisfy the orthogonality condition

$$\int_{-1}^{+1} P_m(x)P_n(x)dx = \frac{2}{2n+1}\,\delta_{mn}, \tag{4.38}$$

or expressed explicitly in spherical coordinates,

$$\begin{aligned}\int_{-1}^{+1} P_m(\cos\theta)P_n(\cos\theta)d(\cos\theta) &= \int_0^{\pi} P_m(\cos\theta)P_n(\cos\theta)\sin\theta d\theta \\ &= \frac{2}{2n+1}\,\delta_{mb} = \begin{cases} \dfrac{2}{2n+1} & (\text{if } m=n,) \\ 0 & (\text{if } m\neq n),\end{cases}\end{aligned} \tag{4.39}$$

[1] Mathematically, Legendre's differential equation (4.35) arises naturally from solution of the Laplace and related partial differential equations using separation of variables in spherical coordinates. The eigenfunctions of the angular part of the Laplacian operator acting on Φ on the left side of Eq. (4.25) are spherical harmonics (see Section 3.8.1); modulo multiplicative constants, Legendre polynomials are the subset of spherical harmonics left invariant by rotations about the polar axis. Viewed in this way, the Legendre polynomials are intimately connected to rotational symmetry. Indeed, many of their properties are found most easily using symmetry and group theory methods, which in turn implies that they have deep physical and geometrical meaning.

[2] The normalization is chosen to make all Legendre polynomials equal to one at $\cos\theta = 1$.

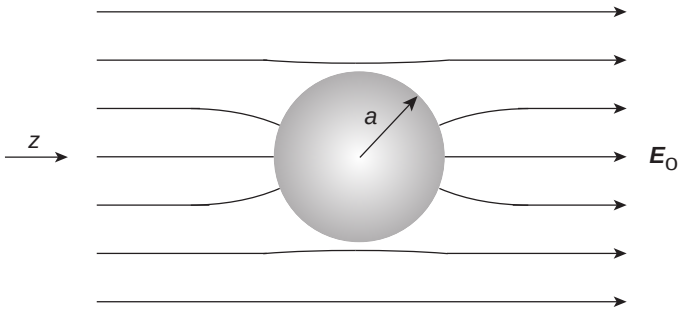

Fig. 4.7 A conducting sphere of radius a in an external electric field $\boldsymbol{E}_0$ directed along the $\boldsymbol{z}$ axis, with axial symmetry assumed around the z axis.

which are important in evaluating the coefficients in the expansion Eq. (4.37).

Example 4.2 Consider the conducting sphere of radius a in an electric field illustrated in Fig. 4.7. Inside the sphere the field will be zero, far outside it will be the undisturbed field $\boldsymbol{E}_0$, and near the sphere the field will be distorted by polarization. Let's solve the 2D Laplace equation for the exterior field by separation of variables in spherical coordinates, assuming axial symmetry. We take as boundary conditions

$$\Phi = 0 \qquad (r = a) \tag{4.40a}$$

$$\Phi = -E_0 r\cos\theta \qquad (r = \infty) \tag{4.40b}$$

At the radius of the sphere $r = a$, from Eqs. (4.37) and (4.40a)

$$\Phi(r,\theta) = \sum_{n=0}^{\infty} A_n r^n P_n(\cos\theta) + \sum_{n=0}^{\infty} B_n r^{-(n+1)} P_n(\cos\theta) = 0. \tag{4.40c}$$

The coefficients A_n and B_n may be evaluated using the orthogonality relation (4.39) for the Legendre polynomials. Multiplying Eq. (4.40c) by $P_m(\cos\theta)$ and integrating over $d(\cos\theta)$, from Eq. (4.39) the only non-vanishing terms are those for which $n = m$, implying that

$$\begin{aligned} 0 &= A_n a^n \int_{-1}^{+1} P_n^2(\cos\theta) d(\cos\theta) + B_n a^{-(n+1)} \int_{-1}^{+1} P_n^2(\cos\theta) d(\cos\theta) \\ &= A_n a^n \left(\frac{2}{2n+1}\right) + B_n a^{-(n+1)} \left(\frac{2}{2n+1}\right), \end{aligned}$$

which requires the coefficients to be related by

$$B_n = -A_n a^{2n+1}. \tag{4.41}$$

Therefore, from Eqs. (4.40c) and (4.41),

$$\Phi(r,\theta) = \sum_{n=0}^{\infty} A_n \left(r^n - \frac{a^{2n+1}}{r^{n+1}}\right) P_n(\cos\theta). \tag{4.42}$$

Now as $r \to \infty$ the second term in parentheses in Eq. (4.42) becomes negligible compared with the first and the boundary condition (4.40b) requires that

$$-E_0 r\cos\theta = -E_0 r P_1(\cos\theta) = \sum_{n=0}^{\infty} A_n r^n P_n(\cos\theta), \tag{4.43}$$

where we have used $P_1(\cos\theta) = \cos\theta$ from Table 4.1. Thus, the only non-zero term on the right side is $n = 1$, implying that

$$A_1 = -E_0,$$

with all other $A_n = 0$. Then from Eq. (4.41) all the B_n are zero except for

$$B_1 = -A_1 a^3 = E_0 a^3,$$

and the potential at any point (r, θ) is given by

$$\begin{aligned}\Phi(r,\theta) &= -E_0 r\cos\theta + E_0\frac{a^3\cos\theta}{r^2} \\ &= -E_0\left(1 - \frac{a^3}{r^3}\right) r\cos\theta,\end{aligned} \tag{4.44}$$

where the first term is the potential corresponding to the applied field E_0 and the second term is the induced polarization potential. The electric field components follow from Eq. (4.44) by taking the gradient [see Eq. (A.48) for the gradient in spherical coordinates],

$$E_r = -\frac{\partial\Phi}{\partial r} = E_0\left(1 + \frac{2a^3}{r^3}\right)\cos\theta, \tag{4.45}$$

$$E_\theta = -\frac{1}{r}\frac{\partial\Phi}{\partial\theta} = -E_0\left(1 - \frac{a^3}{r^3}\right)\sin\theta. \tag{4.46}$$

At the surface of the conductor we know that

$$E_r|_{r=a} = \frac{\sigma}{\epsilon_0},$$

so solving for σ and using Eq. (4.45) with $r = a$ gives

$$\sigma = 3\epsilon_0 E_0\cos\theta, \tag{4.47}$$

for the induced charge density.

4.1.3 Separation of Variables in Cylindrical Coordinates

This section is under construction.

4.2 Variational Methods

This section is under construction.

4.3 Solution by Numerical Methods

While the traditional emphasis of a book such as this one has been on analytical solutions, problems that are tractable by analytical means are often made so by invoking assumptions that are only approximately justified:

- capacitor plates of infinite extent,
- solenoids of infinite length,
- matter of simplified structure and uniform distribution,
- oversimplified boundary conditions, ...

But problems in the real world often don't conform to these restrictions. Furthermore, both desktop-level and high-performance computing platforms have made rapid advances

1. in speed and efficiency, and
2. in development of programming tools that make it increasingly easier to bend computers to the will of physicists.

Most dramatic in the latter category is the use of generative AI to write and debug code for numerical solution of classical electromagnetic problems that would be very difficult to solve analytically (see Appendix E). In this book we have taken a unified modern view that one should understand how to solve problems analytically, but one should also develop the ability to solve more complicated problems numerically.

In Section 3.4.2 we listed concisely some standard numerical approaches to solving electromagnetic problems. In this section we expand that into an overview of the dominant numerical methods and the computational optimizations essential for handling complex E&M systems. Presenting these methods with a focus on modern computational paradigms like adaptive mesh integration and vectorization and parallelization bridges the gap between abstract theory and practical physics. For the static and quasistatic fields emphasized in these initial chapters,[3] we are primarily concerned with solving the Poisson equation, or its charge-free counterpart, the Laplace equation. Some more technical aspects of these solutions are discussed in Appendix F and we shall address numerical methods for more general time-dependent problems in Section 15.3.

4.3.1 The Finite Difference Method

Finite difference methods (FDM) are the most intuitive numerical approach to solving differential equations numerically. They involve

- discretizing the continuous domain into a regular grid and
- approximating the Laplacian operator using Taylor series expansions on that grid.

[3] See Section 10.2.1 for a definition of quasistatic limits.

In 2D Cartesian coordinates, the discrete update equation using the Jacobi relaxation method for the Poisson equation (see the discussion of iterative solvers in Appendix F.1) takes the form,

$$\Phi_{i,j}^{(k+1)} = \frac{1}{4}\left(\Phi_{i+1,j}^{(k)} + \Phi_{i-1,j}^{(k)} + \Phi_{i,j+1}^{(k)} + \Phi_{i,j-1}^{(k)}\right) + \frac{\Delta^2}{4\epsilon_0}\rho_{i,j}, \tag{4.48}$$

where k is the iteration index, Δ is the grid spacing, and $\Phi_{i,j}^{(k)}$ denotes the solution at the gridpoint (i,j) after the kth iteration. The Jacobi method is conceptually simple but its convergence to a solution is typically slow and standard solvers usually implement *Successive Over-Relaxation (SOR)*, which accelerates convergence by extrapolating the newly computed value using an an empirically chosen over-relaxation parameter (see the discussion in Appendix F.2).

4.3.2 Finite Element Method

The *finite element method (FEM)* is a standard approach for more complex problems such as

- waveguides,
- cavities, or
- boundaries for topological insulators,

that may not conform neatly to rectangular or cylindrical grids. Instead of discretizing the differential equation directly, FEM relies on the variational principle (see Section 4.2), and minimizes the electrostatic energy functional over the domain.

1. The starting point for the finite element method is typically to replace the differential equation written in its normal "strong form" with its weak or variational form, as described in Appendix F.5.
2. The region is broken down into a mesh of unstructured elements (typically triangles or tetrahedrons).
3. The potential Φ is approximated as a linear combination of localized basis functions.
4. This transforms the PDE into a large, usually sparse,[4] system of linear algebraic equations: $A\boldsymbol{x} = \boldsymbol{b}$, which can be solved efficiently by the highly optimized linear algebra packages found on all modern computers.

Problem 14.5 illustrates a numerical FEM solution of a waveguide problem, with the solution displayed in Fig. 14.3. The constant triangular mesh that was used in this solution is shown in Fig. 4.8. Note that the entire rectangular area corresponding to the waveguide is covered by tiny triangles.

[4] A *sparse matrix* is one in which the large majority of entries are equal to zero. There are specialized algorithms that can greatly expedite sparse-matrix solutions relative to generic matrix solvers (for example, the *Python* sparse-matrix solver `scipy.sparse`). Conversely, a dense matrix is one with many non-zero entries. Other things being equal, equations containing dense matrices typically cannot be solved as fast as those with sparse matrices, and problems containing dense matrices tend to scale much more poorly with problem size than those involving sparse matrices.

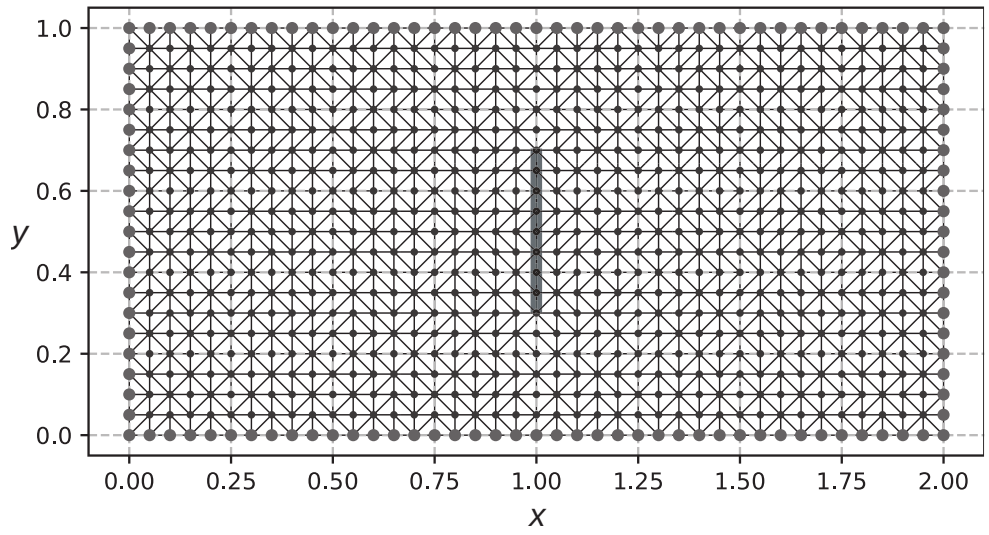

Fig. 4.8 Constant triangular mesh used in the FEM calculation of Fig. 14.3. Nodes are indicated by dots (larger dots on the outer edges where Dirichlet constraints are applied). The vertical dark gray line indicating a slice of the mesh at $x = 1$ and $y = 0.30 - 0.75$ will be used in Fig. 4.9 below.

The finite element method typically starts by replacing the PDE to be integrated with a weak form that has only C^1 or C^2 continuity. For example, in Problem 14.5, the FEM solution begins by constucting the weak form of Poisson's equation for an element e as

$$\sum_j \Phi_j \int_e \boldsymbol{\nabla} N_i \cdot \boldsymbol{\nabla} N_j \, d\Omega = \int_e \frac{\rho}{\epsilon_0} N_i \, d\Omega,$$

where N_i and N_j are linear shape functions on a triangular element. This weak form is only C^0 continuous, which implies that on each triangular element of the mesh in Fig. 4.8 the potential is continuous across boundaries between triangles, but the electric field, which is proportional to the gradient of the potential, is constant over a mesh element but discontinuous at the boundaries of mesh elements. This is illustrated in Fig. 4.9.

4.3.3 Boundary Element Method (BEM)

When dealing with open boundary problems (where fields extend to infinity), or problems where the sources are strictly located on surfaces (like perfect conductors), the boundary element method (BEM) [also termed the *method of moments (MOM)*; see Section 15.3.2], is highly efficient.

> The boundary element method relies on *Green's theorem* to recast the differential volume problem into an integral surface problem.

Then one need only discretize the boundaries (surfaces) of the objects, not the empty

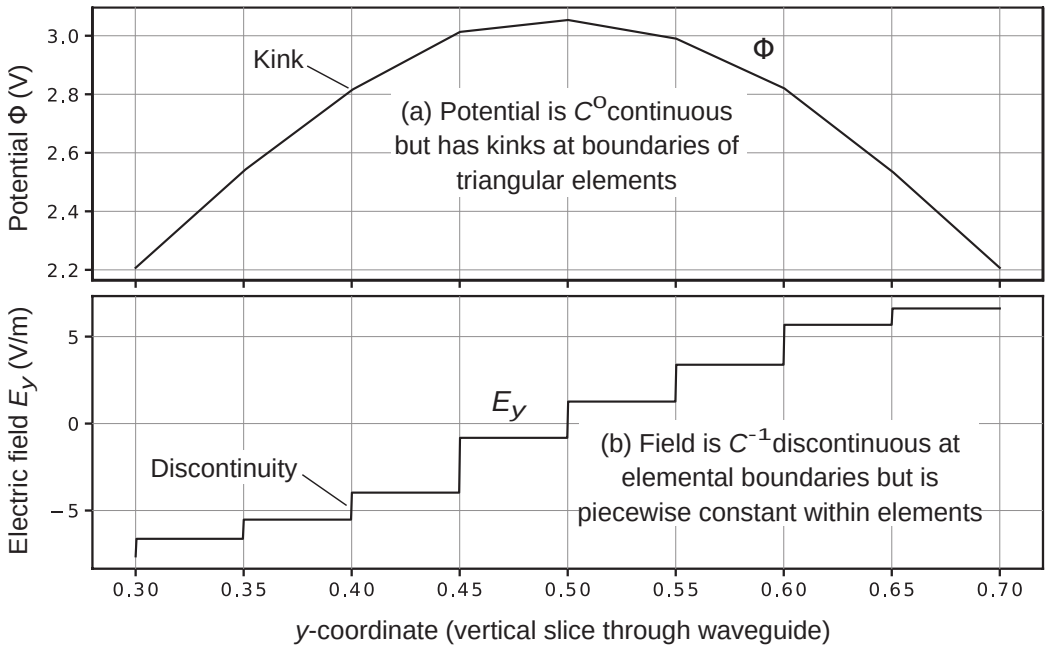

Fig. 4.9 A vertical slice through the waveguide FEM mesh in Fig. 4.8. From Fig. 4.8 each triangle has a vertical height of 0.05, so each vertical gray line in the y-coordinate of these graphs corresponds to the boundary of a triangular element. (a) The potential Φ is continuous with constant slope within elements, but has kinks (change in slope) at each elemental boundary; a kink in Φ is marked at $y = 0.40$. (b) The electric field $\boldsymbol{E}$ is constant within elements but discontinuous at elemental boundaries, since it is minus the gradient of the potential; a discontinuity in E_y is marked at $y = 0.40$.

volume of space around them. This converts a 3D problem into a 2D surface problem, greatly reducing the number of unknowns, though it results in a dense matrix rather than a sparse one.

4.4 Algorithmic Optimizations

In addition to the raw power increase as computers have evolved, various algorithmic optimizations have been introduced that can greatly increase the throughput for numerical simulation in E&M and other scientific problems. This is particularly important for languages like *Python* that are intepreted rather than compiled, and therefore are not intrinsically very fast.

4.4.1 Vectorization

When developing solvers such as those described above in high-level interpreted environments like *Python*, explicit loops over large spatial grids will inhibit performance substan-

tially. Vectorization leverages optimized compiled backends through *Python* libraries like `NumPy` to execute operations across entire arrays simultaneously using *Single Instruction, Multiple Data (SIMD)* architecture, as described in Box 4.1.

Example 4.3 In a 2D Jacobi iteration, instead of executing sequential nested loops, the entire interior grid can be updated in one fell vectorized swoop using array slicing techniques (See Appendix F.1 for a description of the Jacobi iteration procedure).

The *Python* implementation of vectorization is much faster than typical non-vectorized *Python* implementations for several basic reasons.

1. *Minimal interpreter overhead:* It avoids type-checking and dynamic dispatch for a multitude of element.
2. *Access to contiguous memory:* `NumPy` arrays occupy a flat, sequential block of memory, allowing the processor to stream data directly into vector registers.
3. *Hardware-level SIMD:* Under the hood, the underlying C library loads multiple 64-bit doubles into vector registers, performing the required arithmetic in parallel at the hardware level.

Thus for compute-intensive tasks, it will often be advantageous in Python code to invoke vectorization.

4.4.2 Parallelization and Domain Decomposition

For high-resolution 3D problems, single-core execution is too slow and it is necessary to leverage parallel execution (subtasks running simultaneously rather than sequentially) on multiple computing cores.

Shared Memory (OpenMP): Useful for distributing loop iterations (or array operations) across multiple CPU cores on a single machine.

Distributed Memory (MPI): For massive grids, the physical domain is divided into subdomains (*Domain Decomposition*). Each node computes its local interior and only exchanges boundary data with adjacent nodes at the end of each iteration step.

GPU Acceleration: The matrix operations required in finite difference method (FDM) and finite element method (FEM) calculations are inherently highly parallelizable. Utilizing

Box 4.1 SIMD Architecture

A SIMD (*single instruction, multiple data*) architecture allows a CPU or GPU to execute a single instruction on multiple data points simultaneously, which may be contrasted with the usual SISD (*single instruction single data*) approach.

SIMD versus SISD

Suppose we wish to add two arrays of 4 numbers each (a total of 4 pairwise addition operations).

1. *Traditional SISD:* The processor must execute an `ADD` command, fetching and calculating 4 pairs of numbers sequentially.
2. *SIMD:* The processor loads all 4 pairs of numbers into a special wide *vector register* and executes a single vector `ADD` command that adds all 4 pairs at essentially the same time.

Neglecting small overheads, SIMD is 4 times faster for this simple example.

Use Cases

Generally, SIMD shines for workloads that are *data-parallel*, meaning that the same mathematical operation is being applied to each member of a massive dataset. Modern processors implement SIMD using dedicated hardware blocks and ultra-wide registers called *vector registers* able to handle large amounts of data at once. However SIMD isn't effective for all computing problems. Two issues can cause SIMD implementations to struggle.

1. *Conditional branching friction:* If a large amount of `if-else` conditional logic must be processed, this can force compiler work-arounds that compromise the parallel processing in vectorized loops.
2. *Memory alignment:* Efficient loading of data into vector registers requires data to be structured contiguously in memory; scattered or poorly aligned data layouts can negate the vectorization speedup.

If these issues are present, SIMD may afford no significant advantages.

Writing Efficient SIMD Code

In summary, the key guidelines for writing efficient SIMD code (in *Python* or any language) are that one should

1. organize data *highly contiguously in memory*,
2. avoid loop dependencies (step i depends on results from step $i-1$), and
3. minimize conditional branching (`if-else` statements).

Python code written with strict attention to these rules can often execute orders of magnitude faster than a code solving the same problem by executing sequential loops over arrays.

graphical processing units (GPUs)[5] allows thousands of cores to compute node updates simultaneously, offering orders-of-magnitude speedups for dense linear algebra problems.

4.4.3 Efficient Grid Points and Integration Steps

Uniform numerical spatial grids can be computationally wasteful because high resolution is required only where gradients are large or quantities are changing rapidly. Likewise, constant numerical integration timesteps are easy to implement but are often computationally wasteful because accuracy and stability limitations on the optimal size of an integration timestep can vary by large amounts over the course of an integration. Numerical simulations can be made much more efficient by employing spatial grids and integration timesteps that adapt automatically to local spatial and temporal conditions. Modification of the spatial grid in response to local conditions in a numerical simulation is called *adaptive mesh refinement*, and a corresponding modification of the timestep size is called *adaptive quadrature*.

Adaptive Mesh Refinement (AMR) in PDE Solvers: Algorithms dynamically subdivide the spatial grid in regions of high error or steep gradients (near point charges, sharp corners, or domain boundaries) while keeping a coarse mesh in regions where the field is smooth.

Adaptive Quadrature in Integral Solvers: In direct numerical integrations, adaptive integration step sizes automatically adjust the step width based on the local curvature of the integrand, ensuring precision near singularities without wasting compute cycles in empty space.

These numerical methods and optimization strategies are discussed further in Appendices E and F, and are exhibited in the *Numerical and GenAI Problems* sections of the exercises at the end of each chapter.

Background and Further Reading

An introduction to the material of this chapter may be found in Griffiths [33] or Purcell and Morin [62]. More advanced treatments may be found in Jackson [41], Garg [31], Chaichian et al [23], and Zangwill [77].

[5] *Graphical processing units (GPUs)* were developed for the fast update of video-screen pixels required for smooth motion graphics, but it was quickly realized that they excel at a variety of computational tasks. A GPU is a massively parallel processor that can execute many *lightweight threads* (subprocesses requiring a limited number of computational steps and limited fast memory) in parallel with high efficiency. If a large computing problem can be factored into many lightweight tasks that can run in parallel, it can be executed very quickly on a GPU. Many linear algebra problems fall into this category and they often can be computed very efficiently with GPUs. On the fastest current supercomputers, often 90% or more of their benchmark speed is provided by their GPUs.

Problems

4.1 A surface charge density specified by a function $\sigma(\theta)$ is pasted onto an empty 3D spherical shell of radius R. Assume axial symmetry and use separation of variables in the Laplace equation to derive a general formula for the potential Φ as a function of $\sigma(\theta)$ inside and outside the shell radius R.

4.2 One form of *Earnshaw's theorem* (see Section 3.2.1) states that, for any electric field $\boldsymbol{E}$, the average of the scalar potential Φ over any sphere that lies entirely in a charge-free region is equal to the value of the potential at the center of the sphere. For a charge Q outside a sphere of radius $r_0 = |\boldsymbol{r}|$ as in the following diagram,

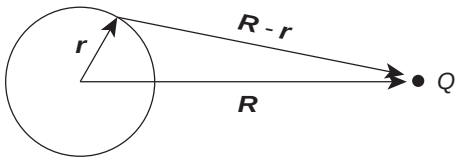

the potential averaged over the sphere $\langle\Phi\rangle$ is given by

$$\langle\Phi\rangle = \frac{1}{4\pi r_0^2}\int \frac{1}{4\pi\epsilon_0}\frac{Q}{|\boldsymbol{R}-\boldsymbol{r}|}\, r^2\delta(r-r_0)dr\, d\Omega.$$

This could be integrated directly, but instead prove Earnshaw's theorem by evaluating the integral using the spherical harmonic expansion

$$\frac{1}{|\boldsymbol{x}-\boldsymbol{x}'|} = 4\pi\sum_{l=0}^{\infty}\sum_{m=-l}^{l}\frac{1}{2l+1}\frac{r_<^l}{r_>^{l+1}}\, Y_{lm}^*(\theta',\phi')Y_{lm}(\theta,\phi),$$

given in Eq. (3.57). ***

4.3 Consider the following figure,

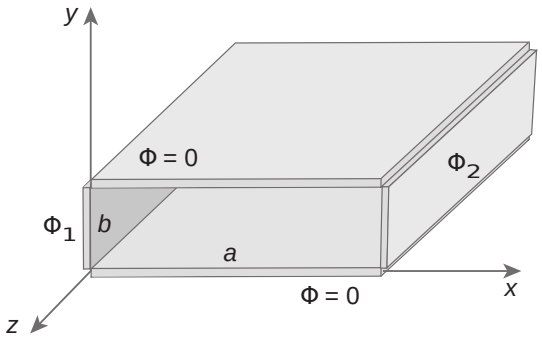

which illustrates grounded ($\Phi = 0$) parallel-plane electrodes of width a and separated by a distance b, which are terminated on the left and right sides with plane electrodes at potentials Φ_1 and Φ_2, and the top and bottom sides are held at potentials $\Phi = 0$. The electrodes are assumed to be infinite in the direction perpendicular

to the page. Calculate the potential in the region between the parallel-plane electrodes.

4.4 Assume a sphere of radius R parameterized by spherical coordinates (r, θ, ϕ), with a surface charge layer of density

$$\sigma(\theta) = kP_1(\cos\theta) = k\cos\theta,$$

where k is a constant and $P_1(\cos\theta)$ is a Legendre polynomial. Use the Laplace equation assuming axial symmetry (no ϕ dependence) to find expressions for the potential $\Phi(r, \theta)$ inside and outside of R. *Hint*: This problem will be easy if you work Problem 4.1 first. ***

Numerical and GenAI Problems

4.5 We solved Problem 4.3 by separation of variables. Prompt your *GenAI* to solve the same problem by numerical integration of the Laplace equation and reproduce the plot displayed in Fig. 4.6.

5 Electrostatics in Conducting Matter

There are a number of categories for the classification of matter in materials science. One of the most fundamental distinctions is between[1]

1. *insulators* (often termed *dielectrics* in electromagnetism), which correspond to matter having charge carriers that are tightly bound and do not transport electrical charge well, and
2. *conductors*, which have delocalized charge carriers that are free to transport electrical charge efficiently; conductors are also often called *metals*.

In atomic matter the charge carriers are typically electrons, electron holes, or ions, but for purposes of being definite in discussion, we shall normally assume electrons to be the charge carriers, unless otherwise stated.

5.1 Properties of Conductors

The extremely high mobility of charge carriers in good conductors underlies much of their basic behavior. A good conductor is expected to exhibit the following properties (see Problem 2.3),[2]

1. electric fields and electric charge density vanish inside a conductor;
2. if a conductor has any excess charge, it must reside on its surface;
3. any exterior electric field is normal to the surface of a conductor;
4. a conductor is an equipotential (all interior regions have the same electrical potential);
5. if the conductor has an irregular shape, any surface charge density will be concentrated in regions where curvature is largest.

Let us now discuss these properties of a good conductor in a little more detail.

[1] There are also things in between such as *semimetals* or *semiconductors* that transport charge poorly, or transport it only under certain conditions, some insulating materials like *Mott insulators* or *topological insulators* that have mechanisms different from those governing simple insulators, or *superconductors* that do a super job of carrying current without resistance. We will leave finer details of classification to materials science for now and concentrate on the electromagnetic behavior of simple and idealized conductors and insulators.

[2] We are assuming that the conductor in question is in equilibrium; brief transients violating these expected properties are possible if equilibrium is disturbed.

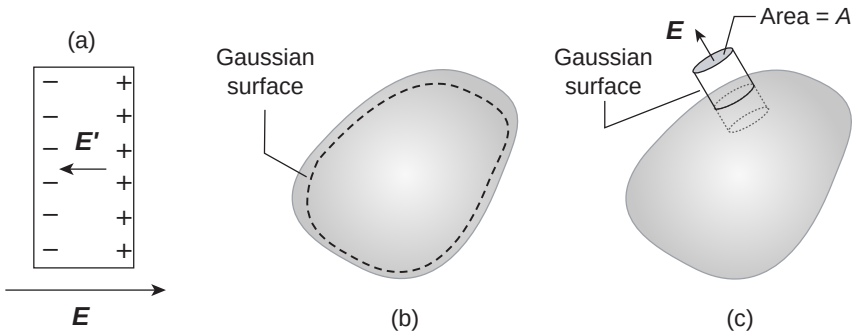

Fig. 5.1 (a) Conducting slab in a uniform electric field $\boldsymbol{E}$. (b) Gaussian surface (dashed curve) inside a conductor. (c) Cylindrical Gaussian surface perpendicular to the surface of a conductor.

5.1.1 Electric Fields Vanish Inside a Conductor

Intuitively, $\boldsymbol{E} = 0$ inside a conductor because if there were an electric field inside the conductor it would accelerate electrons, violating the assumption of electrostatic equilibrium. More precisely, consider Fig. 5.1(a) where a conducting slab is immersed in an external electric field $\boldsymbol{E}$ oriented horizontally. Initially the external field will attract negative charges to the left side of the slab, leaving a net positive charge on the right side. This *polarization of charge* within the slab will create an internal electric field $\boldsymbol{E}'$ that opposes the external field $\boldsymbol{E}$ (remember the convention that the electric field vector points from positive to negative charge). This piling up of negative charges on one side and positive charges on the opposite side in response to application of an external electric field is called an *induced charge*. Charge will continue to flow within the slab until the induced internal electric field $\boldsymbol{E}'$ exactly cancels the external field $\boldsymbol{E}$, leaving a net zero electric field inside the conductor. Because this is a conductor the charge carriers are extremely mobile and the generation of internal fields that oppose and cancel the external field typically occurs on a timescale sufficiently short that usually it can be assumed to be instantaneous.

5.1.2 Charge Density Is Zero Inside a Conductor

Just as the electric field vanishes inside a conductor, the charge density ρ is also zero there. Consider the Gaussian surface shown in Fig. 5.1(b). From Gauss's law with zero internal electric field (Point 1 above),

$$\oint_S \boldsymbol{E} \cdot \boldsymbol{n}\, da = \oint_S 0 \cdot \boldsymbol{n}\, da = 0 = \frac{Q}{\epsilon_0},$$

where Q is the total charge enclosed by the surface. Hence the absence of an electric field means necessarily that the charge density $\rho = 0$ inside a conductor.

5.1.3 Excess Charge Resides on the Surface

That any excess charge must reside at the surface of the conductor is a consequence of Gauss's law and follows immediately from the requirement that $\rho = 0$ inside the conductor. Since the Gaussian surface (dashed curve) in Fig. 5.1(b) can be place arbitrarily close to the surface, it follows that any excess charge can exist only at the surface of a conductor.

5.1.4 Any Exterior Electric Field is Normal to the Surface

No electric field exists inside a conductor; if any electric field exists *outside an isolated conductor* it is necessarily

- generated by the excess surface charge, and is
- perpendicular to the surface of the conductor.

Consider Fig. 5.1(c), where a cylindrical Gaussian surface has been placed with the end faces parallel to the surface of the conductor that is partially inside and partially outside the conductor. If at a point on the surface the electric field $\boldsymbol{E}$ had a component tangent to the surface of the conductor, this would cause electrons to move along the surface and disturb electrostatic equilibrium.

1. Thus $\boldsymbol{E}$ is perpendicular the the surface of the conductor and there is no flux through the curved part of the Gaussian cylinder.
2. There also is no flux through the flat face of the cylinder *inside the conductor*, because $\boldsymbol{E}$ is zero there.

Hence any net flux passes only through the flat face of the Gaussian cylinder outside the conductor. Applying Gauss's law to this surface,

$$\oint_S \boldsymbol{E}\cdot\boldsymbol{n}\,da = \int_{\text{base}} |\boldsymbol{E}|da = EA = \frac{Q}{\epsilon_0} \quad\longrightarrow\quad E = \frac{Q}{\epsilon_0 A} = \frac{\sigma}{\epsilon_0}$$

where $\sigma = Q/A$ is the surface charge density and A is the area of the endplate of the cylinder. It follows that any electric field

1. must lie *outside the conductor*,
2. must have a *magnitude proportional to the surface charge density*, and
3. must have an *orientation that is normal locally to the surface.*

5.1.5 A Conductor is an Equipotential

A conductor necessarily has the same same potential Φ at each point in the conductor. This follows immediately because for any two points either within the conductor or on its surface,

$$\Phi(\boldsymbol{A}) - \Phi(\boldsymbol{B}) = -\int_{\boldsymbol{A}}^{\boldsymbol{B}} \boldsymbol{E}\cdot d\boldsymbol{l} = 0,$$

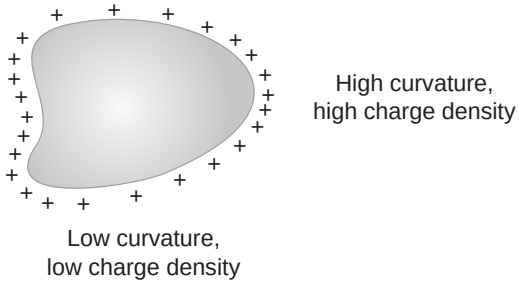

Fig. 5.2 Curvature and distribution of local surface charge for a conductor. Charge accumulates where curvature of the surface is largest.

because we have established previously that $\boldsymbol{E} = 0$ in the interior and on the surface.

5.1.6 Surface Charge Density and Curvature

If a conductor is of irregular shape and has a net surface charge, the local density σ of the charge will be greatest where the surface has the *largest local curvature* (that is, the *smallest radius of curvature*). Consider an irregularly shaped conductor, as in Fig. 5.2, and partition the surface into small elements of area da_i subtending equal angles measured from the center of the conductor. Points 1 and 3 above then require that $\sigma_i\, da_i$ be constant, and since da_i depends on the radius of curvature, the smaller the radius of curvature (the larger the curvature) the greater the electric field and the local surface charge density σ.

This relationship between curvature and local surface charge density can be understood physically as being caused by local charges repelling each other and arranging themselves to achieve electrostatic equilibrium by minimizing the repulsion, subject to the constraint of no electric field inside the conductor and all excess charge being distributed on the surface. This is illustrated in Fig. 5.3. In Fig. 5.3(a) the spherical conductor has constant curvature over its surface so the charge and electric field are distributed uniformly. In a region with small radius of curvature (large curvature), the limit of which may be exemplified by a sharp point as in Fig. 5.3(b), the local surface area is very small and charges are repelled outward (away from the surface), allowing a large charge accumulation near the point.[3] Electric field lines are perpendicular to the surface of the conductor and the strongest electric fields (hence the greatest accumulation of surface charge) occur at the sharpest points.

[3] This is the principle that allows *lightning rods* (elevated and grounded metal rods with sharp points) to protect buildings by drawing charge from the surrounding air and dissipating it to ground, thereby minimizing the chance of a catastrophic lightning strike on the building. Conversely, high-voltage power lines are designed with smooth rounded surfaces to minimize leakage of charge into the surrounding air. Attempts to find a simple analytic formula to describe the relationship between surface curvature and charge density for an isolated conductor may be found in Ref. [21].

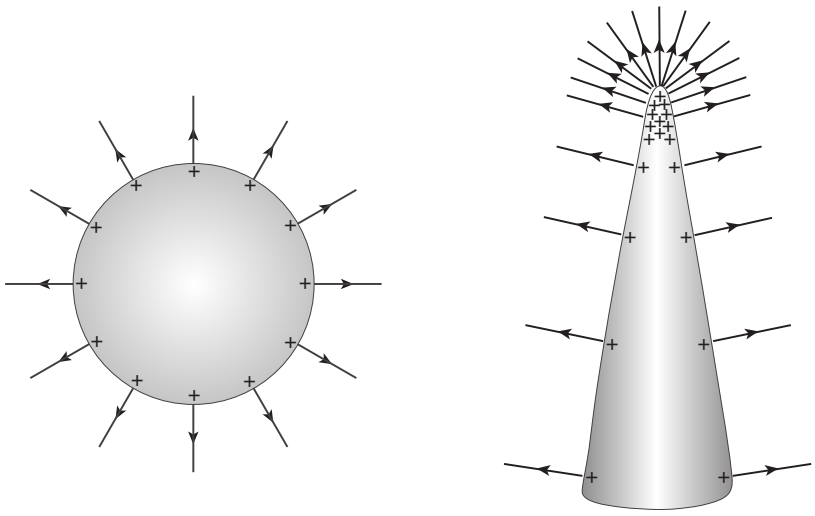

(a) Constant curvature (b) Large curvature near lightning rod tip

Fig. 5.3 Curvature, electric field lines, and charge distribution (a) for a conductor with a surface of uniform curvature, and (b) near a pointed surface on a conductor.

5.2 Capacitance

From the equations of electrostatics the source charge Q is proportional to the scalar potential Φ, with the constant proportionality termed the *capacitance* C. For an isolated conductor carrying a charge Q with potential Φ, the capacitance is

$$C = \frac{Q}{\Phi}. \tag{5.1}$$

In the SI system of units the charge is measured in coulombs, the potential in volts, and the capacitance in *farads* (F),[4] with $1\,\mathrm{F} \equiv 1$ coulomb/volt.

5.2.1 Parallel Plate Capacitors

Capacitance is also a useful concept in dealing with the charges and potentials associated with more than one conductor. The generic example is the *parallel plate capacitor* illustrated in Fig. 5.4. For two conductors the capacitance is defined to be the charge on the positive plate divided by the difference in potential between the two plates. If the difference in potential for two conductors denoted by V,

$$V \equiv \Phi_+ - \Phi_-, \tag{5.2}$$

[4] The farad is a very large unit for many phenomena, so it is common to employ microfarads ($1\ \mu\mathrm{F} = 10^{-6}$ F) and picofarads ($1\ \mathrm{pF} = 10^{-9}$ F) as units of capacitance in practical calculations.

Box 5.1 A Simple Model of a Lightning Rod

A lightning rod functions by enhancing the localized electric field at its tip, initiating a conductive channel (a *leader*) in the air. Let's model a lightning rod of length L as a very thin vertical line charge extending from the ground ($z = 0$) to a height $z = L$.

Linear Charge Density

Charges on a conductor migrate to the extremities to minimize repulsion, so the linear charge density $\lambda(z)$ is not uniform. We can parameterize this charge distribution as

$$\lambda(z) = \lambda_0 \left(\frac{z}{L}\right)^n,$$

where $n \geq 0$ is a parameter controlling how heavily the charge is concentrated at the tip. The ground is modeled as an infinite, perfectly conducting plane at $z = 0$.

Applying the Method of Images

To satisfy the equipotential ground plane condition at $z = 0$, we introduce an image line charge from $z = 0$ to $z = -L$ with charge density

$$\lambda_{\text{image}}(z) = -\lambda(-z).$$

The potential at an observation point (r, z) due to a differential source element dz' at height z' on the rod, plus its corresponding image element at $-z'$, is:

$$\Phi(r, z) = \frac{1}{4\pi\epsilon_0} \int_0^L \lambda(z') \left(\frac{1}{\sqrt{r^2 + (z - z')^2}} - \frac{1}{\sqrt{r^2 + (z + z')^2}} \right) dz'$$

The electric field components can be obtained by taking the numerical gradient of the resulting 2D potential field. In Problem 5.9 you are asked to investigate this model of a lightning rod using numerical integration of this model.

the capacitance for a parallel plate capacitor is given by

$$C = \frac{Q}{V} \qquad \text{(Two conductors)}. \tag{5.3}$$

For the capacitor in Fig. 5.4 the capacitance depends only on its geometry,

$$C = \frac{\epsilon_0 A}{s} \qquad \text{(Parallel plate capacitor)}, \tag{5.4}$$

where A is the surface area of a plate and s is the separation between the plates (which we assume to be parallel to each other, and of equal area) .

As will be discussed in Section 6.1, the capacitance of a parallel plate capacitor like that shown in Fig. 5.4 can be increased significantly by replacing the gap between the elec-

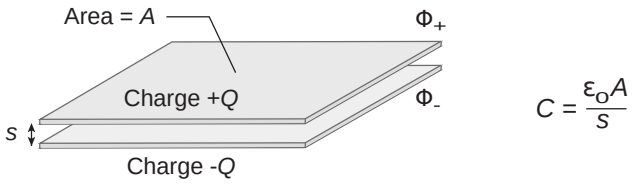

Fig. 5.4 A parallel plate capacitor with a charge $+Q$ and a potential Φ_+ on its upper plate and a charge $-Q$ and potential Φ_- on its lower plate.

trodes with a layer of insulating (dielectric) material, such as teflon. This is a consequence of the electric field polarizing the charge distribution in the dielectric layer lying between the plates (see Box 6.1).

5.2.2 Energy Stored in a Capacitor

Charging a capacitor by connecting the two plates in Fig. 5.4 to the poles of a battery stores energy in the electric field that is created between the oppositely-charged electrodes of the device. The amount of energy in the field may be determined by computing the work done to charge the capacitor to a particular level. Consider the parallel plate capacitor of Fig. 5.4. If at some point in the charging process the charge on the positive plate is q, from Eqs. (2.37) and (5.3) the work increment dW required to add the next charge increment dq is given by

$$dW = \left(\frac{q}{C}\right) dq, \tag{5.5}$$

and the total work that must be done to charge the plate from $q = 0$ to $q = Q$ is given by integration,

$$W = \int dW = \int_0^Q \left(\frac{q}{C}\right) dq = \frac{Q^2}{2C}. \tag{5.6}$$

Therefore, using $Q = CV$ from Eq. (5.3), the work required to charge to a potential difference V between the electrodes is

$$W = \frac{1}{2}CV^2, \tag{5.7}$$

From Eq. (5.4), this takes the specific form

$$W = \frac{1}{2}\frac{A\epsilon_0}{d}V^2, \tag{5.8}$$

for a parallel plate capacitor, where A is the area of a plate and d is the separation of the plates.

Background and Further Reading

Problems

5.1 Consider a sphere containing a single point charge Q located a distance r' from the origin along the z-axis.

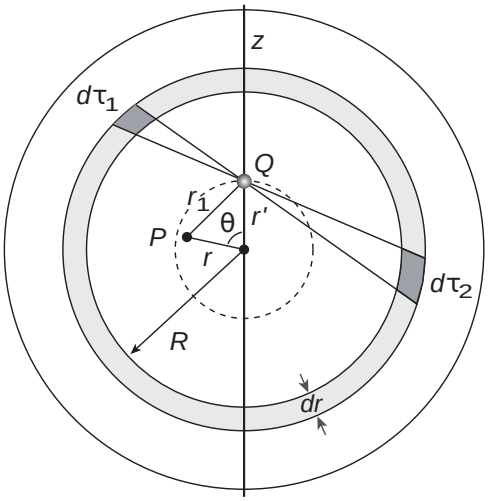

Calculate the average electric field inside the sphere. *Hint*: Separate the volume of the sphere τ into the part outside Q plus the part inside Q, as indicated by the dashed circle in the figure, and show by qualitative argument that the contribution from outside the dashed circle is zero.

5.2 Consider the spherical capacitor shown in the following figure,

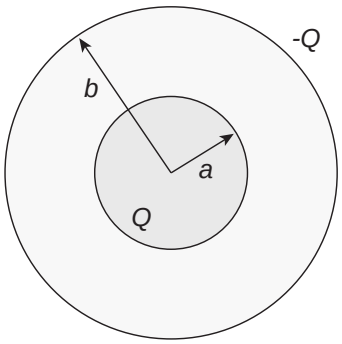

where the outer spherical conducting shell has radius b and charge $-Q$, and the innner spherical conducting shell has radius a and charge $+Q$. What is the capacitance of this device? ***

5.3 A capacitor consists of concentric cylinders with radii a for the inner cylinder and b for the outer cylinder.

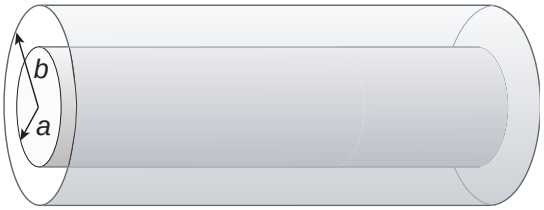

Derive a formula for the capacitance per unit length assuming the inner cylinder to be positively charged with a charge density of λ coulombs per unit length.

5.4 A conducting sphere of radius a is grounded and placed in a uniform electric field $\boldsymbol{E}$ directed along the x axis.

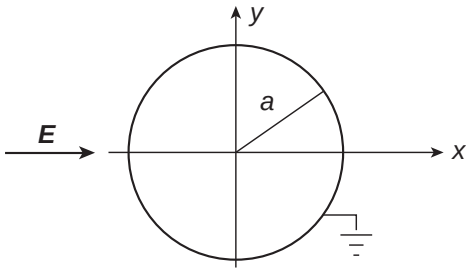

Derive a formula for the resulting electric field at all points, and sketch the corresponding field lines. ***

5.5 In Example 4.2 we illustrated solving for the electric field for the problem of a conducting spherical ball immersed in an initially uniform electric field. In Problem 5.4 we addressed the same problem, except with the added stipulation that the ball was grounded (note that the solution for Problem 5.4 is given in the *Student Solution Manual*). Discuss the differences and the underlying physics for these two cases.

5.6 Suppose that in Problem 5.5 and Example 4.2 we replace the *hollow conducting spherical shell* with a *solid conducting spherical ball* of the same radius R. Prove formally that the electric potential $\Phi(\mathbf{r})$ and the electric field $\boldsymbol{E}(\boldsymbol{r})$ everywhere outside the sphere ($r > R$) would be completely unchanged. *Hint*: Gauss's Law and the First Uniqueness Theorem.

5.7 A lightning rod [see Fig. 5.3(b)] functions by enhancing the localized electric field at its tip, initiating a conductive channel (called a *leader*) in the air. Let's model a lightning rod of length L as a thin vertical line charge extending from the ground ($z = 0$) to a height $z = L$, and assume the ground to be at zero potential. Charges on a conductor migrate to the extremities to minimize repulsion, so the linear charge density $\lambda(z)$ is not uniform. Parameterize this charge distribution as

$$\lambda(z) = \lambda_0 \left(\frac{z}{L}\right)^n,$$

where $n \geq 0$ is a parameter controlling how heavily the charge is concentrated at the top, and assume the ground to be an infinite, perfectly conducting plane at $z = 0$. Use the method of image charges to show that in this model the potential is

given at a point (r, z) in cylindrical coordinates by

$$\Phi(r,z) = \frac{1}{4\pi\epsilon_0}\int_0^L \lambda(z')\left(\frac{1}{\sqrt{r^2+(z-z')^2}} - \frac{1}{\sqrt{r^2+(z+z')^2}}\right)dz'.$$

In Problem 5.9 you will be asked to evaluate this integral and its gradient numerically to study the potential and electric field around this model of a lightning rod.

Numerical and GenAI Problems

5.8 Prompt your generative AI to use the method of images to solve for the electric potential and electric field near a conducting sphere placed in a uniform electric field with a single point charge placed nearby for (a) the case where the sphere is grounded and (b) the case where the sphere is ungrounded (isolated). Generate appropriate plots to illustrate your findings.

5.9 For the model of a lightning rod studied in Problem 5.7, prompt your *GenAI* to write Python code to evaluate numerically the integral expression

$$\Phi(r,z) = \frac{1}{4\pi\epsilon_0}\int_0^L \lambda(z')\left(\frac{1}{\sqrt{r^2+(z-z')^2}} - \frac{1}{\sqrt{r^2+(z+z')^2}}\right)dz'$$

for the potential, and to evaluate numerically the gradient of this potential to determine the electric field around the lightning rod. Use this code to generate appropriate graphics and study how the field and potential around the rod depend on the parameter n controlling the distribution of charge in the lightning rod.

6 Electrostatics in Dielectric Matter

To this point we have considered electrostatics primarily in vacuum, except for the presence of electrical charges, and of conducting matter in a few instances. But many important applications of electromagnetic theory involve interactions in non-conducting (dielectric) matter. There are two fundamental differences between conductors and dielectrics, and their electrostatic behavior.

1. Conductors have available many electrons that are very mobile because they are not bound in atoms or molecules. In constrast, ideal dielectrics have no free electrons.
2. Dielectrics typically can have electric fields in their interior, but conductors suppress any internal electric fields.

Therefore, this chapter begins to address how the properties of dielectric matter influence the equations of electrostatics. We will find that electric fields in matter are largely dipole fields, with the the net dipole moment having two basic sources:

1. Some molecules have an *intrinsic dipole moment*, and an external electric field exerts a torque that tends to align those moments with the field.
2. An electric field produces dipoles by polarizing matter, even if the atoms or molecules have no significant dipole moment in the absence of the applied field. This polarization effect is characterized by a quantity called the *atomic polarizability*.

In either case the material my be characterized in terms of a *polarization* P and an *electric susceptibility*, which is proportional to the ratio of P to the electric field. The primary effect of the polarization is to create a surface charge density in dielectric material. A considerable amount can be learned about the nature of dielectrics by examining the effect of this induced surface charge density on capacitors.

6.1 Dielectrics

As illustrated in Box 6.1, a capacitor with dielectric material between the metal plates has increased capacitance because of this induced surface charge (with the practical implications of reducing the size of the capacitor, or increasing its working voltage). Let us investigate in more depth the effect of a dielectric on a capacitor. A parallel-plate capacitor with no material between the plates has a capacitance C defined by

$$C = \frac{Q}{\Phi_{12}} = \frac{\epsilon_0 A}{s}, \tag{6.1}$$

Box 6.1 Capacitors and Dielectrics

The simplest parallel-plate capacitor has two separated parallel metal plates with nothing in between, as illustrated in Fig. (a) below.

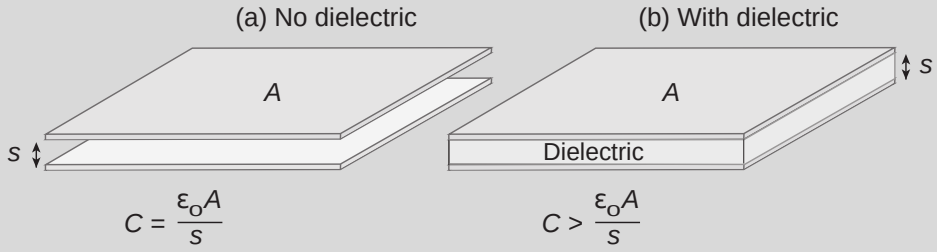

Inserting a dielectric between the plates of the capacitor as in Fig. (b) increases the capacitance because the induced surface charge on the dielectric produced by the electric field between the plates partially cancels the opposite charge on the adjacent plate. Understanding this mechanism leads to fundamental insight into the role of an electric field in a dielectric, as described in Section 6.1.1.

where Q is the magnitude of the charge on the plates (positive Q on one plate and negative Q on the other), Φ_{12} is the difference in electrical potential between the two plates, A is the surface area of a plate, and s is the separation of the plates.

6.1.1 Capacitors and Dielectrics

Now suppose that a layer of dielectric material is placed between the capacitor plates, as illustrated in Box 6.1. The capacitance may still be defined by the ratio of the charge to the potential difference between the plates, $C = Q/\Phi_{12}$, but now the *actual value of* C *will be increased* over that found for no dielectric between the plates. The presence of the dielectric between the plates allows more charge Q to accumulate on the plates and therefore greater capacitance, for the same potential difference, plate area, and separation of the plates. Qualitatively, this influence of the dielectric on the capacitance is not difficult to understand. The material of the dielectric consists of atoms or molecules with negatively charged electrons and positively charged nuclei.

1. The electric field between the plates polarizes the charge distribution of the dielectric.
2. Assuming the charge on the upper plate to be positive, negative charges in the dielectric will be pulled upward and positive charges pushed down, as illustrated in Fig. 6.1.
3. This exposes a layer of uncompensated negative charge near the top and a layer of uncompensated positive charge near the bottom of the dielectric.[1]

[1] As will be quantified shortly, this displacement of charge is *very small*. Remember that we are dealing with a dielectric where the electrons are bound up in atoms and molecules. There is no significant population of free charge carriers, as would be the case with a metallic conductor.

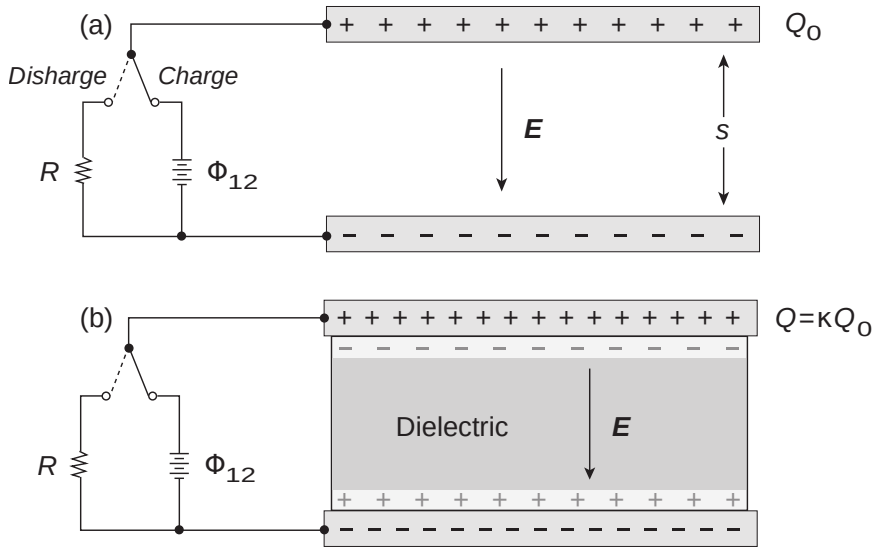

Fig. 6.1 Effect on capacitor of a dielectric between the plates. (a) No dielectric. (b) With dielectric. The switch allows charging and discharging the capacitor. Adapted from Ref. [62].

4. The charge Q on the upper plate will increase because of the induced top layer of negative charge below it in the dielectric.
5. We shall show later that Q increases until the algebraic sum of Q and the induced charge in the upper layer is equal to the total charge on the top plate Q_0 before the dielectric was inserted.
6. It follows that the total charge Q in the top layer is *larger than the charge* Q_0 of the top plate in Fig. 6.1(a) before the dielectric was inserted.
7. Thus, the charge is the Q that appears in Eq. (6.1) and is, in the circuit of Fig. 6.1, the charge supplied by the battery to charge the capacitor.

The induced charge layer is not part of the charge Q appearing in Eq. (6.1). If the switch in the circuit of Fig. 6.1 is used to discharge the fully-charged capacitor though the resistance R, the charge Q will be dissipated.

Thus the induced charge present in the charged capacitor is absorbed back into the normal structure of the dielectric in the discharged capacitor.

6.1.2 Dielectric Constants

Different dielectric materials would be expected to have different efficiencies for increasing the charge capacity of a capacitor, according to the ease with which electrons can be displaced with respect to the atomic nuclei in the dielectric matter by the applied electric

Table 6.1 Dielectric constants κ for some substances

Substance	Conditions	κ
Vacuum	(Definition)	1.00000
Air	gas, 0° C, 1 atm	1.00059
Water vapor	gas, 110° C, 1 atm	1.0126
Liquid water	liquid, 20° C	80.4
Silicon	solid 20° C	11.7
Polyethelene	solid, 20° C	$2.25 - 2.3$
Porcelain	solid 20° C	$6.0 - 8.0$

field. The factor Q/Q_0 by which the charge and thus the capacitance is increased by inserting a particular material between the capacitor plates is called the *dielectric constant* κ of that material:

$$Q = \kappa Q_0 \quad \longleftrightarrow \quad C = \kappa C_0. \tag{6.2}$$

Dielectric constants are ratios of charges and thus dimensionless; a few values of κ are given in Table 6.1 for some representative substances. The dielectric constant of the vacuum is defined to be $\kappa = 1$, typical gases have κ slightly larger than one, and liquids and solids can have dielectric constants varying widely in the range $\kappa \sim 1 - 100$. The remarkably large value $\kappa = 80.4$ for water merits an explanation that will be given later.

6.1.3 Bound Charge and Free Charge

In considering the effect of a dielectric on a capacitor, it is useful to introduce some terminology distinguishing between the charge associated with the dielectric itself and the mobile charges that can charge the plates. Those charges associated intrinsically with the dielectric are termed *bound charges*; those charges that are mobile and not bound in the dielectric are termed *free charges.* The *bound charges are not mobile* because they are attached physically to the atoms and molecules making up the dielectric.[2] *Bound charges can be polarized by electric fields* causing tiny charge displacements in the charged capacitor, but if the capacitor is discharged the bound charges remain with the dielectric, which becomes unpolarized as the electric field vanishes (assuming no permanent dipole moment for the substance of the dielectric); *the bound charges are not part of the charge Q on the capacitor plates.* Conversely, the free charges may be viewed as those charges that we have some agency over in an experiment (for example, through manipulation of the electrical circuit in Fig. 6.1 by using the switch to charge or discharge the capacitor).

[2] We assume that fields are not large enough to cause ionization and breakdown of the dielectric (possibly accompanied by smoke and fire, which would be unseemly in a theoretical discusssion).

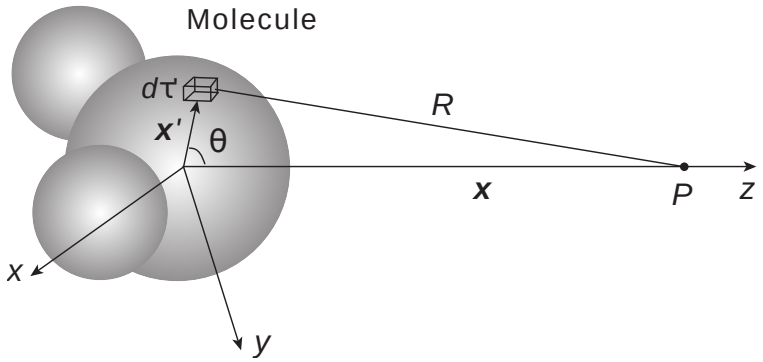

Fig. 6.2 Diagram for calculation of the potential at point P produced by a molecular charge distribution.

6.2 Moments of a Molecular Charge Distribution

Let's consider the potential Φ_P at a distant point P produced by the molecular electrical charge distribution of Fig. 6.2,

$$\Phi_P = \frac{1}{4\pi\epsilon_0}\int \frac{\rho(\boldsymbol{x}')}{R}\, d\tau', \tag{6.3}$$

where the integral is over all of the charge distribution. From the law of cosines (A.63) the distance R is given by

$$R = (r^2 + r'^2 - 2rr'\cos\theta)^{1/2}, \tag{6.4}$$

where we define $r = |\boldsymbol{x}|$ and $r' = |\boldsymbol{x}'|$, and Eq. (6.3) becomes

$$\Phi_P = \frac{1}{4\pi\epsilon_0}\int (r^2 + r'^2 - 2rr'\cos\theta)^{-1/2}\rho(\boldsymbol{x}')\, d\tau'. \tag{6.5}$$

Let us now expand this expression for the potential in multipole moments.

6.2.1 Multipole Expansion of the Potential

For a distant point P we have $r \gg r'$ and a binomial expansion gives (see Problem 3.2)

$$\frac{1}{R} = (r^2 + r'^2 - 2rr'\cos\theta)^{-1/2} = \frac{1}{r}\left[1 + \frac{r'}{r}\cos\theta + \left(\frac{r'}{r}\right)^2 \frac{3\cos^2\theta - 1}{2} + O\left(\left[\frac{r'}{r}\right]^3\right)\right]. \tag{6.6}$$

Then from Eqs. (6.3) and (6.6) the potential can be written as

$$\Phi_P = \frac{1}{4\pi\epsilon_0}\left[\frac{1}{r}\int \rho d\tau' + \frac{1}{r^2}\int r'\cos\theta\rho d\tau' + \frac{1}{r^3}\int r'^2\frac{3\cos^2\theta - 1}{2}\rho\, d\tau' + \cdots\right], \tag{6.7}$$

where the constant $r = |\boldsymbol{x}|$ has been brought outside the integrals (the integration variable is $\boldsymbol{x}'$). Now this is a power series in $1/r$ with coefficients that are constants depending only on integrals over the charge distribution and independent of the distance to P. Thus the potential can be written as a power series (multipole expansion) with constant coefficients

$$\Phi_P = \frac{1}{4\pi\epsilon_0}\left[\frac{C_0}{r} + \frac{C_1}{r^2} + \frac{C_2}{r^3} + \cdots\right], \tag{6.8}$$

where the coefficients C_i are the integrals over the internal charge distribution in Eq. (6.7). The electric field then follows from $\boldsymbol{E} = -\boldsymbol{\nabla}\Phi_P$.

6.2.2 Dominence of Monopole and Dipole Terms

At large distance from the source, the rapid convergence of terms in Eq. (6.8) implies that only low-order multipoles dominate. Behavior of the electric potential Φ at large distance from the source typically will be *dominated by the first term that has a non-zero coefficient* in the multipole expansion (6.8). Let us examine the coefficients in Eq. (6.8). The monopole coefficient $C_0 = \int \rho(\boldsymbol{x}')d\tau'$ is the total charge. For a neutral atom or molecule, $C_0 = 0$. If the atom or molecules is ionized so that $\rho \neq 0$, the monopole term will always dominate at large enough distance. If the atom or molecule is charge-neutral so that $\rho = 0$, the dipole term with $C_1 = \int r' \cos\theta\rho(\boldsymbol{x}')d\tau'$ dominates since $C_0 = 0$. Furthermore, if the charge distribution is charge-neutral the value of C_1 is independent of the choice of origin.[3]

> As we shall see, for our main task here of understanding the behavior of dielectrics, in a multipole expansion only the monopole strength (the total charge) and the dipole strength of the molecular building blocks of the dielectric are important in determining its electric-field properties. Thus, for the properties of dielectrics all multipole moments of the charge distribution of order beyond the dipole can usually be ignored.

As noted in the introduction to this chapter, a net dipole moment can come about because of induced polarization by an electric field, or because of molecules that have a permanent dipole moment. We shall now consider induced moments in Section 6.3 and permanent dipole moments in Section 6.4.

6.3 Induced Dipole Moments

The simplest atom is hydrogen, consisting of one nucleus (a proton) and one electron. The nucleus is so small compared with the electron cloud that in hydrogen and in more

[3] Generally, the value of a multipole moment may depend on the origin chosen for the coordinate system. But for the special case of a dipole moment in a charge-neutral dielectric, the value of the dipole moment is always independent of the choice of origin.

complicated atoms and molecules the nuclei can be approximated as point charges. Quantum mechanically the electron in hydrogen must be viewed as a cloud of negative charge with smoothly varying density (with the integrated charge equal to the electron charge e). The density falls off exponentially on the boundaries, so it makes sense to view the charge clouds of atoms and molecules as having approximate classical radii and shapes.

6.3.1 Polarization of the Electron Cloud

The electron cloud of the undisturbed hydrogen atom is spherically symmetric, but if it is placed in an electric field pointing upward along a z-axis the atomic charge cloud will be polarized, with the negative electrons pulled down and the positive nucleus pushed up. This distorted atom will have an electric dipole moment because the center of mass of the electron cloud will be displaced a small amount Δz from the nucleus, giving a net dipole moment of magnitude $\sim e\Delta z$, where e is the total electron charge. Example 6.1 estimates the size of this distortion in actual atoms.

Example 6.1 A very rough estimate of how much distortion will be caused by a field of strength E may be made by noting that a strong electric field already exists holding the unperturbed H atom together, which may be estimated as

$$E \simeq \frac{e}{4\pi\epsilon_0 a^2},$$

where a is a characteristic atomic length scale (for example, some multiple of the Bohr radius). If it is assumed that a field of the same order of magnitude would be required to produce significant distortion, the distortion may be estimated to be

$$\frac{\Delta z}{a} \simeq \frac{E}{e/4\pi\epsilon_0 a^2}.$$

Typically, $e/4\pi\epsilon_0 a^2 \sim 10^{11}$ volts/m, which is enormous (thousands of times larger than any field that can be produced at present in a laboratory); the distortion of the atom $\Delta z/a$ induced by electrical polarization will be tiny indeed!

The *dipole moment vector* $\boldsymbol{p}$ induced by an electric field $\boldsymbol{E}$ will point in the direction of the field and the magnitude of the induced dipole moment is generally proportional to the electric field (at least if the field is not too strong, which we assume to be the case).

6.3.2 Atomic Polarizabilities

The factor relating the dipole moment vector $\boldsymbol{p}$ to $\boldsymbol{E}$ is termed the *atomic polarizability* α,

$$\boldsymbol{p} = \alpha \boldsymbol{E}. \tag{6.9}$$

More generally, in a molecules the polarization may be asymmetric with respect to different axes and the scalar coefficient α in this equation must be replaced by a *polarizability tensor*, as described in Box 6.2. It is common to report atomic polarizabilities as the quantity $\alpha/4\pi\epsilon_0$ (which has units of volume) rather than as α itself.[4] Some atomic polarizabilities are given in Table 6.2, listed in order of atoms with increasing total electron number. The large variations in polarizabilities that are evident in Table 6.2 may be attributed to differences in total electron number and in valence electronic structure. For example, the noble gas elements He, Ne, and Ar have small polarizabilities because their outer electrons are more tightly bound than for other elements, but the polarizabilities increase in the sequence He to Ne to Ar because of an increase in the total electron number. As another example, the elements Na and K each have one loosely bound electron outside a closed electronic shell and that electron is very susceptible to perturbation by an electric field. As a result, Na and K have very large polarizabilities ($\kappa = 27$ and $\kappa = 34$, respectively).

Example 6.2 Let's estimate the amount of charge displacement in an atom induced by a typical electric field. From the polarizability of atomic hydrogen given in Table 6.2, the magnitude of the dipole moment induced by an electric field of strength one megavolt / meter is $p < 10^{-34}$ coulomb-meters.

Thus the characteristic atomic and molecular polarizations induced by applied electric fields are extremely small.

6.4 Permanent Dipole Moments of Polar Molecules

Some molecules have asymmetric shapes and exhibit permanent dipole moments in their normal ground state, even in the absence of an external field; a few examples are shown in Fig. 6.3. Molecules that have a permanent dipole moment are termed *polar molecules*. As a rule, the intrinsic dipole moments of polar molecules are much larger than the dipole moments induced by laboratory electric fields for either non-polar or polar molecules.

Example 6.3 As shown in Fig. 6.3, the magnitude of the (permanent) dipole moment for the polar molecule HCl is $p = |\boldsymbol{p}| = 3.43 \times 10^{-30}$ coulomb-meters (which is equivalent to shifting the charge of one electron by a distance of 2×10^{-9} cm [62]). From Example 6.2, the magnitude of the dipole moment in hydrogen induced by an electric field of magnitude one megavolt per meter is $p < 10^{-34}$ coulomb-meters. This result is a characteristic one and permanent dipole moments are typically multiple orders of magnitude larger than

[4] Beware: both α and $\alpha/4\pi\epsilon_0$ are sometimes called the "atomic polarizability" in the literature.

Box 6.2 **Asymmetric Polarization**

Molecules can be very asymmetric and may have different polarizabilities along different axes. For example, the linear molecule carbon dioxide (CO_2) illustrated in the following figure

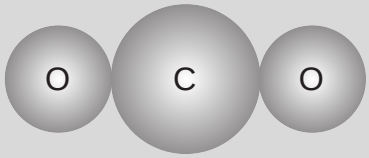

has a polarizability more than twice as large if the field is applied along its long axis than if it is applied perpendicular to that. In the most general case of a highly asymmetric molecule the simple relation (6.9) between the polarization vector and the electric field vector must be replaced by a tensor equation that can be expressed as a matrix–vector multiply,

$$\boldsymbol{p} = \begin{pmatrix} p_x \\ p_y \\ p_z \end{pmatrix} = \begin{pmatrix} \alpha_{xx} & \alpha_{xy} & \alpha_{xz} \\ \alpha_{yx} & \alpha_{yy} & \alpha_{yz} \\ \alpha_{zx} & \alpha_{zy} & \alpha_{zz} \end{pmatrix} \begin{pmatrix} E_x \\ E_y \\ E_z \end{pmatrix},$$

which is equivalent to the simultaneous equations

$$\begin{aligned} p_x &= \alpha_{xx}E_x + \alpha_{xy}E_y + \alpha_{xz}E_z, \\ p_y &= \alpha_{yx}E_x + \alpha_{yy}E_y + \alpha_{yz}E_z, \\ p_z &= \alpha_{zx}E_x + \alpha_{zy}E_y + \alpha_{zz}E_z. \end{aligned}$$

Thus the scalar coefficient α in Eq. (6.9) has been replaced by a polarizability tensor $\mathcal{A}$ that has the components

$$\mathcal{A} = \begin{pmatrix} \alpha_{xx} & \alpha_{xy} & \alpha_{xz} \\ \alpha_{yx} & \alpha_{yy} & \alpha_{yz} \\ \alpha_{zx} & \alpha_{zy} & \alpha_{zz} \end{pmatrix},$$

expressed as a matrix in the current basis.

Table 6.2 Atomic polarizabilities $(\alpha/4\pi\epsilon_0)$ in units of 10^{-30} m^3

Element:	H	He	Li	Be	C	Ne	Na	Ar	K
	0.66	0.21	12	9.3	1.5	0.4	27	1.6	34

those induced by laboratory electric fields.

In a uniform electric field polar molecules will have their dipole vectors partially aligned

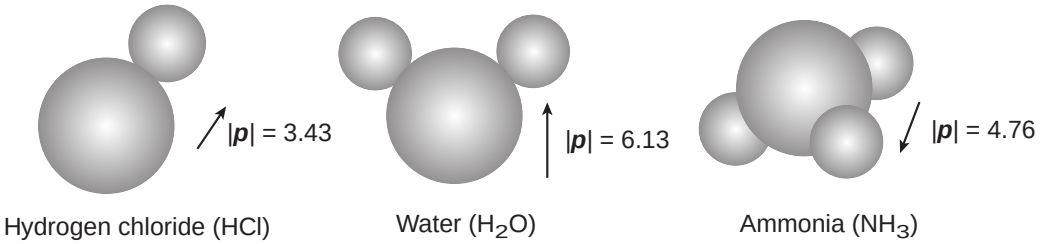

Fig. 6.3 Approximate geometry of the electron cloud and the observed dipole moment vector $\boldsymbol{p}$ for some polar molecules. Magnitudes $p = |\boldsymbol{p}|$ of the dipole moment vector are in units of 10^{-30} coulomb-meters (adapted from Ref. [62]).

with the field. The net force on the dipole vanishes, because the force on the negative end exactly cancels the force on the positive end (see Fig. 6.4), but the torque $\boldsymbol{N}$ acting on the dipole is

$$\boldsymbol{N} = \boldsymbol{p} \times \boldsymbol{E}, \tag{6.10}$$

where $\boldsymbol{p}$ is the dipole moment vector. The direction of $\boldsymbol{N}$ is so as to align the dipole moment of a polar molecule with the electric field. Perturbations such as thermal fluctuations tend to inhibit this alignment, so the typical physical outcome is an equilbrium with the dipoles partially aligned with the field.

6.5 Polarization Density

We have discussed two basic mechanism that lead to polarization of a dielectric: (1) distortion of the charge distribution by an electric field, which induces many tiny dipoles pointing in the same direction as the field if the dielectric substance consists of atoms or non-polar molecules, and (2) alignment of the existing intrinsic dipole moments by an electric field if the substance consists of polar molecules.[5] The net effect of either is to

[5] An applied field induces polarization for polar and non-polar molecules. However, any induced polarization for a polar molecule is usually very small compared with its intrinsic polarization and can be neglected.

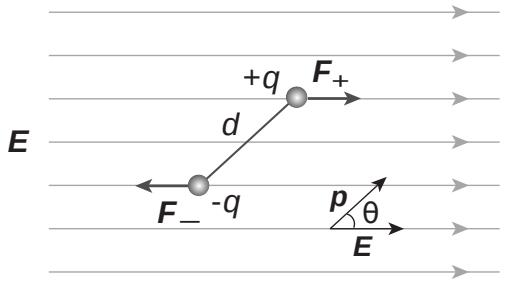

Fig. 6.4 Torque applied to a molecule with an intrinsic dipole moment in a uniform electric field.

produce a set of dipoles aligned or partially aligned with the electric field. Our primary interest here is in the effect of this polarization, without regard to the mechanism by which it was produced. Therefore, a measure of polarization for matter can be formed by asking how many dipoles N of average dipole moment $\boldsymbol{p}$ there are in a unit volume, without regard to their source. The total dipole strength of an infinitesimal volume element is then $\boldsymbol{p}N\,d\tau$ and the *polarization density* $\boldsymbol{P}$ can be defined by

$$\boldsymbol{P} \equiv \boldsymbol{p}N = \left(\frac{\text{Number of dipole moments}}{\text{Unit volume}}\right), \tag{6.11}$$

which has units of C-m/m^3 = C/m^2. The *polarization-charge density* ρ_{pol} is given by minus the divergence of the polarization density,

$$\rho_{\text{pol}}(\boldsymbol{x}) = -\boldsymbol{\nabla} \cdot \boldsymbol{P}(\boldsymbol{x}). \tag{6.12}$$

The electric field is discontinuous across the surface of the dielectric (see Sections 6.9 and 6.11), so there must be a surface charge density given by the difference between the density (6.12) evaluated for the two media at the boundary that is given by

$$\sigma_{\text{pol}} = -(\boldsymbol{P}_2 - \boldsymbol{P}_1) \cdot \hat{\boldsymbol{n}} \tag{6.13}$$

where $\boldsymbol{P}_i$ is the polarization in Medium i and $\hat{\boldsymbol{n}}$ is a unit vector that is normal to the boundary and points from Medium 1 to Medium 2.

6.6 Field Outside Polarized Matter

Let's now estimate the electric potential associated with the polarized dielectric material, considering separately the regions outside and inside of the dielectric matter. If it is assumed that the dielectric was assembled from neutral matter so that there is no net charge, there will be no monopole term in the multipole expansion (6.8). Therefore to good approximation only the dipole moments need be considered as sources of a field. Consider a thin vertical cylinder of dielectric matter in an electric field, as illustrated in Fig. 6.5. The polarization $\boldsymbol{P}$ is uniform and points in the positive z direction, and we wish to calculate the electric potential at the point A. An element of the cylinder of height dz in Fig. 6.5(a) has a dipole moment

$$\boldsymbol{p} = \boldsymbol{P}d\tau = \boldsymbol{P}\,da\,dz, \tag{6.14}$$

and its contribution to the potential at point A is

$$d\Phi_A = \frac{P\,\cos\theta da\,dz}{4\pi\epsilon_0 r^2}. \tag{6.15}$$

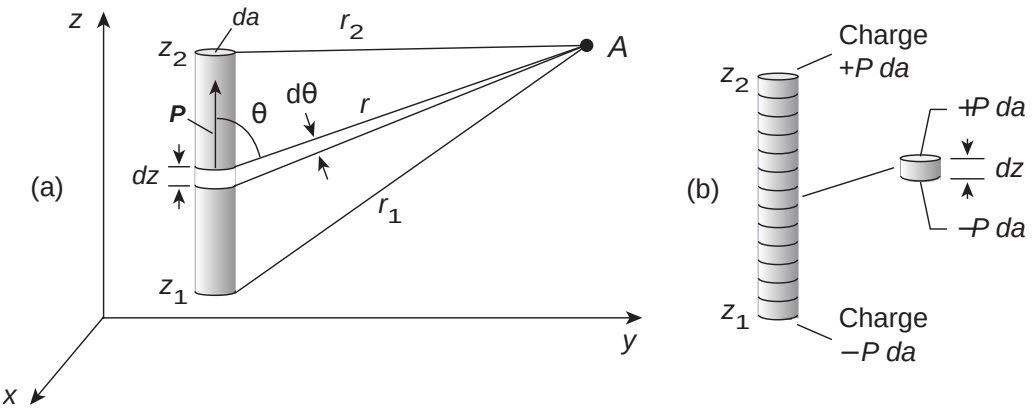

Fig. 6.5 (a) A column of polarized material with cross section da observed at a distant point A produces the same field as two charges, one at each end of (b). Adapted from Ref. [62].

Then the potential at the point A produced by the entire column of polarized matter is obtained by integration,

$$\begin{aligned}\Phi_A &= \frac{P\,da}{4\pi\epsilon_0}\int_{z_1}^{z_2}\frac{dz\cos\theta}{r^2} \\ &= \frac{-P\,da}{4\pi\epsilon_0}\int_{z_1}^{z_2}\frac{dr}{r^2} \\ &= \frac{Pda}{4\pi\epsilon_0}\left(\frac{1}{r_2}-\frac{1}{r_1}\right). \end{aligned} \tag{6.16}$$

But this the same as a potential produced by a positive point charge Pda at the top of the column at a distance r_2 from A and a negative point charge $-Pda$ placed at the bottom of the column a distance r_1 from A (see the dipole potential example in Box 3.3). A column of uniformly polarized matter produces the same potential and thus the same electric field at an external point A as a dipole consisting of two concentrated charges of magnitude Pda at the two ends of the column.

We can make Eq. (6.16) plausible by the heuristic argument illustrated in Fig. 6.5(b). Consider making the cylinder shown in Fig. 6.5(a) by stacking on top of each other small cylinder segments of height dz, with a charge of $+P\,da$ on its top face and $-P\,da$ on its bottom face. But now within the column the $+$ charge on the top of a segment will be cancelled by the $-$ charge on the bottom of the next segment up, except for the top-most segment, which will have an uncompensated charge on its top face of $+P\,da$, and the bottom-most segment, which will have an uncompensated charge on its bottom face of $-P\,da$. Thus the column of tiny dipoles will appear to be a single large dipole with end charges $+P\,da$ and $-P\,da$, separated by a distance $z_2 - z_1$. Note that nowhere in this derivation have we assumed that A is particularly distant; we have only assumed that the distance to A is much larger than the lengths of the individual microscopic dipoles and much larger than the width of the column in Fig. 6.5(a), both of which are very small.

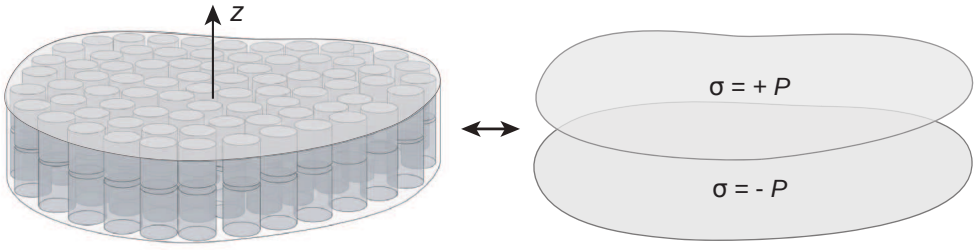

(a) Block of polarized dielectric (b) Top and bottom layers of surface charge

Fig. 6.6 (a) A block of dielectric polarized by an electric field in the z direction, rendered in a volumetric approximation using packed cylinders from the analysis in Fig. 6.5. (b) Two sheets of surface charge density $\pm P$ at the positions of the top and bottom surfaces of the block in (a). By the arguments given in the text and Fig. 6.5, (a) and (b) are equivalent because for each packed cylinder in (a) the interiors cancel out, leaving only the effective charges at the top and bottom of each cylinder, which is equivalent to the two layers of surface charge in (b).

We can take a slab of dielectric and divide it up infinitesimally into such columns and integrate over them to conclude that the electric field outside the slab is the same as if two sheets of surface charge were located at the positions of the top and bottom of the slab, carrying constant surface charge density $\sigma = +P$ and $\sigma = -P$, respectively. See Fig. 6.6.

6.7 Field Inside Polarized Matter

It may be expected that the field *inside polarized dielectric matter* could be quite complicated, and inside the dielectric it can't assumed that a point is at a much larger distance than the size of the dipoles. However, we may surmise that the electrostatic properties are governed by averages rather than the detailed local microscopic structure. Therefore, let us average over a region that is *macroscopically small but microscopically large*.[6] The spatial average of $\boldsymbol{E}$ over a volume V inside the polarized matter is given by

$$\langle \boldsymbol{E} \rangle_V = \frac{\int \boldsymbol{E}\, d\tau}{\int d\tau} = \frac{1}{V} \int \boldsymbol{E}\, d\tau, \tag{6.17}$$

where the volume $V = \int d\tau$. This average field $\langle \boldsymbol{E} \rangle_V$ is a *macroscopic quantity* formed from a spatial average of the *microscopic quantity* $\boldsymbol{E}(\boldsymbol{x})$ appearing in the integrand of Eq.

[6] That is, a region that is large enough to suppress statistical sampling fluctuations, but small enough that $\boldsymbol{P}$ doesn't vary substantially over the averaging volume. If d is the characteristic size of atoms, L is the chosen averaging scale, and R is the size of the sample, then a suitable macroscopic description of averaged field quantities requires that $d \ll L \ll R$. The basic reason that the averaging procedure preserves important properties of the fields such as $\boldsymbol{\nabla} \times \boldsymbol{E} = 0$ is that derivative operations commute with averaging operations. A more detailed discussion of the procedure of averaging microscopic quantities to produce macroscopic quantities may be found in Section 6.6 of Jackson [41] and Section 3.1 of Wald [74].

(6.17). Let us summarize some important properties of the macroscopic (that is, averaged) electric field.

1. The fundamental relation (2.27) that is obeyed by the microscopic electric field,

$$\boldsymbol{\nabla} \times \boldsymbol{E} = 0 \tag{6.18}$$

   remains valid for the macroscopic electric field.

2. This implies that the macroscopic electric field is still *derivable from a scalar potential*, through $\boldsymbol{E} = -\boldsymbol{\nabla}\boldsymbol{\Phi}$ (see Section 2.6).

3. If an electric field is applied to a medium consisting of a large number of atoms or molecules. The dominant multipole mode response to the applied field is again dipole, with an electric *polarization* $\boldsymbol{P}$ corresponding to the density of dipoles in Eq. (6.11),

$$\boldsymbol{P}(\boldsymbol{x}) = \sum_i N_i \langle \boldsymbol{p}_i \rangle,$$

   where $\boldsymbol{p}_i$ is the dipole moment of the ith species (atoms or molecules), the average $\langle \cdots \rangle$ is taken over a small volume centered on $\boldsymbol{x}$, and N_i is the average number per unit volume of the ith species at $\boldsymbol{x}$.

6.8 The Electric Displacement D

The macroscopic potential or field can be built up by linear superposition of contributions from each macroscopically small volume element ΔV at the variable point $\boldsymbol{x}'$. If macroscopic multipole moments higher than dipole may be ignored, then from Eq. (3.67), the macroscopically averaged potential is

$$\Delta\Phi(\boldsymbol{x}, \boldsymbol{x}') = \frac{1}{4\pi\epsilon_0}\left[\frac{\rho(\boldsymbol{x}')}{|\boldsymbol{x}-\boldsymbol{x}'|}\Delta V + \frac{\boldsymbol{P}(\boldsymbol{x}')\cdot(\boldsymbol{x}-\boldsymbol{x}')}{|\boldsymbol{x}-\boldsymbol{x}'|^3}\Delta V\right], \tag{6.19}$$

assuming $\boldsymbol{x}$ to lie outside ΔV. Setting $\Delta V \to d^3x'$ and integrating over all space gives the potential

$$\Phi(\boldsymbol{x}) = \frac{1}{4\pi\epsilon_0}\int d^3x' \left[\frac{\rho(\boldsymbol{x}')}{|\boldsymbol{x}-\boldsymbol{x}'|} + \boldsymbol{P}(\boldsymbol{x}')\cdot\boldsymbol{\nabla}'\left(\frac{1}{|\boldsymbol{x}-\boldsymbol{x}'|}\right)\right], \tag{6.20}$$

where the prime on $\boldsymbol{\nabla}'$ indicates that the $\boldsymbol{\nabla}$ operator acts on $\boldsymbol{x}'$ instead of $\boldsymbol{x}$. An integration of the second term by parts leads to

$$\Phi(\boldsymbol{x}) = \frac{1}{4\pi\epsilon_0}\int d^3x' \frac{1}{|\boldsymbol{x}-\boldsymbol{x}'|}\left[\rho(\boldsymbol{x}') - \boldsymbol{\nabla}'\cdot\boldsymbol{P}(\boldsymbol{x}')\right], \tag{6.21}$$

which represents the potential generated by an effective charge distribution $\tilde{\rho}(\boldsymbol{x}') = \rho(\boldsymbol{x}') - \boldsymbol{\nabla}' \cdot \boldsymbol{P}(\boldsymbol{x}')$.[7] Then Gauss's law (1.1a) reads

$$\boldsymbol{\nabla} \cdot \boldsymbol{E} = \frac{1}{\epsilon_0} \left[\rho - \boldsymbol{\nabla}' \cdot \boldsymbol{P}(\boldsymbol{x}')\right], \tag{6.22}$$

which reduces to Eq. (1.1a) in the absence of polarization. If we define the *electric displacement* $\boldsymbol{D}$ by

$$\boldsymbol{D} \equiv \epsilon_0 \boldsymbol{E} + \boldsymbol{P}, \tag{6.23}$$

Eq. (6.22) can be written as

$$\boldsymbol{\nabla} \cdot \boldsymbol{D} = \rho. \tag{6.24}$$

Solution for potentials or fields requires that the relations that connect the displacement $\boldsymbol{D}$ and the electric field $\boldsymbol{E}$ be specified.

6.8.1 Constituitive Relationships

The relationships that connect D and E are called *constitutive relations*. It is common to make two assumptions in these relationships.

1. The response to the applied field is linear, $\boldsymbol{P} \propto \boldsymbol{E}$.
2. The medium is isotropic, so that $\boldsymbol{P}$ is parallel to $\boldsymbol{E}$ and the coefficient of proportionality has no angular dependence,

$$\boldsymbol{P} = \epsilon_0 \chi_\mathrm{e} \boldsymbol{E}, \tag{6.25}$$

   where χ_e is termed the *electric susceptibility* of the medium.

With these assumptions the displacement $\boldsymbol{D}$ and the electric field $\boldsymbol{E}$ are related by

$$\boldsymbol{D} = \epsilon \boldsymbol{E} \qquad \epsilon \equiv \epsilon_0 (1 + \chi_\mathrm{e}), \tag{6.26}$$

where ϵ is the *electric permittivity* and

$$\kappa \equiv \frac{\epsilon}{\epsilon_0} = 1 + \chi_\mathrm{e} \tag{6.27}$$

is called the *dielectric constant*. Then the polarization can be written

$$\boldsymbol{P} = (\epsilon - \epsilon_0) \boldsymbol{E}. \tag{6.28}$$

If the dielectric medium is *uniform in addition to being isotropic*, then ϵ is independent of position and the divergence equation (6.24) can be written

$$\boldsymbol{\nabla} \cdot \boldsymbol{E} = \frac{\rho}{\epsilon}, \tag{6.29}$$

which is Gauss's law (1.1a) with ϵ_0 replaced by $\epsilon = \epsilon_0(1 + \chi_\mathrm{e})$. Equations (6.24) and

[7] The divergence term appears in the effective charge density $\tilde{\rho}$ because for non-uniform polarization there can be a net increase or decrease of charge within any small volume; see Section 6.9. As was noted in Eq. (6.12), the polarization-charge density at a point $\boldsymbol{x}$ in polarized media is given by $\rho_\mathrm{pol}(\boldsymbol{x}) = -\boldsymbol{\nabla} \cdot \boldsymbol{P}(\boldsymbol{x})$.

(6.18) are the macroscopic counterparts of the microscopic equations (1.1a) and (2.27), respectively.

For a medium fulfilling all the conditions specified above, solutions for electrostatics problems in that medium are equivalent to the corresponding solutions found previously for vacuum, except that the electric fields must be reduced by a factor ϵ_0/ϵ. Physically this reduction is a consequence of polarized atoms producing fields in the medium that oppose the applied field.

One consequence of immediate relevance to our prior discussion is that the capacitance of a parallel-plate capacitor is increased by a factor ϵ/ϵ_0 if the empty space between the electrodes is filled with a material having dielectric constant ϵ/ϵ_0 (neglecting the effect of fringing fields). Example 6.4 illustrates.

Example 6.4 From Eq. (6.26), inserting a dielectric layer in a parallel-plate capacitor alters the electric field, changing the capacitance from C_0 to

$$C = \kappa C_0 = \frac{\epsilon}{\epsilon_0} C_0 = (1 - \chi_e) C_0. \tag{6.30}$$

For the capacitor described in Section 5.2.1, the capacitance with a dielectric layer between the plates is

$$C = \frac{\epsilon}{\epsilon_0} C_0 = \frac{\epsilon}{\epsilon_0} \frac{A\epsilon_0}{d} = \frac{A\epsilon}{d}. \tag{6.31}$$

The corresponding work required to charge a parallel-plate capacitor that was given in Section 5.2.2 is modified to

$$W = \frac{Q^2}{2C} = \frac{1}{2} C V^2 = \frac{1}{2} \frac{A\epsilon}{d} V^2, \tag{6.32}$$

which is ϵ/ϵ_0 times the work required to charge the capacitor without the dielectric layer that was given in Eq. (5.8).

6.8.2 Boundary Conditions

If a system contains different media, boundary conditions must be considered for both $\boldsymbol{D}$ and $\boldsymbol{E}$ at all interfaces between different media. This will be addressed in more depth in Section 6.11, but the results for electrostatics are that the normal components of $\boldsymbol{D}$, and the tangential components of $\boldsymbol{E}$ on either side of an interface between Medium 1 and Medium 2, must satisfy the boundary conditions (for either static or time-varying fields)

$$(\boldsymbol{D}_2 - \boldsymbol{D}_1) \cdot \boldsymbol{n} = \sigma, \tag{6.33a}$$

$$(\boldsymbol{E}_2 - \boldsymbol{E}_1) \times \boldsymbol{n} = 0, \tag{6.33b}$$

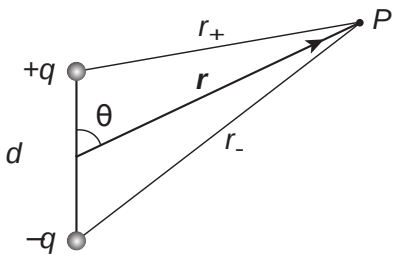

Fig. 6.7 Coordinate system for an electric dipole. The distance from the dipole to P is $\boldsymbol{r} = \boldsymbol{x} - \boldsymbol{x}'$ and $r \equiv |\boldsymbol{r}|$.

where $\boldsymbol{n}$ is a unit normal to the surface pointing from Medium 1 to Medium 2, and σ is the macroscopic surface-charge density on the boundary surface (which does not include the polarization charge discussed in following sections).

6.9 Surface and Volume Bound Charges

The potential created by a single dipole can be written

$$\Phi(\boldsymbol{x}) = \frac{1}{4\pi\epsilon_0}\frac{\boldsymbol{p}\cdot\hat{\boldsymbol{r}}}{r^2}, \tag{6.34}$$

where from Fig. 6.7, $r = |\boldsymbol{r}|$ where $\boldsymbol{r} = \boldsymbol{x} - \boldsymbol{x}'$, and $\boldsymbol{p}$ is the dipole moment vector. The total potential contributed by dipoles then follows by integration,

$$\Phi(\boldsymbol{x}) = \frac{1}{4\pi\epsilon_0}\int_V \frac{\boldsymbol{P}(\boldsymbol{x}')\cdot\hat{\boldsymbol{r}}}{r^2}\,d\tau', \tag{6.35}$$

where $d\tau' \equiv d^3x'$ and $\boldsymbol{P}$ is the dipole moment density. This can be rewritten using

$$\boldsymbol{\nabla}'\left(\frac{1}{r}\right) = \frac{\hat{\boldsymbol{r}}}{r^2} \tag{6.36}$$

in the form

$$\Phi(\boldsymbol{x}) = \frac{1}{4\pi\epsilon_0}\int_V \boldsymbol{P}\cdot\boldsymbol{\nabla}'\left(\frac{1}{r}\right)d\tau', \tag{6.37}$$

which can be integrated using the product rule in Eq. (A.18c)

$$\boldsymbol{\nabla}'\cdot(f\boldsymbol{A}) = f(\boldsymbol{\nabla}'\cdot\boldsymbol{A}) + \boldsymbol{A}\cdot(\boldsymbol{\nabla}' f).$$

Setting $f = 1/r$ and $\boldsymbol{A} = \boldsymbol{P}$, and integrating both sides over the volume V, the product rule becomes

$$\int_V \boldsymbol{\nabla}'\cdot\left(\frac{\boldsymbol{P}}{r}\right)d\tau' = \int_V \frac{1}{r}(\boldsymbol{\nabla}'\cdot\boldsymbol{P})d\tau' + \int_V (\boldsymbol{P}\cdot\boldsymbol{\nabla}')\frac{1}{r}d\tau'. \tag{6.38}$$

Now apply the divergence theorem (A.34)

$$\oint_S \boldsymbol{A}\cdot\boldsymbol{n}\,da = \int_V \boldsymbol{\nabla}\cdot\boldsymbol{A}\,d^3x,$$

to the term on the left side of Eq. (6.38) to give

$$\oint_S \frac{1}{r}\,\boldsymbol{P}\cdot\boldsymbol{n}\,da' = \int_V \frac{1}{r}(\boldsymbol{\nabla}'\cdot\boldsymbol{P})d\tau' + \int_V (\boldsymbol{P}\cdot\boldsymbol{\nabla}')\frac{1}{r}d\tau', \tag{6.39}$$

multiply both sides by $1/4\pi\epsilon_0$ and rearrange to give

$$\frac{1}{4\pi\epsilon_0}\int_V (\boldsymbol{P}\cdot\boldsymbol{\nabla}')\frac{1}{r}d\tau' = \frac{1}{4\pi\epsilon_0}\oint_S \frac{1}{r}\,\boldsymbol{P}\cdot\boldsymbol{n}\,da' - \frac{1}{4\pi\epsilon_0}\int_V \frac{1}{r}(\boldsymbol{\nabla}'\cdot\boldsymbol{P})d\tau', \tag{6.40}$$

and finally, upon comparing with Eq. (6.37),

$$\Phi(\boldsymbol{x}) = \frac{1}{4\pi\epsilon_0}\oint_S \frac{1}{r}\,\boldsymbol{P}\cdot\boldsymbol{n}\,da' - \frac{1}{4\pi\epsilon_0}\int_V \frac{1}{r}(\boldsymbol{\nabla}'\cdot\boldsymbol{P})d\tau'. \tag{6.41}$$

Thus we see that

1. The first term of Eq. (6.41) looks like the potential generated by a surface charge

$$\sigma_{\mathrm{b}} \equiv \boldsymbol{P}\cdot\hat{\boldsymbol{n}}, \tag{6.42}$$

   with $\hat{\boldsymbol{n}}$ the unit vector normal to the surface and the subscript "b" indicating that it originates in the bound charges.
2. The second term of Eq. (6.41) looks like the potential generated by a volume charge of magnitude

$$\rho_{\mathrm{b}} = -\boldsymbol{\nabla}\cdot\boldsymbol{P}. \tag{6.43}$$

Hence Eq. (6.41) can be written

$$\Phi = \frac{1}{4\pi\epsilon_0}\oint_S \frac{\sigma_{\mathrm{b}}}{r}\,da' + \frac{1}{4\pi\epsilon_0}\int_V \frac{\rho_{\mathrm{b}}}{r}\,d\tau', \tag{6.44}$$

and the potential Φ and electric field $\boldsymbol{E}$ of a polarized object are equivalent to that produced by a volume charge density $\rho_{\mathrm{b}} = -\boldsymbol{\nabla}\cdot\boldsymbol{P}$ plus a surface charge density $\sigma_{\mathrm{b}} = \boldsymbol{P}\cdot\hat{\boldsymbol{n}}$. Notice that the volume charge density ρ_{b} involves derivatives of the polarization $\boldsymbol{P}$; thus it contributes only if the polarization is spatially non-uniform [see Eq. (6.21)].

Example 6.5 Let's use the result of Eq. (6.44) to determine the potential inside and outside a uniformly polarized sphere of radius R. Since we assume uniform polarization the second (volume-charge) term, which is non-zero only if the derivative of the polarization density is finite, makes no contribution and the potential is generated entirely by the surface charge defined in Eq. (6.42),

$$\sigma_{\mathrm{b}} = \boldsymbol{P}\cdot\hat{\boldsymbol{n}} = P\cos\theta, \tag{6.45}$$

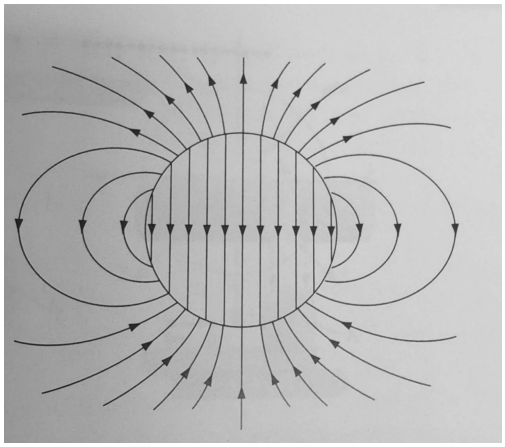

Fig. 6.8 Electric field for a uniformly polarized sphere determined in Example 6.5. [*NOTE: Replot on white background.]*

where the z-axis has been chosen as the direction of polarization. Thus, we need to evaluate the potential for a sphere with the surface charge (6.45) painted on it. This problem was already solved in Problems 4.1 and 4.4, with the result that

$$\Phi(r,\theta) = \begin{cases} \dfrac{Pr}{3\epsilon_0}\cos\theta & (r \le R), \\ \dfrac{PR^3}{3\epsilon_0 r^2}\cos\theta & (r \ge R). \end{cases} \tag{6.46}$$

The electric field is then given by $\boldsymbol{E} = -\boldsymbol{\nabla}\Phi$. Note that since $r\cos\theta = z$, inside the sphere the field is uniform:

$$\boldsymbol{E} = -\boldsymbol{\nabla}\Phi = -\frac{P}{3\epsilon_0}\,\hat{\boldsymbol{z}} = -\frac{1}{3\epsilon_0}\boldsymbol{P} \qquad (r < R). \tag{6.47}$$

Outside the sphere the field has a dipole form

$$\Phi = \frac{1}{4\pi\epsilon_0}\frac{\boldsymbol{p}\cdot\hat{\boldsymbol{r}}}{r^2} \qquad (r \ge R), \tag{6.48}$$

where the dipole moment is equal to the total dipole moment of the sphere,

$$\boldsymbol{p} = \frac{4}{3}\pi R^3 \boldsymbol{P}, \tag{6.49}$$

since $\boldsymbol{P}$ is the dipole moment density.

Curves of constant electric field strength for the electric field of the uniformly polarized sphere computed in Example 6.5 are plotted in Fig. 6.8.

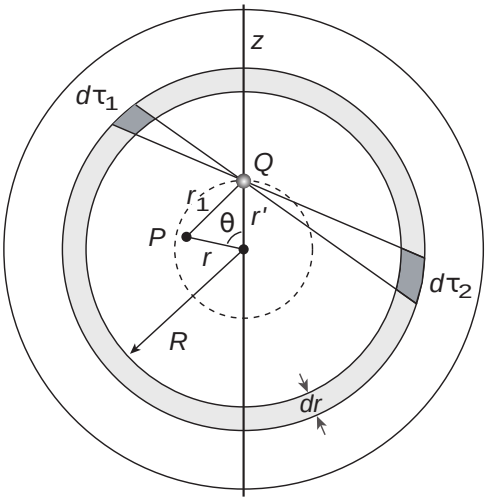

Fig. 6.9 A point charge Q located at a distance r' from the center of a sphere of radius R.

6.10 Average Electric Fields in Matter

The influence of matter on electrostatics will in most cases require some amount of averaging over the detailed and complex microscopic interactions in the matter. Hence one fundamental task will be to compute the electric field averaged over some volume of matter. Let's begin by consider a sphere containing a single point charge Q located a distance r' from the origin along the z-axis, as illustrated in Fig. 6.9 [25]. By symmetry the average field over the entire volume must be along the z-axis The average field is then

$$\langle E_z \rangle = \frac{\int_\tau E_z \, d\tau}{\int_\tau d\tau} = \frac{1}{\tau} \int_\tau E_z \, d\tau,$$

where τ is the volume of the sphere. It is convenient to separate the integral into two parts: one over the spherical shell from radii r' to R (outside the dashed circle in the above diagram) and one over the sphere of radius r' (inside the dashed circle).

The integral over the outer volume vanishes, by the following qualitative argument. Consider the concentric shell at radius R with thickness dr. The solid angle element intercepts the volume elements $d\tau_1$ and $d\tau_2$ in the shaded shell of thickness dr. The value of E_z decreases quadratically with distance from Q but $d\tau$ increases quadratically with distance, so their product remains constant. But E_z is positive at $d\tau_1$ but negative at $d\tau_2$, so the two contributions cancel. A similar argument can be make for all shells and the entire outer shell with $r > r'$ contributes zero.

To calculate the integral over the inner volume (inside the dashed circle), consider the point P in Fig. 6.9. The potential at P is

$$\Phi = \frac{1}{4\pi\epsilon_0} \frac{Q}{r_1} = \frac{1}{4\pi\epsilon_0} \frac{Q}{|\boldsymbol{x} - \boldsymbol{x}'|},$$

where from Fig. 6.9 that $r_1 = |\boldsymbol{x} - \boldsymbol{x}'|$. Thus, we may expand in the multipole expansion

given in Eq. (3.54),

$$\frac{1}{|\boldsymbol{x}-\boldsymbol{x}'|}=\sum_{l=0}^{\infty}\frac{r_<^l}{r_>^{l+1}}P_l(\cos\theta)=\sum_{l=0}^{\infty}\frac{r^l}{(r')^{l+1}}P_l(\cos\theta)$$

where we've used from Fig. 6.9 that $r<r'$. Writing this expansion out and substituting the explicit values for the Legendre polynomials from Table 4.1,

$$\Phi=\frac{Q}{4\pi\epsilon_0}\frac{1}{r'}\left[1+\frac{r}{r'}\cos\theta+\frac{1}{2}\frac{r^2}{r'^2}(3\cos^2\theta-1)+\frac{1}{2}\frac{r^3}{r'^3}(5\cos^3\theta-3\cos\theta+\cdots\right].$$

The electric field is minus the gradient of the potential, so we need to evaluate $E_z=-\partial\Phi/\partial z$. Utilizing

$$r\cos\theta=z\qquad\frac{\partial r}{\partial z}=\frac{\partial}{\partial z}(x^2+y^2+z^2)^{1/2}=\frac{z}{r}=\cos\theta$$

the preceding multipole expansion can be written in terms of z and the derivative taken to give the expansion for the electric field

$$E_z=-\frac{Q}{4\pi\epsilon_0 r'^2}\left[1+\frac{2z}{r'}+\frac{3}{2r'^2}(3z^2-r^2)+\cdots\right]$$

Then we may compute the average by integrating term by term in this series. The first term gives

$$\langle E_z\rangle_1=-\frac{Q}{4\pi\epsilon_0 r'^2}\int_0^{\pi}\int_0^{r'}2\pi r^2\sin\theta\,dr\,d\theta=-\frac{Qr'}{3\epsilon_0\tau}.$$

All of the higher-order terms give zero, so we obtain

$$\langle E_z\rangle=-\frac{Qr'}{3\epsilon_0\tau}=-\frac{Qr'}{3\epsilon_0}\frac{3}{4\pi R^3}=-\frac{Qr'}{4\pi\epsilon_0 R^3}=-\frac{p}{4\pi\epsilon_0 R^3},$$

where the volume is $\tau=\frac{4}{3}\pi R^3$ and the dipole moment p of the charge Q is $p=Qr'$. This result was for a single charge on the z-axis. For an arbitrary charge distribution the same result is obtained, except that

$$\langle E_z\rangle=-\frac{p_{\text{total}}}{4\pi\epsilon_0 R^3},$$

where p_{total} is the total dipole moment of the arbitrary charge distribution within the sphere of radius R.

6.11 Boundary Conditions at Interfaces

In advanced applications one often must consider problems in which media with different properties are spatially adjacent and boundary conditions at all interfaces must be accounted for. We may do so by using the vacuum Maxwell equations modified to reflect the influence of the medium on classical electrodynamics. As we now discuss, the in-medium Maxwell equations may be expressed in either differential or integral form.

6.11.1 Differential Form of Maxwell Equations in Medium

In a medium that may be polarized by electric or magnetic fields, the *vacuum Maxwell equations* (1.1) are modified to the *Maxwell equations in medium*, expressed in differential form,

$$\boldsymbol{\nabla} \cdot \boldsymbol{D} = \rho \qquad \text{(Gauss's law)}, \tag{6.50a}$$

$$\boldsymbol{\nabla} \times \boldsymbol{E} + \frac{\partial \boldsymbol{B}}{\partial t} = 0 \qquad \text{(Faraday's law)}, \tag{6.50b}$$

$$\boldsymbol{\nabla} \cdot \boldsymbol{B} = 0 \qquad \text{(No magnetic charges)}, \tag{6.50c}$$

$$\boldsymbol{\nabla} \times \boldsymbol{H} - \frac{\partial \boldsymbol{D}}{\partial t} = \boldsymbol{J} \qquad \text{(Ampère–Maxwell law)}, \tag{6.50d}$$

where $\boldsymbol{D}$ is defined in Eq. (6.23) and $\boldsymbol{H}$ is defined in Eq. (9.11).[8] The Maxwell equations (6.50) in differential form can be cast in integral form using the divergence theorem and Stokes' theorem.

6.11.2 Integral Form of Maxwell Equations in Medium

Let V be a finite volume bounded by a closed surface (or surfaces) S, let da be an area element of that surface, and let $\boldsymbol{n}$ be a unit normal at da, pointing out of the volume. The divergence theorem (2.20)

$$\oint_S \boldsymbol{A} \cdot \boldsymbol{n}\, da = \int_V \boldsymbol{\nabla} \cdot \boldsymbol{A}\, d^3x,$$

applied to Eq. (6.50a) yields

$$\oint_S \boldsymbol{D} \cdot \boldsymbol{n}\, da = \int_V \rho\, d^3x, \tag{6.51}$$

with Eq. (6.51) being an integral form of Gauss's law requiring that the total flux $\boldsymbol{D}$ out through the surface be equal to the charge contained in the volume. Likewise, applying the divergence theorem to Eq. (6.50c) yields the integral equation

$$\oint_S \boldsymbol{B} \cdot \boldsymbol{n}\, da = 0, \tag{6.52}$$

where Eq. (6.52) is the magnetic analog of Eq. (6.51), requiring that there be no net flux B through the closed surface S because no magnetic charges are known to exist.

In a similar manner, suppose that C is a closed contour spanned by an open surface S', $d\boldsymbol{l}$ is a line element on C, da is an area element on S', and $\boldsymbol{n}'$ is a unit vector pointing in a direction given by the right-hand rule (see Box 2.3). Applying Stokes' theorem (2.25),

$$\int_S (\boldsymbol{\nabla} \times \boldsymbol{A}) \cdot \boldsymbol{n}\, da = \oint_C \boldsymbol{A} \cdot d\boldsymbol{l},$$

[8] The vacuum Maxwell equations (1.1) can be recovered from the Maxwell equations in medium (6.50) by substituting $\boldsymbol{D} = \epsilon_0 \boldsymbol{E}$ and $\boldsymbol{H} = \boldsymbol{B}/\mu_0$ into Eqs. (6.50), remembering from Eq. (2.4) that $\mu_0 \epsilon_0 = 1/c^2$.

to Eq. (6.50b) gives

$$\oint_C \boldsymbol{E} \cdot d\boldsymbol{l} = -\int_S \frac{\partial \boldsymbol{B}}{\partial t} \cdot \boldsymbol{n}' da, \tag{6.53}$$

which is an integral form of Faraday's law of magnetic induction. Likewise, applying Stokes' theorem to Eq. (6.50d) gives

$$\oint_C \boldsymbol{H} \cdot d\boldsymbol{l} = \oint_{S'} \left(\boldsymbol{J} + \frac{\partial \boldsymbol{D}}{\partial t} \right) \cdot \boldsymbol{n}' da \tag{6.54}$$

which is an integral form of the Ampère–Maxwell law of magnetic fields. Summarizing equations (6.51)-(6.54), the integral forms of Maxwell's equations in medium are

$$\oint_S \boldsymbol{D} \cdot \boldsymbol{n}\, da = \int_V \rho\, d^3x \qquad \text{(Gauss's law)} \tag{6.55a}$$

$$\oint_C \boldsymbol{E} \cdot d\boldsymbol{l} = -\int_S \frac{\partial \boldsymbol{B}}{\partial t} \cdot \boldsymbol{n}' da, \qquad \text{(Faraday's law)} \tag{6.55b}$$

$$\oint_S \boldsymbol{B} \cdot \boldsymbol{n}\, da = 0, \qquad \text{(No magnetic charges)} \tag{6.55c}$$

$$\oint_C \boldsymbol{H} \cdot d\boldsymbol{l} = \oint_{S'} \left(\boldsymbol{J} + \frac{\partial \boldsymbol{D}}{\partial t} \right) \cdot \boldsymbol{n}' da \qquad \text{(Ampère–Maxwell law)} \tag{6.55d}$$

Equations (6.55) may be used to determine the relationship of normal and tangential components of the fields on either side of an interface between media having different electromagnetic properties, as we shall now illustrate following the discussion in Jackson [41].

6.11.3 Matching Conditions at Boundaries

Consider Fig. 6.10, where there is a boundary between Medium 1 and Medium 2 and we allow the most general possibility that the interface at the boundary can have both a surface charge σ and a surface current density $\boldsymbol{K}$. To facilitate the analysis, an infinitesimal cylindrical Gaussian pillbox of volume V straddles the surface between the two media. In addition, an infinitesimal rectangular contour C has long sides on either side of the boundary and is oriented so that the normal to the rectangular surface points out of the page and is tangent to the interface.

Let us first apply equations (6.55a) and (6.55c) to the cylindrical Gaussian pillbox in Fig. 6.10. In the limit that the pillbox is assumed to be very shallow the side of the cylinder does not contribute to the integrals on the left side of Eqs. (6.55a) and (6.55c). If the top and bottom of the cylinder are are assumed to be parallel to the interface and to each have area Δa, then the integral on the left side of Eq. (6.55a) is given by

$$\oint_S \boldsymbol{D} \cdot \boldsymbol{n}\, da = (\boldsymbol{D}_2 - \boldsymbol{D}_1) \cdot \boldsymbol{n}\, \Delta a.$$

Now, applying a similar argument to the left side of Eq. (6.55c), the integral is given by

$$\oint_S \boldsymbol{B} \cdot \boldsymbol{n}\, da = (\boldsymbol{B}_2 - \boldsymbol{B}_1) \cdot \boldsymbol{n}\, \Delta a.$$

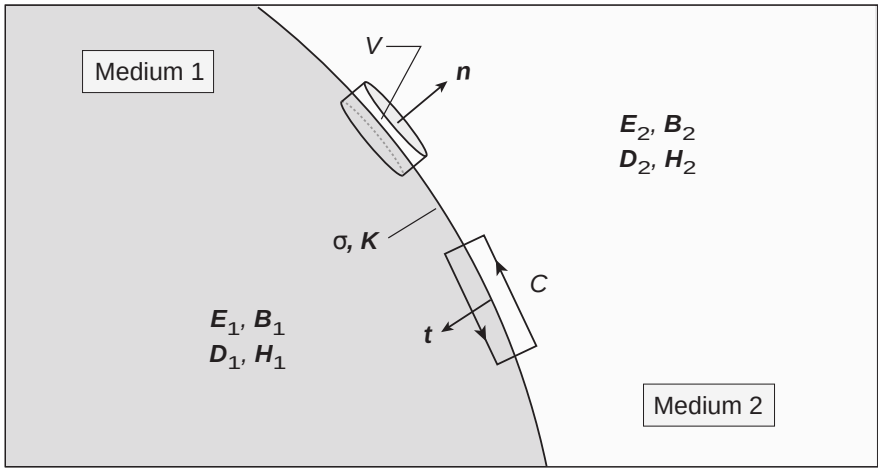

Fig. 6.10 Schematic illustration of a boundary surface between two different media that is assumed to carry surface charge σ and surface current density $\boldsymbol{K}$. The infinitesimal Gaussian cylinder of volume V is assumed to lie half in one medium and half in the other, with the normal to its surface $\boldsymbol{n}$ pointing from Medium 1 into Medium 2. The infinitesimal rectangular contour C is assumed to lie partly in one medium and partly in the other, with its plane perpendicular to the surface so that its normal $\boldsymbol{t}$ (pointing out of the page in the figure) is tangent to the surface. Adapted from Ref. [41].

If the charge density ρ is singular at the interface and produces an idealized surface charge density σ, the integral on the right side of Eq. (6.55a) evaluates to

$$\int_V \rho \, d^3x = \sigma \Delta a,$$

and the normal components of $\boldsymbol{D}$ and $\boldsymbol{B}$ on the two sides of the interface are related to each other by

$$(\boldsymbol{D}_2 - \boldsymbol{D}_1) \cdot \boldsymbol{n} = \sigma, \tag{6.56a}$$

$$(\boldsymbol{B}_2 - \boldsymbol{B}_1) \cdot \boldsymbol{n} = 0. \tag{6.56b}$$

Thus, stating Eqs. (6.56) in words:

1. the normal component of the magnetic field $\boldsymbol{B}$ is continuous across the interface, but
2. the discontinuity of the normal component of the electric displacement $\boldsymbol{D}$ at any point on the interface is equal to the surface charge density σ at that point.

In a similar manner, the infinitesimal rectangular contour C in Fig. 6.10 can be used in conjunction with Stokes' theorem to determine the discontinuities in the tangential components of $\boldsymbol{E}$ and $\boldsymbol{H}$. In the limit that the short sides of the rectangular loop may be

neglected and each long side is of length Δl and parallel to the interface, the integral on the left side of Eq. (6.55b) is

$$\oint_C \boldsymbol{E} \cdot d\boldsymbol{l} = (\boldsymbol{t} \times \boldsymbol{n}) \cdot (\boldsymbol{E}_2 - \boldsymbol{E}_1)\Delta l.$$

Likewise, the integral on the left side of Eq. (6.55d) is

$$\oint_C \boldsymbol{H} \cdot d\boldsymbol{l} = (\boldsymbol{t} \times \boldsymbol{n}) \cdot (\boldsymbol{H}_2 - \boldsymbol{H}_1)\Delta l.$$

The right side of Eq. (6.55b) vanishes because in the limit of vanishing length of the short side of the rectangular contour $\partial \boldsymbol{B}/\partial t$ is finite while $\Delta t \to 0$. Because there is an idealized surface current density $\boldsymbol{K}$ flowing exactly on the boundary, the integral on the right side of Eq. (6.55d) is equal to

$$\oint_{S'} \left(\boldsymbol{J} + \frac{\partial \boldsymbol{D}}{\partial t}\right) \cdot \boldsymbol{t}\, da = \boldsymbol{K} \cdot \boldsymbol{t}\Delta l,$$

where the second term vanishes by the same argument as that given above for the right side of Eq. (6.55b). Therefore, the tangential components of $\boldsymbol{E}$ and $\boldsymbol{H}$ on either side of the media interface are related by

$$(\boldsymbol{t} \times \boldsymbol{n}) \cdot (\boldsymbol{E}_2 - \boldsymbol{E}_1) = 0 \qquad (\boldsymbol{t} \times \boldsymbol{n}) \cdot (\boldsymbol{H}_2 - \boldsymbol{H}_1) = \boldsymbol{K} \cdot \boldsymbol{t},$$

and using the identity (A.4), this implies that

$$\boldsymbol{n} \times (\boldsymbol{E}_2 - \boldsymbol{E}_1) = 0, \tag{6.57a}$$

$$\boldsymbol{n} \times (\boldsymbol{H}_2 - \boldsymbol{H}_1) = \boldsymbol{K}, \tag{6.57b}$$

where in Eq. (6.57b) it is understood that the surface current only has components parallel to the interface at each point. Thus, stating Eqs. (6.57) in words:

1. the tangential component of the electric field $\boldsymbol{E}$ is continuous across an interface, but
2. the tangential component of $\boldsymbol{H}$ is discontinuous across the interface by an amount having magnitude $|\boldsymbol{K}|$ and direction $\boldsymbol{K} \times \boldsymbol{n}$.

The discontinuity equations (6.56) and (6.57) for the fields $\boldsymbol{B}$, $\boldsymbol{E}$, $\boldsymbol{D}$, and $\boldsymbol{H}$ allow solving the Maxwell equations in different regions having potentially different electromagnetic properties, and then connecting the solutions to obtain the fields evaluated over all of the space. FigureboundaryCond summarizes

6.12 Dielectric Boundary Value Problems

Methods developed in previous chapters may be adapted to handle the presence of dielectrics in boundary value problems. Let us illustrate, in the process displaying techniques that are applicable to a variety of problems.

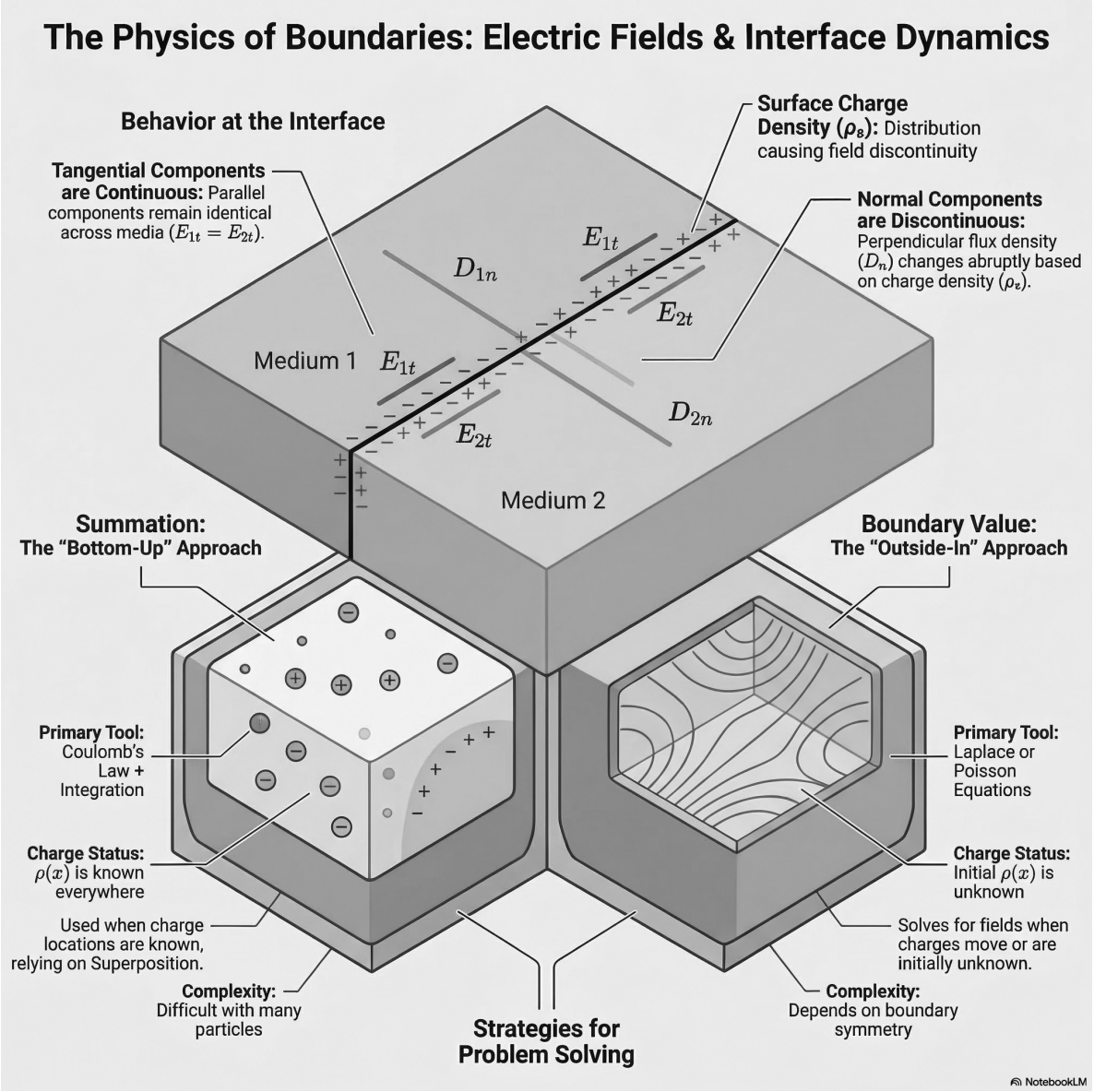

Fig. 6.11 Electric fields and interface boundary conditions, and contrast of summation and boundary value approaches to solving electrostatic problems. [*Note: Produced by NotebookLM; redraw to increase size of small fonts and try on white background.*]

6.12.1 Dielectric Ball in External Electric Field

A ball with dielectric constant $\kappa = \epsilon/\epsilon_0$ is placed in an initially uniform electric field directed along the z axis, as illustrated in Fig. 6.12, with the assumption that there are no free charges inside or outside of the ball. Let's determine the scalar potential Φ and the electric field $\boldsymbol{E}$ using the Laplace equation with appropriate boundary conditions. Exploiting axial symmetry about the z axis and solving the Laplace equation in spherical

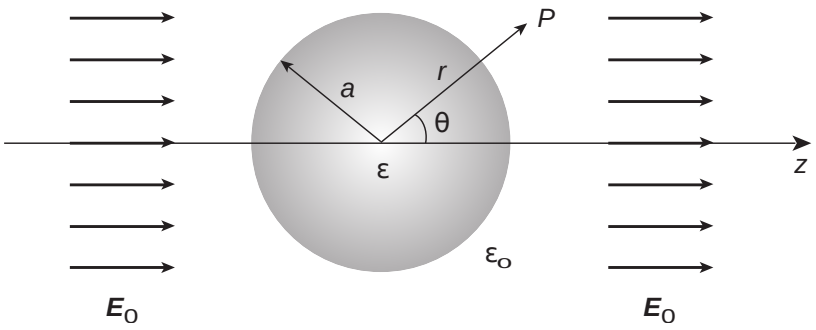

Fig. 6.12 A dielectric ball of radius a and dielectric constant $\kappa = \epsilon/\epsilon_0$ placed in an initially uniform external electric field $\boldsymbol{E}_0$ directed along the $\boldsymbol{z}$ axis. Used in the example discussed in Section 6.12.

coordinates by separation of variables (see Section 4.1.2), general solutions are of the form given by Eq. (4.37),

$$\Phi(r,\theta) = \sum_{l=0}^{\infty} (A_l r^l + B_l r^{-(l+1)}) P_l(\cos\theta).$$

However, there are no charges at the origin and the requirement that $\Phi(r,\theta)$ be finite there demands that for the interior solution, $B_l = 0$, and the interior solution is of the form

$$\Phi_{\text{in}}(r,\theta) = \sum_{l=0}^{\infty} A_l r^l P_l(\cos\theta), \tag{6.58}$$

and the exterior solution is of the form

$$\Phi_{\text{out}}(r,\theta) = \sum_{l=0}^{\infty} (B_l r^l + C_l r^{-(l+1)}) P_l(\cos\theta),$$

with the constants A_l, B_l, and C_l to be determined by imposing boundary conditions. At infinity, we must have [see Eq. (4.40b)],

$$\Phi(r \to \infty) = -E_0 z = -E_0 r\cos\theta = -E_0 r P_1(\cos\theta).$$

This requires that

$$-E_0 r P_1(\cos\theta) = [B_l r^l + C_l r^{-(l+1)}] P_l(\cos\theta) \simeq B_l r^l P_l(\cos\theta),$$

since the C_l term vanishes as $r \to \infty$. Multiplying both sides by $P_1(\cos\theta)$ and integrating,

$$-E_0 r \int P_1(\cos\theta) P_1(\cos\theta) d(\cos\theta) = B_l r^l \int P_1(\cos\theta) P_l(\cos\theta) d(\cos\theta).$$

Using the orthogonality relation (4.38),

$$\int_{-1}^{+1} P_k(\cos\theta) P_l(\cos\theta) d(\cos\theta) = \frac{2}{2l+1}\,\delta_{kl},$$

all terms vanish except for $l = 1$ and we obtain $B_1 = -E_0$, with all other B_l equal to zero. Thus, the exterior solution becomes,

$$\Phi_{\text{out}}(r,\theta) = -E_0 r^l P_1(\cos\theta) + \sum_{l=0}^{\infty} C_l r^{-(l+1)} P_l(\cos\theta). \tag{6.59}$$

Now let's use the boundary conditions at the edge of the sphere to fix the other constants, by requiring the matching conditions at the surface $r = a$ for tangential and normal components of Φ,

$$-\frac{1}{a}\frac{\partial \Phi_{\text{in}}}{\partial \theta}\bigg|_{r=a} = -\frac{1}{a}\frac{\partial \Phi_{\text{out}}}{\partial \theta}\bigg|_{r=a} \qquad (\text{Tangential}), \tag{6.60}$$

$$-\epsilon\frac{\partial \Phi_{\text{in}}}{\partial r}\bigg|_{r=a} = -\epsilon_0\frac{\partial \Phi_{\text{out}}}{\partial r}\bigg|_{r=a} \qquad (\text{Normal}). \tag{6.61}$$

We must substitute the expansions (6.58) and (6.59) into these matching equations and solve to determine the constants. First consider the tangential matching. Substituting (6.58) and (6.59) into Eq. (6.60) gives

$$-\frac{1}{a}\frac{\partial}{\partial\theta}\sum_{l=0}^{\infty} A_l r^l P_l(\cos\theta)\bigg|_{r=a} = -\frac{1}{a}\frac{\partial}{\partial\theta}\left[B_l r^l P_1(\cos\theta) + \sum_{l=0}^{\infty} C_l r^{-(l+1)}\right]_{r=a} P_l(\cos\theta),$$

which simplifies to

$$\sum_{l=0}^{\infty} a^l A_l \frac{\partial}{\partial\theta} P_l(\cos\theta) = -aE_0\frac{\partial}{\partial\theta}P_1(\cos\theta) + \sum_{l=0}^{\infty} a^{-(l+1)} C_l \frac{\partial}{\partial\theta} P_l(\cos\theta). \tag{6.62}$$

Let's convert the derivatives of Legendre polynomials $P_n(x)$ to associated Legendre polynomials $P_n^m(x)$ using the general relationship [17],

$$P_n^m(x) = (1-x^2)^{m/2}\frac{d^m}{dx^m}P_n(x), \tag{6.63}$$

which, upon specializing to $m = 1$, yields

$$\frac{dP_n(x)}{dx} = (1-x^2)^{-1/2}P_n^1(x), \tag{6.64}$$

or, upon letting $x = \cos\theta$,

$$\frac{dP_n(\cos\theta)}{d\theta} = -P_n^1(\cos\theta). \tag{6.65}$$

Then Eq. (6.62) becomes

$$-\sum_{l=0}^{\infty} a^l A_l P_l^1(\cos\theta) = -aE_0 P_1^1(\cos\theta) + \sum_{l=0}^{\infty} a^{-(l+1)} C_l P_l^1(\cos\theta). \tag{6.66}$$

We will now exploit the orthogonality properties of the associated Legendre polynomials, which obey the relationship [17],

$$\int_{-1}^{+1} P_p^m(x) P_q^m(x) dx = K_{qm}\delta_{pq} \qquad K_{qm} \equiv \frac{2}{2q+1}\frac{(q+m)!}{(q-m)!}, \tag{6.67}$$

or in spherical coordinates

$$\int_0^\pi P_p^m(\cos\theta)P_q^m(\cos\theta)\sin\theta d\theta = K_{qm}\,\delta_{pq}. \tag{6.68}$$

There are two solutions for Eq. (6.66),

1. a *special solution* for $l = 1$, and
2. a *general solution* for all $l \neq 1$.

Special solution $(l = 1)$*:* To obtain the special solution let $x = \cos\theta$, multiply both sides by $P_1^1(x)$, and integrate to give

$$-\sum_{l=0}^{\infty} a^l A_l \int P_1^1(x)P_l^1(x)dx = -aE_0 \int P_1^1(x)P_1^1(x)dx + \sum_{l=0}^{\infty} a^{-(l+1)}C_l \int P_l^1(x)P_1^1(x)dx.$$

Utilizing Eq. (6.67), this gives

$$-\sum_{l=0}^{\infty} a^l A_l \delta_{1l} = -aE_0 + \sum_{l=0}^{\infty} a^{-(l+1)}C_l\delta_{1l},$$

and finally $aA_1 = -aE_0 + a^{-2}C_1$, so that

$$A_1 = -E_0 + \frac{C_1}{a^3} \qquad \text{(Special solution for } l = 1\text{)}. \tag{6.69}$$

General solution $(l \neq 1)$*:* To obtain the general solution, set $x = \cos\theta$, multiply both sides of Eq. (6.66) by $P_k^1(x)$, and integrate to give

$$-\sum_{l=0}^{\infty} a^l A_l \int P_k^1(x)P_l^1(x)dx = -aE_0 \int P_k^1(x)P_1^1(x)dx + \sum_{l=0}^{\infty} a^{-(l+1)}C_l \int P_k^1(x)P_l^1(x)dx.$$

Utilizing the orthogonality relation (6.67), this gives $a^l A_l = a^{-(l+1)}C_l$, which rearranges to

$$A_l = \frac{C_l}{a^{2l+1}} \quad \text{(General solution for } l \neq 1\text{)}. \tag{6.70}$$

Two relations [Eqs. (6.69) and (6.70)] have been obtained among the coefficients using the *tangential matching condition* (6.60) but the contraints imposed by matching at the boundary have not been exhausted: we may use the *normal matching condition* (6.61) to obtain additional constraints on the coefficients. Upon substituting the expansions (6.58) and (6.59) into Eq. (6.61),

$$\epsilon \sum_{l=0}^{\infty} l a^{l-1} A_l P_l(x) = \epsilon_0 B_1 P_1(x) + \sum_{l=0}^{\infty} -(l+1)C_l a^{-(l+2)}P_l(x). \tag{6.71}$$

As before, there are two solutions,

1. a *special solution,* when $l = 1$, and
2. a *general solution,* when $l \neq 1$.

Special solution ($l = 1$)*:* The special solution may be found by multiplying Eq. (6.71) by $P_1(x)$ and integrating. Upon exploiting orthogonality properties the result is another relationship among coefficients:

$$\frac{\epsilon}{\epsilon_0} A_1 = -E_0 - 2\,\frac{C_1}{a^3} \quad \text{(Special solution for } l = 1\text{)}. \tag{6.72}$$

General solution ($l \neq 1$)*:* The general solution may be obtained by multiplying both sides of Eq. (6.71) by $P_k(x)$, integrating, and exploiting the orthogonality constraints (4.38) to give

$$\frac{\epsilon}{\epsilon_0} l A_l = -(l+1)\frac{C_l}{a^{2l+1}} \quad \text{(General solution for } l \neq 1\text{)}. \tag{6.73}$$

We have obtained four equations—(6.69), (6.70), (6.72), and (6.73)—by exploiting boundary matching conditions on the fields; these must be solved simultaneously for the unknown coefficients. We note that Eqs. (6.70) and (6.73) can be satisfied only if $A_l = C_l = 0$ for all $l \neq 1$, and solving the other two equations (6.69) and (6.72) simultaneously for $l = 1$ gives

$$A_1 = -\left(\frac{3}{\epsilon/\epsilon_0 + 2}\right) E_0 \qquad C_1 = \left(\frac{\epsilon/\epsilon_0 - 1}{\epsilon/\epsilon_0 + 2}\right) a^3 E_0. \tag{6.74}$$

Inserting these results into Eqs. (6.58) and (6.59) gives for the *interior and exterior scalar potentials*

$$\Phi_{\text{in}} = -\left(\frac{3}{2 + \epsilon/\epsilon_0}\right) E_0\, r\cos\theta = -\left(\frac{3}{2 + \epsilon/\epsilon_0}\right) E_0\, z \qquad \text{(Interior potential)}, \tag{6.75a}$$

$$\Phi_{\text{out}} = -E_0\, z + \left(\frac{\epsilon/\epsilon_0 - 1}{\epsilon/\epsilon_0 + 2}\right) E_0\, a^3 \frac{\cos\theta}{r^2} \qquad \text{(Exterior potential)}, \tag{6.75b}$$

The electric fields then follow from $\boldsymbol{E} = -\boldsymbol{\nabla}\Phi$,

$$E_{\text{in}} = \left(\frac{3}{\epsilon/\epsilon_0 + 2}\right) E_0 \qquad \text{(Interior electric field)}, \tag{6.76a}$$

$$E_{\text{out}} = E_0 - \frac{P}{4\pi\epsilon_0 r^3} \qquad \text{(Exterior electric field)}, \tag{6.76b}$$

as shown in Problem 6.5. From these results we conclude that for the interior electric field

1. E_{in} is a constant that is proportional to the constant exterior field E_0,
2. if $\epsilon = \epsilon_0$, the interior field is equal to the exterior field, $E_{\text{in}} = E_0$, and
3. if $\epsilon > \epsilon_0$, then the strength of the interior field is reduced relative to that of the exterior field, $E_{\text{in}} < E_0$.

In Eq. (6.75b) for the external field, it is clear that the first term is just the unperturbed exterior field $\boldsymbol{E}_0$ and the second term is a correction associated with a potential generated by the polarized dielectric sphere. If the induced electric dipole moment $\boldsymbol{p}$ [see Eq. (3.59)] of the polarized sphere is taken to have magnitude

$$p = 4\pi\epsilon_0 \left(\frac{\epsilon/\epsilon_0 - 1}{\epsilon/\epsilon_0 + 2}\right) a^3 E_0, \tag{6.77}$$

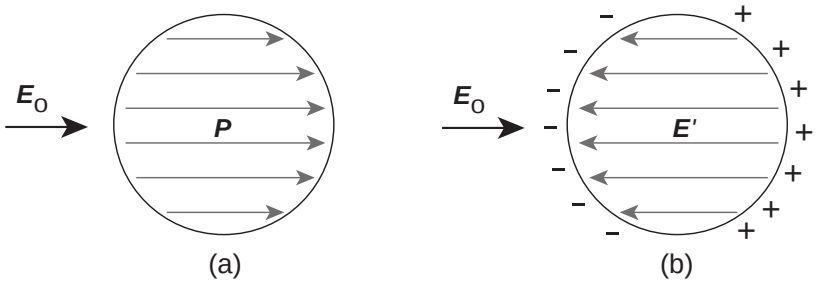

Fig. 6.13 (a) Polarization of a dielectric ball by an external electric field $\boldsymbol{E}_0$. (b) The polarization of charge induces a field $\boldsymbol{E}'$ inside the sphere that opposes and partially cancels the applied field $\boldsymbol{E}_0$.

then the exterior potential (6.75b) can be written

$$\Phi_{\text{out}} = -E_0\, z + \frac{p}{4\pi\epsilon_0}\frac{\cos\theta}{r^2}, \tag{6.78}$$

making clear that the external potential is the unperturbed external potential (first term) modified by a potential corresponding to an induced electric dipole at the origin that is associated with the polarized dielectric sphere. From Eqs. (6.25) and (6.27), the polarization $\boldsymbol{P}$ is given by

$$\boldsymbol{P} = (\epsilon - \epsilon_0)\boldsymbol{E}, \tag{6.79}$$

and from Eq. (6.11) the polarization may also be defined as the density of dipole moments. Then from Eq. (6.77), the polarization of the dielectric sphere is given by

$$\begin{aligned}\boldsymbol{P} = (\epsilon - \epsilon_0)\boldsymbol{E} &= \left(\frac{\text{dipole moments}}{\text{unit volume}}\right) = \frac{p}{\frac{4}{3}\pi a^3} \\ &= 3\epsilon_0\left(\frac{\epsilon/\epsilon_0 - 1}{\epsilon/\epsilon_0 + 2}\right)\boldsymbol{E}_0.\end{aligned} \tag{6.80}$$

As you are asked to show in Problem 6.6, the surface charge on the polarized dielectric in Fig. 6.12 is then given by

$$\sigma_{\text{pol}} = 3\epsilon_0\left(\frac{\epsilon/\epsilon_0 - 1}{\epsilon/\epsilon_0 + 2}\right)E_0\cos\theta. \tag{6.81}$$

The results of this extended example of a spherical dielectric in an external electric field are displayed graphically in Figs. 6.13 and 6.14.

As indicated schematically in Fig. 6.13(a), the external field E_0 aligned in the z direction polarizes the dielectric sphere, with the polarization vector $\boldsymbol{P}$ given in Eq. (6.80) and oriented in the direction of the external field. The polarization is the density of induced dipole moments (6.77). This corresponds to the polarization of charge illustrated in Fig. 6.13(b) with positive charge accumulating on the right side of the sphere and negative charge on the left side. The polarization of charge indicated in Fig. 6.13(b) induces an electric field $\boldsymbol{E}'$ that opposes the applied field $\boldsymbol{E}_0$ but does not completely cancel it for

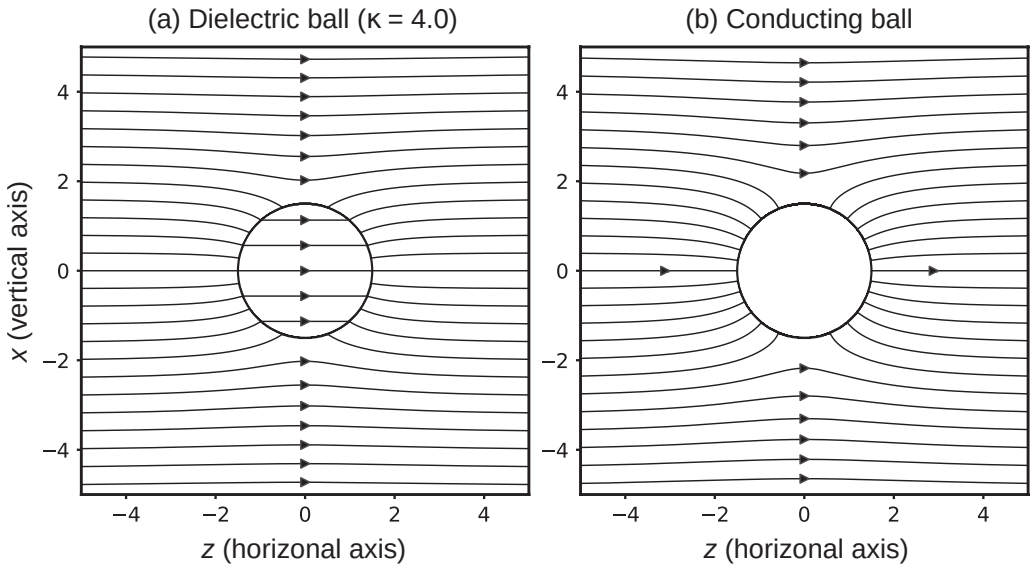

Fig. 6.14 (a) Electric field lines for dielectric filled sphere with dielectric constant $\kappa = 4.0$ in an external electric field $\boldsymbol{E}_0$ directed along the z axis. (b) Electric field lines for a conducting filled sphere in an external electric field $\boldsymbol{E}_0$ directed along the z axis. The conducting ball completely excludes the electric field (no field lines inside). The dielectric ball has a uniform electric field inside, but it is reduced in strength from the applied field (lower density of field lines inside relative to outside the dielectric ball).

the dielectric-filled sphere as would be the case for a conducting metal-filled sphere. The electric field $\boldsymbol{E}_{\text{in}}$ inside the sphere is given by Eq. (6.76) and is constant. If $\epsilon > \epsilon_0$ the electric field inside acts in the opposite direction as the applied field and is reduced in strength by a factor $3/(\epsilon/\epsilon_0 + 2)$ relative to the applied field. This is indicated schematically in Fig. 6.14(a), where we note that

1. The field inside $\boldsymbol{E}_{\text{in}}$ points in the same direction as the applied field $\boldsymbol{E}_0$, but is reduced in strength by the induced field $\boldsymbol{E}'$ acting against the applied field.
2. This reduction in strength for the interior field is indicated by the decreased density of field lines inside the sphere relative to the outside.
3. There is a discontinuity of the electric field lines at the boundary of the sphere because of the surface charge with density given by Eq. (6.81) that has accumulated there as a consequence of polarization by the external field.

As indicated in Eqs. (6.77) and (6.78), in the presence of the dielectric the external potential has two contributions:

1. the original potential due to the external field, and
2. a correction term that may be interpreted as the potential generated by an effective electric dipole centered on the dielectric sphere, which has been produced by the charge polarization.

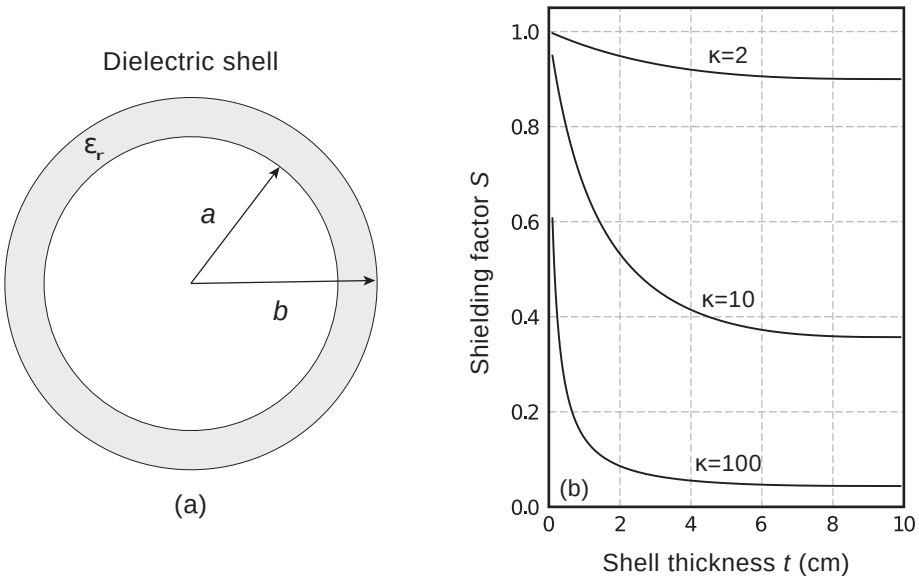

Fig. 6.15 (a) A concentric shell containing a dielectric with dielectric constant $\kappa = \epsilon/\epsilon_0 > 1$ in the gray areas. (b) Shielding factor $S = |\boldsymbol{E}|/|\boldsymbol{E}_0|$ for different values of the dielectric constant κ as a function of the shell thickness $t = b - a$ in cm for the dielectric shell.

At large distance the potential is that of the original applied field $\boldsymbol{E}_0$, but near the sphere the field lines in Fig. 6.14(a) are distorted by the increasing importance of the second term in Eq. (6.78), which grows rapidly as the sphere is approached since it scales as r^{-2}.

6.12.2 A Spherical Dielectric Shell

Let us repeat the analysis of the previous two sections, but for a spherical shell of dielectric material as illustrated in Fig. 6.15(a) with inner radius a, outer radius b, and dielectric constant $\kappa \equiv \epsilon/\epsilon_0 > 1$ (this is also termed the relative permittivity). The solution may be found by solving the Laplace equation in spherical coordinates. The details are worked out in Problems 6.7, 6.8, and 6.12, and have many similarities with the method of solution for the dielectric spherical ball problem in Section 6.12.1; the primary difference is that in the present case matching conditions must be imposed on both the inner and outer boundaries of the dielectric shell. Because of azimuthal symmetry and the $-E_0 r\cos\theta$ form of the external potential at infinity, upon expanding the solution in Legendre polynomials only the $l = 1$ terms survive (see Section 6.12.1). Defining the potential in three distinct regions corresponding to the boundaries in Fig. 6.15(a),

$$\Phi_1(r,\theta) = A_1 z = A_1 r\cos\theta \qquad (r < a), \tag{6.82a}$$

$$\Phi_2(r,\theta) = \left(B_1 r + \frac{C_1}{r^2}\right)\cos\theta \qquad (a < r < b), \tag{6.82b}$$

$$\Phi_3(r,\theta) = \left(-E_0 r + \frac{D_1}{r^2}\right)\cos\theta \qquad (r > b), \tag{6.82c}$$

and the unknown constants A_1, B_1, C_1, and D_1 may be determined by imposing boundary conditions at $r = a$ and $r = b$. Then the electric field follows from $\boldsymbol{E} = -\boldsymbol{\nabla}\Phi$. As shown in Problem 6.7, the solution for the electric field in the cavity inside the shell is then given by

$$\boldsymbol{E}_{\text{cav}} = -\boldsymbol{\nabla}\Phi_1 = \frac{9\kappa}{(2\kappa+1)(\kappa+2) - 2\left(\frac{a}{b}\right)^3(\kappa-1)^2}\,\boldsymbol{E}_0, \tag{6.83}$$

where $\boldsymbol{E}_0$ is the undisturbed applied electric field. Because $\kappa > 1$, the coefficient multiplying $\boldsymbol{E}_0$ is less than 1, demonstrating that a dielectric shell partially shields its interior from external electric fields due to the bound surface charge that forms on the inner and outer interfaces of the dielectric shell.

Equation 6.83 indicates that a dielectric shell shields its interior from external electric fields. Utilizing Eq. (6.83), we may define a *shielding factor* for the cavity inside a dielectric shell by

$$S \equiv \frac{|\boldsymbol{E}_{\text{cav}}|}{|\boldsymbol{E}_0|} = \frac{9\kappa}{(2\kappa+1)(\kappa+2) - 2\left(\frac{a}{b}\right)^3(\kappa-1)^2}, \tag{6.84}$$

where $\boldsymbol{E}_0$ is the undisturbed applied electric field outside the dielectric shell and $\boldsymbol{E}_{\text{cav}}$ is the electric field in the shielded cavity. Problem 6.12 investigates the effectiveness of this shielding, with examples of S as a function of ϵ for the material and the thickness of the dielectric shell $t = b - a$ displayed in Fig. 6.15(b). Example 6.6 illustrates a practical application of this information.

Example 6.6 Figure 6.15(b) illustrates the behavior of the shielding factor S defined in Eq. (6.84) for different materials and shell thickness. One sees that if we wish to operate a sensitive device in the shielded cavity of a dielectric shell of thickness 10 cm or less that suppresses external electric fields to only a few percent of their external value, we must use dielectric material with $\kappa = \epsilon/\epsilon_0$ of order 100. Materials exist with dielectric constants ~ 100 or more. One example is titanium dioxide (TiO_2), which has $\kappa \sim 86 - 173$ at room temperature. There are specialized high-κ materials that can exhibit dielectric constants of thousands or even tens of thousands under particular conditions. These materials are typically *ferroelectric* or *paraelectric*, meaning that they are characterized by spontaneous electric polarization (see Section 8.1) that can be reversed by an external field, implying massive effective dielectric constants. The classic example is barium titanate ($BaTiO_3$), which is used in multilayer ceramic capacitors and can exhibit $\kappa \sim 1200 - 10,000$ at room temperature. However, these very high-κ materials exhibit strong dependence on the frequency of the fields. Barium titanate has $\kappa \sim 10,000$ only for low-frequency fields. For frequencies in the microwave or optical region, κ drops dramatically to characteristic values of $\kappa \sim 10$ or less.

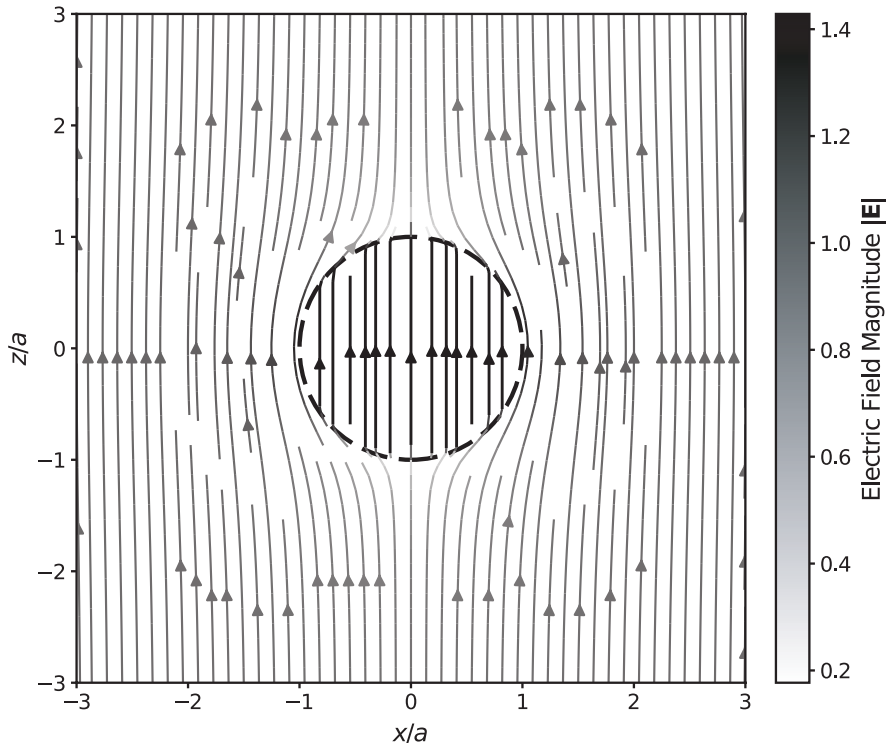

Fig. 6.16 Electric field for a spherical bubble of vacuum ($\epsilon = \epsilon_0$) in a uniform dielectric background with $\kappa = \epsilon/\epsilon_0 = 10$. The darker grayscale for larger electric field in the grayscale colormap indicates that the field is stronger inside the bubble than outside. [*NOTE: The actual density of field lines inside the sphere is also greater, but that isn't apparent since Python plotting has left gaps in the lines drawn. Need to apply Stokes Stream plotting or something similar in Python to fix this.*]

6.12.3 A Vacuum Bubble in a Dielectric Medium

Let us consider the problem of a spherical bubble immersed in a dielectric background, which is worked out in Problem 6.9, with results summarized in Fig. 6.16.[9] Notice that for the solution,

1. The field inside the dashed boundary is uniform (straight, vertical lines).
2. Although it is easier to see in color, the darker grayscale for stronger electric field indicates that the field is stronger inside the bubble (1.43 times stronger than $\boldsymbol{E}_0$ inside the bubble for $\kappa = 10$). This is because the induced surface charge on the boundary of the spherical bubble for this case creates a field that is enhanced relative to the external field $\boldsymbol{E}_0$.
3. The surrounding field lines are distorted near the cavity.

[9] This problem of a spherical bubble of normal vacuum immersed in a uniform dielectric is essentially the inverse of the spherical dielectric ball surrounded by vacuum worked out in Section 6.12.1. As a consequence, we can use similar methods of solution for the two problems.

These effects are a consequence of the bound positive charge induced on the upper hemisphere of the cavity and the bound negative charge induced on its lower hemisphere.

Background and Further Reading

Good introductions to the material of this chapter may be found in Griffiths [33]. More advanced treatments may be found in Jackson [41], Garg [31], Chaichian et al [23], and Zangwill [77].

Problems

6.1 Two concentric conducting spheres of inner and outer radii a and b, respectively, carry charges $\pm Q$. The empty space between the spheres is half-filled by a hemispherical shell of dielectric having dielectric constant ϵ/ϵ_0.

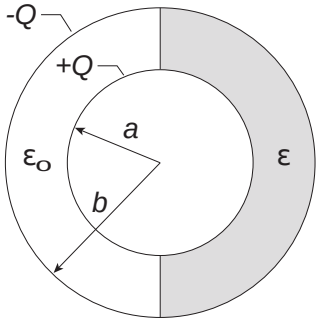

(a) Find the electric field in the region between the spheres. (b) Calculate the surface-charge distribution on the inner sphere. (c) Calculate the polarization-charge density induced on the surface of the dielectric at $r = a$. ***

6.2 Two long coaxial conducting cylinders of radii a and b are lowered vertically into a dielectric liquid.

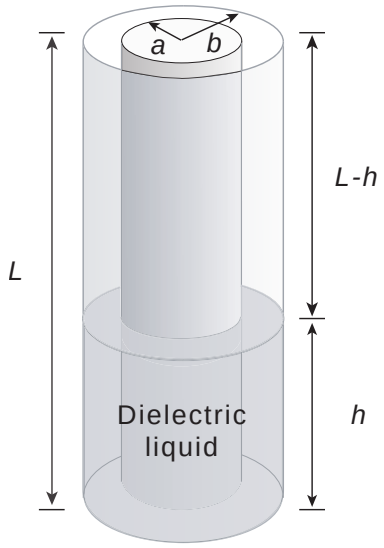

If the liquid rises an average height of h between the electrodes when a potential difference V is established between them, show that the susceptibility of the dielectric liquid is given by

$$\chi_e = \frac{(b^2 - a^2)\rho g h \ln(b/a)}{\epsilon_0 V^2},$$

where ρ is the density of the liquid, g is the acceleration due to gravity, and the susceptibility of the air is neglected.

6.3 A parallel-plate capacitor has plates of area A separated by a distance d and the plates are charged to a potential difference V using a battery.

a. With the charging battery *disconnected,* a dielectric sheet that has exactly the same width and length as a plate is inserted between the plates. Find the work done on the dielectric sheet; is it pulled in or must it be pushed in?

b. Repeat the experiment and analysis of part (a), but with the charging battery *connected* to the plates.

You may assume the capacitor plates to have infinite extent relative to the width of the gap between the plates.

6.4 A point charge q is located in free space a distance d from the center of a dielectric sphere of radius a, with $a < d$. Find the potential at all points in space as an expansion in spherical harmonics with expansion coefficients evaluated. ***

6.5 Prove that for the dielectric ball in an external electric field considered in Section 6.12, the interior and exterior electric fields are given by Eqs. (6.76a) and (6.76b), respectively. ***

6.6 For the dielectric ball in an external electric field

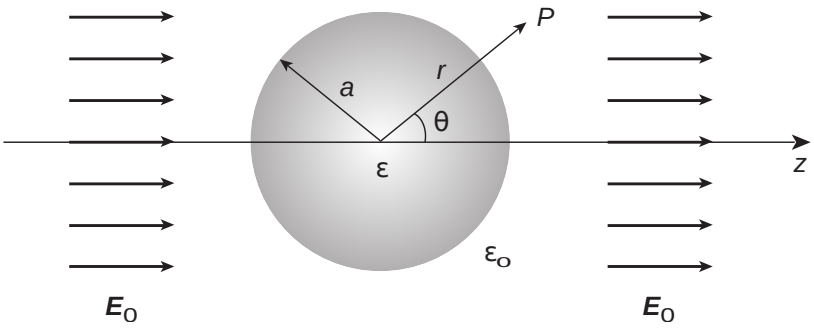

that is analyzed in Section 6.12, show that the surface charge density induced by the polarization is given by,

$$\sigma_{\text{pol}} = 3\epsilon_0 \left(\frac{\epsilon/\epsilon_0 - 1}{\epsilon/\epsilon_0 + 2} \right) E_0 \cos\theta,$$

where ϵ characterizes the interior and ϵ_0 characterizes the exterior permittivity.

6.7 Consider a hollow dielectric sphere (a spherical shell) with inner radius a, outer radius b, and relative permittivity $\epsilon_{\text{r}} = \epsilon/\epsilon_0$, as illustrated in the following figure.

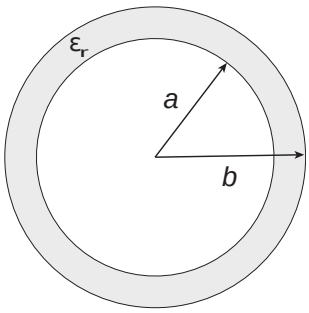

(a) The shell is placed in a region of space that initially contained a uniform electric field $\boldsymbol{E}_0 = E_0\hat{\boldsymbol{z}}$. Assuming that no free charge is present, determine the electric potential everywhere and show that the electric field inside the central cavity is given by

$$\boldsymbol{E}_{\text{cav}} = \frac{9\epsilon_{\text{r}}}{(2\epsilon_{\text{r}}+1)(\epsilon_{\text{r}}+2) - 2\left(\frac{a}{b}\right)^3(\epsilon_{\text{r}}-1)^2}\,\boldsymbol{E}_0.$$

(b) Verify that the solution for the interior electric field has the correct limiting behavior: as $a \to 0$ the shell should vanish entirely, leaving a solid dielectric sphere (spherical ball); as $a \to b$, the shell vanishes entirely, which should leave the undisturbed initial field $\boldsymbol{E}_0$. ***

6.8 For the dielectric shielding problem described in Problem 6.7, define a shell thickness $t = b - a$ and a *shielding factor* S as the magnitude of the cavity field relative to the external field: $S = |\boldsymbol{E}_{\text{cav}}|/|\boldsymbol{E}_0|$.

a. Using the formula for $\boldsymbol{E}_{\text{cav}}$ from Problem 6.7, evaluate the shielding ratio analytically in the limit of a vanishing shell ($t \to 0$); is the result physically reasonable?
b. Evaluate the shielding ratio analytically in the limit of a solid sphere ($t \to b$); compare this asymptotic value to the field inside a solid dielectric sphere, which is given in Eq. (6.76a).

6.9 Consider an infinite, linear, isotropic, homogeneous dielectric medium with relative permittivity $\epsilon_{\text{r}} = \epsilon/\epsilon_0 > 1$. A spherical cavity of radius a (in which $\epsilon = \epsilon_0$) is hollowed out of this medium. Far away from the cavity, the electric field is uniform, $\boldsymbol{E}_{\text{bulk}} = E_0\hat{\boldsymbol{z}}$. Determine the electric field inside the cavity, and in the surrounding medium, and plot it using *Python*, *gnuplot* or another software package. ***

Numerical and GenAI Problems

6.10 In introductory discussions we usually idealize parallel-plate capacitors as having infinite plate size relative to the size of the gap between them. In the real world capacitors have plates of finite size and the actual potential and fields differ from the idealized analytical result.

a. Assume two infinitesimally thin conducting plates of length L, separated by a gap distance d in a vacuum. The plates extend infinitely into the page so this can be treated as a 2D problem. Assume no dielectric layer and no free charge in the gap between the plates.

b. Use your *GenAI* to write *Python* code to calculate by numerical integration with a finite difference method FDM (see Section 4.3.1 and Appendix F.4) the potential Φ and electric field $\boldsymbol{E}$ in a 2D domain near the capacitor.
c. Use your code to investigate how changing the ratio d/L influences deviation of the resulting potential and electric field relative to the idealized solution that would be obtained analytically by assuming $L \to \infty$.
d. Discuss how the code was implemented and debugged, how you checked the validity of the AI-generated results, and the physical meaning of your results; include appropriate *Python*-generated plots illustrating your results.

Hint: To get sufficient resolution to see the detailed behavior of the fields in the 2D domain near the capacitor will require integration over a 2D grid with many points, so investigate with the *GenAI* how to make the relatively slow interpreted *Python* code of a minimal FDM scheme faster by (1) using an adaptive mesh for numerical integration (see Section 4.4.3) and by (2) vectorizing the finite-difference algorithm (see Section 4.4.1 and Box 4.1).

6.11 Repeat Problem 6.4 for a point charge near a dielectric sphere, but now solve it numerically , using your *GenAI* to write appropriate *Python* code. Check your answers against the analytical results of Problem 6.4.

6.12 The analytical solution for the electric field in the interior cavity of a spherical shell containing dielectric matter was obtained in Problem 6.7. As in Problem 6.8, define a *shielding factor* S as the magnitude of the cavity field relative to the external field: $S = |\boldsymbol{E}_{\text{cav}}|/|\boldsymbol{E}_0|$.

a. *Computational Implementation:* Write, or prompt your *GenAI* to write, a *Python* script to calculate the shielding ratio S, assuming a fixed outer radius $b = 10.0$ cm. Plot S as a function of the shell thickness $t = b - a$ for three different dielectric materials having $\epsilon_{\text{r}} = 2$, $\epsilon_{\text{r}} = 10$, and $\epsilon_{\text{r}} = 100$, respectively.
b. *Design Constraint:* If you needed to suppress the external electric field inside a sensitive detector cavity to less than 5% of its original strength, what minimum relative permittivity $\epsilon_{\text{r}} \equiv \epsilon/\epsilon_0$ would be required if design constraints limit your shell thickness to $t = \frac{1}{2}b$ or less? What are some candidate materials having ϵ_{r} that large?

6.13 Repeat Problem 6.10, but now assume that the capacitor has more ideal behavior ($L \gg d$) and that a dielectric layer has been inserted between the plates. Investigate how changing the dielectric layer influences the potential and electric field in a 2D domain near the capacitor.

7 Steady Currents

An important class of problems in electrostatics corresponds to situations where the source of the electric field $\boldsymbol{E}$ is a steady flow of electrical charge. In this chapter we shall study electrostatics in the presence of such steady-current sources.

7.1 Steady-Current Conditions

The current I passing through an arbitrary surface S is given by

$$I = \int_S d\boldsymbol{S} \cdot \boldsymbol{J}. \tag{7.1}$$

where $\boldsymbol{J}$ is the current density. Generally the charge density ρ and the current density $\boldsymbol{J}$ are required to satisfy the continuity equation (1.3),

$$\frac{\partial \rho}{\partial t} + \boldsymbol{\nabla} \cdot \boldsymbol{J} = 0,$$

which ensures *local conservation of charge* by demanding that electrical charge variation in some arbitrarily small volume be caused by flow of electrical current through the surface of that volume. If we restrict consideration to charge densities having no explicit time dependence, $\partial\rho/\partial t = 0$ and the continuity equation simplifies to the *steady-current condition*

$$\boldsymbol{\nabla} \cdot \boldsymbol{J} = 0 \qquad \text{(Steady-current condition)}. \tag{7.2}$$

Currents satisfying (7.2) can produce static electric and static magnetic fields, which can be studied independently because the Maxwell equations (1.1) do not mix static electric and magnetic fields. The field lines of a current density $\boldsymbol{J}$ consistent with Eq. (7.2) must satisfy the condition that every field line

- begins and ends at infinity, or
- closes on itself, implying that
- any field line entering an infinitesimal volume of space must also exit that volume.

Figure 7.1 shows an example of field lines for a current satisfying these conditions. The resemblance of Fig. 7.1 to streamlines for fluid flow is obvious, and the analogy of a steady current as a flow of fluid is often a useful one as long as the details of microscopic interactions between particles in an ordinary fluid can be ignored. If the motion of a charge density is characterized by a velocity field $\boldsymbol{v}(\boldsymbol{x})$ we may write

$$\boldsymbol{J}(\boldsymbol{x}) = \rho(\boldsymbol{x})\boldsymbol{v}(\boldsymbol{x}). \tag{7.3}$$

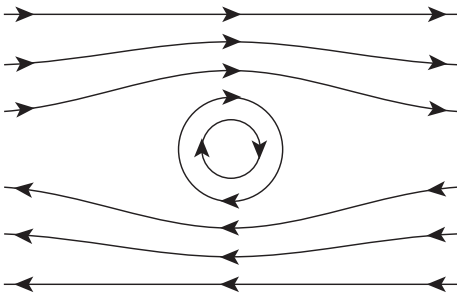

Fig. 7.1 Field lines of a current density that satisfies the condition (7.2) for a steady current. The resemblance to streamlines for flow of an ordinary fluid is apparent.

If the charge density can be viewed as moving rigidly with a uniform velocity $\boldsymbol{v} = v_0$, the current can be expressed as

$$\boldsymbol{J}(\boldsymbol{x}) = \rho(\boldsymbol{x})v_0, \tag{7.4}$$

and Eq. (7.3) is termed the *convection current density*. If N different species carrying charges q_i, with number densities n_i and uniform velocities v_i contribute to the current, the current density is a sum of the different contributions

$$\boldsymbol{J} = \sum_{i=1}^{N} q_i n_i b_i. \tag{7.5}$$

We shall most often exemplify using currents with a single kind of charge carrier, but currents with such mixed charge carriers—perhaps with different charge signs for the constituent carriers—may be found in some realistic applications such as in biological and astrophysical settings.

7.2 Vacuum Currents

We begin with the simplest currents, which can be viewed as a stream of particles flowing in a vacuum, with no influence from any fields or surrounding matter. The properties of vacuum currents may be explored by considering the operation of the *vacuum diode* illustrated in Fig. 7.2(a), which is a parallel plate capacitor with one plate heated so that it expels electrons by *thermionic emission*.[1] These devices may be as unfamiliar to the reader as horse-drawn buggies because they have been replaced by semiconductors in most modern consumer electronics, but a theoretical analysis of the vacuum diode provides substantial insight into the nature of vacuum currents. In particular, vacuum diodes illustrate clearly a characteristic property of vacuum currents: the current is limited ultimately by interactions between the charge-carrying particles in the current itself.

[1] Thermionic emission is the ejection of particles from the surface of a heated metal because the thermal energy of the metal gives some particles sufficient kinetic energy to escape, with the rate of ejection increasing with temperature. We consider only the case of the emitted particles being electrons.

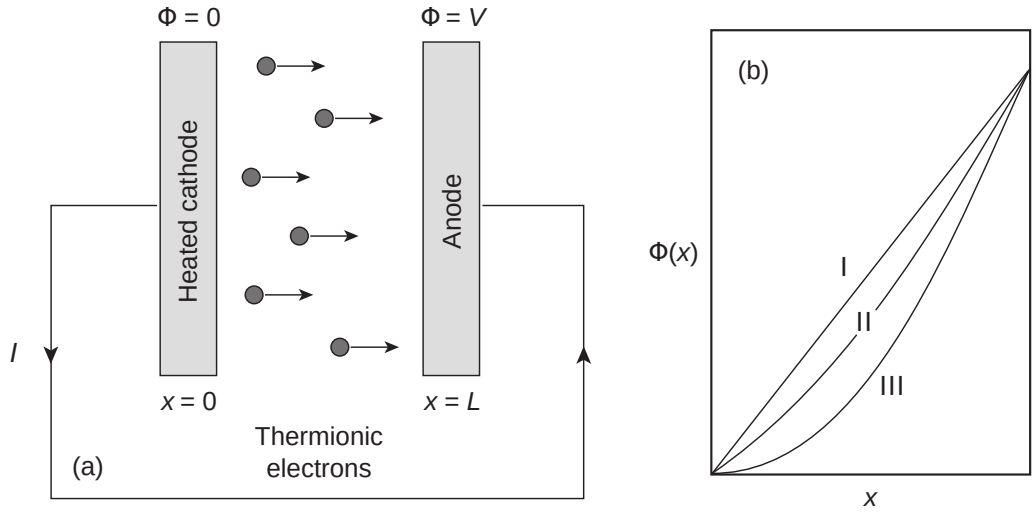

Fig. 7.2 (a) A vacuum diode. The heated cathode emits electrons thermionically that strike the anode, causing a current to flow in the circuit. (b) Curves for the electric potential Φ between the plates for (I) low, (II) medium, and (III) high thermionic electron density.

In our analysis a vacuum will be assumed to exist between the plates in Fig. 7.2(a), and for simplicity the thermionic electrons are taken to have negligible velocity when produced. A vacuum diode behaves differently at different cathode temperatures, which corresponds to different rates of electron emission from the heated plate, as will now be discussed.

7.2.1 Vacuum Diodes at Low Temperature

At low cathode temperatures the rate of electron emission, and thus the density of electrons between the plates, is small. The emitted electrons accelerate in the potential $\Phi(x) = xV/L$, and if the electron density is negligible the behavior of the electrons corresponds to the usual solution of the Laplace equation (2.58) between the plates of a capacitor that is illustrated by Curve I in Fig. 7.2(b). The current per electron in the gap is estimated in Problem 7.2 to be

$$I = \frac{e}{L}\, v, \tag{7.6}$$

where L is the plate separation and v is the average speed of electrons in the gap.

7.2.2 Vacuum Diodes at Intermediate Temperatures

If the temperature of the cathode is raised the rate of electron emission increases, as does the current in the gap since each additional electron makes a contribution given by Eq. (7.6). Eventually, the charge density in the gap created by the emitted electrons can no

longer be ignored; a *space charge*[2] builds up in the gap, and the solution for the potential is no longer given by the Laplace equation $\nabla^2\Phi = 0$, but rather by the Poisson equation (2.54),

$$\nabla^2\Phi = -\frac{\rho}{\epsilon_0}. \tag{7.7}$$

The transition of the solution from Laplace to Poisson is a signal that the Coulomb repulsion between the emitted electrons in the gap associated with the charge density ρ (which is negative) can no longer be ignored. In one dimension $\nabla^2 = d^2/dx^2$ is a curvature and the Poisson equation (7.7) implies that the potential $\Phi(x)$ begins to develop a positive curvature between the plates as a result of the (negative) space charge built up there (physically because the Coulomb interaction between the charges in the gap begins to retard their acceleration), leading to the behavior that is exemplified by Curve II in Fig. 7.2(b).

7.2.3 Vacuum Diodes at High (Saturation) Temperature

Despite the retarding effect of the accumulating space charge the charge density and current continue to increase as the temperature of the cathode is raised, although more slowly than at lower temperatures. Eventually, however, a temperature is reached where $d\Phi/dx \to 0$ at $x = 0$, which is exemplified by Curve 3 in Fig. 7.2(b). The *current saturates* at this point, since there is no electric field at the cathode ($x = 0$) to accelerate additional emitted electrons.

7.2.4 Space Charge and the Child–Langmuir Law

The saturated saturated steady current illustrated by Curve III in Fig. 7.2(b) still satisfies Eq. (7.2), meaning that

$$\rho(x)v(x) = \text{ constant} \tag{7.8}$$

everywhere. Furthermore, because we assumed $v(0) = 0$, the kinetic energy of each electron is

$$\frac{1}{2}mv^2(x) = e\,\Phi(x). \tag{7.9}$$

Combining these results with the Poisson equation (7.7) leads to the *Child–Langmuir law* specifying the space-charge limited current density,

$$|\boldsymbol{J}| = \frac{4}{9}\sqrt{\frac{2e}{m}}\frac{\epsilon_0 V^{3/2}}{L^2}, \tag{7.10}$$

as you are asked to show in Problem 7.3.

[2] *Space charge* is a general term used to indicate a volume of uncompensated charge that builds up in an otherwise electrically neutral region of space.

7.3 Currents in Matter

Electrical currents flowing in neutral matter are generally more complex than those flowing in a vacuum, requiring the full power of quantum mechanics and statistical mechanics for an adequate theoretical understanding. Nevertheless, it is empirically well established that the current density for many systems can be described well by *Ohm's law*, which is based on classical considerations and is described in the following subsection.

7.3.1 Ohm's Law

To make a current flow some force must push on the charges (continuously if, as is usually the case, there is any resistance to the charge flow). For most materials the current density $\boldsymbol{J}$ is proportional to the force per unit charge $\boldsymbol{f}$,

$$\boldsymbol{J} = \sigma \boldsymbol{f}, \tag{7.11}$$

where the constant of proportionality σ depends on the nature of the medium and is called the *conductivity*. Often the reciprocal of the conductivity, $\rho = \sigma^{-1}$, which is called the *resistivity*, is used instead. If the force is electromagnetic in origin,

$$\boldsymbol{J} = \sigma(\boldsymbol{E} + \boldsymbol{v} \times \boldsymbol{B}), \tag{7.12}$$

where $\boldsymbol{E}$ is the electric field, $\boldsymbol{B}$ is the magnetic field, and $\boldsymbol{v}$ is the velocity. Except for special circumstances such as in relativistic plasmas, the velocity is small and the $\boldsymbol{v} \times \boldsymbol{B}$ term can be neglected, leaving

$$\boldsymbol{J} = \sigma \boldsymbol{E} \qquad \text{(Ohm's law)}. \tag{7.13}$$

This is called *Ohm's law*.[3] For a cylindrical wire of cross-sectional area A and conductivity σ, if the potential difference between the ends is V the electric field and current density are uniform and the total current is given

$$I \equiv JA\sigma EA = \frac{\sigma A}{V}. \tag{7.14}$$

In this and similar examples the total current flow in the wire from one point to another is proportional to the potential difference between the points,

$$V = IR \qquad \text{(Ohm's law)}, \tag{7.15}$$

where the constant of proportionality R is called the *resistance*. This is the most familiar form of Ohm's law. The resistance depends on the geometry and the conductivity of the medium; in the example given above $R = L/\sigma A$, where L is the length. In more complex situations (for example, crossed electric and magnetic fields) the simple scalar form of Ohm's law described here is replaced by a tensor formulation, as described in Box 7.1.

[3] Ohm's law is not a true "law" in the same sense as say Coulomb's law or the law of gravity. It is a "rule of thumb" that is often but not always obeyed. The subset of conductors that do obey Ohm's law are called *ohmic conductors*.

Box 7.1 Resistivity and Conductivity Tensors

In the simplest cases the current and the electric field may be assumed collinear and the elementary form of *Ohm's law* described in Section 7.3.1 holds: $V = IR$, where V is voltage, I is current, and R is resistance. This can also be expressed in terms of the electric field E and current density j as $j = \sigma E$ where σ is the scalar *conductivity,* or the inverted expression $E = \rho j$, where the scalar *resistivity* ρ is given by $\rho = \sigma^{-1}$. In more complex situations such as in the Hall effect described in Box 8.1 where there are both electric and magnetic fields, the resistivities and related quantities become tensors. Restricting to two dimensions for the Hall problem, the rank-2 resistivity tensor ρ and rank-2 conductivity tensor σ may be expressed as the matrices

$$\rho = \begin{pmatrix} \rho_{11} & \rho_{12} \\ \rho_{21} & \rho_{22} \end{pmatrix} = \begin{pmatrix} \rho_{xx} & \rho_{xy} \\ \rho_{yx} & \rho_{yy} \end{pmatrix} \qquad \sigma = \begin{pmatrix} \sigma_{11} & \sigma_{12} \\ \sigma_{21} & \sigma_{22} \end{pmatrix} = \begin{pmatrix} \sigma_{xx} & \sigma_{xy} \\ \sigma_{yx} & \sigma_{yy} \end{pmatrix},$$

where the components are $\rho_{ij} = E_i/j_j$ and $\sigma_{ij} = j_i/E_j$, with ρ and σ related by matrix inversion, $\rho = \sigma^{-1}$. Then $E_i = \rho_{ij} j_j$ and $j_i = \sigma_{ij} E_j$, or

$$\begin{pmatrix} E_x \\ E_y \end{pmatrix} = \begin{pmatrix} \rho_{xx} & \rho_{xy} \\ \rho_{yx} & \rho_{yy} \end{pmatrix} \begin{pmatrix} j_x \\ j_y \end{pmatrix} \qquad \begin{pmatrix} j_x \\ j_y \end{pmatrix} = \begin{pmatrix} \sigma_{xx} & \sigma_{xy} \\ \sigma_{yx} & \sigma_{yy} \end{pmatrix} \begin{pmatrix} E_x \\ E_y \end{pmatrix},$$

written out explicitly. Notice that if $\rho_{xy} = \rho_{yx}$ vanishes the resistivity matrix becomes diagonal and we revert to the simple Ohm's law description of Section 7.3.1, with a scalar resistivity.

7.3.2 The Drude Model of Metallic Conduction

An unavoidable difficulty for any classical treatment of electromagnetism is that important phenomena involving interaction with matter, such as the dielectric or magnetic properties of various materials, depend essentially on the microscopic structure of the matter, which requires arguments from quantum theory and quantum statistical mechanics that are outside the scope of classical electrodynamics and classical mechanics. In a presentation of classical electrodynamics, one is forced then into one of two alternatives:

1. graft sufficient quantum theory and results into the presentation, assuming that the reader has sufficient understanding of quantum theory, or
2. approximate quantum phenomena by classical or semiclassical models.

An example of the second alternative is the *Drude model of electrical conduction* [26, 27], which predates modern quantum mechanics by 25 years, but is still used in condensed matter physics to give a qualitative overview of metallic conduction [19]. We begin this section with a brief introduction to the Drude model.

Although at the time there was little precise theoretical justification, in the year 1900

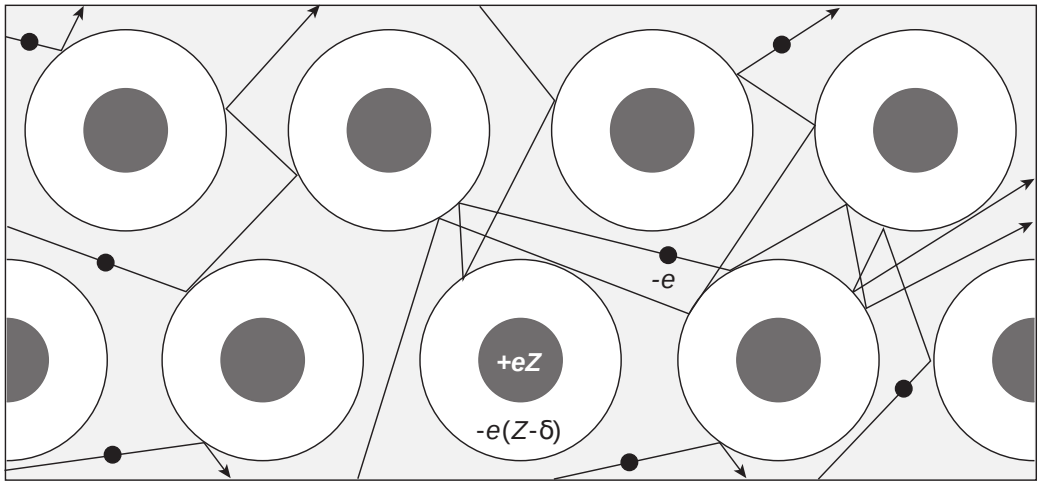

Fig. 7.3 Drude model of electrical conduction in metal with atoms of atomic number Z, which is basically a classical analysis of a pinball machine in which the ions are stationary and act as the posts of the machine and the valence electrons are detached from the ions, free to roam through the crystal lattice and scatter from the ions as in a pinball machine. In this diagram (which is *not to scale*) each large circle is an ion, which consists of the dark gray nucleus with charge $+eZ$, surrounded by a white region containing the core electrons carrying charge $-e(Z-\delta)$, where δ is the number of electrons ionized from each ion. The small black balls indicate electrons that have been freed from the ions and scatter randomly from the fixed ions. In this example an electric field has been assumed that causes a net drift of the randomly scattering electrons to the right.

Drude proposed a model of metallic conduction that *assumed* the heavy, positively charged ions (atomic nucleus plus core electrons in modern language) to be fixed spatially in a crystal lattice, and that the light valence electrons became detached from the ions and wandered freely, scattering randomly from the fixed ions as in a *miniature pinball machine;* Fig. 7.3 illustrates.[4] These free (valence) electrons are called the *conduction electrons*, and in the Drude model they are viewed as forming a gas. There are four basic assumptions that enter into this *Drude model*.

1. Between collisions with ions the conduction electrons move freely in straight lines, if there are no applied fields. If external fields are applied, the electrons move according

[4] As indicated in Fig. 7.3, the number of ionized valence electrons per atom is denoted by δ, which will depend on the valence of the atoms comprising the metal. For example, metallic copper in a $+1$ valence state has $\delta(\mathrm{Cu}) = 1$ and metallic iron in a $+2$ valence state has $\delta(\mathrm{Fe}) = 2$. One should bear in mind that when the Drude model was formulated in 1900 the electron had only recently been discovered as a distinguishable particle (by J. J. Thomson in 1897), but it was not yet certain that atoms even existed, or what their structure was if they did. In particular, it is clear that our discussion above distinguishing core electrons from valence electrons in atoms is an interpolation into the Drude model of knowledge that would only come later: even the rudimentary Bohr model of the atom was still 15 years in the future, and it would be another 25 years before quantum mechanics would be invented when Drude published his model.

to Newton's laws of motion in those fields (this is called the *independent electron approximation*), neglecting fields produced by other electrons or ions (this is called the *free electron approximation*). The independent electron approximation is found to be fairly good in many contexts, but even a qualitative understanding of the behavior of metals often requires improving on the free electron approximation.

2. As in kinetic theory, collisions are assumed to alter electron velocity instantaneously.[5] Although the simple picture of Fig. 7.3 with instantaneous interactions misses the mark in details, many qualitative features of metallic behavior survive.
3. A parameter τ called the *relaxation time* or *mean collision time* is of fundamental importance in the Drude model. The probability per unit time for an electron collision to occur is τ^{-1} so that the probability that an electron experiences a collision in a time interval dt is dt/τ. With these assumptions, an electron chosen at random at a given time will travel an average time τ before the next collision, and will have traveled an average time τ since its last collision. In the simplest approximation, the relation time τ is assumed *independent of electron position and velocity*. Perhaps surprisingly, this assumption often works reasonably well.
4. Electrons reach thermal equilibrium only through collisions. After each collision an electron emerges with a velocity having a random direction and a magnitude proportional to the local temperature at the site of the collision.

The following example illustrates an application of the Drude model to the relationship of current, voltage, and resistance for a current flowing in a wire.

Example 7.1 According to the empirical Ohm's law described in Section 7.3.1, for a current I flowing in a wire, $V = IR$, where V is the voltage drop and R is the resistance, which depends on the geometry of the wire but is independent of V and I. Let us show that the Drude model provides a reasonable understanding of Ohm's law, and allows an estimate of the resistance R. The dependence of the resistance on the geometry of the wire can be eliminated by introducing the *resistivity* ρ, which depends only on the nature of the metal in the wire, through the requirement that it be the constant of proportionality between the electric field $\boldsymbol{E}$ and the current density $\boldsymbol{J}$ that it induces,

$$\boldsymbol{E} = \rho \boldsymbol{J}, \tag{7.16}$$

where we assume the simplest case that $\boldsymbol{E}$ and $\boldsymbol{J}$ are parallel. [If they were not parallel, the scalar resistivity in Eq. (7.16) would become a *resistivity tensor*, as described in Box 7.1.] The magnitude of $\boldsymbol{J}$ is the charge per unit time crossing a unit area perpendicular to the current. For uniform flow of a current I through a wire of length L and cross sectional area A, the current density will be $J = I/A$ and since the voltage drop along the wire is EL, from Eq. (7.16) $V = I\rho L/A$ and the resistance is related to the resistivity of the

[5] As illustrated in Problem 7.1, the density of the "gas of conduction electrons" is typically of order 1000 times larger than that of classical gases at standard temperature and pressure; nevertheless, the Drude model assumes the normal kinetic theory of gases to apply in relatively unaltered form.

metal and the geometry of the wire by

$$R = \frac{\rho L}{A}. \tag{7.17}$$

If n electrons per unit volume, each carrying charge $-e$ move with velocity $\boldsymbol{v}$, in a time dt the charge passing through a cross section A will be $-nevAdt$, so the current density is

$$\boldsymbol{J} = -ne\boldsymbol{v}. \tag{7.18}$$

In the absence of an applied field electrons may be expected to move randomly in all directions and the velocity $\boldsymbol{v}$ in Eq. (7.18) averages to zero, but if an electric field $\boldsymbol{E}$ is applied there will be a non-zero net velocity of the electrons opposite the direction of $\boldsymbol{E}$ (since the electron charge is negative).

This velocity can be computed as follows. For a typical electron at time zero, let Δt be the time elapsed since its last collision. Its velocity will be a sum of the velocity $\boldsymbol{v}_0$ after the last collision plus a velocity $-e\boldsymbol{E}\delta t/m$ (where m is the electron mass) gained from the electric field. Since the Drude model assumes the direction of the velocity after the previous collision to be random, $\boldsymbol{v}_0$ averages to zero and the average electronic velocity is given entirely by the average of $-e\boldsymbol{E}\Delta t/m$. But the average of Δt is the Drude relaxation time τ and therefore the average velocity is

$$\overline{\boldsymbol{v}} = -\frac{e\boldsymbol{E}\tau}{m}, \tag{7.19}$$

and the current density is

$$\boldsymbol{J} = \sigma\boldsymbol{E} \qquad \sigma \equiv \frac{ne^2\tau}{m}, \tag{7.20}$$

where $\sigma = \rho^{-1}$ is called the *conductivity*. [As for the resistivity, if $\boldsymbol{E}$ and $\boldsymbol{J}$ are not parallel the scalar conductivity of Eq. (7.20) becomes a *conductivity tensor*, as described in Box 7.1.] The Drude relaxation time is then

$$\tau = \frac{m}{\rho n e^2}, \tag{7.21}$$

from which measured resistivities ρ can be used to estimate relaxation times. These are found to be $\tau \sim 10^{-14}$ seconds for many metals at room temperature.

The Drude model describes some conduction phenomena qualitatively, but fails dramatically for others. The successes point to aspects of conduction theory that can be understood in simple classical terms, such in Example 7.1; the failures can be understood and ameliorated only with the aid of modern quantum theories of electrical conduction.

Background and Further Reading

The properties of vacuum diodes are described in Ref. [77]. An introduction to the Drude model of classical conduction may be found in Ref. [19].

Problems

7.1 In the Drude model, estimate the number density of the gas of conduction electrons for a typical metal like copper. Compare with the number density for a typical gas by calculating the number density for air molecules under standard conditions.

7.2 For the vacuum diode of Fig. 7.2(a), assume that the cathode temperature is low enough that electron density between the plates is small. Find an expression for the average current per electron in the gap between the plates in terms of plate separation L and average electron speed v.

7.3 Using Eqs. (7.8) and (7.9), and the Poisson equation (7.7), prove the space-charge limiting result given in Eq. (7.10). ***

Numerical and GenAI Problems

8 Magnetostatics in Vacuum

Chapters 2-6 have dealt with the subject of electrostatics. The basic goal of electrostatics is that we have some set of discrete source charges $\{q_i\}$, or a localized continuous distribution of charge $\rho(\boldsymbol{x})$, that are *stationary* with respect to a chosen reference frame, and we desire to calculate the electric field produced by those charges at arbitrary locations in space. This can be accomplished using the principle of superposition: calculate the contribution of each source charge q_i or infinitesimal piece of a continuous charge $d\rho(\boldsymbol{x})$ to the electric field at some point, and sum them to get the total electric field at that point. We have developed a number of sophisticated ways to do this beyond brute force summation or integration, but that is the essential idea. In this chapter we wish to expand upon this idea by the (seemingly) elemental extension of allowing the source charges to move.

8.1 Magnetostatics versus Electrostatics

The introduction of charges in motion (currents) may seem an innocuous change on its surface, but it adds to the electric field associated with the stationary source charges a new *magnetic field* associated with their motion, and a host of associated phenomena (*magnetism*) having a phenomenology that is often very different from that of electrostatics; so much so that it took many centuries after electrostatic and magnetic phenomena were first identified in nature to realize that they are not separate subjects but are in fact different manifestations of the same basic physical principles. Although we shall emphasize the unity of electricity and magnetism from multiple perspectives later in this book, for now it is useful to consider *magnetostatics* (magnetic effects produced by steady currents) in isolation.

Magnetostatics is more subtle and complex than electrostatics. From Maxwell's equations (1.1), a time-independent current distribution $\boldsymbol{J}(\boldsymbol{x})$ is a source of a vector field $\boldsymbol{B}(\boldsymbol{x})$ called the *magnetic field* that satisfies the differential equations[1]

$$\boldsymbol{\nabla} \cdot \boldsymbol{B}(\boldsymbol{x}) = 0, \tag{8.1a}$$

$$\boldsymbol{\nabla} \times \boldsymbol{B}(\boldsymbol{x}) = \mu_0 \boldsymbol{J}(\boldsymbol{x}). \tag{8.1b}$$

Applying the divergence operation to both sides of Eq. (8.1b) using the vector identity

[1] Equations (8.1) specify the divergence and the curl of the vector field $\boldsymbol{B}(\boldsymbol{x})$. This should be sufficient to specify $\boldsymbol{B}(\boldsymbol{x})$ uniquely by the Helmholtz theorem of Section 3.3.6, provided that the fields and sources are sufficiently well-behaved.

$\boldsymbol{\nabla} \cdot (\boldsymbol{\nabla} \times \boldsymbol{A}) = 0$ of Eq. (A.6) gives

$$\boldsymbol{\nabla} \cdot (\boldsymbol{\nabla} \times \boldsymbol{B}(\boldsymbol{x})) = 0 = \mu_0 \boldsymbol{\nabla} \cdot \boldsymbol{J}(\boldsymbol{x}). \tag{8.2}$$

Thus, magnetostatic current densities satisfy $\boldsymbol{\nabla} \cdot \boldsymbol{J}(\boldsymbol{x}) = 0$. In electrostatics stationary charges produce *electric fields constant in time*; in magnetostatics stationary (unchanging) currents produce *magnetic fields that are constant in time*. The more complex nature of magnetostatics relative to electrostatics arises in part because magnetostatics involves a current density that is a vector and the force law [given in Eq. (8.4) below] involves a cross product of vectors, in contrast to the scalar quantities and operations inherent in electrostatics. From a physics perspective magnetism is also complicated by there being two fundamentally different types of currents that can produce magnetic effects:

1. currents that results from moving charges, and
2. currents that result from the quantum spins of point-like particles (*magnetization currents*), which have no suitable classical analogs.[2]

It follows that *magnetizable matter* exhibits much greater variety than *polarizable matter* (Ch. 6), both in its fundamental attributes and in the way that it responds to external fields.

> For example, permanent magnetism (*ferromagnetism*), caused by spontaneous breaking of angular momentum symmetry by macroscopic alignment of spins, occurs much more commonly than than the dielectric counterpart of *ferroelectricity* where a material spontaneously polarizes in the absence of an external electric field [77].

From the static (all time derivatives are set to zero) vacuum Maxwell equations (1.1), the basic equations governing electrostatics are

$$\boldsymbol{\nabla} \times \boldsymbol{E}(\boldsymbol{x}) = 0 \tag{8.3a}$$

$$\boldsymbol{\nabla} \cdot \boldsymbol{E}(\boldsymbol{x}) = \frac{\rho(\boldsymbol{x})}{\epsilon_0}. \tag{8.3b}$$

Comparing with the basic equations (8.1) governing magnetostatics, we see that the formal roles of the divergence and curl operators are interchanged between electrostatics and magnetostatics. As a purely practical matter, this leads to methods and corresponding results for magnetostatics that are quite different from the methods and corresponding results in electrostatics. Table 8.1 summarizes the basic difference betwen electrostatic problems and magnetostatic problems.

Finally, though, let us note that from a fundamental point of view special relativity tells us that (despite the differences described above) the distinction between electric $\boldsymbol{E}$

[2] Quantum-mechanical orbital angular momentum can be viewed semiclassically as charge in motion on a classical orbit (think of the Bohr model of the hydrogen atom), but quantum spin angular momentum has no corresponding classical analog that is completely faithful to the underlying quantum physics. Intrinsic spin is inherently quantum in nature and any attempt to treat it classically raises issues at a fundamental level.

Table 8.1 Magnetostatics versus electrostatics in vacuum

	Electrostatics	Magnetostatics
Field source	Stationary charge density ρ	Steady current density $\boldsymbol{J}$
Fundamental field	The electric field $\boldsymbol{E}$	The magnetic field $\boldsymbol{B}$
Divergence (source/sink)	$\boldsymbol{\nabla} \cdot \boldsymbol{E} = \rho/\epsilon_0$	$\boldsymbol{\nabla} \cdot \boldsymbol{B} = 0$ (no magnetic charge)
Curl (circulation)	$\boldsymbol{\nabla} \times \boldsymbol{E} = 0$	$\boldsymbol{\nabla} \times \boldsymbol{B} = \mu_0 \boldsymbol{J}$

fields and magnetic $\boldsymbol{B}$ fields amounts to nothing more than a choice of observer reference frame.

> What looks like an electric field when observed from one inertial frame looks like a magnetic field when observed from a different inertial frame, and vice versa. Thus the distinction between electric and magnetic phenomena can't be fundamental, because it isn't consistent with special relativity and Lorentz invariance.

We shall take that up in later chapters addressing the special theory of relativity, Lorentz transformations, and the formulation of the Maxwell equations in a manifestly Lorentz-covariant manner. For now we note that in the low-energy world of most everyday and laboratory experience,[3] there is utility in a formalism that distinguishes between electric and magnetic phenomena through the use of equations that are (secretly) Lorentz covariant, but are not manifestly so.

8.2 Magnetic Forces

A magnetic field $\boldsymbol{B}$ generated by source charges in motion and the electric field $\boldsymbol{E}$ associated with those charges lead to a force $\boldsymbol{F}$ that is found to act on a test charge q having relative velocity v according to the *Lorentz force law*,

$$\boldsymbol{F} = q(\boldsymbol{E} + \boldsymbol{v} \times \boldsymbol{B}) \qquad \text{(Lorentz force law).} \tag{8.4}$$

[3] Although it is not completely apparent from the appearance of the equations in SI units without examining the constants carefully [recall from Eq. (2.4) that the SI constants μ_0 and ϵ_0 are related to each other through the speed of light c], *magnetic fields are intrinsically much weaker than electric fields under typical laboratory conditions.* But this is largely because the characteristic speeds of charged particles are much less than the speed of light c in those circumstances. If the speed of charged particles approaches c, magnetic forces and electric forces become comparable in intrinsic strength. (see Probs. 8.10 and 8.11 in this regard). This is a consequence of special relativity, which requires not only space and time, but also electric and magnetic phenomena, to enter the theory on an equal footing, and whether a field is seen as electric or magnetic by an observer depends on the inertial frame of that observer.

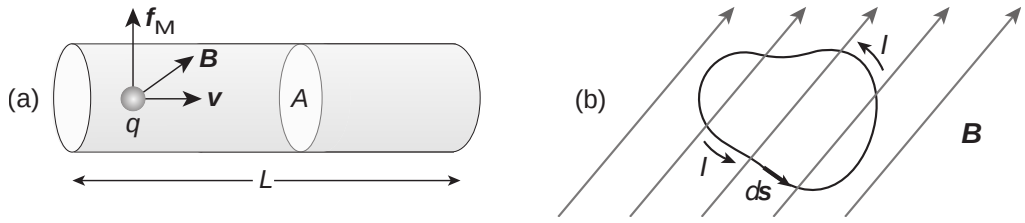

Fig. 8.1 (a) The magnetic force $\boldsymbol{f}_{\mathrm{M}}$ acting on a charged particle moving with velocity $\boldsymbol{v}$ in a segment of conductor of length L and cross-sectional area A, subject to a magnetic field $\boldsymbol{B}$. (b) Current loop carrying a steady current I in a uniform magnetic field $\boldsymbol{B}$. The vector line segment $d\boldsymbol{s}$ has a magnitude equal to the segment length and direction equal to the local current direction.

As you are asked to show in Problem 9.2, the magnetic force acting on a single charged particle in the short segment of conductor illustrated in Fig. 8.1(a) is

$$\boldsymbol{f}_{\mathrm{M}} = q\boldsymbol{v} \times \boldsymbol{B}, \tag{8.5}$$

and is directed upward by the right-hand rule for the cross product. The total magnetic force acting on the segment in Fig. 8.1(a) is given by

$$\boldsymbol{F}_{\mathrm{M}} = I(\boldsymbol{L} \times \boldsymbol{B}), \tag{8.6}$$

where $\boldsymbol{L}$ has magnitude L and direction equivalent to that of the current, and the magnitude of the current is $I = nqvA$. A finite length of wire having uniform cross section can be partitioned into segments of length ds as in Fig. 8.1(b), and the total force acting on the wire is found to be

$$\boldsymbol{F}_{\mathrm{M}} = I \int_a^b (d\boldsymbol{s} \times \boldsymbol{B}), \tag{8.7}$$

where a and b are the endpoints. For the special case of a steady current, uniform magnetic field $\boldsymbol{B}$, and a closed loop ($a = b$), the force acting on the loop is

$$\boldsymbol{F}_{\mathrm{M}} = I \oint (d\boldsymbol{s} \times \boldsymbol{B}) = I \left(\oint d\boldsymbol{s} \right) \times \boldsymbol{B} = 0, \tag{8.8}$$

which vanishes because for a closed loop the set of length-element vectors $d\boldsymbol{s}$ forms a closed polygon so $\oint d\boldsymbol{s} = 0$.

> For any closed current loop in a uniform magnetic field the total magnetic force acting on the loop is zero.

Although in a uniform field the net force on current loops vanishes, the *net torque* does not, as you are asked to show in Problem 9.3.

The quite different phenomenology of magnetism relative to electrostatics in everyday experience is partially due to characteristic charged-particle velocities being much less than the speed of light in typical observations (see Section 8.1), and partially due to

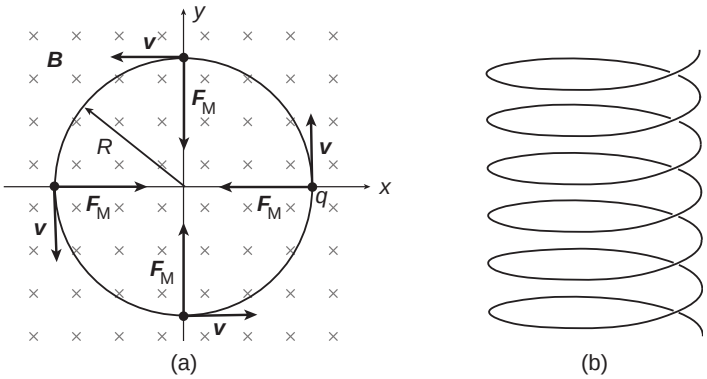

Fig. 8.2 (a) Cyclotron motion caused by magnetic field $\boldsymbol{B}$ pointing into the page along the z axis acting on a charge q with a velocity $\boldsymbol{v}$, as explained in Box 8.1. We have used the standard notation of $\otimes$ or $\times$ to indicate a magnetic field pointing into the page (and $\odot$ to indicate one pointing out of the page). (b) An electric field $\boldsymbol{E}$ perpendicular to the magnetic field converts circular cyclotron motion into spiral motion because of

the nature of the Lorentz force law (8.4), which mixes the effect of the electric field and magnetic field in a non-trivial way. The characteristic motion of a charged particle in a magnetic field is circular, as illustrated in Box 8.1 and Fig. 8.2. Two important physical consequences of the force law (8.4) are illustrated in Box 8.1, *cyclotron orbits* and the classical *Hall effect*.

8.3 Work and the Lorentz Force

How much work can be done by the Lorentz force? We calculated previously in Eq. (2.37) that the work done if a test charge is moved in an electric field is the product of the charge and the difference in electric potential over the path. If we repeat that calculation using the Lorentz force (8.4) with $\boldsymbol{B} = 0$ the same result is obtained (which is reassuring!). On the other hand, let's set $\boldsymbol{E} = 0$ in Eq. (8.4) and calculate the work done by the magnetic part of the Lorentz force on a test charge. If a charge Q moves a distance $d\boldsymbol{L} = \boldsymbol{v}dt$, then the amount of work done by the magnetic field is

$$dW = \boldsymbol{F} \cdot d\boldsymbol{L} = Q(v \times \boldsymbol{B}) \cdot \boldsymbol{v}\, dt = 0. \tag{8.9}$$

The magnetic field does no work, since the cross product $\boldsymbol{v} \times \boldsymbol{B}$ is perpendicular to the velocity $\boldsymbol{v}$, so that the scalar product $(v \times \boldsymbol{B}) \cdot \boldsymbol{v}$ *vanishes identically.* As exemplified in the cyclotron motion discussed in Box 8.1, magnetic forces can *alter the direction* of charged-particle velocity but *not its magnitude.*

Box 8.1 Motion of Charged Particles in Magnetic and Electric Fields

Characteristic *cyclotron motion* of a charged particle in a magnetic field is circular with the centripetal acceleration that curves the path provided by the magnetic force.

Cyclotron Motion

As illustrated in Fig. 8.2(a) and Problem 8.12, the magnetic field $\boldsymbol{B}$, oriented into the page, produces through the $q\boldsymbol{v} \times \boldsymbol{B}$ component of the Lorentz force (8.4) a centripetal force directed toward the center of the circle for a particle of charge q and velocity $\boldsymbol{v}$, causing the particle to be deflected in a circular path without changing its speed (implying that the magnetic field does no work). The motion becomes more complex if an electric field is present also. For both an electric field and magnetic field, the circular cyclotron motion due to the magnetic field can be converted into a the spiral motion depicted in Fig. 8.2(b) by the $q\boldsymbol{E}$ component of the Lorentz force.

Classical and Quantum Hall Effects

An important consequence of the Lorentz force is exemplified by the *classical Hall effect*, depicted in the following diagram for a 2D conductor.

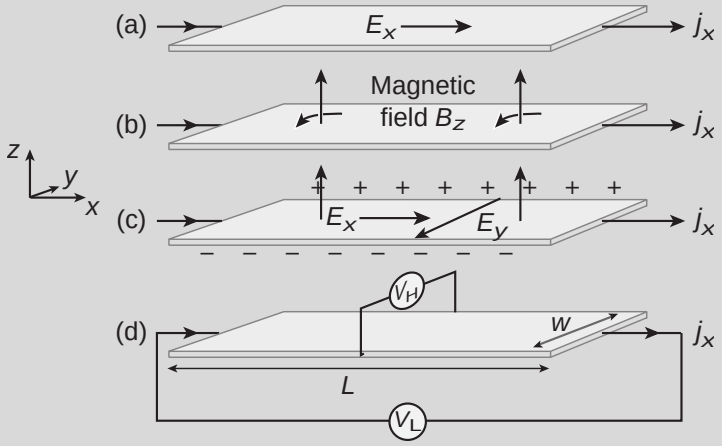

(a) A current density j_x is produced by an applied electric field E_x. (b) A uniform magnetic field $\boldsymbol{B}$ applied in the $+z$ direction deflects electrons in the current in the $-y$ direction (Lorentz force). (c) Negative charge accumulate on one edge and positive charge on the opposite edge, producing a transverse electric field E_y (*Hall field*) and associated force that just cancels the Lorentz force; thus in equilibrium current flows only in the x direction. (d) Typically the longitudinal voltage V_{L} and the transverse Hall voltage V_{H} are measured. The *Hall resistance* R_{H} (inferred from $R_{\mathrm{H}} = V_{\mathrm{H}}/wj_x$) depends on the sign and density of charge carriers. Thus the Hall effect is a diagnostic for charge carriers in materials. At very high magnetic fields, the classical Hall effect is modified dramatically by quantum mechanics. Corresponding *quantum Hall experiments* revealed topological effects that initiated the topological matter revolution in modern condensed matter and materials science.

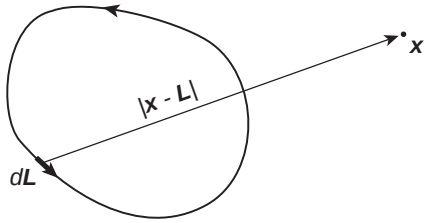

Fig. 8.3 Current loop carrying a steady current I for Eq. (8.11).

If a magnetic field appears to us to be doing work, Eq. (8.9) indicates that we have misunderstood what is happening. Often, when at first glance a magnetic field appears to be doing work, what is actually happening is that a magnetic field is acting to alter the direction of motion, which then permits an electric field to do the observed work.

The magnetic field may enable the work to be done by changing the direction of motion, but the actual work is done by an electric field, never by the magnetic field acting alone.

8.4 The Biot–Savart Law

The magnetic field $\boldsymbol{B}(\boldsymbol{x})$ of a steady line current described by the density $\boldsymbol{J}(\boldsymbol{x})$ is given by the empirical *Biot–Savart law*,

$$\boldsymbol{B}(\boldsymbol{x}) = \frac{\mu_0}{4\pi} \int \frac{\boldsymbol{J}(\boldsymbol{x}') \times (\boldsymbol{x} - \boldsymbol{x}')}{|\boldsymbol{x} - \boldsymbol{x}'|^3}\, d^3x' = \frac{\mu_0}{4\pi} \int \frac{\boldsymbol{J}(\boldsymbol{x}') \times \hat{\boldsymbol{R}}}{R^2}\, d^3x', \tag{8.10}$$

where the *permeability of free space* μ_0 is defined in Eq. (1.2) and the second form employs the compact notation of Eqs. (2.10) and (2.11). The law embodied in Eq. (8.10) was formulated by Jean-Baptiste Biot and Félix Savart in 1820. The SI unit for $\boldsymbol{B}$ is the *tesla* (T), where $1\,\mathrm{T} \equiv 1\,\mathrm{N\,A^{-1}\,m^{-1}}$. Although discouraged by champions of international standards, it is common also to use the gaussian (CGI) unit of *gauss* (G) for $\boldsymbol{B}$, even when using SI units overall, where $1\,\text{tesla} = 10^4\,\text{gauss}$.[4] The integral in Eq. (8.10) can be performed analytically only for simple geometrical arrangements. When a steady current is flowing in a 1D wire the magnitude of the current I must be constant. If $\boldsymbol{L}$ is a vector that points to a line element $d\boldsymbol{L}$ of the wire as in Fig. 8.3, substitution of $I d\boldsymbol{L}$ for $\boldsymbol{J} d^3x$ in Eq. (8.10) yields the Biot–Savart law in the form

$$\boldsymbol{B}(\boldsymbol{x}) = \frac{\mu_0 I}{4\pi} \int \frac{d\boldsymbol{L} \times (\boldsymbol{x} - \boldsymbol{L})}{|\boldsymbol{x} - \boldsymbol{L}|^3} = \frac{\mu_0 I}{4\pi} \int \frac{d\boldsymbol{L} \times \hat{\boldsymbol{R}}}{R^2}, \tag{8.11}$$

which is valid for a steady current.

[4] For reference, the magnetic field at the surface of the Earth is of order one gauss ($\sim 10^{-4}$ T), and the strongest known magnetic fields are $\sim 10^{16}$ gauss ($\sim 10^{12}$ T), which are observed in highly magnetized, rapidly rotating neutron stars called *magnetars*.

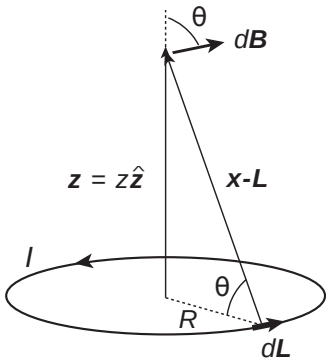

Fig. 8.4 Geometry for Biot–Savart calculation of the magnetic field on the symmetry axis of a circular current loop, as illustrated in Example 8.1.

Example 8.1 Let us use the Biot–Savart law (8.11) to calculate the magnetic field produced along the z axis by the circular current loop in Fig. 8.4. The components of $d\boldsymbol{B}$ that are perpendicular to the z symmetry axis cancel one another when the entire loop is traversed, but the z components add with the same magnitude for each line increment $d\boldsymbol{L}$, which gives

$$\boldsymbol{B}(z) = \hat{\boldsymbol{z}}\,\frac{\mu_0 I}{4\pi}\,\frac{\cos\theta}{R^2+z^2}\oint dL = \hat{\boldsymbol{z}}\,\frac{\mu_0 I}{2}\,\frac{R^2}{(R^2+z^2)^{3/2}}, \tag{8.12}$$

where $\oint dL = 2\pi R$ and $\cos\theta = R/\sqrt{R^2+z^2}$ were used. This non-zero value of $\boldsymbol{B}$ on the symmetry axis contrasts with the value of zero for the electric field $\boldsymbol{E}$ found for the corresponding electrostatics problem of a uniformly charged ring. The difference follows from the cross product in the Biot–Savart formula that isn't present in the electric field formula. This causes contributions to $\boldsymbol{B}(z=0)$ from opposite sides of the ring to add constructively for the magnetic field, but to subtract and cancel each other for the electric field. This example is one illustration of the basic differences between electric fields produced by stationary charges and magnetic fields produced by charges in motion.

Both Coulomb's law and the Biot–Savart law are empirical, with each tailored to account for the corresponding electrostatic and magnetostatic data, respectively.

> The Biot–Savart law may be viewed as the empirical starting point for magnetostatics, just as Coulomb's law may be viewed as the empirical starting point for electrostatics.

Both laws exhibit an inverse-square distance dependence, but otherwise they differ substantially because of the vector character of the magnetic law.

8.4.1 Magnetic Flux

Similar to the case for electric flux defined in Eq. (2.49), it is convenient to introduce the *magnetic flux* $\mathcal{F}_{\mathrm{M}}$ through a surface S, which is defined as the normal component of $\boldsymbol{B}$ integrated over S,

$$\mathcal{F}_{\mathrm{M}} = \int_S \boldsymbol{B} \cdot d\boldsymbol{a}. \tag{8.13}$$

In electrostatics one can use lines of force to describe an electric field. In a similar way, for magnetic fields, one can draw lines of the magnetic field, which are everywhere tangent to the direction of $\boldsymbol{B}$ at that point.

8.4.2 Application to Long Straight Wires

Since steady currents normally flow in closed loops, the integral in the Biot–Savart law is typically evaluated over a closed curve. However, the Biot–Savart law can also be applied to infinitely long wires carrying a steady current. Let us use the Biot-Savart law to calculate the magnetic field due to current in a very long straight wire carrying a steady current I, as illustrated in Fig. 8.5. An element $Id\boldsymbol{L}$ of the current will produce a magnetic field $d\boldsymbol{B}$ with magnitude

$$dB = \frac{\mu_0 I}{4\pi} \frac{dL \sin\phi}{r^2},$$

as illustrated in Fig. 8.5. Expressing the variables dL, $\sin\phi$, and r^2 in terms of the angle θ, the magnitude of B is given by

$$B = \frac{\mu_0 I}{4\pi\rho} \int_{-\pi/2}^{+\pi/2} \cos\theta d\theta = \frac{\mu_0 I}{2\pi\rho}, \tag{8.14}$$

where we've assumed the length of the wire to be infinite. The corresponding magnetic field lines are concentric circles, as illustrated in Fig. 8.6.

This result can be generalized easily to calculate the force acting between the two long parallel wires illustrated in Fig. 8.7, as you are asked to show in Problem 8.7. The resulting

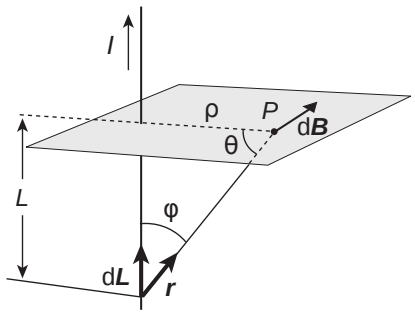

Fig. 8.5 Magnetic field $d\boldsymbol{B}$ produced by an element $Id\boldsymbol{L}$ of an infinitely long straight wire. The vector $d\boldsymbol{B}$ lies in a plane perpendicular to the wire at the point P.

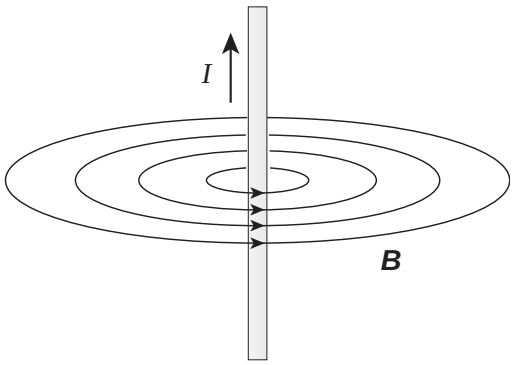

Fig. 8.6 Magnetic field $\boldsymbol{B}$ produced around an infinitely long straight wire carrying a steady current I.

force per unit length is

$$\frac{dF}{dI_a} = \frac{\mu_0 I_a I_b}{2\pi d}, \tag{8.15}$$

with the force attractive if the currents I_a and I_b flow in the same direction and repulsive if they flow in opposite directions.[5]

8.5 Differential Form of the Biot–Savart Law

The Biot–Savart law (8.10) for a line current in integral form,

$$\boldsymbol{B}(\boldsymbol{x}) = \frac{\mu_0}{4\pi} \int \frac{\boldsymbol{J}(\boldsymbol{x}') \times (\boldsymbol{x} - \boldsymbol{x}')}{|\boldsymbol{x} - \boldsymbol{x}'|^3} \, d^3x',$$

[5] Until the year 2019, this equation provided the official definition of the ampere (amp) unit of current in the SI system: one ampere is the current passing through two long parallel wires 1 meter apart with thickness negligible relative to their separation that produces a magnetic force of 2×10^{-7} newtons per meter. In a 2019 revision of the SI units system, the elementary charge e was fixed to be exactly $1.602176634 \times 10^{19}$ C, and an ampere (amp) was defined to be an electric current equivalent to one Coulomb (C) of charge moving past a reference point per second.

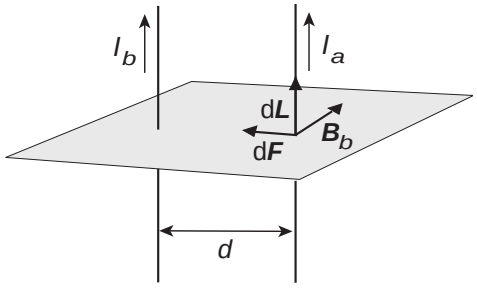

Fig. 8.7 Geometry for calculating the force per unit length acting between two long, straight parallel wires.

contains (in principle) a complete description of magnetostatics for line currents, but is not always the most convenient form for solving problems. In many situations a differential equation is more convenient to use. Let us find a form of the Biot–Savart law expressed as a differential equation, following the presentation in Jackson [41]. From Eq. (A.11),

$$\frac{\boldsymbol{x}-\boldsymbol{x}'}{|\boldsymbol{x}-\boldsymbol{x}'|^3} = -\boldsymbol{\nabla}\left(\frac{1}{|\boldsymbol{x}-\boldsymbol{x}'|}\right) = \boldsymbol{\nabla}'\left(\frac{1}{|\boldsymbol{x}-\boldsymbol{x}'|}\right), \tag{8.16}$$

which allows converting the Biot–Savart equation (8.10) into

$$\begin{aligned}\boldsymbol{B}(\boldsymbol{x}) &= \frac{\mu_0}{4\pi}\int \frac{\boldsymbol{J}(\boldsymbol{x}')\times(\boldsymbol{x}-\boldsymbol{x}')}{|\boldsymbol{x}-\boldsymbol{x}'|^3}\,d^3x' \\ &= \frac{\mu_0}{4\pi}\,\boldsymbol{\nabla}\times\int \frac{\boldsymbol{J}(\boldsymbol{x}')}{|\boldsymbol{x}-\boldsymbol{x}'|}\,d^3x',\end{aligned} \tag{8.17}$$

where $\boldsymbol{\nabla}$ has been pulled out of the integral because it operates on $\boldsymbol{x}$ but not $\boldsymbol{x}'$.[6] Now take the divergence of Eq. (8.17)

$$\boldsymbol{\nabla}\cdot\boldsymbol{B} = \frac{\mu_0}{4\pi}\,\boldsymbol{\nabla}\cdot\boldsymbol{\nabla}\times\int \frac{\boldsymbol{J}(\boldsymbol{x}')}{|\boldsymbol{x}-\boldsymbol{x}'|}\,d^3x'.$$

But from Eq. (A.6) we have the identity $\boldsymbol{\nabla}\cdot(\boldsymbol{\nabla}\times\boldsymbol{A}) = 0$ so

$$\boldsymbol{\nabla}\cdot\boldsymbol{B} = 0, \tag{8.18}$$

which may be termed the *first law of magnetostatic*s [and is the third Maxwell equation (1.1c), corresponding to the absence of magnetic charges]. Next, take the curl of $\boldsymbol{B}$ in Eq. (8.17),

$$\boldsymbol{\nabla}\times\boldsymbol{B} = \frac{\mu_0}{4\pi}\,\boldsymbol{\nabla}\times\boldsymbol{\nabla}\times\int \frac{\boldsymbol{J}(\boldsymbol{x}')}{|\boldsymbol{x}-\boldsymbol{x}'|}\,d^3x'. \tag{8.19}$$

Using the vector identity $\boldsymbol{\nabla}\times(\boldsymbol{\nabla}\times\boldsymbol{A}) = \boldsymbol{\nabla}(\boldsymbol{\nabla}\cdot\boldsymbol{A}) - \nabla^2\boldsymbol{A}$ of Eq. (A.8), this becomes

$$\begin{aligned}\boldsymbol{\nabla}\times\boldsymbol{B} &= \frac{\mu_0}{4\pi}\,\boldsymbol{\nabla}\int \boldsymbol{J}(\boldsymbol{x}')\cdot\boldsymbol{\nabla}\left(\frac{1}{|\boldsymbol{x}-\boldsymbol{x}'|}\right)d^3x' - \frac{\mu_0}{4\pi}\int \boldsymbol{J}(\boldsymbol{x})\,\nabla^2\left(\frac{1}{|\boldsymbol{x}-\boldsymbol{x}'|}\right)d^3x' \\ &= -\frac{\mu_0}{4\pi}\boldsymbol{\nabla}\int \boldsymbol{J}(\boldsymbol{x}')\cdot\boldsymbol{\nabla}'\left(\frac{1}{|\boldsymbol{x}-\boldsymbol{x}'|}\right)d^3x' + \mu_0\boldsymbol{J}(\boldsymbol{x}),\end{aligned} \tag{8.20}$$

where we have used the identities of Eq. (A.11),

$$\boldsymbol{\nabla}\left(\frac{1}{|\boldsymbol{x}-\boldsymbol{x}'|}\right) = -\boldsymbol{\nabla}'\left(\frac{1}{|\boldsymbol{x}-\boldsymbol{x}'|}\right) \qquad \nabla^2\left(\frac{1}{|\boldsymbol{x}-\boldsymbol{x}'|}\right) = -4\pi\delta(\boldsymbol{x}-\boldsymbol{x}') \tag{8.21}$$

[6] Remember that in these manipulations, using our standard notation, the integrations are over the *primed coordinates*, but applied gradient, divergence, and curl operations ($\boldsymbol{\nabla}$, $\boldsymbol{\nabla}\cdot$, and $\boldsymbol{\nabla}\times$, respectively, without primes) are taken with respect to the *unprimed coordinates*. This is made explicit in the notation exemplified in Eqs. (A.11) of Appendix A, where $\boldsymbol{\nabla} \equiv \boldsymbol{\nabla}_x$ operates on the $\boldsymbol{x}$ coordinates while $\boldsymbol{\nabla}' \equiv \boldsymbol{\nabla}_{x'}$ operates on the $\boldsymbol{x}'$ coordinates. However, we will usually use the abbreviated notation $\boldsymbol{\nabla} \equiv \boldsymbol{\nabla}_x$ and $\boldsymbol{\nabla}' \equiv \boldsymbol{\nabla}_{x'}$.

(with $\boldsymbol{\nabla}$ operating on $\boldsymbol{x}$ and $\boldsymbol{\nabla}'$ operating on $\boldsymbol{x}'$) in the last step. Integrating the remaining integral in Eq. (8.20) by parts then gives

$$\boldsymbol{\nabla} \times \boldsymbol{B} = \mu_0 \boldsymbol{J} + \frac{\mu_0}{4\pi} \boldsymbol{\nabla} \int \frac{\boldsymbol{\nabla}' \cdot \boldsymbol{J}(\boldsymbol{x}')}{|\boldsymbol{x} - \boldsymbol{x}'|} \, d^3x'. \tag{8.22}$$

But for steady-state magnetism $\boldsymbol{\nabla} \cdot \boldsymbol{J} = 0$ and we obtain finally

$$\boldsymbol{\nabla} \times \boldsymbol{B} = \mu_0 \boldsymbol{J} \qquad \text{(Ampére's law)}, \tag{8.23}$$

which may be termed the *second law of magnetostatics* [and is the fourth Maxwell equation (1.1d), if electric fields don't depend on time (Ampère's law)].

The preceding proof shows that in magnetostatics the Biot–Savart law is the integral solution of Ampére's law, in the same sense that in electrostatics Coulomb's law is the integral solution of Gauss's law. To be precise, in electrostatics

1. Gauss's Law ($\boldsymbol{\nabla} \cdot \boldsymbol{E} = \rho/\epsilon_0$) is the fundamental local differential equation governing electrostatics, and
2. Coulomb's law,

$$\boldsymbol{E} = \frac{1}{4\pi\epsilon_0} \int \frac{\rho \hat{\boldsymbol{R}}}{R^2} \, d^3x',$$

is the brute-force integral solution that can be used to find the field when the charge distribution is known.

In an analogous way for magnetostatics,

1. Ampére's law ($\boldsymbol{\nabla} \times \boldsymbol{B} = \mu_0 \boldsymbol{J}$) is the fundamental local differential equation governing magnetostatics, and
2. the Biot–Savart law,

$$\boldsymbol{B} = \frac{\mu_0}{4\pi} \int \frac{\boldsymbol{J} \times \hat{\boldsymbol{R}}}{R^2} \, d^3x',$$

is the brute-force integral solution that can be used to find the magnetic field when the current distribution $\boldsymbol{J}$ is known.

Let us now consider the use of Ampère's law to solve some basic problems in magnetostatics.

8.6 Magnetostatics Using Ampère's Law

Just as it is sometimes useful to employ Gauss's law in integral form, it is handy to have an integral form of Ampère's law. The integral equivalent of Ampère's law (8.23) may be obtained from Stokes' theorem (2.25),

$$\int_S (\boldsymbol{\nabla} \times \boldsymbol{A}) \cdot \boldsymbol{n} \, da = \oint_C \boldsymbol{A} \cdot d\boldsymbol{l},$$

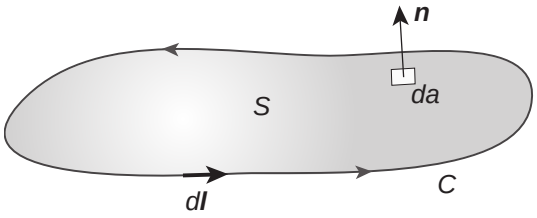

Fig. 8.8 The 2D surface S and the contour C bounding the surface for Stokes' theorem. An infinitesimal line element on C is indicated by dl and an infinitesimal surface element on S is indicated by da, with the normal to da denoted by $\boldsymbol{n}$. The path in the line integration is traversed in a right-hand rule sense relative to $\boldsymbol{n}$, as indicated by arrows.

for the vector field $\boldsymbol{A}$, where S is an arbitrary open surface bounded by a closed curve C and where $\boldsymbol{n}$ is the normal to S. Figure 8.8 illustrates. Applying Stokes' theorem to Eq. (8.23) we find,

$$\int_S (\boldsymbol{\nabla} \times \boldsymbol{B}) \cdot \boldsymbol{n}\, da = \oint_C \boldsymbol{B} \cdot d\boldsymbol{l} = \mu_0 \int_S \boldsymbol{J} \cdot \boldsymbol{n}\, da, \tag{8.24}$$

and therefore Eq. (8.23) becomes

$$\oint_C \boldsymbol{B} \cdot d\boldsymbol{l} = \mu_0 \int_S \boldsymbol{J} \cdot \boldsymbol{n}\, da. \tag{8.25}$$

Using that the total current I passing through the closed curve C is given by the surface integral on the right side of Eq. (8.25),

$$I = \int_S \boldsymbol{J} \cdot \boldsymbol{n}\, da, \tag{8.26}$$

gives us Ampère's law in integral form,[7]

$$\oint_C \boldsymbol{B} \cdot d\boldsymbol{l} = \mu_0 I \qquad \text{(Ampère's law)}. \tag{8.27}$$

We found in our study of electrostatics that Gauss's law can often be used to find the electric field quickly in highly symmetric cases. Ampére's law can be employed in an analogous way for magnetostatic problems that have high symmetry. The following example illustrates.

Example 8.2 Let's determine the magnetic field for the long solenoid illustrated in Fig. 8.9, with n closely wound turns per unit length on a cylinder of radius R and carrying a steady current I. Because the solenoid is tightly wound, each coil may be assumed to

[7] Because both integral and differential forms of multiple laws appear in this discussion, there is ample room for confusion. To be clear, $\boldsymbol{\nabla} \times \boldsymbol{B} = \mu_0 \boldsymbol{J}$ is not the differential form of the Biot–Savart law; it is the *differential form of the integral version of Ampere's Law*, $\oint \boldsymbol{B} \cdot d\boldsymbol{l} = \mu_0 I_{\text{enc}}$. The Biot–Savart law may then be viewed as the mathematical hammer you can swing to solve that differential equation if your physical system lacks the symmetry to use the Ampère Law loop integral.

be perpendicular to the symmetry axis of the cylinder. One expects then on symmetry and general grounds that the magnetic field is oriented along the cylinder axis, and that it must be zero at large distances from the solenoid. Let's apply Ampère's law (8.27) to the two rectangular *Ampèrian loops* shown in the diagram.[8] Loop 1 is completely outside the solenoid and encloses no current, $I_{\text{enc}} = 0$, with its left side a distance a and its right side a distance b from the central axis of the cylinder. Applying Ampère's law to it

$$\oint \boldsymbol{B} \cdot dl = [B(a) - B(b)]L = \mu_0 I_{\text{enc}} = 0,$$

where $B = |\boldsymbol{B}|$. Thus,

1. $B(a) = B(b)$ and the magnetic field outside is independent of the distance from the solenoid, but
2. the boundary conditions require that $B = 0$ at infinity,

which implies that $B = 0$ *everywhere outside the solenoid*. Loop 2 is halfway inside the solenoid and Ampère's law gives

$$\oint \boldsymbol{B} \cdot dl = BL = \mu_0 I_{\text{enc}} = \mu_0 nIL,$$

where B is the field inside the solenoid, since there is no contribution from the half rectangle outside the cylinder because $B = 0$ there. Thus inside the solenoid the field is uniform, $\boldsymbol{B} = \mu_0 nI\hat{\boldsymbol{z}}$, where $\hat{\boldsymbol{z}}$ is a unit vector along the cylinder axis, and outside the solenoid the magnetic field vanishes.

[8] We shall refer to such constructions employed in the use of Ampère's law as *Ampèrian loops*, by analogy with the *Gaussian surfaces* introduced in Section 2.5 in the use of Gauss's law.

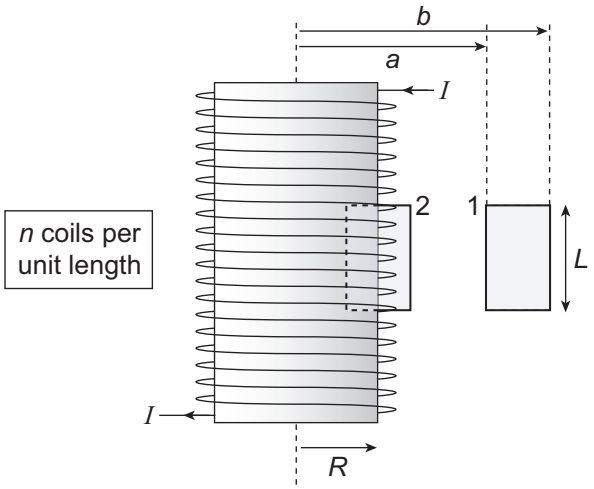

Fig. 8.9 Analysis of a long, tightly wound solenoid using Ampère's law. Two rectangular loops are shown, Loop 1 is outside the solenoid and Loop 2 overlaps half inside and half outside of the solenoid.

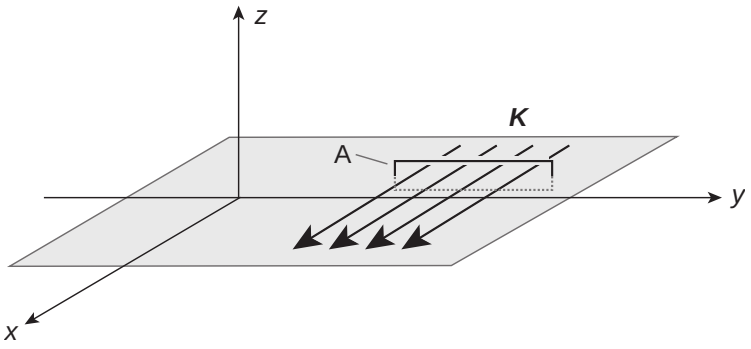

Fig. 8.10 Using the Biot–Savart law in Example 8.3 to find the magnetic field produced by an infinite sheet of surface current $\boldsymbol{K} = K\hat{\boldsymbol{x}}$ in the $x-y$ plane. The rectangle A is an Amperian loop used to determine the magnetic field $\boldsymbol{B}$ produced by the sheet of charge through Ampère's law.

Like Gauss's law, Ampère's law for steady currents is generally *valid*, but it is *useful* only if there is sufficient symmetry to allow B to be pulled out of the integral $\oint \boldsymbol{B} \cdot d\boldsymbol{l}$ so that Eq. (8.27) to be solved easily for the magnetic field.

8.7 Surface Currents and Volume Currents

The integral form of the Biot–Savart Law for line currents given in Eq. (8.10) may be generalized easily to apply to surface currents and volume currents. For a 2D surface current $\boldsymbol{K}$, the Biot–Savart law takes the form

$$\boldsymbol{B}(\boldsymbol{x}) = \frac{\mu_0}{4\pi} \int \frac{\boldsymbol{K}(\boldsymbol{x}') \times (\boldsymbol{x} - \boldsymbol{x}')}{|\boldsymbol{x} - \boldsymbol{x}'|^3}\, da' = \frac{\mu_0}{4\pi} \int \frac{\boldsymbol{K}(\boldsymbol{x}') \times \hat{\boldsymbol{R}}}{R^2}\, da' \tag{8.28}$$

while for a 3D volume current $\boldsymbol{J}$

$$\boldsymbol{B}(\boldsymbol{x}) = \frac{\mu_0}{4\pi} \int \frac{\boldsymbol{J}(\boldsymbol{x}') \times (\boldsymbol{x} - \boldsymbol{x}')}{|\boldsymbol{x} - \boldsymbol{x}'|^3}\, d^3x' = \frac{\mu_0}{4\pi} \int \frac{\boldsymbol{J}(\boldsymbol{x}') \times \hat{\boldsymbol{R}}}{R^2}\, d^3x', \tag{8.29}$$

where the second form of each expression employs the compact notation of Eqs. (2.10) and (2.11).

Example 8.3 Let us use Eq. (8.28) to calculate the magnetic field due to a surface current $\boldsymbol{K} = K\hat{\boldsymbol{x}}$ in the $x-y$ plane, as illustrated in Fig. 8.10. From the Biot–Savart law the magnetic field must be perpendicular to $\boldsymbol{K}$ so it cannot have an x component and cannot have a z component by symmetry in y since any vertical contribution at $+y$ would be cancelled by one at $-y$. Thus the magnetic field has only y components and

by the right-hand rule it points left above the plane of Fig. 8.10 and right below it. The rectangular Ampèrian loop A is parallel to the yz plane and is half above and half below the xy surface. Applying Ampère's law (8.27) to the loop A gives

$$\oint_C \boldsymbol{B} \cdot d\boldsymbol{l} = 2BL = \mu_0 I_{\text{enc}} = \mu_0 K L,$$

where L is the width of the rectangle and I_{enc} is the current enclosed by the rectangle. Thus $B = \frac{1}{2}\mu_0 K$ and the magnetic field produced by the sheet of current $\boldsymbol{K} = K\hat{\boldsymbol{x}}$ in Fig. 8.10 is

$$\boldsymbol{B} = \begin{cases} +\dfrac{1}{2}\,\mu_0 K\hat{\boldsymbol{y}} & (z < 0), \\ -\dfrac{1}{2}\,\mu_0 K\hat{\boldsymbol{y}} & (z > 0), \end{cases} \tag{8.30}$$

where $\hat{\boldsymbol{y}}$ is a unit vector in the y direction.

In Example 8.3, the magnetic field produced by a uniform sheet of current is independent of the distance from the surface containing the current in Example 8.3, just as would be the case for the electric field produced by a uniform surface charge in electrostatics.

8.8 Vector Potentials and Gauge Invariance

We have seen in the preceding section that the basic laws of magnetostatics are defined in differential form through Eqs. (8.23) and (8.18),

$$\boldsymbol{\nabla} \times \boldsymbol{B} = \mu_0 \boldsymbol{J}, \qquad \boldsymbol{\nabla} \cdot \boldsymbol{B} = 0, \tag{8.31}$$

which must be solved for the magnetic field $\boldsymbol{B}$. In electrostatics the electric potential Φ proved to be an extremely useful quantity because the electric field can be derived from it by taking the gradient, $\boldsymbol{E} = -\boldsymbol{\nabla}\Phi$. The electric potential Φ is a scalar quantity and it is often termed the *scalar potential* [we have indeed used the terms "(electric) potential" and "scalar potential" interchangeably]. For the *special case that the current density is zero in a region*, it is possible to define a *magnetic scalar potential* Φ_{M} such that the magnetic field is given by $\boldsymbol{B} = -\boldsymbol{\nabla}\Phi_{\text{M}}$.[9] Then in Eq. (8.31) $\boldsymbol{\nabla} \times \boldsymbol{B} = 0$, and $\boldsymbol{\nabla} \cdot \boldsymbol{B} = 0$ reduces to the Laplace equation for Φ_{M}, implying that the methods for solving Laplace's equation developed for electrostatics in Chs. 2-6 become applicable. However, this approach has limited utility because it is valid only for regions where the current density vanishes. As we now discuss, an approach with potentially broader application may be developed by exploiting the second equation above, $\boldsymbol{\nabla} \cdot \boldsymbol{B} = 0$. This will allow defining a *vector potential* $\boldsymbol{A}$, from which the magnetic field $\boldsymbol{B}$ can be derived by taking the curl of $\boldsymbol{A}$.

[9] If $\boldsymbol{J} = 0$ then $\boldsymbol{\nabla} \times \boldsymbol{B} = 0$ and by the Helmholtz theorem $B = -\boldsymbol{\nabla}\Phi_{\text{M}}$.

8.8.1 Magnetic Fields and the Vector Potential

We begin by noting that $\boldsymbol{\nabla} \cdot \boldsymbol{B} = 0$ will hold everywhere if $\boldsymbol{B}$ is the curl of some vector field $\boldsymbol{A}$ (which we call the *vector potential*),

$$\boldsymbol{B}(\boldsymbol{x}) = \boldsymbol{\nabla} \times \boldsymbol{A}(\boldsymbol{x}), \tag{8.32}$$

since then the identity $\boldsymbol{\nabla} \cdot (\boldsymbol{\nabla} \times \boldsymbol{A}) = 0$ ensures that the divergence of $\boldsymbol{B}$ vanishes under all conditions. In fact, $\boldsymbol{B}$ was already written in this form in Eq. (8.17),

$$\boldsymbol{B}(\boldsymbol{x}) = \frac{\mu_0}{4\pi} \boldsymbol{\nabla} \times \int \frac{\boldsymbol{J}(\boldsymbol{x}')}{|\boldsymbol{x} - \boldsymbol{x}'|} \, d^3x', \tag{8.33}$$

and upon comparing Eqs. (8.32) and (8.33), a vector potential $\boldsymbol{A}$ consistent with the phenomenology of magnetism takes the general form

$$\boldsymbol{A}(\boldsymbol{x}) = \frac{\mu_0}{4\pi} \int \frac{\boldsymbol{J}(\boldsymbol{x}')}{|\boldsymbol{x} - \boldsymbol{x}'|} \, d^3x' + \boldsymbol{\nabla}\chi(\boldsymbol{x}), \tag{8.34}$$

where the addition of the *arbitrary scalar function* $\chi(\boldsymbol{x})$ has no effect on $\boldsymbol{\nabla} \cdot \boldsymbol{B} = 0$ because of the identity $\boldsymbol{\nabla} \times (\boldsymbol{\nabla} f) = 0$ [see Eq. (A.7)] for a scalar function f.

8.8.2 Gauge Transformations

Since $\chi(\boldsymbol{x})$ is an arbitrary scalar function of $\boldsymbol{x}$, the vector potential $\boldsymbol{A}$ can be transformed freely according to

$$\boldsymbol{A} \to \boldsymbol{A} + \boldsymbol{\nabla}\chi, \tag{8.35}$$

which has no effect on the magnetostatic equation $\boldsymbol{\nabla} \cdot \boldsymbol{B} = 0$ because identically $\boldsymbol{\nabla} \cdot (\boldsymbol{\nabla} \times \boldsymbol{\nabla}\chi) = 0$. The addition of the gradient of an arbitrary scalar function ψ to the vector potential $\boldsymbol{A} \to \boldsymbol{A} + \boldsymbol{\nabla}\chi$ as in Eq. (8.35) is called a *gauge transformation* and the invariance of the laws of electromagnetism under this transformation is called *gauge invariance*. The *gauge symmetry* associated with this invariance has large implications for classical electromagnetism and quantum electrodynamics, and a generalization of this gauge symmetry is of fundamental importance in relativistic quantum field theories, particularly for the Standard Model of elementary particle physics. We will elaborate on these aspects of electromagnetism as the prototypical gauge field theory in Ch. 21.

From the Helmholtz theorem (Section 3.3.6), a vector field with suitable boundary conditions is specified uniquely by its curl and its divergence. From Eq. (8.32), specifying the magnetic field requires only the curl of $\boldsymbol{A}$. Thus we are free to make gauge transformations on the vector potential such that $\boldsymbol{\nabla} \cdot \boldsymbol{A}$ has any convenient functional form, without affecting the magnetic field and thus without altering the physics of classical electromagnetism. Substituting $\boldsymbol{B} = \boldsymbol{\nabla} \times \boldsymbol{A}$ into Eq. (8.23) gives

$$\boldsymbol{\nabla} \times (\boldsymbol{\nabla} \times \boldsymbol{A}) = \mu_0 \boldsymbol{J},$$

which becomes

$$\boldsymbol{\nabla}(\boldsymbol{\nabla} \cdot \boldsymbol{A}) - \nabla^2 \boldsymbol{A} = \mu_0 \boldsymbol{J}, \tag{8.36}$$

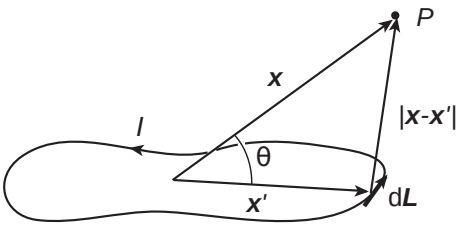

Fig. 8.11 A small current loop that produces a vector potential $\boldsymbol{A}(\boldsymbol{x})$ and corresponding magnetic field $\boldsymbol{B}(\boldsymbol{x})$ at the point P, where it is assumed for this discussion that $\boldsymbol{x} \gg \boldsymbol{x}'$.

upon invoking the identity $\boldsymbol{\nabla} \times (\boldsymbol{\nabla} \times \boldsymbol{A}) = \boldsymbol{\nabla}(\boldsymbol{\nabla} \cdot \boldsymbol{A}) - \nabla^2 \boldsymbol{A}$ given in Eq. (A.8). Now gauge invariance implies that for the magnetic field we are free to choose any useful functional form for $\boldsymbol{\nabla} \cdot \boldsymbol{A}$. Let now use this freedom to simplify Eq. (8.36).

8.8.3 The Coulomb Gauge Condition

An obvious simplification allowed by gauge invariance is to choose a gauge for which

$$\boldsymbol{\nabla} \cdot \boldsymbol{A} = 0 \qquad \text{(Coulomb gauge condition)}, \tag{8.37}$$

is satisfied, which defines the *Coulomb gauge* (also known as the *radiation gauge* or the *transverse gauge*, for reasons that will be explained later). In Coulomb gauge, Eq. (8.36) is transformed into the (vector) Poisson equation,

$$\nabla^2 \boldsymbol{A} = -\mu_0 \boldsymbol{J} \qquad \text{(Coulomb gauge)}. \tag{8.38}$$

From application of the Poisson equation in electrostatics we expect that the solution for $\boldsymbol{A}$ in Coulomb gauge is given by the first term of Eq. (8.34) with $\chi =$ constant,

$$\boldsymbol{A}(\boldsymbol{x}) = \frac{\mu_0}{4\pi} \int \frac{\boldsymbol{J}(\boldsymbol{x}')}{|\boldsymbol{x} - \boldsymbol{x}'|}\, d^3x', \tag{8.39}$$

provided that the $\boldsymbol{J}(\boldsymbol{x}') \to 0$ sufficiently rapidly at infinity. Classical gauge transformations will be discussed in more depth in Ch. 11.

8.9 Magnetic Fields of Localized Currents

We now consider a current distribution that is localized in a region of space that is of small size compared to the distance to an observer; Fig. 8.11 illustrates, where a loop that is small compared with the distance to an observer at P carries a steady current I. A full treatment of this problem by analogy with electric multipole expansions is possible using *vector spherical harmonics*, which are an extension of normal scalar spherical harmonics designed specifically for use with vector fields. They are described briefly in Box 8.2. We

Box 8.2 Vector Spherical Harmonics

Vector spherical harmonics are an extension of regular (scalar) spherical harmonics designed for ease of use with vector fields. Generally the components of vector spherical harmonics are complex-valued functions expressed in terms of spherical basis vectors. Following the conventions of Ref. [20], three vector spherical harmonics may be defined

$$\mathbf{Y}_{lm} = Y_{lm}\hat{\boldsymbol{r}} \qquad \boldsymbol{\Psi}_{lm} = r\boldsymbol{\nabla}Y_{lm} \qquad \boldsymbol{\Phi}_{lm} = \boldsymbol{r}\times\boldsymbol{\nabla}Y_{lm},$$

where $\boldsymbol{r}$ is the radial vector in spherical coordinates. The purpose of the radial factors is to ensure that the vector spherical harmonics have the same dimensions as ordinary spherical harmonics, and that they do not depend on the radial coordinate. These new vector fields facilitate separation of radial from angular coordinates in spherical coordinates, permitting a multipole expansion of the electric field $\boldsymbol{E}$ of the form

$$\boldsymbol{E} = \sum_{l=0}^{\infty}\sum_{m=-l}^{+l}\left(E^r_{lm}(r)\boldsymbol{Y}_{lm} + E^{(1)}_{lm}(r)\boldsymbol{\Psi}_{lm} + E^{(2)}_{lm}(r)\boldsymbol{\Phi}_{lm}\right),$$

The component labels indicate that $E^r_{lm}(r)$ is the radial component, and $E^{(1)}_{lm}(r)$ and $E^{(2)}_{lm}(r)$ are transverse components of the vector field (with respect to the vector $\boldsymbol{r}$).

shall confine ourselves instead to employing a lowest-order multipole expansion using normal spherical harmonics. The results will be of considerable practical significance because it will be found that magnetism in matter (if quantum spin effects can be ignored) is well approximated classically by the magnetic dipole moment in a multipole expansion of atomic-scale current loops.

8.9.1 Multipole Expansion of the Vector Potential

Let us assume that $\boldsymbol{x} \gg \boldsymbol{x}'$ and expand the denominator of Eq. (8.39) in a multipole series of the form (3.54) for the current distribution in Fig. 8.11,

$$\frac{1}{|\boldsymbol{x}-\boldsymbol{x}'|} = \frac{1}{r}\sum_{n=0}^{\infty}\left(\frac{r'}{r}\right)^n P_n(\cos\theta)d\boldsymbol{l}, \tag{8.40}$$

where $r \equiv |\boldsymbol{x}|$, $r' \equiv |\boldsymbol{x}'|$, and θ is indicated in Fig. 8.11. Thus the vector potential can be expanded as

$$\boldsymbol{A}(\boldsymbol{x}) = \frac{\mu_0 I}{4\pi}\left[\frac{1}{r}\oint d\boldsymbol{l}' + \frac{1}{r^2}\oint r'\cos\theta d\boldsymbol{l}' + \frac{1}{r^3}\oint (r')^2\left(\frac{3}{2}\cos^2\theta - \frac{1}{2}\right) d\boldsymbol{l}' + \cdots\right]. \tag{8.41}$$

The first term in Eq. (8.41) vanishes because the integral of the current vector over all orientations will average to zero.[10] This reflects that the first term in the multipole expansion is the monopole term, which measures the total "charge"; but there are no magnetic monopoles because there is no magnetic charge consistent with the Maxwell equations ($\boldsymbol{\nabla}\cdot\boldsymbol{B} = 0$). Defining the *magnetic moment* $\boldsymbol{m}$ by the integral

$$\boldsymbol{m} = \frac{1}{2}\int \boldsymbol{x}' \times \boldsymbol{J}(\boldsymbol{x}')\, d^3x', \tag{8.42}$$

and the *magnetic moment density* or *magnetization* $\boldsymbol{M}(\boldsymbol{x})$ by

$$\boldsymbol{M}(\boldsymbol{x}) = \frac{1}{2}\left[\boldsymbol{x}\times\boldsymbol{J}(\boldsymbol{x})\right], \tag{8.43}$$

for $I = |\boldsymbol{J}|$ the multipole expansion (8.41) of the vector potential can be written as

$$\boldsymbol{A}(\boldsymbol{r}) = \frac{\mu_0}{4\pi}\frac{\boldsymbol{m}\times\hat{\boldsymbol{r}}}{r^2} + \text{ higher-order multipole terms},$$

where the first term has the form of a *magnetic dipole*. The higher-order multipoles in this expression have increasingly larger powers of $|\boldsymbol{x}|$ in their denominators and at large distances from the current source the vector potential for a steady-state current distribution can be approximated well by retaining only the magnetic dipole term (see Problem 8.8,

$$\boldsymbol{A}(\boldsymbol{r}) = \frac{\mu_0}{4\pi}\frac{\boldsymbol{m}\times\hat{\boldsymbol{r}}}{r^2}. \tag{8.44}$$

Then the magnetic field may be found by taking the curl of $\boldsymbol{A}$, giving the components (see Problem 8.9)

$$\boldsymbol{B}_r = \frac{\mu_0 m}{2\pi r^3}\cos\theta \qquad \boldsymbol{B}_\theta = \frac{\mu_0 m}{4\pi r^3}\sin\theta \qquad \boldsymbol{B}_\phi = 0. \tag{8.45}$$

Because the dipole term dominates the multipole expansion in typical situations, it is common to refer to the magnetic dipole moment as *simply the magnetic moment*.

8.9.2 Magnetic Dipole Moment of a Current Loop

If the current as assumed to correspond to an arbitrary closed loop confined to a plane the magnitude of the magnetic moment takes a simple form that is independent of the shape of the loop,

$$|\boldsymbol{m}| = IA, \tag{8.46}$$

[10] This argument is intuitive; a more formal proof that the first term vanishes is given in Section 5.6 of Ref. [41].

where I is the current and A is the area enclosed by the planar current loop. If the current distribution is due to charged particles with charges q_i, masses M_i, and velocities $\boldsymbol{v}_i$, the current density is

$$\boldsymbol{J} = \sum_i q_i \boldsymbol{v}_i \delta(\boldsymbol{x} - \boldsymbol{x}_i),$$

where $\boldsymbol{x}_i$ is the position of the ith particle, and the magnetic moment is

$$\boldsymbol{m} = \frac{1}{2} \sum_i q_i (\boldsymbol{x}_i \times \boldsymbol{v}_i).$$

But the orbital angular momentum of particle i is $\boldsymbol{L}_i = M_i(\boldsymbol{x}_i \times \boldsymbol{v}_i)$ and the magnetic moment becomes

$$\boldsymbol{m} = \sum_i \frac{q_i}{2M_i} \boldsymbol{L}_i. \tag{8.47}$$

If all the particles have the same charge-to-mass ratio $q_i/M_i = e/M$,

$$\boldsymbol{m} = \frac{e}{2M} \sum_i \boldsymbol{L}_i = \frac{e}{2M} \boldsymbol{L}, \tag{8.48}$$

where $\boldsymbol{L}$ is the total orbital angular momentum. Equation (8.48) is the well-known classical connection between angular momentum and magnetic moment. It holds approximately for orbital angular momentum even on the atomic scale, but fails for moments arising from intrinsic particle spin, which is a uniquely quantum effect that is beyond the scope of our present discussion of classical electromagnetism.

Background and Further Reading

Good introductions to the material of this chapter may be found in Griffiths [33]. More advanced treatments may be found in Jackson [41], Garg [31], Chaichian et al [23], and Zangwill [77].

Problems

8.1 A localized current distribution of cylindrical symmetry has a current flowing only in the azimuthal direction, with a current density $\boldsymbol{J} = J(r,\theta)\hat{\boldsymbol{\phi}}$. The current is zero both outside the cylinder and near the origin. Working in Coulomb gauge, show that the corresponding vector potential $\boldsymbol{A}$ has only an azimuthal component with

$$A_\phi^{\text{in}}(r,\theta) = -\frac{\mu_0}{4\pi}\sum_l m_l r^l P_l^1(\cos\theta),$$

where $P_l^1(\cos\theta)$ is an associated Legendre polynomial and the multiple moments are given by

$$m_l = \begin{cases} -\dfrac{1}{l(l+1)}\displaystyle\int r^{-l-1}P_l^1(\cos\theta)J(r,\theta)\,d^3x & (\text{interior}), \\ -\dfrac{1}{l(l+1)}\displaystyle\int r^{l}P_l^1(\cos\theta)J(r,\theta)\,d^3x & (\text{exterior}), \end{cases}$$

for the interior and exterior solutions, respectively.

8.2 A cylindrical solenoid of length L and radius a carries a current I through N turns per unit length.

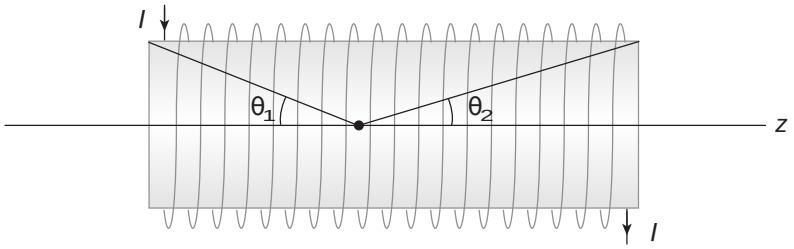

Show that in the limit $NL \to \infty$, the magnetic field is

$$B_z = \frac{\mu_0 NI}{2}(\cos\theta_1 + \cos\theta_2)$$

at the point defined on the cylinder axis by the angles θ_1 and θ_2 in the preceding figure.

8.3 It was asserted in Eq. (8.39) that the vector potential in Coulomb gauge is given by

$$\boldsymbol{A}(\boldsymbol{x}) = \frac{\mu_0}{4\pi}\int \frac{\boldsymbol{J}(\boldsymbol{x}')}{|\boldsymbol{x}-\boldsymbol{x}'|}\,d^3x',$$

provided that the current distribution $\boldsymbol{J}(\boldsymbol{x}')$ vanishes sufficiently rapidly at infinity. Prove that this solution does indeed satisfy the Coulomb gauge condition.

8.4 Show that a vector potential $\boldsymbol{A} = \frac{1}{2}\boldsymbol{B}_0 \times \boldsymbol{x}$ produces a magnetic field $\boldsymbol{B}_0$. ***

8.5 (a) Starting from the classical Lorentz-force equation, show that $E_y = v_x B_z$ in the Hall effect experimental diagram shown in Box 8.1.

(b) The electron velocity $\boldsymbol{v}$ in the Hall experiment depends on interactions with the lattice in the 2D Hall device. In the classical *Drude model* of electron transport

(see Section 7.3.2) the force is given by $\boldsymbol{F} = m(d\boldsymbol{v}/dt + \boldsymbol{v}/\tau)$, where m is the effective electron mass and τ is the Drude-model relaxation time. Assuming steady-state electron flow and defining the *cyclotron frequency* $\omega_c \equiv e\,B/m$, show that the classical equations of motion for Hall-device electrons in the Drude approximation are

$$v_x = -\frac{e\tau}{m}\,E_x - \omega_c \tau v_y \qquad v_y = -\frac{e\tau}{m}\,E_y + \omega_c \tau v_x \qquad v_z = -\frac{e\tau}{m}\,E_z,$$

where e is the electronic charge, m is the electron mass, $\boldsymbol{B}$ is the magnetic field, and $\boldsymbol{E}$ is the electric field.

(c) Use the results from parts (a) and (b) to show that in the figure of Box 8.1,

$$E_y = -\frac{eB\tau}{m} E_x.$$

Hint: At equilibrium, $v_y = 0$.

(d) The current density $\boldsymbol{J}$ in the Drude model is

$$\boldsymbol{J} = \frac{e^2 n_e}{m}\,\tau \boldsymbol{E} = \sigma \boldsymbol{E} \qquad \sigma \equiv \frac{e^2 n_e \tau}{m},$$

where n_e is the electron number density, σ is the conductance, and τ is the Drude-model relaxation time. Using the figure in Box 8.1, prove that

$$E_y = \frac{V_H}{w} \qquad I = w j_x \qquad R_H \equiv \frac{V_H}{I} = -\frac{B}{e n_e} \qquad R_L \equiv \frac{V_L}{I} = \frac{L}{w\sigma},$$

where V_H is the *Hall voltage* (associated with the induced electric field E_y), I is the total current, J_x is the current density in the x direction, $q = -e$ was assumed for electrons, R_H is the *Hall resistance,* and R_L is the *longitudinal resistance* (along the x axis) of the Hall device shown in Box 8.1.

8.6 (a) Show that for a 2D Hall device like the one shown in Box 8.1, with length L and width w, that $J = \sigma E$ (where J is the current density, E is the electric field, and σ is the conductivity) is equivalent to the simple form of Ohm's law, $V = IR$. *Hint*: See Section 7.3.1 and Box 7.1.

(b) Show that for the Hall device shown in Box 8.1, the resistance components $R_{ij} = V_i/I_j$ and resistivity components $\rho_{ij} = E_i/j_j$ are related by

$$R_{yx} = \rho_{yx} \qquad R_{xx} = (L/w)\rho_{xx}.$$

Verify the final forms of the ρ and σ tensors in Box 7.1. s***

8.7 Show that the magnitude of the force per unit length acting between two infinitely long parallel wires carrying steady currents I_a and I_b, respectively, and separated by a distance d,

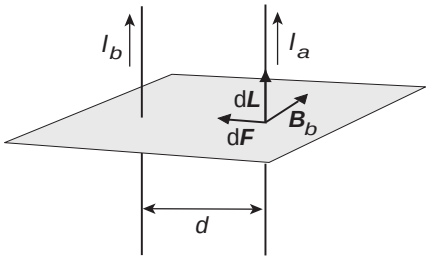

is given by

$$\frac{dF}{dI_a} = \frac{\mu_0 I_a I_b}{2\pi d},$$

and is attractive if the currents are in the same direction and repulsive if they are in the opposite directions.

8.8 Prove that for the current loop in Fig. 8.11 the vector potential is at large distance from the source is given by

$$\boldsymbol{A}(\boldsymbol{r}) = \frac{\mu_0}{4\pi}\frac{\boldsymbol{m}\times\hat{\boldsymbol{r}}}{r^2},$$

where we define $r \equiv |\boldsymbol{x}|$ and $r' \equiv |\boldsymbol{x}'|$. *Hint*: Use a multipole expansion assuming $r \gg r'$, and that

$$\oint(\hat{\boldsymbol{r}}\cdot\boldsymbol{r}')d\boldsymbol{L}' = -\hat{\boldsymbol{r}}\times\int d\boldsymbol{a}' = -\hat{\boldsymbol{r}}\times\boldsymbol{a}$$

in Fig. 8.11, where $\boldsymbol{a}$ is the "vector area" of the loop. ***

8.9 Find the formula for the magnetic field corresponding to the vector potential derived in Problem 8.8

8.10 Consider two parallel, infinite line charges λ separated by a distance d and and moving in the same direction at a speed v, as viewed in the laboratory frame. The following figure illustrates.

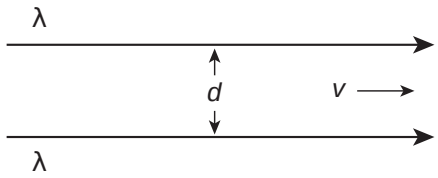

Show that for the electrostatic repulsion between the charges to be equal in magnitude to the magnetic attraction, the velocity v must be equal to the speed of light c. *Hint*: Remember that the SI constants ϵ_0 and μ_0 are related to each other through c. ***

8.11 A large parallel plate capacitor has a uniform charge $+Q$ on its upper plate and a uniform charge $-Q$ on its lower plate, and the entire capacitor is moving to the right at a constant speed v, as viewed in the laboratory frame. The following figure illustrates.

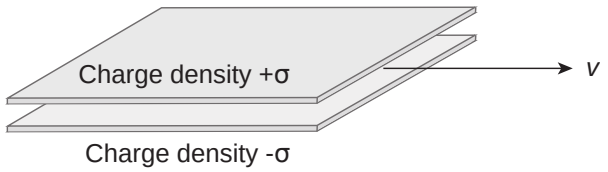

Show that for the electrostatic repulsion between the plates to exactly balance the magnetic attraction, v must be equal to the speed of light c. *Hint*: Approximate the plates of the capacitor as infinite 2D sheets of current.

8.12 Consider a particle with positive charge q and mass m moving in a uniform magnetic field $\boldsymbol{B}$ directed into the page with initial velocity $\boldsymbol{v}$ in the $x-y$ plane perpendicular to the field and to the x axis, as illustrated in the following diagram.

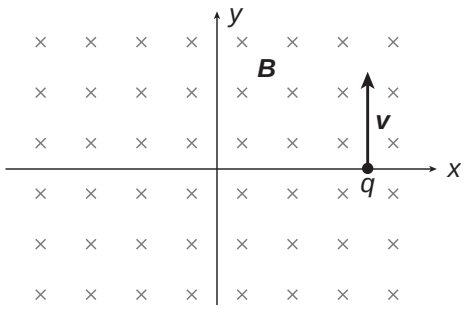

Show that the resulting force acting on the particle has constant magnitude $F_{\mathrm{M}} = qvB$, with orientation perpendicular to both $\boldsymbol{B}$ and $\boldsymbol{v}$. Thus show that the positively charged particle executes clockwise circular motion in the $x-y$ plane with the force always directed toward the center of a circular orbit of radius $R = mv^2/qvB$, with orbital period $T = 2\pi m/qB$. ***

8.13 (a) A semicircular conducting wire loop of radius R carries a steady counterclockwise current I and a uniform magnetic field $\boldsymbol{B}$ is applied in the vertical direction:

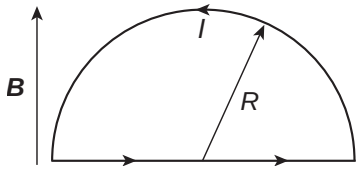

What are the magnitude and direction of the magnetic forces acting on the straight and curved parts of the wire; what is the total magnetic force acting on the loop?

(b) In the following diagram

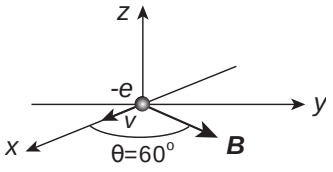

an electron with charge $q = -e$ is moving in the positive direction on the x-axis at a speed of $v = 5 \times 10^6$ m s^{-1} and is subject to a magnetic field $\boldsymbol{B}$ with a magnitude of $B = 0.03$ T and an orientation lying in the $x - y$ plane at an angle of 60° relative to the x-axis. Determine the acceleration vector of the electron.

8.14 A rectangular loop consists of $N = 100$ closely wrapped turns and has dimensions $a = 0.4$ m and $b = 0.3$ m. The loop is hinged along the y-axis and its plane makes an angle of $\theta = 30^\circ$ with the x-axis.

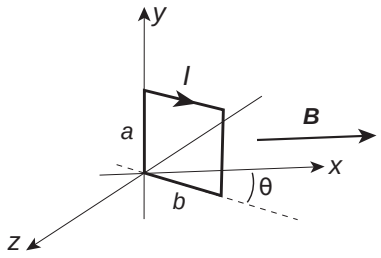

What is the magnitude of the torque exerted on the loop by a uniform magnetic field $B = 0.8$ T directed along the x-axis when the steady current is $I = 1.2$ A in the direction shown? What is the expected direction of rotation for the loop? ***

8.15 Consider a cylindrical wire of radius R carrying a uniform current density $\boldsymbol{J} = J_0 \hat{\boldsymbol{z}}$. For a point inside the wire the vector potential can be expressed as:

$$\boldsymbol{A} = -\frac{\mu_0 J_0 s^2}{4} \hat{\boldsymbol{z}} \qquad (s < R),$$

where s is the radial distance in cylindrical coordinates. Use the divergence theorem to verify that the net flux of $\boldsymbol{A}$ through the surface of a closed cylinder of length L and radius $s < R$ is zero, which is consistent with the Coulomb gauge condition.

Numerical and GenAI Problems

9 Magnetostatics in Matter

Just as it was shown in Ch. 6 that electric fields can polarize matter electrostatically, magnetic fields can polarize matter magnetically. In classical electromagnetism all magnetic phenomena have their origin in the motion of electrical charges. At the microscopic level, we may view magnetism as being produced by small current loops (for example, electrons in orbits around nuclei in atoms) that may be modeled as tiny magnetic dipoles. Ordinarily the effects of these dipoles cancel out because of random orientation of atoms, but if a magnetic field is applied to the matter it can cause a net alignment of the dipoles so that the matter becomes magnetically polarized (*magnetized*). For the electric polarization of matter, the polarization is usually in the direction of the $\boldsymbol{E}$ field. Magnetic polarization of matter is more complex and varied than electric polarization of matter. For example,

1. *paramagnetic materials* acquire a magnetization in the *same direction* as the applied field $\boldsymbol{B}$, while
2. *diamagnetic materials* acquire a magnetization in the direction *opposite the applied field*, and
3. *ferromagnetic materials* can become *permanent magnets* by retaining their magnetization after the polarizing field has been removed, with the retained magnetization then depending on the *entire magnetic history* of the material.

As a consequence of these features, the discussion of magnetized matter is more complex than the discussion of electrically polarized matter.

9.1 Aligning Current Loops in Magnetic Fields

In classical electromagnetism, magnetic interactions in matter are assumed to be a consequence of small current loops arising at the atomic and molecular level.[1] As shown in

[1] Some early investigators were enamored of the idea that magnetic effects were attributable to Coulomb-like interactions with magnetic dipoles formed from north and south magnetic poles, analogous to electric dipoles formed from a positive and negative electric charge (this is often called the *Gilbert model*). Today we know that there is no evidence for fundamental positive or negative magnetic charges and a more realistic picture of classical magnetism is based on small loops of electrical current (this is often called the *Ampèrian model*). These fictitious magnetic charges can be used as a basis for theoretical approaches that lead to correct answers for a restricted set of problems. (For example, see Section 9.3.4, where a solution of the Poisson equation for a special case of magnetism with no free currents exhibits a magnetic field with dipole character arising from polarization concentrating positive and negative "magnetic charges" on opposite sides of a sphere.) But they are limited in range of application, and have limited explanatory power because they are based on a fiction. In our discussion we shall always have in mind the Ampèrian picture of classical magnetism arising from tiny current loops.

Probs. 9.2 and 9.3, these current loops experience *no net force* in a uniform magnetic field if they carry steady currents, but they do experience *a net torque* that tends to align them with the magnetic field. It is this alignment of current loops by the magnetic field that leads to magnetization of matter. If the magnetic interaction is expanded in a multipole series (see Section 8.9), only the lowest orders contribute when observing from a large distance. For a magnetic interaction, the $l = 0$ monopole term is the total "charge", but there are no magnetic charges (no magnetic monopoles) so the $l = 0$ term vanishes and the lowest-order magnetic multipole is the dipole with $l = 1$. Thus, to good approximation we may treat the current loops as a set of magnetic dipoles.[2] Just as found for electric multipole moments in Section 6.2.2, the low-order moments dominate for a distant observer. The difference here is that there is no monopole moment for magnetism, so it is dominated typically by the magnetic dipole moments.

Thus the current loops may be replaced by magnetic dipoles in the analysis of magnetized matter. The magnetic dipole moment vector $\boldsymbol{m}$ for a loop carrying a current I is defined by

$$\boldsymbol{m} = I \int d\boldsymbol{a} = I\boldsymbol{a}, \tag{9.1}$$

where $\boldsymbol{a}$ is the *vector area of a surface* S bounded by the loop:

$$\boldsymbol{a} = \int_S d\boldsymbol{a} = \frac{1}{2} \oint \boldsymbol{r} \times d\boldsymbol{l}, \tag{9.2}$$

where the second integral is around the boundary curve of the area S. If the loop is flat, $\boldsymbol{a}$ has a magnitude equal to the usual area enclosed and the direction of $\boldsymbol{a}$ (and of $\boldsymbol{m}$) is given by the right-hand rule applied to the direction of the current in the loop. Then the magnitude of the magnetic dipole moment vector $\boldsymbol{m}$ is

$$|\boldsymbol{m}| = Ia, \tag{9.3}$$

where I is the magnitude of the current and a is the area bounded by the loop. The torque $\boldsymbol{\tau}$ exerted on a current loop of area $\boldsymbol{a}$ carrying current I, or on the corresponding magnetic dipole moment $\boldsymbol{m}$, is

$$\boldsymbol{\tau} = I\boldsymbol{a} \times \boldsymbol{B} = \boldsymbol{m} \times \boldsymbol{B}, \tag{9.4}$$

with the direction given by the right-hand rule applied to the direction of the current within the loop.

9.2 Ampère's Law in Polarized Matter

In the previous chapter we have dealt with steady-state magnetic fields in a microscopic manner, assuming that the current density $\boldsymbol{J}$ is a known function of position. In macroscopic problems dealing with magnetic effects in materials, this will often not be true

[2] Retaining only the dipoles and not higher-order multipoles is justified if the distance to the observer greatly exceeds the size of the current loop. This is almost always true, since the current loops are atomic-scale.

since the magnetic polarization of the matter will modify current densities. Now we must develop methods to solve for the fields in the presence of such polarization.

9.2.1 Macroscopic Averaging

The atomic currents in matter produce rapidly fluctuating current densities on a microscopic scale. Just as discussed in Section 6.7 for electric fields in matter, only averages over small macroscopic volumes are known and only these enter into the classical equations of electromagnetism. The first step in introducing averaging in matter for electric fields in Section 6.7 was to note that the averaging procedure preserves the crucial relation $\boldsymbol{\nabla} \times \boldsymbol{E} = 0$, which ensures that the macroscopic electric field is still derivable from a scalar potential through $\boldsymbol{E} = -\boldsymbol{\nabla}\Phi$. In a similar manner, for magnetic fields the macroscopic averaging procedure leads to the same equation $\boldsymbol{\nabla} \cdot \boldsymbol{B} = 0$ that we introduced in Eq. (8.18). Thus, the averaging procedure preserves the notion of a vector potential $\boldsymbol{A}(\boldsymbol{x})$, from which we can derive the macroscopic magnetic field by taking the curl, $\boldsymbol{B} = \boldsymbol{\nabla} \times \boldsymbol{A}$.

The basic effect of magnetization is to establish currents within a material and on its surface such that these currents produce the field due to magnetization. The average macroscopic magnetization or magnetic (dipole) moment density is

$$\boldsymbol{M}(\boldsymbol{x}) = \sum_i N_i \langle \boldsymbol{m}_i \rangle, \tag{9.5}$$

where $\langle \boldsymbol{m}_i \rangle$ is the magnetic moment averaged over a small volume around the point $\boldsymbol{x}$. In addition to the bulk magnetization we may assume that there is a macroscopic current density $\boldsymbol{J}(\boldsymbol{x})$ produced by the flow of free charge in the medium. Then the vector potential resulting from averaging over a small volume ΔV around $\boldsymbol{x}'$ will take the form

$$\Delta \boldsymbol{A}(\boldsymbol{x}) = \frac{\mu_0}{4\pi} \left[\frac{\boldsymbol{J}(\boldsymbol{x}')}{|\boldsymbol{x} - \boldsymbol{x}'|} + \frac{\boldsymbol{M}(\boldsymbol{x}') \times (\boldsymbol{x} - \boldsymbol{x}')}{|\boldsymbol{x} - \boldsymbol{x}'|^3} \right] \Delta V, \tag{9.6}$$

where the first term represents the contribution of the flow of free charge and the second term represents the contribution from the magnetic dipoles in the medium described by Eq. (8.44). Letting ΔV tend to d^3x', the total vector potential at $\boldsymbol{x}$ is given by an integral over all space,

$$\boldsymbol{A}(\boldsymbol{x}) = \frac{\mu_0}{4\pi} \int \left[\frac{\boldsymbol{J}(\boldsymbol{x}')}{|\boldsymbol{x} - \boldsymbol{x}'|} + \frac{\boldsymbol{M}(\boldsymbol{x}') \times (\boldsymbol{x} - \boldsymbol{x}')}{|\boldsymbol{x} - \boldsymbol{x}'|^3} \right] d^3x'. \tag{9.7}$$

The second (magnetization) term in the integrand can then be cast in another form by utilizing the identity Eq. (8.16) to write it as

$$\int \frac{\boldsymbol{M}(\boldsymbol{x}') \times (\boldsymbol{x} - \boldsymbol{x}')}{|\boldsymbol{x} - \boldsymbol{x}'|^3} \, d^3x' = \int \boldsymbol{M}(\boldsymbol{x}') \times \boldsymbol{\nabla}' \left(\frac{1}{|\boldsymbol{x} - \boldsymbol{x}'|} \right) d^3x'.$$

Integration of this integral by parts then allows Eq. (9.7) to be written

$$\boldsymbol{A}(\boldsymbol{x}) = \frac{\mu_0}{4\pi} \int \frac{[\boldsymbol{J}(\boldsymbol{x}') + \boldsymbol{\nabla}' \times \boldsymbol{M}(\boldsymbol{x}')]}{|\boldsymbol{x} - \boldsymbol{x}'|} \, d^3x', \tag{9.8}$$

where a surface term has been discarded by assuming $\boldsymbol{M}(\boldsymbol{x}')$ to be localized and well behaved.

9.2.2 Auxiliary Field $\boldsymbol{H}$ and Constituitive Relations

From the results in the preceding section we see that the magnetization contributes an effective current density

$$\boldsymbol{J}_{\mathrm{M}} = \boldsymbol{\nabla} \times \boldsymbol{M}. \tag{9.9}$$

Then $\boldsymbol{J} + \boldsymbol{J}_{\mathrm{M}}$ plays the role of the effective current such that

$$\boldsymbol{\nabla} \times \boldsymbol{B} = \mu_0(\boldsymbol{J} + \boldsymbol{\nabla} \times \boldsymbol{M}). \tag{9.10}$$

It is then convenient to define a new macroscopic field $\boldsymbol{H}$ by[3]

$$\boldsymbol{H} \equiv \frac{1}{\mu_0}\boldsymbol{B} - \boldsymbol{M}. \tag{9.11}$$

The introduction of $\boldsymbol{H}$ in the presence of magnetically polarized materials is a matter of convenience, analogous to the introduction in Section 6.7 of $\boldsymbol{D}$ to account for electrically polarized materials in electrostatics. The *fundamental fields* in classical electromagnetism are the electric field $\boldsymbol{E}$ and the magnetic field $\boldsymbol{B}$.[4] The *derived fields* $\boldsymbol{D}$ and $\boldsymbol{H}$ are introduced as a convenient way to take into account the average contributions to charge density and current of the atomic-level charges and currents. Then the macroscopic fields in medium that replace the microscopic fields of Eqs. (8.31) are

$$\begin{aligned} \boldsymbol{\nabla} \times \boldsymbol{H} &= \boldsymbol{J}, \\ \boldsymbol{\nabla} \cdot \boldsymbol{B} &= 0, \end{aligned} \tag{9.12}$$

which are analogous to the macroscopic fields for electrostatics in medium

$$\begin{aligned} \boldsymbol{\nabla} \times \boldsymbol{E} &= 0, \\ \boldsymbol{\nabla} \cdot \boldsymbol{D} &= \rho, \end{aligned} \tag{9.13}$$

that were derived in Sections 6.7 and 6.8.

[3] We have routinely termed $\boldsymbol{B}$ the magnetic field. Some authors instead call $\boldsymbol{H}$ the magnetic field, which requires finding another name for $\boldsymbol{B}$. For example, Jackson [41] calls $\boldsymbol{H}$ the *magnetic field* and calls $\boldsymbol{B}$ the *magnetic induction*. This is a question of terminology, not physics, and arguments can be made from a theoretical or experimental perspective in favor of either naming convention. Because the fundamental fields are $\boldsymbol{E}$ and $\boldsymbol{B}$, and the auxiliary fields $\boldsymbol{D}$ and $\boldsymbol{H}$ are derived quantities, we have adopted the convention here of calling $\boldsymbol{B}$ the magnetic field, with no specific name for $\boldsymbol{H}$ (except "$\boldsymbol{H}$-field"). Likewise $\boldsymbol{E}$ is termed the electric field and $\boldsymbol{D}$ the displacement field (but the common name "displacement" for $\boldsymbol{D}$ survives for historical, not descriptive, reasons).

[4] This statement applies specifically to *classical* electromagnetism. As will be discussed further in Ch. 21, in quantum mechanics one finds that the scalar potential Φ and the vector potential $\boldsymbol{A}$ (or a 4-vector having Φ and $\boldsymbol{A}$ as components in a Lorentz-covariant theory) should be viewed as more fundamental than the electric and magnetic fields, for two basic reasons. (1) There are experiments where probes that never see the magnetic field are influenced by the vector potential (the Aharonov–Bohm effect), and (2) the fundamental coupling of electromagnetism to charged particles is through the vector and scalar potentials (the *minimal coupling prescription*; also called *minimal substitution*).

Just as for Eqs. (9.13), the description of macroscopic magnetostatics in Eqs. (9.12) requires constituitive relationships, in this case between the fundamental field $\boldsymbol{B}$ and the derived field $\boldsymbol{H}$. For paramagnetic and diamagnetic materials that are isotropic, the relationship may be assumed linear,

$$\boldsymbol{B} = \mu \boldsymbol{H}, \tag{9.14}$$

where the constant μ is characteristic of the medium and is called the *magnetic permeability*. It is also common to characterize the magnetic properties of the medium in terms of the *magnetic susceptibility* χ, which is related to the magnetic permeability μ by

$$\chi = \left(\frac{\mu}{\mu_0} - 1 \right). \tag{9.15}$$

Typically for paramagnetic materials $\mu > 1$ and for diamagnetic materials $\mu < 1$, with μ/μ_0 differing from unity by a part in $\sim 10^5$ for either case. As a consequence, diamagnetism and paramagnetism are small effects in normal matter. The physical reasons for paramagnetism and diamagnetism are discussed in Box 9.1 and in Fig. 9.1.

The case of ferromagnetic materials is more involved than simple paramagnetism or diamagnetism. In ferromagnetic substances the magnetic susceptibility χ (or the magnetic permeability μ) is positive but not constant; it depends on the applied field $\boldsymbol{H}$, and typically can take large values. When an external field is applied to a ferromagnetic material the system acquires a magnetization $\boldsymbol{M}$ aligned with the applied field. The origin of permanent ferromagnetism (magnetism that remains in the absence of an external field) is an essentially quantum-mechanical effect where many spins align spontaneously to form a highly collective state.[5] Ferromagnets may exhibit *hysteresis*, where the magnetic field $\boldsymbol{B}$ is not a single-valued function of $\boldsymbol{H}$ and the state of the system may depend on its preparation history; Fig. 9.2 illustrates. These complex behaviors lead to a constituitive relationship

$$\boldsymbol{B} = \boldsymbol{F}[\boldsymbol{H}], \tag{9.16}$$

where the notation $\boldsymbol{F}[\boldsymbol{H}]$ indicates that $\boldsymbol{F}$ has a *non-linear dependence on* $\boldsymbol{H}$. The complicated nonlinear relationship of $\boldsymbol{B}$ and $\boldsymbol{H}$ in ferromagnetic materials means that magnetic boundary-value problems are generally more difficult to deal with than corresponding boundary value problems in electrostatics.

9.2.3 Magnetic Boundary-Value Conditions

Boundary conditions for $\boldsymbol{B}$ and $\boldsymbol{H}$ at media interfaces were considered in Section 6.11; Eqs. (6.56b) and (6.57b) indicate that normal components of $\boldsymbol{B}$ and tangential components

[5] This is an example of quantum-mechanical *spontaneous symmetry breaking*, which is characterized by a ground state wavefunction that does not have the full symmetry of the Hamiltonian for a system. In the case of permanent ferromagnetism, the correct Hamiltonian is rotationally invariant (implying conservation of angular momentum) but the ferromagnetic wavefunction has spins aligned in a preferred direction, even if no external field is present, which breaks rotational invariance. Thermal fluctuations can destroy this collective alignment of spins, so in permanent ferromagnets the collective magnetic state disappears above a critical temperature called the *Curie temperature* T_c. For $T > T_c$, a ferromagnet then behaves as a paramagnet. An introduction to spontaneously broken symmetry may be found in Chs. 17 and 18 of Ref. [38].

Box 9.1 Diamagnetism and Paramagnetism

Materials characterized by small magnetic susceptibilities $|\chi| \ll 1$ are called *paramagnetic* if $\chi > 0$, and *diamagnetic* if $\chi < 0$. Magnetization in diamagnetic and paramagnetic media typically depends linearly on the applied magnetic field.

Physical Origin of Diamagnetism

In diamagnetic media an external field $\boldsymbol{H}$ creates a magnetization $\boldsymbol{M}$ opposite to $\boldsymbol{H}$, so $\chi < 0$. Physically, external fields induce currents associated with orbital motion in the diamagnetic material. (The external field also interacts with electron spins, but this is a much smaller effect than the interaction with orbital currents.) The field created by the moving charges *opposes* the applied field $\boldsymbol{H}$ (*Lenz's law*). Thus, the magnetic field is decreased inside the material and magnetic lines of force are expelled from the medium. This diamagnetic effect is particularly dramatic in *superconductors*, where the magnetic field is expelled completely (*Meissner effect*), except for a thin surface layer where the magnetic field decays exponentially over a distance called the *London penetration depth*).

Diamagnetism on Steroids: Diamagnetic effects are greatly amplified in a *superconductor* because the induced currents flow without resistance. In quantum field theory the normally massless photon acquires an *effective mass* through interaction with the medium, which causes it to penetrate the superconductor with exponentially decaying probability. This acquisition of effective mass by photons is a non-relativistic model of the *Higgs mechanism*, whereby a massless gauge boson (the photon) acquires a mass. As we shall discuss in Ch. 21, this *Higgs mode of spontaneous symmetry breaking* is fundamental for the Standard Model of elementary particle physics.

Physical Origin of Paramagnetism

Some materials have magnetic dipoles associated with intrinsic spins (a quantum-mechanical effect). Application of an external field $\boldsymbol{H}$ then partially aligns the dipoles with the applied field, thereby *enhancing the internal field*. (This ordering is opposed by thermal fluctuations, so the fraction of alignment is temperature dependent.) Such materials are called *paramagnetic*. The net effect is that the lines of magnetic force are "drawn in" to paramagnetic material.

Magnetic Field Lines for Diamagnets and Paramagnets

The contrasting behavior of diamagnetic and paramagnetic matter in magnetic fields can be characterized by their magnetic field lines [23], as illustrated in Fig. 9.1. The diamagnetic matter in (a) expels the magnetic field but the paramagnetic matter in (b) enhances the density of field lines within the sample.

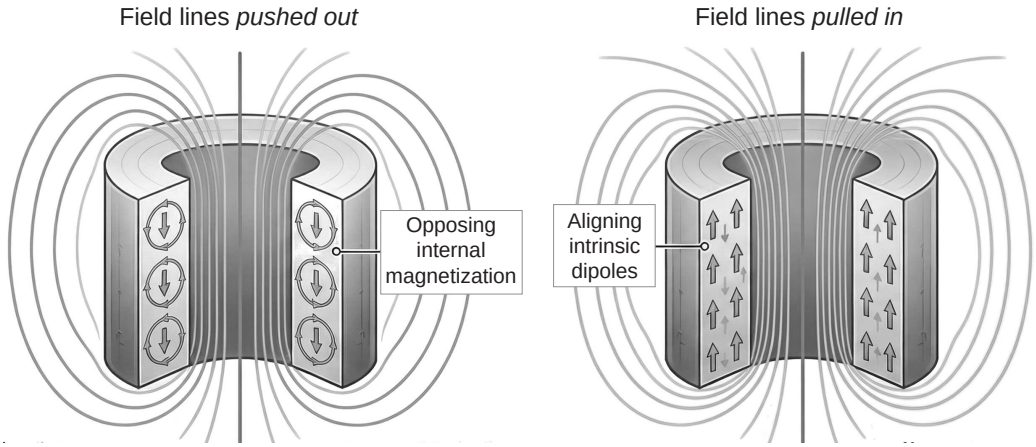

Fig. 9.1 Interaction of diagmagnetic and paramagnetic materials with external magnetic fields. (a) Diamagnetic matter repels the magnetic field slightly, causing a small reduction of the density of field lines inside the material. (b) Paramagnetic matter attracts the magnetic field slightly, causing a small increase in the density of field lines in the sample.

of $\boldsymbol{H}$ on opposite sides of a boundary between medium 1 and medium 2 are related by

$$(\boldsymbol{B}_2 - \boldsymbol{B}_1) \cdot \boldsymbol{n} = 0, \tag{9.17a}$$

$$\boldsymbol{n} \times (\boldsymbol{H}_2 - \boldsymbol{H}_1) = \boldsymbol{K}, \tag{9.17b}$$

where $\boldsymbol{n}$ is a unit normal vector pointing from region 1 into region 2 and $\boldsymbol{K}$ is the surface current density. If media satisfy the linear constituitive relation (9.14) and have finite conductivities so that $\boldsymbol{J} = \sigma \boldsymbol{E}$ and $\boldsymbol{K} = 0$, boundary conditions can be expressed as

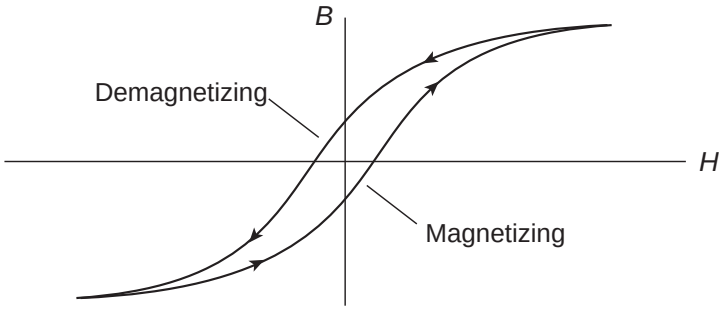

Fig. 9.2 Schematic illustration of magnetic hysteresis for a ferromagnetic state. If the system is magnetized by slowly increasing the applied magnetic field up to a maximum and then demagnetized by decreasing it, the system is said to exhibit hysteresis if the demagnetizing path isn't the reverse of the magnetizing path. In that case, the relation between B and H is not single-valued and the state of the system depends on its preparation history.

[41],

$$\boldsymbol{B}_2 \cdot \boldsymbol{n} = \boldsymbol{B}_1 \cdot \boldsymbol{n} \qquad \boldsymbol{B}_2 \times \boldsymbol{n} = \frac{\mu_2}{\mu_1} \boldsymbol{B}_1 \times \boldsymbol{n}, \tag{9.18}$$

or as

$$\boldsymbol{H}_2 \cdot \boldsymbol{n} = \frac{\mu_1}{\mu_2} \boldsymbol{H}_1 \cdot \boldsymbol{n} \qquad \boldsymbol{H}_2 \times \boldsymbol{n} = \boldsymbol{H}_1 \times \boldsymbol{n}. \tag{9.19}$$

If $\mu_1 \gg \mu_2$ the boundary conditions on $\boldsymbol{H}$ for highly-permeable material are essentially the same as for the electric field at the surface of a conductor, which permits electrostatic potential theory to be applied to magnetic field problems. In the next section we shall address methods of solving magnetostatic boundary value problems.

9.3 Magnetostatic Boundary-Value Problems

Magnetostatic boundary value problems require solving Eqs. (9.12) subject to constitutive relations as in Eqs. (9.14) and (9.16). Especially because of the range of constituitive relations that are possible for magnetic and magnetized materials, a variety of situations can occur and a survey of possible methods of attack is useful. We summarize some approaches following the presentation in Jackson [41].

9.3.1 Solutions Using a Vector Potential

Because $\boldsymbol{\nabla} \cdot \boldsymbol{B} = 0$, it is always possible introduce a vector potential $\boldsymbol{A}(\boldsymbol{x})$ such that $\boldsymbol{B} = \boldsymbol{\nabla} \times \boldsymbol{A}$. Then if we have a non-linear constituitive relation (9.16) the resulting differential equation

$$\boldsymbol{\nabla} \times \boldsymbol{H}[\boldsymbol{\nabla} \times \boldsymbol{A}] = \boldsymbol{J}$$

is generally very difficult to solve. However, if the constituitive relation is linear, $\boldsymbol{B} = \mu \boldsymbol{H}$, the preceding equation becomes

$$\boldsymbol{\nabla} \times \left(\frac{1}{\mu} \boldsymbol{\nabla} \times \boldsymbol{A} \right) = \boldsymbol{J}. \tag{9.20}$$

For a region of space in which μ is constant, the vector identity $\boldsymbol{\nabla} \times (\boldsymbol{\nabla} \times \boldsymbol{A}) = \boldsymbol{\nabla}(\boldsymbol{\nabla} \cdot \boldsymbol{A}) - \nabla^2 \boldsymbol{A}$ of Eq. (A.8) may be used to write this as

$$\boldsymbol{\nabla}(\boldsymbol{\nabla} \cdot \boldsymbol{A}) - \nabla^2 \boldsymbol{A} = \mu \boldsymbol{J}, \tag{9.21}$$

and invoking the Coulomb gauge condition (8.37) by setting $\boldsymbol{\nabla} \cdot \boldsymbol{A} = 0$, we obtain the Poisson equation

$$\nabla^2 \boldsymbol{A} = -\mu \boldsymbol{J}. \tag{9.22}$$

Comparing with Eq. (8.38) in vacuum, this is a Poisson equation with a current density modified by the medium, which is similar to a Poisson equation for uniform dielectric media with an effective charge density (ϵ/ϵ_0). Matching of solutions for Eq. (9.22) across

interfaces between different (linear) media can be implemented using the boundary conditions (9.18) or (9.19).

9.3.2 Solutions Using a Magnetic Scalar Potential

As mentioned in Section 8.8, for the special case $\boldsymbol{J} = 0$ where the current density vanishes in a region of interest, $\boldsymbol{\nabla} \times \boldsymbol{H} = 0$, suggesting the introduction of a *magnetic scalar potential* Φ_{M} such that

$$\boldsymbol{H} = -\boldsymbol{\nabla}\Phi_{\mathrm{M}}. \tag{9.23}$$

If the medium is linear and μ is constant the magnetic scalar potential satisfies the Laplace equation

$$\nabla^2\Phi_{\mathrm{M}} = 0, \tag{9.24}$$

for which the boundary conditions (9.18) are appropriate. This method is of limited utility since it applies only if $\boldsymbol{J} = 0$. One use case is the magnetic field external to a closed loop of current. Another is the hard ferromagnet that will be considered in Section 9.3.3. The condition that $\boldsymbol{J} = 0$ in magnetism is often stated concisely as "$\boldsymbol{H}$ is conservative", which has several important consequences that are summarized in Box 9.2.

9.3.3 Solutions for Hard Ferromagnets

A *hard ferromagnet* is one having a magnetization sufficiently stable that is largely independent of applied field for moderate field strengths. This suggests an approximation where the ferromagnet can be assumed to have a specified fixed magnetization $\boldsymbol{M}(\boldsymbol{x})$, using either magnetic scalar potential methods or magnetic vector potential methods.

Using the Magnetic Scalar Potential: Since $\boldsymbol{J} = 0$ for a hard ferromagnetic, the magnetic scalar potential method of Section 9.3.2 is applicable. Then $\boldsymbol{\nabla} \cdot \boldsymbol{B} = 0$ becomes

$$\boldsymbol{\nabla} \cdot \boldsymbol{B} = \mu_0 \boldsymbol{\nabla} \cdot (\boldsymbol{H} + \boldsymbol{M}) = 0, \tag{9.25}$$

where Eq. (9.11) was used, and since $\boldsymbol{H} = -\boldsymbol{\nabla}\Phi_{\mathrm{M}}$ from Eq. (9.23), we obtain a *magnetic Poisson equation*,

$$\nabla^2\Phi_{\mathrm{M}} = \boldsymbol{\nabla} \cdot \boldsymbol{M} = -\rho_{\mathrm{M}}, \tag{9.26}$$

where an *effective magnetic-charge density*

$$\rho_{\mathrm{M}} \equiv -\boldsymbol{\nabla} \cdot \boldsymbol{M} \tag{9.27}$$

has been introduced. By analogy with the second term of Eq. (6.21) for electrically polarized matter, if there are no boundary surfaces the expected solution is [41]

$$\Phi_{\mathrm{M}}(\boldsymbol{x}) = -\frac{1}{4\pi}\int \frac{\boldsymbol{\nabla}' \cdot \boldsymbol{M}(\boldsymbol{x}')}{|\boldsymbol{x} - \boldsymbol{x}'|}\, d^3x = -\frac{1}{4\pi}\boldsymbol{\nabla} \cdot \int \frac{\boldsymbol{M}(\boldsymbol{x}')}{|\boldsymbol{x} - \boldsymbol{x}'|}\, d^3x, \tag{9.28}$$

where the second form results from applying the identity Eq. (8.16) and an integration by parts, which is justified if $\boldsymbol{M}$ is localized and well behaved.

Box 9.2 Conservative H Fields in Magnetostatics

In magnetostatics, stating that *the $\boldsymbol{H}$ field is conservative* is shorthand for *$\boldsymbol{H}$ has no curl:* $\boldsymbol{\nabla} \times \boldsymbol{H} = 0$. This mathematical property radically simplifies how we can conceptualize and calculate the field.

1. Graphically, the field lines exhibit no local circulation (no "swirling").
2. Work done in moving between two points is independent of the path taken, just as in electrostatics (Section 2.8.1); hence the appelation "conservative".
3. over any loop that encloses no net free current, $\oint \boldsymbol{H} \cdot d\boldsymbol{l} = 0$.
4. *The mathematical machinery of electrostatics can be applied to magnetism.* Because the curl of any scalar gradient is identically zero, a curl-free $\boldsymbol{H}$ field allows us to define a *magnetic scalar potential*, Φ_{m}, with $\boldsymbol{H} = -\boldsymbol{\nabla}\Phi_{\mathsf{m}}$.

This latter point is a massive analytical advantage; instead of wrestling with

- the *vector potential* $\boldsymbol{A}$, and
- the coupled partial differential equations of the *Biot–Savart law*,

we have a *scalar boundary value problem*. Since $\boldsymbol{\nabla} \cdot \boldsymbol{B} = 0$, for linear, isotropic, homogeneous matter $\boldsymbol{\nabla} \cdot \boldsymbol{H} = 0$ and Φ_{m} obeys Laplace's equation, $\boldsymbol{\nabla}^2 \Phi_{\mathsf{m}} = 0$.

Physical Applications

Although treating $\boldsymbol{H}$ as conservative has limited general utility because it requires $\boldsymbol{J} \equiv 0$, it is a method of choice for certain physical systems:

1. *Permanent magnets:* It is the primary method for calculating fields inside and outside of magnetized materials (like ferromagnets) where the magnetization $\boldsymbol{M}$ is known, but there are no free currents $\boldsymbol{J}$ driving the system.
2. *Magnetic circuits:* It is highly effective for fields in the air gaps of transformers or motors.

However, the topology of the current-free region does introduce a subtle caveat.

Topological Nuances

Consider the space around an infinite, straight, current-carrying wire. Outside the wire $\boldsymbol{J}_f = 0$, so $\boldsymbol{\nabla} \times \boldsymbol{H} = 0$ locally, but for a line integral along a closed loop entirely enclosing the wire, Ampère's law implies that $\oint \boldsymbol{H} \cdot d\boldsymbol{l} = I_{\mathsf{enc}} \neq 0$.

> Then, because the integral is non-zero, the scalar potential Φ_{m} becomes a *multivalued function*, changing by I_{enc} over each cycle of $\oint$.

Hence, even if $\boldsymbol{H}$ is conservative locally, a *uniquely defined global scalar potential* requires the manifold to be *simply connected (no holes)*.

Although physical magnetization distributions generally don't have discontinuities, it is sometimes useful to idealize a problem and treat $\boldsymbol{M}(\boldsymbol{x})$ as if it is discontinuous. We can then model a hard ferromagnet as having a volume V and a surface S, with $\boldsymbol{M}(\boldsymbol{x})$ finite inside but falling to zero at the surface S. Application of the divergence theorem to the surface indicates that in this idealization there is an effective magnetic surface-charge density given by [41]

$$\sigma_{\mathrm{M}} = \boldsymbol{n} \cdot \boldsymbol{M}, \tag{9.29}$$

where $\boldsymbol{n}$ is the outward normal at the surface. Then the first form of the potential (9.28) is modified to

$$\Phi_{\mathrm{M}}(\boldsymbol{x}) = -\frac{1}{4\pi} \int_V \frac{\boldsymbol{\nabla}' \cdot \boldsymbol{M}(\boldsymbol{x}')}{|\boldsymbol{x} - \boldsymbol{x}'|}\, d^3x + \frac{1}{4\pi} \oint_S \frac{\boldsymbol{n}' \cdot \boldsymbol{M}(\boldsymbol{x}')}{|\boldsymbol{x} - \boldsymbol{x}'|}\, da'. \tag{9.30}$$

An important special case is for uniform magnetization of the volume. Then $\boldsymbol{J}' = 0$ inside the volume and the first term of Eq. (9.30) vanishes, leaving only the surface term,

$$\Phi_{\mathrm{M}}(\boldsymbol{x}) = \frac{1}{4\pi} \oint_S \frac{\boldsymbol{n}' \cdot \boldsymbol{M}(\boldsymbol{x}')}{|\boldsymbol{x} - \boldsymbol{x}'|}\, da' = \frac{1}{4\pi} \oint_S \frac{\sigma(\boldsymbol{x}')}{|\boldsymbol{x} - \boldsymbol{x}'|}\, da', \tag{9.31}$$

where Eq. (9.29) was used.

Thus, introduction of a *sharp boundary* for the volume of a uniformly magnetized object induces an *effective magnetic surface-charge density* σ_{M} on the boundary that is given by Eq. (9.29).

Using the Magnetic Vector Potential: If we choose to satisfy $\boldsymbol{\nabla} \cdot \boldsymbol{B}$ automatically by introducing a vector potential $\boldsymbol{A}$ and defining the magnetic field by $\boldsymbol{B} = \boldsymbol{\nabla} \times \boldsymbol{A}$, then the first of Eqs. (9.12) is

$$\boldsymbol{\nabla} \times \boldsymbol{H} = \boldsymbol{\nabla} \times \left(\frac{1}{\mu_0} \boldsymbol{B} - \boldsymbol{M} \right) = 0, \tag{9.32}$$

which becomes upon introduction of $\boldsymbol{B} = \boldsymbol{\nabla} \times \boldsymbol{A}$,

$$\frac{1}{\mu_0} (\boldsymbol{\nabla} \times \boldsymbol{\nabla} \times \boldsymbol{A}) = \boldsymbol{\nabla} \times \boldsymbol{M},$$

and upon using the identity $\boldsymbol{\nabla} \times (\boldsymbol{\nabla} \times \boldsymbol{A}) = \boldsymbol{\nabla}(\boldsymbol{\nabla} \cdot \boldsymbol{A}) - \nabla^2 \boldsymbol{A}$ on the left side and Eq. (9.9) on the right side,

$$\boldsymbol{\nabla}(\boldsymbol{\nabla} \cdot \boldsymbol{A}) - \nabla^2 \boldsymbol{A} = \mu_0 \boldsymbol{J}_{\mathrm{M}}, \tag{9.33}$$

where $\boldsymbol{J}_{\mathrm{M}}$ is the effective magnetic current density defined in Eq. (9.9). Transforming to Coulomb gauge (8.37) by setting $\boldsymbol{\nabla} \cdot \boldsymbol{A} = 0$ then leads to a Poisson equation for the vector potential,

$$\nabla^2 \boldsymbol{A} = -\mu_0 \boldsymbol{J}_{\mathrm{M}}. \tag{9.34}$$

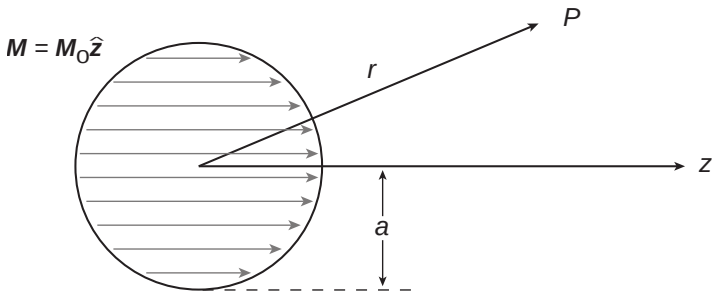

Fig. 9.3 A uniformly magnetized spherical ball of radius a, with a sharp surface and a surface magnetic charge density $\sigma_{\rm M}(\theta)$; $\boldsymbol{M} = \boldsymbol{M}_0\hat{\boldsymbol{z}}$ is parallel to the z axis, so that $\sigma_{\rm M} = \boldsymbol{n}\cdot\boldsymbol{M} = M_0\cos\theta$.

If there are no bounding surfaces, the solution is

$$\boldsymbol{A}(\boldsymbol{x}) = \frac{\mu_0}{4\pi}\int \frac{\boldsymbol{\nabla}'\times\boldsymbol{M}(\boldsymbol{x}')}{|\boldsymbol{x}-\boldsymbol{x}'|}\,d^3x \tag{9.35}$$

[compare Eq. (9.8) with $\boldsymbol{J}=0$]. If the magnetization is discontinuous (as in the uniformly magnetized sphere with sharp surface that is discussed in Section 9.3.4), it is necessary to add a surface integral to Eq. (9.28). For the case of $\boldsymbol{M}$ falling to zero at the surface S bounding the volume V, starting from Eq. (9.7) the proper generalization of Eq. (9.35) may be shown to be [41]

$$\boldsymbol{A}(\boldsymbol{x}) = \frac{\mu_0}{4\pi}\int_V \frac{\boldsymbol{\nabla}'\times\boldsymbol{M}(\boldsymbol{x}')}{|\boldsymbol{x}-\boldsymbol{x}'|}\,d^3x + \frac{\mu_0}{4\pi}\oint_S \frac{\boldsymbol{M}(\boldsymbol{x}')\times\boldsymbol{n}'}{|\boldsymbol{x}-\boldsymbol{x}'|}\,da'. \tag{9.36}$$

For the special case that the magnetization is constant over the volume V, the volume term is zero and only the second (surface integral) term can contribute in Eq. (9.36).

9.3.4 Example: Uniformly Magnetized Sphere

As an example of solving boundary problems in magnetostatics using the methods just discussed, let us consider a spherical ball with uniform permanent magnetization that has a sharp transition at the surface from magnetized to non-magnetized matter; Fig. 9.3 illustrates. We shall illustrate solutions using both the magnetic scalar potential method and the magnetic vector potential method.

Solution Using the Magnetic Scalar Potential: The sphere is uniformly magnetized, so there are no volume currents and the scalar magnetic potential method of Section 9.3.2 is applicable. As discussed in Section 9.3.3, there will be a surface charge $\sigma_{\rm M} = \boldsymbol{n}\cdot\boldsymbol{M}$ associated with the sharp transition from magnetized to un-magnetized material. Assuming that $\boldsymbol{M} = M_0\hat{\boldsymbol{z}}$ so that $\sigma_{\rm M} = \boldsymbol{n}\cdot\boldsymbol{M} = \boldsymbol{M}_0\cos\theta$ in spherical coordinates,

from Eq. (9.28) the scalar magnetic potential is

$$\Phi_{\rm M}(r,\theta) = \frac{1}{4\pi}\oint_S \frac{\sigma(\boldsymbol{x}')}{|\boldsymbol{x}-\boldsymbol{x}'|}\,da' = \frac{M_0 a^2}{4\pi}\int \frac{\cos\theta}{|\boldsymbol{x}-\boldsymbol{x}'|}\,d\Omega'.$$

Inserting the multipole expansion

$$\frac{1}{|\boldsymbol{x}-\boldsymbol{x}'|} = \sum_{l=0}^{\infty} \frac{r_<^l}{r_>^{l+1}}\,P_l(\cos\theta)$$

of Eq. (3.54), and using that $P_1(\cos\theta) = \cos\theta$ gives

$$\begin{aligned}\Phi_{\rm M}(r,\theta) &= \frac{M_0 a^2}{4\pi}\int \frac{P_1(\cos\theta)}{|\boldsymbol{x}-\boldsymbol{x}'|}\,d\Omega' \\ &= \frac{M_0 a^2}{4\pi}\sum_{l=0}^{\infty}\frac{r_<^l}{r_>^{l+1}}\int P_l(\cos\theta)P_1(\cos\theta)\,d\Omega' \\ &= \frac{1}{3}M_0 a^2\,\frac{r_<}{r_>^2}\,P_1(\cos\theta) = \frac{1}{3}M_0 a^2\,\frac{r_<}{r_>^2}\cos\theta, \end{aligned} \tag{9.37}$$

where the orthogonality condition of Eq. (4.39) has eliminated all terms in the sum except for $l=1$, and $r_<$ and $r_>$ are the smaller and larger of r and a, respectively.

Interior solution: Inside the sphere, $r_< = r$ and $r_> = a$, so the magnetic scalar potential is given by

$$\Phi_{\rm M}^{\rm in} = \frac{1}{3}M_0 r\cos\theta = \frac{1}{3}M_0 z.$$

Then from Eq. (9.23)

$$\boldsymbol{H}_{\rm in} = -\boldsymbol{\nabla}\Phi_{\rm M}^{\rm in} = -\frac{\partial}{\partial z}\left(\frac{1}{3}M_0 z\right)\hat{\boldsymbol{z}} = -\frac{1}{3}M_0\hat{\boldsymbol{z}} = -\frac{1}{3}\boldsymbol{M},$$

and from Eq. (9.11),

$$\boldsymbol{B}_{\rm in} = \mu_0(\boldsymbol{H}_{\rm in}+\boldsymbol{M}) = \mu_0\left(-\frac{1}{3}\boldsymbol{M}+\boldsymbol{M}\right) = \frac{2\mu_0}{3}\boldsymbol{M}.$$

Therefore, the interior solution is

$$\Phi_{\rm M}^{\rm in} = \frac{1}{3}M_0 z \qquad \boldsymbol{H}_{\rm in} = -\frac{1}{3}\boldsymbol{M} \qquad \boldsymbol{B}_{\rm in} = \frac{2\mu_0}{3}\boldsymbol{M}, \tag{9.38}$$

where we see that the fields are constant inside the sphere, with $\boldsymbol{B}$ parallel and $\boldsymbol{H}$ antiparallel to $\boldsymbol{M}$.

Exterior solution: For the exterior solution, $r_< = a$ and $r_> = r$, giving from Eq. (9.37) for the exterior potential,

$$\Phi_{\rm M}^{\rm out} = \frac{1}{3}M_0 a^3\frac{\cos\theta}{r^2}, \tag{9.39}$$

which may be recognized as a dipole potential with dipole moment

$$\boldsymbol{m} = \frac{4\pi a^3}{3}\boldsymbol{M}. \tag{9.40}$$

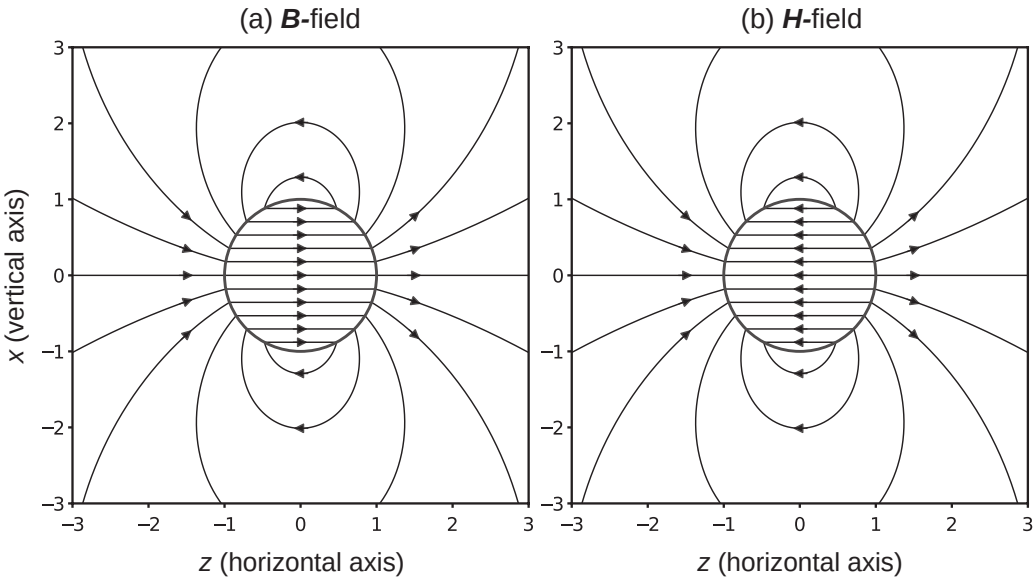

Fig. 9.4 Lines of $\boldsymbol{B}$ and $\boldsymbol{H}$ for a uniformly magnetized sphere having a sharp boundary.

Then, proceeding as above the exterior solution is

$$\boldsymbol{H}_{\text{out}} = -\boldsymbol{\nabla}\Phi_{\text{M}}^{\text{out}} = -\frac{1}{3}\frac{a^3}{r^3}\,\boldsymbol{M} \quad \boldsymbol{B}_{\text{out}} = \mu_0(\boldsymbol{H}+\boldsymbol{M}) = \left(\frac{3r^3-a^3}{3r^3}\right)\mu_0\,\boldsymbol{M}. \tag{9.41}$$

The $\boldsymbol{B}$ and $\boldsymbol{H}$ fields for the interior and exterior solutions are plotted in Fig. 9.4.

Physical interpretation: The $\boldsymbol{B}$ field is strictly solenoidal ($\boldsymbol{\nabla}\cdot\boldsymbol{B} = 0$ everywhere). Its field lines form continuous, unbroken loops. Conversely, the $\boldsymbol{H}$ field is conservative (that is irrotational), and can be described as the gradient of a scalar potential, similar to an electrostatic field in this current-free problem. The divergence $\boldsymbol{\nabla}\cdot\boldsymbol{H} = -\boldsymbol{\nabla}\cdot\boldsymbol{M} \equiv \rho_{\text{M}}$ acts as an effective *"magnetic charge density"* ρ_{M}. Recalling that the magnetization M in Fig. 9.3 points to the right in the $+z$ direction,

1. On the right of the sphere, $\boldsymbol{M}$ points outward, creating an *effective positive magnetic surface charge.*
2. On the left, it points inward and creates an *effective negative surface charge.*

Thus, the internal $\boldsymbol{H}$ field points *leftwards* (from positive to negative magnetic charge), strictly opposing the magnetization $\boldsymbol{M}$. This internal field is commonly called the *demagnetizing field.* [6]

[6] Although there is no evidence to date for free magnetic charge (no magnetic monopoles), it is common in quantum many-body systems for interactions to create collective states that behave effectively as a known or conjectured elementary particle. These states are termed "emergent", because they don't exist in the non-interacting many-body wavefunction, but they *emerge* when interactions are turned on. For example, in certain condensed matter systems excitations having the character of magnetic monopoles have been identified, and the analog of a conjectured elementary particle called a *Majorana fermion* has been sought eagerly in condensed matter (for its intrinsic interest, but also because it could enable some attractive approaches to quantum computing). Here we see that the there is no free charge (either electric or magnetic), but the

The preceding solution using the magnetic scalar potential formalism is applicable only if $\boldsymbol{J} = 0$. However, the vector potential method is applicable whether a free current is present or not, so let's now rederive the preceding result using the vector potential method.

Solution Using the Vector Potential: The vector potential and Eq. (9.36) can be used to obtain the solution for the problem posed in Fig. 9.3. The magnetization is assumed to be uniform inside the sphere, so that the volume current $\boldsymbol{J}_{\mathrm{M}} = 0$ and the first (volume) term in Eq. (9.36) makes no contribution. However, there is a surface charge because of the sharp boundary on the magnetized matter so the second term in Eq. (9.36) will be non-zero and

$$\boldsymbol{A}(\boldsymbol{x}) = \frac{\mu_0}{4\pi} \oint_S \frac{\boldsymbol{M}(\boldsymbol{x}') \times \boldsymbol{n}'}{|\boldsymbol{x} - \boldsymbol{x}'|}\, da'. \tag{9.42}$$

Using the notation $(\boldsymbol{\epsilon}_1, \boldsymbol{\epsilon}_2, \boldsymbol{\epsilon}_3) = (\hat{\boldsymbol{x}}, \hat{\boldsymbol{y}}, \hat{\boldsymbol{z}})$ for cartesian basis vectors and $(\boldsymbol{\epsilon}_r, \boldsymbol{\epsilon}_\theta, \boldsymbol{\epsilon}_\phi) = (\hat{\boldsymbol{r}}, \hat{\boldsymbol{\theta}}, \hat{\boldsymbol{\phi}})$ for spherical basis vectors, since $\boldsymbol{M} = M_0 \boldsymbol{\epsilon}_3$ we have

$$\boldsymbol{M}(\boldsymbol{x}') \times \boldsymbol{n}' = M_0 \sin\theta' \boldsymbol{\epsilon}_\phi = M_0 \sin\theta' (-\sin\phi \boldsymbol{\epsilon}_1 + \cos\phi' \boldsymbol{\epsilon}_2),$$

where Eq. (A.42) was used. The problem has azimuthal (ϕ) symmetry about the z-axis. If the observing point P is chosen to lie in the x-y plane, then only the y component of $\boldsymbol{M} \times \boldsymbol{n}$ survives integration over the azimuth so $(-\sin\phi' \boldsymbol{\epsilon}_1 + \cos\phi' \boldsymbol{\epsilon}_2) \to \cos\phi' \boldsymbol{\epsilon}_2$, which gives an azimuthal component of the vector potential

$$A_\phi = \frac{\mu_0}{4\pi} M_0 a^2 \int \frac{\sin\theta' \cos\phi'}{|\boldsymbol{x} - \boldsymbol{x}'|}\, d\Omega', \tag{9.43}$$

where the components of $\boldsymbol{x}'$ are $(r' = a, \theta', \phi')$, confining the integration to the surface of the sphere. Since

$$Y_{11}(\theta', \phi') = -\sqrt{\frac{3}{8\pi}} \sin\theta' e^{i\phi'} = -\sqrt{\frac{3}{8\pi}} \sin\theta' (\cos\phi' + i \sin\phi'),$$

we may write

$$\sin\theta' \cos\phi' = -\sqrt{\frac{8\pi}{3}}\, \mathrm{Re}[Y_{11}(\theta', \phi')],$$

where $\mathrm{Re}(x)$ denotes the real part of x. Thus,

$$A_\phi = -\sqrt{\frac{3}{8\pi}} \frac{\mu_0}{4\pi} M_0 a^2 \int \frac{\mathrm{Re}[Y_{11}(\theta', \phi')]}{|\boldsymbol{x} - \boldsymbol{x}'|}\, d\Omega'.$$

Then if the denominator is expanded using Eq. (3.57),

$$\frac{1}{|\boldsymbol{x} - \boldsymbol{x}'|} = 4\pi \sum_{l=0}^{\infty} \sum_{m=-l}^{l} \frac{1}{2l+1} \frac{r_<^l}{r_>^{l+1}} Y_{lm}^*(\theta', \phi') Y_{lm}(\theta, \phi),$$

magnetic polarization has created *bound currents* that mimic a magnetic dipole consisting of a positive magnetic charge and a negative magnetic charge, separated by some distance (the magnetic analog of an electric dipole). None of these examples violate the Maxwell equations because they correspond to emergent states, not free elementary particles.

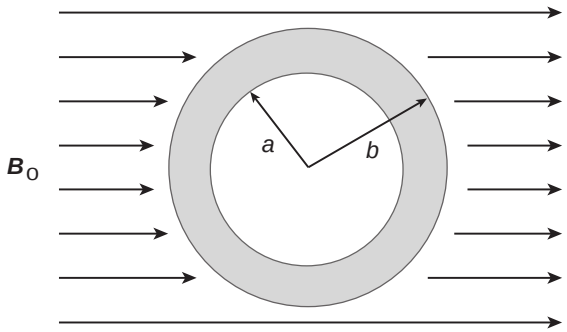

Fig. 9.5 A shell of material with permeability μ is placed in a previously uniform magnetic field $\boldsymbol{B}_0$. If the shell contains highly permeable material, the cavity inside the shell is shielded strongly from the exterior magnetic field.

the spherical harmonic orthogonality relation (3.62),

$$\int_0^{2\pi} d\phi \int_0^{\pi} Y^*_{l'm'}(\theta,\phi) Y_{lm}(\theta,\phi) \sin\theta d\theta = \delta_{l'l}\delta_{m'm},$$

ensures that only the $l = 1, m = 1$ term survives the summation and the vector potential is

$$A_\phi(\boldsymbol{x}) = \frac{\mu_0}{3} M_0 a^2 \left(\frac{r_<}{r_>^2}\right) \sin\theta. \tag{9.44}$$

For the inside solution, $r_< = r$ and $r_> = a$, so

$$A^{\text{in}}_\phi(\boldsymbol{x}) = \frac{\mu_0}{3} M_0 r \sin\theta. \tag{9.45}$$

You are asked to calculate the corresponding $\boldsymbol{B}$ and $\boldsymbol{H}$ fields for the interior of the sphere in Problem 9.1.

9.3.5 Example: A Shell of Permeable Matter

By placing a shell of permeable matter in a magnetic field, it is possible to shield the interior of the shell from the magnetic field. Consider Fig. 9.5, where the shell contains material of permeability μ. Let us find the fields $\boldsymbol{B}$ and $\boldsymbol{H}$ for this arrangement. There are no free currents so the magnetic scalar potential method of Section 9.3.2 is applicable. From Eq. (9.23), $\boldsymbol{H} = -\boldsymbol{\nabla}\Phi_{\text{M}}$, and since $\boldsymbol{B} = \mu\boldsymbol{H}$, the equation $\boldsymbol{\nabla}\cdot\boldsymbol{B} = 0$ is replaced by $\boldsymbol{\nabla}\cdot\boldsymbol{H} = 0$ in all regions. Therefore, the magnetic potential Φ_{M} satisfies the Laplace equation everywhere, and the problem reduces to solving the Laplace equation subject to the boundary conditions of Eq. (9.19) at $r = a$ and $r = b$.

Exterior solution: If $r > b$, the potential is of the form

$$\Phi_{\text{M}} = -H_0 r\cos\theta + \sum_{l=0}^{\infty} \frac{\alpha_l}{r^{l+1}} P_l(\cos\theta) \qquad (r > b), \tag{9.46}$$

which gives a uniform field $\Phi_{\text{M}} = \boldsymbol{H}_0$ at large distance.

Interior solution: By similar considerations, the potential must take the form

$$\Phi_{\rm M} = \sum_{l=0}^{\infty} \left(\beta_l r^l + \gamma_l \frac{1}{r^{l+1}} \right) P_l(\cos\theta). \qquad (a < r < b), \tag{9.47a}$$

$$\Phi_{\rm M} = \sum_{l=0}^{\infty} \delta_l r^l P_l(\cos\theta) \qquad (r < a). \tag{9.47b}$$

in interior regions.

Matching boundary conditions: The boundary conditions at $r = a$ and $r = b$ require the components H_θ and B_r to be continuous, which implies that

$$\frac{\partial \Phi_{\rm M}}{\partial \theta}(b_+) = \frac{\partial \Phi_{\rm M}}{\partial \theta}(b_-) \qquad \frac{\partial \Phi_{\rm M}}{\partial \theta}(a_+) = \frac{\partial \Phi_{\rm M}}{\partial \theta}(a_-), \tag{9.48a}$$

$$\mu_0 \frac{\partial \Phi_{\rm M}}{\partial r}(b_+) = \mu \frac{\partial \Phi_{\rm M}}{\partial r}(b_-) \qquad \mu \frac{\partial \Phi_{\rm M}}{\partial r}(a_+) = \mu_0 \frac{\partial \Phi_{\rm M}}{\partial r}(a_-), \tag{9.48b}$$

where the notation b_+ means the limit $r \to b$ approached from $r > b$ and the notation b_- means means the limit $r \to b$ approached from $r < b$, with a similar convention for $a_\pm$. The four conditions (9.48) determine the unknown constants in Eqs. (9.46) and (9.47). One finds that all coefficients with $l \neq 1$ vanish and the $l = 1$ coefficients satisfy the simultaneous equations

$$\begin{gathered} \alpha_1 - b^3\beta_1 - \gamma_1 = b^3 H_0, \\ 2\alpha_1 + \mu' b^3 \beta_1 - 2\mu'\gamma_1 = -b^3 H_0, \\ a^3\beta_1 + \gamma_1 - a^3\delta_1 = 0, \\ \mu' a^3 \beta_1 - 2\mu'\gamma_1 - a^3\delta_1 = 0, \end{gathered} \tag{9.49}$$

where $\mu' \equiv \mu/\mu_0$, which may be solved simultaneously for the unknown coefficients. For example, the solution of Eqs. (9.49) for α_1 and δ_1 are [41],

$$\begin{aligned} \alpha_1 &= \left(\frac{(2\mu'+1)(\mu'-1)}{(2\mu'+1)(\mu'+2) - 2\,\dfrac{a^3}{b^3}\,(\mu'-1)^2} \right) (b^3 - a^3) H_0, \\ \delta_1 &= -\left(\frac{9\mu'}{(2\mu'+1)(\mu'+2) - 2\,\dfrac{a^3}{b^3}\,(\mu'-1)^2} \right) H_0. \end{aligned} \tag{9.50}$$

The corresponding magnetic field lines are shown in Fig. 9.6. For this solution the potential outside the shell corresponds to the original uniform field $\boldsymbol{H}_0$ plus a dipole field with dipole moment α_1 parallel to $\boldsymbol{H}_0$. In the cavity inside the shell there is a uniform field parallel to $\boldsymbol{H}_0$ and equal in magnitude to $-\delta_1$. If $\mu \gg \mu_0$, the dipole moment α_1 and the inner field $-\delta_1$ tend to

$$\alpha_1 \longrightarrow b^3 H_0 \qquad -\delta_1 \longrightarrow \frac{9\mu_0}{2\mu(1 - a^3/b^3)} H_0. \tag{9.51}$$

Thus the field in the inner cavity of Fig. 9.6 is proportional to μ^{-1}, and a shield made of

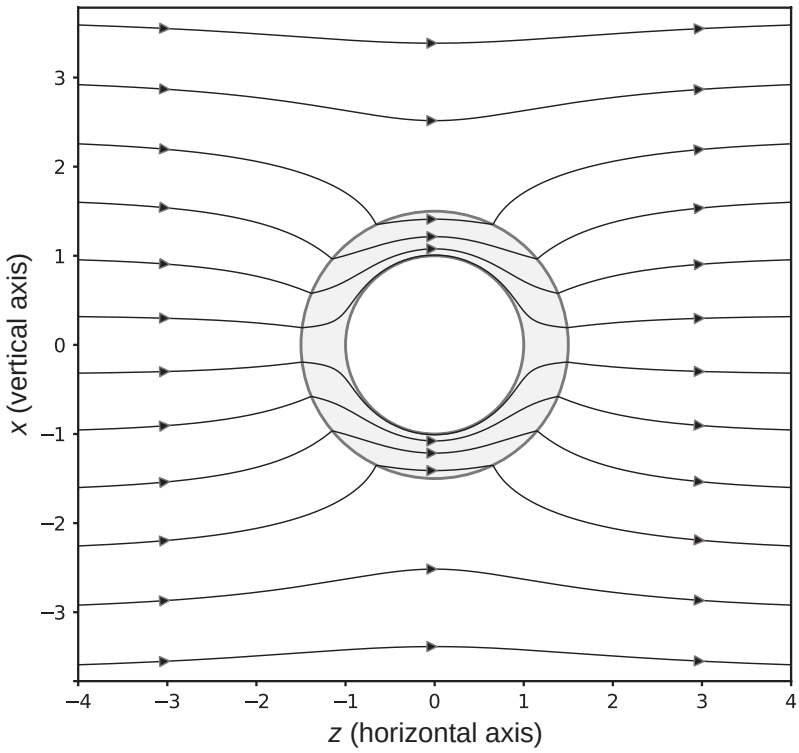

Fig. 9.6 The magnetic shielding effect of a shell containing highly permeable material ($\mu = 1000\mu_0$). Lines for the magnetic field $\boldsymbol{B}$ are shown. Note the absence of field lines in the cavity inside the shell, indicating strongly suppressed magnetic field there.

highly permeable material causes a large reduction of the magnetic field inside the cavity. Figure 9.6 illustrates that even thin shells of material with $\mu/\mu_0 \sim 10^3 - 10^6$ can greatly reduce the strength of an applied magnetic field inside the shell.

Background and Further Reading

The presentation in this chapter has followed Jackson [41] rather closely. See also Garg [31], Chaichian et al [23], and Zangwill [77].

Problems

9.1 Find the fields $\boldsymbol{B}_{\text{in}}$ and $\boldsymbol{H}_{\text{in}}$ corresponding to the vector potential of Eq. (9.45),

$$A_\phi^{\text{in}}(\boldsymbol{x}) = \frac{\mu_0}{3} M_0 r \sin\theta,$$

inside the sphere of Fig. 9.3.

9.2 Classical magnetism can be viewed as resulting from current loops in matter. Analyze the magnetic forces acting on a rectangular current loop carrying a steady current I in a uniform magnetic field $\boldsymbol{B}$. Show that the total magnetic force acting on the loop is

$$\boldsymbol{F}_{\text{M}} = I \oint (d\boldsymbol{s} \times \boldsymbol{B}),$$

and that the total force vanishes for a loop carrying a steady current in a uniform magnetic field. ***

9.3 In Problem 9.2 and Section 8.2 we showed that there is no net force acting on a loop carrying a steady current that is immersed in a uniform magnetic field. Show that there *is however a net torque* acting on current loops in uniform magnetic fields, and that the net effect of this torque is to align magnetic dipole moments with the applied magnetic field by aligning the normal vector of the plane of current loops with $\boldsymbol{B}$.

9.4 Determine the magnetic dipole moment $\boldsymbol{m}$ of the current loop in the following figure,

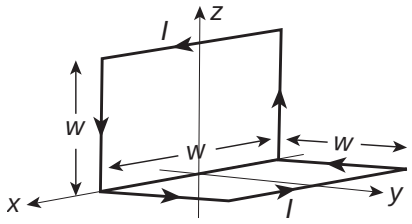

where the current is I and all sides are of equal width w.

9.5 Suppose a non-conducting thick spherical shell with inner radius a and outer radius b that has a uniform charge density ρ embedded in it. The shell is then spun at constant angular velocity ω about the z axis, creating a steady volume current density $\boldsymbol{J}(r,\theta) = kr\sin\theta\hat{\boldsymbol{\phi}}$ within the shell ($a \le r \le b$), where $k = \rho\omega$ is assumed constant. Furthermore, no currents are present in the central cavity ($r < a$) or in the exterior region ($r > b$).

a. Solve the vector Poisson equation to determine the magnetic vector potential $\boldsymbol{A}(r,\theta)$ everywhere in space.

b. Calculate the magnetic field $\boldsymbol{B}$ inside the central cavity ($r < a$), inside the shell ($a \le r \le b$), and outside the shell ($r > b$). Discuss the physical nature of the fields in each region.

Hint: Evaluate the vector potential using the Coulomb gauge (require that $\boldsymbol{A}$ satisfies the condition $\boldsymbol{\nabla} \cdot \boldsymbol{A} = 0$).

9.6 A sphere of radius a carries a uniform permanent magnetization $\boldsymbol{M} = M_0 \hat{\boldsymbol{z}}$ and we assume that there are no free currents present anywhere in the domain of the problem.

a. Using the magnetic scalar potential Φ_{M}, determine the magnetic fields $\boldsymbol{H}$ and $\boldsymbol{B}$ both inside and outside the sphere.
b. Discuss the physical difference between the behavior of the $\boldsymbol{B}$ and $\boldsymbol{H}$ fields at the boundary of the sphere.

Numerical and GenAI Problems

10 Dynamical Charges and Currents

In the discussion to this point we have considered primarily static charges (no relative motion) as sources of electric fields and steady-state charge currents (no change in time) as the source of magnetic fields. However, many important electromagnetic phenomena involve the motion of charges and/or non-steady electrical currents. Hans Christian Ørsted (1777-1827) discovered the magnetic effect of the electric current, establishing the first connection between electric and magnetic phenomena, and André–Marie Ampère (1775-1827) extended that work, finding in 1823 the circuit law between electric current passing through a loop and magnetic field around the loop and establishing a formula describing the interaction of two currents. However, it was Michael Faraday who performed the most quantitative experiments on time-dependent electric and magnetic field, and their relationship, beginning in 1831. As we shall see, these experiments verified that a time-varying electric field produces a magnetic field and a time-varying magnetic field produces an electric field, and paved the way for the understanding of classical electromagnetism that was elucidated fully by Maxwell.

10.1 Faraday and the Law of Induction

Faraday extended the earlier insights of Ørsted, Biot, Savart, and Ampère by concentrating on time-varying electric and magnetic phemomena. In a nutshell, Faraday's essential observations were that

1. a transient current is produced in a test circuit if *a steady current in a nearby circuit is turned off;*
2. a transient current is also produced in a test circuit if *a nearby circuit with a steady current is moved* relative to the first circuit;
3. a transient current is produced in a test circuit if *a permanent magnet is moved into or out of the circuit.*

In summary, Faraday established experimentally that a current flows in a test circuit if a current in a nearby circuit changes over time, or if the two circuits move with respect to each other, or if a magnetic field varies near the test circuit. Faraday interpreted these results as originating in a *changing magnetic flux* that

1. is produced an electric field around the test circuit,
2. which leads to an *electromotive force* $\mathcal{E}$ (EMF) that drives a current in the test circuit governed by Ohm's law (see Section 7.3.1).

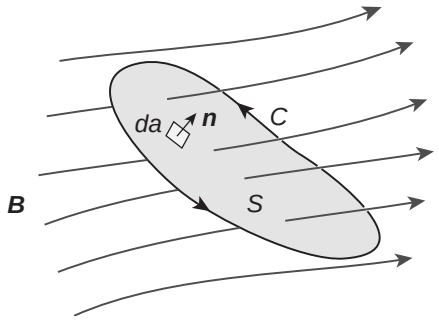

Fig. 10.1 Magnetic flux through a circuit C bounding a surface S, with a unit normal to the surface $\boldsymbol{n}$ and surface element da.

Thus, Faraday's results and his interpretation of those results represent the first steps in the unification of electricity and magnetism into a single theory of *electromagnetism*.

> Faraday's unified principle of induction—that motion and changing magnetic fields can be converted into electrical current—isn't just a historical curiosity. It remains the fundamental operating principle behind nearly all generation of electricity, the power grid, and modern electrical motors.

Faraday was a gifted experimentalist with incisive intuition, but he had little formal training in the sciences or in mathematics. Maxwell, Heaviside, and others are largely responsible for expressing Faraday's brilliant insights and measurements in more mathematical language (concise enough to fit on tee-shirts). Let us now look at a mathematical formulation of Faraday's results.

10.2 Mathematical Content of Faraday's Results

Consider Fig. 10.1, where the magnetic flux[1] passing through the area enclosed by the circuit indicated by the contour C is

$$\mathcal{F}_{\mathrm{M}} = \int_S \boldsymbol{B} \cdot \boldsymbol{n}\, da \tag{10.1}$$

and the electromotive force $\mathcal{E}$ around the circuit that causes a current flow according to Ohm's law is

$$\mathcal{E} = \oint_C \boldsymbol{E}' \cdot d\boldsymbol{l}, \tag{10.2}$$

[1] Faraday originally envisioned invisible "lines of force" radiating from magnets and currents. In the hands of more mathematically minded physicists like Maxwell, these notions became our modern concept of a field. Magnetic flux may then be interpreted physically as a measure of the total number of what we would now call (magnetic) field lines that pierced the area of a wire loop, as suggested by Fig. 10.1.

where $\boldsymbol{E}'$ is the electric field at element $d\boldsymbol{l}$ of the circuit C. All of Faraday's observations listed above may be explained by the *Faraday flux rule*

$$\mathcal{E} = -k\,\frac{d\mathcal{F}_{\rm M}}{dt}, \tag{10.3}$$

between the rate of change of the magnetic flux $d\mathcal{F}_{\rm M}/dt$ and the EMF $\mathcal{E}$, where k is a constant of proportionality that can be determined by requiring Galilean invariance at low velocities.[2] This indicates that $k = 1$ in SI units (and $k = c^{-1}$ in Gaussian units). Therefore, in SI units

$$\mathcal{E} = -\frac{d\mathcal{F}_{\rm M}}{dt}, \tag{10.4}$$

where the units of flux and EMF are

$$[\mathcal{F}_{\rm M}] = \text{ 1 weber (Wb) = 1 volt-second} \qquad [\mathcal{E}] = \text{ volt (V)} \tag{10.5}$$

and where the sign in Eq. (10.4) is specified by *Lenz's law*.[3]

> ***Lenz's law:*** The induced current and corresponding magnetic field are in a direction so as to oppose changing the flux through the circuit.

Combining Eq. (10.4) with Eqs. (10.1) and (10.2) gives Faraday's law in integral form,

$$\oint_C \boldsymbol{E}' \cdot d\boldsymbol{l} = -\frac{d}{dt}\int_S \boldsymbol{B}\cdot\boldsymbol{n}\,da \qquad \text{(Faraday's law)}, \tag{10.6}$$

indicating that the induced EMF is proportional to the *total time derivative* of the magnetic flux.[4] Notice that this reduces to the result $\oint_c \boldsymbol{E}\cdot d\boldsymbol{l} = 0$ of Eq. (2.26) for the static case with $d\boldsymbol{B}/dt = 0$. Equation (10.6) represents a form of Faraday's law with broad implications. If we view C as a geometrical closed path not necessarily coincident with an electrical circuit, Eq. (10.6) may be viewed as a relationship among the fields $\boldsymbol{B}$ and $\boldsymbol{E}'$.

If the circuit C is moving with some velocity, the total time derivative must take that motion into account, since the flux through the circuit can change for two reasons:

1. the flux varies with time at a given point, or
2. translation of the circuit changes the location of the circuit in an external field that may have a spatial dependence.

This can be taken into account by computing the *convective derivative*,

$$\frac{d}{dt} = \frac{\partial}{\partial t} + \boldsymbol{v}\cdot\boldsymbol{\nabla}, \tag{10.7}$$

[2] As we shall see in Chs. 17-18, the Maxwell equations are covariant under Lorentz transformations, not Galilean transformations. But Lorentz transformations reduce to Galilean transformations in the limit $v \ll c$, so requiring Galilean invariance for low velocities is a legitimate way to determine the constant k.

[3] Lenz's law can be stated in more picturesque form: "Nature abhors a change in flux" [33]. For a dramatic example of just how much Nature detests changes in magnetic flux, see Problem 10.1.

[4] The flux can be changed by changing the magnetic field, or the shape, position, or orientation of the circuit. The total time derivative d/dt appearing in Eq. (10.6) accounts for all such possibilities. Note that $\boldsymbol{E}'$ is the electric field at $d\boldsymbol{l}$ *in the coordinate system where* $d\boldsymbol{l}$ *is at rest.*

where $\boldsymbol{v}$ is the velocity and the partial derivative in the first term on the right side has the usual meaning that it is the derivative with respect to a variable (time in this case) with all other variables held constant. Then the total time derivative of the moving circuit is [41],

$$\frac{d}{dt}\int_S \boldsymbol{B}\cdot\boldsymbol{n}\,da = \int_S \frac{\partial \boldsymbol{B}}{\partial t}\cdot\boldsymbol{n}\,da + \oint_C (\boldsymbol{B}\times\boldsymbol{v})\cdot d\boldsymbol{l}, \tag{10.8}$$

which can be used to write Eq. (10.6) in the form

$$\oint_C [\boldsymbol{E}' - (\boldsymbol{v}\times\boldsymbol{B})]\cdot d\boldsymbol{l} = -\int_S \frac{\partial \boldsymbol{B}}{\partial t}\cdot\boldsymbol{n}\,da. \tag{10.9}$$

This is Faraday's law applied to the moving circuit C, but if we think of the circuit C and surface S being instantaneously at a certain point, then application of Eq. (10.6) to that circuit at fixed location gives,

$$\oint_C \boldsymbol{E}\cdot d\boldsymbol{l} = -\int_S \frac{\partial \boldsymbol{B}}{\partial t}\cdot\boldsymbol{n}\,da, \tag{10.10}$$

where $\boldsymbol{E}$ is now the electric field in the laboratory frame. Galilean invariance (valid at low velocities) then requires the left sides of Eqs. (10.9) and (10.10) to be equivalent.

If the circuit is held fixed in a reference frame so that the electric and magnetic fields are defined in the same frame, Faraday's law (10.6) in integral form can be transformed into a differential equation. From Stoke's theorem,

$$\oint_C \boldsymbol{E}'\cdot d\boldsymbol{l} = \int_S (\boldsymbol{\nabla}\times\boldsymbol{E}')\cdot\boldsymbol{n}\,da,$$

and Eq. (10.6) may be written as

$$\int_S \left(\boldsymbol{\nabla}\times\boldsymbol{E} + \frac{\partial \boldsymbol{B}}{\partial t}\right)\cdot\boldsymbol{n}\,da = 0.$$

But the circuit C and surface S are arbitrary, so the expression in parentheses must vanish identically, giving

$$\boldsymbol{\nabla}\times\boldsymbol{E} + \frac{\partial \boldsymbol{B}}{\partial t} = 0 \qquad \text{(Faraday's law)}, \tag{10.11}$$

which is Faraday's law (1.1b) in differential form. Note that this is the time-dependent generalization of $\boldsymbol{\nabla}\times\boldsymbol{E} = 0$ from Eq. (2.27) in electrostatics. In a static system the curl of $\boldsymbol{E}$ vanishes but that is no longer true in the presence of a time-dependent magnetic field.

10.2.1 Quasistatic Approximations

It is often possible to treat a time-varying electromagnetic field in a *quasistatic approximation*, where the system simplifies because part of the time dependence is ignored, which usually is easier to solve than the full time-dependent problem.

Separation of Scales: A quasistatic approximation is a perturbative expansion of the Maxwell equations that decouples the electric and magnetic fields by formally taking the speed of light $c \to \infty$. It is valid when the characteristic timescale τ on which sources are varying is much larger than the electromagnetic transit time over the characteristic length scale of the system, L. If the transit time is $\tau_{\text{em}} = L/c$, the quasistatic regime requires

$$\tau \gg \frac{L}{c} \quad \text{or equivalently} \quad \omega \ll \frac{c}{L} \tag{10.12}$$

where $\omega \sim 1/\tau$ is the characteristic frequency of the system. In this limit, electromagnetic retardation effects are negligible.[5] The fields effectively propagate instantaneously, so that the spatial distribution of the fields at any moment is determined by the configuration of the sources at that same moment. But the sources are time-dependent so the fields are also time-dependent; hence the designation "quasistatic". This approximation reduces the dynamic Maxwell equations to a form more similar to electrostatics or magnetostatics.

Expansion Parameter: To formalize the preceding ideas, Maxwell's equations can be expanded in terms of a dimensionless small parameter $\alpha = \omega L/c$. The full Maxwell equations couple $\boldsymbol{E}$ and $\boldsymbol{B}$ through both

- the *displacement current*, proportional to $\partial \boldsymbol{E}/\partial t$, and
- *Faraday induction*, proportional to $\partial \boldsymbol{B}/\partial t$.

Depending on the physical nature of the sources and energy distribution in the system, the formulation splits naturally into two distinct Galilean (that is, $v \ll c$) limits: the *Electro-Quasistatic (EQS)* limit and the *Magneto-Quasistatic (MQS)* limit.

The Electro-Quasistatic Limit: The EQS limit applies when the system is driven primarily by time-varying charge distributions (ρ) and high voltages. Then the electric energy density greatly exceeds the magnetic energy density, $\epsilon_0 E^2 \gg \mu_0^{-1} B^2$, inductive effects may be ignored, charge relaxation is fast, and general capacitive electric-field effects dominate.[6] The magnetic induction term in Faraday's law is of order α^2 relative to the electric field and may be discarded at zeroth order. Then the governing equations reduce to

$$\boldsymbol{\nabla} \cdot \boldsymbol{D} = \rho \qquad \boldsymbol{\nabla} \times \boldsymbol{E} \approx 0. \tag{10.13}$$

Because the curl of $\boldsymbol{E}$ is zero, the electric field can be expressed using only a scalar potential, $\boldsymbol{E} = -\boldsymbol{\nabla}\Phi$, which satisfies an instantaneous Poisson equation: $\nabla^2 \Phi = -\rho/\epsilon$. The displacement current $\partial \boldsymbol{D}/\partial t$ and any small conduction currents $\boldsymbol{J}$ are retained to

[5] *Retardation effect* is jargon for a property of the electromagnetic field that depends on the observation that, because of causality and the finite speed of light, a signal detected at some time t was emitted at an earlier time (the retarded time) given by Eq. (11.46). See Section 11.4.2.

[6] A *capacitive effect* refers generically to the capability of a system of conductors to store electric charge and energy in an electric field when a potential difference (voltage) is applied. This causes the system to oppose sudden changes in voltage, acting as a temporary reservoir of electric energy. An *inductive effect* refers generically to the generation of electric fields by time-varying magnetic fields in Faraday's law ($\partial \boldsymbol{B}/\partial t$), typically while neglecting the reciprocal effect of displacement currents ($\partial \boldsymbol{D}/\partial t$) in Ampère's law.

compute the small, first-order magnetic field via Ampère's law,

$$\boldsymbol{\nabla} \times \boldsymbol{H} = \boldsymbol{J} + \frac{\partial \boldsymbol{D}}{\partial t}.$$

However, this induced $\boldsymbol{H}$ does not feed back into $\boldsymbol{E}$.

The Magneto-Quasistatic Limit: The MQS limit applies when the magnetic energy density greatly exceeds the electric energy density ($\mu_0^{-1} B^2 \gg \epsilon_0 E^2$), for example if the system is primarily driven by large, time-varying currents $\boldsymbol{J}$. Inductive effects dominate, magnetic diffusion is fast,[7] and the system is typically near charge neutrality ($\rho \approx 0$). The displacement current in the Ampère–Maxwell law is of order α^2 relative to the conduction current and may be discarded at zeroth order, leaving as the governing equations,

$$\boldsymbol{\nabla} \cdot \boldsymbol{B} = 0 \qquad \boldsymbol{\nabla} \times \boldsymbol{H} \approx \boldsymbol{J}. \tag{10.14}$$

The magnetic field is determined instantaneously by the Biot–Savart law, and Faraday's law is retained fully to calculate the induced electric field,

$$\boldsymbol{\nabla} \times \boldsymbol{E} = -\frac{\partial \boldsymbol{B}}{\partial t}. \tag{10.15}$$

This $\boldsymbol{E}$ field drives eddy currents in conductors, but its associated displacement current is too weak to feed back into generating more $\boldsymbol{B}$.

Quasistatic Approximation in Coulomb Gauge: In Coulomb gauge ($\boldsymbol{\nabla} \cdot \boldsymbol{A} = 0$), the exact equations for the scalar potential Φ and vector potential $\boldsymbol{A}$ are

$$\nabla^2 \Phi = -\frac{\rho}{\epsilon_0} \tag{10.16a}$$

$$\nabla^2 \boldsymbol{A} - \frac{\partial^2 \boldsymbol{A}}{\partial t^2} = -\mu_0 \boldsymbol{J} + \frac{1}{c^2} \boldsymbol{\nabla} \left(\frac{\partial \Phi}{\partial t} \right) \tag{10.16b}$$

The scalar potential Φ is always instantaneous in Coulomb gauge (see Section 11.3.2 and Box 11.3), so it always fulfills the quasistatic conditions; thus we impose the quasistatic approximation on the vector potential by taking the formal limit $c \to \infty$. This eliminates the retardation term $(1/c^2)\partial^2 \boldsymbol{A}/\partial t^2$ and the last term on the right side in Eq. (10.16b). In the MQS limit, the transverse part of the current $\boldsymbol{J}$ dominates, yielding an instantaneous vector potential $\nabla^2 \boldsymbol{A} \approx -\mu_0 \boldsymbol{J}$. In the EQS limit, the current $\boldsymbol{J}$ is extremely small and $\boldsymbol{A}$ is negligible or computed purely as a first-order correction, leaving the physics dominated by the instantaneous scalar potential Φ. Table 10.1 summarizes the regimes of the quasistatic approximation in electrodynamics.

10.2.2 Sources of EMF and Special Relativity

The Faraday flux rule (10.2) states that the electromotive force $\mathcal{E}$ around a closed conducting loop is equal to the negative rate of change of the magnetic flux through that loop, but this accounts for two entirely different physical mechanisms for generating an EMF.

[7] Magnetic diffusion refers to the process by which a magnetic field penetrates into, or decays within, an electrically conducting medium. This phenomenon is the opposite of the "frozen-in" magnetic field behavior seen in perfect conductors or perfectly conducting fluids (as in ideal magnetohydrodynamics), where the field lines move together with the material.

Table 10.1 Summary of quasistatic regimes in electrodynamics

Feature	Electro-Quasistatic (EQS)	Magneto-Quasistatic (MQS)
Dominant source	Charge density $\rho(t)$	Current density $\boldsymbol{J}(t)$
Dominant field	Electric ($\boldsymbol{E}$)	Magnetic ($\boldsymbol{B}$)
Neglected term	Magnetic induction ($\partial\boldsymbol{B}/\partial t$)	Displacement current ($\partial\boldsymbol{D}/\partial t$)
Physical applications	RC circuits, dielectrics, plasmas, microfluids	RL circuits, transformers, eddy currents, magnetohydrodynamics

1. *Motional EMF:* This occurs when a circuit or conductor moves through a static magnetic field. As the wire moves through space, the mobile electrons inside the conductor are dragged along with it. Because they are moving through a magnetic field, these charges experience the magnetic component of the Lorentz force, which pushes the electrons along the length of the wire, leading to a separation of charge that drives a current.

2. *Transformer EMF:* This occurs when the conducting loop remains stationary, but the magnetic flux through it changes over time. The charges in the loop are not initially moving, meaning that the magnetic Lorentz force cannot be responsible for pushing them. Instead, by Faraday's law a changing magnetic field induces a circulating, non-conservative electric field in space, which exerts an electric force on the charges, driving the current around the loop.

That these two very different physical processes are both governed by the same flux rule (10.3) constituted a major conceptual puzzle in classical physics. Maxwell recognized this dual nature in 1861 and provided separate physical explanations for each case.

Decades later, Einstein noted that the amount of induced current depends entirely on the *relative motion* between the magnet and the conductor, but classical theory uses different explanations (motional EMF vs. transformer EMF) depending on the subjective choice of which object is "moving" and which is "stationary". As will be explained in Ch. 18, Einstein recognized that this conundrum could be resolved only if whether one saw an electric or magnetic field depended on the inertial frame of the observer. This insight into Faraday's law suggested that there is no "preferred" stationary frame (no luminiferous aether), which provided a key foundational motivation for Einstein in developing his special theory of relativity.

As we shall discuss in Section 18.8, special relativity shows explicitly that, because of Lorentz contraction, electricity and magnetism are two sides of the same coin: a field that looks magnetic in the inertial frame of one observer may be seen as electric or some mixture of electric and magnetic in the inertial frame of another observer. This is contrary to our low-velocity experience (where relativity has negligible effect) that electric and magnetic forces differ fundamentally in their phenomenology.

10.3 Electromagnetic Induction

10.3.1 Self-Inductance

10.3.2 Mutual Inductance

Background and Further Reading

See Griffith [33] and Tong [72] for an introduction, and Garg [31] and Zangwill [77] for more advanced discussions.

Problems

10.1 Consider a metal ring placed on top of a strong solenoid (enhanced by an iron core), as illustrated in the following figure.

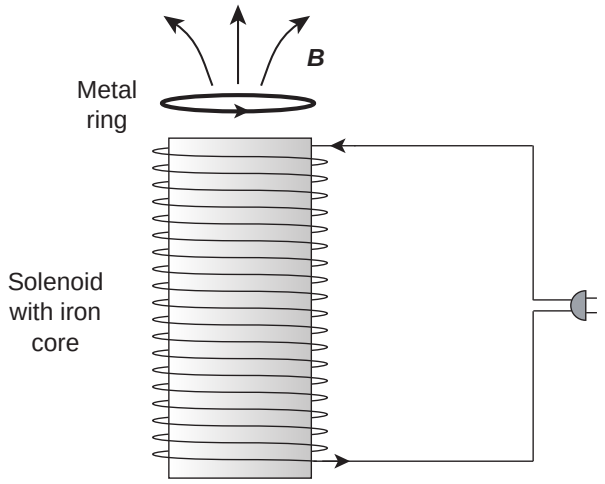

If the solenoid is plugged in the metal ring will jump into the air, by as much as several feet in typical demonstrations. (a) Explain why. (b) What would happen if a gap were placed in the ring? (c) What would happen if the metal ring were replaced by a wooden ring? (d) What would happen if the ring were cooled in liquid nitrogen before turning on the switch? *Hint*: See Refs. [65, 70] for a discussion of this demonstration, and the video [6] for an actual demonstration. ***

10.2 A thin spherical shell of radius a and uniform surface conductivity σ is placed in a spatially uniform but time-varying external magnetic field

$$\boldsymbol{B}_{\text{ext}}(t) = B_0 e^{-i\omega t}\hat{\boldsymbol{z}}.$$

Assuming that the quasistatic approximation $\omega a \ll c$ holds (see Section 10.2.1), show analytically that the total magnetic field inside the shell is directed along the z axis and is frequency-dependent,

$$\boldsymbol{B}_{\text{in}}(t) = \frac{B_0}{\sqrt{1+\omega^2\tau^2}}\cos(\omega t - \delta)\hat{\boldsymbol{z}},$$

where ω is the frequency of the electromagnetic radiation, $\tau \equiv \frac{1}{3}\mu_0\sigma a$ is a characteristic relaxation time of the spherical shell, and $\delta = \arctan(\omega\tau)$ is a phase shift. Discuss the physical significance of the resulting field inside the shell and its frequency dependence. *Hint*: Because of the quasistatic approximation you can assume that there are no free volume currents and that the displacement current can be neglected.

Numerical and GenAI Problems

10.3 Prompt your *GenAI* to create an interactive animation of the jumping ring demonstration described in Problem 10.1. *Hint*: If you are unfamiliar with the effect, watch a YouTube video of a laboratory demonstration; for example see Ref. [6]. Use that to guide your prompt to the *GenAI*.

11 Maxwell's Equations

The preceding chapters have provided a systematic explanation and validation of the various pieces of electromagnetic theory that James Clerk Maxwell synthesized into what we now call the *Maxwell equations*. To this point we have treated electricity and magnetism largely as separate subjects. As Faraday's discoveries that were discussed in Ch. 10 make clear, this distinction begins to fail when one moves from static to time-dependent phenomena, and we will now begin to address a unified picture of electromagnetism, valid for electric and magnetic phenomena in both static and dynamical contexts. In this chapter we take the Maxwell equations to be the basis for all classical understanding of electromagnetism and address systematically their broader scientific and technical implications.

11.1 The Not-Quite Maxwell Equations

The basic equations of electricity and magnetism that we have studied in Chs. 2-9 can be summarized (in medium, in differential form, in SI units) as

$$\boldsymbol{\nabla} \cdot \boldsymbol{D} = \rho \qquad \text{(Gauss's law)}, \tag{11.1a}$$

$$\boldsymbol{\nabla} \times \boldsymbol{E} + \frac{\partial \boldsymbol{B}}{\partial t} = 0 \qquad \text{(Faraday's law)}, \tag{11.1b}$$

$$\boldsymbol{\nabla} \cdot \boldsymbol{B} = 0 \qquad \text{(No magnetic charges)}, \tag{11.1c}$$

$$\boldsymbol{\nabla} \times \boldsymbol{H} = \boldsymbol{J} \qquad \text{(Ampère's law)}, \tag{11.1d}$$

Expressed here in modern notation, these were the fundamental equations of electromagnetism as they stood in the mid-1800s when James Clerk Maxwell set about his synthesis of electromagnetic understanding. A comparison shows that these are almost, but not quite, the Maxwell equations that were introduced in Eqs. (6.50). The difference lies in the fourth equation (Ampère's law), where a term $-\partial \boldsymbol{D}/\partial t$ is missing relative to the fourth Maxwell equation (6.50d).

11.1.1 Ampère's Law and the Displacement Current

It is important to recognize that all but Faraday's law in Eqs. (11.1) were derived from data taken under steady-state conditions, so we should expect that modifications might be required for the description of time-dependent fields. Maxwell realized that the fundamental equations of electromagnetism (11.1) known in his time were inconsistent as they then stood. Since the divergence of a curl vanishes by a basic vector-calculus identity,

$\boldsymbol{\nabla} \cdot (\boldsymbol{\nabla} \times \boldsymbol{H}) = 0$, it follows from Ampère's law (11.1d) for steady currents that

$$\boldsymbol{\nabla} \cdot \boldsymbol{J} = \boldsymbol{\nabla} \cdot (\boldsymbol{\nabla} \times \boldsymbol{H}) = 0. \tag{11.2}$$

But from the continuity equation (1.3) ensuring conservation of charge,

$$\frac{\partial \rho}{\partial t} = -\boldsymbol{\nabla} \cdot \boldsymbol{J},$$

so $\boldsymbol{\nabla} \cdot \boldsymbol{J} = 0$ can hold only if the charge density doesn't change with time. Therefore, Maxwell modified Ampère's law to accomodate a time dependence by introducing a *displacement current* term $\partial \boldsymbol{D}/\partial t$,[1]

$$\boldsymbol{\nabla} \times \boldsymbol{H} = \boldsymbol{J} \quad \longrightarrow \boldsymbol{\nabla} \times \boldsymbol{H} = \boldsymbol{J} + \frac{\partial \boldsymbol{D}}{\partial t}, \tag{11.3}$$

thus converting Eqs. (11.1) into what we now call the Maxwell equations (6.50) (in medium, in differential form),[2]

$$\boldsymbol{\nabla} \cdot \boldsymbol{D} = \rho \qquad \text{(Gauss's law)}, \tag{11.4a}$$

$$\boldsymbol{\nabla} \times \boldsymbol{E} + \frac{\partial \boldsymbol{B}}{\partial t} = 0 \qquad \text{(Faraday's law)}, \tag{11.4b}$$

$$\boldsymbol{\nabla} \cdot \boldsymbol{B} = 0 \qquad \text{(No magnetic charges)}, \tag{11.4c}$$

$$\boldsymbol{\nabla} \times \boldsymbol{H} - \frac{\partial \boldsymbol{D}}{\partial t} = \boldsymbol{J} \qquad \text{(Ampère–Maxwell law)}, \tag{11.4d}$$

where the last equation is now called the *Ampère–Maxwell law*. It still is the same law as before when applied to steady-state phenomena, but addition of the displacement current term means that a changing electric field can generate a magnetic field, even if there is no current. Thus, it is the converse of Faraday's law, where a changing magnetic field can produce an electric field. As you were asked to show way back in Problem 1.1, these (Maxwell) equations are now consistent with the continuity equation. Taking the divergence of both sides of the Ampère–Maxwell law,

$$\boldsymbol{\nabla} \cdot (\boldsymbol{\nabla} \times \boldsymbol{H}) = \boldsymbol{\nabla} \cdot \boldsymbol{J} + \frac{\partial (\boldsymbol{\nabla} \cdot \boldsymbol{D})}{\partial t},$$

and using $\boldsymbol{\nabla} \cdot \boldsymbol{D} = \rho$ from Gauss's law and the identity $\boldsymbol{\nabla} \cdot (\boldsymbol{\nabla} \times \boldsymbol{H}) = 0$ from Eq. (A.6), this becomes

$$\frac{\partial \rho}{\partial t} + \boldsymbol{\nabla} \cdot \boldsymbol{J} = 0,$$

which is the continuity equation (1.3).

[1] As elaborated in Box 11.1, Maxwell's original detailed physical reason for the displacement term and corresponding name is partially bogus, being based on a now-discredited mechanical model of electric and magnetic fields in the fictitious aether. However, his insight that the displace term is required was seminal, and the name itself survives in the modern form of the Maxwell equations.

[2] Recall that the vacuum Maxwell equations (1.1) in differential form can be recovered by substituting $\boldsymbol{D} = \epsilon_0 \boldsymbol{E}$ and $\boldsymbol{H} = \boldsymbol{B}/\mu_0$ into these equations, remembering from Eq. (2.4) that $\mu_0 \epsilon_0 = 1/c^2$, and that the Maxwell equations in medium in integral form are given by Eqs. (6.55).

Box 11.1 Maxwell, Steampunk, and the Displacement Current

Maxwell's reasons for introducing the displacement current were based partially on a now-discredited mechanical model of the (fictitious) aether, which was thought in the 19th century to be the special medium through which electromagnetic waves traveled. These ideas of a mechanical aether have strong overlap with the modern literary and animé genre called *steampunk*, which is a fictional alternative history in which modern electrical and internal combustion technologies fail to develop and all mechanical devices (including flying machines) are driven by steam, as described in Ref. [58]. A schematic illustration of Maxwell's mechanical model (the "elastic vortex aether") is illustrated in the following figure.

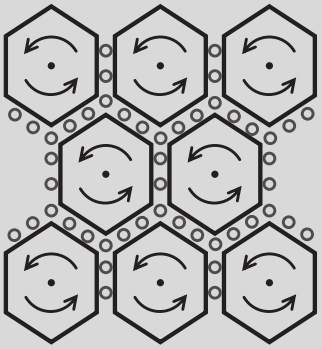

Maxwell calculated that his elastic vortex aether propagated transverse waves at a speed of $3.107 \times 10^8\,\mathrm{m\,s^{-1}}$, which was close to the $3.149 \times 10^8\,\mathrm{m\,s^{-1}}$ for the speed of light that Hippolyte Fizeau had measured in 1847 using a rotating toothed wheel with mirror apparatus. Maxwell remarked [51, 52],

> "we can scarcely avoid the inference that light consists of the transverse undulations of the same medium which is the cause of electric and magnetic phenomena" ,

which was the first direct claim that light had an electromagnetic origin. The displacement term in the Maxwell equations and the electromagnetic origin of light have stood the test of time, despite their origin in a fictitious steampunk-like mechanical model of vortices and idle wheels inspired by the cogs and gears in the machinery of the Victorian age.

Local Conservation of Charge: Physically the continuity equation requires that changes in electrical charge in some arbitrary volume are caused by flow of charge through the surface bounding that volume.

1. This requires conservation of charge within a volume of space that can be arbitrarily small, thus implying that *charge is conserved locally*.
2. A charge that disappears from one point in space and instantly reappears at another point is consistent with *global charge conservation*, but not with *local charge conservation*.

The reason requires relativistic quantum field theory for its full explanation:

Maxwell's equations (11.4), supplemented by the Lorentz force law (1.4)

$$\boldsymbol{F} = q(\boldsymbol{E} + \boldsymbol{v} \times \boldsymbol{B}),$$

to describe electromagnetic forces, and Newton's laws of motion to translate force into experimentally observable particle motion are thought to describe all of classical electromagnetism.

11.1.2 Implications of the Ampère–Maxwell Law

As was introduced in Section 1.4, Maxwell's seemingly small change in the Ampère law turns out to have enormous implications for both our classical and quantum understanding of electromagnetism.

1. Maxwell's addition of $\partial \boldsymbol{D}/\partial t$ to Ampère's law (and Faraday's induction experiments) effectively brought together the previously separate subjects of electricity and magnetism. Ampère's law is only about magnetism, but both the polarized electric field $\boldsymbol{D}$ and the polarized magnetic field $\boldsymbol{H}$ appear in the Ampère–Maxwell law, while $\boldsymbol{E}$ and $\boldsymbol{B}$ both appear in Faraday's law.

   > Changing electric fields produce magnetic fields and changing magnetic fields produce electric fields, and we may now speak meaningfully of the unified subject of *electromagnetism*.

2. The fundamental equations of electromagnetism are now consistent with (local) conservation of electrical charge.
3. This modification will lead eventually to the greatest triumph of Maxwell's theory (see Section 13.2.1):

   > The Maxwell equations have wave solutions, and the corresponding electromagnetic waves may be interpreted as light,

   which *unifies* the field of electricity, not only with the field of magnetism, but also with the field of optics.
4. That Maxwell's equations obey the continuity equation and thus conserve charge locally leads to the idea of *electromagnetic gauge invariance*, which will provide powerful tools for dealing with classical electromagnetism, and will underlie a quantum field theory of electromagnetism (*quantum electrodynamics* or QED).
5. Electromagnetic gauge invariance will eventually be generalized to more sophisticated local gauge invariance in the weak and strong interactions, resulting in the relativistic quantum field theory that we term the *Standard Model* of elementary particle physics.

Many of these topics are beyond the scope of classical electromagnetism, but it is important to appreciate that they have their historical and scientific antecedents in that discipline. A general introduction to modern relativistic quantum field theory and many of these topics specifically may be found in Ref. [34].

11.2 Vector and Scalar Potentials

In our discussions of electrostatics and magnetostatics we introduced the scalar potential Φ (Section 2.6) and the vector potential $\boldsymbol{A}$ (Section 8.8). The Maxwell equations (11.4) are a set of coupled first-order differential equations relating the components of the electric and magnetic fields. To solve those coupled differential equations it is often convenient to introduce the potentials $\boldsymbol{A}$ and Φ, which satisfy some of the Maxwell equations identically and leave a smaller number of second-order differential equations to solve.

Consider the two homogeneous equations (the ones equal to zero on the right side) in Eqs. 11.4. As we have noted in Section 8.8, since $\boldsymbol{\nabla} \cdot \boldsymbol{B} = 0$, the magnetic field $\boldsymbol{B}$ can be described as the curl of a vector potential $\boldsymbol{A}$,[3]

$$\boldsymbol{B} = \boldsymbol{\nabla} \times \boldsymbol{A}. \tag{11.5}$$

Then Faraday's law (11.4b) may be written as,

$$\boldsymbol{\nabla} \times \left(\boldsymbol{E} + \frac{\partial \boldsymbol{A}}{\partial t} \right) = 0. \tag{11.6}$$

Since the curl of the quantity $\boldsymbol{E} + \partial \boldsymbol{A}/\partial t$ in parentheses vanishes, it can be written as the gradient of a scalar function; let's choose it to be minus the scalar potential Φ,

$$\boldsymbol{E} + \frac{\partial \boldsymbol{A}}{\partial t} = -\boldsymbol{\nabla}\Phi,$$

which rearranges to

$$\boldsymbol{E} = -\boldsymbol{\nabla}\Phi - \frac{\partial \boldsymbol{A}}{\partial t}. \tag{11.7}$$

For simplicity, let us restrict consideration to the vacuum form of the Maxwell equations that is given in Eq. (1.1), which are formulated in terms of the electric field $\boldsymbol{E}$ and the magnetic field $\boldsymbol{B}$,

$$\boldsymbol{\nabla} \cdot \boldsymbol{E} = \frac{\rho}{\epsilon_0} \qquad \text{(Gauss's law)}, \tag{11.8a}$$

$$\boldsymbol{\nabla} \times \boldsymbol{E} + \frac{\partial \boldsymbol{B}}{\partial t} = 0 \qquad \text{(Faraday's law)}, \tag{11.8b}$$

$$\boldsymbol{\nabla} \cdot \boldsymbol{B} = 0 \qquad \text{(No magnetic charges)}, \tag{11.8c}$$

$$\boldsymbol{\nabla} \times \boldsymbol{B} - \frac{1}{c^2}\frac{\partial \boldsymbol{E}}{\partial t} = \mu_0 \boldsymbol{J} \qquad \text{(Ampère–Maxwell law)}. \tag{11.8d}$$

[3] Recall the reason: if $\boldsymbol{B} = \boldsymbol{\nabla} \times \boldsymbol{A}$, then by taking the divergence of both sides $\boldsymbol{\nabla} \cdot \boldsymbol{B} = \boldsymbol{\nabla} \cdot (\boldsymbol{\nabla} \times \boldsymbol{A}) = 0$, where the identity (A.6) was used. Thus the condition $\boldsymbol{\nabla} \cdot \boldsymbol{B} = 0$ is guaranteed if $\boldsymbol{B}$ derives from the curl of a vector potential.

Substituting $\boldsymbol{B} = \boldsymbol{\nabla} \times \boldsymbol{A}$ and $\boldsymbol{E} = -\boldsymbol{\nabla}\Phi - \partial \boldsymbol{A}/\partial t$ into the Maxwell equations (11.8), we find using the identities $\boldsymbol{\nabla} \cdot (\boldsymbol{\nabla} \times \boldsymbol{B}) = 0$ and $\boldsymbol{\nabla} \times \boldsymbol{\nabla}\Phi = 0$, that the homogeneous equations (11.8b) and (11.8c) are *satisfied identically*, while the inhomogeneous equations (11.8a) and (11.8d) are transformed into coupled second-order differential equations,

$$\nabla^2\Phi + \frac{\partial}{\partial t}(\boldsymbol{\nabla} \cdot \boldsymbol{A}) = -\frac{\rho}{\epsilon_0}, \tag{11.9a}$$

$$\nabla^2 \boldsymbol{A} - \frac{1}{c^2}\frac{\partial^2 \boldsymbol{A}}{\partial t^2} - \boldsymbol{\nabla}\left(\boldsymbol{\nabla} \cdot \boldsymbol{A} + \frac{1}{c^2}\frac{\partial \Phi}{\partial t}\right) = -\mu_0 \boldsymbol{J}, \tag{11.9b}$$

where the identity $\boldsymbol{\nabla} \times (\boldsymbol{\nabla} \times \boldsymbol{A}) = \boldsymbol{\nabla}(\boldsymbol{\nabla} \cdot \boldsymbol{A}) - \nabla^2 \boldsymbol{A}$ has been used. Thus the problem has been converted into solving the two coupled equations (11.9). These equations can be decoupled by a suitable gauge transformation, as will now be shown.

11.3 Exploiting Gauge Symmetry

In Section 8.8 we showed that the magnetic field is invariant under a gauge transformation on the vector potential,

$$\boldsymbol{A} \to \boldsymbol{A}' = \boldsymbol{A} + \boldsymbol{\nabla}\chi,$$

where χ is an arbitrary scalar function. But in general the Maxwell equations involve both magnetic and electric fields. If the electric field is to be unaltered under this gause transformation of the magnetic field the scalar potential must be changed at the same time according to

$$\Phi \to \Phi' = \Phi - \frac{\partial \chi}{\partial t}.$$

Gauge Transformation: A *classical gauge transformation* on the electromagnetic field is defined by the simultaneous transformations

$$\boldsymbol{A} \to \boldsymbol{A} + \boldsymbol{\nabla}\chi \qquad \Phi \to \Phi - \frac{\partial \chi}{\partial t}, \tag{11.10}$$

on the vector potential $\boldsymbol{A}$ and the scalar potential Φ, where χ is an arbitrary scalar function. A gauge transformation leaves the electric and magnetic fields, and thus Maxwell's equations, unchanged.

Notice that in the gauge transformation (11.10) the same scalar function χ must be used in both equations, but the choice of χ is arbitrary.

Mathematically, the invariance of electromagnetism under the gauge transformation (11.10) means that an electromagnetic field may be viewed as an *equivalence class* of potentials $\{\Phi, \boldsymbol{A}\}$, where equivalence classes are defined in Box 11.2. Thus, on the set of all possible electromagnetic potentials $\{(\Phi_1, \boldsymbol{A}_1), (\Phi_2, \boldsymbol{A}_2), \cdots\}$ we may define an equivalence relation "related by the gauge transformation of Eq. (11.10)" and the equivalence

Box 11.2 Equivalence Classes

A very useful concept for a set is that of an *equivalence class*, which is predicated on there being an *equivalence relation* defined between set members. Equivalence classes are of utility when one wishes to refer to a subset of things that are "the same" for our considerations, in that they all exhibit a specific property.

For example, if for the set of all balls of a solid color we define an equivalence relation "having the same color", then the subset of all yellow balls would be one equivalence class of the set of all balls of a solid color, and the subset of all black balls would be another.

When a set S has an equivalence relation defined on it the set may be partitioned naturally into disjoint (non-overlapping) equivalence classes, with elements a and b belonging to the same equivalence class if and only if they are equivalent. Formally, equivalence is a binary relation $\sim$ between members of a set S exhibiting

1. *Reflexivity:* for each $a \in \mathrm{S}$, one has $a \sim a$.
2. *Symmetry:* for each $a, b \in \mathrm{S}$, if $a \sim b$, then $b \sim a$.
3. *Transitivity:* for each $a, b, c \in \mathrm{S}$, if $a \sim b$ and $b \sim c$, then $a \sim c$.

Since mathematical groups are sets with added structure, equivalence classes may be defined in a similar way for groups.

class is the set of all electromagnetic potentials related to each other by a gauge transformation. The objects of the class then are "equivalent" in the sense that all members of the equivalence class give the same electric and magnetic fields, and thus lead to the same classical electromagnetic physics when inserted in the Maxwell equations.

11.3.1 Lorenz Gauge

Suppose that we now take advantage of the invariance of electromagnetism under gauge transformations and choose a set of potentials $\{\Phi, \boldsymbol{A}\}$ that satisfy the *Lorenz condition*

$$\boldsymbol{\nabla} \cdot \boldsymbol{A} + \frac{1}{c^2} \frac{\partial \Phi}{\partial t} = 0 \qquad \text{(Lorenz gauge)}. \tag{11.11}$$

A constraint like Eq. (11.11) is termed a *gauge-fixing condition* and imposing such a constraint is termed *fixing the gauge*. The gauge choice implied by Eq. (11.11) is called the *Lorenz gauge*.[4] If the Lorenz gauge condition is inserted into the coupled equations (11.9),

[4] The *Lorenz gauge* (named for Danish physicist and mathematician Ludvig Lorenz) has often mistakenly been called the *Lorentz gauge*, after the better-known Dutch physicist Hendrik Lorentz (who shared the

the equations decouple and solving the Maxwell equations has now been reduced to solving two second-order differential equations,

$$\nabla^2\Phi - \frac{1}{c^2}\frac{\partial^2\Phi}{\partial t^2} = -\frac{\rho}{\epsilon_0}, \tag{11.12a}$$

$$\nabla^2\boldsymbol{A} - \frac{1}{c^2}\frac{\partial^2\boldsymbol{A}}{\partial t^2} = -\mu_0\boldsymbol{J}, \tag{11.12b}$$

which are *uncoupled:* solution of Eq. (11.12a) gives the scalar potential Φ independent of the vector potential $\boldsymbol{A}$, while solution of Eq. (11.12b) gives the vector potential, independent of the scalar potential. Equations (11.12) along with the gauge condition (11.11) are completely equivalent in physical content to the original Maxwell equations (11.4).

It is always possible to find potentials $\{\Phi, \boldsymbol{A}\}$ that satisfy the Lorenz condition. Suppose that we have a solution with gauge potentials that satisfies Eqs. (11.9), but does not satisfy Eqs. (11.11). Then, make a gauge transformation to new potentials $\{\Phi', \boldsymbol{A}'\}$ and require the new potentials to satisfy the Lorentz condition

$$\boldsymbol{\nabla}\cdot\boldsymbol{A}' + \frac{1}{c^2}\frac{\partial\Phi'}{\partial t} = 0 = \boldsymbol{\nabla}\cdot\boldsymbol{A} + \frac{1}{c^2}\frac{\partial\Phi}{\partial t} + \nabla^2\chi - \frac{1}{c^2}\frac{\partial^2\chi}{\partial t^2}.$$

Thus, if a scalar function χ can be found that satisfies

$$\nabla^2\chi - \frac{1}{c^2}\frac{\partial^2\chi}{\partial t^2} = -\left(\boldsymbol{\nabla}\cdot\boldsymbol{A} + \frac{1}{c^2}\frac{\partial\Phi}{\partial t}\right), \tag{11.13}$$

the new potentials will satisfy the Lorenz gauge conditions (11.11) and the simultaneous equations (11.12).

The Lorenz condition Eq. (11.11) does not exhaust the gauge degrees of freedom in Lorenz gauge. The *restricted gauge transformation*

$$\boldsymbol{A} \to \boldsymbol{A} + \boldsymbol{\nabla}\chi \qquad \Phi \to \Phi - \frac{\partial\chi}{\partial t}, \tag{11.14}$$

where the scalar function χ (which is arbitrary for general gauge transformations) is *restricted to those that satisfy the constraint*

$$\nabla^2\chi - \frac{1}{c^2}\frac{\partial^2\chi}{\partial t^2} = 0, \tag{11.15}$$

preserves the Lorenz condition if $\{\boldsymbol{A}, \Phi\}$ satisfies it to begin with. Thus the Lorenz gauge corresponds to an entire family of of gauge conditions that satisfy Eq. (11.11). The Lorenz gauge is often used for two reasons:

1902 Nobel Prize in physics for the theoretical explanation of the Zeeman effect). The present author must confess to being among the many who have made this error, referring to the "Lorentz" rather than "Lorenz" gauge in an early book [34]. Ludvig Lorenz did significant work on electromagnetism contemporary with, but independent of, Maxwell. For example, he proposed independently that electromagnetic waves might be lightwaves. An overview of Lorenz's scientific work is given in Ref. [46], and the history of his work and the incorrect attribution of his famous gauge to Lorentz is discussed in Ref. [42].

1. It leads to the decoupled equations (11.12) that treat Φ and $\boldsymbol{A}$ on an equal footing.
2. As will be elaborated in Ch. 17, the Lorenz gauge condition is manifestly invariant under Lorentz transformations, which fits naturally into special relativity.[5]

There are infinitely many valid gauge transformations that can be made using Eq. (11.10) with different choices for the scalar function χ. However, only some prove to be useful. One of use is the transformation to Lorenz gauge described in this section. Another that we have already encountered in Section 8.8 is the transformation to Coulomb gauge.

11.3.2 Coulomb Gauge

We have already introduced the *Coulomb gauge condition* in Eq. (8.37),

$$\boldsymbol{\nabla} \cdot \boldsymbol{A} = 0 \qquad \text{(Coulomb gauge condition)}.$$

From Eq. (11.9a), in Coulomb gauge the scalar potential obeys a Poisson equation

$$\nabla^2 \Phi = -\frac{\rho}{\epsilon_0}, \tag{11.16}$$

which has a solution

$$\Phi(\boldsymbol{x}, t) = \frac{1}{4\pi\epsilon_0} \int \frac{\rho(\boldsymbol{x}', t)}{|\boldsymbol{x} - \boldsymbol{x}'|}\, d^3x'. \tag{11.17}$$

This is the instantaneous Coulomb potential caused by the charge density $\rho(\boldsymbol{x})$, which is the motivation for the appelation *Coulomb gauge*.

> As Box 11.3 discusses, the Coulomb potential (11.17) suggests instantaneous transmission of information in a universe where lightspeed c is the speed limit. In Chs. 17-21 we will resolve this issue and show that electromagnetism is in fact causal because *no information is being transmitted at a speed greater than the speed of light* c.

From Eq. (11.9b), in Coulomb gauge the vector potential obeys

$$\nabla^2 \boldsymbol{A} - \frac{1}{c^2}\frac{\partial^2 \boldsymbol{A}}{\partial t^2} = -\mu_0 \boldsymbol{J} + \frac{1}{c^2}\frac{\partial \Phi}{\partial t}. \tag{11.18}$$

As guaranteed by the Helmholtz theorem for any vector (see Section 3.3.6), the current density can be decomposed as a sum of two terms

$$\boldsymbol{J} = \boldsymbol{J}_{\mathrm{L}} + \boldsymbol{J}_{\mathrm{T}}, \tag{11.19}$$

where the terms have the following properties:

1. The component $\boldsymbol{J}_{\mathrm{L}}$ has vanishing curl, $\boldsymbol{\nabla} \times \boldsymbol{J}_{\mathrm{L}} = 0$; it is called the *longitudinal current* or the *irrotational current*.

[5] Note that the equations are in (Ludvig) *Lorenz gauge*, but we shall see in Ch. 17 that they are invariant under (Hendrik) *Lorentz transformations*. This perhaps helps to explain the historical confusion in the name of the gauge.

Box 11.3 Causality and the Coulomb and Gravitational Potentials

Causality (that actions must precede results) is a fundamental principle underlying all of modern science. The Coulomb potential of Eq. (11.17) appears to violate that principle.

Causality and the Coulomb Potential

The Coulomb potential in Eq. (11.17) is said to be "instantaneous" because the associated force acts without delay at any $\boldsymbol{x}$ corresponding to a distance $|\boldsymbol{x}-\boldsymbol{x}'|$ from the source. This is inconsistent with special relativity and relativistic quantum field theory, which require that a force be transmitted by a virtual particle (the photon in this case) communicated at a speed less than or equal to the speed of light c.

Causality and the Newtonian Gravitational Potential

The Newtonianian gravitational potential has the form of a Coulomb potential with masses playing the role of charges, and has the same causality problem: it implies that the gravitational force acts instantaneously over any distance. The solution of this problem in gravitational physics is replacement of Newtonian gravity with general relativity, which generalizes special relativity and requires that the transmission speed of the gravitational force be equal to the speed of light. This prediction of general relativity has been confirmed by observations, as we now describe.

The Speed of Light and the Speed of Gravity

In 2017 the ground-based Ligo–Virgo detectors observed gravitational wave GW170817.[a] But there was more to come: 1.7 seconds later, two satellites in orbit around the Earth, the Fermi Gamma-ray Space Telescope (Fermi) and International Gamma-Ray Astrophysics Laboratory (INTEGRAL), detected a *burst of gamma-rays* from the same portion of the sky as the source of the gravitational wave. Detailed observations of the afterglow of the gamma-ray burst at many wavelengths, and comprehensive analysis of the gravitational and electromagnetic data sets, concluded that the gravitational wave and the gamma-ray burst were caused by a binary neutron star merger 40 megaparsecs (130 million lightyears) away in the galaxy NGC 4993.

That the gravitational and electromagnetic signals arrived within 1.7 seconds of each other after traveling a distance of 40 megaparsecs implied that the speed of gravity (for the gravitational waves) and the speed of light c (for the gamma-rays) differ by no more than 3 parts in 10^{15}. Thus, we conclude that *the speed of gravity is* c (as predicted by the general theory of relativity). More extensive discussion of physical implications for GW170817 may be found in Ref. [35] and in Section 24.7 of Ref. [36].

[a] The name GW170817 indicates that the gravitational wave (GW) was observed in the year 20(17), in the (08)th month of that year, on the (17)th day of that month.

2. The component $\boldsymbol{J}_{\mathrm{T}}$ has vanishing divergence, $\boldsymbol{\nabla}\cdot\boldsymbol{J}_{\mathrm{T}}=0$; it is called the *transverse current* or the *solenoidal current*.

The longitudinal and transverse currents are given explicitly by

$$\boldsymbol{J}_{\mathrm{L}}=-\frac{1}{4\pi}\boldsymbol{\nabla}\int\frac{\boldsymbol{\nabla}'\cdot\boldsymbol{J}(\boldsymbol{x}',t)}{|\boldsymbol{x}-\boldsymbol{x}'|}\,d^3x', \tag{11.20a}$$

$$\boldsymbol{J}_{\mathrm{T}}=\frac{1}{4\pi}\boldsymbol{\nabla}\times\boldsymbol{\nabla}\times\int\frac{\boldsymbol{J}(\boldsymbol{x}',t)}{|\boldsymbol{x}-\boldsymbol{x}'|}\,d^3x'. \tag{11.20b}$$

From Eq. (11.17) and the continuity equation (1.3),

$$\frac{1}{c^2}\boldsymbol{\nabla}\frac{\partial\Phi}{\partial t}=\mu_0\boldsymbol{J}_{\mathrm{T}}, \tag{11.21}$$

which gives upon insertion into Eq. (11.9b) and using the identity $\boldsymbol{\nabla}(\boldsymbol{\nabla}\cdot\boldsymbol{A})=0$ and Eq. (11.19),

$$\nabla^2\boldsymbol{A}-\frac{1}{c^2}\frac{\partial^2\boldsymbol{A}}{\partial t^2}=-\mu_0\boldsymbol{J}_{\mathrm{T}}. \tag{11.22}$$

Thus, in Coulomb gauge the source for the equation for $\boldsymbol{A}$ can be expressed entirely in terms of the transverse current $\boldsymbol{J}_{\mathrm{T}}$. For this reason, the Coulomb gauge is sometimes termed the *transverse gauge*. The Coulomb gauge is also sometimes called the *radiation gauge*, because one finds that in describing electromagnetic radiation by quantum electrodynamics, only the vector potential (which is determined by the transverse components) need be quantized.

> Notice that Eq. (11.22) has the form of a wave equation with the speed of the wave equal to c, which is the behavior expected for electromagnetic waves. However, the discussion given above implies that for the scalar potential the propagation speed is infinite. The full resolution of this seeming paradox is beyond our scope because it requires relativistic quantum field theory, but in essence the propagating classical field has only transverse components and one finds that in quantum electrodynamics only the vector potential (and thus only the transverse components) need be quantized.

As we will see in Ch. 17, Lorentz covariance is most transparent if the 3-vector potential $\boldsymbol{A}$ and the scalar potential Φ are combined into a spacetime 4-vector A^μ with the components of the 4-vector given by

$$A^\mu=(A^0,A^1,A^2,A^3)=(\Phi,\boldsymbol{A})=(\Phi,A^1,A^2,A^3), \tag{11.23}$$

where Φ is the scalar potential and $\boldsymbol{A}$ is the 3-vector potential with components $A^i(i=1,2,3)$. In the 4-vector the first component A^0 is called the *timelike component* and the other three components (A^1,A^2,A^3) are called the *spacelike components* of the 4-vector.[6]

[6] A small terminology inconsistency must be dealt with. We have been calling the 3-vector $\boldsymbol{A}$ the vector

It was asserted above that only the *two transverse components* of the vector (typically chosen to be A_1 and A_2 for $\boldsymbol{A}$ and A^2 and A^3 for A^μ) are required to describe propagating waves. But a 3-vector like $\boldsymbol{A}$ normally has three components, and a 4-vector like A^μ has four components. So how can a propagating photon have only two rather than three or four degrees of freedom? A systematic discussion of relativistic quantum field theory applied to electrons and photons (QED) is beyond our present scope. However, the short answer is that it is found in QED that in a covariant gauge like Lorenz gauge there are four states of polarization, but the contributions from timelike and longitudinal polarizations enter with equal magnitudes but opposite signs and exactly cancel each other, leaving only the transverse contributions for a free propagating photon. (This is called the *Gupta–Bleuler mechanism* in quantum electrodynamics.) A massive vector field would have three spatial polarization components. As we will see, the reduction to two spatial polarizations is a consequence of the *photon being identically massless:* massive vector fields have three states of polarization but massless vector fields have only two. An enormous amount of highly consequential physics follows from this fact. Regrettably, we have neither the space nor the foundation to explore that here, but readable accounts may be found in Refs. [16, 64, 63, 34].

11.4 Retarded Green Function

From Eqs. (11.12), it is clear that the key to solving Maxwell's equations in Lorenz gauge is to be able to solve the wave equation with a source f,

$$\Box\psi = -f, \tag{11.24}$$

where we introduce for convenience the *d'Alembertian operator* $\Box$ with[7]

$$\Box \equiv -\frac{1}{c^2}\frac{\partial^2}{\partial t^2} + \nabla^2, \tag{11.25}$$

because if one knows how to solve (11.24), one can solve Eqs. (11.12). Lorenz gauge has been assumed, so Eq. (11.11) must also be satified, but the retarded solution of Eqs. (11.12) with sources that will be found shortly will in fact satisfy Eq. (11.11) automatically, provided that the solution decreases rapidly enough at infinity. Generalizing the electrostat-

potential, but relativistically it will be more convenient to work with the 4-vector potential A^μ (which makes more obvious the requirement of relativity that space and time enter on an equal footing); see Section 18.9.3. We adopt a policy that where it is clear that we are working non-relativistically, $\boldsymbol{A}$ will often be called the vector potential, while if it is clear that we are working in a relativistic context, A^μ will often be called the vector potential. If there is a chance for confusion the explicit names "3-vector potential" for $\boldsymbol{A}$ and "4-vector potential" for A^μ will be used. Similar terminology considerations apply to other quantities such as the 3-vector current $\boldsymbol{J}$ and the 4-vector current J^μ, each of which is called "the current vector" in various contexts.

[7] The d'Alembertian operator $\Box$ is a Lorentz-invariant combination of the second derivatives with respect to space and time that will be of significant utility in discussing the relationship of the Maxwell equations to Lorentz invariance and special relativity in Ch. 17.

ics case, a Green function $G(t, \boldsymbol{x}; t'\boldsymbol{x}')$ can be defined by

$$\Box\, G(t, \boldsymbol{x};\, t'\boldsymbol{x}') = -\delta(\boldsymbol{x} - \boldsymbol{x}')\delta(t - t'), \tag{11.26}$$

where the derivative operators in $\Box$ are understood to operate on the unprimed variables, and in contrast to Eq. (3.27) for electrostatics, the Green function depends on $(t', \boldsymbol{x}')$ and $(t, \boldsymbol{x})$ and there is a delta function in $t' - t$ as well as in $\boldsymbol{x} - \boldsymbol{x}'$. If we can obtain a Green function, a solution ψ of Eq. (11.24) is given by the principle of superposition,

$$\psi(t, \boldsymbol{x}) = \int G(t, \boldsymbol{x}; t'\boldsymbol{x}')f(t', \boldsymbol{x}')\, d^3x'\, dt', \tag{11.27}$$

assuming that the integral converges. Let us seek a solution of Eq. (11.26) using *Fourier transforms*, guided by the discussion in Wald [74].

11.4.1 Fourier Transforms

For an integrable function $F : \mathbb{R} \to \mathbb{R}$, define its *Fourier transform* $\hat{F}$ as[8]

$$\hat{F}(k) = \frac{1}{\sqrt{2\pi}} \int_{-\infty}^{+\infty} F(x)e^{-ikx}dx. \tag{11.28}$$

Fourier transforms can also be extended to distributions such as the Dirac delta function; for example, the Fourier transform of the delta function is,

$$\hat{\delta}_{x_0}(k) = \frac{1}{\sqrt{2\pi}}\, e^{ilx_0}. \tag{11.29}$$

Assuming a function to be smooth and to fall off fast enough at infinity, the original function $F(x)$ can be recovered by the *inverse Fourier transform*,

$$F(x) = \frac{1}{\sqrt{2\pi}} \int_{-\infty}^{+\infty} \hat{F}(k)e^{+ikx}dk. \tag{11.30}$$

This formula applies also to distributions and the inverse of the Fourier transform for a delta function is

$$\delta_{x_0}(x) = \frac{1}{\sqrt{2\pi}} \int_{-\infty}^{+\infty} \hat{\delta}_{x_0}(k)e^{+ikx}dk = \frac{1}{2\pi} \int_{-\infty}^{+\infty} e^{-ikx_0}e^{+ikx}\, dk. \tag{11.31}$$

One of the most useful properties of Fourier transforms is that differentiation in real space corresponds to multiplication by ik in Fourier transform space. For example,

$$\widehat{\frac{dF}{dx}}\,(k) = ik\hat{F}(k), \tag{11.32}$$

for the Fourier transform of $dF(x)/dt$, as you are asked to show in Problem 11.1.

[8] There are different conventions for choosing the normalization factor in defining Fourier transforms. The definitions in Eqs. (11.28) and(11.30) employ the "symmetric convention", which uses a normalization factor of $1/\sqrt{2\pi}$ for both the transform (11.28) and the inverse transform (11.30). Note that a simple example of a solution using Green functions for a driven mechanical oscillator was described in Box 3.2, where a different normalization for Fourier transforms was used.

Thus a partial differential equation with constant coefficients expressed in real space can be converted to a corresponding algebraic equation in Fourier transform space.

Now let's solve Eq. (11.26) for G using Fourier transform methods.

11.4.2 Green Functions Using Fourier Transforms

To simplify notation let us temporarily set $x' = t' = 0$ and $c = 1$, and define the 4D Fourier transform of G as[9]

$$\hat{G}(\omega, \boldsymbol{k}) = \frac{1}{(2\pi)^2} \int_{-\infty}^{+\infty} G(t, \boldsymbol{x}) e^{+i\omega t} e^{-i\boldsymbol{k}\cdot\boldsymbol{x}} dt\, d^3x. \tag{11.33}$$

Taking the Fourier transform of Eq. (11.26) with respect to t and $\boldsymbol{x}$, using Eq. (11.29) with $x_0 = 0$, and using Eq. (11.32) yields

$$(\omega^2 - k^2)\, \hat{G}(\omega, \boldsymbol{k}) = -\frac{1}{4\pi^2}, \tag{11.34}$$

where $k \equiv |k|$. Naively, this suggest the solution

$$\hat{G}(\omega, \boldsymbol{k}) = -\frac{1}{4\pi^2} \frac{1}{(\omega^2 - k^2)} = -\frac{1}{4\pi^2} \frac{1}{(\omega + k)(\omega - k)}, \tag{11.35}$$

but division by $(\omega^2 - k^2)$ is illegal since it is possible that $\omega = k$. To see the difficulty clearly, let's attempt to take the inverse transform of $\hat{G}$ with respect to ω (but not $\boldsymbol{k}$). This is a Fourier transform with respect to space but not time; denoting it as $\tilde{G}$,

$$\begin{aligned} \tilde{G}(t, \boldsymbol{k}) &= \frac{1}{\sqrt{2\pi}} \int_{-\infty}^{+\infty} \hat{G}(\omega, \boldsymbol{k}) e^{-i\omega t}\, d\omega \\ &= -\frac{1}{4\pi^2\sqrt{2\pi}} \int_{-\infty}^{+\infty} \frac{e^{-i\omega t}}{(\omega + k)(\omega - k)}\, d\omega, \end{aligned} \tag{11.36}$$

where Eq. (11.35) was used. This has *logarithmic divergences* of the integral[10] if $\omega \to \pm k$, so it is ill-defined.

The fundamental reason that the integral in (11.36) is not well defined as it stands is that many different Green functions satisfy Eq. (11.26), so a unique solution for G in (11.36) cannot be expected without providing further information to identify the particular Green function that we seek. To proceed it is necessary to regularize the integration in Eq. (11.36) in such a way that

1. equation (11.34) remains valid,

[9] By convention the time Fourier transform is defined by integrating with $e^{+i\omega t}$ rather than with $e^{-i\omega t}$ for compatibility with the 4-momentum vector $k^\mu = (\omega/c, \boldsymbol{k})$ of special relativity that will be introduced in Ch. 17.

[10] All diverges spell trouble, some more than others. The prototypical logarithmic divergence occurs in an integral of the form $f(x) = \int_{x_0}^{x} d\Lambda/\Lambda$, which diverges as $x \to \infty$. As divergences go, logarithmic divergences such as this one are relatively mild, growing only as $f(x) \sim \log(x)$ at large x.

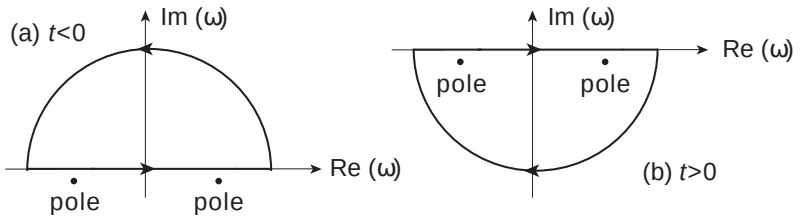

Fig. 11.1 Contour integration paths for the the retarded Green function. (a) Path for $t < 0$, which encloses no poles and thus gives zero for the integral. (b) Path for $t > 0$, which encloses both poles so that the integral is equal to the sum of the residues at the two poles.

2. the right side of Eq. (11.36) becomes well defined, and
3. the resulting solution has the desired boundary and causality properties.

One way to do this is to displace the poles at $\omega = \pm k$ into the complex ω plane and evaluate the resulting contour integral. There is more than one way to do this, each leading to a different Green function. The Green function that we seek is the *retarded Green function*, which will be appropriate for the situation where there is only outgoing radiation from a source. To get this solution the poles should be displaced into the lower half of the complex ω-plane; thus we define the *retarded Green function* by

$$\tilde{G}(t, \boldsymbol{k})_{\text{ret}} = -\frac{1}{4\pi^2\sqrt{2\pi}} \int_{-\infty}^{+\infty} \frac{e^{-i\omega t}}{(\omega + k + i\epsilon)(\omega - k + i\epsilon)}\, d\omega, \tag{11.37}$$

where ϵ is positive and it is understood that the limit $\epsilon \to 0$ is to be taken after the integral is evaluated. Viewing the integral in Eq. (11.37) as a contour integral in the complex ω-plane, if $t < 0$ the integration contour can be closed by a large semicircle in the upper half plane since the exponential factor is damped there ($e^{i\omega t} \to 0$, as $\omega \to +i\infty$), which is illustrated in Fig. 11.1(a). The poles are in the negative half-plane so the contour does not enclose them and by the *Cauchy residue theorem*,

$$\tilde{G}(t, \boldsymbol{k})_{\text{ret}} = 0 \qquad (t < 0). \tag{11.38}$$

That the Green function vanishes for $t = 0$ is characteristic of the retarded solution, corresponding to outgoing but no incoming radiation. This solution is relevant physically if there is no radiation present when the source is turned on.

By similar reasoning, for $t > 0$ the integration contour can be closed in the lower half-plane, as is illustrated in Fig. 11.1(b). Now the integration contour encloses poles at $\omega = \pm k - i\epsilon$ and by the Cauchy residue theorem the integral evaluates to $2\pi i$ times a sum of residues at the two poles. The residue res $f(a)$ of a function $f(z)$ at a pole $z = a$ is given by

$$\text{res}\, f(a) = \frac{1}{(m-1)!} \lim_{z \to 0} \left(\frac{d^{m-1}}{dz^{m-1}} (z-a)^m f(z) \right), \tag{11.39}$$

where m is the order of the pole (exponent on the denominator factor tending to zero at

the pole) and a is the location of the pole (with $a \neq \infty$). In Eq. (11.37) the poles are of order $m = 1$ and we obtain

$$\tilde{G}(t, \boldsymbol{k})_{\text{ret}} = \frac{2\pi i}{4\pi^2\sqrt{2\pi}} \left(\frac{e^{-ikt}}{2k} - \frac{e^{+ikt}}{2k} \right) = \frac{1}{2\pi\sqrt{2\pi}} \frac{\sin kt}{k} \qquad (t > 0). \tag{11.40}$$

The retarded Green function in real (position) space then results from taking the inverse Fouriertransform of Eq. (11.40) with respect to k (see Problem 11.2),

$$\begin{aligned} G(t, \boldsymbol{x})_{\text{ret}} &= \frac{1}{(2\pi)^{3/2}} \frac{1}{2\pi\sqrt{2\pi}} \int \frac{\sin kt}{k} \, e^{i\boldsymbol{k}\cdot\boldsymbol{x}} d^3k \\ &= \frac{\delta(t - |\boldsymbol{x}|)}{4\pi \, |\boldsymbol{x}|} \qquad (t > 0). \end{aligned} \tag{11.41}$$

Restoring t', $\boldsymbol{x}'$, and c, this result becomes

$$G(t, \boldsymbol{x}; t', \boldsymbol{x}')_{\text{ret}} = \begin{cases} 0 & (t < t'), \\ \dfrac{\delta(t - t' - |\boldsymbol{x} - \boldsymbol{x}'| / c)}{4\pi \, |\boldsymbol{x} - \boldsymbol{x}'|} & (t > t'). \end{cases} \tag{11.42}$$

This can be written in a more compact way if we define the *retarded time* by

$$t_{\text{det}} = t - \frac{|\boldsymbol{x} - \boldsymbol{x}'|}{c} \qquad \text{(retarded time)}, \tag{11.43}$$

This propagator now has the desired causal behavior.[11]

Using the language of special relativity that will be introduced in Section 18.5, the Green function $G(t, \boldsymbol{x}; t', \boldsymbol{x}')_{\text{ret}}$ is non-zero only *on the future lightcone* of the source point $(t', \boldsymbol{x}')$, meaning that it vanishes unless

$$|\boldsymbol{x} - \boldsymbol{x}'| = c(t - t').$$

That is, if a field satisfying the wave equation $\Box\psi = -f$ of Eq. (11.24) is zero at early times and

1. a δ-function source is placed at $(t', \boldsymbol{x}')$, then
2. the resulting disturbance of the field (electromagnetic waves) will propagate away from the source at the speed of light.

Because the retarded Green function respects the principle of causality (that cause precedes effect), it is said to be a *causal Green function.*

[11] The retarded time has a simple meaning. When there is a local change in an electromagnetic field, the field at some distant point doesn't reflect that change instantaneously. Instead, the signal of a change in the field propagates as electromagnetic waves moving at the speed of light and there is a time delay in its action at a distant point; the time at the distant point minus the time for the signal to propagate is termed the *retarded time.* It is the time at which a source must have produced a signal for it to reach a detector at the current time t.

Thus, light propagating in a vacuum corresponds to a wave solution of the Maxwell equations that is fixed by the theory to have a constant speed of propagation $v = c$, independent of inertial frame. Electricity, magnetism, and optics are now unified in the science of electromagnetism, with optics now the science of waves in the electromagnetic field.

11.4.3 Causal Potential Solutions

The retarded solution of Eq. (11.24) is the solution obtained by inserting the retarded Green function (11.42) in Eq. (11.27),

$$\begin{aligned}\psi(t,\boldsymbol{x}) &= \int G(t,\boldsymbol{x};t'\boldsymbol{x}')f(t',\boldsymbol{x}')\,d^3x'\,dt' \\ &= \frac{1}{4\pi}\int \frac{f(t-|\boldsymbol{x}-\boldsymbol{x}'|/c,\boldsymbol{x}')}{|\boldsymbol{x}-\boldsymbol{x}'|}\,d^3x'. \end{aligned} \tag{11.44}$$

This can also be written more compactly as

$$\psi(t,\boldsymbol{x}) = \frac{1}{4\pi}\int \frac{f(t',\boldsymbol{x}')_{\text{ret}}}{|\boldsymbol{x}-\boldsymbol{x}'|}\,d^3x', \tag{11.45}$$

where the notation means that $f(t',\boldsymbol{x}')$ is to be evaluated at the retarded time

$$t' = t - \frac{|\boldsymbol{x}-\boldsymbol{x}'|}{c} \qquad \text{(retarded time)}, \tag{11.46}$$

and where t' isn't independent but rather is a function of t, $\boldsymbol{x}$, and $\boldsymbol{x}'$.[12] Written in this form, the retarded solution looks like a solution of the Poisson equation, but evaluated at the retarded time (11.43).

The Maxwell equations (11.12a) and (11.12b) for the scalar and vector potentials are of the form (11.24), so we can write immediately the corresponding retarded solutions,

$$\Phi(t,\boldsymbol{x}) = \frac{1}{4\pi\epsilon_0}\int \frac{[\rho(t',\boldsymbol{x}']_{\text{ret}}}{|\boldsymbol{x}-\boldsymbol{x}'|}\,d^3x', \tag{11.47a}$$

$$\boldsymbol{A}(t,\boldsymbol{x}) = \frac{\mu_0}{4\pi}\int \frac{[\boldsymbol{J}(t',\boldsymbol{x}']_{\text{ret}}}{|\boldsymbol{x}-\boldsymbol{x}'|}\,d^3x'. \tag{11.47b}$$

Finally, substitution of Eqs. (11.47a) and (11.47b) in Eq. (11.11) and some manipulation indicates that these solutions are indeed consistent with the Lorenz gauge condition (see Problem 11.3). Therefore, we may conclude that the solution of the Maxwell equations for a charge density ρ and a current density $\boldsymbol{J}$, and no initial incoming radiation, is given by Eqs. (11.47). This has been shown here in for the special case of Lorenz gauge, but the Maxwell equations are invariant under gauge transformations so this solution may be taken to be valid generally.

[12] In Eq. (11.45), the integration is not over all of space at an instant of time (as the notation might suggest). Rather, it is restricted to the *surface defined by the past lightcone of the spacetime point* $(t,\boldsymbol{x})$, since only points on the past lightcone can be causally connected to $(t,\boldsymbol{x})$ by a signal traveling at lightspeed (see the discussion of lightcones and causality in Ch. 17).

11.4.4 Retarded and Advanced Solutions

Our choice for contour integration path in Fig. 11.1 led to the retarded Green function defined in Eq. (11.42). Other solutions for the Green function result from different contour integration choices in Fig. 11.1. For example, if we had displaced the poles infinitesimally above the $\mathrm{Im}\,\omega$ axis we would have obtained the *advanced solution*, which takes the form

$$G(t,\boldsymbol{x};t',\boldsymbol{x}')_{\text{adv}} = \begin{cases} 0 & (t<t'), \\ \dfrac{\delta(t-t'+|\boldsymbol{x}-\boldsymbol{x}'|/c)}{4\pi\,|\boldsymbol{x}-\boldsymbol{x}'|} & (t>t'). \end{cases} \tag{11.48}$$

This can be written in a more compact way if we define the *advanced time* by

$$t_{\text{adv}} = t + \frac{|\boldsymbol{x}+\boldsymbol{x}'|}{c} \qquad \text{(advanced time)}, \tag{11.49}$$

Now the physical interpretation is that the observer sees a signal at time t only if it is emitted at a *future time* specified by Eq. (11.46), which violates all of our understanding of causality.

That both the retarded and advanced solutions for Eq. (11.24) are acceptable mathematically is a consequence of the Maxwell equations being *time-reversal invariant* (see Box 1.1). Thus, both the retarded and advanced solutions are *mathematically valid*, because they correspond to reversing the direction of time in time-symmetric equations. However, we would reject the advanced solution for realistic situations, not because it fails to satisfy the Maxwell equations, but rather because it fails to satisfy the causality constraints that we expect for a physically reasonable solution. We conclude that the solution of Eq. (11.24) that is of practical significance is the one obtained by inserting the retarded Green function in Eq. (11.27),

$$\begin{aligned} \psi(t,\boldsymbol{x}) &= \int G_{\text{ret}}(t,\boldsymbol{x};t'\boldsymbol{x}')f(t',\boldsymbol{x}')\,d^3x'\,dt' \\ &= \frac{1}{4\pi}\int \frac{f(t-|\boldsymbol{x}-\boldsymbol{x}'|/c,\boldsymbol{x}')}{|\boldsymbol{x}-\boldsymbol{x}'|}\,d^3x', \end{aligned} \tag{11.50}$$

with G_{ret} defined in (11.42).

Background and Further Reading

Much of this chapter is based on the presentations in Jackson [41], Garg [31], and Wald [74]. Further useful discussion may be found in Refs. [23, 33, 77, 72]. The quite interesting history of Maxwell's original formulation of his equations, and their subsequent evolution in notation and interpretation under the influence of Oliver Heaviside, G. F. Fitzgerald, Oliver Lodge, J. W. Gibbs, and others may be found in Hunt [39].

Problems

11.1 One of the most useful aspects of Fourier transforms is that differentiation in real space corresponds to multiplication by a factor ik in Fourier transform space, which converts differential equations into algebraic equations. As an example, prove that

$$\widehat{\frac{dF}{dx}}\,(k) = ik\,\hat{F}(k),$$

for the Fourier transform of dF/dx. ***

11.2 Supply and explain the steps in verifying the result of Eq. (11.41).

11.3 Prove that Eqs. (11.47) are consistent with the Lorenz gauge condition (11.11). ***

11.4 For problems with a magnetic field oriented along the z axis, two gauge choices that can be made for the vector potential $\boldsymbol{A} = (A_x, A_y, A_z)$ are

$$\boldsymbol{A} = (0,\, Bx,\, 0) \qquad \text{(Landau gauge)},$$
$$\boldsymbol{A} = \frac{1}{2}\,B(-y,\, x,\, 0) \qquad \text{(Symmetric gauge)}.$$

Demonstrate that both of these gauges lead to the same magnetic field $\boldsymbol{B} = (B_x, B_y, B_z) = (0, 0, B)$, where $B = |\boldsymbol{B}|$.

11.5 Demonstrate by explicit calculation that a local gauge transformation,

$$\boldsymbol{A}'(\boldsymbol{x}, t) = \boldsymbol{A}(\boldsymbol{x}, t) + \boldsymbol{\nabla}\chi(\boldsymbol{x}, t) \qquad \Phi'(\boldsymbol{x}, t) = \Phi(\boldsymbol{x}, t) - \frac{\partial\chi(\boldsymbol{x}, t)}{\partial t}$$

on the vector and scalar potentials has no effect on the corresponding electric and magnetic fields entering the Maxwell equations.

Numerical and GenAI Problems

12 Symmetries and Conservation Laws

In Box 1.1 we summarized concisely the symmetries that the equations of classical electromagnetism exhibit. In this chapter we elaborate on the corresponding conservation laws that are implied by the symmetries of the Maxwell equations. The prototype conservation law in electromagnetism is charge conservation, exmplified in the continuity equation (1.3)

$$\frac{\partial \rho}{\partial t} + \boldsymbol{\nabla} \cdot \boldsymbol{J} = 0 \qquad \text{(Continuity equation)},$$

discussed in Section 1.3, which relates the change of charge density in a local region to flow of charge through the boundaries of that region. Various other electromagnetic conservation laws can be formulated in a similar manner.

12.1 Conservation of Charge

12.2 Conservation of Energy

12.3 Conservation of Momentum

12.4 Conservation of Angular Momentum

12.5 Noether's Theorem

This section is under construction.

No problems yet for this chapter.

13 Electromagnetic Waves in Vacuum

Perhaps the aspect of classical electromagnetism with the greatest everyday import is that the Maxwell equations have wave solutions that can propagate through space carrying energy, momentum, and angular momentum at the speed of light. The continuous flow of life-sustaining energy from the Sun, your smartphone, and the satellite navigation system in your car are but a few implications. These propagating fields are termed *free fields*, because the electric field lines do not terminate in charges and the magnetic field lines do not encircle current. In the 19th century it was commonly held that waves required a medium for transmission, based on experience with waves like those in water that *did* propagate through a medium. Thus was hypothesized a medium specifically for transmission of the electromagnetic waves predicted by Maxwell's theory that was called the *luminiferous aether* or just *aether* for short,[1] and electromagnetic waves were hypothesized to travel in a preferred inertial frame that was at rest with respect the aether. The aether hypothesis held sway for decades, but its death knell sounded from both observational and theoretical quarters as the 19th century turned into the 20th century:

1. The *Michelson–Morley light interferometry experiment* in 1887 found no evidence for motion of the Earth through the aether (absence of the hypothesized *aether drift*).
2. The publication of Einstein's *special theory of relativity* in 1905 rendered the aether superfluous, by asserting that there are no preferred inertial frames and that electromagnetic waves in vacuum traveled at a constant speed c *in every inertial frame*.

The idea that electromagnetic waves travel at the same speed in all inertial frames was radical, but correct, and special relativity implied that both electromagnetism and particle mechanics were governed by Lorentz invariance. With the aether now irrelevant, let us speak of it no more and consider electromagnetic waves, in vacuum, in this chapter, and then in matter in the following chapter.

13.1 The Classical Wave Equation

Wave phenomena in classical physics are described by a *wave equation*, which is a second-order partial differential equation that in one spatial dimension and cartesian coordinates

[1] To accomplish its task, while remaining faithful to the rest of observed reality, the aether was required to possess rather miraculous properties. It was assumed that the aether filled all of space but that it was invisible (since no one could see it), that it was rigid (because electromagnetic waves are transverse and normal transverse waves require a rigid body for transmission), and that it influenced only electromagnetic waves (so that it didn't disturb our understanding of non-electromagnetic phenomena).

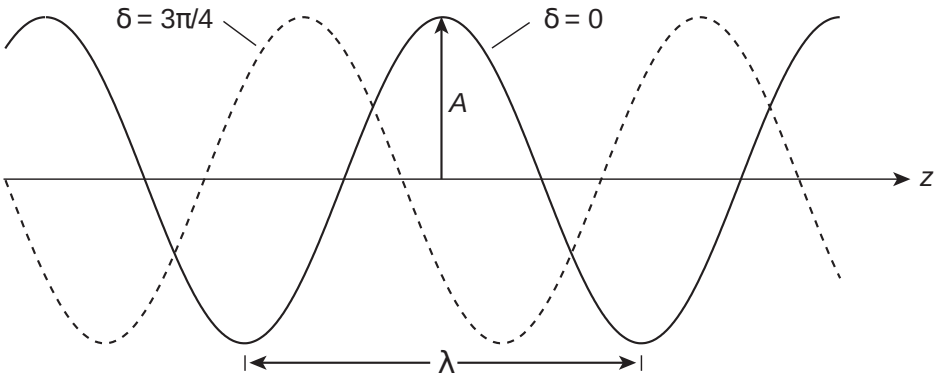

Fig. 13.1 Sinusoidal solutions (13.4) of a 1D wave equation with amplitude A and wavelength $\lambda = 2\pi$. The solid curve has phaseshift $\delta = 0$ and the dashed curve has a phaseshift $\delta = 3\pi/4$. The two waves have the same amplitude and wavelength, but they are shifted in phase by $3\pi/4$.

takes the form

$$\frac{\partial^2\psi(z,t)}{\partial x^2} - \frac{1}{v^2}\frac{\partial^2\psi(z,t)}{\partial t^2} = \mathcal{F}(z,t), \tag{13.1}$$

where $\psi(z,t)$ is a scalar field, v is the speed of the wave,[2] and we have allowed the possibility of a source term $\mathcal{F}(z,t)$. The 1D classical wave equation admits solutions of the form

$$\psi(z,t) = \psi(z \pm vt), \tag{13.2}$$

with the $\pm$ sign indicating whether the wave is traveling in the positive or negative z direction. The wave equation is linear, meaning that a sum of solutions is also a solution, and the most general 1D solution is of the form

$$\psi(z,t) = f(z+vt) + g(z-vt), \tag{13.3}$$

which represents a superposition of left-going (negative-z direction) and right-going (positive-z direction) waves.

Example 13.1 The sinusoidal waveform

$$\psi(z,t) = A\cos[k(z-vt)+\delta], \tag{13.4}$$

that is illustrated in Fig. 13.1 is a representative and instructive solution of the classical wave equation (13.1), both because many simple wave solutions have a similar form, and because complex waveforms can be built up by a linear combination of such waves (*Fourier series*). As illustrated in Fig. 13.1, the *amplitude* A is the maximum displacement

[2] Specifically v is the *phase velocity* of the wave described by the function ψ, which will depend on the nature of the wave. For example, for transverse waves on a string $v = (T/\mu)^{1/2}$, where T is the string tension and μ is the mass per unit length of the string, while we shall see that electromagnetic waves in vacuum propagate at the speed of light c.

of the wave. The argument of the cosine function is called the *phase* of the wave, and k is the *wave number*, which is related to the wavelength λ by

$$k = \frac{2\pi}{\lambda} \qquad \text{(Wavenumber)}, \tag{13.5}$$

with the wavelength displayed in Fig. 13.1. As illustrated in Fig. 13.1, if the wave is assumed to be propagating to the right in the positive x direction, the *phaseshift* δ represents a shift to the left (a delay) of the waveform. As time passes the the entire wave proceeds to the right in Fig. 13.1 with a constant speed v, such that a distance $\Delta x = 2\pi/k$ corresponds to one complete cycle of the cosine function, and one wavelength. At a fixed point x, the wave amplitude vibrates up and down, executing one complete cycle in a *period* T given by

$$T = \frac{2\pi}{kv}. \tag{13.6}$$

The corresponding *frequency* ν represents the number of oscillations per unit time and is given by

$$\nu = \frac{1}{T} = \frac{k\nu}{2\pi} = \frac{\nu}{\lambda}, \tag{13.7}$$

which may also be expressed as the *angular frequency* ω, with

$$\omega \equiv 2\pi\nu = k\nu, \tag{13.8}$$

which allows Eq. (13.4) to be written more concisely as

$$\psi(x,t) = A\cos(kz - \omega t + \delta). \tag{13.9}$$

It is sometimes useful to write a waveform in complex notation using the *Euler formula*,

$$e^{i\theta} = \cos\theta + i\sin\theta, \tag{13.10}$$

which allows writing Eq. (13.9) in the form

$$\psi(z,t) = \text{Re}\left(Ae^{i(kz-\omega t+\delta)}\right), \tag{13.11}$$

where $\text{Re}(\cdots)$ takes the real part of a complex argument.

Extending to three dimensions, Eq. (13.1) generalizes to the 3D wave equation

$$\left(\frac{\partial^2}{\partial x^2} + \frac{\partial^2}{\partial y^2} + \frac{\partial^2}{\partial z^2} - \frac{1}{c^2}\frac{\partial^2}{\partial t^2}\right)\psi(\boldsymbol{x}) = \mathcal{F}(\boldsymbol{x},t),, \tag{13.12}$$

which can be written in the compact form

$$\Box\,\psi(\boldsymbol{x}) = f, \tag{13.13}$$

by utilizing the d'Alembertian operator $\Box$ given in Eq. (11.25) and the Laplacian operator ∇^2 defined in Eq. (2.55),

$$\Box \equiv -\frac{1}{c^2}\frac{\partial^2}{\partial t^2} + \nabla^2 \qquad \nabla^2 = \frac{\partial^2}{\partial x^2} + \frac{\partial^2}{\partial y^2} + \frac{\partial^2}{\partial z^2}.$$

Let us now consider wave solutions of the Maxwell equations, first in vacuum, and then in medium.

13.2 Electromagnetic Waves in Vacuum

Electromagnetic waves are solutions of the Maxwell equations in the absence of sources. Removing the source terms ρ/ϵ_0 and $\mu_0 \boldsymbol{J}$ from the vacuum Maxwell equations (1.1) gives the *source-free Maxwell equations* in vacuum,

$$\boldsymbol{\nabla} \cdot \boldsymbol{E} = 0, \tag{13.14a}$$

$$\boldsymbol{\nabla} \times \boldsymbol{E} = -\frac{\partial \boldsymbol{B}}{\partial t}, \tag{13.14b}$$

$$\boldsymbol{\nabla} \cdot \boldsymbol{B} = 0, \tag{13.14c}$$

$$\boldsymbol{\nabla} \times \boldsymbol{B} = \frac{1}{c^2}\frac{\partial \boldsymbol{E}}{\partial t}. \tag{13.14d}$$

We may interpret these four equations in the following way:

1. The two equations (13.14b) and (13.14d) involving curls are coupled partial differential equations describing the time evolution of the electric field $\boldsymbol{E}(\boldsymbol{x}, t)$ and magnetic field $\boldsymbol{B}(\boldsymbol{x}, t)$, respectively.
2. The two equations (13.14a) and (13.14c) involving divergences provide initial conditions for the integration of (13.14b) and (13.14d), and we may deduce from them that

   $$\frac{\partial}{\partial t}\left(\boldsymbol{\nabla} \cdot \boldsymbol{E}\right) = 0 \qquad \frac{\partial}{\partial t}\left(\boldsymbol{\nabla} \cdot \boldsymbol{B}\right) = 0. \tag{13.15}$$

   Thus if the fields are free of divergence initially because of conditions set by Eqs. (13.14a) and (13.14c), they will remain divergence-free as time evolves in the integration because of Eq. (13.15).

We shall now show that there are solutions of the source-free Maxwell equations in vacuum (13.14) that are vector versions of the classical wave solution for a scalar field. However, these wave solutions for the $\boldsymbol{E}$ and $\boldsymbol{B}$ fields

1. are 3D vector fields, and
2. the vector $\boldsymbol{E}$ and $\boldsymbol{B}$ fields are not independent because they are coupled through one of the first-order Maxwell equations, for example the Faraday equation (13.14b).

Thus the physics of electromagnetic wave solutions may be expected to be much richer than that of a scalar wave equation.

13.2.1 Wave Equations for the Fields

First, applying the curl operation to Eq. (13.14b) and using the vector identity of Eq. (A.8),

$$\boldsymbol{\nabla} \times (\boldsymbol{\nabla} \times \boldsymbol{A}) = \boldsymbol{\nabla}(\boldsymbol{\nabla} \cdot \boldsymbol{A}) - \nabla^2 \boldsymbol{A}, \tag{13.16}$$

we obtain

$$\boldsymbol{\nabla}\times(\boldsymbol{\nabla}\times\boldsymbol{E}) = \boldsymbol{\nabla}(\boldsymbol{\nabla}\cdot\boldsymbol{E}) - \nabla^2\boldsymbol{E} = -\boldsymbol{\nabla}\times\left(\frac{\partial\boldsymbol{B}}{\partial t}\right)$$
$$= -\frac{\partial}{\partial t}(\boldsymbol{\nabla}\times\boldsymbol{B}) = -\frac{1}{c^2}\frac{\partial^2\boldsymbol{E}}{\partial t^2},$$

where Eq. (13.14d) was used in the last step. Thus,

$$\boldsymbol{\nabla}(\boldsymbol{\nabla}\cdot\boldsymbol{E}) - \nabla^2\boldsymbol{E} = -\frac{1}{c^2}\frac{\partial^2\boldsymbol{E}}{\partial t^2}.$$

But from the 1st vacuum Maxwell equation $\boldsymbol{\nabla}\cdot\boldsymbol{E} = 0$, and we obtain finally,

$$\nabla^2\boldsymbol{E} = \frac{1}{c^2}\frac{\partial^2\boldsymbol{E}}{\partial t^2}, \tag{13.17}$$

Next apply the curl operation to Eq. (13.14d) and use the identity (13.16) to obtain in a similar manner

$$\boldsymbol{\nabla}\times(\boldsymbol{\nabla}\times\boldsymbol{B}) = \boldsymbol{\nabla}(\boldsymbol{\nabla}\cdot\boldsymbol{B}) - \nabla^2\boldsymbol{B} = \frac{1}{c^2}\boldsymbol{\nabla}\times\left(\frac{\partial\boldsymbol{E}}{\partial t}\right)$$
$$= \frac{1}{c^2}\frac{\partial}{\partial t}(\boldsymbol{\nabla}\times\boldsymbol{E}) = -\frac{1}{c^2}\frac{\partial^2\boldsymbol{B}}{\partial t^2},$$

where Eq. (13.14b) was used in the last step. But from the 3rd vacuum Maxwell equation, $\boldsymbol{\nabla}\cdot\boldsymbol{B} = 0$, and we obtain

$$\nabla^2\boldsymbol{B} = \frac{1}{c^2}\frac{\partial^2\boldsymbol{B}}{\partial t^2}. \tag{13.18}$$

Finally, collecting the results in Eqs. (13.17) and (13.18), the wave solutions of the Maxwell equations are expressed by

$$\nabla^2\boldsymbol{E} - \frac{1}{c^2}\frac{\partial^2\boldsymbol{E}}{\partial t^2} = 0, \tag{13.19a}$$

$$\nabla^2\boldsymbol{B} - \frac{1}{c^2}\frac{\partial^2\boldsymbol{B}}{\partial t^2} = 0, \tag{13.19b}$$

from which one sees that each cartesian component of $\boldsymbol{E}$ and $\boldsymbol{B}$ satisfies a scalar wave equation of the form (13.1) with no source term ($\mathcal{F} = 0$). Thus the coupled first-order Maxwell equations (13.14b) and (13.14d) have been decoupled in the vector wave equations (13.19), but at a price of the decoupled equations becoming second-order PDEs.[3]

Equations (13.19) indicate that each cartesian component of $\boldsymbol{E}(\boldsymbol{x},t)$ and $\boldsymbol{B}(\boldsymbol{x},t)$ satisfies a scalar wave equation of the form (13.1), but this is no longer true in spherical or cylindrical coordinates. Functions that happen to satisfy Eqs. (13.19) are not automatically guaranteed to be solutions of the Maxwell equations (13.19); they only describe valid electric and magnetic fields if they satisfy also the divergence conditions of Eqs.

[3] Note that the wave equations (13.19) require second derivatives of the fields, which appear only because of the displacement term $(1/c^2)\partial\boldsymbol{E}/\partial t$ that Maxwell added to Ampère's law to convert it into the Ampère–Maxwell law given in Eq. (13.14d). Thus one of the several fundamental consequences following from Maxwell's modification of Ampère's law that were discussed in Section 11.1.2 is the existence of electromagnetic wave solutions of the Maxwell equations that we have just found.

(13.14a) and (13.14c), and satisfy Eqs. (13.14b) and (13.14d) when coupled together. These Maxwell-equation constraints are easy to demonstrate for simple plane-wave solutions of Eqs. (13.19), but more difficult for more complicated situations such as spherical waves or beam-like solutions. In such cases it may be simpler to use a set of wave equations based on the electromagnetic potentials rather than the fields, as illustrated in the next section.

13.2.2 Wave Equations for Potentials

An uncoupled description of electromagnetic waves can be obtained using the potentials rather than the fields. The gauge ambiguity requires that we choose a gauge to work in; we shall illustrate for the two most common choices, the Coulomb gauge and the Lorenz gauge.

Coulomb Gauge: For example, if we work in Coulomb gauge the gauge constraint $\boldsymbol{\nabla}\cdot\boldsymbol{A} = 0$ of Eq. (8.37) for the vector potential $\boldsymbol{A}$ implies that $\nabla^2\Phi = 0$, which has a solution $\Phi = 0$, and the electric field in the presence of a vector potential is the electrostatic result given in Eq. (2.35) minus a time derivative of the vector potential:

$$\boldsymbol{E} = -\boldsymbol{\nabla}\Phi - \frac{\partial \boldsymbol{A}}{\partial t}. \tag{13.20}$$

Thus, substituting

$$\boldsymbol{B} = \boldsymbol{\nabla}\times\boldsymbol{A} \qquad \boldsymbol{E} = -\frac{1}{c}\frac{\partial \boldsymbol{A}}{\partial t}.$$

into the Faraday law (13.14b) and applying $\boldsymbol{\nabla}\cdot\boldsymbol{A} = 0$ once again gives

$$\nabla^2\boldsymbol{A} - \frac{1}{c^2}\frac{\partial^2\boldsymbol{A}}{\partial t^2} = 0, \tag{13.21}$$

which can be solved for $\boldsymbol{A}$ and the electric and magnetic fields can then be obtained by applying the $\partial/\partial t$ and curl operations to $\boldsymbol{A}$.

Lorenz Gauge: In a similar way, the Lorenz gauge condition of Eq. (11.11)

$$\boldsymbol{\nabla}\cdot\boldsymbol{A} + \frac{1}{c^2}\frac{\partial\Phi}{\partial t} = 0, \tag{13.22}$$

can be used to deduce the wave equations

$$\nabla^2\Phi - \frac{1}{c^2}\frac{\partial^2\Phi}{\partial t^2} = 0, \tag{13.23}$$

$$\nabla^2\boldsymbol{A} - \frac{1}{c^2}\frac{\partial^2\boldsymbol{A}}{\partial t^2} = 0, \tag{13.24}$$

for the scalar potential Φ and vector potential $\boldsymbol{A}$ in Lorenz gauge.

13.2.3 Monochromatic Plane-Wave Solutions

Comparing Eqs. (13.1) and (13.19), we may interpret the solutions of Eqs. (13.19) as waves in the electric and magnetic fields propagating at the speed of light c in vacuum, with the

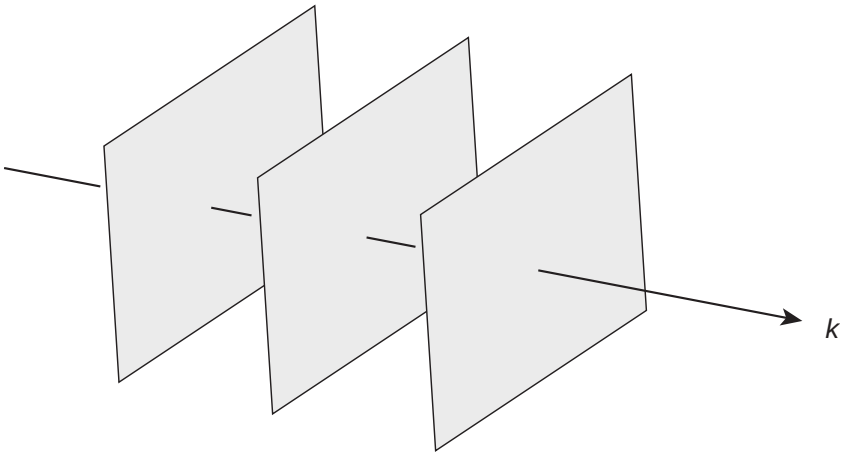

Fig. 13.2 For a plane wave the fields are constant on any plane transverse to the direction of propagation given by $\boldsymbol{k}$.

wavespeed c arising because of the relationship in Eq. (2.4) between the SI constants ϵ_0 and μ_0, and the speed of light,

$$c = \frac{1}{\sqrt{\epsilon_0 \mu_0}} = 3.0 \times 10^8 \,\mathrm{m\,s^{-1}}. \tag{13.25}$$

The essential nature of these wave solutions may be illustrated by considering sinusoidal waves of a single angular frequency ω (monochromatic waves), since more complex waveforms correspond to a Fourier superposition of such waves. We assume these monochromatic and sinusoidal waves to propagate in the positive-z, direction, and assume them to be *plane-waves* (no x and y dependence); so-called, because the fields are uniform over a plane perpendicular to the direction of propagation,[4] as illustrated schematically in Fig. 13.2. For plane waves the wave equations for $\boldsymbol{E}$ and $\boldsymbol{B}$ can be solved directly relatively easily as in Section 13.2.1, so it isn't necessary to solve for the potentials first, as in Section 13.2.2.

Using the exponential notation introduced in Eq. (13.11), the fields $\boldsymbol{E}$ and $\boldsymbol{B}$ corresponding to wave solutions of Eqs. (13.19) may be expressed in the general form,

$$\boldsymbol{E}(\boldsymbol{x}, t) = \boldsymbol{\mathcal{E}}_0 e^{i(\boldsymbol{k}\cdot\boldsymbol{x} - \omega t)}, \tag{13.26a}$$

$$\boldsymbol{B}(\boldsymbol{x}, t) = \boldsymbol{\mathcal{B}}_0 e^{i(\boldsymbol{k}\cdot\boldsymbol{x} - \omega t)}, \tag{13.26b}$$

where $\boldsymbol{\mathcal{E}}_0$ and $\boldsymbol{\mathcal{B}}_0$ are complex vectors [that have absorbed the phaseshift δ of Eq. (13.4)], and $\boldsymbol{k}$ is the *wavevector*, with

$$\boldsymbol{k} = \frac{\omega}{c}\hat{\boldsymbol{n}} \qquad \boldsymbol{\mathcal{E}}_0 \perp \hat{\boldsymbol{n}} \qquad \boldsymbol{\mathcal{B}}_0 = \hat{\boldsymbol{k}} \times \boldsymbol{\mathcal{E}}_0, \tag{13.27}$$

where $\hat{\boldsymbol{n}}$ is the direction of wave propagation. Generally every solution of the Maxwell equations satisfies Eqs. (13.26), but not every solution of Eqs. (13.26) is consistent with the

[4] Monochromatic plane waves are a fiction, since no physical wave can have infinite extent. However, they are a useful fiction because (1) they are simple mathematically, (2) realistic waves often resemble plane waves in a local-enough region, and (3) linear combinations of plane waves can approximate physical waves.

Maxwell equations, which impose additional constraints. Taking the wave propagation direction to be along the z-axis, from Eq. (13.19a) the wave equation for the z component of $\boldsymbol{E}$ is

$$\frac{\partial^2 E_z}{\partial z^2} - \frac{1}{c^2}\frac{\partial^2 E_z}{\partial t^2} = 0, \tag{13.28}$$

and the constraint $\boldsymbol{\nabla} \cdot \boldsymbol{E} = 0$ of Eq. (13.14a) imposes $\partial E_z/\partial t = 0$, so E_z is independent of z and the wave equation (13.28) reduces to

$$\frac{\partial^2 E_z}{\partial t^2} = 0. \tag{13.29}$$

Integrating gives $E_z = at + b$, where a and b are constants. The first term at can be discarded as unphysical because it grows in time without bound, leaving E_z equal to a constant, which we choose to be zero. By a similar procedure, we can choose $B_z = 0$. Therefore,

$$E_z = B_z = 0. \tag{13.30}$$

In addition, Faraday's law requires a relationship between electric and magnetic fields,

$$\boldsymbol{B}(\boldsymbol{x}, t) = \frac{1}{c}\,\hat{\boldsymbol{n}} \times \boldsymbol{E}(\boldsymbol{x}, t). \tag{13.31}$$

where $\hat{\boldsymbol{n}}$ is the direction of wave propagation. In summary, for a plane wave traveling in the direction $\hat{\boldsymbol{n}}$,

$$\boldsymbol{E} \perp \hat{\boldsymbol{n}} \qquad \boldsymbol{B} \perp \hat{\boldsymbol{n}} \qquad \boldsymbol{B}(\boldsymbol{x}, t) = \frac{1}{c}\,\hat{\boldsymbol{n}} \times \boldsymbol{E}(\boldsymbol{x}, t). \tag{13.32}$$

These results indicate that

1. electromagetic waves are *transverse:* oscillations in the electric and magnetic fields are
   - perpendicular to the direction of wave propagation,
   - perpendicular to each other, and
   - in phase with each other.
2. The fields $\boldsymbol{B}$ scaled by a factor of c and $\boldsymbol{E}$ have the same magnitude at all points of spacetime, $B_0 = E_0/c$.

A transverse electromagnetic field propagating in the vacuum along the z-axis with the electric field oscillating in the $x - z$ plane is illustrated schematically in Fig. 13.3.

13.2.4 Energy and Momentum

From Ch. 12, the general expression for the energy density u associated with an electromagnetic wave is

$$u = \frac{1}{2}\left(\epsilon_0 E^2 + \frac{1}{\mu_0} B^2\right), \tag{13.33}$$

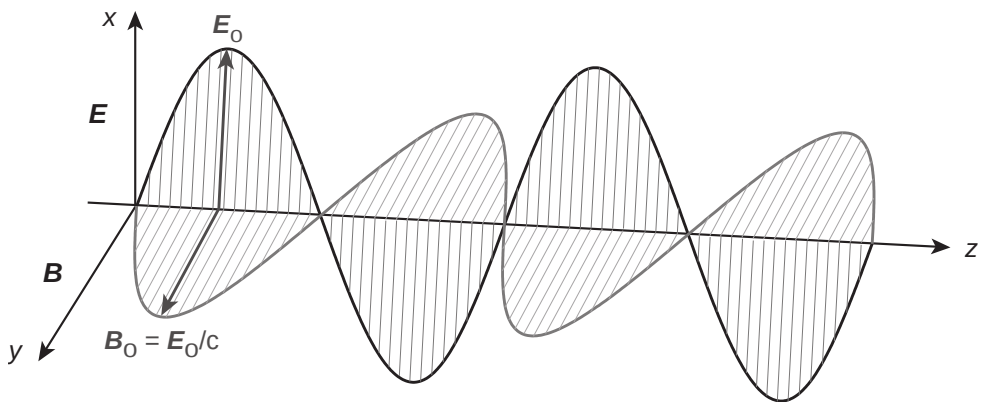

Fig. 13.3 An electromagnetic wave in vacuum propagating along the z axis. The electric field $\boldsymbol{E}$ oscillates sinusoidally in the $x-z$ plane, implying that the magnetic field $\boldsymbol{B}$ oscillates sinusoidally in the $y-z$ plane, in phase with the electric field, with the strength of the waves related by $cB_0 = E_0$ at each spacetime point.

where E and B are the magnitudes of the electric and magnetic fields, respectivley. From Eq. (13.32), for monochromatic plane waves

$$B^2 = \frac{1}{c^2}E^2 = \mu_0\epsilon_0 E^2, \tag{13.34}$$

and the contributions of the electric and magnetic fields to the energy density are equal,

$$\begin{aligned} u = \epsilon_0 E^2 &= \epsilon_0 \left(\mathrm{Re} E_0 e^{i(kz-\omega t+\delta)}\right)^2 \\ &= \epsilon_0 E_0^2 \cos^2(kz-\omega t+\delta). \end{aligned} \tag{13.35}$$

The energy flux density associated with an electromagnetic wave (energy per unit area per unit time) is given by the Poynting vector

$$\boldsymbol{S} = \frac{1}{\mu_0}(\boldsymbol{E}\times\boldsymbol{B}), \tag{13.36}$$

and for a monochromatic plane wave propagating in the z-direction,

$$\boldsymbol{S} = c\epsilon_0 E_0^2 \cos^2(kz-\omega t+\delta)\hat{\boldsymbol{z}} = cu\hat{\boldsymbol{z}}. \tag{13.37}$$

The corresponding momentum density is

$$\boldsymbol{g} = \frac{1}{c^2}\boldsymbol{S}, \tag{13.38}$$

and for monochromatic plane waves propagating in the $\hat{\boldsymbol{z}}$ direction,

$$\boldsymbol{g} = \frac{1}{c}\epsilon_0 E_0^2 \cos^2(kz-\omega t+\delta)\hat{\boldsymbol{z}} = \frac{1}{c}u\,\hat{\boldsymbol{z}}. \tag{13.39}$$

Typically for electromagnetic waves the period is so short[5] that any macroscopic measurement will encompass many cycles and for energy and momentum densities we are

[5] For example, in the visible spectrum the characteristic wavelength of yellow light is $\sim 6\times10^{-7}$ m, corresponding to a frequency of $\sim 5\times10^{-14}$ Hz.

interested in their average value over a cycle. The average of the rapidly oscillating cosine squared function over one period is

$$\langle \cos^2(kz - 2\pi t/T + \delta)\rangle = \frac{1}{T}\int_0^T \cos^2(kz - 2\pi t/T + \delta)dt = \frac{1}{2}, \tag{13.40}$$

where $\langle\ \rangle$ denotes the average over one cycle. Thus, the energy density, Poynting vector, and momentum density averaged over one cycle become

$$\langle u\rangle = \frac{1}{2}\epsilon_0 E_0^2, \tag{13.41}$$

$$\langle \boldsymbol{S}\rangle = \frac{1}{2}c\epsilon_0 E_0^2\,\hat{\boldsymbol{z}}, \tag{13.42}$$

$$\langle \boldsymbol{g}\rangle = \frac{1}{2c}\epsilon_0 E_0^2\,\hat{\boldsymbol{z}}, \tag{13.43}$$

for a wave propagating in the $\hat{\boldsymbol{z}}$ direction.

13.3 Polarization of Electromagnetic Waves

The polarization of an electromagnetic wave characterizes the orientation of its field vectors over time. This polarization can be measured (see Section 13.3.6) and is often of considerable physical interest, since the polarization carries information about how the wave was formed, and about the environments that it has encountered while propagating from the source.[6] By convention, the polarization of electromagnetic waves is defined by the plane in which the electric field $\boldsymbol{E}$ is oscillating, as illustrated in Fig. 13.4.

13.3.1 The Polarization Ellipse

Restricting consideration to monochromatic plane electromagnetic waves propagating in vacuum, we shall now show that as the phase of the wave advances by 2π, the tip of the electric field vector traces out an ellipse in the plane perpendicular to the propagation direction $\boldsymbol{k}$ that is called the *polarization ellipse*. Let us define real unit vectors $\hat{\boldsymbol{\epsilon}}_1$ and $\hat{\boldsymbol{\epsilon}}_2$ such that $(\hat{\boldsymbol{\epsilon}}_1, \hat{\boldsymbol{\epsilon}}_2, \hat{\boldsymbol{k}})$ constitutes a right-handed orthogonal triad,

$$\hat{\boldsymbol{\epsilon}}_1 \cdot \hat{\boldsymbol{\epsilon}}_2 = 0 \qquad \hat{\boldsymbol{\epsilon}}_1 \times \hat{\boldsymbol{\epsilon}}_2 = \hat{\boldsymbol{k}}. \tag{13.44}$$

The vectors $(\hat{\boldsymbol{\epsilon}}_1, \hat{\boldsymbol{\epsilon}}_2)$ constitute a polarization basis for $\boldsymbol{\mathcal{E}}_0$ in Eq. (13.26a) and the electric field may be expressed as

$$\boldsymbol{E}(\boldsymbol{x}, t) = (\mathcal{E}_1\hat{\boldsymbol{\epsilon}}_1 + \mathcal{E}_2\hat{\boldsymbol{\epsilon}}_2)\, e^{i(\boldsymbol{k}\cdot\boldsymbol{x} - \omega t)}, \tag{13.45}$$

[6] For example, the polarization of the cosmic microwave background (CMB) radiation that is observed coming from all directions in the sky by satellite observatories provides a key test for cosmological theories of the origin of the Universe, since the CMB is thought to be the cooling remnant of the big bang itself. It has also been proposed that the CMB may carry a polarization imprint of perturbations due to gravitational waves produced in the big bang.

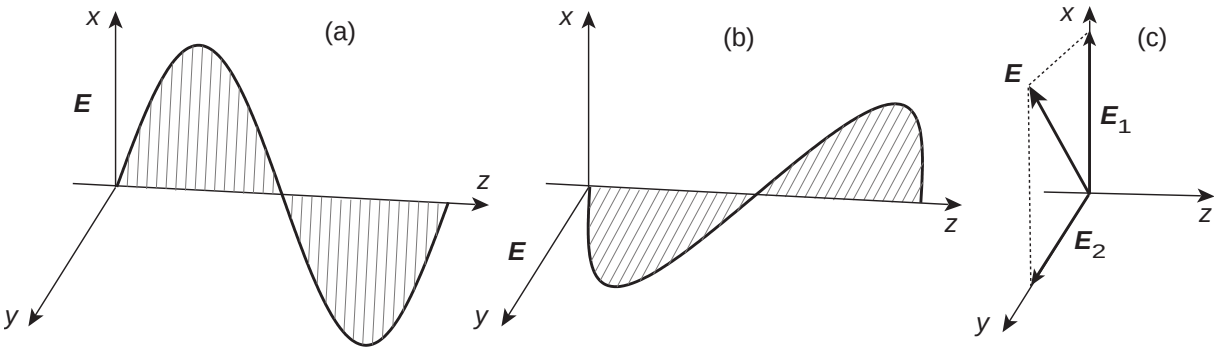

Fig. 13.4 Polarization of transverse electromagnetic wave propagating in the positive z direction. (a) "Vertical" polarization of electric field in the $x-z$ plane. (b) "Horizontal" polarization of electric field in the $y-z$ plane. These are examples of linear or plane polarization. (c) General polarization defined by plane of the electric field vibrations, which can be resolved into two mutually perpendicular components, $\boldsymbol{E}_1$ and $\boldsymbol{E}_2$.

where the complex numbers $\mathcal{E}_1$ and $\mathcal{E}_2$ may be parameterized as

$$\mathcal{E}_1 = Ae^{i\delta_1} \qquad \mathcal{E}_2 = Be^{i\delta_2}, \tag{13.46}$$

in terms of the real numbers A, B, δ_1, and δ_2. Then

$$\mathrm{Re}\boldsymbol{E} = A\cos(\phi+\delta_1)\hat{\boldsymbol{\epsilon}}_1 + B\cos(\phi+\delta_2)\hat{\boldsymbol{\epsilon}}_2 \equiv E_1\hat{\boldsymbol{\epsilon}}_1 + E_2\hat{\boldsymbol{\epsilon}}_2, \tag{13.47}$$

where we have defined

$$\phi \equiv \boldsymbol{k}\cdot\boldsymbol{x} - \omega t, \tag{13.48}$$

and it may be shown (Problem 13.1) that Eqs. (13.45)-(13.48) imply that

$$\left(\frac{E_1}{A}\right)^2 + \left(\frac{E_2}{B}\right)^2 - 2\left(\frac{E_1}{A}\right)\left(\frac{E_2}{B}\right)\cos\delta = \sin^2\delta, \tag{13.49}$$

where we define

$$\delta \equiv \delta_2 - \delta_1. \tag{13.50}$$

Equation (13.49) specifies an ellipse in the $\hat{\boldsymbol{\epsilon}}_1 - \hat{\boldsymbol{\epsilon}}_2$ plane, with the eccentricity and orientation of the ellipse determined by the parameters δ and the ratio B/A. All possible polarizations of a monochromatic, plane electromagnetic wave in vacuum are then described by the polarization ellipse (13.49) with arbitrary values of parameters.

There are some special cases of the general polarization ellipse of Eq. (13.49) corresponding to two limits of the eccentricity e of an ellipse (which lies between 0 and 1, by definition) that are of note. The first is that the limit of an ellipse as $e \to 1$ is a straight line. The second is that an ellipse becomes a circle in the limit that $e \to 0$. Let us now discuss these two special cases.

13.3.2 Linear (Plane) Polarization

The ellipse described by Eq. (13.49) becomes a straight line if the orthogonal electric field components have the same phase or are 180° out of phase, which corresponds to the restriction

$$\delta = \delta_2 - \delta_1 = m\pi \qquad (m = 0, 1, 2, ...). \tag{13.51}$$

This special case corresponds to *linear (or plane) polarization*, because the electric field vector for a linearly polarized electromagnetic wave points in the *same direction for all values of* $\boldsymbol{x}$ *and* t [see Problem 13.2(a)]. The waves in Figs. 13.4(a) and 13.4(b) are examples of such *plane-polarized* waves. Any plane-polarized wave can be decomposed into a sum of two components that are plane-polarized in mutually perpendicular directions and that have the same phase. In Fig. 13.4(c), $\boldsymbol{E}$ has been resolved into two mutually perpendicular x and y components, $\boldsymbol{E}_1$ and $\boldsymbol{E}_2$, respectively, that have the same phase.

13.3.3 Circular Polarization

The other special case of Eq. (13.49) of specific interest is that an ellipse becomes a circle in the limit that the eccentricity tends to zero. If two plane-polarized waves that differ in phase are added, the maxima of $\boldsymbol{E}_1$ and $\boldsymbol{E}_2$ occur at different times and the tip of the vector $\boldsymbol{E}$ describes an ellipse as the phase of the wave advances by 2π; such a wave is described by the general ellipse (13.49) with arbitrary parameter values and is said to have *elliptical polarization*. As we have seen, if the phases of the two components are made equivalent the ellipse degenerates to a straight line corresponding to plane polarization. However, if $\boldsymbol{E}_1$ and $\boldsymbol{E}_2$ have the same amplitudes but are out of phase by $\pm\frac{\pi}{2}$, the ellipse becomes a circle and the wave is said to be *circularly polarized*. If the orthogonal field components are 90° out of phase but of equal amplitude,

$$\mathcal{A} \equiv \sqrt{2}A = \sqrt{2}B \qquad \delta = \delta_2 - \delta_1 = \frac{m\pi}{2} \qquad (m = \pm 1, \pm 3, ...). \tag{13.52}$$

Then, as you are asked to show in Problem 13.2(b), the wave is described in a plane containing $\boldsymbol{x}$ by

$$\mathrm{Re}[\boldsymbol{E}_{\pm}(0, t)] = \frac{\mathcal{A}}{\sqrt{2}}(\hat{\boldsymbol{\epsilon}}_1 \cos\omega t \pm \hat{\boldsymbol{\epsilon}}_2 \sin\omega t). \tag{13.53}$$

As illustrated in Fig. 13.5, for the corresponding circularly polarized light the tip of the electric field vector executes a spiraling motion as the wave advances. Because of the sign ambiguity in Eq. (13.53), for a circularly polarized wave the tip of the electric field vector rotates clockwise or counterclockwise in a circle as the wave propagates. For an *observer looking toward the source*, we define the wave to be

1. *right circularly polarized (RCP)* if the vector $\boldsymbol{E}$ rotates clockwise as the wave propagates, and
2. *left circularly polarized (LCP)* if it rotates counterclockwise.

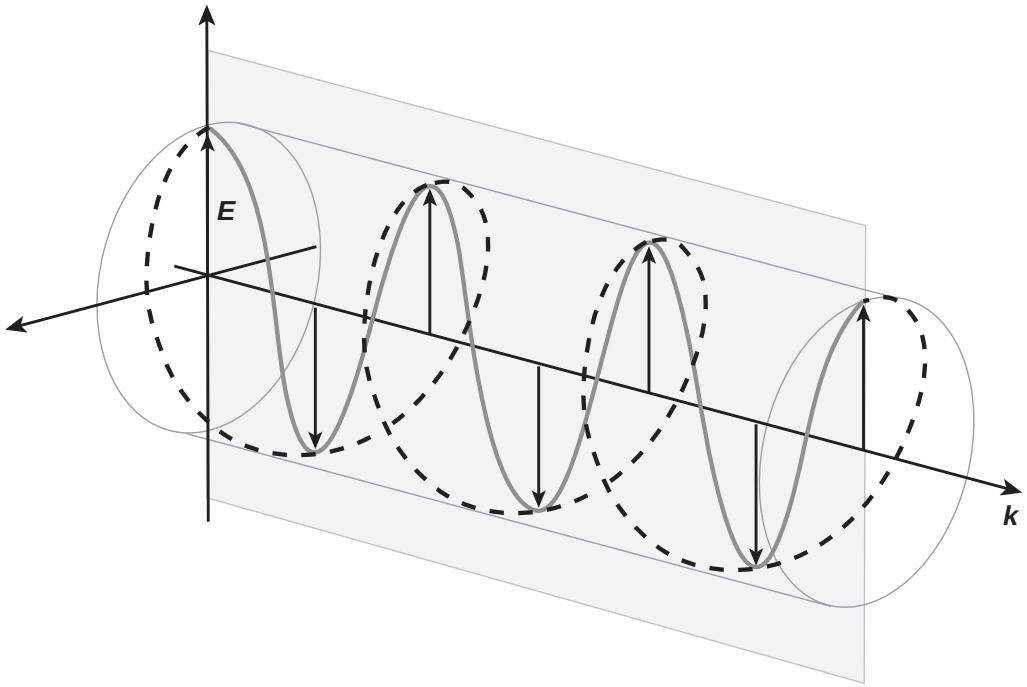

Fig. 13.5

Snapshot at fixed time of $\boldsymbol{E}(x,0)$ of a monochromatic, circularly-polarized, plane wave propagating in the direction given by $\boldsymbol{k}$. The magnitude of the electric field is indicated by the solid gray curve. The tip of the $\boldsymbol{E}$ vector executes a spiral motion around the $\boldsymbol{k}$ axis as the wave propagates, as indicated by the dashed curve. This wave is left circularly polarized (LCP), since the sense of rotation is counterclockwise, as viewed in the direction of the source.

The wave in Fig. 13.5 is thus left circularly polarized (LCP), since for an observer looking toward the source $\boldsymbol{E}$ appears to be rotating counterclockwise. The corresponding RCP wave looks the same as Fig. 13.5, except that the sense of the spiral would be opposite because it would appear to be rotating clockwise for the same observer. In some subfields of physics such as optics a convention for LCP/RCP may be employed that reverses these definitions. Generally, in discussing LCP/RCP one must specify whether one is defining the sense of rotation by looking upstream at the source, or downstream toward the destination of the wave, since these points of view reverse the definitions. Here we define LCP/RCP by looking upstream at the source, with RCP corresponding to clockwise rotation and LCP to counterclockwise rotation of $\boldsymbol{E}$.

13.3.4 Circular Polarization Basis

It can be useful to combine the cartesian basis vectors $\hat{\boldsymbol{\epsilon}}_1$ and $\hat{\boldsymbol{\epsilon}}_2$ into the complex conjugate pairs

$$\hat{\boldsymbol{\epsilon}}_+ = \frac{1}{\sqrt{2}}(\hat{\boldsymbol{\epsilon}}_1 + i\hat{\boldsymbol{\epsilon}}_2) \qquad \hat{\boldsymbol{\epsilon}}_- = \frac{1}{\sqrt{2}}(\hat{\boldsymbol{\epsilon}}_1 - i\hat{\boldsymbol{\epsilon}}_2), \tag{13.54}$$

which satisfy the relations

$$\hat{\boldsymbol{\epsilon}}_{\pm}^{*}\hat{\boldsymbol{\epsilon}}_{\pm} = 1 \qquad \hat{\boldsymbol{\epsilon}}_{\pm}^{*} \cdot \hat{\boldsymbol{\epsilon}}_{\mp} = 0.$$

Equation (13.53) is the real part of the complex field (evaluated at $\boldsymbol{x} = 0$),

$$\boldsymbol{E}_{\pm}(\boldsymbol{x}, t) = \mathcal{A}\left(\frac{\hat{\boldsymbol{\epsilon}}_1 \pm i\hat{\boldsymbol{\epsilon}}_2}{\sqrt{2}}\right) e^{i(\boldsymbol{k}\cdot\boldsymbol{x}-\omega t)}, \tag{13.55}$$

so $\hat{\boldsymbol{\epsilon}}_{+}$ is a pure LCP wave and $\hat{\boldsymbol{\epsilon}}_{-}$ is a pure RCP wave. Thus the expansion

$$\boldsymbol{E}(\boldsymbol{x}, t) = \left(\mathcal{E}_{+}\hat{\boldsymbol{\epsilon}}_{+} + \mathcal{E}_{-}\hat{\boldsymbol{\epsilon}}_{-}\right) e^{i(\boldsymbol{k}\cdot\boldsymbol{x}-\omega t)}, \tag{13.56}$$

is just as legitimate as the expansion (13.45), and either of the orthogonal bases $(\hat{\boldsymbol{\epsilon}}_1, \hat{\boldsymbol{\epsilon}}_2)$ or $(\hat{\boldsymbol{\epsilon}}_{+}, \hat{\boldsymbol{\epsilon}}_{-})$ may be used to expand monochromatic plane waves in states of definite linear or circular polarization.

13.3.5 Helicity and Circular Polarization

The RCP/LCP labeling for circular polarization of light originates in the field of optics. In modern physics, it may be more natural to define circular polarization instead in terms of the projection of the angular momentum carried by the light wave on the axis of propagation, which is termed *helicity*.[7] With our convention of looking in the direction of the source at the oncoming wave,

1. *Left circular polarization (LCP)* corresponds to *positive helicity*, and a circular-polarization basis state

$$\hat{\boldsymbol{\epsilon}}_{+} = \frac{1}{\sqrt{2}}(\hat{\boldsymbol{\epsilon}}_1 + i\hat{\boldsymbol{\epsilon}}_2), \tag{13.57}$$

   which corresponds to a *positive projection* of the photon spin on the direction of propagation.
2. *Right circular polarization (RCP)* corresponds to *negative helicity*, and basis state

$$\hat{\boldsymbol{\epsilon}}_{-} = \frac{1}{\sqrt{2}}(\hat{\boldsymbol{\epsilon}}_1 - i\hat{\boldsymbol{\epsilon}}_2), \tag{13.58}$$

   which corresponds to a *negative projection* of the photon spin on the direction of propagation.

Our conventions and terminology for discussing circular polarization of light are given in Table 13.1.

[7] From quantum field theory we know that the quanta of electromagnetic radiation (photons) carry an intrinsic spin of $1\hbar$, and because photons are *massless* there are only two projection states on the propagation axis for the spin, $\pm 1\hbar$, which we can map to a helicity label $\pm$. A *massive* spin-1 particle would have three projection states: $0, \pm 1$. Understanding the reasons for this difference requires a detailed look at the spacetime symmetry of the Lorentz and Poincaré groups, which is well beyond our present scope, but we will remark that the gauge symmetry of electromagnetism that is a central theme of our discussion in this book can only exist because the photon is massless. The interested reader may find the relevant discussion of these matters in Chapters 13-15 of Ref. [38].

Table 13.1 Conventions for circularly polarized light

Label	Optical designation*	Helicity	Basis vector†
RCP	Right circular polarization	Negative helicity ($h=-1$)	$\epsilon_- = \epsilon_1 - i\epsilon_2$
LCP	Left circular polarization	Positive helicity ($h=+1$)	$\epsilon_+ = \epsilon_1 + i\epsilon_2$

*Observer assumed looking in direction of light source at oncoming wave.
†Expressed in terms of linear polarization basis (ϵ_1, ϵ_2).

13.3.6 Measuring Polarization: Stokes Parameters

At low frequencies the parameters A, B, and δ defining the polarization ellipse (13.49) can be extracted rather directly from data. At optical and higher frequencies it is usual to instead extract the polarization parameters from the *Stokes parameters* s_i, which are related to the parameters A, B, and δ of the polarization ellipse as follows.

$$\begin{aligned} s_0 &= A^2 + B^2 \qquad & s_1 &= A^2 - B^2, \\ s_2 &= 2AB\cos\delta \qquad & s_3 &= 2AB\sin\delta, \end{aligned} \tag{13.59}$$

with the constraint $s_0^2 = s_1^2 + s_2^2 + s_3^2$, so only three of the s_i are independent. The utility of the Stokes parameters is that each parameter is quadratic in the fields and can be related directly to wave intensities measured in different orthogonal bases. Consider the $\hat{\boldsymbol{\epsilon}}_1 - \hat{\boldsymbol{\epsilon}}_2$ coordinate system used in Eq. (13.45).

1. Let I_0 and I_{90} be intensities measured in detectors sensitive to horizontal and vertical linear polarizations, respectively, for the $\hat{\boldsymbol{\epsilon}}_1 - \hat{\boldsymbol{\epsilon}}_2$ coordinate system.
2. Let I_{+45} and I_{-45} be intensities measured in detectors sensitive to linear polarizations measured at angles ± 45 degrees, respectively, relative to the $\hat{\boldsymbol{\epsilon}}_1 - \hat{\boldsymbol{\epsilon}}_2$ axes.
3. Let I_{RCP} and I_{LCP} be intensities measured by detectors sensitive to right and left circular polarizations, respectively.

Then, as you are asked to prove in Problem 13.3,

$$\begin{aligned} s_0 &= I_0 + I_{90} \qquad & s_1 &= I_0 - I_{90}, \\ s_2 &= I_{+45} - I_{-45} \qquad & s_3 &= I_{\text{RCP}} - I_{\text{LCP}}. \end{aligned} \tag{13.60}$$

This shows that (1) *six intensity measurements* are sufficient to determine the amplitudes and phases of the complex electric field components E_1 and E_2 appearing in Eqs. (13.44) - (13.49), and that (2) a simple physical interpretation can be attached to each Stokes parameter:

1. s_0 is the total intensity.
2. s_1 indicates the preference for horizontal (+) over vertical (−) linear polarization.
3. s_2 indicates the preference for $+45^\circ$ over -45° linear polarization.
4. s_3 indicates the preference for right-circular (+) over left-circular (−) polarization.

It will prove useful later to assemble the four Stokes parameters s_i into a 4×1 column vector

$$\boldsymbol{S} = \begin{pmatrix} s_0 \\ s_1 \\ s_2 \\ s_3 \end{pmatrix} \tag{13.61}$$

that is called the *Stokes vector*, which parameterizes all possible states of polarization for light.

Example 13.2 A Stokes vector

$$\boldsymbol{S} = \begin{pmatrix} s_0 \\ s_1 \\ s_2 \\ s_3 \end{pmatrix} = \begin{pmatrix} 1 \\ 0 \\ 0 \\ 0 \end{pmatrix}$$

corresponds to completely unpolarized light. Reason:

1. s_1 measures the time-averged intensity of the wave; it must be a positive number if the wave exists.
2. s_1 measures the preference for horizontal over vertical linear polarization. Unpolarized light consists of rapidly and randomly shifting polarization states, the time-averaged intensity of the horizontal and vertical components cancel each other out and $s_1 = 0$ for unpolarized light.
3. s_2 measures the preference for $+45^\circ$ over -45° linear polarization. For the same reason as above, unpolarized light exhibits no bias toward either diagonal axis, resulting in $s_2 = 0$.
4. s_3 measures the preference for RCP over LCP. Unpolarized light has an equal probability of containing clockwise and counterclockwise rotational states over time, yielding a net zero difference, so $s_3 = 0$ for unpolarized light.

Hence a Stokes vector with $s_0 \neq 0$ and $s_1 = s_2 = s_3 = 0$ corresponds to completely unpolarized light.

13.3.7 The Poincaré Sphere

Mathematically, the Stokes parameters define a one-to-one relationship between each possible polarization state and a unique point on the surface of a 2-sphere of radius s_0 called the *Poincaré sphere*, which is illustrated in Fig. 13.6. The Stokes parameters map the polarization ellipse parameters A, B, and δ of Eq. (13.49) into a unique point on the Poincaré sphere.

1. *Linear polarization:* all states of linear polarization lie on the equator;
2. *Right circular polarization:* all RCP states lie at the south pole;

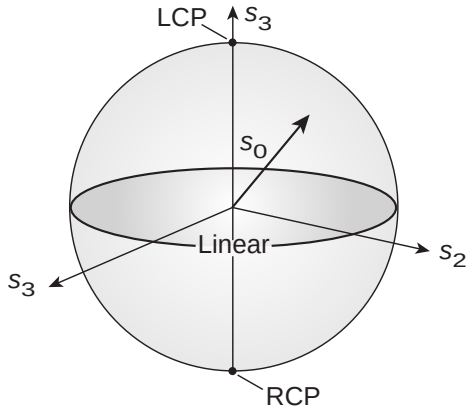

Fig. 13.6 A Poincaré sphere of radius s_0 that is in one-to-one correspondence with values of the Stokes parameters defined in Eqs. (13.59) and (13.60).

3. *Left circular polarization:* all LCP states lie at the north pole;
4. *Elliptical polarization:* all other points lying between the poles and the equator correspond to general elliptical polarization in Fig. 13.6.

Representation of polarization on the Poincaré sphere permits easy visualization of complex polarization changes, such as those that occur in fiber optics applications or upon passing through a polarizer. The sphere can also be animated, to track evolution of a polarization state.

13.3.8 The Mueller Matrix

In view of the Stokes vector defined in Eq. (13.61), it is natural to formulate the polarization of light as a linear algebra problem. The two most common matrix formalisms applied to light polarization are

1. *The Jones calculus,* which uses 2×2 complex matrices acting on the complex electric field vector. It is highly effective for tracking phase and interference, but it can only describe fully polarized light.
2. *The Mueller calculus,* which uses 4×4 real matrices (*Mueller matrix*) acting on intensities parameterized by the Stokes parameters. It can handle unpolarized or partially polarized light in addition to fully polarized light, because it works with time-averaged intensities rather than instantaneous fields.

Let us describe use of the Mueller calculus to track the effect of an optical element (polarizer, waveplate,[8] scattering medium, ...) on polarization of the light passing through

[8] A *waveplate* (also termed a *retarder*) is a transparent, birefringent (see Box 14.1) optical component that manipulates the polarization state of light by introducing a controlled phase shift between two orthogonal polarization components. By introducing this *retardance*, waveplates can change linearly polarized light to circular/elliptical polarization, or rotate the angle of linear polarization without altering the intensity or direction of the beam.

it. We define a *Mueller matrix* M that represents an optical element acting linearly on the Stokes vector $\boldsymbol{S}$ defined in Eq. (13.49) to convert it into a new Stokes vector $\boldsymbol{S}'$ with modified polarization: $\boldsymbol{S}' = M\boldsymbol{S}$. Explicitly,

$$\begin{pmatrix} s_0' \\ s_1' \\ s_2' \\ s_3' \end{pmatrix} = \begin{pmatrix} M_{00} & M_{01} & M_{02} & M_{03} \\ M_{10} & M_{11} & M_{12} & M_{13} \\ M_{20} & M_{21} & M_{22} & M_{23} \\ M_{30} & M_{31} & M_{32} & M_{33} \end{pmatrix} \begin{pmatrix} s_0 \\ s_1 \\ s_2 \\ s_3 \end{pmatrix}, \tag{13.62}$$

which transforms an input polarization state on the right side labeled by the Stokes parameters s_i into an output polarization state on the left side labeled by Stokes parameters s_i' that has been modified by an optical element represented by the matrix M.

Each of the 16 elements of the Mueller matrix has a physical interpretation. For example, M_{00} represents the unpolarized transmittance or reflectance of the optical element, and M_{10}, M_{20}, and M_{30}, describe the ability of the element to create polarized light from unpolarized light. For an ideal linear polarizer with its transmission axis oriented horizontally, the Mueller matrix is:

$$M_{\text{linear}} = \frac{1}{2} \begin{pmatrix} 1 & 1 & 0 & 0 \\ 1 & 1 & 0 & 0 \\ 0 & 0 & 0 & 0 \\ 0 & 0 & 0 & 0 \end{pmatrix}.$$

For an ideal quarter-wave plate (which introduces a 90° phase shift) with its fast axis horizontal, the Mueller matrix is

$$M_{\text{QWP}} = \begin{pmatrix} 1 & 0 & 0 & 0 \\ 0 & 1 & 0 & 0 \\ 0 & 0 & 0 & 0 \\ 0 & 0 & 0 & 1 \end{pmatrix}.$$

In more complex cases, such as reflection at a dielectric interface or scattering through a dusty medium—the Mueller matrix can become fully populated, describing a complex mixture of partial polarization, retardance, and attenuation.

Background and Further Reading

The discussion of polarization in this chapter is patterned loosely after the presentation in Zangwill [77].

Problems

13.1 Beginning from Eqs. (13.45)-(13.48), prove that the most general polarization of a monochromatic plane electromagnetic wave propagating in the vacuum is described by the polarization ellipse of Eq. (13.49).

13.2 (a) Show that for linearly (plane) polarized monochromatic plane electromagnetic waves the electric field vector points in the same fixed direction for all values of the coordinates $\boldsymbol{x}$ and t.

(b) Show that for circularly polarized monochromatic plane electromagnetic waves the electric field vector satisfies

$$\mathrm{Re}[\boldsymbol{E}_{\pm}(0,t)] = \frac{\mathcal{A}}{\sqrt{2}}(\hat{\boldsymbol{\epsilon}}_1 \cos\omega t \pm \hat{\boldsymbol{\epsilon}}_2 \sin\omega t),$$

where for circular polarization,

$$\mathcal{A} \equiv \sqrt{2}A = \sqrt{2}B \qquad \delta = \delta_2 - \delta_1 = \frac{m\pi}{2} \qquad (m = \pm 1, \pm 3, ...),$$

which corresponds to the spiral motion illustrated in Fig. 13.5.

13.3 Prove the relationships between measured intensities and the Stokes parameters given in Eq. (13.60).

13.4 Prove the dispersion relation (14.7). *Hint*: Take the curl of the relation $\boldsymbol{k} \times \boldsymbol{E} = \omega\mu\boldsymbol{H}$ given in Eq. (14.6b).

Numerical and GenAI Problems

14 Electromagnetic Waves in Matter

Having established the basic properties of electromagnetic waves propagating in vacuum in the preceding chapter, let us now turn to the behavior of those waves in the presence of matter. It will be useful to begin by considering the simplest possibility, where we assume that the electrical permittivity ϵ, magnetic permeability μ, and ohmic conductivity σ are all constant. Realistic matter is *frequency dispersive*, meaning that the permitivitty ϵ is a function of frequency $\epsilon = \epsilon(\omega)$, which means that plane waves propagate with different phase velocities if they have different frequencies. Nevertheless, it is useful to first consider simple matter, where if $\sigma = 0$ plane waves are *non-dispersive* and all frequencies travel at the same phase velocity, because many essential features of real matter are captured in a simple non-dispersive model. This is particularly true with respect to reflection, refraction, and interference effects occurring at the boundaries that separate different types of matter.

14.1 Electromagnetic Waves in Simple Matter

Wave propagation in linear, isotropic, non-dispersive matter looks superficially a lot like propagation in vacuum. The Maxwell equations in medium are

$$\boldsymbol{\nabla} \cdot \boldsymbol{D} = \rho, \tag{14.1a}$$

$$\boldsymbol{\nabla} \times \boldsymbol{E} = -\frac{\partial \boldsymbol{B}}{\partial t}, \tag{14.1b}$$

$$\boldsymbol{\nabla} \cdot \boldsymbol{B} = 0, \tag{14.1c}$$

$$\boldsymbol{\nabla} \times \boldsymbol{H} = \boldsymbol{J} + \frac{\partial \boldsymbol{D}}{\partial t}, \tag{14.1d}$$

where ρ is the free charge and $\boldsymbol{J}$ is the free current. For the present discussion we assume that there is no free charge and no free current, and furthermore assume the medium to be linear and homogeneous, obeying the equations

$$\boldsymbol{D} = \epsilon \boldsymbol{E} \qquad \boldsymbol{B} = \mu \boldsymbol{H}. \tag{14.2}$$

The constituitive relations (14.2) imply that there are only two independent fields, which we choose to be $\boldsymbol{E}$ and $\boldsymbol{H}$, with the polarization $\boldsymbol{P}$ and magnetization $\boldsymbol{M}$ of the medium then given by

$$\boldsymbol{P} = (\epsilon - \epsilon_0)\boldsymbol{E} \qquad \boldsymbol{M} = \left(\frac{\mu}{\mu_0} - 1\right)\boldsymbol{H}, \tag{14.3}$$

and the source-free Maxwell equations expressed in terms of $\boldsymbol{E}$ and $\boldsymbol{H}$ are

$$\boldsymbol{\nabla}\cdot\boldsymbol{E}=0 \qquad \boldsymbol{\nabla}\cdot\boldsymbol{H}=0, \tag{14.4a}$$

$$\boldsymbol{\nabla}\times\boldsymbol{E}=-\mu\frac{\partial\boldsymbol{H}}{\partial t} \qquad \boldsymbol{\nabla}\times\boldsymbol{H}=\epsilon\frac{\partial\boldsymbol{E}}{\partial t}. \tag{14.4b}$$

As in the discussion of waves in vacuum in Section 13.2.3, we assume as a starting point monochromatic plane waves,

$$\boldsymbol{E}(\boldsymbol{x},t)=\boldsymbol{E}e^{i(\boldsymbol{k}\cdot\boldsymbol{x}-\omega t)} \qquad \boldsymbol{H}(\boldsymbol{x},t)=\boldsymbol{H}e^{i(\boldsymbol{k}\cdot\boldsymbol{x}-\omega t)}, \tag{14.5}$$

which produces four constraints upon substitution in Eqs. (14.4),

$$\boldsymbol{k}\cdot\boldsymbol{E} \qquad \boldsymbol{k}\cdot\boldsymbol{H}=0, \tag{14.6a}$$

$$\boldsymbol{k}\times\boldsymbol{E}=\omega\mu\boldsymbol{H} \qquad \boldsymbol{k}\times\boldsymbol{H}=-\omega\epsilon\boldsymbol{E}. \tag{14.6b}$$

These imply that Eq. (14.5) corresponds to a transverse electromagnetic wave, so our discussion of polarization in Section 13.3 applies without modification. From Problem 13.4, the wave frequency ω is related to the wave vector $\boldsymbol{k}$ by a *dispersion relation*,

$$\omega(\boldsymbol{k})=\frac{c}{n}\,k, \tag{14.7}$$

where c is the speed of light and

$$n=c\sqrt{\mu\epsilon}. \tag{14.8}$$

is the *index of refraction.*

14.2 Reflection and Refraction at Interfaces

From general experience with waves, we expect that a plane electromagnetic wave incident on a sharp boundary between two different dielectric materials produces a reflected and a transmitted (refracted) wave if the wavelength is small compared with the curvature of the interface; Fig. 14.1 illustrates. At an introductory level this can be understood in terms of geometrical optics and ray tracing. Here we shall go beyond that and explore how the boundary conditions derived from kinematics of fields and the dynamics implied by the Maxwell equations lead to refraction, diffraction, absorption, and dispersion of electromagnetic waves.

In Fig. 14.1, $z=0$ is the boundary between Medium 1 characterized by parameters (ϵ_1,μ_1) and Medium 2 characterized by parameters (ϵ_1,μ_1). We may expect that at the boundary the incident wave splits into a reflected wave propagating in Medium 1 and a transmitted wave propagating in Medium 2. Therefore, the electric fields in the two media are given by

$$\boldsymbol{E}_2(\boldsymbol{x},t)=E_{\mathrm{T}}e^{i(\boldsymbol{k}_{\mathrm{T}}\cdot\boldsymbol{x}-\omega_{\mathrm{T}}t)} \qquad \text{(Medium 1)}, \tag{14.9a}$$

$$\boldsymbol{E}_1(\boldsymbol{x},t)=E_{\mathrm{I}}e^{i(\boldsymbol{k}_{\mathrm{I}}\cdot\boldsymbol{x}-\omega_{\mathrm{I}}t)}+E_{\mathrm{R}}e^{i(\boldsymbol{k}_{\mathrm{R}}\cdot\boldsymbol{x}-\omega_{\mathrm{R}}t)} \qquad \text{(Medium 2)}. \tag{14.9b}$$

When a plane wave is incident on a planar interface between two linear, isotropic, and

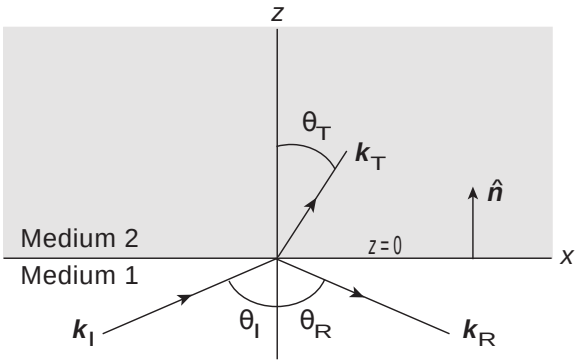

Fig. 14.1 Propagation of a monochromatic electromagnetic plane wave at a straight boundary between two dielectric materials, with $\hat{\boldsymbol{n}}$ the unit normal at the boundary. The wavevectors are $\boldsymbol{k}_\mathrm{I}$ for the incident wave, $\boldsymbol{k}_\mathrm{R}$ for the reflected wave, and $\boldsymbol{k}_\mathrm{T}$ for the transmitted (refracted) wave.

homogeneous media, the physics is governed by conservation of the *tangential components of the electric and magnetic fields*. At the interface between Medium 1 and Medium 2, the matching conditions in the absence of free charge or current are

$$\hat{\boldsymbol{n}} \cdot (\boldsymbol{D}_1 - \boldsymbol{D}_2) = 0 \qquad \hat{\boldsymbol{n}} \cdot (\boldsymbol{B}_1 - \boldsymbol{B}_2) = 0, \tag{14.10a}$$

$$\hat{\boldsymbol{n}} \times (\boldsymbol{E}_1 - \boldsymbol{E}_2) = 0 \qquad \hat{\boldsymbol{n}} \times (\boldsymbol{H}_1 - \boldsymbol{H}_2) = 0, \tag{14.10b}$$

which may be used to determine the properties of the transmitted and reflected waves. The fundamental rules governing electromagnetic reflection and refraction at a boundary between media arise from requiring the phase of the waves to be synchronized across the entire boundary for all times. Specifically, if the interface is the $z = 0$ plane, then $e^{i(\boldsymbol{k}\cdot\boldsymbol{r}-\omega t)}$ must match at the boundary. This phase-matching constraint has three immediate implications:

1. the incident, reflected, and transmitted waves must have the *same frequency* and their *wavevectors must be coplanar*,
2. the incident, reflected, and transmitted waves must obey the *law of reflection*, and
3. the incident, reflected, and transmitted waves must obey *Snell's law*,

as we shall now demonstrate.

14.2.1 Frequency Matching and Coplanar Vectors

Using I to denote the incident wave, R to denote the reflected wave, and T to denote the transmitted wave, the matching conditions (14.10) cannot be satisfied at all points and all times in the $z = 0$ boundary plane unless

$$\omega_\mathrm{I} = \omega_\mathrm{T} = \omega_\mathrm{R} \equiv \omega. \tag{14.11}$$

Thus the boundary conditions impose the constraint that the *incident, transmitted and reflected waves must all have the same frequency* ω. Furthermore, the phase-matching constraint at the boundary requires that

$$\boldsymbol{k}_{\mathrm{I}} \cdot \boldsymbol{x}\big|_{z=0} = \boldsymbol{k}_{\mathrm{T}} \cdot \boldsymbol{x}\big|_{z=0} = \boldsymbol{k}_{\mathrm{R}} \cdot \boldsymbol{x}\big|_{z=0}\,, \tag{14.12}$$

which imposes the conditions

$$k_{\mathrm{Ix}} = k_{\mathrm{Tx}} = k_{\mathrm{Rx}}, \tag{14.13a}$$

$$k_{\mathrm{Iy}} = k_{\mathrm{Ty}} = k_{\mathrm{Ry}}. \tag{14.13b}$$

In Fig. 14.1, $\boldsymbol{k}_{\mathrm{I}}$ and $\hat{\boldsymbol{n}}$ lie in the $x - z$ plane, so $k_{\mathrm{Iy}} = 0$ and thus from Eq. (14.13b) $k_{\mathrm{Ty}} = k_{\mathrm{Ry}} = 0$. Hence, *the three wavevectors* $\boldsymbol{k}_{\mathrm{I}}$, $\boldsymbol{k}_{\mathrm{T}}$, and $\boldsymbol{k}_{\mathrm{R}}$ *lie in the same plane*, which is commonly termed the *plane of incidence.*

14.2.2 Law of Reflection and Snell's Law

From the matching of the tangential components of the wave vectors in Eq. (14.13b), we obtain,

$$\theta_{\mathrm{I}} = \theta_{\mathrm{R}} \qquad \text{(Law of reflection)}, \tag{14.14}$$

$$n_1 \sin\theta_{\mathrm{I}} = n_2 \sin\theta_{\mathrm{T}} \qquad \text{(Snell's law)}, \tag{14.15}$$

where the index of refraction for medium i is defined by

$$n_i = \sqrt{\frac{\epsilon_i \mu_i}{\epsilon_0 \mu_0}}. \tag{14.16}$$

The preceding results are kinematic in nature, as they follow from the properties of the fields alone and did not invoke the Maxwell equations. To determine things like the amplitudes of the reflected and refracting waves we must consider dynamical phenomena that are consequences of the Maxwell equations.

14.3 The Fresnel Equations

To find the amplitudes of reflected and transmitted waves, it is convenient to decompose the electric field into two fundamental polarizations relative to the plane of incidence,[1]

1. *s-polarization* (also termed *Transverse Electric or TE polarization)*, and

[1] A plane wave with arbitrary polarization can be decomposed into a sum of two plane waves having mutually orthogonal polarizations. The s and p designations for the polarization comes from the German language (reflecting the significant role played by German scientists in 19th century optics). The "s" in "s-polarization" derives from the German *senkrecht,* meaning perpendicular. In this polarization the electric field is perpendicular to the plane of incidence. It is also called transverse electric or TE polarization because the electric field is transverse to the plane of incidence. The "p" in "p-polarization" derives from the German *parallel*, which has the same meaning as the English word with the same spelling; in this polarization the electric field lies parallel to the plane of incidence. It is also called transverse magnetic (TM) polarization because the auxiliary magnetic field vector $\boldsymbol{H}$ is transverse to the plane of incidence in this polarization.

2. *p-polarization* (also termed *Transverse Magnetic or TM Polarization*).

The names derive from the orientation of the electric field vector $\boldsymbol{E}$ relative to the plane of incidence (the plane containing the incident, reflected, and transmitted wave vectors), as we now describe.

14.3.1 Transverse Electric and Magnetic Polarizations

The reflection and transmission coefficients for Fresnel states can be derived from boundary conditions.

s-Polarization (TE - Transverse Electric): The electric field $\boldsymbol{E}$ is perpendicular to the plane of incidence. Applying the boundary conditions (the tangential components of $\boldsymbol{E}$ and $\boldsymbol{H}$ are continuous) yields the reflection coefficient r_{s} and transmission coefficient t_{s} for s-polarized waves in the form

$$r_{\mathrm{s}} = \frac{n_1 \cos\theta_{\mathrm{I}} - n_2 \cos\theta_{\mathrm{T}}}{n_1 \cos\theta_{\mathrm{I}} + n_2 \cos\theta_{\mathrm{T}}} \qquad t_{\mathrm{s}} = \frac{2n_1 \cos\theta_{\mathrm{I}}}{n_1 \cos\theta_{\mathrm{I}} + n_2 \cos\theta_{\mathrm{T}}}. \tag{14.17}$$

p-Polarization (TM - Transverse Magnetic): The electric field $\boldsymbol{E}$ lies within the plane of incidence. Applying the boundary conditions gives the reflection coefficient r_{p} and transmission coefficient t_{p} for p-polarized waves in the form,

$$r_{\mathrm{p}} = \frac{n_2 \cos\theta_{\mathrm{I}} - n_1 \cos\theta_{\mathrm{T}}}{n_2 \cos\theta_{\mathrm{I}} + n_1 \cos\theta_{\mathrm{T}}} \qquad t_{\mathrm{p}} = \frac{2n_1 \cos\theta_{\mathrm{I}}}{n_2 \cos\theta_{\mathrm{I}} + n_1 \cos\theta_{\mathrm{T}}}. \tag{14.18}$$

The matching conditions on the normal components of $\boldsymbol{D}$ and $\boldsymbol{B}$ provide no new information and Eqs. (14.17) and (14.18) are known as the *Fresnel equations*. The use of Eqs. (14.17) and (14.18) requires also Snell's law (14.15), to compute the refracted angle θ_{T} from the incident angle θ_{I}.

14.3.2 Stokes Parameters from Fresnel States

It will prove convenient to express the Stokes parameters in terms of the Fresnel states described above. The orthogonal polarization basis vectors map directly to

- the *p-polarization direction* (parallel to the plane of incidence), and
- the *s-polarization direction* (perpendicular to the plane of incidence).

Let the complex electric field components be E_{p} and E_{s}, with a relative phase difference

Table 14.1 Stokes parameters s_i from Fresnel parameters $(E_\mathrm{p}, E_\mathrm{s}, \delta)$

Stokes s_i	$s_i(E_\mathrm{p}, E_\mathrm{s}, \delta = \delta_1 - \delta_2)$	Physical meaning
s_0	$s_0 = \lvert E_\mathrm{p}\rvert^2 + \lvert E_\mathrm{s}\rvert^2$	Total intensity
s_1	$s_1 = \lvert E_\mathrm{p}\rvert^2 - \lvert E_\mathrm{s}\rvert^2$	Strength of p-polarization relative to s-polarization
s_2	$s_2 = 2\,\mathrm{Re}(E_\mathrm{p}E_\mathrm{s}^*) = 2\lvert E_\mathrm{p}\rvert\lvert E_\mathrm{s}\rvert\cos\delta$	Preference for linear polarization at $+45^\circ$ over -45°
s_3	$s_3 = 2\,\mathrm{Im}\,(E_\mathrm{p}E_\mathrm{s}^*) = 2\lvert E_\mathrm{p}\rvert\lvert E_\mathrm{s}\rvert\sin\delta,$	Preference for RCP over LCP

between them of $\delta = \delta_\mathrm{s} - \delta_\mathrm{p}$. The Stokes vector[2] $\boldsymbol{S} = (s_0, s_1, s_2, s_3)^\mathrm{T}$ is then defined by the intensities and phase correlations of these two components:

1. The total intensity of the wave is $s_0 = |E_\mathrm{p}|^2 + |E_\mathrm{s}|^2$.
2. The intensity difference between the two states is $s_1 = |E_\mathrm{p}|^2 - |E_\mathrm{s}|^2$; a positive value indicates a dominance of p-polarization, while a negative value indicates a dominance of s-polarization.
3. The preference for linear polarization at $+45^\circ$ over -45° (relative to the p-axis) is indicated by $s_2 = 2\,\mathrm{Re}(E_\mathrm{p}E_\mathrm{s}^*) = 2|E_\mathrm{p}||E_\mathrm{s}|\cos\delta$, which captures the in-phase correlation between the p and s components.
4. The preference for right-circular polarization over left-circular polarization is indicated by $s_3 = 2\,\mathrm{Im}\,(E_\mathrm{p}E_\mathrm{s}^*) = 2|E_\mathrm{p}||E_\mathrm{s}|\sin\delta$, which captures the out-of-phase (90°) correlation between the p and s components.

These relationships between the Fresnel and Stokes parameters are summarized in Table 14.1.

14.4 Key Physical Phenomena

The reflection and transmission coefficients derived in Section 14.3 lead to several important phenomena.

[2] It is awkward to write out a 4-component column vector in text, so here we avoid displaying a column vector by employing the equivalence

$$\boldsymbol{S} = (s_0, s_1, s_2, s_3)^\mathrm{T} = \begin{pmatrix} s_0 \\ s_1 \\ s_2 \\ s_3 \end{pmatrix},$$

to write it as the transpose of the corresponding row vector (s_0, s_1, s_2, s_3); this formats much better inline than a column vector.

14.4.1 Brewster's Law and Brewster's Angle

Brewster's Law describes the condition under which the p-polarized component of an electromagnetic wave (meaning that the electric field lies within the plane of incidence) is entirely absent from the reflected wave when striking a dielectric interface. Physically, this total extinction occurs when the reflected ray and the transmitted (refracted) ray are exactly 90° apart. The law was proposed by Scottish physicist Sir David Brewster in 1815, after observing disappearance of the p-polarized component of light at specific incident angles. *Brewster's Angle* θ_B is the specific angle of incidence at which Brewster's law is satisfied. The mathematical relationship defining Brewster's angle is derived by applying Snell's law with the 90° geometric constraint $\theta_\mathrm{T} = \frac{\pi}{2} - \theta_\mathrm{B}$, which yields

$$\tan\theta_\mathrm{B} = \frac{n_2}{n_1}, \tag{14.19}$$

where n_1 is the refractive index of the incident medium and n_2 is the refractive index of the transmitting medium. At this angle, the p-polarized component vanishes completely and the reflected light is *100% s-polarized* (meaning that it is linearly polarized perpendicular to the plane of incidence).

Example 14.1 Water has refractive index $n \approx 1.33$ and a Brewster angle $\theta_\mathrm{B} \sim 53^\circ$; glass has a refractive index $n \approx 1.5$ and a Brewster angle $\theta_\mathrm{B} \sim 57^\circ$.

14.4.2 Total Internal Reflection

When light travels from a more dense medium to a less dense medium ($n_1 > n_2$),

1. Snell's law implies that for angles greater than a *critical angle* θ_c defined by

$$\theta_\mathrm{c} = \arcsin\left(\frac{n_2}{n_1}\right), \tag{14.20}$$

   there is *no real solution for* θ_t.
2. While the energy is totally reflected ($|r|^2 = 1$), the *boundary conditions still require a field in the second medium.*

This field in the second medium is the *evanescent wave*, which propagates along the interface but decays exponentially in the z-direction: $E \sim e^{-\kappa z}$.

14.4.3 Phase Shifts

1. *External Reflection ($n_1 < n_2$):* At normal incidence, the reflected wave undergoes a phase shift of π.
2. *Internal Reflection ($n_1 > n_2$):* Beyond θ_c defined in Eq. (14.20), the reflection coefficients become complex numbers with a magnitude of 1.

The resulting phase shifts between s and p components can be utilized to convert linear polarization into circular polarization.

14.5 Transport of Energy

The flow of energy is described by the *Poynting vector* (see Section 13.2.4),

$$\boldsymbol{S} = \boldsymbol{E} \times \boldsymbol{H}. \tag{14.21}$$

Conservation of energy then requires that the component of the Poynting vector normal to the interface be conserved ($R + T = 1$), where

$$R = |r|^2 \qquad \text{(Reflectance)}, \tag{14.22}$$

$$T = \frac{n_2 \cos\theta_t}{n_1'' \cos\theta_i} |t|^2 \qquad \text{(Transmittance)}, \tag{14.23}$$

where the geometric factor multiplying $|t|^2$ in the expression for T accounts for spreading of the beam area caused by refraction.

The remainder of this section is under construction.

14.6 Radiation Pressure

Absorption or reflection of an electromagnetic wave from a surface exerts a force on that surface by transferring linear momentum from the wave to the surface; the corresponding force per unit area is called *radiation pressure*.

This section is under construction.

14.7 The Faraday Effect

Circular birefringence occurs when a material exhibits two distinct indices of refraction for left and right circularly polarized light, respectively, as elaborated in Box 14.1. It enables the *Faraday effect,* which is one of the most direct experimental demonstrations that light corresponds to electromagnetic waves. The essence of the Faraday effect is that a static magnetic field $\boldsymbol{B}$ breaks time-reversal symmetry and induces a non-diagonal dielectric tensor, and this rotates the plane of polarization for linearly polarized light.

14.7.1 The Microscopic Origin

The Faraday effect arises from the Zeeman splitting of electronic energy levels within the medium. When an external magnetic field is applied, the motion of electrons is modified by the Lorentz force. This creates a distinction between the responses to left-circularly polarized (LCP) and right-circularly polarized (RCP) light. In a classical Drude–Lorentz model, the equation of motion for an electron in a magnetic field $\boldsymbol{B} = B_z\hat{z}$ is

$$m\frac{d^2\boldsymbol{r}}{dt^2} + m\gamma\frac{d\boldsymbol{r}}{dt} + m\omega_0^2\boldsymbol{r} = -e(\boldsymbol{E} + \boldsymbol{v}\times\boldsymbol{B}). \tag{14.24}$$

For a wave propagating along the z-direction, this leads to different effective indices of refraction, n_+ and n_-, for the two circular polarizations. Any linearly polarized wave can be decomposed into two counter-rotating circular components. If the medium is circularly birefringent, these components travel at different phase velocities k,

$$\text{LCP } (+): \quad k_+ = \frac{\omega}{c}n_+ \qquad \text{RCP } (-): \quad k_- = \frac{\omega}{c}n_- \,. \tag{14.25}$$

As the wave propagates over a distance L, a phase shift develops between the two components. When they are recombined as they exit the medium, the circularly polarized components will combine again in a state that is linearly polarized, but the linear polarization vector will now be rotated by an angle θ relative to the linear polarization of the original light wave,

$$\theta = \frac{\omega L}{2c}(n_- - n_+), \tag{14.26}$$

which is exactly half the accumulated phase difference and depends on the properties of the material, the frequency of the light, and the distance traveled through the medium by the light.

14.7.2 Key Characteristics

The Faraday effect exhibits some key characteristics and has various scientific and technical applications.

Non-Reciprocity: Unlike optical activity found in chiral molecules (see Box 14.2), the Faraday effect is *non-reciprocal:* If a beam is reflected back through the medium, the rotation does not cancel out; it *doubles*. This property is heavily exploited in the design of optical isolators and circulators.

Dielectric Tensor: The presence of $\boldsymbol{B}$ introduces off-diagonal, imaginary components to the permittivity tensor ϵ_{ij}, such that:

$$\boldsymbol{D} = \epsilon\boldsymbol{E} + i\boldsymbol{g}\times\boldsymbol{E} \tag{14.27}$$

where $\boldsymbol{g}$ is the gyration vector proportional to $\boldsymbol{B}$.

Plasma and Astrophysics: In a dilute plasma (such as the interstellar medium), the rotation depends on the wavelength squared (λ^2), allowing astronomers to measure galactic magnetic fields by observing the "rotation measure" of distant radio sources.

Box 14.1 Circular Birefringence

Circular birefringence is a phenomenon where a material exhibits two distinct indices of refraction—one for left-circularly polarized (LCP) light, n_+, and another for right-circularly polarized (RCP) light, n_-. Because the phase velocity of light is inversely proportional to its refractive index ($v = c/n$), LCP and RCP waves travel at different speeds through the material.

Optical Rotation Dynamics

To see why this results in a rotation, recall that any linearly polarized light wave can be decomposed into an equal superposition of an LCP wave and an RCP wave. When these two circular components enter a circularly birefringent medium:

1. *Phase accumulation:* Because $n_+ \neq n_-$, the two circular waves propagate with different wave numbers: $k_+ = (\omega/c)n_+$ and $k_- = (\omega/c)n_-$.
2. *Phase shift:* After traveling a distance L through the medium, a relative phase difference develops between the LCP and RCP components, given by $\Delta\phi = (k_- - k_+)L$.
3. *Recombination:* When the light exits the material, the LCP and RCP components recombine. Because of the newly introduced phase shift, their vector sum is still linearly polarized, but its plane of polarization has been rotated.

The angle of rotation θ is given in Eq. (14.26) and corresponds to exactly half the accumulated phase difference.

Physical Origin

Circular birefringence in materials typically arises from two distinct physical mechanisms, one violating mirror symmetry and one violating time reversal symmetry.

1. *Natural optical activity (spatial asymmetry):* Occurs in materials that lack mirror symmetry (chiral media), such as solutions of chiral molecules or crystals with helical lattice structures. The spatial handedness of the structure interacts differently with the left- and right-handed helicities of the light fields. This effect preserves time-reversal symmetry.
2. *The Faraday effect (time-reversal asymmetry):* A static magnetic field applied to a magneto-optic material breaks time-reversal symmetry, inducing a gyroelectric or gyromagnetic response. The magnetic field effectively biases the cyclotron motion of the electrons, forcing a distinction in how the medium responds to fields rotating in the same sense versus the opposite sense of the electron precession.

The Faraday effect is discussed in Section 14.7, natural optical activity is described in Box 14.2, and magneto-optic material is described in Section 14.8.

Box 14.2 Optically Active Matter and Chiral Molecules

Optically active matter can rotate the plane of linearly polarized light as it passes through the matter. As discussed in Box 14.1, there are two main physical origins: the *Faraday effect*, described in Section 14.7, which breaks time-reversal symmetry, and *natural optical activity*, which stems from the spatial geometry of the material itself and preserves time-reversal symmetry.

Chiral Molecules

A molecule having no internal plane of symmetry is *chiral*, meaning that it cannot be superimposed on its mirror image through any combination of translations or rotations. Consider a pair of human hands: they are mirror images, but no orientation of the left and right hands in 3D space will have perfect overlap; for this reason, chirality is often called "handedness".[a] The two distinct, non-superimposable mirror images of a chiral molecule are called *enantiomers*. They have identical physical properties but differ in how they interact with other chiral objects and with polarized light. Many vital biological molecules are chiral; for instance, the amino acids making up human proteins are almost exclusively left-handed, while naturally occurring sugars are right-handed.

Optically Active Matter

A material must possess a net handedness to be optically active, meaning that it must contain an *excess of one enantiomer over the other*.

1. If the substance rotates the polarization plane to the right (clockwise, when looking directly into the oncoming light beam), it is termed *dextrorotatory*.
2. If it rotates the plane to the left (counter-clockwise), it is termed *levorotatory*.

A solution containing a 50/50 mixture of left-handed and right-handed enantiomers (termed a *racemic mixture*) will not be optically active because the clockwise rotation caused by half of the molecules will be canceled by the counter-clockwise rotation caused by the other half.

Why Chirality Rotates Light

Chiral molecules create optically active matter because of the circular birefringence described in Box 14.1. Linearly polarized light is a 1:1 superposition of left-circularly polarized (LCP) and right-circularly polarized (RCP) light. As these circular components propagate, their electric field vectors sweep out left-handed and right-handed helical paths, respectively (see Fig. 13.5). Because a chiral molecule itself has a specific handedness, it presents a spatially asymmetric environment, which causes the right-handed circularly polarized wave to interact with the molecule's electron cloud differently than the left-handed circularly polarized wave does.

[a] Chirality also is fundamental in elementary particle physics, where neutrinos are found to be left-handed and antineutrinos right-handed with respect to spin projection in the direction of motion. This leads to maximal violation of parity (symmetry of the wavefunction under spatial reflection of the coordinate system through the origin) in the weak interactions.

14.8 Magneto-Optic Material

A *magneto-optic material* is any medium whose optical properties—specifically its index of refraction or its interaction with the polarization state of light—are modified by the presence of a static external magnetic field or an intrinsic net magnetization. The fundamental characteristic of magneto-optic materials is that the magnetic field breaks time-reversal symmetry. This macroscopic breaking of symmetry means the material responds differently to electromagnetic waves propagating forward versus backward, or to waves rotating clockwise versus counter-clockwise (yielding effects like the Faraday effect in transmission, or the Magneto-Optic Kerr Effect in reflection).

14.8.1 Gyroelectric Response

A *gyroelectric response* occurs when an applied magnetic field (or intrinsic magnetization) causes the material's permittivity tensor ϵ to become anisotropic and complex-Hermitian. In an isotropic, non-magnetic medium, ϵ is a simple scalar; in a gyroelectric medium with a static magnetic field applied along the z-axis, ϵ becomes a tensor with components

$$\epsilon_{ij} = \begin{pmatrix} \epsilon_{xx} & i\epsilon_{xy} & 0 \\ -i\epsilon_{xy} & \epsilon_{xx} & 0 \\ 0 & 0 & \epsilon_{zz} \end{pmatrix}. \tag{14.28}$$

The off-diagonal, imaginary components ($i\epsilon_{xy}$) represent the gyroelectric coupling. Physically, this means that an electric field applied in the x-direction induces a displacement field $\boldsymbol{D}$ that has a component in the y-direction. This cross-coupling is driven by the Lorentz force acting on bound or free electrons, and causes the different phase velocities for left- and right-circularly polarized light discussed in Box 14.1.

In the visible and infrared optical regimes, the interaction of light with matter is overwhelmingly dominated by the electric field acting on electrons. Therefore, most magneto-optic effects at optical frequencies have a gyroelectric origin.

14.8.2 Gyromagnetic Response

A *gyromagnetic response* is the magnetic analog of the gyroelectric response described in Section 14.8.1. It occurs when a magnetic field causes the material's permeability μ (normally a scalar), to become an anisotropic and complex-hermitian tensor.[3] With a biasing

[3] A matrix A is *hermitian* (or *self-adjoint*) if it is equal to its own conjugate transpose. In matrix notation, $A = A^\dagger$, where the *hermitian conjugate* $A^\dagger$ of A is defined by
1. transposing the matrix (interchanging rows and columns), and
2. taking the complex conjugate of each element ($i \to -i$).

magnetic field along the z-axis, the components of the permeability tensor take the form

$$\mu_{ij} = \begin{pmatrix} \mu_{xx} & i\mu_{xy} & 0 \\ -i\mu_{xy} & \mu_{xx} & 0 \\ 0 & 0 & \mu_{zz} \end{pmatrix}. \tag{14.29}$$

In this case, an oscillating $\boldsymbol{H}$ field from an electromagnetic wave in the x-direction induces a magnetic field $\boldsymbol{B}$ with a component in the y-direction. This is driven by the precession of magnetic dipoles (spins) around the static biasing field. Gyromagnetic responses are typically negligible at visible optical frequencies because magnetic dipoles cannot precess fast enough to track the rapidly oscillating magnetic field of the light wave ($\sim 10^{14}$ Hz). However, the gyromagnetic response is pronounced and technologically vital at microwave and radio frequencies ($\sim 10^{9}$ Hz), particularly in materials like ferrites used for microwave isolators and circulators.[4]

14.9 Polarization of Light by Reflection

Polarization of light by reflection is best understood as a consequence of the Fresnel equations (Section 14.3) and the differing boundary conditions for fields oscillating parallel or perpendicular to the plane of incidence. When unpolarized light—which can be viewed as a stochastic superposition of s-polarized and p-polarized components—strikes a dielectric interface, the material response depends on the orientation of the electric field relative to the surface.

14.9.1 The Physical Mechanism

Polarization by reflection occurs because the dipoles in the second medium are driven by the refracted wave. These oscillating dipoles then reradiate energy to create the reflected wave.

1. *The dipole null:* Classically, an oscillating dipole does not radiate along its axis of oscillation.

For an individual element of the matrix this means $a_{ij} = a_{ji}^*$, where $*$ indicates the complex conjugate. The matrix is *complex hermitian* if the elements can be complex numbers and *real hermitian* if the entries are restricted to real numbers; however, in physics one often uses simply "hermitian" for either case.

[4] Microwave *isolators* and *circulators* are components used in radio frequency and microwave engineering to control the direction of signal flow, often with a purpose of protecting sensitive equipment from damaging high-power signals. They are practical engineering applications of the gyromagnetic response and the breaking of time-reversal symmetry discussed in this section. These devices operate at microwave frequencies (roughly 300 MHz to 300 GHz), so the primary interaction is not with the electric field (as in optical Faraday rotation) but with the magnetic field of the wave. Isolators are dual-port devices that typically act as one-way valves for electromagnetic energy, and are often used to protect microwave sources from reflections. Circulators are multiport devices where power entering any one port is transmitted strictly to the next port in the rotation sequence, and isolated from all others; their purpose often is to prevent sensitive devices from accidentally receiving damaging high-power signals.

2. *The p-component:* As the angle of incidence changes, the orientation of the induced dipoles in the second medium changes. At a specific angle, the direction of the reflected ray aligns perfectly with the axis of the dipoles that would be responsible for the p-polarized reflection. Since these dipoles cannot radiate in that direction, the p-polarized reflection vanishes.
3. *The s-component:* The dipoles driven by s-polarized light always oscillate perpendicular to the plane of incidence (and thus perpendicular to the direction of the reflected ray), so they always radiate, regardless of the angle.

14.9.2 Brewster's Law

The condition for the total extinction of the p-polarized component at an interface for a special angle of incidence θ_B is known as *Brewster's law*. This occurs when the reflected and transmitted rays are exactly 90° apart: $\theta_T = \frac{\pi}{2} - \theta_R$. Applying Snell's Law (14.15) for an incident angle $\theta_R = \theta_B$ gives

$$n_1 \sin\theta_B = n_2 \sin\theta_B = n_2 \sin\left(\frac{\pi}{2} - \theta_B\right) = n_2 \cos\theta_B,$$

and dividing by $n_1 \cos\theta_B$ then gives

$$\tan\theta_B = \frac{n_2}{n_1}, \tag{14.30}$$

which defines *Brewster's angle*, θ_B. At the Brewster angle the reflected light is 100% linearly polarized (s-polarized).[5]

14.10 Waveguides

Electromagnetic waves subject to no constraints expand naturally into 3D space, causing their intensities to decrease according to the inverse square law. An electromagnetic *waveguide* is a long enclosure that guides waves by restricting the direction in which their energy can be transmitted. To keep our discussion simple we will assume waveguides to be perfect conductors, and will concentrate on the most common case of rectangular cross-section. Electromagnetic wave solutions in waveguides represent a shift from the plane-wave approximations of free space to boundary-value problems governed by Maxwell's equations in the bounded geometry of the waveguide. A mode of propagation is a solution of the wave equation (the Helmholtz equation) subject to the waveguide boundary conditions. As we shall see, when EM waves are confined within a perfectly conducting structure, the boundary conditions restrict the allowed modes of propagation.

[5] This is the basis for a standard method for producing polarized light in laboratory settings using a "pile-of-plates" polarizer, which is a device that produces linearly polarized light by transmitting light through a stack of tilted transparent plates. The plates are typically oriented at Brewster's angle, where each surface reflects a portion of s-polarized light, causing the transmitted beam to become increasingly enriched with p-polarized light.

14.10.1 General Helmholtz Formulation

Consider first a a hollow, infinitely long, metallic cylinder with a uniform cross-section and aligned along the z-axis. The interior is filled with a lossless dielectric (μ, ϵ), and the walls are assumed to be perfect electric conductors. We seek harmonic wave solutions corresponding to fields propagating in the $+z$ direction that take the form

$$\boldsymbol{E}(\boldsymbol{x}, t) = \boldsymbol{E}_0(x, y)e^{i(k_z z - \omega t)} \qquad \boldsymbol{B}(\boldsymbol{x}, t) = \boldsymbol{B}_0(x, y)e^{i(k_z z - \omega t)} \tag{14.31}$$

Where k_z is the wave vector along the guide axis and ω is the angular frequency. Inside the waveguide, both $\boldsymbol{E}$ and $\boldsymbol{B}$ must satisfy the wave equation. If we split the Laplacian ∇^2 into transverse parts ∇_{T}^2 and longitudinal parts ∇_{L}^2,

$$\nabla^2 = \nabla_{\mathrm{T}}^2 + \nabla_{\mathrm{L}}^2 = \nabla_{\mathrm{T}}^2 + \frac{\partial^2}{\partial z^2}, \tag{14.32}$$

the longitudinal components E_z and B_z govern the entire field structure through the 2D Helmholtz equations,

$$\left(\nabla_{\mathrm{T}}^2 + \gamma^2\right) E_z = 0 \qquad \left(\nabla_{\mathrm{T}}^2 + \gamma^2\right) B_z = 0, \tag{14.33}$$

where $\nabla_{\mathrm{T}}^2 = \dfrac{\partial^2}{\partial x^2} + \dfrac{\partial^2}{\partial y^2}$ and

$$\gamma^2 \equiv \mu\epsilon\omega^2 - k_z^2 = k^2 - k_z^2. \tag{14.34}$$

is the *transverse wave number*.

14.10.2 Decomposing into Transverse Fields

The transverse field components $(\boldsymbol{E}_{\mathrm{T}}, \boldsymbol{B}_{\mathrm{T}})$ can be determined by taking gradients of the longitudinal components (E_z, B_z). Isolating the transverse parts of Maxwell's curl equations (the Faraday and Ampère laws) gives

$$\boldsymbol{E}_{\mathrm{T}} = \frac{i}{\gamma^2}\left(k_z \nabla_{\mathrm{T}} E_z - \omega \hat{\boldsymbol{z}} \times \nabla_{\mathrm{T}} B_z\right),$$
$$\boldsymbol{B}_{\mathrm{T}} = \frac{i}{\gamma^2}\left(k_z \nabla_{\mathrm{T}} B_z + \mu\epsilon\omega \hat{\boldsymbol{z}} \times \nabla_{\mathrm{T}} E_z\right).$$

This decouples the solutions into two independent families of modes,

1. *Transverse electric (TE) modes:* $E_z = 0$ everywhere and the fields are completely specified by B_z.
2. *Transverse magnetic (TM) modes:* $B_z = 0$ everywhere and the fields are completely specified by E_z.

Transverse electromagnetic (TEM) modes, corresponding to $E_z = B_z = 0$, cannot exist inside a perfectly conducting hollow waveguide because the boundary conditions would force the interior electrostatic potential to be constant, implying zero fields.

14.10.3 Rectangular Metallic Waveguides

Let us apply these general ideas to the specific case of a waveguide having rectangular cross-section with dimensions $x \in [0, a]$ and $y \in [0, b]$, where we assume $a > b$.

TM Modes ($B_z = 0$): For TM modes, we may solve for $E_z(x, y)$ using separation of variables. Setting $E_z = X(x)Y(y)$, we must solve

$$\left(\frac{\partial^2}{\partial x^2} + \frac{\partial^2}{\partial y^2} + \gamma^2\right) E_z = 0. \tag{14.35}$$

The perfect conductor boundary condition requires the tangential electric field to vanish at the walls, which means that $E_z = 0$ at $x = 0$ and $x = a$, as well as at $y = 0$, and $y = b$. Application of these conditions restricts the solutions to sinusoidal functions,

$$E_z(x, y) = E_0 \sin\left(\frac{m\pi x}{a}\right) \sin\left(\frac{n\pi y}{b}\right), \tag{14.36}$$

where the positive integers $m = 1, 2, 3...$, and $n = 1, 2, 3...$, label the mode: TM_{mn}. If either m or n is zero, E_z vanishes entirely and there are no TM_{m0} or TM_{0n} modes.

TE Modes ($E_z = 0$): For TE modes, we may solve for $B_z(x, y)$, with boundary conditions that require the normal component of $\boldsymbol{B}$ to vanish at the conductor walls, $\hat{\boldsymbol{n}} \cdot \boldsymbol{B} = 0$. From Maxwell's equations, this implies that the normal derivative of B_z must vanish at the walls, $\partial B_z/\partial n = 0$, which is a Neumann boundary condition. Applying separation of variables with these boundary conditions yields a solution

$$B_z(x, y) = B_0 \cos\left(\frac{m\pi x}{a}\right) \cos\left(\frac{n\pi y}{b}\right), \tag{14.37}$$

where m and n are integers starting from zero ($m, n = 0, 1, 2...$), but the specific case $m = n = 0$ is excluded because it results in uniform static fields that do not propagate. Therefore, the lowest TE mode is either TE_{10} or TE_{01}.

14.10.4 Cutoff Frequency and Dispersion

For both TE and TM modes, substituting the sinusoidal solutions (14.36) and (14.37) back into the Helmholtz equation (14.33) yields the eigenvalue equation for the transverse wave number:

$$\gamma^2 = \left(\frac{m\pi}{a}\right)^2 + \left(\frac{n\pi}{b}\right)^2 \tag{14.38}$$

Recalling that $k_z^2 = k^2 - \gamma^2$, we can solve for the *longitudinal propagation constant* k_z:

$$k_z = \sqrt{\mu\epsilon\omega^2 - \left[\left(\frac{m\pi}{a}\right)^2 + \left(\frac{n\pi}{b}\right)^2\right]}. \tag{14.39}$$

The Frequency Cutoff: For wave propagation to occur, k_z must be real. If the operational frequency ω is too low, the term under the square root becomes negative, making k_z imaginary ($k_z = i\alpha$). The wave then transitions into an evanescent wave, decaying exponentially along the guide axis ($e^{-\alpha z}$) without transferring net energy. The threshold

corresponding to $k_z = 0$ defines the cutoff frequency ω_{mn}^{c} for a given mode labeled by m and n,

$$\omega_{mn}^{\mathrm{c}} = \frac{1}{\sqrt{\mu\epsilon}}\sqrt{\left(\frac{m\pi}{a}\right)^2 + \left(\frac{n\pi}{b}\right)^2}. \tag{14.40}$$

Waveguide Phase and Group Velocities: From Eq. (14.39), k_z depends non-linearly on ω, implying that a waveguide is an inherently dispersive mediums, even if the interior dielectric is perfectly lossless.

1. *Phase velocity:* The speed at which the wavefronts appear to travel along the z-axis is the phase velocity v_{p}, given by

$$v_{\mathrm{p}} = \frac{\omega}{k_z} = \frac{v_0}{\sqrt{1 - \left(\frac{\omega_{\mathrm{c}}}{\omega}\right)^2}} > v_0, \tag{14.41}$$

   where $v_0 = 1/\sqrt{\mu\epsilon}$ is the speed of light in the unbounded medium.[6]
2. *Group velocity:* The speed at which signal energy and information actually propagate down the waveguide is the group velocity v_g, which is given by

$$v_{\mathrm{g}} = \frac{d\omega}{dk_z} = v_0\sqrt{1 - \left(\frac{\omega_{\mathrm{c}}}{\omega}\right)^2} < v_0. \tag{14.42}$$

   An elegant consequence of this relation is that $v_{\mathrm{p}}v_{\mathrm{g}} = v_0^2$.

In Problem 14.5 we shall use the finite element method (FEM) to solve numerically for the electric field and the potential for the rectangular waveguide shown in Fig. 14.2. The potential and electric field resulting from that calculation are displayed in Fig. 14.3 and the constant triangular mesh employed in the FEM calculations is shown in Fig. 4.8.

14.10.5 The Dominant Mode TE_{10}

In practical applications it is common to operate waveguides under *single-mode conditions* such that only a single mode can propagate, which prevents distortion of signals by intermodal dispersion.[7] The mode with the lowest cutoff frequency is called the *dominant mode*. Assuming the convention $a > b$ for our rectangular waveguide, the lowest cutoff configuration corresponds to $m = 1, n = 0$. The TE_{10} mode has a cutoff frequency of

$$\omega_{10}^{\mathrm{c}} = \frac{\pi}{a\sqrt{\mu\epsilon}} \implies f_{10}^{\mathrm{c}} = \frac{v_0}{2a}, \tag{14.43}$$

where f is the frequency and ω is the corresponding angular frequency. This implies that the long dimension a must be exactly equal to a half-wavelength ($\frac{1}{2}\lambda_0$) at the cutoff

[6] The *phase velocity* v_{p} exceeds the speed of light v_0, but this does not violate special relativity because phase carries no information. The *group velocity* characterizes the rate of information transport, so its magnitude is required be less than the speed of light.

[7] *Intermodal dispersion* (also called *modal dispersion*) can occur in waveguides when a signal pulse is broadened because different modes travel down the waveguide at different speeds.

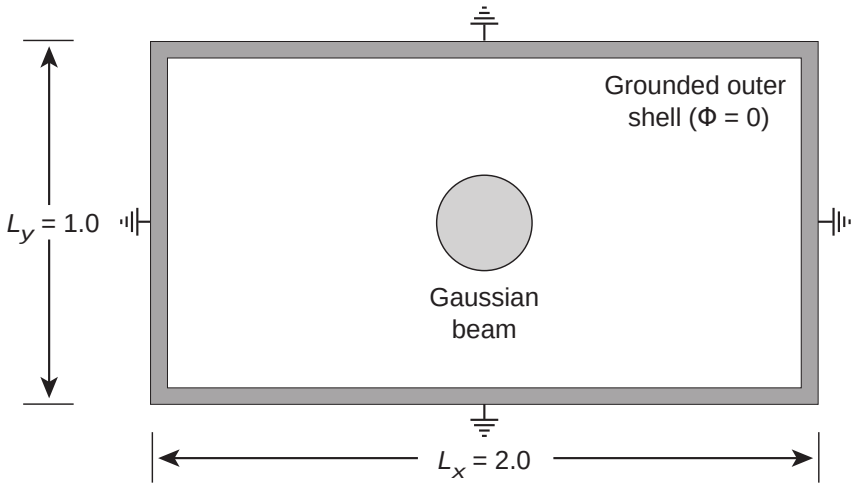

Fig. 14.2 Cross-section of a rectangular waveguide with a conducting outer shell that is grounded, with a gaussian-shaped central charge beam. Problem 14.5 solves for the electric field and potential using the finite element method (see Section 4.3.2).

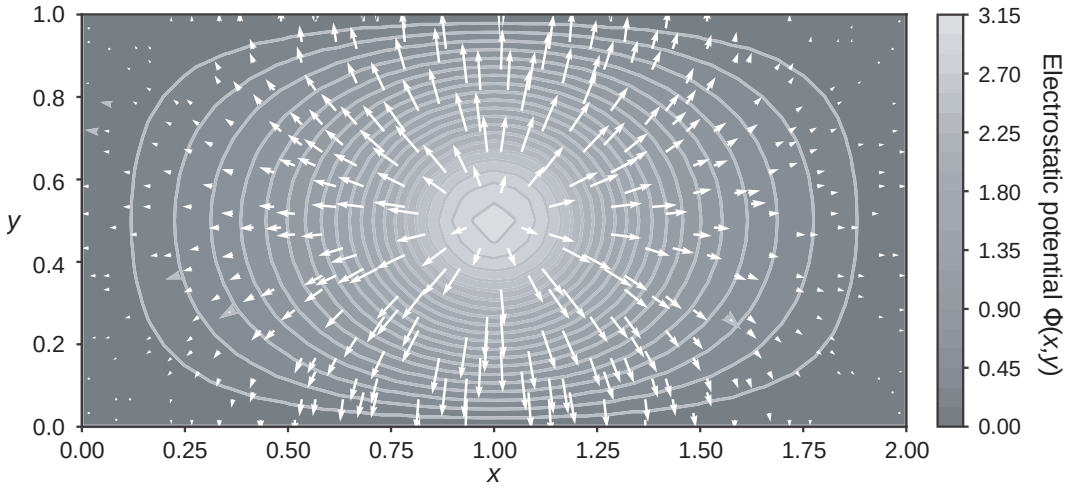

Fig. 14.3 Electric field (arrows) and electric potential contours inside the waveguide of Fig. 14.2. Calculated using the finite element method in Problem 14.5.

frequency. For the TE_{10} mode, setting $m = 1$ and $n = 0$ in the field equations yields the non-zero field components

$$B_z = B_0 \cos\left(\frac{\pi x}{a}\right) e^{i(k_z z - \omega t)} \qquad E_y = -\frac{i\omega\mu a}{\pi} B_0 \sin\left(\frac{\pi x}{a}\right) e^{i(k_z z - \omega t)},$$
$$B_x = -\frac{ik_z a}{\pi} B_0 \sin\left(\frac{\pi x}{a}\right) e^{i(k_z z - \omega t)}. \tag{14.44}$$

The electric field points entirely along the transverse y-direction, reaching its peak amplitude in the center of the guide at $x = \frac{1}{2}a$, and falling smoothly to zero at the conducting side walls, which satisfies the boundary conditions seamlessly.

Background and Further Reading

The discussion of polarization is patterned loosely after the presentation in Zangwill [77].

Problems

14.1 A monochromatic plane wave with Stokes parameters $\boldsymbol{S} = (s_0, s_1, s_2, s_3)$ is incident at an angle θ_i on a planar dielectric interface separating two non-magnetic media with refractive indices n_1 and n_2, respectively.

a. Using the Fresnel reflection coefficients r_s and r_p, derive the 4×4 reflection Mueller matrix M (see Section 13.3.8) such that the Stokes parameters of the reflected wave are given by $\boldsymbol{S}' = M\boldsymbol{S}$.

b. Evaluate M at Brewster's angle, θ_B. If the incident light is completely unpolarized, verify that the reflected light is 100% s-polarized, and express the reflected intensity s_0' in terms of n_1, n_2, and the incident intensity s_0.

Hint: Begin by decomposing the wave into transverse electric and transverse magnetic polarizations with respect to the plane of incidence, as described in Section 14.3.

14.2 Consider a monochromatic plane wave propagating in a gyroelectric medium (see Section 14.8.1) that is characterized by a static magnetic field applied along the z-axis. The medium has a permeability μ_0 and is characterized by the permittivity tensor ϵ_{ij} given in Eq. (14.28).

a. Assuming the wave propagates along the z-axis ($\boldsymbol{k} = k\hat{z}$), substitute the constitutive relation $\boldsymbol{D} = \epsilon\boldsymbol{E}$ into the source-free Maxwell equations to derive the wave equation for the electric field.

b. Solve the resulting eigenvalue problem to find the dispersion relations $\omega(k)$ for the allowed propagating modes.

c. Prove that these eigenmodes correspond to left-circularly polarized (LCP) and right-circularly polarized (RCP) waves, and show that they travel at different phase velocities in the medium.

14.3 A linearly polarized plane wave enters a circularly birefringent medium of length L that exhibits the Faraday effect. The indices of refraction for the LCP and RCP components are n_+ and n_-, respectively. Derive the Stokes parameters (s_1, s_2, s_3) of the wave as a function of the propagation distance z inside the medium, assuming that the wave is initially polarized along the x-axis at $z = 0$. ***

Numerical and GenAI Problems

14.4 For the Faraday effect Problem 14.3, prompt your *GenAI* to write a *Python* script using `NumPy` and `Matplotlib` (or `Plotly` for 3D interactivity) to compute numerically and plot the continuous trajectory of the wave's polarization state on the Poincaré sphere as it propagates from $z = 0$ to $z = L$. Choose sample parameters where the total rotation angle is $\theta = 3\pi/2$. *Hint*: The solution for Problem 14.3 is given in the *Student Solutions Manual*.

14.5 Consider the metallic, rectangular waveguide shown in Fig. 14.2, with grounded conducting shell and a charged beam at the center of the waveguide giving a gaussian distribution of charge around the center of the waveguide.

a. Prompt your *GenAI* to solve the Poisson equation using the finite elements method (FEM; see Section 4.3.2) for the electrostatic potential and electric field inside the waveguide shown in Fig. 14.2. Make an appropriate plot of the potential and electric field corresponding to the solution.
b. Display the FEM grid for this problem. You should be able to obtain something like Fig. 4.8.
c. Prompt your *GenAI* to examine a portion of the grid and show that in each triangular element the potential has constant slope but the slope changes at the elemental boundary, while the electric field is constant within an element, but jumps discontinuously at the elemental boundaries.

Hint: The finite element method typically requires sparse-matrix solutions, so use the standard libraries `numpy`, `scipy`, and `matplotlib`, which will allow invoking the sparse-matrix solver `scipy.sparse`. ***

15 Electromagnetic Radiation

15.1 Introduction

15.2 Time Domain and Frequency Domain

Two complementary points of view may be adopted for electromagnetic phenomena. As described more extensively in Box 15.1, these correspond to

1. a *time domain* perspective, which represents events as they occur in real time, describing them mathematically with the standard Maxwell equations, and
2. a *frequency domain* perspective, which represents phenomena in terms of steady-state oscillation at specific frequencies and replaces derivatives with algebraic operations on complex numbers called *phasors*,[1]

with the two perspectives providing complementary and equally valid views that are related to each other by Fourier transforms, as summarized by Table 15.1.

15.3 Time Dependent Numerical Methods

Numerical methods commonly applied to static and quasistatic electromagnetic problems were summarized in Section 4.3. For fully time-varying E&M problems two general numerical approaches are favored:

1. The *finite-difference time-domain FDTD* method is used to solve Maxwell's equations in the time domain.
2. The method of moments (MOM), which was termed the boundary element method (BEM) in Section 4.3, is used in the frequency domain.

Let us give a brief description of these two methods.

[1] A *phasor* is a complex number representing a sinusoidal function whose amplitude A and initial phase θ are time-invariant, while frequency ω is fixed. It replaces time-varying sinusoidal functions with static complex numbers that capture only magnitude and phase.

Box 15.1 Time and Frequency Domains

Time and frequency domains differ in how we observe and describe evolution of the fields. They represent alternative views of electromagnetic phenomena that are related mathmatically by Fourier transforms.

The Time Domain

The *time domain* represents phenomena as they unfold in real-time.

> ***Perspective:*** The electric field $\boldsymbol{E}(\boldsymbol{x}, t)$ and magnetic field $\boldsymbol{B}(\boldsymbol{x}, t)$ are functions of position and time. You are watching a "movie" of the fields: pulses propagate, waves reflect off surfaces, and transients decay. Analysis employs the standard form of Maxwell's Equations, which include partial derivatives with respect to time (e.g., $\partial \boldsymbol{B}/\partial t$ and $\partial \boldsymbol{D}/\partial t$).

This domain is natural for studying transient effects such as lightning strikes, digital pulse propagation in high-speed circuits, or ultra-short laser pulses. *Finite-Difference Time-Domain (FDTD)* is a standard numerical tool, stepping through time to see how a wave moves through a grid.

The Frequency Domain

The *frequency domain* represents electromagnetic phenomena in terms of their steady-state oscillation at specific frequencies. We treat a signal, not as a sequence of events in time, but as a sum of sinusoidal waves (sine and cosine) with varying frequencies, amplitudes, and phases.

> ***Perspective:*** Instead of a movie, you are looking at a "spectrum." The system is assumed to have reached a *steady-state*, and we wish to know how it responds to a specific frequency. Time derivatives are replaced by algebraic operations using complex numbers called *phasors*. Specifically, $\partial/\partial t$ becomes $j\omega$ (where ω is the angular frequency), which transforms Maxwell's partial differential equations into the Helmholtz equations.

Standard for antenna design, microwave engineering, and optics, where one is often more interested in the "bandwidth" or "gain" of a device at a specific frequency than in the specific oscillations. The *Method of Moments (MoM)* is a common approach, solving for response to a single frequency at a time.

The Connection: Fourier Analysis

The time and frequency domains are *mathematically equivalent, as they are linked by Fourier transforms*. A "sharp" time-domain event (lightning bolt) contains a broad range of frequencies in the frequency domain, while a time-domain sine wave appears as a sharp vertical line in the frequency domain.

Table 15.1 Comparing time and frequency domain perspectives

Feature	Time domain	Frequency domain
Independent variable	Time (t)	Frequency (f or ω)
Mathematical tool	Differential equations	Complex algebra (phasors)
Optimal applications	Transients, non-linear effects, pulses, ...	Steady-state, resonances, filters, ...
Characteristic visual representation	Oscilloscope trace	Spectrum analyzer plot[†]

[†]A graph that displays amplitude versus frequency for a wave.

15.3.1 Finite-Difference Time-Domain Method

Finite-difference time-domain (FDTD) is a grid-based method that solves Maxwell's equations numerically in the time domain. Both space and time are discretized, using a "staggered grid" where electric field (E) components and magnetic field (H) components are offset from one another. The algorithm then solves the curl equations

$$\boldsymbol{\nabla} \times \boldsymbol{E} = -\frac{\partial \boldsymbol{B}}{\partial t} \qquad \boldsymbol{\nabla} \times H = \boldsymbol{J} + \frac{\partial \boldsymbol{D}}{\partial t},$$

numerically using a *leap-frog algorithm* (which is described in more depth in Box 15.2):

- the E-field is solved at a given instant in time, then
- the H-field is solved at the next half-time step.

Because it is a time-domain method, a single simulation run with a pulse can provide the frequency response across a wide range of spectrum through a Fourier transform. It is conceptually straightforward and handles complex, inhomogeneous, or nonlinear materials very effectively. The main drawback is that the method requires a grid over the entire volume of space, which can be computationally expensive for models involving large distances or requiring resolution of fine geometric details.

15.3.2 The Method of Moments

The *method of moments (MoM)* [also known as the *boundary element method (BEM)*; see Section 4.3.3] is a numerical technique used to solve integral forms of Maxwell's equations, typically in the frequency domain. Unlike FDTD, which grids the entire volume of space, the boundary element method relies on Green's theorem to recast the differential volume problem into an integral surface problem. Then MoM requires only the surface of the objects (or the volume of dielectric bodies) to be discretized. It converts the governing integral equations into a linear system of algebraic equations, $Ax = b$. It calculates the induced currents on the surface of a conductor and then uses those currents to determine the resulting electromagnetic fields in the surrounding space. Some key strengths:

Box 15.2 The Leap-Frog Integration Algorithm

A *leap-frog integration algorithm* is a numerical method used to solve equations of motion for physical systems such as Newton's laws, Hamiltonian dynamics, or wave equations. The name comes from the way the positions and velocities "leap" over one another in time, alternating update steps.

Staggered Timesteps

In a standard Euler integration method, the position x and velocity v are evaluated at the same time t. In a leap-frog scheme, positions and velocities are staggered on a half-time step, with positions evaluated at integer time steps,

$$t, t + \Delta t, t + 2\Delta t, \ldots,$$

and velocities evaluated at half-integer time steps,

$$t - \frac{1}{2}\Delta t, t + \frac{1}{2}\Delta t, t + \frac{3}{2}\Delta t, \ldots$$

Because the velocity is known exactly halfway through the interval, it gives a more accurate update for the position across that entire interval.

Leap-Frog Advantages

The leap-frog algorithm has two desirable mathematical properties:

1. *Time-reversability:* The algorithm run forward N steps and then backward N steps will return exactly to the starting position. Standard explicit methods like Euler or Runge–Kutta don't do this because of numerical drift.
2. *Geometric conservation:* The leap-frog algorithm doesn't conserve energy exactly, but numerical error does not grow without bound. Instead of spiraling into a star or flying out into space due to numerical friction, an orbit simulated via leap-frog will cleanly oscillate around the true path indefinitely.

Application in Electromagnetism

The leap-frog scheme is called the *Yee Algorithm* in FDTD. It uses a leap-frog update of the electric field $\boldsymbol{E}$ and magnetic field $\boldsymbol{H}$, interleaving them both in time steps $\frac{1}{2}\Delta t$ and spatial grids $\frac{1}{2}\Delta x$) to preserve the curl structure of Maxwell's equations without unphysical dissipation.

1. It is very efficient for radiation and scattering problems (such as antenna design) because it inherently satisfies the outgoing-wave radiation condition at infinity without requiring artificial absorbing boundary conditions to prevent reflections.
2. It is the gold standard for analyzing complex wire antennas and metallic structures.

The main shortcoming of MOM is that the matrix A becomes very large and dense (filled with non-zero values) as the complexity or size of the system increases, which can lead to high memory requirements and longer solve times compared to sparse-matrix methods like *finite element analysis*.

15.4 Dipole Radiation

15.5 Scattering and Diffraction

Deviations for scattering of electromagnetic waves (EM) from the Fresnel model of reflection and transmission (refraction) at flat interfaces that was described in Section 14.3 are termed *scattering* or *diffraction*, with the distinction between the two being somewhat subjective. A common assumption is that scattering occurs when EM waves interact with smooth objects and diffraction occurs when EM waves interact with objects having sharp edges.

15.5.1 Introduction

This section is under construction.

15.5.2 Scattering Cross Section

This section is under construction.

15.5.3 Thomson Scattering

Thomson scattering corresponds to the scattering of an electromagnetic wave from a free electron, which may be viewed as the classical, non-relativistic limit of quantum *Compton scattering*.[2] It is an important process for physical environments where strong ionization produces many free electrons, as in stars.[3]

[2] *Compton scattering* is a quantum process in which a high-energy photon collides with a loosely bound electron, transferring some of its energy. As a result, the electron recoils and the scattered photon continues in a new direction with less energy, and hence a longer wavelength. At very low energy Compton scattering becomes equivalent to classical Thomson scattering.

[3] Because of strong *thermal ionization* and *pressure ionization* (the latter a quantum process that can ionize densely packed atoms, even at zero temperature), stars are expected to be completely ionized, except near their surfaces. The strong scattering of electromagnetic radiation from the copious number of free electrons in the plasma makes stellar matter extremely opaque to light. For example, in the deep interior of the Sun the mean free path of a photon before interacting with an electron is only of order millimeters. This high *opacity* of stellar matter plays a fundamental role in all aspects of the structure and evolution of stars [37]. Thomson scattering makes a significant contribution to stellar opacity, especially at higher temperatures and lower densities,

The remainder of this section is under construction.

15.5.4 Rayleigh Scattering

Mie scattering is a formalism derived from the Maxwell equations that describes the scattering of electromagnetic radiation by spherical particles that are similar in size or larger than the wavelength of the radiation. *Rayleigh scattering* is a subset of Mie scattering corresponding to the elastic scattering of light by particles having diameters a that are much smaller than the wavelength λ of the light ($a \ll \lambda$). The blue color of the sky, the red and orange colors of sunsets, and the propensity to sunburn on a sunny day even if you limit direct exposure to sunlight are all at least partially consequences of Rayleigh scattering of sunlight from molecules in the Earth's atmosphere (primarily oxygen and nitrogen).[4]

The Dipole Approximation: Gas particles typically have small magnetic moments compared with their electric dipole moments, so the scattering is almost pure electric dipole. When an electromagnetic wave interacts with a small, non-absorbing dielectric sphere (like a gas molecule), the oscillating electric field $\boldsymbol{E} = \boldsymbol{E}_0 e^{-i\omega t}$ induces an oscillating electric dipole moment $\boldsymbol{p}$,

$$\boldsymbol{p} = \alpha \boldsymbol{E}, \tag{15.1}$$

where α is the polarisability of the particle. For a sphere of radius a and refractive index n, the polarizability is given by

$$\alpha = 4\pi\epsilon_0 a^3 \left(\frac{n^2-1}{n^2+2}\right). \tag{15.2}$$

This induced dipole acts as a miniature antenna, re-radiating energy in all directions except along the axis of oscillation. The power P radiated by an oscillating dipole is proportional to the fourth power of the frequency (ω^4), implying an inverse fourth-power dependence on wavelength λ. The scattering cross-section σ_s is given by

$$\sigma_s = \frac{2\pi^5}{3}\frac{a^6}{\lambda^4}\left(\frac{n^2-1}{n^2+2}\right)^2, \tag{15.3}$$

Angular Distribution and Polarization: For unpolarized incident light, the intensity of the scattered light I at a distance r and angle θ from the incident beam is given by

$$I = I_0 \frac{1+\cos^2\theta}{2r^2}\left(\frac{2\pi}{\lambda}\right)^4 \left(\frac{n^2-1}{n^2+2}\right)^2 a^6. \tag{15.4}$$

The $(1+\cos^2\theta)$ term indicates that scattering is symmetric in the forward ($\theta = 0$) and backward ($\theta = \pi$) directions. At an observation angle of $\theta = 90^\circ$, the $\cos^2\theta$ term for

[4] The sunburn argument might seem counter-intuitive. The strong Rayleigh scattering of short-wavelength UV radiation *reduces the direct UV* that you receive from the Sun, but it contributes to a diffuse secondary source of UV that bathes you from all sides. Hence, even while in the shade you are being hit by Rayleigh-scattered UV from the full hemisphere of the visible sky and your integrated dosage of solar UV is greater than that accumulated while in direct sunlight.

one component vanishes. Consequently, light scattered at right angles to incident light is 100% linearly polarized.

Physical Implications: The λ^{-4} dependence on wavelength for the intensity in Eq. (15.4) implies that shorter wavelengths of visible light (blue/violet) scatter much more efficiently than longer wavelengths (red) from molecules in the Earth's atmosphere. Quantitative, it is found that blue light is Rayleigh scattered approximately 10 times more than red light scattering. Thus, when we look up at the sky the strongly scattered light that we see has been scattered down to us and is predominantly blue light; consequently, the clear day sky appears blue to us. Conversely, at sunset the Sun is near the horizon and the path of light through the atmosphere to our eyes is large, and most of the blue light is scattered out of the direct line of sight, leaving the transmitted red and orange light to reach our eyes; thus we perceive sunsets as being dominated by these colors. The Rayleigh scattering approximation is generally valid if

$$\frac{2\pi a}{\lambda} \ll 1, \tag{15.5}$$

where a is the diameter of the particle. If particles are much larger than air molecules, such as for water droplets in clouds, the scattering is dominated by the more general Mie theory, which is less wavelength dependent. Thus clouds and fog tend to appear white to us. On a macroscopic scale, Rayleigh scattering is intimately linked to the refractive index of a medium. The closeness of molecules in a liquid or solid leads to destructive interference in most directions, which is why a pure crystal doesn't scatter light significantly despite being made of atoms.

15.5.5 Absorption and Dispersion

This section is under construction.

15.6 Radiation from a Single Particle

15.6.1 Liénard–Wiechert Potentials

15.6.2 Syncrotron Radiation

This section is under construction.

No problems yet for this chapter.

Numerical and GenAI Problems

16 Coordinate-Free Representations

Practical physics problems are often most conveniently solved by expanding vector or tensor quantities in a well-chosen basis. For example, a time honored approach that has often been followed in the preceding chapters of this book is to solve electromagnetic boundary value problems by expanding in a basis of orthogonal polynomials, and then exploiting the orthonormality of the basis functions to evaluate the sum. However, vectors and more generally tensors are *geometrical objects* that exist independent from expression in any particular basis, and we must admit that the clearly useful practical approach of expanding in a basis obscures some of the elegance of these geometrical objects.[1]

16.1 Introduction

Mathematicians—often more attuned to elegance and beauty, and less constrained by practicality of application than physicists—have striven for almost two centuries to formulate mathematical quantities in a coordinate-free manner that allows fundamental statements to be made about geometrical objects that are unencumbered by the scaffolding of specific coordinate systems. While less familiar to most physicists than traditional vector and tensor calculus expanded in a basis, this endeavor has led to a coordinate-free framework that is often less practical for the solution of specific physics problems, but able to express fundamentals of such problems more elegantly and succinctly. It is to the advantage of physicists to at least understand the basics and language of this more mathematical approach.

16.2 Electromagnetism's New Clothes

In the remainder of this book, we shall be exploring broader themes in electromagnetism that are less about solution of specific problems (though we shall still do some of those) and more about a deeper understanding of how classical electromagnetism is related to modern physics and mathematics. We shall often express those themes initially in the coordinate-free mathematical approach associated with concepts from topology and differential geometry like vectors and dual vectors, differential forms, exterior calculus,

[1] Indeed, no less a physicist than Einstein emphasized in the development of special and particularly general relativity that coordinates are merely labels with no physical content, and that the physics lies in the geometry of curved spacetime, not in an arbitrary choice of coordinate system to represent that geometry.

Hodge star operators, covariant derivatives, connections, fiber bundles, ..., but then show clearly the relationship to the same concepts expressed in traditional vector calculus language. This chapter provides a minimal introduction to this mathematical approach and a familiarity with at least the terminology used here is important in understanding the remaining chapters.

16.3 Sets

Although most readers will be familiar with the basics of set theory, an understanding of sets will often be implicit in our discussion, so it is useful to give formal definitions to begin with. The basic properties of sets are summarized in Box 16.1, which is adapted from Ref. [38]. More advanced set properties such as open and closed sets, or equivalence classes for sets, will be addressed as they are needed in our discussion.

16.3.1 Maps between Sets

A *map* $\phi : M \to N$ from a set M to a set N may be viewed as a generalization of a function[2] that assigns to each element of M *exactly one element* of N (where M and N could be the same or different sets). In the map $\phi : M \to N$

1. ϕ defines the mapping operation,
2. M is called the *domain* of the map,
3. N is called the *codomain* of the map,
4. the set of points in N that points in M get mapped to is the *image* of the map (it is a subset of the codomain), and
5. the *inverse image* of a subset of the codomain is the set of all elements of the domain that map to the subset of the codomain.

The general nature of the mapping between two sets is often described using a terminology that is illustrated in Fig. 16.1.

1. A map is *injective* (also termed *into*) if an element in N is related to no more than one element in M, but N can have unmatched elements.
2. A map is *surjective* (also termed *onto*) if at least one element of M is associated with each element of N.
3. A map is *bijective* if each element of M has a matching element in N and each element in N has a matching element in M.

Of particular importance to our discussion is that a bijective map is one-to-one (1:1) and thus *invertible*. Figure 16.2 illustrates an invertible map. The inverse map $\phi^{-1} : M \to N$ of a map $\phi : M \to N$ is defined by the requirement that

$$(\phi^{-1} \circ \phi)(m) = m, \tag{16.1}$$

[2] We shall be loose in our discussion and view maps and functions as the same things.

Box 16.1 **Basic Properties of Sets [38]**

A *set* is a collection of distinct objects considered as an entity. The members of a set are called *elements* and they can be almost anything (including other sets). The number of members is called the *cardinality* of the set.

Defining elements of a set: A set may be populated with elements in two ways.

1. List the elements explicitly: $A = \{$ red, yellow, green$\}$.
2. Specify a rule: "the negative integers greater than -4". A common rule is to specify a property $P(x)$ that all members x of a set have using *set-builder notation:* $\{x|P(x)\}$ means "the set of all x such that the property $P(x)$ is true". *Example:* If $P(x)$ is the property "x is a prime number", then $\{x|P(x)\} = \{x|\, x$ is a prime number$\}$ = the set of all prime numbers.

Set membership: $x \in A$ indicates that x is a member of set A and $x \notin A$ means that it isn't. These may be read 'x is in A' and 'x is not in A', respectively.

Equivalence: Sets are *equivalent* iff (which means "if and only if") they have precisely the same elements. We assume each element to be listed only once, so $\{a, a, b, c\}$ and $\{a, b, c\}$ are equivalent sets. Likewise, the order of elements doesn't matter, so $\{a, b, c\}$ and $\{b, a, c\}$ are equivalent sets.

Null set: The *null set* is the set having no elements, often denoted by $\emptyset$ or $\{\}$.

Subsets: Set B is a *subset* of set A if each element of B is in A. The notation $B \subset A$ indicates that B is a subset of A. Equivalently $A \supset B$ indicates that A is a superset of B (contains B as a subset). Every set has itself and the null set as subsets. If $B \subset A$ but A and B are not equivalent and $B \neq \{\emptyset\}$, B is a *proper subset* of A.

Union and intersection: The *union* $A \cup B$ of two sets A and B is the set containing all elements that are in A or B, or in both A and B. The *intersection* $A \cap B$ of sets A and B is the set of only those elements contained in both A and B. The union and intersection of two sets are conveniently represented in terms of *Venn diagrams*:

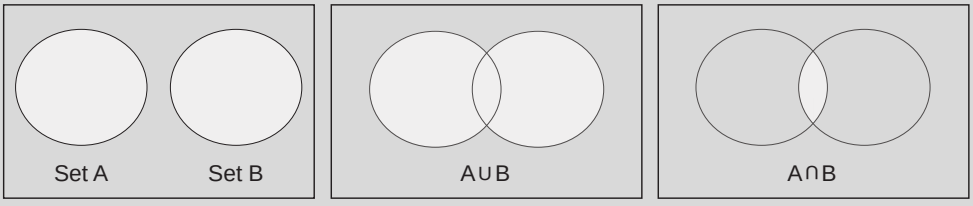

Cartesian product: A cartesian product $X \times Y$ of sets X and Y is the set of ordered pairs (x, y) with $x \in X$ and $y \in Y$. The prototype is $\mathbb{R}^2 = \mathbb{R}^1 \times \mathbb{R}^1$, where $\mathbb{R}^1$ is the real number line and $\mathbb{R}^2$ is the 2D cartesian plane. If X is of dimension m and Y is of dimension n, the cartesian product $X \times Y$ is a set of dimension $m \times n$.

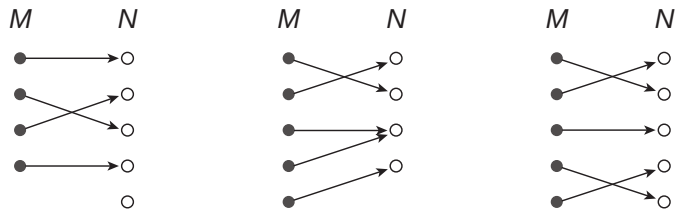

(a) Injective ("into") (b) Surjective ("onto") (c) Bijective

Fig. 16.1 Terminology associated with a mapping $\phi : M \to N$ between two sets M and N. (a) Injective ("into") means that an element in N can have unmatched elements, but an element in N is related to no more than one element in M. (b) Surjective ("onto") means that at least one element of M is associated with each element of N. (c) Bijective ("one-to-one") means that each element of M has a matching element in N, and each element in N has a matching element in M. Bijective maps are invertible because they represent a 1:1 relationship between elements of the two sets.

where $m \in M$.

16.3.2 Differentiation and Continuity of Maps

Of particular interest for maps in physical applications is whether they are *differentiable*. A standard notation is to label a map C^p if all component functions in the map are differentiable to order p and continuous. Thus, a map that is C^∞ is continuous and differentiable to all orders. Two sets M and N are said to be *diffeomorphic* if

1. a C^∞ map $\phi : M \to N$ exists, and
2. the inverse map $\phi^{-1} : M \to N$ exists and is C^∞.

The map $\phi : M \to N$ is then said to be a *diffeomorphism*. Diffeomorphism is the precise formulation of the idea that two topological spaces are equivalent if they can be deformed continuously into each other. The best notion that two spaces correspond to the same manifold is that they are diffeomorphic.

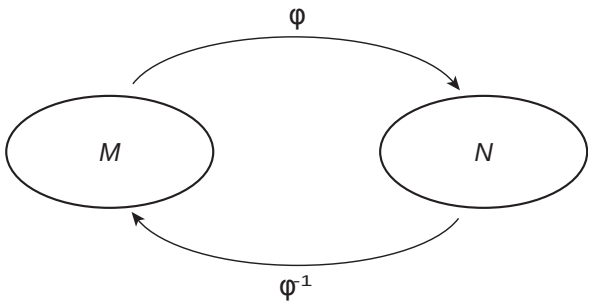

Fig. 16.2 If $\phi : M \to N$ is 1:1, it may be inverted using the inverse map $\phi^{-1} : M \to N$ defined by Eq. (16.1).

16.4 Vector Spaces and Linear Transformations

Our goal is to develop a theory of *tensors* and a *tensor calculus* that may be used to describe a broad range of physical phenomena from a geometrical perspective. We begin by defining a *vector space*.

16.4.1 Vector Spaces

The notion of a *vector space* (also termed a *linear space* or a *linear vector space*) will play a fundamental role in our discussion.[3]

Axiomatic Definition: A *vector space* $\mathbb{V}$ over a field $\mathbb{K}$ (typically the real or complex numbers) is a set with two operations defined:

- *addition of vectors* (a map $\mathbb{V} \times \mathbb{V} \to \mathbb{V}$ of the vector space to itself), and
- *multiplication by scalars* (a map $\mathbb{C} \times \mathbb{V} \to \mathbb{V}$, where $\mathbb{C}$ is the set of complex numbers),

which satisfies the following axioms [56]:

1. $\boldsymbol{u} + \boldsymbol{v} = \boldsymbol{v} + \boldsymbol{u}$;
2. $(\boldsymbol{u} + \boldsymbol{v}) + \boldsymbol{w} = \boldsymbol{u} + (\boldsymbol{v} + \boldsymbol{w})$;
3. a zero vector $\mathbf{0}$ exists, such that $\boldsymbol{u} + \mathbf{0} = \boldsymbol{u}$;
4. for each $\boldsymbol{u}$ there is a corresponding $-\boldsymbol{u}$ such that $\boldsymbol{u} + (-\boldsymbol{u}) = \mathbf{0}$;
5. $\alpha(\boldsymbol{u} + \boldsymbol{v}) = \alpha\boldsymbol{u} + \alpha\boldsymbol{v}$;
6. $(\alpha + \beta)\boldsymbol{u} = \alpha\boldsymbol{u} + \beta\boldsymbol{u}$;
7. $(\alpha\beta)\boldsymbol{u} = \alpha(\beta\boldsymbol{u})$;
8. $1\boldsymbol{u} = \boldsymbol{u}$;

where the vectors $\boldsymbol{u}, \boldsymbol{v}, \boldsymbol{w} \in \mathbb{V}$, the scalars $\alpha, \beta \in \mathbb{K}$, and 1 is the unit element of K.

A More Intuitive Definition: From a more intuitive perspective, we may think of a linear vector space as a set of objects (the vectors) that can be multiplied by numbers and added together in a linear way, while exhibiting *closure:* any such operations on elements of the set give back a linear combination of elements. For arbitrary vectors $\boldsymbol{A}$ and $\boldsymbol{B}$, and arbitrary scalars a and b, one expects then that expressions reflecting linearity like

$$(a + b)(\boldsymbol{A} + \boldsymbol{B}) = a\boldsymbol{A} + a\boldsymbol{B} + b\boldsymbol{A} + b\boldsymbol{B} \tag{16.2}$$

should be satisfied. These rules are not very restrictive and many familiar collections

[3] *Vector space* and *linear space* (and the somewhat redundant *linear vector space*) may all be viewed as synonyms because they refer to the same algebraic structure. "Vector space" originates in physics and geometry, and is the older and more common term. "Linear space" is often the preferred term in more abstract branches of mathematics because the objects in the space need not look like traditional physics vectors (as illustrated in Example 16.1). The essential point is not whether the objects in the space would look like vectors to a physicist, but rather that they exhibit the defining mathematical property of being able to form linear combinations by adding elements together and multiplying them by scalars, and the resulting states are members of the same space (closure condition).

of quantities not usually thought of as vectors by non-mathematicians qualify as vector spaces; Example 16.1 illustrates.

Example 16.1 A vector space of fundamental importance is n-dimensional euclidean space, $\mathbb{R}^n$, which is the set of all n-tuples of the real numbers, $(a^1, a^2, \dots, a^n)$ where $a^i \in \mathbb{R}$ (see Box 16.2 for the definition of an n-tuple). This qualifies as a vector space. For example, it is closed under addition,

$$(\boldsymbol{u}^1, \boldsymbol{u}^2, \dots, \boldsymbol{u}^n) + (\boldsymbol{w}^1, \boldsymbol{w}^2, \dots, \boldsymbol{w}^n) = (\boldsymbol{u}^1 + \boldsymbol{w}^1, \boldsymbol{u}^2 + \boldsymbol{w}^2, \dots, \boldsymbol{u}^n + \boldsymbol{w}^n),$$

meaning that adding two n-tuples results in a third n-tuple that belongs to the same space. Likewise,

$$a(\boldsymbol{u}^1, \boldsymbol{u}^2, \dots, \boldsymbol{u}^n) = (a\boldsymbol{u}^1, a\boldsymbol{u}^2, \dots, a\boldsymbol{u}^n),$$

meaning that multiplication of an n-tuple by a scalar gives another n-tuple that belongs to the same space.

The preceding rules give the minimal requirements to be a vector space but vector spaces employed in physics often have additional structure defined beyond the minimal requirements listed above, like an inner product and a norm, which we will invoke when required.

Basis Vectors: A *basis* for a vector space is a set of vectors that *span the space* (any vector is a linear combination of basis vectors) and that are *linearly independent* (no basis vector is a linear combination of other basis vectors). The number of basis vectors is equal to the *dimensionality* of the vector space.

16.4.2 Linear Transformations

Consider a transformation $T : U \to V$, which is a function from U to V. If U and V are vector spaces, The transformation T is linear if for any two elements u_1 and u_2 of U,

$$T(au_1 + bu_2) = aT(u_1) + bT(u_2), \tag{16.3}$$

where a and b are arbitrary scalars. Example 16.2 illustrates a quintessential linear transformation.

Example 16.2 Let U be $\mathbb{R}^n$ and $V = \mathbb{R}^m$. Then, if A is an $m \times n$ matrix, $\boldsymbol{u} \in \mathbb{R}^n$ is a vector, and $\boldsymbol{v} \in \mathbb{R}^m$ is a vector, the matrix transformation

$$A\boldsymbol{u} = \boldsymbol{v},$$

satisfies

$$A(a\boldsymbol{u}_1 + b\boldsymbol{u}_2) = aA\boldsymbol{u}_1 + bA\boldsymbol{u}_2,$$

and is a linear transformation.

Box 16.2 n-tuples

An *n-tuple* is an ordered sequence of n elements, where n is a non-negative integer. It may be thought of as a list with the specific items and their order strictly prescribed. An n-tuple is typically specified by enclosing elements with parentheses and separating them with commas: $(a_1, a_2, ... a_n)$. For low values of n there often is a common name for an n-tuple: a 2-tuple often goes by the name *ordered pair*, a 3-tuple is an *ordered triplet*, and so on.

An n-tuple differs from a set (see Box 16.1) in two essential ways: (1) Unlike a set, the order of items in a n-tuple matters: $(1, 2)$ and $(2, 1)$ are different n-tuples. (2) Sets care only about unique elements, but an n-tuple can contain multiple instances of the same element: $(1, 1, 2)$ is a valid n-tuple and it is distinct from the n-tuple $(1, 2)$. Some common uses of n-tuples in various contexts include

1. *Mathematics:* The coordinates of an n-dimensional space are specified by an n-tuple; for example, the ordered pair (x, y) uniquely identifies a point in a 2D space.
2. *Linear algebra:* An n-dimensional row or column vector in linear algebra is an n-tuple of numbers.
3. *Relational database:*, A single row of data is an n-tuple; for example, a user's name, age, marital status, and ID number constitute a 4-tuple of data.

Note in these examples that an n-tuple does the job unambiguously but a set would not, either because the order of elements is not prescribed by a set, or because sets don't recognize duplicate entries as being distinct.

Linearity of transformations will be important to later tasks such as defining tensors.

16.5 Differentiable Manifolds

In this section we shall formalize the concept of a manifold in terms of a collection (*atlas*) of open sets (*charts*), the union of which covers the manifold completely and smoothly. We follow generally the discussion of manifolds in Refs. [57, 22, 38, 60, 28].

16.5.1 Composition of Two Maps

In Section 16.3.1 we introduced mapping between sets. Given two maps $\phi : A \to B$ and $\phi : B \to C$ among sets A, B, and C, the *composition* of the two maps (see Box 16.3) is

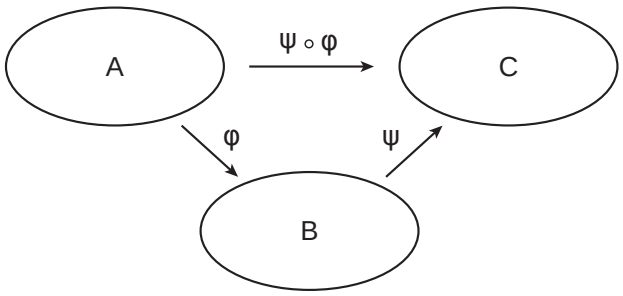

Fig. 16.3 Composition $\psi \circ \phi : A \to C$ of the maps $\phi : A \to B$ and $\psi : B \to C$, as defined by Eq. (16.4).

denoted by $\psi \circ \phi : A \to C$ and is defined by the condition that

$$(\psi \circ \phi)(a) = \psi(\phi(a)), \tag{16.4}$$

where $a \in A$ and $\phi(a) \in B$, so that $(\psi \circ \phi)(a) \in C$. Thus composition of the maps ϕ and ψ is equivalent to

1. mapping an element of A to an element of B using ϕ, and then
2. mapping the result to an element of C using ψ,

as represented by the diagram in Fig. 16.3 and discussed in Box 16.3.

16.6 Vectors

Points in a manifold (which we will label generically by $\mathbb{S}$) exist independent of their being labeled by a coordinate systems. Vectors and one-forms are fundamental entities in the geometry of manifolds that are defined at points in the manifold and are also independent of any specific coordinate system.

16.7 One-Forms

16.8 Tensors

16.9 Differentiation on Manifolds

The remainder of this section is under construction.

Box 16.3 **Composition**

Composition combines two or more maps into a new, single map. It is a "chaining process", where the output of the first map is the input to the second map.

> ***A Composition Machine:*** Think of machines on an assembly line. If machine A takes p as input and produces q, and machine B takes q as input and produces r, then if machines A and B are chained the resulting machine (composition of machines A and B) takes p and produces r directly.

That is the meaning of the composition diagram shown in Fig. 16.3.

Formal Definition of Composition

Composition takes two maps and produces a third map. Let A, B, and C be sets. Suppose that we have two mappings,

1. $f : A \to B$, which maps an element $x \in A$ to an element $f(x) \in B$,
2. $g : B \to C$, which maps an element $y \in B$ to an element $g(y) \in C$.

The *composition* of g and f, denoted as $g \circ f$ (read as "g composed with f" or "g of f"), is a new function that maps set A directly to set C,

$$g \circ f : A \to C.$$

For all x in A, it is defined by

$$(g \circ f)(x) = g(f(x)).$$

Composition has the following properties:

1. *Domain/Codomain Restriction:* For the composition $g \circ f$ to be valid, the codomain (or at least the range) of the first function f must be a subset of the domain of the second function g.
2. *Composition Isn't Commutative:* Generally $g \circ f \neq f \circ g$; always evaluate from right to left in $g \circ f$ [inside out in $g(f(x))$].
3. *Composition Is Associative:* In composing three or more mappings, the grouping does not matter: $h \circ (g \circ f) = (f \circ g) \circ f$.

A Simple Example

Define two mappings on the set of real numbers, $f(x) = x^2$ and $g(x) = x + 1$. Then the composition $(g \circ f)(x)$ means that we plug $f(x)$ into g:

$$(g \circ f)(x) = g(f(x)) = g(x^2) = x^2 + 1.$$

Notice that if we evaluate instead

$$(f \circ g)(x) = f(g(x)) = f(x + 1) = (x + 1)^2,$$

illustrating by explicit example that composition generally does not commute.

Background and Further Reading

Tromp [73] gives an overview of many of the ideas addressed here. A geometrical view of tensors from a physics perspective may be found in Carrol [22], Misner, Thorne, and Wheeler [54], and Schutz [66].

Problems

No problems yet for this chapter.

16.1

17 Spacetime Tensors

These lectures constitute a graduate-level course in classical electromagnetism. The distinction between classical and modern physics turns on whether the dynamics are described by quantum mechanics and quantum field theory or classical mechanics and classical field theory, and by non-relativistic mechanics or relativistic mechanics. Traditionally classical electromagnetism excludes quantum theory (except for a few quantum concepts involving the microscopic structure of matter), but special relativity has been considered part of the discussion of classical electromagnetism. Accordingly, this chapter will introduce Minkowski spacetime and a differential geometry and spacetime tensor formalism that is the mathematical foundation of the theory of relativity. Then in Ch. 18 we will introduce the special theory of relativity and demonstrate explicitly the Lorentz covariance of Maxwell's equations. Finally, Ch. 21 will use the gauge-invariant and Lorentz-covariant formulation of classical electromagnetism in terms of the Maxwell equations to paint electromagnetism as a relativistic gauge field theory that, when quantized, is the harbinger of the Standard Model of elementary particle physics.

It is possible to introduce special relativity in a minimal way and then use that to demonstrate the Lorentz invariance of the Maxwell equations in less space than we will use here. However, we choose to give a more thorough introduction to the differential geometry and tensor formalism underlying the theory of relativity. In particular, the tensor formalism will be developed in a way that is compatible with curved spacetime, and therefore with general relativity. Then, we will approximate by restricting to flat spacetime to recover the theory of special relativity. This approach has several advantages:

1. At the level of expertise required for our discussion it does not take much longer to develop the formalism in a way compatible with either flat or curved spacetime than to describe special relativity minimally.
2. The resulting formalism gives more satisfying insight into special relativity and its relationship with Newtonian mechanics, general relativity, and the Maxwell equations.
3. Developing the formalism in this way gives the reader a solid foundation to take on more advanced topics such as general relativity.

Let us begin the discussion with an overview of 4-dimensional spacetime.

17.1 Minkowski Spacetime and Spacetime Tensors

The most elegant formulation of special relativity is in terms of a 4-dimensional spacetime manifold called *Minkowski space*, and in terms of *spacetime tensors* that are a consequence

of the differential geometry of that manifold. Let us review Minkowski space and spacetime tensors defined for that manifold.

17.1.1 Transformations between Inertial Systems

In 1905 Einstein published the *special theory of relativity*, which was to revolutionize our conception of space and time. His motivation for the special theory was a conviction that the laws of physics must be independent of coordinate system for the observer (the *principle of relativity*), and that transformations between inertial frames (coordinate systems in which Newton's first law is valid) should be the same for particles and for light. Newtonian mechanics already implied a principle of relativity for space: the laws of mechanics were unchanged by a *Galilean transformation* between inertial frame. The most general Galilean transformation for $\boldsymbol{x} = (x, y, z)$ may be written

$$\boldsymbol{x}' = \boldsymbol{x}'(\boldsymbol{x}, t) = \boldsymbol{x} - \boldsymbol{v}t \qquad t' = t'(\boldsymbol{x}, t) = t, \tag{17.1}$$

so for motion along the x axis,

$$x' = x - vt \qquad y' = y \qquad z' = z \qquad t' = t, \tag{17.2}$$

where primed coordinates and unprimed coordinates represent the two inertial frames, the velocity is v, and a single universal time $t = t'$ is assumed for all inertial frames. But Einstein (as well as others such as Lorentz) realized that there is a problem in that these common-sense notions of relative motion between inertial frames were consistent with the motion of billiard balls and projectiles, but were inconsistent with the theory of light, which was well understood in 1905 to correspond to an electromagnetic wave described by Maxwell's equations.

A striking aspect of the Maxwell theory was that it admitted wave solutions and these waves traveled with a speed that was a *constant of the theory* (and thus independent of inertial frame for the observer). When the constant was evaluated it was found to be equal to the speed of light, which led to Maxwell's electromagnetic waves being identified with light. The beauty of Maxwell's equations greatly impressed Einstein, but they presented a problem of interpretation for classical physics.

> By the Galilean transformations, the speed of light should depend upon the inertial frame of the observer; but not by Maxwell's equations because the speed of light is a constant of the theory.

The interpretation that emerged in the 1800s to reconcile this discrepancy was that electromagnetic waves must move through some medium. (How could a wave travel through nothing?) This hypothesized medium was called the *(luminiferous) aether*, and it possessed quite magical properties: it was required to be an invisible, rigid (because transverse waves don't propagate through fluids) substance permeating all of space, but relevant only for light propagation, so as not to disturb other physical laws. Then the constant

Box 17.1 Rise and Fall of the Luminiferous Aether

The idea of the luminiferous aether originated in optics in the 1700s (luminiferous means "light-bearing"), long before light was understood to be an electromagnetic phenomenon.

Origin in Optics

Christiaan Huygens proposed a wave theory of light in 1690, and because all waves studied to that point required a medium for propagation, he proposed a subtle, massless medium permeating all of space that carried light waves. The idea was bolstered by

1. Thomas Young's double-slit experiment and
2. mathematical treatments by Augustin-Jean Fresnel in the early 1800s,

which established firmly that light was a transverse wave, suggesting the need of a medium to support those transverse undulations.

Maxwell Weds the Aether to Electromagnetism

Maxwell was the first to unite the optical aether with the electromagnetic field. He constructed a complex mechanical model of the aether, which he envisioned as a fluid filled with spinning "molecular vortices" that representing magnetic fields, separated by "idle wheels" that represented electric particles (see the diagram in Box 11.1). Through this mechanical aether model, he derived what we now recognize as the foundational equations of electromagnetism. In particular, his famous theoretical discovery that electromagnetic waves were expected to propagate at the speed of light was first obtained using a version of his aether model that removed some of the mechanical scaffolding but retained the underlying dynamical medium.

Downfall of the Aether Hypothesis

This alliance of electromagnetism and the aether model persisted until

1. the Michaelson–Morley experiment in 1887 called into question the existence of the aether and
2. Einstein's theory of special relativity in 1905,challenged the need for an aether.

speed of electromagnetic waves could be understood as an artifact of the special aether rest frame in which light propagated. The history of this idea is summarized in Box 17.1.

It is now understood that light waves are propagating disturbances in electric and magnetic fields that do not require a physical medium, and that the aether is a fiction. But in

the latter part of the 19th century it was widely believed to exist, and various attempts were made to detect the motion of the Earth relative to the aether (an effect called the *aether drift*). Using light interferometry, Michelson and Morley showed in 1887 that there was no evidence for motion of the Earth with respect to the hypothetical aether, thus casting serious doubt on its existence.[1]

17.1.2 Lorentz Transformations

Without the aether fiction, Maxwell's equations for light and the Galilean invariance exhibited by material particles were clearly at odds. Others had hinted at a solution (notably Hendrik Lorentz and Henri Poincaré) but it was Einstein who first concluded that the Maxwell theory was correct and that it was the *Galilean transformations* that required modification to reconcile mechanics and electromagnetism. Thus he put forth the bold and unqualified assertions that

1. physical law is the same in all coordinate systems, so there are no preferred inertial frames, and
2. the speed of light is *constant in all inertial frames*

that are the foundation of the 1905 *special theory of relativity*. Requiring the speed of light c be an invariant independent of inertial frame dictated replacement of Galilean transformations (17.2) with *Lorentz transformations,*

$$\begin{aligned} x' &= \gamma(x - vt) \qquad y' = y \qquad z' = z, \\ t' &= \gamma\left(t - \frac{vx}{c^2}\right) \qquad \gamma \equiv \frac{1}{\sqrt{1 - v^2/c^2}}, \end{aligned} \tag{17.3}$$

where a boost along the x axis is assumed and γ is called the *Lorentz γ-factor*. Notice that the Galilean transformations remain quite correct in the low-velocity world since in the limit $v/c \to 0$ the factor $\gamma \to 1$ and the Lorentz transformations (17.3) become equivalent to the Galilean transformations (17.2). Notice also that time transforms non-trivially under Lorentz transformations, with the Lorentz transformations *mixing the space and time coordinates*. This is in stark contrast to the Galilean transformations, where there is a universal time shared by all observers.

The mathematician Hermann Minkowski (once Einstein's teacher) then proposed that in special relativity separate notions of space and time should be abandoned in favor of a *4-dimensional spacetime* parameterized by *spacetime coordinates*

$$(x^0, x^1, x^2, x^3) \equiv (ct, x, y, z), \tag{17.4}$$

where the superscripts are indices, not exponents. (The reason for placing indices as superscripts will explained shortly.) In a 1908 presentation entitled *Raum und Zeit* (*Space*

[1] Nevertheless, efforts persisted for years to salvage the aether hypothesis. Einstein originally took the aether hypothesis seriously, but abandoned it at some point before he published the special theory of relativity. Einstein claimed that the Michelson–Morley result had no influence on his formulation of the special theory of relativity. Surely Einstein knew of the Michelson–Morley results, but he seems to have felt that this was not as important as his own reasoning in coming to the special theory of relativity.

and Time) Minkowski introduced 4-dimensional spacetime using a now-legendary phrasing:

> *The views of space and time which I wish to lay before you have sprung from the soil of experimental physics, and therein lies their strength. They are radical. Henceforth space by itself, and time by itself, are doomed to fade away into mere shadows, and only a kind of union of the two will preserve an independent reality.*
>
> Hermann Minkowski (1908)

Now time, scaled by the speed of light so that it has the same units as the other three coordinates, is just another coordinate in 4-dimensional spacetime. Minkowski's formulation showed that special relativity is rather simple in 4-dimensional spacetime, but becomes complicated when projected onto 3-dimensional space.[2]

17.1.3 Minkowski Space

Allowing the coordinates (x^0, x^1, x^2, x^3) to range over all their possible values traces out the manifold of 4-dimensional spacetime called *Minkowski space*. In this space the square of the infinitesimal distance ds^2 between two points (ct, x, y, z) and $(ct+cdt, x+dx, y+dy, z+dz)$ is given by

$$\begin{aligned} ds^2 = \sum_{\mu\nu} \eta_{\mu\nu} dx^\mu dx^\nu &= -c^2dt^2 + dx^2 + dy^2 + dz^2, \\ &= -(dx^0)^2 + (dx^1)^2 + (dx^2)^2 + (dx^3)^2, \end{aligned} \tag{17.5}$$

which is called the *line element* of the Minkowski space. Notice that in this equation ds^2 means $(ds)^2$, and dx^2 means $(dx)^2$, but the superscripts in (dx^0, dx^1, dx^2, dx^3) are indices and not powers. The *metric tensor* of Minkowski space $\eta_{\mu\nu}$ appearing in Eq. (17.5) may be expressed as the diagonal matrix

$$\eta_{\mu\nu} = \begin{pmatrix} -1 & 0 & 0 & 0 \\ 0 & 1 & 0 & 0 \\ 0 & 0 & 1 & 0 \\ 0 & 0 & 0 & 1 \end{pmatrix}. \tag{17.6}$$

The line element (17.5) or the metric tensor $\eta_{\nu\mu}$ determine the geometry of Minkowski space because they specify distances, distances can be used to define angles, and that is geometry.

The pattern of plus and minus signs on the right side of Eq. (17.5), or on the diagonal of the matrix in Eq. (17.6), defines the *signature of the metric*. For Minkowski space the signature that we adopt is $(-+++)$. Some authors define the signature as the difference

[2] An English translation of the full presentation may be found at `https://en.wikisource.org/wiki/Translation:Space_and_Time`. Minkowski undoubtedly would have made further contributions to the development of special and general relativity, but he died unexpectedly of peritonitis only months after his famous Space and Time lecture.

of the number of $+$ and $-$ signs, which conveys similar information. A metric such as (17.6) where the signs in the signature pattern are not all the same is termed an *indefinite metric*. Equally common is the choice $(+\ -\ -\ -)$ for the Minkowski-space signature, which leads to the same physical results as our choice if all signs are carried through consistently. The central point for the indefinite metric of Minkowski spacetime is that the last three terms have the same sign and that the sign of the first term differs from that of the other three (assuming the usual modern convention of displaying the timelike coordinate in the first position and the spacelike coordinates in the last three positions).

The fundamental difference between the *geometry of 4D Minkowski space* and that of 4D Euclidean space lies in the metric signature, which is just the signature of the unit matrix $(+\ +\ +\ +)$ for 4-dimensional euclidean space, compared with the indefinite Minkowski-metric signature $(-\ +\ +\ +)$.

Most of the "strange" features of special relativity (space contraction, time dilation, relativity of simultaneity, the twin "paradox", ...) follow directly from this difference in geometry implied by the Euclidean-space positive definite metric and the Minkowski-space indefinite metric.

17.2 Symmetry under Coordinate Transformations

A physical system has a symmetry under some operation if after the operation the system is indistinguishable from the system before the operation. The theory of relativity may be viewed as a symmetry under coordinate transformations. Relativity is ultimately a statement that physics is independent of our choice of coordinate system: two observers, referencing their measurements to two different coordinate systems, should deduce from their observations the *same laws of physics*. General relativity requires invariance of the laws of physics under the most general possible coordinate transformations, while special relativity requires a symmetry under only the subset of coordinate transformations that are between inertial frames. Hence, to understand relativity it is important consider coordinate systems, transformations between coordinate systems, and the properties of those transformations.

17.3 Spacetime Tensors and Covariance

The *principle of relativity* implies that coordinates should be viewed as *arbitrary labels,* so that the laws of physics are independent of the coordinate system in which they are formulated. We may implement this coordinate independence by formulating the laws of

physics in terms of equations that are *covariant* with respect to the coordinate transformations.[3] The term *covariance* implies that a set of equations maintains the same mathematical form under a specified set of transformations. Covariance can be stated most concisely in terms of *tensors,* which we may think of as generalizing the idea of vectors. We now give an introduction to tensors, tensor notation, and tensor properties for 4D spacetime, and illustrate with an application of the tensor formalism to Lorentz covariance, which will lead to the theory of special relativity.

17.3.1 Spacetime Coordinates

Relativity implies that space and time enter physical descriptions on comparable footings, so it is useful to unify them into a 4-dimensional continuum termed *spacetime*. Spacetime is an example of a *differentiable manifold,* as described in Box 17.2 (adapted from Ref. [36]). Spacetime points are defined by coordinates having four components, the first labeling the time t multiplied by the speed of light c, the other three labeling the spatial coordinates:

$$x \equiv x^\mu = (x^0, x^1, x^2, x^3) = (ct, \mathbf{x}), \tag{17.7}$$

where $\mathbf{x}$ denotes a 3-vector with components (x^1, x^2, x^3) labeling the spatial position. The first component x^0 is termed *timelike* and the last three components (x^1, x^2, x^3) are termed *spacelike*. As for earlier discussion, the upper or lower placement of indices is meaningful. Bold symbols will denote (ordinary) vectors defined in the three spatial degrees of freedom, and 4-component vectors in spacetime will be denoted in non-bold symbols. The modern convention is to number the indices beginning with zero rather than one. The coordinate systems of interest will be subject only to the requirements that they assign a coordinate uniquely and be differentiable to sufficient order at each point of spacetime.

A point in an n-dimensional manifold can be labeled using a coordinate system of n parameters, but the choice of coordinate system is arbitrary. Points may be relabeled by a *passive coordinate transformation* that switches the coordinate labels of the points, $x^\mu \to x'^\mu$, with x^μ and x'^μ labeling the *same point* but in two different coordinate systems. Our generic concern is with a transformation between one set of spacetime coordinates denoted by (x^0, x^1, x^2, x^3), and a new set

$$x'^\mu = x'^\mu(x) \qquad (\mu = 0, 1, 2, 3), \tag{17.8}$$

where $x = x^\mu$ denotes the original (untransformed) coordinates. This notation is an

[3] Covariance is a property defined relative to a particular set of transformations. There is a subtle difference in meaning between *invariance* and *covariance*, with respect to a set of transformations. As we shall discuss further in Box 18.3, invariance means that the physical observables of the system are not changed by the transformations. Covariance means that the system is formulated mathematically so that the form of the equations does not change under the transformations. *Manifest covariance* means that the invariance is *manifest* in the formulation of the theory (can be "seen at a glance"). Thus, a system could be covariant under some set of transformations, but not manifestly covariant because the covariance is obscured by the way the equations are written. This is the case with the Maxwell equations. As we shall see in Section 18.9, it isn't clear whether the Maxwell equations written in their usual form (1.1) are covariant under Lorentz transformation (because they are not formulated in standard Lorentz 4-vector notation), but they are, and they can be re-written so that the Lorentz covariance is manifest.

Box 17.2 Manifolds

Loosely, a manifold is a space. More formally, an *n-dimensional manifold* is a set that can be parameterized continuously by n independent real coordinates for each point (member of the set). Physics is usually concerned with *differentiable manifolds,* which are continuous and differentiable (to a suitable order). Again, more formally: a manifold is continuous if for every point there are neighboring points having infinitesimally different coordinates, and differentiable if a scalar field can be defined on the manifold that is everywhere differentiable. Special and general relativity assume spacetime to be a *Riemannian manifold:* a continuous, differentiable manifold with geometry described by a metric tensor of quadratic form that may depend on spacetime coordinates.

Coordinates, charts, and atlases

A *coordinate system* or *chart* associates n real parameter values (labels) uniquely with each point of an n-dimensional manifold M through a one-to-one mapping from $\mathbb{R}^n$ (cartesian product of n copies of the real numbers $\mathbb{R}$) to M. For example, the set of continuous rotations about a single axis defines a one-dimensional manifold parameterized by an angle $\phi \in \mathbb{R}$. The one-to-one association of points in the n-dimensional manifold with the values of their parameter labels is analogous to mapping points of the manifold to points of an n-dimensional euclidean space. Thus, *locally* a manifold looks like euclidean space in its most general properties, such as dimensionality and differentiability (but not necessarily in geometry, since this depends on whether the manifold has a metric and its nature).

A single coordinate system is usually insufficient to give a unique correspondence between points and coordinate labels for all but the simplest manifolds. For example, the latitude–longitude system for the Earth (viewed as a 2-sphere, S^2) is degenerate at the poles where all values of longitude correspond to a single point. In such cases the manifold must be parameterized by overlapping *coordinate patches* (*charts*), with *transition functions* between the different sets of coordinates for points in each overlap region. An *atlas* is a collection of charts sufficient to parameterize an entire manifold. For the latitude–longitude example it may be shown that the atlas must contain at least two overlapping charts to parameterize the full manifold uniquely.

Curves and surfaces

Subsets of points within a manifold can be used to define *curves* and *surfaces*, which represent *submanifolds* of the full manifold. Often it is convenient to represent these parametrically, with an m-dimensional submanifold parameterized by m parameters. A curve is a one-dimensional submanifold parameterized by a single parameter, while a *hypersurface* is a surface of one less dimension than the full manifold, parameterized by $n-1$ real numbers.

economical form of

$$x'^{\mu} = f^{\mu}(x^0, x^1, x^2, x^3) \qquad (\mu = 0, 1, ...), \tag{17.9}$$

where the single-valued, continuously-differentiable function f^{μ} assigns new (primed) coordinates (x'^0, x'^1, x'^2, x'^3) to a point of the manifold with old coordinates (x^0, x^1, x^2, x^3), which may be abbreviated to $x'^{\mu} = f^{\mu}(x)$ and, even more tersely, to Eq. (17.8). The coordinates in Eq. (17.8) are just labels so the laws of physics cannot depend on them. Hence the system x'^{μ} is not privileged and Eq. (17.8) should be invertible.

The generalized form of the Einstein summation convention that we introduced earlier will be assumed for all subsequent equations: for any term on one side of an equation any index that is repeated, once as a superscript and once as a subscript, implies a summation over that index. A superscript (subscript) in a denominator counts as a subscript (superscript) in a numerator. We will use Greek indices $(\alpha, \beta, ...)$ to denote the full set of spacetime indices running over 0, 1, 2, 3, while roman indices $(i, j, ...)$ will denote the indices 1, 2, 3 running only over the spatial coordinates. Thus x^{μ} means any of the components x^0, x^1, x^2, x^3, but x^i means any of the components x^1, x^2, x^3.

17.3.2 Vectors in Non-Euclidean Space

Spacetime is characterized by a non-euclidean manifold. In euclidean space we are used to representing vectors as directed line segments of finite length. This picture will not do in curved spacetime, which is locally but not globally, euclidean so extended straight lines have no clear meaning. Thus we need a more general way to define vectors that works in both euclidean and (possibly curved) non-euclidean manifolds. The standard solution is to define vectors for an n-dimensional manifold, not in manifold itself, but in n-dimensional euclidean *tangent spaces*, with an independent tangent space T_P attached to each point P of the manifold. This is illustrated in Fig. 17.1 for 1D and 2D spheres.[4] Just as vectors may be defined in tangent spaces attached to each point of a manifold, dual vectors my be defined in *cotangent spaces* T_P^* attached to each point of a manifold.

A *tangent bundle* TM for a manifold M is a manifold constructed from the disjoint union of all the tangent spaces T_P defined on the manifold M. Likewise, a contangent bundle for a manifold M is the disjoint union of all the cotangent spaces defined on the manifold. Such bundles and their generalization form the basis of the theory of *fiber bundles*. We will sometimes use the bundle terminology but will not use the theory of fiber bundles directly in our discussion.

17.3.3 Coordinates in Spacetime

A universal coordinate system can be chosen in euclidean space, with basis vectors that are mutually orthogonal and constant, and these constant basis vectors can be normalized to unit length for convenience. Much of ordinary physics may be described using such an

[4] The idea conveyed by Fig. 17.1 in which planes tangent to a 2D surface are shown embedded in a 3D space is useful conceptually, but defining the tangent space at each point is an *intrinsic process* with respect to a manifold and does not require embedding it in a higher-dimensional manifold, as will be shown below.

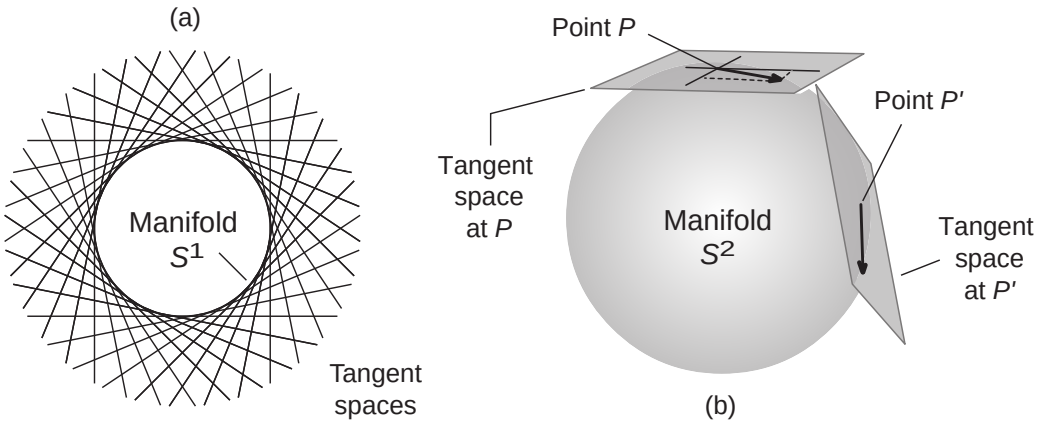

Fig. 17.1 Tangent spaces in curved manifolds, illustrated (a) for the manifold S^1 and (b) for the manifold S^2. As illustrated for S^2, vectors (indicated by arrows) are defined in the tangent spaces at each point, not in the curved manifold. Embedding the 1D tangent-space manifold in 2D euclidean space and the 2D tangent space in 3D euclidean space is for visualization purposes only; the tangent space has a specification that is intrinsic to the manifold.

orthonormal basis. The situation is more complicated in non-euclidean (possibly curved) manifolds. Because of the position-dependent metric of curved spacetime, it is most convenient to choose basis vectors that depend on position and that need not be orthogonal, and it usually is not useful to normalize them since they are position dependent.

The key to specifying vectors in curved space (which will also work in flat space) is to separate the "directed" part from the "line segment" part of the usual conception of a vector as a directed line segment, because the direction for vectors of infinitesimal length can be defined consistently in curved or flat spaces using *directional derivatives.*

17.3.4 Coordinate and Non-Coordinate Bases

Consider a curve in a differentiable manifold along which one coordinate x^μ varies while all others $x^\nu (\nu \neq \mu)$ are held constant. This curve will be termed *the coordinate curve* x^μ. Four such coordinate curves will pass through any point P in a spacetime manifold, corresponding to the coordinate curves x^μ with $\mu = (0, 1, 2, 3)$. A set of position-dependent basis vectors $e_\mu (\mu = 0, 1, 2, 3)$ can be defined at an arbitrary point P in the manifold by

$$e_\mu = \underset{\delta x^\mu \to 0}{\text{Lim}} \frac{\delta s}{\delta x^\mu}, \tag{17.10}$$

where δs is the infinitesimal distance along the coordinate curve x^μ between the point P with coordinate x^μ and a nearby point Q with coordinate $x^\mu + \delta x^\mu$. For a parameterized

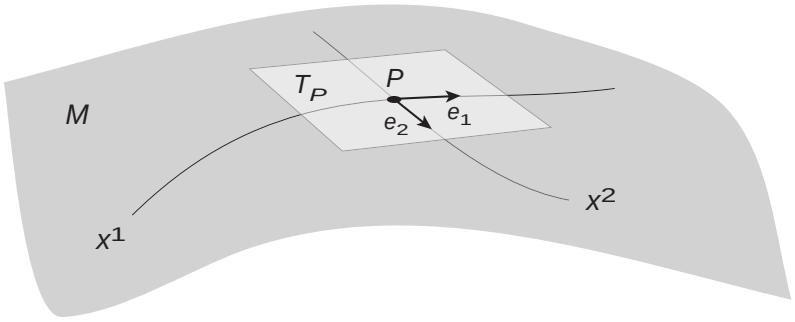

Fig. 17.2 Tangent space T_P at a point P for a curved 2D manifold M. The vectors tangent to the coordinate curves at each point define a coordinate or holonomic basis. This figure is a generalization of Fig. 17.1 to an arbitrary curved 2D manifold with a position-dependent, non-orthogonal (coordinate) basis. This embedding of M in 3D euclidean space is for visualization purposes only; the basis vectors e_1 and e_2 of the tangent space are specified by directional derivatives of the coordinate curves evaluated entirely in M at the point P, as described in Eqs. (17.10)–(17.13).

curve $x^\mu(\lambda)$ having a tangent vector t with components $t^\mu = dx^\mu/d\lambda$,

$$t = t^\mu e_\mu = \frac{dx^\mu}{d\lambda}\, e_\mu,$$

the directional derivative of an arbitrary scalar function $f(x^\mu)$ defined in the neighborhood of the curve is

$$\frac{df}{d\lambda} \equiv \operatorname*{Lim}_{\epsilon\to 0}\left[\frac{f\left(x^\mu(\lambda+\epsilon)\right) - f(x^\mu\left(\lambda\right))}{\epsilon}\right] = \frac{dx^\mu}{d\lambda}\frac{\partial f}{\partial x^\mu} = t^\mu \frac{\partial f}{\partial x^\mu},$$

and since $f(x)$ is arbitrary this implies the operator relation

$$\frac{d}{d\lambda} = \frac{dx^\mu}{d\lambda}\frac{\partial}{\partial x^\mu} = t^\mu \frac{\partial}{\partial x^\mu}. \tag{17.11}$$

Hence the components t^μ are associated with a unique directional derivative and the partial derivative operators $\partial/\partial x^\mu$ may be identified with the basis vectors e_μ,

$$e_\mu = \frac{\partial}{\partial x^\mu} \equiv \partial_\mu, \tag{17.12}$$

which permits an arbitrary vector to be expanded as

$$V = V^\mu e_\mu = V^\mu \frac{\partial}{\partial x^\mu} = V^\mu \partial_\mu. \tag{17.13}$$

Position-dependent basis vectors specified in this way define a *coordinate basis* or *holonomic basis;* a basis using orthonormal coordinates is then termed a *non-coordinate basis* or an *anholonomic basis.* A coordinate basis is illustrated schematically in Fig. 17.2 for a generic curved 2D manifold.

The definition of a vector in terms of directional derivatives evaluated at a point of the manifold is valid in any curved or flat differentiable manifold. It replaces the standard idea of a vector as the analog of a displacement vector between two points, which does not generalize to curved manifolds.

From Eq. (17.10) the separation between nearby points is $ds = e_\mu(x)dx^\mu$, from which

$$ds^2 = ds \cdot ds = (e_\mu \cdot e_\nu)dx^\mu dx^\nu = g_{\mu\nu}dx^\mu dx^\nu$$

with the metric tensor $g_{\mu\nu}$ defined by,

$$e_\mu(x) \cdot e_\nu(x) \equiv g_{\mu\nu}(x). \tag{17.14}$$

The scalar product of vectors A and B in a coordinate basis is given by

$$A \cdot B = (A^\mu e_\mu) \cdot (B^\nu e_\nu) = g_{\mu\nu}A^\mu B^\nu. \tag{17.15}$$

Equation (17.14) may be taken as a definition of a vector coordinate basis $\{e_\mu\}$.

The preceding discussion has been specifically for vectors and involves defining a basis for the tangent space T_P at each point P using the tangents $\partial/\partial x^\mu$ to coordinate curves passing through P. A similar intrinsic procedure can be invoked to construct a basis for dual vectors in the cotangent space T_P^* at a point P using gradients to define basis vectors. This leads to equations analogous to (17.14)–(17.15), but with the indices of the basis vectors in the upper position. A set of dual basis vectors e^μ may be used to expand dual vectors ω as[5]

$$\omega = \omega_\mu e^\mu, \tag{17.16}$$

allowing the metric tensor with upper indices to be defined through

$$e^\mu(x) \cdot e^\nu(x) \equiv g^{\mu\nu}(x), \tag{17.17}$$

with the scalar product of arbitrary dual vectors α and β given by

$$\alpha \cdot \beta = g^{\mu\nu}\alpha_\mu\beta_\nu. \tag{17.18}$$

Equation (17.17) may be taken as a definition of a dual-vector coordinate basis $\{e^\mu\}$.

Just as Eqs. (17.14) or (17.17) are characteristic of a coordinate basis, an orthonormalized non-coordinate basis is specified by the requirement

$$e_{\hat\mu}(x) \cdot e_{\hat\nu}(x) = \eta_{\hat\mu\hat\nu}, \tag{17.19}$$

where $\eta = \text{diag}\{-1, 1, 1, 1\}$. In this expression, hats on indices indicate explicitly that this is an orthonormal and not coordinate basis. Our discussion will seldom require display of explicit basis vectors but usually we will assume implicitly the use of a coordinate basis such that Eqs. (17.10)–(17.18) are valid.

[5] The same symbol e will be used for vector and dual vector basis vectors, with the index in the lower position for a vector basis and upper position for a dual vector basis.

17.3.5 Tensors and Coordinate Transformations

In formulating special and general relativity we are interested in how quantities that enter physical descriptions change when the spacetime coordinates are transformed as in Eq. (17.8). This requires understanding the transformations of fields, their derivatives, and their integrals. To this end, it is useful to introduce spacetime *tensors.* These have a fundamental definition without reference to specific coordinate systems. but it often proves convenient to view tensors as objects expressed in a basis with components that carry some number of upper and lower indices, and that change in a specific way under coordinate transformations. This more practical interpretation of tensors will be developed below.[6]

The *rank* of a tensor will be given a more fundamental definition below but practically it is equal to the total number of indices required to label its components when evaluated in a basis. Thus scalars are tensors of rank zero and vectors or dual vectors are tensors of rank one. This may be generalized to tensors carrying more than one index. Tensors carrying only lower indices are termed *covariant tensors,* tensors carrying only upper indices are termed *contravariant tensors,* and tensors carrying both lower and upper indices are termed *mixed tensors.*

> ***Tensor Types:*** It is convenient to indicate the *type* of a tensor by the ordered pair (p, q), where p is the number of contravariant (upper) indices for components, q is the number of covariant (lower) indices for components, and the rank of the tensor is $p + q$. In principle p and q can take any non-negative value, but practically most physical applications of tensors involve ranks of four or less.

Thus a dual vector is a tensor of type $(0, 1)$ with a rank of one, while the Kronecker delta δ^{ν}_{μ} is a mixed tensor of type $(1, 1)$ and rank 2.

17.3.6 Tensors as Linear Maps to Real Numbers

The characterization of tensors in terms of their transformation properties in a particular represention that will be discussed in Section 17.4 below is the most pragmatic approach to the mathematics required to solve realistic problems. However, mathematicians prefer to define tensors in a more abstract manner that makes manifest that they are independent of representation in a particular coordinate system. This approach, which frequently goes by the name *index-free formalism*, is described in this section.

[6] Hermann Minkowski introduced the use of tensors for the theory of special relativity. In his original special relativity paper, Einstein had not used tensors and at first he dismissed Minkowski's tensor formulation of special relativity as needlessly pedantic. However, Einstein soon realized the power of this new (for physicists, not for mathematicians) approach and adopted the framework of tensors and differential geometry in his later formulation of general relativity.

Fundamentally, a tensor of type (n, m) has input slots for n vectors and m dual vectors, and acts linearly on these inputs to produce a real number.

For example, if ω is a $(0, 1)$ tensor (that is, a dual vector) and A and B are $(1, 0)$ tensors (that is, vectors), linearity implies

$$\omega(aA + bB) = a\omega(A) + b\omega(B) \in \mathbb{R}, \tag{17.20}$$

where a and b are arbitrary scalars and $\mathbb{R}$ denotes the set of real numbers. This definition makes no reference to components of the vectors or dual vectors, so the tensor map must give the same real number, irrespective of any choice of coordinate system.

Thus, a tensor may be viewed as a *function of the vectors and dual vectors themselves,* rather than as a function of their components, or as an *operator* that accepts vectors and dual vectors as input and outputs a real number.

Example 17.1 As a warmup exercise, consider a real-valued function of the coordinates $f(x)$. Since this function takes no vectors or dual vectors as input and yields a real number (the value of the function at x) as output, it is a tensor of rank zero (a scalar).

Let's now give a few less-trivial examples of how this approach works, beginning with vectors and dual vectors.

17.3.7 Vectors and Dual Vectors

Vector spaces are discussed in Box 17.3. Suppose a vector field to be defined on a manifold such that each point P has associated with it a vector V that may be expanded in a vector basis e_μ,

$$V = V^\mu e_\mu, \tag{17.21}$$

and that there is a corresponding dual vector field ω defined at each point P that may be expanded in a dual-vector basis e^μ,

$$\omega = \omega_\mu e^\mu, \tag{17.22}$$

where the basis vectors e_μ are defined in the tangent space T_P and the basis dual vectors e^μ are defined in the cotangent space T_P^* at each point P of the manifold, as described in Section 17.3.2. Hence the e_μ are basis vectors in the tangent bundle and the e^μ are basis vectors in the cotangent bundle. The vector spaces for V and ω are said to be *dual* in the following sense.

Box 17.3 Vector spaces

A *vector space* has a precise axiomatic definition in mathematics, but for our purposes it will be sufficient to view it more loosely as a set of objects (the vectors) that can be multiplied by real numbers and added together in a linear way while exhibiting *closure:* any such operations on elements of the set give back a linear combination of elements. For arbitrary vectors A and B, and arbitrary scalars a and b, one expects then that expressions like

$$(a+b)(A+B) = aA + aB + bA + bB$$

should be satisfied. A few other things are necessary: a zero vector that serves as an identity under vector addition, an inverse for every vector, and the usual assortment of associativity, distributivity, and commutativity rules, for example; but it is clear that it isn't very hard to be a vector space. Vector spaces of use in physics often have additional structure like a norm and inner product, but that is over and above the minimal requirements for being a bonafide vector space.

A *basis* for a vector space is a set of vectors that *span the space* (any vector is a linear combination of basis vectors) and that are *linearly independent* (no basis vector is a linear combination of other basis vectors). The number of basis vectors is the *dimension* of the space. For spacetime the vector spaces of interest will be defined at each point of the manifold and will be of dimension four.

Duality of Vectors and Dual Vectors: For a manifold, the space of vectors (tangent bundle) consists of all linear maps of dual vectors to the real numbers; conversely, the space of dual vectors (cotangent bundle) consists of all linear maps of vectors to the real numbers.

This *duality* of vector and dual vector spaces can be implemented systematically by requiring the basis vectors to satisfy

$$e^\mu(e_\nu) = e^\mu \cdot e_\nu = \delta^\mu_\nu, \tag{17.23}$$

where the Kronecker delta is given by

$$\delta^\mu_\nu = \begin{cases} 1 & \mu = \nu \\ 0 & \mu \neq \nu \end{cases} .$$

Note that $A(B)$, which indicates the action of A on B, can be expressed in the alternative form $\langle A, B\rangle$, so Eq. (17.23) is also commonly written as $\langle e^\mu,\, e_\nu\rangle = \delta^\mu_\nu$. From Eqs. (17.20)–

(17.23) it follows that a dual vector ω acts on a vector V in the manner

$$\begin{aligned}\omega(V) = \langle \omega,\, V\rangle &= \omega_\mu e^\mu(V^\nu e_\nu)\\ &= \omega_\mu V^\nu e^\mu(e_\nu)\\ &= \omega_\mu V^\nu \delta^\mu_\nu\\ &= \omega_\mu V^\mu \in \mathbb{R},\end{aligned} \tag{17.24}$$

where $\mathbb{R}$ denotes the real numbers.[7] This illustrates clearly that a dual vector is an operator that accepts a vector as an argument and produces a real number (the scalar product $\omega_\mu V^\mu$, which is unique and independent of basis) as output. By the same token, a vector is an operator that accepts a dual vector as an argument and produces a real number equal to the scalar product, $V(\omega) = \omega_\mu V^\mu$. These definitions involve no uncontracted indices, so the results are independent of any basis choice. This suggests that vectors and dual vectors may be defined fundamentally in terms of linear maps to the real numbers:

1. A *dual vector* is an operator that acts linearly on a vector to return a real number.
2. A *vector* is as an operator that acts linearly on a dual vector to return a real number.

For those having a knowledge of linear algebra or quantum mechanics this may sound vaguely familiar, as suggested by the following example.

Example 17.2 In the language of linear algebra, vectors may be represented as column vectors and dual vectors as row vectors, and their matrix product is a number. For example,

$$A \equiv (a\ \ b) \qquad B \equiv \begin{pmatrix} c \\ d \end{pmatrix} \qquad AB = (a\ \ b)\begin{pmatrix} c \\ d \end{pmatrix} = ac + bd \in \mathbb{R}$$

may be regarded as the dual vector A acting linearly on the vector B to produce the real number $ac + bd$: $A(B) \in \mathbb{R}$. For Dirac notation in quantum mechanics, $|a\rangle$ may be viewed as representing a vector and $\langle a|$ as representing a dual vector *in Hilbert space*, and mathematically the vector space of $\langle a|$ is the dual of the vector space of $|a\rangle$ (see Ref. [66]). Thus the overlap $\langle f|\ i\rangle$ is a number, and a matrix element $\langle f|\, M\, |i\rangle$ is a map from vectors and dual vectors of Hilbert space to the real numbers.

17.3.8 Evaluating Components in a Basis

The preceding definitions of vectors and dual vectors are independent of any choice of basis, but practically it often is convenient to work in a basis. The components of a vector

[7] As has been noted previously, basis vectors are defined in the tangent bundle and basis dual vectors are defined in the cotangent bundle of the manifold. Thus for applications in spacetime our concern is really with the action of vector fields on dual vector fields and vice versa, in which case what is returned is not a real number but rather a scalar field of real numbers defined over the manifold. We trust that the reader is sophisticated enough at this point to realize when "thing" really means "field of things".

or dual vector in a specific basis are obtained by evaluating them with respect to the corresponding basis vectors and dual basis vectors; for example,

$$V^\mu = V(e^\mu) = e^\mu \cdot V \qquad \omega_\mu = \omega(e_\mu) = e_\mu \cdot \omega, \tag{17.25}$$

which follows from Eq. (17.23). Equations such as (17.25) may be interpreted (for example) as a vector accepting a basis vector e^μ as input and acting linearly on it to return a real number that is the component of the vector evaluated in that basis.

Example 17.3 The validity of Eqs. (17.25) may be checked easily:

$$e^\mu \cdot V = e^\mu \cdot (V^\alpha e_\alpha) = V^\alpha e^\mu(e_\alpha) = V^\alpha \delta^\mu_\alpha = V^\mu,$$
$$e_\mu \cdot \omega = e_\mu \cdot (\omega_\alpha e^\alpha) = \omega_\alpha e_\mu(e^\alpha) = \omega_\alpha \delta^\alpha_\mu = \omega_\mu,$$

where the expansions (17.21)–(17.22), the linearity requirement (17.20), and the orthogonality condition (17.23) were employed.

Vector and dual vector components as in Eq. (17.25), and more generally tensor components, are then found to obey the same transformation laws and tensor calculus that will be presented in following sections as alternative defining characteristics of tensors. Example 17.4 illustrates for dual vectors and vectors.

Example 17.4 Consider a coordinate transformation $x^\mu \to x'^\mu$ on a dual vector $\omega = \omega_\mu e^\mu$ and on a vector $V = V^\mu e_\mu$. The basis dual vectors e^μ and basis vectors e_μ transform as

$$e^\mu \to e'^\mu = \frac{\partial x'^\mu}{\partial x^\nu}\, e^\nu \qquad e_\mu \to e'_\mu = \frac{\partial x^\nu}{\partial x'^\mu}\, e_\nu.$$

How do the components ω_μ transform? This may be determined by noting that the dual vector ω is a geometrical object having an existence independent of representation in a specific coordinate system, so it must be invariant under coordinate transformations. This will be ensured only if the components of ω transform as

$$\omega_\nu \to \omega'_\nu = \frac{\partial x^\alpha}{\partial x'^\nu}\, \omega_\alpha,$$

since then the dual vector ω is invariant under $x^\mu \to x'^\mu$:

$$\begin{aligned}
\omega' &= \omega'_\mu e'^\mu \\
&= \frac{\partial x^\alpha}{\partial x'^\mu}\, \omega_\alpha \frac{\partial x'^\mu}{\partial x^\nu}\, e^\nu \\
&= \frac{\partial x^\alpha}{\partial x'^\mu} \frac{\partial x'^\mu}{\partial x^\nu}\, \omega_\alpha e^\nu \\
&= \omega_\alpha e^\nu \delta^\alpha_\nu \\
&= \omega_\alpha e^\alpha = \omega.
\end{aligned}$$

This transformation law for the components ω_ν is the same one that will be used to *define* a dual vector in Eq. (17.31). By a similar proof, vector components V^μ may be shown to have the transformation law (17.33).

In later sections, such transformation laws will be offered as a *definition* of tensors. In the index-free picture currently under discussion tensors are defined instead as linear maps of some number of vectors and dual vectors to the real numbers, with the transformation laws and associated tensor calculus that will be discussed in Sections 17.4–17.7 following as a *consequence* of that definition.

Let us now greatly simplify keeping track of the distinction between upper indices and lower indices on tensors by demonstrating that the metric tensor map may be used to establish a one-to-one relationship between a vector in the tangent space and a corresponding dual vector in the cotangent space.

17.3.9 Identification of Vectors and Dual Vectors

Consider the metric tensor, viewed as a rank-2 covariant tensor that accepts two vector inputs and acts on them (multi-)linearly to give a real number. Schematically, this may be written as the operator $g(\cdot\,,\,\cdot)$, where the dots indicate the input slots for the two vectors. Suppose that a vector V is inserted into only *one* of the slots, giving $g(V,\,\cdot)$. What is this object? It has one open slot that can accept a vector, on which it will act linearly to return a real number. But that should sound familiar: it is the definition of a dual vector! Because it is associated directly with the vector V, let us call this dual vector $\tilde{V} \equiv g(V\,,\,\cdot)$. The components of this dual vector may be evaluated by inserting a basis vector as argument in the usual way,

$$\begin{aligned} V_\mu \equiv \tilde{V}(e_\mu) &= g(V, e_\mu) \\ &= g(V^\nu e_\nu, e_\mu) \\ &= V^\nu g(e_\nu, e_\mu) \\ &= g_{\mu\nu} V^\nu. \end{aligned} \tag{17.26}$$

Likewise, by using that $g_{\mu\nu}$ and $g^{\mu\nu}$ are matrix inverses, $V^\mu = g^{\mu\nu} V_\nu$. Summing over repeated indices in tensor products is called *contraction*. Thus, the properties of the metric tensor allow vectors and dual vectors to be treated effectively as if they were both vectors, one with an upper index and one with a lower index, with the two related by contraction with the metric tensor,

$$V_\mu = g_{\mu\nu} V^\nu \qquad V^\mu = g^{\mu\nu} V_\nu. \tag{17.27}$$

This is of great practical importance since it allows the same symbol to be used for a vector and its corresponding dual vector, and it reduces the handling of vectors and dual vectors to keeping proper track of the vertical position of indices in the Einstein summation convention. This identification works only for manifolds with metric tensors but that is no limitation for special or general relativity, which deal *only* with metric spaces.

Once the operations of raising and lowering indices by contraction with the metric tensor are established through Eq. (17.27), the scalar product between two vectors U and V can be calculated as the *complete contraction* $U_\alpha V^\alpha$ of one of the vectors with the dual vector associated with the other vector:

$$g(U,V) = g_{\mu\nu}U^\mu V^\nu = U_\nu V^\nu. \tag{17.28}$$

The scalar product has no indices left after contraction and is said to be *fully contracted*. Because tensors of higher rank are products of vectors and dual vectors, the preceding discussion is easily generalized and contraction with the metric tensor can be used to raise or lower any index for a tensor of any rank. For example,

$$A^{\mu\nu} = g^{\mu\alpha}g^{\nu\beta}A_{\alpha\beta} \qquad A_{\mu\nu\lambda\sigma} = g_{\mu\rho}A^\rho{}_{\nu\lambda\sigma}.$$

Since indices can be raised or lowered at will by a metric, tensors may be thought of as objects of a particular tensorial rank, irrespective of their particular vertical arrangement of indices (for example, the identification of vectors and dual vectors discussed above). Of course this is true only in the abstract; index placement matters when tensors are evaluated in a basis.

17.3.10 Index-Free versus Component Transformations

The material in this section has been a brief introduction to the index-free formulation of tensors favored by mathematicians. The discussion above and that in Section 17.4 indicates that the index-free formalism leads to the same transformation laws for tensors. Thus the practical outcome will be the same with application of either approach to the issues addressed in these lectures, but index-free concepts provide a more solid mathematical foundation for physical results while often the component transformation approach affords a more direct path to obtaining them.

17.4 Tensors Specified by Transformation Laws

In the preceding discussion tensors have been introduced at a fundamental level through linear maps from vectors and dual vectors to the real numbers, but it was shown also that these linear maps imply that when tensors of a given type are expressed in an arbitrary basis (see Section 17.3.8) their components obey well-defined transformation laws under change of coordinates. This view of tensors as groups of quantities obeying particular transformation laws is often the most practical for physical applications because

1. it is less abstract and requires less new mathematics for the novice,
2. a physical interpretation often requires expression of the problem in a well-chosen basis anyway, and
3. the component index formalism has a built-in error checking mechanism of great practical utility in solving problems: failure of indices to balance on the two sides of an equation is a sure sign of an error.

This section summarizes the use of tensors to formulate invariant equations by exploiting the transformation properties of their components. Tensors may be viewed as generalizing the idea of scalars and vectors, so let's begin with these more familiar quantities.

17.4.1 Scalar Transformation Law

Consider the behavior of fields under the coordinate transformations introduced in Section 17.3.1. The simplest possibility is that the field has a single component at each point of the manifold, with a value that is unchanged by the transformation (17.8),

$$\phi'(x') = \phi(x). \tag{17.29}$$

Quantities such as $\phi(x)$ that are unchanged under the coordinate transformation are called *scalars*. As the notation indicates, scalar quantities are generally functions of the coordinates but their value at a given point does not change if the coordinate system changes.[8] Scalar quantities may be expected to play a central role in physical theories because measurable observables must be scalars if the goal of formulating physical laws such that they do not depend on the coordinate labels is to be fulfilled.

17.4.2 Dual Vector Transformation Law

It is useful to define two kinds of spacetime vectors having distinct transformation laws. Both will be termed vectors because sets of each type separately obey the axioms to form a *vector space,* as discussed in Box 17.3. By the argument in Section 17.3.9, the same symbol will be used for both but they will be distinguished by vertical placement of indices. By the rules of ordinary partial differentiation the gradient of a scalar field $\phi(x)$ obeys

$$\frac{\partial \phi(x)}{\partial x'^{\mu}} = \frac{\partial \phi(x)}{\partial x^{\nu}} \frac{\partial x^{\nu}}{\partial x'^{\mu}}. \tag{17.30}$$

Now consider a vector having a transformation law mimicking that of the scalar field gradient (17.30),

$$A'_{\mu}(x') = \frac{\partial x^{\nu}}{\partial x'^{\mu}} A_{\nu}(x) \qquad \text{(dual vector)}. \tag{17.31}$$

A quantity transforming in this way is termed a *dual vector* (it also goes by the names *one-form*, *covariant vector,* or *covector*). Understand clearly that in (17.31) the two sides of the equation refer to the *same point* in spacetime. Thus, the argument is x' on the left side and x on the right side, and these label the same spacetime point in two different coordinate systems. Before continuing we stop to note that even the relatively simple expressions that have been introduced so far emphasize the importance of the compact notation that we are using. For example, Eq. (17.31) is a concise way to write the matrix

[8] This may be contrasted with the behavior of the components of a vector under coordinate transformation, which will be discussed shortly. Geometrically the components of a vector are projections of the vector on particular coordinate axes. Thus, if the coordinate system is changed the components of a vector at a given point typically change their values, but the length of the vector, which is a scalar, is invariant.

equation

$$\begin{pmatrix} A'_0 \\ A'_1 \\ A'_2 \\ A'_3 \end{pmatrix} = \begin{pmatrix} \partial x^0/\partial x'^0 & \partial x^1/\partial x'^0 & \partial x^2/\partial x'^0 & \partial x^3/\partial x'^0 \\ \partial x^0/\partial x'^1 & \partial x^1/\partial x'^1 & \partial x^2/\partial x'^1 & \partial x^3/\partial x'^1 \\ \partial x^0/\partial x'^2 & \partial x^1/\partial x'^2 & \partial x^2/\partial x'^2 & \partial x^3/\partial x'^2 \\ \partial x^0/\partial x'^3 & \partial x^1/\partial x'^3 & \partial x^2/\partial x'^3 & \partial x^3/\partial x'^3 \end{pmatrix} \begin{pmatrix} A_0 \\ A_1 \\ A_2 \\ A_3 \end{pmatrix}.$$

Furthermore, although we usually suppress it in the notation, the partial derivatives appearing in these transformation equations *depend on spacetime coordinates* in the general case and all partial derivatives are understood implicitly to be evaluated at a specific point P labeled by x in one coordinate system and x' in the other.

17.4.3 Vector Transformation Law

Now consider application of the rules of partial differentiation to transformation of the differential,

$$dx'^{\mu} = \frac{\partial x'^{\mu}}{\partial x^{\nu}}\, dx^{\nu}. \tag{17.32}$$

This suggests a second vector transformation rule,

$$A'^{\mu}(x') = \frac{\partial x'^{\mu}}{\partial x^{\nu}}\, A^{\nu}(x) \qquad \text{(vector)}. \tag{17.33}$$

A quantity behaving in this way is termed a *vector*.[9] Most physical quantities that are thought of loosely as "vectors" (displacement or velocity, for example) are vectors in the restricted sense defined by the transformation law (17.33).

Example 17.5 Equations (17.31) and (17.33) may be viewed as matrix equations,

$$A'_{\mu}(x') = \hat{U}^{\nu}_{\mu} A_{\nu}(x) \qquad A'^{\mu}(x') = U^{\mu}_{\nu} A^{\nu}(x), \tag{17.34}$$

with the matrices $U = \partial x'/\partial x$ and $\hat{U} = \partial x/\partial x'$ obeying $\hat{U}U = I$, where I is the unit matrix. In these transformations the matrix U is called the *Jacobian matrix* and the matrix $\hat{U}$ is called the *inverse Jacobian matrix*.

17.4.4 Duality of Vectors and Dual Vectors

The preceding discussion distinguishes two kinds of "vectors": dual vectors, which carry a lower index and transform like (17.31), and vectors, which carry an upper index and transform like (17.33). In particular instances vectors and dual vectors may be considered

[9] Some authors call vectors *contravariant vectors*, indicating explicitly that when expanded in a basis the component index is in the upper position, and call dual vectors *covariant vectors*, indicating explicitly that the component index is in the lower position.

equivalent as a practical matter (albeit with some loss of mathematical rigor), but generally they are not. However, the duality discussed in Section 17.3.9 allows us to use the same symbol for vectors and dual vectors, with the distinction between them residing in upper and lower positioning of indices in the summation convention.

17.5 Scalar Product of Vectors

The introduction of vectors and dual vectors, and their relationship through the metric tensor, allows a natural definition of a scalar product

$$A \cdot B \equiv A_\mu B^\mu, \tag{17.35}$$

where the dual vector A_μ and the corresponding vector A^μ are related through the metric tensor according to $A_\mu = g_{\mu\nu}A^\nu$. This product transforms as a scalar because from Eqs. (17.31) and (17.33),

$$\begin{aligned} A' \cdot B' = A'_\mu B'^\mu &= \frac{\partial x^\nu}{\partial x'^\mu} A_\nu \frac{\partial x'^\mu}{\partial x^\alpha} B^\alpha = \frac{\partial x^\nu}{\partial x'^\mu}\frac{\partial x'^\mu}{\partial x^\alpha} A_\nu B^\alpha \\ &= \frac{\partial x^\nu}{\partial x^\alpha} A_\nu B^\alpha = \delta^\nu_\alpha A_\nu B^\alpha = A_\alpha B^\alpha = A \cdot B, \end{aligned} \tag{17.36}$$

where the Kronecker delta δ^ν_μ is given by

$$\delta^\mu_\nu = \frac{\partial x'^\mu}{\partial x'^\nu} = \frac{\partial x^\mu}{\partial x^\nu} = \begin{cases} 1 & \mu = \nu \\ 0 & \mu \neq \nu \end{cases}, \tag{17.37}$$

which is a rank-2 tensor with the unusual property that its components take the same value in all coordinate systems.

17.6 Tensors of Higher Rank

Three types of rank-2 tensors $(0,2)$, $(1,1)$, and $(2,0)$ may be distinguished; they have the transformation laws

$$T'_{\mu\nu} = \frac{\partial x^\alpha}{\partial x'^\mu}\frac{\partial x^\beta}{\partial x'^\nu} T_{\alpha\beta}, \tag{17.38}$$

$$T'^\nu_{\ \mu} = \frac{\partial x^\alpha}{\partial x'^\mu}\frac{\partial x'^\nu}{\partial x^\beta} T^\beta_{\ \alpha}, \tag{17.39}$$

$$T'^{\mu\nu} = \frac{\partial x'^\mu}{\partial x^\alpha}\frac{\partial x'^\nu}{\partial x^\beta} T^{\alpha\beta}. \tag{17.40}$$

These transformation rules may be generalized easily to tensors of any rank. In such a generalization,

1. Each upper index on the left side requires a right-side "factor" of the form $\partial x'^\mu/\partial x^\nu$ (prime in the numerator), and

Table 17.1 Some tensor transformation laws

Tensor	Transformation law
Scalar	$\phi' = \phi$
Dual vector	$A'_\mu = \dfrac{\partial x^\nu}{\partial x'^\mu} A_\nu$
Vector	$A'^\mu = \dfrac{\partial x'^\mu}{\partial x^\nu} A^\nu$
Covariant rank-2	$T'_{\mu\nu} = \dfrac{\partial x^\alpha}{\partial x'^\mu} \dfrac{\partial x^\beta}{\partial x'^\nu} T_{\alpha\beta}$
Contravariant rank-2	$T'^{\mu\nu} = \dfrac{\partial x'^\mu}{\partial x^\alpha} \dfrac{\partial x'^\nu}{\partial x^\beta} T^{\alpha\beta}$
Mixed rank-2	$T'^\nu{}_\mu = \dfrac{\partial x^\alpha}{\partial x'^\mu} \dfrac{\partial x'^\nu}{\partial x^\beta} T^\beta{}_\alpha$

2. each lower index on the left side requires a right-side "factor" of the form $\partial x^\mu / \partial x'^\nu$ (prime in the denominator).

This "position of the left-side index equals position of the right-side primed coordinate" rule for the partial derivative factors is a useful aid in remembering the forms of the tensor transformation equations. Transformation laws for tensors through rank 2 are summarized in Table 17.1.

17.7 The Metric Tensor

A rank-2 tensor of special importance is the metric tensor $g_{\mu\nu}$, because it is associated with the line element

$$ds^2 = g_{\mu\nu} dx^\mu dx^\nu \tag{17.41}$$

that determines the *geometry of the manifold.* The metric tensor is symmetric in its indices ($g_{\mu\nu} = g_{\nu\mu}$) and satisfies the $(0, 2)$ tensor transformation law

$$g'_{\mu\nu} = \frac{\partial x^\alpha}{\partial x'^\mu} \frac{\partial x^\beta}{\partial x'^\nu} g_{\alpha\beta}. \tag{17.42}$$

The contravariant form of the metric tensor $g^{\mu\nu}$ is defined by the requirement

$$g_{\mu\alpha} g^{\alpha\nu} = \delta^\nu_\mu, \tag{17.43}$$

so $g_{\mu\nu}$ and $g^{\mu\nu}$ are *matrix inverses.* Contractions with the metric tensor may be used to raise and lower (any number of) tensor indices; for example,

$$A^\mu = g^{\mu\nu} A_\nu \qquad A_\mu = g_{\mu\nu} A^\nu \qquad T^\mu{}_\nu = g_{\nu\alpha} T^{\mu\alpha} \qquad T^\alpha{}_{\beta\gamma} = g^{\alpha\mu} g_{\gamma\epsilon} T_{\mu\beta}{}^\epsilon. \tag{17.44}$$

Thus, the scalar product of vectors may be expressed as

$$A \cdot B = g_{\mu\nu} A^\mu B^\nu \equiv A_\nu B^\nu = g^{\mu\nu} A_\mu B_\nu \equiv A^\nu B_\nu. \tag{17.45}$$

Because such products are scalars, they are unchanged by coordinate-system transformations. A specific example of such a conserved quantity is an invariant length such as the line element of Eq. (17.41).

In mixed-tensor expressions like the third or fourth ones in Eq. (17.44) the relative horizontal order of upper and lower indices can be important. For example, in $T^\mu{}_\nu = g_{\nu\alpha} T^{\mu\alpha}$ the notation indicates that the mixed tensor on the left side of the equation was obtained by lowering the rightmost index of $T^{\mu\alpha}$ on the right side (since in $T^\mu{}_\nu$ the lower index ν is to the right of the upper index μ). This distinction is immaterial if the tensor is symmetric under exchange of indices but which index is lowered or raised by contraction matters for tensors that are antisymmetric under index exchange (see Section 17.8): $T^\mu{}_\nu = g_{\nu\alpha} T^{\mu\alpha}$ and $T_\nu{}^\mu = g_{\nu\alpha} T^{\alpha\mu}$ are equivalent if T is symmetric, but different if T is antisymmetric.

Vectors and dual vectors are distinct entities that are defined in different spaces (see Section 17.3.2). However, Eqs. (17.43)–(17.45) make it clear that for the *special case of a manifold with metric,* indices on any tensor may be raised or lowered at will by contraction with the metric tensor, as in Eq. (17.44). Defining a metric establishes a relationship that permits vectors and dual vectors to be treated as if they were (in effect) different representations of the same vector. Our discussion will usually proceed as if A^μ and A_μ are different forms of the same vector that are related by contraction with the metric tensor, while secretly remembering that they really are different, and that it is only for metric spaces that this conflation is not likely to land us in trouble.

The preceding discussion makes clear why the convention in much of nonrelativistic physics to ignore the mathematical distinction between vectors and dual vectors causes few problems. For example, the gradient operator is commonly termed a vector in elementary physics but Section 17.4.2 shows that it is actually a dual vector. However, physics almost always assumes that a manifold has a metric, so vectors and dual vectors are related trivially through the metric tensor and no lasting harm is done by calling the gradient a vector if the bookkeeping is done correctly in equations. Specifically, the gradient dual vector may be converted to the corresponding vector by contracting with the metric tensor to raise the index. The issue is particularly simple if the problem is formulated in euclidean space using cartesian coordinates, in which case the metric tensor is just the unit matrix and the components of the vector and dual vector are the same. The mathematician is required to be more circumspect because the definition of a manifold does not automatically imply existence of a metric to enable this identification.

17.8 Symmetric and Antisymmetric Tensors

The symmetry of tensors under an exchange of indices is often important. A rank-2 tensor can always be decomposed into a symmetric and antisymmetric part according to the

identity

$$T_{\alpha\beta} = \tfrac{1}{2}(T_{\alpha\beta} + T_{\beta\alpha}) + \tfrac{1}{2}(T_{\alpha\beta} - T_{\beta\alpha}), \tag{17.46}$$

where the first term is symmetric and the second term antisymmetric under exchange of indices. For completely symmetric and completely antisymmetric rank-2 tensors

$$T_{\alpha\beta} = \pm T_{\beta\alpha} \qquad T^{\alpha\beta} = \pm T^{\beta\alpha},$$

where the plus sign holds if the tensor is symmetric and the minus sign if it is antisymmetric. More generally, a tensor of rank two or higher is said to be *symmetric* in any two of its indices if exchanging those indices leaves the tensor invariant and *antisymmetric* (or *skew-symmetric*) in any two indices if it changes sign upon switching those indices.

17.9 Algebraic Tensor Operations

Various algebraic operations are permitted for tensors in equations. These valid operations include:

1. *Multiplication by a scalar:* A tensor may be multiplied by a scalar (meaning that each component is multiplied by the scalar) to produce a tensor of the same rank. For example, $aA^{\mu\nu} = B^{\mu\nu}$, where a is a scalar and $A^{\mu\nu}$ and $B^{\mu\nu}$ are rank-2 contravariant tensors.
2. *Addition or subtraction:* Two tensors of the same type may be added or subtracted (meaning that their components are added or subtracted) to produce a new tensor of the same type. For example, $A^{\mu} - B^{\mu} = C^{\mu}$, where A^{μ}, B^{μ}, and C^{μ} are vectors.
3. *Multiplication:* Two or more tensors may be multiplied by forming products of their components. The rank of the resultant tensor will be the product of the ranks of the tensor factors. For example, $A_{\mu\nu} = U_{\mu}V_{\nu}$, where $A_{\mu\nu}$ is a rank-2 covariant tensor and U_{μ} and V_{ν} are dual vectors.
4. *Contraction:* For a tensor or tensor product with covariant rank n and contravariant rank m, a tensor of covariant rank $n-1$ and contravariant rank $m-1$ may be formed by setting one upper and one lower index equal and taking the implied sum. For example, $A = A^{\mu}{}_{\mu}$, where A is a scalar and $A^{\mu}{}_{\nu}$ is a mixed rank-2 tensor, or $A_{\mu} = g_{\mu\nu}A^{\nu}$, where the metric $g_{\mu\nu}$ is a rank-2 covariant tensor, A^{ν} is a vector, and A_{μ} is a dual vector.

In addition to these algebraic manipulations, it will often be necessary to integrate or differentiate in tensor expressions. This *tensor calculus* is addressed in the following section.

17.10 Tensor Calculus on Curved Manifolds

To formulate physical theories in terms of tensors requires the ability to manipulate tensors mathematically. In addition to the algebraic rules for tensors described in preced-

ing sections, we must formulate a prescription to integrate tensor equations and one to differentiate them. Tensor calculus is mostly a straightforward generalization of normal calculus but additional complexity arises for two reasons:

1. It must be ensured that integration and differentiation preserve the symmetries and invariances embodied in the tensor equations.
2. To preserve the utility of the tensor formalism, it must be ensured that the results of these operations on tensor quantities are themselves tensor quantities.

As will now be shown, the first requirement implies a simple modification of the rules for ordinary integration while the second implies a less-simple modification with far-reaching mathematical and physical implications for the rules of partial differentiation.

17.10.1 Invariant Integration

Under a change of coordinates the volume element for integration over the spacetime coordinates changes according to

$$d^4x' = \det\left(\frac{\partial x'}{\partial x}\right) d^4x = J d^4x, \tag{17.47}$$

where $d^4x \equiv dx^0 dx^1 dx^2 dx^3$ and $J \equiv \det(\partial x'/\partial x)$ is the Jacobian determinant (determinant of the 4×4 matrix of partial derivatives relating the x and x' coordinates; see Example 17.5). Notice that the right side of Eq. (17.42) may be viewed as a triple matrix product and recall that the determinant of a matrix product is the product of determinants. Thus Eq. (17.42) implies that the determinant of the metric tensor $g \equiv \det g_{\mu\nu}$ transforms as $g' = J^{-2} g$. Hence $J = \sqrt{|g|}/\sqrt{|g'|}$, where the absolute value signs are necessary because the determinant of $g_{\mu\nu}$ is negative in 4D spacetime with Lorentzian metric signature [see Eq. (18.6)], and this result may be substituted into Eq. (17.47) to give $\sqrt{|g'|}\, d^4x' = \sqrt{|g|}\, d^4x$. This implies that an *invariant volume element,*

$$dV = \sqrt{|g|}\, d^4x, \tag{17.48}$$

must be employed in tensor integration to ensure that the results are invariant under a change of coordinate system. A simple demonstration of using invariant integration to determine an area for a 2-dimensional curved manifold is given in Example 17.6.

Example 17.6 The metric for a 2-dimensional spherical surface (the 2-sphere S^2) is specified by the line element $d\ell^2 = R^2 d\theta^2 + R^2 \sin^2\theta d\phi^2$, which may be written as the matrix equation

$$d\ell^2 = \begin{pmatrix} d\theta & d\phi \end{pmatrix} \begin{pmatrix} R^2 & 0 \\ 0 & R^2 \sin^2\theta \end{pmatrix} \begin{pmatrix} d\theta \\ d\phi \end{pmatrix}.$$

The area of the 2-sphere may then be calculated as

$$\begin{aligned} A &= \int_0^{2\pi} d\phi \int_0^{\pi} \sqrt{\det g_{ij}}\, d\theta \\ &= \int_0^{2\pi} d\phi \int_0^{\pi} R^2 \sin\theta d\theta = 4\pi R^2, \end{aligned}$$

where the metric tensor g_{ij} is the 2×2 matrix in the first equation for the line element. In this 2-dimensional example the sign of the determinant is positive, so no absolute value is required under the radical in Eq. (17.48).

Thus, the extension of ordinary integration to integration over tensor fields requires only that the volume element be made invariant according to the prescription in Eq. (17.48). What about the derivatives of tensor quantities? This is a more complicated issue that we must now address.

17.10.2 Partial Derivatives

Before proceeding it will be useful to introduce a more compact way to write partial derivatives. Two shorthand notations are in common use, as illustrated by the following examples.[10]

$$\partial_\mu \phi = \phi_{,\mu} \equiv \frac{\partial \phi(x)}{\partial x^\mu} \qquad \partial'_\mu \phi' = \phi'_{,\mu} \equiv \frac{\partial \phi'(x')}{\partial x'^\mu} \qquad \partial^\mu \phi = \phi^{,\mu} \equiv \frac{\partial \phi(x)}{\partial x_\mu}. \tag{17.49}$$

All three of the notations exhibited for partial derivatives in these equations will be used at various places in this book. Let us now consider the covariance of the partial derivative operation applied to tensors.

The transformation law for the derivative of a scalar is given by Eq. (17.30), which is just the transformation law (17.31); therefore the derivative of a scalar is a dual vector and scalars and their first derivatives have well-defined tensorial properties. So far, so good, but now consider the derivative of a dual vector,

$$\begin{aligned} A'_{\mu,\nu} &\equiv \frac{\partial A'_\mu}{\partial x'^\nu} = \frac{\partial}{\partial x'^\nu}\left(A_\alpha \frac{\partial x^\alpha}{\partial x'^\mu}\right) \\ &= \frac{\partial A_\alpha}{\partial x'^\nu}\frac{\partial x^\alpha}{\partial x'^\mu} + A_\alpha \frac{\partial^2 x^\alpha}{\partial x'^\nu \partial x'^\mu} \\ &= \frac{\partial A_\alpha}{\partial x^\beta}\frac{\partial x^\beta}{\partial x'^\nu}\frac{\partial x^\alpha}{\partial x'^\mu} + A_\alpha \frac{\partial^2 x^\alpha}{\partial x'^\nu \partial x'^\mu} \\ &= A_{\alpha,\beta}\frac{\partial x^\beta}{\partial x'^\nu}\frac{\partial x^\alpha}{\partial x'^\mu} + A_\alpha \frac{\partial^2 x^\alpha}{\partial x'^\nu \partial x'^\mu}. \end{aligned} \tag{17.50}$$

The first term in the last line transforms as a (rank-2) tensor but the second term does not since it involves second derivatives, ultimately because the partial-derivative matrix implementing the transformation is *position dependent* in curved spacetime. In flat space it

[10] Higher-order derivatives can be denoted by additional subscripts. For example $\partial^2\phi/\partial x^\mu \partial x^\nu = \phi_{,\mu\nu}$.

is possible to choose coordinates where the second term vanishes but in curved spacetime it cannot be transformed away globally. By a similar procedure it is found that the partial derivatives of vectors and all higher-order tensors exhibit a similar pathology:

> With the exception of derivatives of scalars, ordinary partial differentiation of tensors is *not a covariant operation in curved spacetime* because it fails to preserve the tensor structure of equations.

This will complicate the formalism immensely because the utility of the tensor framework rests on the preservation of tensor structure under transformations. It is desirable to define a new covariant derivative operation that does this automatically. In general the terms that violate the tensor transformation laws for partial derivatives of tensors will involve second derivatives, as in Eq. (17.50). The non-tensorial contributions can be eliminated systematically by introducing additional fields on the manifold, which can be done in more than one way, each leading to a different form of covariant differentiation. Three common approaches are (1) *covariant derivatives* and (2) *absolute derivatives,* which use derivatives of the metric tensor field to cancel non-tensorial terms, and (3) *Lie derivatives,* which use derivatives of an auxiliary vector field defined on the manifold to the same end. We will discuss here only covariant derivatives, which will be introduced in Section 17.10.3

17.10.3 Covariant Derivatives

For the manifolds important in general relativity, the most common approach to converting partial differentiation into an operation that preserves tensor structure is to use particular linear combinations of metric-tensor derivatives to create new non-tensorial terms that *exactly cancel* the non-tensorial terms arising from taking the partial derivative. Notice that if the *Christoffel symbols* $\Gamma^{\lambda}_{\alpha\beta}$ are introduced and required to obey a transformation law

$$\Gamma'^{\lambda}_{\alpha\beta} = \Gamma^{\kappa}_{\mu\nu}\frac{\partial x^{\mu}}{\partial x'^{\alpha}}\frac{\partial x^{\nu}}{\partial x'^{\beta}}\frac{\partial x'^{\lambda}}{\partial x^{\kappa}} + \frac{\partial^2 x^{\mu}}{\partial x'^{\alpha}\partial x'^{\beta}}\frac{\partial x'^{\lambda}}{\partial x^{\mu}}, \tag{17.51}$$

it may be shown that

$$\left(A'_{\mu,\nu} - \Gamma'^{\lambda}_{\mu\nu}A'_{\lambda}\right) = \left(A_{\alpha,\beta} - \Gamma^{\kappa}_{\alpha\beta}A_{\kappa}\right)\frac{\partial x^{\alpha}}{\partial x'^{\mu}}\frac{\partial x^{\beta}}{\partial x'^{\nu}}. \tag{17.52}$$

Comparing with Eq. (17.38), the quantity in brackets is seen to transform as a rank-2 covariant tensor. This suggests the utility of introducing a new derivative operation: the *covariant derivative* of a dual vector is defined to be

$$A_{\mu;\nu} \equiv A_{\mu,\nu} - \Gamma^{\lambda}_{\mu\nu}A_{\lambda}, \tag{17.53}$$

where now a subscript comma denotes ordinary partial differentiation and a subscript semicolon denotes covariant differentiation with respect to the variables following it. It

will be useful to introduce also an alternative notation for the covariant derivative,

$$\nabla_\nu A_\mu = A_{\mu;\nu} \equiv \partial_\nu A_\mu - \Gamma^\lambda_{\mu\nu} A_\lambda. \tag{17.54}$$

This covariant derivative of a dual vector then transforms as a covariant tensor of rank 2: neither of its terms is a tensor but their *difference* is. Likewise, the covariant derivative of a vector can be introduced in either of the notations

$$A^\lambda{}_{;\mu} = A^\lambda{}_{,\mu} + \Gamma^\lambda_{\alpha\mu} A^\alpha \qquad \nabla_\mu A^\lambda = \partial_\mu A^\lambda + \Gamma^\lambda_{\alpha\mu} A^\alpha, \tag{17.55}$$

where the result of (17.55) is a mixed rank-2 tensor, and the covariant derivatives of the three possible rank-2 tensors through

$$A_{\mu\nu;\lambda} = A_{\mu\nu,\lambda} - \Gamma^\alpha_{\mu\lambda} A_{\alpha\nu} - \Gamma^\alpha_{\nu\lambda} A_{\mu\alpha}, \tag{17.56}$$

$$A^\mu{}_{\nu;\lambda} = A^\mu{}_{\nu,\lambda} + \Gamma^\mu_{\alpha\lambda} A^\alpha{}_\nu - \Gamma^\alpha_{\nu\lambda} A^\mu{}_\alpha, \tag{17.57}$$

$$A^{\mu\nu}{}_{;\lambda} = A^{\mu\nu}{}_{,\lambda} + \Gamma^\mu_{\alpha\lambda} A^{\alpha\nu} + \Gamma^\nu_{\alpha\lambda} A^{\mu\alpha}, \tag{17.58}$$

or in alternative notation

$$\nabla_\lambda A_{\mu\nu} = \partial_\lambda A_{\mu\nu} - \Gamma^\alpha_{\mu\lambda} A_{\alpha\nu} - \Gamma^\alpha_{\nu\lambda} A_{\mu\alpha}, \tag{17.59}$$

$$\nabla_\lambda A^\mu{}_\nu = \partial_\lambda A^\mu{}_\nu + \Gamma^\mu_{\alpha\lambda} A^\alpha{}_\nu - \Gamma^\alpha_{\nu\lambda} A^\mu{}_\alpha, \tag{17.60}$$

$$\nabla_\lambda A^{\mu\nu} = \partial_\lambda A^{\mu\nu} + \Gamma^\mu_{\alpha\lambda} A^{\alpha\nu} + \Gamma^\nu_{\alpha\lambda} A^{\mu\alpha}, \tag{17.61}$$

where the derivatives in Eqs. (17.56)–(17.61) define rank-3 tensors. In the general case the covariant derivative of a tensor is a tensor of one rank higher than the tensor being differentiated and the heuristic for constructing it is to form the ordinary partial derivative and add one Christoffel symbol term having the sign and form for a dual vector for each lower index, and one having the sign and form for a vector for each upper index of the tensor (see Example 17.7).

In general relativity the Christoffel symbols are equivalent to *connection coefficients* (hence the same notation will be employed for both), which have a geometrical significance on the manifold and can be defined in terms of the derivatives of the metric tensor as

$$\Gamma^\sigma_{\lambda\mu} = \tfrac{1}{2} g^{\nu\sigma} \left(\frac{\partial g_{\mu\nu}}{\partial x^\lambda} + \frac{\partial g_{\lambda\nu}}{\partial x^\mu} - \frac{\partial g_{\mu\lambda}}{\partial x^\nu} \right).$$

Thus the correction terms in Eqs. (17.53)–(17.61) that cancel non-tensorial character are indeed composed of derivatives of the metric tensor, as promised above.

Rules for covariant differentiation: Most of the rules for partial differentiation carry over with suitable generalization for covariant differentiation. For instance, the ordinary (Leibniz) rule for differentiating a product applies also to covariant differentiation,

$$(A_\mu B_\nu)_{;\lambda} = A_{\mu;\lambda} B_\nu + A_\mu B_{\nu;\lambda}. \tag{17.62}$$

The most important exception concerns the results of successive covariant differentiations. Partial derivative operators normally commute: if two are applied successively, the outcome does not depend on the order in which they are applied. However, covariant

derivative operators generally do not commute and two successive covariant differentiations may give results that depend on the order in which they are applied. It may be shown that covariant derivatives, and their non-commuting nature, arise naturally from a prescription for parallel transport of vectors in curved spaces.

Example 17.7 The Leibniz differentiation rule for the product of two vectors may be used to derive the expressions (17.56)–(17.58) for the covariant derivatives of rank-2 tensors from those given for vectors in Eqs. (17.53) and (17.55). For example,

$$\begin{aligned}(U^\alpha V^\beta)_{;\gamma} &= U^\alpha V^\beta_{\ ;\gamma} + U^\alpha_{\ ;\gamma} V^\beta \\ &= U^\alpha V^\beta_{\ ,\gamma} + U^\alpha(\Gamma^\beta_{\rho\gamma} V^\rho) + U^\alpha_{\ ,\gamma} V^\beta + (\Gamma^\alpha_{\rho\gamma} U^\rho)V^\beta \\ &= (U^\alpha V^\beta)_{,\gamma} + \Gamma^\beta_{\rho\gamma}(U^\alpha V^\rho) + \Gamma^\alpha_{\rho\gamma}(U^\rho V^\beta),\end{aligned}$$

where Eq. (17.55) and $U^\alpha V^\beta_{\ ,\gamma} + U^\alpha_{\ ,\gamma} V^\beta = (U^\alpha V^\beta)_{,\gamma}$ were used in the second and third lines, respectively. This is equivalent to

$$A^{\alpha\beta}_{\ \ ;\gamma} = A^{\alpha\beta}_{\ \ ,\gamma} + \Gamma^\beta_{\rho\gamma} A^{\alpha\rho} + \Gamma^\alpha_{\rho\gamma} A^{\rho\beta},$$

where $A^{\alpha\beta} \equiv U^\alpha V^\beta$, which is Eq. (17.58) for the covariant derivative of a contravariant rank-2 tensor.

Carrying out similar manipulations as in this example for the rank-2 tensors $A_{\mu\nu}$ and $A^\nu_{\ \mu}$ suggests the rule given after Eq. (17.61): differentiate in the normal way and add one Christoffel symbol term having the sign and form for a dual vector for each lower index, and one having the sign and form for a vector for each upper index of the tensor.

Implications of covariant differentiation: One rather important consequence of requiring that differentiation preserve tensor structure in the manner described above is that the covariant derivative of the metric tensor vanishes at all points of a manifold,[11]

$$\nabla_\alpha g_{\mu\nu} = g_{\mu\nu;\alpha} = 0. \tag{17.63}$$

This means that in manipulating tensor equations the operation of covariant differentiation commutes with the operation (17.44) of raising or lowering an index by contraction with the metric tensor. For example,

$$g_{\alpha\beta}\nabla_\gamma V^\beta = \nabla_\gamma(g_{\alpha\beta}V^\beta) = \nabla_\gamma V_\alpha.$$

Thus the order of covariant differentiation and contraction with the metric tensor can be interchanged without altering the result.

[11] The validity of Eq. (17.63) is a consequence of particular assumptions concerning the nature of parallel transport in curved spacetime.

17.11 Covariant Equations

The properties of tensors elaborated above ensure that any equation will be form-invariant under general coordinate transformations if it equates tensor components having the same upper and lower indices. For example, if the quantities $A^{\mu}{}_{\nu}$ and $B^{\mu}{}_{\nu}$ each transform as mixed rank-2 tensors according to Eq. (17.39) and $A^{\mu}{}_{\nu} = B^{\mu}{}_{\nu}$ in the x coordinate system, then in the x' coordinate system $A'^{\mu}{}_{\nu} = B'^{\mu}{}_{\nu}$. Likewise, an equation that equates any tensor to zero (that is, sets all its components to zero) in some coordinate system is covariant under general coordinate transformations, implying that the tensor is equal to zero in all coordinate systems. However, equations such as $A^{\nu}{}_{\mu} = 10$ or $A^{\mu} = B_{\mu}$ might hold in particular coordinate systems but generally are not valid in all coordinate systems because they equate tensors of different kinds (a mixed rank-2 tensor with a scalar in the first example and a dual vector with a vector in the second).

The preceding discussion suggests that invariance of a theory under general coordinate transformations will be guaranteed by carrying out the following steps.

1. Formulate all quantities in terms of tensors, with tensor types matching on the two sides of any equation, and with all algebraic manipulations corresponding to valid tensor operations (addition, multiplication, contraction, ...).
2. Redefine any integration to be invariant integration, as discussed in Section 17.10.1.
3. Replace all partial derivatives with the covariant derivatives introduced in Section 17.10.3.
4. Take care to remember that a covariant differentiation generally does not commute with a second covariant differentiation, so the order matters.

This prescription in terms of tensors will provide a powerful formalism for dealing with mathematical relations that would be much more formidable in standard notation.

Background and Further Reading

Significant parts of this chapter have been adapted from Refs. [36] and [38]. The discussion of coordinate transformations in euclidean space is based on the presentation of Ref. [30]. For those relatively new to the use of tensors a clear conceptual introduction to vectors and tensors is give in Ref. [18].

Problems

17.1 Consider the following torus, parameterized by the angles θ and ϕ.

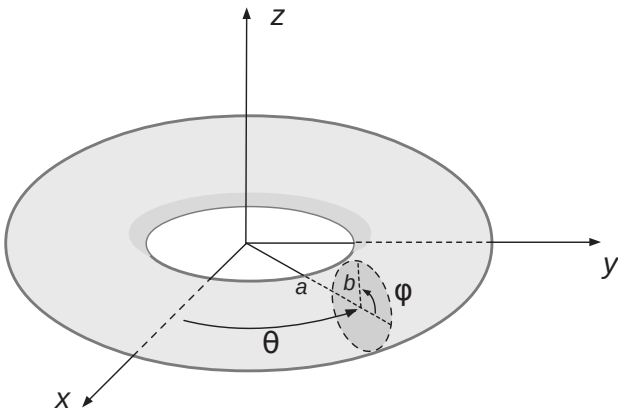

Points on the torus are defined by

$$x = (a + b\cos\phi)\cos\theta \qquad y = (a + b\cos\phi)\sin\theta \qquad z = b\sin\phi,$$

where a and b are constants. Construct the tangent basis vectors for θ and ϕ, and the corresponding metric tensor.

17.2 (a) Verify explicitly that the Lorentz transformation of Eq. (18.20)

$$\begin{aligned} cdt' &= c\cosh\xi dt + \sinh\xi dx \\ dx' &= c\sinh\xi dt + \cosh\xi dx \\ dy' &= dy \\ dz' &= dz \end{aligned}$$

leaves invariant the Minkowski line element ds^2.

(b) Use the Lorentz transformations (18.26) expressed in differential form to obtain the velocity transformation rules consistent with Lorentz invariance. Show that for the special case of two inertial frames moving along the x axis with relative velocity v, the velocity transformation law is

$$u' = \frac{u - v}{1 - uv/c^2},$$

and that this embodies the constancy of the speed of light in all inertial frames, but reduces to the result expected from Galilean invariance for small v.

17.3 *NOTE: Euclidean examples removed from text.* Use tangent and dual basis vectors to construct metric tensor components g^{ij} and g_{ij}, and the line element, for the coordinate system (u, v, w). Verify that the matrices g^{ij} and g_{ij} found for this problem are inverses of each other. ***

17.4 Show that if index raising and lowering operations are *defined* by expressions like

$$T^{\mu}_{\ \nu} = g_{\nu\alpha}T^{\mu\alpha} \qquad T_{\mu\nu} = g_{\mu\alpha}g_{\nu\beta}T^{\alpha\beta},$$

then these are valid tensor operations. That is, show that if these relations are true in one coordinate system they are true in all coordinate systems.

17.5 A theorem useful in various contexts states that if a set of quantities produces a tensor when contracted with a tensor, then that set of quantities is necessarily a tensor. This is called the *quotient theorem.* (a) Use the definition of the scalar product of vectors and the quotient theorem to argue that the metric $g_{\mu\nu}$ is a tensor. (b) Use the quotient theorem to show explicitly that if for an arbitrary vector V^{γ}

$$T^{\alpha}_{\ \beta\gamma}V^{\gamma} = \frac{\partial x'^{\alpha}}{\partial x^{\delta}}\frac{\partial x^{\epsilon}}{\partial x'^{\beta}}T^{\delta}_{\ \epsilon\phi}V^{\phi},$$

then $T^{\alpha}_{\ \beta\gamma}$ is necessarily a tensor of type $(1,2)$. ***

Numerical and GenAI Problems

18 Special Relativity

In this chapter we shall build on the mathematical foundation of Ch. 17 to describe the special theory of relativity and use that to demonstate the Lorentz covariance of the Maxwell equations. Let's begin by noting the natural scientific and historical affinity of the Maxwell equations and the special theory of relativity.

18.1 Maxwell's Equations and Special Relativity

Electrical charges may be viewed as classical objects (for example, as having positions and momenta that are simultaneously well defined) so that quantum mechanics is not required, but the motion of these classical charges could be described by Newtonian mechanics at low velocities, or by special relativity at velocities that are significant fractions of the speed of light c.[1] Historically, classical electromagnetism and special relativity have been intertwined because Einstein was influenced strongly by the beauty and symmetry properties of the Maxwell equations in his formulation of the special theory of relativity. In particular he was motivated by comparing the Lorentz invariance of the Maxwell equations with the Galilean invariance of classical mechanics to propose that it was classical mechanics, not electromagnetism, that required revision if one wanted the laws of electromagnetism and of classical particle motion to be mutually consistent. This led him to propose the radical notion that the speed of light is constant in all inertial frames, which is consistent with Maxwell's equations but not with Newtonian mechanics, and which forms the basis of the special theory of relativity.

18.2 Minkowski Space

A manifold equipped with a prescription for measuring distances is termed a *metric space* and the mathematical function that specifies distances is termed the *metric* for the space.[2]

[1] If strong gravity is important, as it would be in various electromagnetic phenomena in astrophysics (for example, accretion disks for black holes), one must extend the description of charged-particle motion to curved spacetime. This requires use of the *general theory of relativity*. Here we will consider only relativistic electrodynamics in flat spacetime, so special but not general relativity will be necessary. The interested reader will find a tractable introduction to general relativity and its relationship to special relativity in Ref. [35].

[2] Physicists almost always work in metric spaces and usually take existence of a metric for granted (it is hard to do physics without measurement of distance). However, mathematicians are quite familiar with respectible manifolds that need not include a metric among their attributes.

In this section those ideas are applied to flat 4-dimensional spacetime, which is commonly termed *Minkowski space*. Although many concepts will be similar to those for euclidean manifolds, fundamentally new features will enter. Many of these new features are associated with the *indefinite metric* of Minkowski space.

18.2.1 The Indefinite Metric of Spacetime

Although Minkowski space is flat it is not euclidean, for it does not possess a euclidean metric. A metric that can be put into a diagonal form in which the signs of the diagonal entries can all be chosen positive is termed *positive definite*. In contrast, we have see in Ch. 17 that the Minkowski metric has an essential property that the diagonal entries cannot all be chosen positive. Such a metric is termed *indefinite,* and it leads to properties of Minkowski space differing fundamentally from those of euclidean spaces.

18.2.2 Scalar Products and the Metric Tensor

In a particular inertial frame, introduce unit vectors e_0, e_1, e_2, and e_3 that point along the t, x, y, and z axes, respectively, allowing any 4-vector A to be expressed as

$$A = A^0 e_0 + A^1 e_1 + A^2 e_2 + A^3 e_3. \tag{18.1}$$

Thus (A^0, A^1, A^2, A^3) are the (contravariant) components of the 4-vector A.[3] The scalar product of 4-vectors is given by

$$A \cdot B = B \cdot A = (A^\mu e_\mu) \cdot (B^\nu e_\nu) = e_\mu \cdot e_\nu \, A^\mu B^\nu. \tag{18.2}$$

Introducing the definition

$$\eta_{\mu\nu} \equiv e_\mu \cdot e_\nu, \tag{18.3}$$

we may express the scalar product as

$$A \cdot B = \eta_{\mu\nu} A^\mu B^\nu. \tag{18.4}$$

The metric tensor $\eta_{\mu\nu}$ is just a special case of the general metric tensor for spacetime that is generally denoted $g_{\mu\nu}$; however, in flat spacetime $g_{\mu\nu}$ is a constant matrix independent of the coordinates and it is standard to give it the special symbol $\eta_{\mu\nu}$.

18.2.3 The Line Element

The line element ds^2 in Minkowski space measures the square of the distance between points with infinitesimal separation and is given by

$$ds^2 = -c^2 d\tau^2 = \eta_{\mu\nu} dx^\mu dx^\nu = -c^2 dt^2 + dx^2 + dy^2 + dz^2, \tag{18.5}$$

[3] Recall that non-bold symbols denote 4-vectors, bold symbols denote 3-vectors, and that a notation such as A^μ may stand for the full 4-vector, or for a component of it, depending on context.

where τ is the proper time (the time measured by a clock carried in an inertial frame; thus, it is the time measured between events that are at the same spatial point), and where the metric tensor of flat spacetime may be represented by the constant diagonal matrix[4]

$$\eta_{\mu\nu} = \begin{pmatrix} -1 & 0 & 0 & 0 \\ 0 & 1 & 0 & 0 \\ 0 & 0 & 1 & 0 \\ 0 & 0 & 0 & 1 \end{pmatrix} \equiv \text{diag } (-1, 1, 1, 1). \tag{18.6}$$

Then Eq. (18.5) for the line element may be written as the matrix equation

$$ds^2 = (cdt \;\; dx \;\; dy \;\; dz) \begin{pmatrix} -1 & 0 & 0 & 0 \\ 0 & 1 & 0 & 0 \\ 0 & 0 & 1 & 0 \\ 0 & 0 & 0 & 1 \end{pmatrix} \begin{pmatrix} cdt \\ dx \\ dy \\ dz \end{pmatrix}, \tag{18.7}$$

where ds^2 represents the square of the spacetime interval between x and $x + dx$ with

$$x = (x^0, x^1, x^2, x^3) = (ct, x^1, x^2, x^3). \tag{18.8}$$

A point in Minkowski space defines an *event* and the path followed by an object in spacetime is termed the *worldline* for the object. This 4-dimensional spacetime with indefinite metric is termed a *Lorentzian manifold* (or sometimes a *pseudo-euclidean manifold*).

Example 18.1 Given a Minkowski vector with components (A^0, A^1, A^2, A^3), what are the components of the corresponding dual vector? From Eq. (17.44) with $\eta_{\mu\nu}$ substituted for the metric tensor, the indices may be lowered through the contraction $A_\mu = \eta_{\mu\nu} A^\nu$. Therefore, using the metric tensor (18.6) the elements of the corresponding dual vector are $A_\mu = (-A^0, A^1, A^2, A^3)$. This illustrates explicitly that vectors and dual vectors generally are not equivalent in non-euclidean manifolds, but that they are in one-to-one correspondence though contraction with the metric tensor.

18.2.4 Invariance of the Spacetime Interval

Special relativity follows from two assumptions: (1) the speed of light is constant for all observers and (2) the laws of physics cannot depend on spacetime coordinates. The postulate that the speed of light is a constant is equivalent to a statement that the spacetime interval ds^2 of Eq. (18.5) is an invariant that is unchanged by transformations between inertial systems (the Lorentz transformations to be discussed below). This is not true for the euclidean spatial interval $dx^2 + dy^2 + dz^2$, nor is it true for the time interval $c^2 dt^2$; it is true only for the particular combination of spatial and time intervals defined by Eq. (18.5).

[4] We employ here the "mostly plus" signature $(- + + +)$ for the diagonal elements of the metric tensor. Other choices are summarized in Appendix C.

Because of this invariance, Minkowski space is the natural manifold for the formulation of special relativity.[5]

Example 18.2 The metric can be used to determine the relationship between the time coordinate t and the proper time τ. From Eq. (18.5)

$$\begin{aligned} d\tau^2 = \frac{-ds^2}{c^2} &= \frac{1}{c^2}(c^2dt^2 - dx^2 - dy^2 - dz^2) \\ &= dt^2\left\{1 - \frac{1}{c^2}\left[\left(\frac{dx}{dt}\right)^2 + \left(\frac{dy}{dt}\right)^2 + \left(\frac{dz}{dt}\right)^2\right]\right\} \\ &= \left(1 - \frac{v^2}{c^2}\right)dt^2. \end{aligned} \tag{18.9}$$

where v is the magnitude of the velocity. Therefore, the proper time that elapses between coordinate times t_1 and t_2 is

$$\tau_{12} = \int_{t_1}^{t_2}\left(1 - \frac{v^2}{c^2}\right)^{1/2} dt\,. \tag{18.10}$$

The proper time interval τ_{12} is shorter than the coordinate time interval $t_2 - t_1$ because the square root in the integrand of Eq. (18.10) is always less than one. This is the special-relativistic *time dilation effect,* stated in general form. For the special case of constant velocity, (18.10) yields

$$\Delta\tau = \left(1 - \frac{v^2}{c^2}\right)^{1/2}\Delta t, \tag{18.11}$$

which is the formulation of special-relativistic time dilation that is found commonly in textbooks. From this example it is clear that the origin of time dilation in special relativity lies in the geometry of spacetime, specifically in the indefinite nature of the Minkowski metric.

The first postulate of special relativity (constant speed of light for all observers) is ensured by the invariance of the interval (18.5) under transformations between inertial frames. As was suggested by the discussion in Ch. 17, the second postulate (coordinate invariance of physical law) can be ensured by formulating the equations of special relativity in terms of tensors defined in Minkowski space, which we now address.

[5] To summarize: under Galilean transformations in Newtonian mechanics the time interval dt and the euclidean spatial interval $dx^2 + dy^2 + dz^2$ were separately conserved. Under Lorentz transformations space and time are mixed and neither the time interval nor the spatial interval are separately conserved [which renders the concept of simultaneity frame-dependent, as will be discussed in Section 18.7]; only the combined quantity $-c^2dt^2 + dx^2 + dy^2 + dz^2$ (spacetime interval) is conserved [which rescues the concept of causality because all observers agree on the lightcone structure of spacetime, even in the absence of absolute simultaneity, as will be discussed in Section 18.5].

18.3 Tensors in Minkowski space

In Minkowski space the transformations between coordinate systems are particularly simple because they are *independent of spacetime coordinates.* Furthermore, in flat space the correction terms disappear and partial derivatives are equivalent to covariant derivatives. Therefore, the derivatives appearing in the general definitions of Table 17.1 for tensors are constants and the transformation of a coordinate vector x^μ may be expressed as $x'^\mu = \Lambda^\mu{}_\nu x^\nu$, where the matrix $\Lambda^\mu{}_\nu$ does not depend on the spacetime coordinates. Hence, for flat spacetime the tensor transformation laws simplify to

$$\varphi' = \varphi \qquad \text{Scalar} \tag{18.12a}$$

$$A'^\mu = \Lambda^\mu{}_\nu A^\nu \qquad \text{Vector} \tag{18.12b}$$

$$A'_\mu = \Lambda_\mu{}^\nu A_\nu \qquad \text{Dual vector} \tag{18.12c}$$

$$T'^{\mu\nu} = \Lambda^\mu{}_\gamma \Lambda^\nu{}_\delta T^{\gamma\delta} \qquad \text{Contravariant rank-2 tensor} \tag{18.12d}$$

$$T'_{\mu\nu} = \Lambda_\mu{}^\gamma \Lambda_\nu{}^\delta T_{\gamma\delta} \qquad \text{Covariant rank-2 tensor} \tag{18.12e}$$

$$T'^\mu{}_\nu = \Lambda^\mu{}_\gamma \Lambda_\nu{}^\delta T^\gamma{}_\delta \qquad \text{Mixed rank-2 tensor} \tag{18.12f}$$

and so on. Eq. (18.12) In addition, for flat spacetime it is possible to choose a coordinate system for which non-tensorial terms like the second term of Eq. (17.50) can be transformed away so *covariant derivatives are equivalent to partial derivatives* in Minkowski space. In the transformation laws (18.12) the $\Lambda^\mu{}_\nu$ are elements of *Lorentz transformations* that we will now discuss in more detail.

18.4 Lorentz Transformations

Inertial frames enjoy a privileged role in Newtonian mechanics. Newton's first law is unchanged in special relativity and inertial frames can be constructed in the same way as for Newtonian mechanics. What is different about the inertial frames of special relativity is that because of the requirements imposed by the constant speed of light and principle of relativity postulates, the transformations between inertial frames are no longer the Galilean transformations of Newtonian mechanics but rather the *Lorentz transformations.* Hence, the inertial frames of special relativity are often termed *Lorentz frames.* Rotations are an important class of transformations in euclidean space because they *change the direction but preserve the length* of an arbitrary 3-vector. It is desirable to generalize this idea to investigate abstract rotations in the 4-dimensional Minkowski space that change the direction but preserve the length of 4-vectors. As we will now demonstrate, such rotations in Minkowski space are just the Lorentz transformations alluded to above.

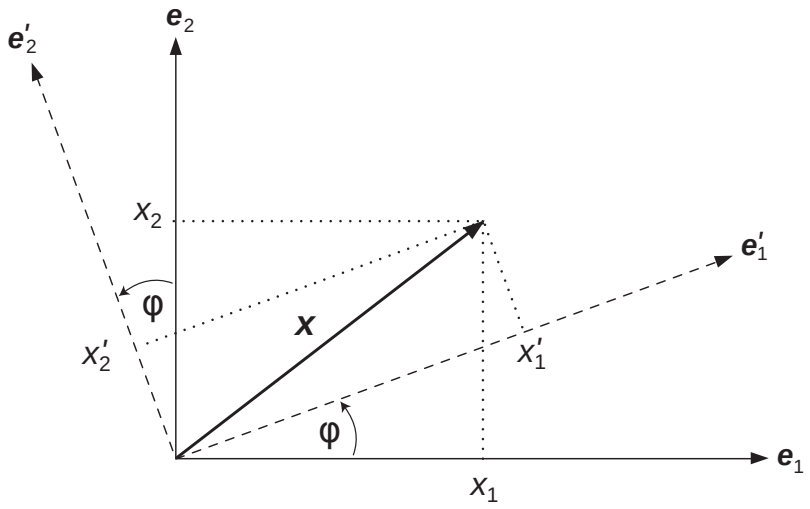

Fig. 18.1 Rotation of 2D euclidean coordinate system.

18.4.1 Rotations in Euclidean Space

First we consider a rotation of the coordinate system in euclidean space, as illustrated in Fig. 18.1. The condition that the length of an arbitrary vector be unchanged by this transformation corresponds to the requirement that the transformation matrix R implementing the rotation act on the metric tensor g_{ij} in the following way

$$Rg_{ij}R^{\mathrm{T}} = g_{ij}, \tag{18.13}$$

where R^{T} denotes the transpose of R. For euclidean space the metric tensor is just the unit matrix so the requirement (18.13) reduces to $RR^{\mathrm{T}} = 1$, which is the condition that R be an orthogonal matrix. Thus, we have obtained the well-known result that rotations in euclidean space are implemented by orthogonal matrices in a rather pedantic manner. But Eq. (18.13) is valid generally, not just for euclidean spaces. Therefore, it may be used as guidance for constructing more general rotations in Minkowski space.

18.4.2 Generalized 4D Minkowski Rotations

By analogy with the above discussion of rotations in euclidean space, which left the length of 3-vectors invariant, let us now seek a set of transformations that leave the length of a 4-vector invariant in the Minkowski space. The coordinate transformation may be written in matrix form,

$$dx'^{\mu} = \Lambda^{\mu}{}_{\nu} dx^{\nu}, \tag{18.14}$$

where the transformation matrix $\Lambda^{\mu}{}_{\nu}$ is expected to satisfy the analog of Eq. (18.13) for the Minkowski metric $\eta_{\mu\nu}$,

$$\Lambda\eta_{\mu\nu}\Lambda^{\mathrm{T}} = \eta_{\mu\nu}, \tag{18.15}$$

or explicitly in terms of components, $\Lambda_\mu{}^\rho \Lambda^\sigma{}_\nu \eta_{\rho\sigma} = \eta_{\mu\nu}$.[6] This property may now be used to construct the elements of the transformation matrix $\Lambda^\mu{}_\nu$. The possible transformations include rotations about the spatial axes (corresponding to rotations within inertial systems) and transformations between inertial systems moving at different constant velocities that are termed Lorentz boosts.

Two inertial frames may differ in displacement, rotational orientation, and uniform velocity. This corresponds to 10 possible transformations between inertial frames: three velocity boosts along the spatial axes, three rotations about the three spatial axes, and four translations in the space and time directions. These 10 transformations form a group called the *Poincaré group* (see Box 18.1). The six Lorentz transformations correspond to the velocity boosts and spatial rotations, and they form a group called the *Lorentz group* that is a subgroup of the Poincaré group, also discussed in Box 18.1. Consider first the simple case of rotations about the z axis.

18.4.3 Lorentz Spatial Rotations

Rotations about a single spatial axis in Minkowski space correspond to a 2-dimensional problem with euclidean metric, so the condition (18.13) may be written as

$$\begin{pmatrix} a & b \\ c & d \end{pmatrix} \begin{pmatrix} 1 & 0 \\ 0 & 1 \end{pmatrix} \begin{pmatrix} a & c \\ b & d \end{pmatrix} = \begin{pmatrix} 1 & 0 \\ 0 & 1 \end{pmatrix}, \tag{18.16}$$

where a, b, c, and d parameterize the transformation matrices. Carrying out the matrix multiplications explicitly on the left side gives

$$\begin{pmatrix} a^2 + b^2 & ac + bd \\ ac + bd & c^2 + d^2 \end{pmatrix} = \begin{pmatrix} 1 & 0 \\ 0 & 1 \end{pmatrix},$$

and comparison of the two sides of the equation implies the conditions

$$a^2 + b^2 = 1 \qquad c^2 + d^2 = 1 \qquad ac + bd = 0.$$

Obviously one choice of parameters that satisfies these conditions is

$$a = \cos\theta \qquad b = \sin\theta \qquad c = -\sin\theta \qquad d = \cos\theta.$$

This leads to the standard result

$$\begin{pmatrix} x'^1 \\ x'^2 \end{pmatrix} = R \begin{pmatrix} x^1 \\ x^2 \end{pmatrix} = \begin{pmatrix} \cos\theta & \sin\theta \\ -\sin\theta & \cos\theta \end{pmatrix} \begin{pmatrix} x^1 \\ x^2 \end{pmatrix}. \tag{18.17}$$

Now we shall apply this same technique to determine the elements of a Lorentz boost transformation.

[6] In this discussion we use the (common) convention that $\eta_{\mu\nu}$ is either a symbol standing for the full tensor or a specific component of the tensor distinguished by indices μ and ν, depending on context. In a matrix equation like (18.15) the order of the factors matters because matrices don't generally commute, but when the matrix equation is written out in terms of sums over component products as in $\Lambda_\mu{}^\rho \Lambda^\sigma{}_\nu \eta_{\rho\sigma} = \eta_{\mu\nu}$ the order of factors can be rearranged at will, since the components of the matrices are just numbers that commute with each other. The matrices Λ are symmetric so horizontal placement of indices isn't crucial, but a typical convention is to define $\Lambda^\mu{}_\nu = \partial x'^\mu / \partial x^\nu$ and $\Lambda_\mu{}^\nu = \partial x^\nu / \partial x'^\mu$ (compare Table 17.1).

Box 18.1 Symmetries and Groups [36]

A group is a set $G = \{x, y, ...\}$ for which a binary operation $a \cdot b = c$ called *group multiplication* is defined that has the following properties

(i) *Closure:* If x and y are elements of G, then $x \cdot y$ is an element of G also.
(ii) *Identity:* An identity element e exists such that $e \cdot x = x \cdot e = x$ for $x \in G$.
(iii) *Existence of an Inverse:* For every group element x there is an inverse x^{-1} in the set such that $xx^{-1} = e$.
(iv) *Associativity:* Multiplication is associative: $(x \cdot y) \cdot z = x \cdot (y \cdot z)$ for $x, y, z \in G$.

For groups of transformations multiplication corresponds to applying first one and then the other transformation. The group definition requires associativity but not commutivity. A group consisting of commutative elements only is *abelian*; otherwise, it is *nonabelian*.

Example: The Lorentz group
There are six independent Lorentz transformations: three rotations about the spatial axes parameterized by real angles, and three boosts along the spatial axes parameterized by boost velocities. Because rotation angles and boost velocities can take continuous real values, the set of Lorentz transformations is infinite. The Lorentz transformations form a group:

1. Two successive transformations are equivalent to some other transformation.
2. Every Lorentz transformation has an inverse that is the transformation in the opposite direction (for example, $v \to -v$ for boosts).
3. The identity corresponds to no transformation.
4. It doesn't matter how three successive transformations are grouped, so multiplication is associative, but the *order* matters, so the Lorentz group is nonabelian.

An important class of groups corresponds to transformations that are continuous (analytical) in their parameters. These are called *Lie groups.* The Lorentz group is a Lie group. Groups also can be classified according to whether their parameter spaces are closed and bounded (*compact groups*) or not (*noncompact groups*). Because boost velocities can approach c asymptotically but never reach it, the Lorentz-group parameter space is not closed (the limit $v = c$ is not part of the set) and the group is noncompact.

Example: The Poincaré group
The Poincaré group is formed by adding to the Lorentz transformations the uniform translations along the four spacetime axes. It is a non-abelian, noncompact Lie group, and contains the Lorentz group as a *subgroup* (a subset of group elements that satisfy the same group postulates as the parent group).

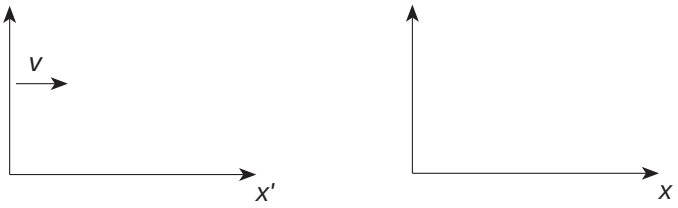

Fig. 18.2 A Lorentz boost along the positive x axis by a velocity v.

18.4.4 Lorentz Boost Transformations

Consider a boost from one inertial system to a second one moving in the positive direction at uniform velocity along the x axis, as illustrated in Fig. 18.2. Since the y and z coordinates will not be affected, this is a 2-dimensional problem in the time coordinate t and the spatial coordinate x. The transformation is of the general form

$$\begin{pmatrix} cdt' \\ dx' \end{pmatrix} = \begin{pmatrix} a & b \\ c & d \end{pmatrix} \begin{pmatrix} cdt \\ dx \end{pmatrix}, \tag{18.18}$$

and the condition (18.15) can be written out explicitly as

$$\begin{pmatrix} a & b \\ c & d \end{pmatrix} \begin{pmatrix} -1 & 0 \\ 0 & 1 \end{pmatrix} \begin{pmatrix} a & c \\ b & d \end{pmatrix} = \begin{pmatrix} -1 & 0 \\ 0 & 1 \end{pmatrix}, \tag{18.19}$$

which is identical in form to the rotation case, except for the indefinite metric. Multiplying the matrices on the left side and comparing with the right side gives the conditions

$$a^2 - b^2 = 1 \qquad -c^2 + d^2 = 1 \qquad -ac + bd = 0,$$

which clearly are satisfied by the parameterization

$$a = \cosh\xi \qquad b = \sinh\xi \qquad c = \sinh\xi \qquad d = \cosh\xi,$$

where ξ is a hyperbolic variable taking the values $-\infty \leq \xi \leq \infty$. Therefore, we may write the boost transformation as

$$\begin{pmatrix} cdt' \\ dx' \end{pmatrix} = \begin{pmatrix} \cosh\xi & \sinh\xi \\ \sinh\xi & \cosh\xi \end{pmatrix} \begin{pmatrix} cdt \\ dx \end{pmatrix}. \tag{18.20}$$

A geometrical interpretation of this result is discussed in Box 18.2.

The Lorentz boost transformation (18.20) can be put into a more familiar form by exchanging the boost parameter ξ for the boost velocity. For convenience, let's replace the differentials in Eq. (18.20) with finite space and time intervals ($dt \to t$ and $dx \to x$). The velocity of the boosted system is $v = x/t$. From Eq. (18.20), the origin ($x' = 0$) of the boosted system is given by

$$x' = ct\sinh\xi + x\cosh\xi = 0.$$

Therefore, $x/t = -c\sinh\xi/\cosh\xi$, from which it may be concluded that

$$\beta \equiv \frac{v}{c} = \frac{x}{ct} = -\frac{\sinh\xi}{\cosh\xi} = -\tanh\xi. \tag{18.21}$$

Box 18.2 **Minkowski rotations**

The respective derivations make clear that the appearance of hyperbolic functions in Eq. (18.20) instead of trigonometric functions as in Eq. (18.17) traces to the role of the indefinite metric diag $(-1, 1)$ in Eq. (18.19) relative to the positive-definite metric diag $(1, 1)$ in Eq. (18.16). The boost transformations are in a sense "rotations" in Minkowski space, but these rotations have unusual properties relative to normal rotations in euclidean space since they mix space and time, and may be viewed as rotations through imaginary angles. These properties follow from the metric because the invariant interval is neither the length of vectors in space nor the length of time intervals, but rather the specific mixture of space and time intervals implied by the Minkowski line element (18.5) with indefinite metric (18.6). This is quite different from Newtonian mechanics, where time is a universal parameter common to all observers and the Galilean transformations conserve only the *space interval*.

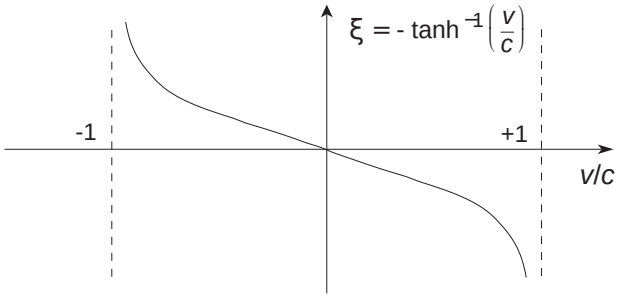

Fig. 18.3 Dependence of the Lorentz parameter ξ on $\beta = v/c$.

This relationship between ξ and β is plotted in Fig. 18.3. Utilizing the identity $1 = \cosh^2 \xi - \sinh^2 \xi$ and the definition

$$\gamma \equiv \left(1 - \frac{v^2}{c^2}\right)^{-1/2} \tag{18.22}$$

of the *Lorentz γ-factor*, we may write

$$\cosh \xi = \sqrt{\frac{\cosh^2 \xi}{1}} = \frac{1}{\sqrt{1 - \sinh^2 \xi / \cosh^2 \xi}} = \frac{1}{\sqrt{1 - v^2/c^2}} = \gamma, \tag{18.23}$$

and from this result and (18.21),

$$\sinh \xi = -\beta \cosh \xi = -\beta\gamma. \tag{18.24}$$

Inserting (18.23)–(18.24) into (18.20) for finite intervals gives

$$\begin{pmatrix} ct' \\ x' \end{pmatrix} = \gamma \begin{pmatrix} 1 & -\beta \\ -\beta & 1 \end{pmatrix} \begin{pmatrix} ct \\ x \end{pmatrix} \tag{18.25}$$

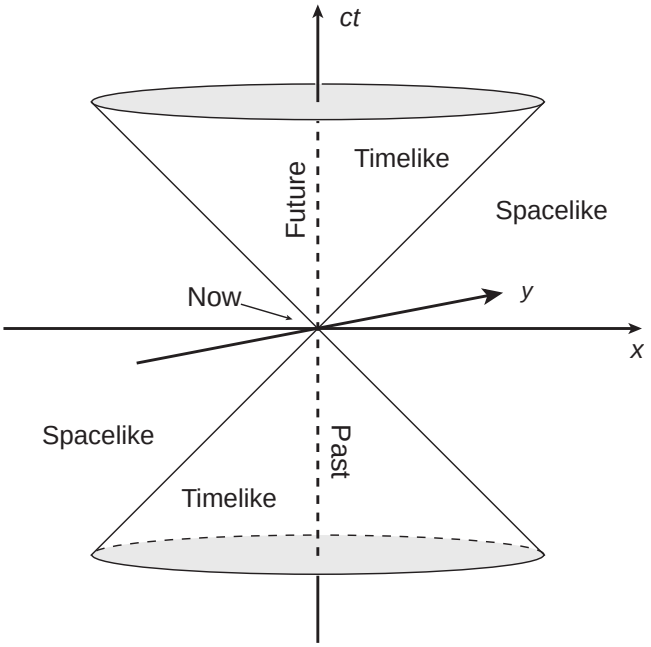

Fig. 18.4 Lightcone diagram for flat spacetime in two space and one time dimensions. The future lightcone is the surface swept out by a spherical light pulse emitted from the origin.

and writing this matrix expression out explicitly gives the Lorentz boost equations (for the specific case of a positive boost along the x axis) in standard textbook form,

$$t' = \gamma\left(t - \frac{vx}{c^2}\right) \qquad x' = \gamma(x - vt) \qquad y' = y \qquad z' = z, \tag{18.26}$$

with the inverse transformation corresponding to the replacement $v \to -v$. By inspection, these reduce to the Galilean boost equations (17.1) if $v/c \to 0$ and it is easy to verify that the Lorentz transformations leave invariant the spacetime interval ds^2.

18.5 Lightcone Diagrams

The line element (18.5) defines a cone, implying that Minkowski spacetime may be classified according to the *lightcone diagram* exhibited in Fig. 18.4. The *lightcone* is a 3-dimensional surface in the 4-dimensional spacetime and intervals relative to the origin may be characterized according to whether they are inside of, outside of, or on the lightcone. Assuming the metric signature $(- + ++)$ employed here, the standard terminology is

- If $ds^2 < 0$ the interval is termed *timelike*.
- If $ds^2 > 0$ the interval is termed *spacelike*.
- If $ds^2 = 0$ the interval is called *lightlike* (or *null*).

These regions for flat spacetime are labeled in Fig. 18.4. This classification can be extended also to surfaces. For example, a *spacelike surface* is a collection of points for which any pair of points has a spacelike separation and a *lightlike surface* is a collection of points for which any pair of points has a lightlike separation. The lightcone classification makes clear the distinction between Minkowski spacetime and a mere 4-dimensional euclidean space in that two points in the Minkowski spacetime may be separated by a distance that when squared could be positive, negative, or zero. This is not possible in a euclidean metric. Notice in particular that for lightlike particles, which have worldlines confined to the lightcone, the square of the spacetime interval between any two points on a worldline is *zero.*

Example 18.3 The Minkowski line element (18.5) in one space and one time dimension [which often is termed $(1+1)$ dimensions] is given by $ds^2 = -c^2dt^2 + dx^2$. Thus, if the spacetime interval is lightlike, $ds^2 = 0$ and

$$-c^2dt^2 + dx^2 = 0 \quad \longrightarrow \quad \left(\frac{dx}{dt}\right)^2 = c^2 \quad \longrightarrow \quad v = \pm c.$$

This result can be generalized easily to the full space, leading to the conclusion that events in Minkowski space separated by a null interval ($ds^2 = 0$) are connected by signals moving at light velocity, $v = c$. If the time axis (ct) and space axes have the same scales, this means that the worldline of a freely-propagating photon (or any massless particle, necessarily moving at light velocity) always makes $\pm 45^\circ$ angles in the lightcone diagram. By similar arguments, events at timelike separations (inside the lightcone) are connected by signals with $v < c$, and those with spacelike separations (outside the lightcone) could be connected only by causality-violating signals with $v > c$.

The lightcone illustrated in Fig. 18.4 was placed at the origin for illustration but each point in the spacetime has its own lightcone. From Example 18.3, the tangent to the worldline of any particle at a point defines the local velocity of the particle at that point and constant velocity implies straight worldlines. Therefore, as illustrated in Fig. 18.5(b), light travels in a straight line in flat spacetime and always on the lightcone because it has constant local velocity, $v = c$, while the worldline for any massive particle must lie inside the local lightcone because it must always have $v \leq c$ (in the jargon, a worldline for a massive particle is always *timelike*). The worldline for the massive particle in Fig. 18.5(a) is curved, indicating an acceleration since the velocity is changing with time. For non-accelerated massive particles the worldline would be straight, but always within the local lightcone.

In the Galilean relativity of Newtonian mechanics an event picks out a hyperplane of simultaneity consisting of all events occurring at the same time as the event. All observers agree on what constitutes this set of simultaneous events because in Galilean relativity simultaneity is independent of the observer. In Einstein's relativity, *simultaneity depends on the observer* and hyperplanes of constant coordinate time have no invariant meaning. However, *all observers agree on the lightcones associated with events,* because the speed of

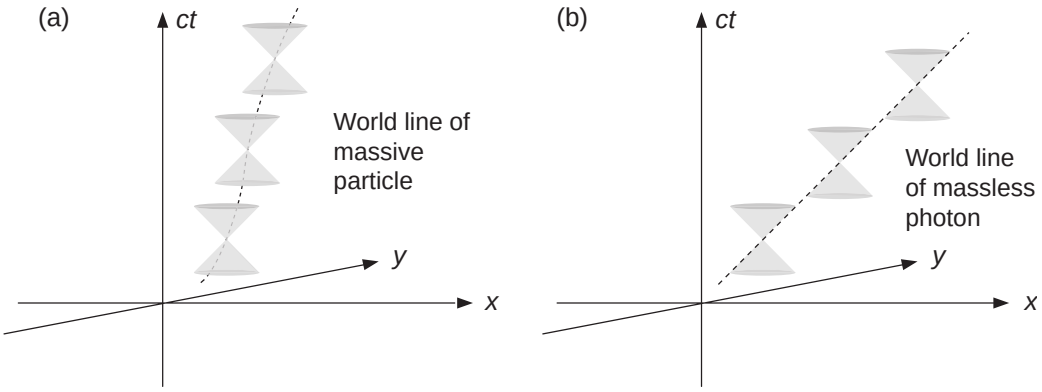

Fig. 18.5 Worldlines for (a) massive (timelike) particles and (b) massless (lightlike) particles. For massive particles the trajectory must always lie inside the local light cone at each point; for massless particles it must always lie on the lightcone at each point.

light is an invariant for all observers. Thus, the *lightcones define an invariant spacetime structure* permitting unambiguous causal classification of events.

18.6 The Causal Structure of Spacetime

The causal properties of Minkowski spacetime are encoded in its invariant lightcone structure. Each spacetime point lies at the apex of its lightcone ("Now" in Fig. 18.4). From Example 18.3, the lightcone defines a set of points that are connected to the origin by signals moving at light velocity c, events inside the lightcone may be connected to the origin by signals moving at $v < c$, and events outside the lightcone may be connected to the origin only by signals having $v > c$. Thus, the event at the origin of a local lightcone may influence any event within its forward lightcone ("Future" in Fig. 18.4) through signals propagating at $v < c$. Likewise, the event at the origin may be influenced by events within its backward lightcone ("Past" in Fig. 18.4) through signals with speeds less than that of light. Conversely, spacelike-separated events may not influence, or have an influence on, the event at the origin except by signals having $v > c$. Finally, events on the lightcone are connected by signals traveling exactly at c. Thus, events at spacelike separations are causally disconnected and the lightcone separates the knowable from the unknowable for an observer at the apex of the lightcone.

This lightcone structure of spacetime ensures that all velocities obey locally the constraint $v \leq c$. Since velocities are defined and measured locally, covariant field theories in either flat or curved spacetime are guaranteed to respect the speed limit $v \leq c$, irrespective of whether velocities appear to exceed c globally. For example, in the Hubble expansion of the Universe galaxies beyond a certain distance (the horizon) appear to recede at velocities in excess of c because of the expansion of space, and light coming to us from near the horizon is stretched in wavelength and takes longer to propagate to us

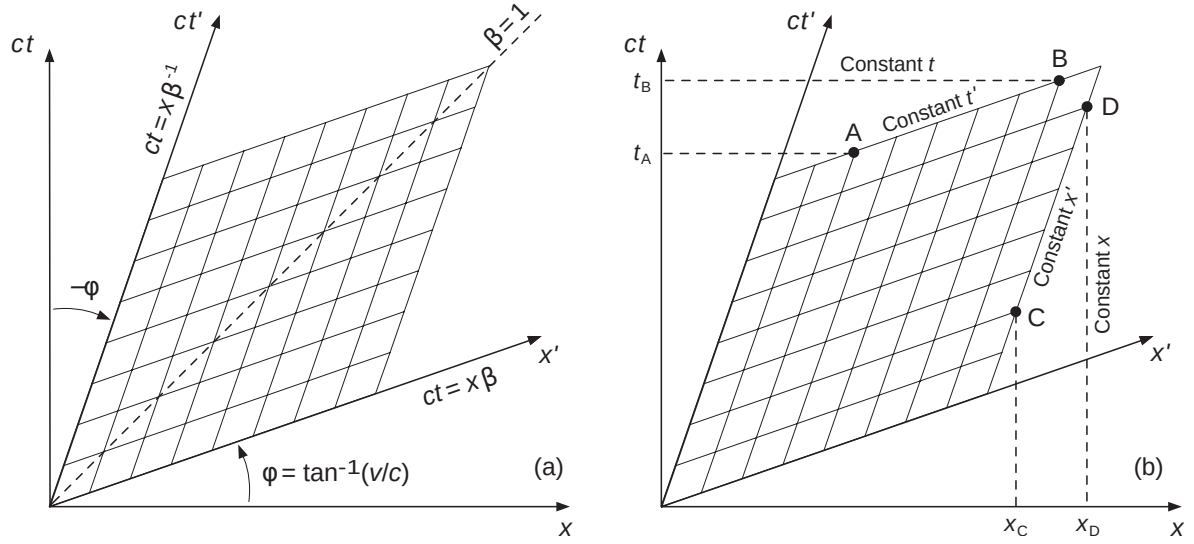

Fig. 18.6 (a) Lorentz boost transformation in a spacetime diagram. (b) Comparison of events in boosted and unboosted reference frames.

than it would in a flat, non-expanding spacetime. However, all local measurements in that expanding, possibly curved spacetime would determine the velocity of light to be c, in accordance with the axioms of special relativity and the associated lightcone structure of spacetime.

From the preceding discussion we may conclude that the axioms of special relativity are fundamentally at odds with the Newtonian concept of absolute simultaneity, since the demand that light have the same speed for all observers necessarily means that the apparent temporal order of two events depends upon the observer. However, the abolishment of absolute simultaneity introduces *no causal ambiguity,* because all observers agree on the lightcone structure of spacetime and hence all observers agree that event A can cause event B only if A lies in the past lightcone of B, for example.

18.7 Lightcones and Lorentz Transformations

It is instructive to examine the action of Lorentz transformations in the lightcone diagram. Restricting to boosts only in the x direction, the relevant part of the spacetime diagram in some inertial frame corresponds to a plot with axes ct and x, as illustrated in Fig. 18.6.

18.7.1 Lorentz Boosts and the Lightcone

What happens to the axes in Fig. 18.6 under a Lorentz boost? From the first two of Eqs. (18.26),

$$ct' = c\gamma\left(t - \frac{vx}{c^2}\right) \qquad x' = \gamma(x - vt). \tag{18.27}$$

The t' axis corresponds to $x' = 0$, which implies from the second of Eqs. (18.27) that $ct = x\beta^{-1}$, with $\beta = v/c$, is the equation of the t' axis in the (ct, x) coordinate system. Likewise, the x' axis corresponds to $t' = 0$, which implies from the first of Eqs. (18.27) that $ct = x\beta$. The x' and ct' axes for the boosted system are also shown in Fig. 18.6(a) for a boost corresponding to a positive value of β. The time and space axes are rotated by the same angle, but in *opposite directions* by the boost (a consequence of the indefinite Minkowski metric). The angle of rotation is related to the boost velocity through $\tan\phi = v/c$.

Many characteristic features of special relativity are apparent from Fig. 18.6. For example, relativity of simultaneity follows directly, as illustrated in Fig. 18.6(b). Points A and B lie on the same t' line, so they are simultaneous in the boosted frame. But from the dashed projections on the ct axis, in the unboosted frame event A occurs before event B. Likewise, points C and D lie at the same value of x' in the boosted frame and so are spatially congruent, but in the unboosted frame $x_{\rm C} \neq x_{\rm D}$. Relativistic time dilation and space contraction effects follow rather directly from these observations, as illustrated in the example below.

Example 18.4 Consider the following schematic representation of the spacetime diagram illustrated in Fig. 18.6, where a rod of length L_0, as measured in its own rest frame (t, x), is oriented along the x axis.

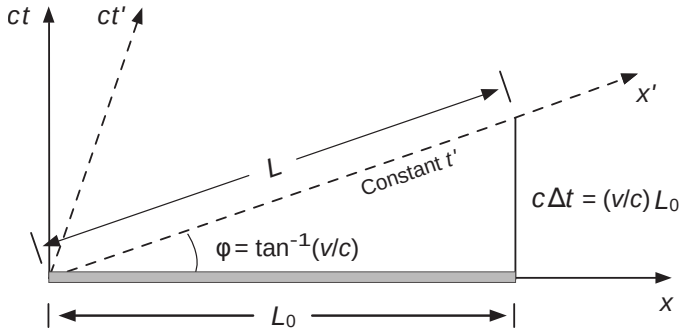

The frame (t', x') is boosted by a velocity v along the $+x$ axis relative to the (t, x) frame. Therefore, in the primed frame the rod will have a velocity v in the negative x' direction. Determining the length L observed in the primed frame requires that the positions of the ends of the rod be measured *simultaneously in that frame.* The axis labeled x' corresponds to constant t' [see Fig. 18.6(b)], so the distance marked as L is the length in the primed frame. This distance *seems* longer than L_0, but this is deceiving because a slice of Minkowski spacetime is being represented on a piece of euclidean paper. Much as a Mercator projection of the globe onto a euclidean sheet of paper gives misleading distance information (Greenland is actually much smaller than Brazil), the metric must be trusted to determine the correct distance in a space. From the Minkowski indefinite metric and the triangle in the figure above, $L^2 = L_0^2 - (c\Delta t)^2$. But from Eq. (18.27) it was found that

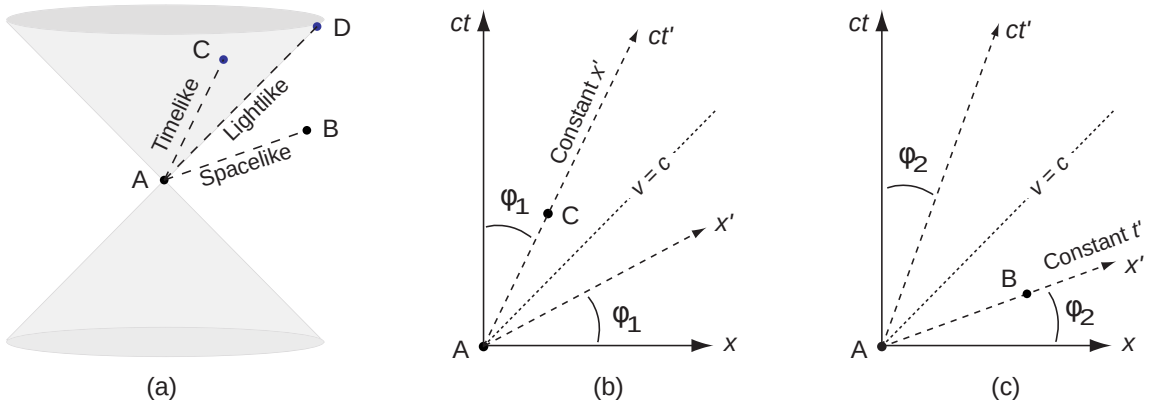

Fig. 18.7 (a) Timelike, lightlike (null), and spacelike separations for events. (b) A Lorentz transformation that brings the timelike separated points A and C of (a) into spatial congruence (they lie along a line of constant x' in the primed coordinate system). (c) A Lorentz transformation that brings the spacelike separated points A and B of (a) into coincidence in time (they lie along a line of constant t' in the primed coordinate system).

the equation for the x' axis is $c\Delta t = (v/c)\, L_0$, from which it follows that

$$L = (L_0^2 - (c\Delta t)^2)^{1/2} = \left(L_0^2 - \left(\frac{v}{c} L_0\right)^2\right)^{1/2} = L_0(1 - v^2/c^2)^{1/2},$$

which is the familiar length-contraction formula of special relativity: L is *shorter* than L_0, even though it appears to be longer in the figure above.

18.7.2 Spacelike and Timelike Intervals

As noted previously, the spacetime interval between any two events may be classified in a relativistically invariant way as timelike, lightlike, or spacelike by constructing the lightcone at one of the points, as illustrated in Fig. 18.7(a). This geometry and that of Fig. 18.6 then suggest another important distinction between events at spacelike separations [the line AB in Fig. 18.7(a)] and timelike separations [the line AC in Fig. 18.7(a)]:

(i) If two events have a timelike separation, a Lorentz transformation exists that can bring them into spatial congruence. Figure 18.7(b) illustrates geometrically a coordinate system (ct', x'), related to the original system by an x-axis Lorentz boost of $v/c = \tan\phi_1$, in which A and C have the same coordinate x'.

(ii) If two events have a spacelike separation, a Lorentz transformation exists that can synchronize the events. Figure 18.7(c) illustrates an x-axis Lorentz boost by $v/c = \tan\phi_2$ to a system in which A and B have the same time t'.

Maximum values of ϕ_1 and ϕ_2 are limited by the $v = c$ line. The Lorentz transformation to bring A into spatial congruence with C exists only if C lies to the left of $v = c$ (C separated

by a timelike interval from A). Likewise, the Lorentz transformation to synchronize A with B exists only if B lies to the right of $v = c$ (B separated by a spacelike interval from A).

18.8 Electromagnetism in Special Relativity

The electromagnetic Lorentz force

$$\boldsymbol{F} = q(\boldsymbol{E} + \boldsymbol{v} \times \boldsymbol{B}),$$

can receive contributions from electric or magnetic fields. In many simple cases a force observed to have magnetic characteristics from one inertial frame exhibits the characteristics of an electrostatic force when observed from a different inertial frame. Since it is a fundamental tenet of special relativity that the laws of physics cannot depend on the intertial frame of the observer, this suggests a fundamental relationship between electricity and magnetism. Let's consider several examples.

18.8.1 A Charge Moving Parallel to a Current

Suppose that we observe a charge moving parallel to a wire that is carrying a steady current from two different perspectives.

1. *In the Lab Frame:* The wire has equal uniform densities of positive and negative charges and is electrically neutral to the test charge. A moving test charge feels a *magnetic force* $\boldsymbol{F}_{\mathrm{B}} = qv \times \boldsymbol{B}$ with $\boldsymbol{B}$ derived in Section 8.4.2, because it is moving through a magnetic field created around the wire by the current.
2. *In Rest Frame of the Charge:* The test charge is stationary with respect to this frame, so $v = 0$ and it doesn't feel any magnetic force. However, in this frame the charges in the wire will appear to be moving backward, and because of *Lorentz contraction* the moving charges in the wire have their spacing compressed compared to the stationary charges, which creates a net charge density in the wire, and a force $\boldsymbol{F}_{\mathrm{E}} = qE$ that is *purely electrostatic*.

This simple thought experiment suggests that electric and magnetic forces are just two sides of the same coin, and whether we see a pure electric, a pure magnetic, or a mixture of electric and magnetic forces is simply a matter of our choice of observing frame.

However, the actual relationship between electricity and magnetism must be more nuanced because not every situation interpreted as magnetism can be so easily transformed into electrostatics just by changing observing frames.

Invariants: In electromagnetism, there are certain quantities that all observers agree on, such as $E^2 - c^2B^2$, because they are invariant under tranformations between inertial frames. If this value is negative in one frame (which means that the magnetic field is

stronger than the electric field in that frame), there is no inertial frame where the magnetic field disappears.

The Electromagnetic Tensor: As we shall see in Section 18.10, special relativity treats the electric field $\boldsymbol{E}$ and magnetic field $\boldsymbol{B}$ as components of a single object, the electromagnetic field tensor ($F^{\mu\nu}$). Just as "length" and "duration" are two sides of the same spacetime interval, relativistically $\boldsymbol{E}$ and $\boldsymbol{B}$ are two sides of the same field.

Intrinsic Magnetism: Some particles, like electrons, have an intrinsic magnetic moment associated with the spin of the particle, which is an intrinsically quantum-mechanical property. This magnetism is fundamental to the particle and cannot be explained simply by the macroscopic movement of charges.

It is fair to say that magnetism is the necessary consequence of applying special relativity to electrostatics, but it is more accurate to say that electricity and magnetism are two parts of a single, unified electromagnetic field that look different depending on your velocity.

18.8.2 A Boosted Line Charge

Let's consider another example. In Problem 2.11 we considered a line charge of uniform linear density λ, which generates an electrostatic field,

$$\boldsymbol{E} = \frac{\lambda}{2\pi\epsilon_0(y^2+z^2)}\begin{pmatrix}0\\ y\\ z\end{pmatrix}. \tag{18.28}$$

if the line lies along the x axis, but there is no magnetic field $\boldsymbol{B}$ because the charges are assumed stationary. Now suppose that an observer moves with constant speed v parallel to the x axis.

18.8.3 A Boosted Point Charge

The effect of a Lorentz transformation on the fields associated with a point electrical charge is illustrated in Fig. 18.8. Initially there is only a radially symmetric electric field and no magnetic field since there is no relative motion of the charge with respect to the observer. But as relative velocity increases for the observer the system develops a magnetic field, and the electric potential is increasingly flattened into a "pancake" by length contraction in the direction of motion.

18.9 Lorentz Covariance of Maxwell's Equations

We conclude this chapter by examining the Lorentz covariance of the Maxwell equations that describe classical electromagnetism. There are several motivations.

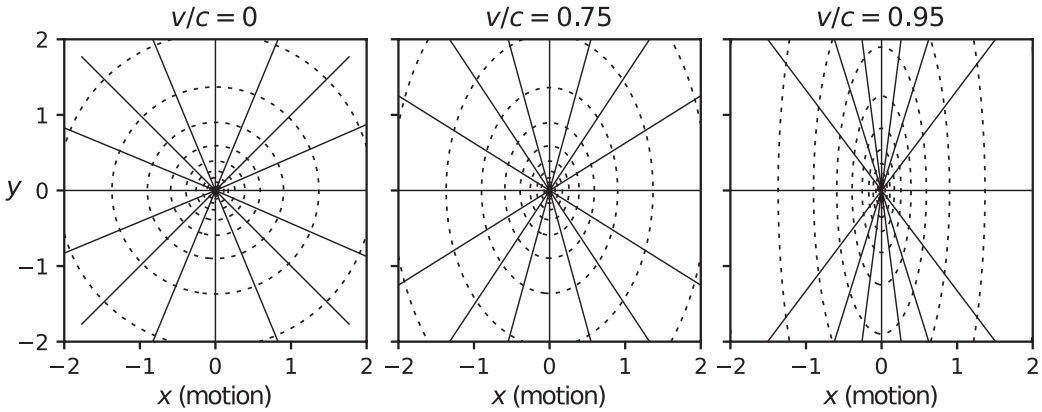

Fig. 18.8 Electric field (solid lines) and electric potential (dotted curves) for a point charge observed at relative velocities $\beta = v/c = 0.00, 0.75, 0.95$ along the x axis, with the observer transverse to the velocity vector of the point charge.

1. It provides a nice example of how useful Lorentz invariance and Lorentz tensors can be in application to a physical problem.
2. It is of *considerable historical interest* because the beauty and properties of the Maxwell equations had strong influence on Einstein in his development of the special theory of relativity.
3. The transformation properties of the Maxwell equations influenced Heaviside and particularly Lorentz in formulating the Lorentz transformations that are integral to the mathematics of special relativity.
4. There are many useful parallels between general relativity and the Maxwell theory, particularly for weak gravity where the Einstein field equations may be linearized.[7]

In the following sections we write the Maxwell equations in standard form, introduce a covariant notation for them, and finally rewrite them in a way that is manifestly Lorentz covariant because all quantities appearing in the equations will be Lorentz tensors. The relationship among invariance and covariance with respect to Lorentz transformations is summarized in Box 18.3 and Table 18.1.

18.9.1 Maxwell Equations in Non-Covariant Form

Let us first write the Maxwell equations in the usual non-covariant way. Departing from our normal SI units, we choose to do this in Heaviside–Lorentz units (see Appendix B.3), which will be recognized as very similar to SI units but with the speed of light set to

[7] For example, this is particularly useful in understanding the propagation of gravitational waves far from strong sources. Then the highly-nonlinear Einstein equations that describe strong gravity can be linearized and the resulting formalism exhibits many similarities to the Maxwell equations of classical electromagnetism (see Section 22.2 of Ref. [36]).

Box 18.3 Invariance and Covariance under Transformations

The terms *invariance* and *convariance* have related but not equivalent meanings and are often confused with each other in casual discussion. Both typically refer to symmetries under a specified set of mathematical transformations. There is a subtle difference in meaning between *invariance* and *covariance*, with respect to a set of transformations.

1. *Invariance means* that the physical observables of the system are not changed by the transformations.
2. *Covariance* means that the system is formulated mathematically so that the form of the equations does not change under the transformations.
3. *Manifest covariance* means that the covariance is *manifest* in the formulation of the theory (can be "seen at a glance").

Thus, a system could be covariant under some set of transformations, but not manifestly covariant because the invariance is obscured by the way the equations are written. This is the case with the Maxwell equations. As we shall see in Section 18.9, it isn't obvious whether the Maxwell equations written in their usual vector calculus form (1.1) are covariant under Lorentz transformation (because they are not formulated in standard Lorentz 4-vector notation), but they are, and they can be re-written so that the Lorentz covariance is manifest. The relationship among invariance, covariance, and manifest invariance or covariance is summarized concisely in Table 18.1.

$c = 1$. The free-space Maxwell equations may be written in Heaviside–Lorentz units as

$$\boldsymbol{\nabla} \cdot \boldsymbol{E} = \rho \tag{18.29a}$$

$$\frac{\partial \boldsymbol{B}}{\partial t} + \boldsymbol{\nabla} \times \boldsymbol{E} = 0 \tag{18.29b}$$

$$\boldsymbol{\nabla} \cdot \boldsymbol{B} = 0 \tag{18.29c}$$

$$\boldsymbol{\nabla} \times \boldsymbol{B} - \frac{\partial \boldsymbol{E}}{\partial t} = \boldsymbol{J}, \tag{18.29d}$$

Table 18.1 Invariance and covariance with respect to a transformation

Term	Meaning	Representative examples
Invariance	Quantities don't change their value under the transformation	Scalars like speed of light or electrical charge under Lorentz transformations
Covariance	Equations or quantities retain their mathematical form after a transformation	Maxwell equations in vector calculus form are *Lorentz covariant,* but are not manifestly so
Manifest	Invariance or covariance can be "seen at a glance" in equations	Maxwell equations in tensor form are *manifestly covariant*

where $\boldsymbol{E}$ is the 3-vector electric field, $\boldsymbol{B}$ is the 3-vector magnetic field, ρ is the scalar charge density, and $\boldsymbol{J}$ is the current 3-vector, with the density and current required to satisfy the usual equation (1.3) of continuity

$$\frac{\partial \rho}{\partial t} + \boldsymbol{\nabla} \cdot \boldsymbol{J} = 0.$$

The Maxwell equations are consistent with the special theory of relativity. However, in the form of Eqs. (18.29) this covariance is *not manifest,* since these equations are formulated in terms of 3-vectors and separate derivatives with respect to space and time, not in terms of Minkowski tensors. It is useful in a number of contexts to reformulate the Maxwell equations in a manner that is manifestly covariant with respect to Lorentz transformations. The usual route to accomplishing this begins by replacing the electric and magnetic fields by new variables, the vector and scalar potentials.

18.9.2 Scalar and Vector Potentials

The electric and magnetic fields appearing in the Maxwell equations may be eliminated in favor of a vector potential $\boldsymbol{A}$ and a scalar potential Φ through the definitions

$$\boldsymbol{B} \equiv \boldsymbol{\nabla} \times \boldsymbol{A} \qquad \boldsymbol{E} \equiv -\boldsymbol{\nabla}\Phi - \frac{\partial \boldsymbol{A}}{\partial t}. \tag{18.30}$$

The vector identities

$$\boldsymbol{\nabla} \cdot (\boldsymbol{\nabla} \times \boldsymbol{B}) = 0 \qquad \boldsymbol{\nabla} \times \boldsymbol{\nabla}\Phi = 0, \tag{18.31}$$

may then be used to show that the second and third Maxwell equations are satisfied identically, and the identity

$$\boldsymbol{\nabla} \times (\boldsymbol{\nabla} \times \boldsymbol{A}) = \boldsymbol{\nabla}(\boldsymbol{\nabla} \cdot \boldsymbol{A}) - \boldsymbol{\nabla}^2 \boldsymbol{A}, \tag{18.32}$$

may be used to write the remaining two Maxwell equations as the coupled second-order differential equations

$$\boldsymbol{\nabla}^2 \Phi + \frac{\partial}{\partial t} \boldsymbol{\nabla} \cdot \boldsymbol{A} = -\rho, \tag{18.33a}$$

$$\boldsymbol{\nabla}^2 \boldsymbol{A} - \frac{\partial^2 \boldsymbol{A}}{\partial t^2} - \boldsymbol{\nabla} \left(\boldsymbol{\nabla} \cdot \boldsymbol{A} + \frac{\partial \Phi}{\partial t} \right) = -\boldsymbol{J}. \tag{18.33b}$$

These equations may then be decoupled by exploiting a fundamental symmetry of electromagnetism termed *gauge invariance.*

18.9.3 Gauge Transformations

Because of the vector identity $\boldsymbol{\nabla} \times \boldsymbol{\nabla}\Phi = 0$, the simultaneous transformations

$$\boldsymbol{A} \to \boldsymbol{A} + \boldsymbol{\nabla}\chi \qquad \Phi \to \Phi - \frac{\partial \chi}{\partial t} \tag{18.34}$$

for an arbitrary scalar function χ do not change the $\boldsymbol{E}$ and $\boldsymbol{B}$ fields; thus, they leave the Maxwell equations invariant. The transformations (18.34) are termed (classical) *gauge*

transformations. This freedom of gauge transformation may be used to decouple Eqs. (18.33). For example, if a set of potentials $(\boldsymbol{A}, \Phi)$ that satisfy

$$\boldsymbol{\nabla} \cdot \boldsymbol{A} + \frac{\partial \Phi}{\partial t} = 0, \tag{18.35}$$

is chosen, the equations decouple to yield

$$\boldsymbol{\nabla}^2 \Phi - \frac{\partial^2 \Phi}{\partial t^2} = -\rho \qquad \boldsymbol{\nabla}^2 \boldsymbol{A} - \frac{\partial^2 \boldsymbol{A}}{\partial t^2} = -\boldsymbol{J}, \tag{18.36}$$

which may be solved independently for $\boldsymbol{A}$ and Φ. A constraint of the sort (18.35) is termed a *gauge condition* and imposing such a constraint is termed *fixing the gauge.* This particular choice of gauge that leads to the decoupled equations (18.36) is termed the *Lorenz gauge.* Another commonly chosen gauge is the *Coulomb gauge*, with a gauge-fixing condition

$$\boldsymbol{\nabla} \cdot \boldsymbol{A} = 0, \tag{18.37}$$

which allows the Maxwell equations (18.33) to be written as the decoupled equations

$$\boldsymbol{\nabla}^2 \Phi = -\rho \qquad \boldsymbol{\nabla}^2 \boldsymbol{A} - \frac{\partial^2 \boldsymbol{A}}{\partial^2 t} = \boldsymbol{\nabla} \frac{\partial \Phi}{\partial t} - \boldsymbol{J}. \tag{18.38}$$

Let us utilize the shorthand notation for derivatives introduced in Eq. (17.49):

$$\partial^\mu \equiv \frac{\partial}{\partial x_\mu} = (\partial^0, \partial^1, \partial^2, \partial^3) = \left(-\frac{\partial}{\partial x^0}, \boldsymbol{\nabla} \right), \tag{18.39a}$$

$$\partial_\mu \equiv \frac{\partial}{\partial x^\mu} = (\partial_0, \partial_1, \partial_2, \partial_3) = \left(\frac{\partial}{\partial x^0}, \boldsymbol{\nabla} \right), \tag{18.39b}$$

where, for example, $\partial^1 = \partial / \partial x_1$ and

$$\boldsymbol{\nabla} \equiv (\partial^1, \partial^2, \partial^3) \tag{18.40}$$

is the 3-divergence. A compact and covariant formalism then results from introducing the 4-vector potential A^μ, the 4-current J^μ, and the d'Alembertian operator $\Box$ through

$$A^\mu \equiv (\Phi, \boldsymbol{A}) = (A^0, \boldsymbol{A}) \qquad J^\mu \equiv (\rho, \boldsymbol{J}) \qquad \Box \equiv \partial_\mu \partial^\mu. \tag{18.41}$$

Thus the time-like component of the 4-vector potential A^μ is the scalar potential Φ and the spacelike components are the 3-vector potential $\boldsymbol{A}$, while the timelike component of the 4-current J^μ is the charge density ρ and the spacelike components are the 3-vector current $\boldsymbol{J}$. Then a gauge transformation takes the form

$$A^\mu \to A^\mu - \partial^\mu \chi \equiv A'^\mu \tag{18.42}$$

and the preceding examples of gauge-fixing constraints become

$$\partial_\mu A^\mu = 0 \quad \text{(Lorenz gauge)} \qquad \boldsymbol{\nabla} \cdot \boldsymbol{A} = 0 \quad \text{(Coulomb gauge)}, \tag{18.43}$$

with the notation in Eq. (18.43) indicating explicitly that

1. the *Lorenz condition is a covariant constraint* because it is formulated in terms of 4-vectors, but

2. the *Coulomb gauge condition is not covariant* because it is formulated in terms of only three of the components of a 4-vector.

The d'Alembertian operator $\Box$ is Lorentz invariant because under Lorentz transformations between coordinate systems,

$$\Box' = \partial'_\mu \partial'^\mu = \Lambda_\mu{}^\nu \Lambda^\mu{}_\lambda \partial_\nu \partial^\lambda = \partial_\mu \partial^\mu = \Box.$$

Thus, the Lorenz-gauge wave equation may be expressed in the compact and manifestly covariant form

$$\Box A^\mu = J^\mu \tag{18.44}$$

and the continuity equation (1.3) becomes becomes

$$\partial_\mu J^\mu = 0, \tag{18.45}$$

when written in covariant form.

The covariance of the Maxwell wave equation (18.44) in the Lorenz gauge, coupled with the general gauge invariance of electromagnetism, ensures that *the Maxwell equations are covariant in all gauges.*

However, as was seen in our original formulation of the Maxwell equations Eq. (1.1) and in the example of the Coulomb gauge, this covariance may not be manifest for a particular choice of notation or gauge. In Section 18.10 we shall address this issue by constructing a manifestly (Lorentz) covariant form of the Maxwell equations.

18.10 Manifestly Covariant Maxwell Equations

Maxwell's equations are covariant with respect to Lorentz transformations. However, the individual electric ($\boldsymbol{E}$) and magnetic ($\boldsymbol{B}$) fields are not invariant with respect to Lorentz transformations; as we have seen in Section18.8, they transform into one another depending on the observer's velocity. For example, a pure electric field in one frame may be seen as a combination of electric and magnetic fields in another.

The Maxwell equations may be cast in a form that is manifestly covariant by appealing to Eqs. (18.30) to construct the components of the electric and magnetic fields in terms of the potentials. Proceeding in this manner, we find that the six independent components of the 3-vectors $\boldsymbol{E}$ and $\boldsymbol{B}$ are elements of an antisymmetric rank-2 *electromagnetic field tensor* (sometimes called the *the Faraday tensor*)

$$F^{\mu\nu} = -F^{\nu\mu} = \partial^\mu A^\nu - \partial^\nu A^\mu, \tag{18.46}$$

where we take as 4-vectors [see Eqs. (18.39) and (18.41)]

$$\partial_\mu = \begin{pmatrix} \partial/\partial(ct) \\ \partial_x \\ \partial_y \\ \partial_z \end{pmatrix} \qquad A^\mu = \begin{pmatrix} \Phi/c \\ A_x \\ A_y \\ A_z \end{pmatrix} \tag{18.47}$$

Let's calculate some tensor components from Eq. (18.46):

$$\begin{aligned} F^{01} &= \partial_0 A^1 - \partial_1 A^0 \\ &= \frac{\partial A_x}{\partial(ct)} - \frac{\partial(\Phi/c)}{\partial x} = \frac{E_x}{c}, \\ F^{12} &= \partial_1 A^2 - \partial_2 A^1 \\ &= \frac{\partial A_y}{\partial x} - \frac{\partial A_x}{\partial y} = B_z, \end{aligned}$$

and so on. These results may be expressed in matrix form as the rank-2 contravariant tensor[8]

$$F^{\mu\nu} = \begin{pmatrix} 0 & E_x/c & E_y/c & E_z/c \\ -E_x/c & 0 & B_z & -B_y \\ -E_y/c & -B_z & 0 & B_x \\ -E_z/c & B_y & -B_x & 0 \end{pmatrix}, \tag{18.48}$$

which can be converted into covariant form by contraction with the metric tensor,

$$F_{\mu\nu} = \eta_{\mu\alpha}\eta_{\nu\beta}F^{\alpha\beta} = \begin{pmatrix} 0 & E_x/c & E_y/c & E_z/c \\ -E_x/c & 0 & -B_z & B_y \\ -E_y/c & B_z & 0 & -B_x \\ -E_z/c & -B_y & B_x & 0 \end{pmatrix}. \tag{18.49}$$

We see that the electric field $\boldsymbol{E}$ and the magnetic field $\boldsymbol{B}$ are *vectors* in three-dimensional euclidean space, but in Minkowski space their six components together form an antisymmetric *rank-2 tensor*. Now let us employ the *completely antisymmetric tensor* (*Levi–Civita* symbol) $\epsilon_{\alpha\beta\gamma\delta}$, which

- has the value $+1$ for $\alpha\beta\gamma\delta = 0123$ and cyclic permutations,
- has the value -1 for odd permutations of the indices, and
- has the value 0 if any two indices are equal,
- and satisfies $\epsilon_{\alpha\beta\gamma\delta} = -\epsilon^{\alpha\beta\gamma\delta}$.

[8] We are using in Eq. (18.48) the "mostly plus" ("East Coast") metric signature diag $(-+++)$. There are switches in signs of some terms if one employs instead the "mostly minus" ("West Coast") metric signature diag $(+---)$. The different metric conventions lead to equivalent results if employed consistently, but can lead to confusion of signs if the conventions are mixed. The Faraday tensor and the dual tensor (18.49) written in both metrics, in both covariant and contravariant forms, may be found Appendix C. It is also common to use $c = 1$ units for these tensors, in which case the factors of $1/c$ multiplying the components of $\boldsymbol{E}$ would be dropped.

Then the *dual field tensor* in contravariant form $\star F^{\mu\nu}$ may be defined by[9]

$$\star F^{\mu\nu} = \tfrac{1}{2}\epsilon^{\mu\nu\gamma\delta}F_{\gamma\delta} = \begin{pmatrix} 0 & B_x & B_y & B_z \\ -B_x & 0 & -E_z/c & E_y/c \\ -B_y & E_z/c & 0 & -E_x/c \\ -B_z & -E_y/c & E_x/c & 0 \end{pmatrix}, \tag{18.50}$$

and the covariant form of the dual tensor is obtained by contracting with the metric tensor to give

$$\star F_{\mu\nu} = \begin{pmatrix} 0 & -B_x & -B_y & -B_z \\ B_x & 0 & -E_z/c & E_y/c \\ B_y & E_z/c & 0 & -E_x/c \\ B_z & -E_y/c & E_x/c & 0 \end{pmatrix}. \tag{18.51}$$

We see that the field strength tensor $F^{\mu\nu}$ and the dual field strength tensor $\star F^{\mu\nu}$ are related by the substitutions $\boldsymbol{E} \to c\boldsymbol{B}$ and $\boldsymbol{B} \to -\boldsymbol{E}/c$ into $F^{\mu\nu}$.

Then using the Faraday tensor and the duel tensor, the two Maxwell equations (18.29a) and (18.29d) may be expressed as a single concise equation,

$$\left.\begin{aligned} \boldsymbol{\nabla}\cdot\boldsymbol{E} &= \rho \\ \boldsymbol{\nabla}\times\boldsymbol{B} - \frac{\partial \boldsymbol{E}}{\partial t} &= \boldsymbol{J} \end{aligned}\right\} \quad \longrightarrow \quad \partial_\mu F^{\mu\nu} = J^\nu, \tag{18.52}$$

and the two Maxwell equations (18.29b) and (18.29c) may be expressed as a second concise equation.

$$\left.\begin{aligned} \frac{\partial \boldsymbol{B}}{\partial t} + \boldsymbol{\nabla}\times\boldsymbol{E} &= 0 \\ \boldsymbol{\nabla}\cdot\boldsymbol{B} &= 0 \end{aligned}\right\} \quad \longrightarrow \quad \partial_\mu \star F^{\mu\nu} = 0. \tag{18.53}$$

The Maxwell equations in this form are now *manifestly covariant* because they are formulated exclusively in terms of Lorentz tensors. We shall have more to say about the *exterior calculus* (differential forms and exterior derivatives) that leads to these results in Section 19.4.4 and Appendix D.

Writing the Maxwell equations in the Lorentz covariant form (18.52) and (18.53) has a number of advantages.

1. We have now shown that the Maxwell equations are in fact covariant under Lorentz transformations and thus completely consistent with the special theory of relativity.
2. The antisymmetry of $F^{\mu\nu}$ implied by the definition (18.46) guarantees that the Faraday tensor (and thus Maxwell electromagnetism) is *gauge invariant*, since a gauge transformation $A^\mu \to A^\mu - \partial^\mu\chi$ on the 4-vector potential A^μ implies that

$$F^{\mu\nu} \to F^{\mu\nu} + \partial^\mu\partial^\nu\chi - \partial^\nu\partial^\mu\chi = F^{\mu\nu}, \tag{18.54}$$

where the last step follows because partial derivatives commute.

[9] The dual tensor is also denoted $\tilde{F}^{\mu\nu}$ in the physics literature; the Hodge star notation $\star F$ is explained in Appendix D.

3. The Maxwell equations manifestly *conserve current:* first $\partial_\mu \partial_\nu F^{\mu\nu} = 0$ because $\partial_\mu \partial_\nu$ is symmetric and $F^{\mu\nu}$ is antisymmetric, and a contraction of a symmetric tensor with an antisymmetric one is identically zero. Then taking the partial derivative of both sides of Eq. (18.52) gives $\partial_\nu \partial_\mu F^{\mu\nu} = 0 = \partial_\nu J^\nu$, which is the continuity equation $\partial_\mu J^\mu = 0$ in our 4-vector notation.
4. Utilizing that $F^{\mu\nu} = -F^{\nu\mu} = \partial^\mu A^\nu - \partial^\nu A^\mu$ and Eq. (18.50), we obtain

$$\partial_\mu \star F^{\mu\nu} = \frac{1}{2}\epsilon^{\mu\nu\gamma\delta}\partial_\mu F_{\gamma\delta} = \frac{1}{2}\epsilon^{\mu\nu\gamma\delta}\partial_\mu(\partial_\gamma A_\delta - \partial_\delta A_\gamma) = 0,$$

where the equivalence to zero follows because the product of two derivatives ($\partial_\mu\partial_\gamma$ or $\partial_\mu\partial_\delta$) is symmetric, but $\epsilon^{\mu\nu\gamma\delta}$ is antisymmetric (it *is* the completely antisymmetric rank-4 tensor, after all). Thus we have shown that Eq. (18.53) is *satisfied identically*, and solution of the Maxwell equations reduces effectively to solving the single equation (18.52): $\partial_\mu F^{\mu\nu} = J^\nu$.

> We have succeeded in reducing the 20 equations that Maxwell needed in the first statement of his eponymous equations down to 4 equations by the introduction of vector calculus (Heaviside), and then to 2 (which is actually only one because one is satisfied identically), using the properties of spacetime tensors. A pretty nice day's work!

The field tensor $F^{\mu\nu}$ expresses the complete physics of the Maxwell equations in covariant form. Therefore, it is useful to consider applying Lorentz transformations directly to the field tensor.

18.11 Lorentz Transformations on the Field Tensor

We have now shown that the Maxwell equations can be derived from the antisymmetric rank-2 tensor $F^{\mu\nu}$. We may thus invoke Lorentz transformations directly on that tensor. The Lorentz transformations are induced by the 4×4 matrices ${\Lambda^\mu}_\nu$ in Eq. (18.12). There are six Lorentz generators, three corresponding to rotations within an inertial frame and three corresponding to boosts between inertial frames. If we restrict boosts to the x-axis, these have the schematic structure illustrated in Eq. (18.55).[10]

$$\underbrace{{\Lambda^\mu}_\nu = \left(\begin{array}{c|ccc} 1 & 0 & 0 & 0 \\ \hline 0 & & & \\ 0 & & R & \\ 0 & & & \end{array}\right)}_{\text{(a) Rotations}} \qquad \underbrace{{\Lambda^\mu}_\nu = \left(\begin{array}{cc|cc} \gamma & -\gamma v/c & 0 & 0 \\ -\gamma v/c & \gamma & 0 & 0 \\ \hline 0 & 0 & 1 & 0 \\ 0 & 0 & 0 & 1 \end{array}\right)}_{\text{(b) Boosts}} \tag{18.55}$$

[10] We adopt a fairly standard convention that in a matrix layout for 2-index quantities, the leftmost index is the row index and the rightmost is the column index, irrespective of whether the indices are arrayed ${A^\mu}_\nu$, $A^{\mu\nu}$, or $A_{\mu\nu}$. In all three of these cases we take μ to be the row index and ν to be the column index.

The rotations are implemented in the three spacelike coordinates by a normal 3D rotation matrix R in the matrix 18.55(a). For boosts along the x-axis the transformation is implemented by a boost matrix 18.55(b), with the upper left quadrant corresponding to the 2×2 matrix worked out in Eq. (18.25),

$$\begin{pmatrix} ct' \\ x' \end{pmatrix} = \gamma \begin{pmatrix} 1 & -\beta \\ -\beta & 1 \end{pmatrix} \begin{pmatrix} ct \\ x \end{pmatrix} = \begin{pmatrix} \gamma & -\gamma v/c \\ -\gamma v/c & \gamma \end{pmatrix} \begin{pmatrix} ct \\ x \end{pmatrix},$$

where $\beta \equiv v/c$. Generally a Lorentz transformation on the Faraday tensor will take the form

$$F'^{\mu\nu} = \Lambda^{\mu}{}_{\alpha} \Lambda^{\nu}{}_{\beta} F^{\alpha\beta}. \tag{18.56}$$

The rotations within the inertial frame implemented by R will clearly transform the electric and magnetic fields like

$$\boldsymbol{E}' = R\boldsymbol{E} \qquad \boldsymbol{B}' = R\boldsymbol{B}, \tag{18.57}$$

as would be expected for rotation of 3-vectors. For the x-axis boosts, we can deduce the transformed components from Eq. (18.48) and 18.55(b), as illustrated in Example 18.5.

Example 18.5 Lets calculate the effect of a boost along the x axis on the Faraday tensor. From Eq. (18.56), the boosted tensor will take the form

$$F'^{\mu\nu} = \Lambda^{\mu}{}_{\alpha} \Lambda^{\nu}{}_{\beta} F^{\alpha\beta}.$$

and from Eq. (18.48) the rest-frame Faraday tensor is

$$F^{\mu\nu} = \begin{pmatrix} F^{00} & F^{01} & F^{02} & F^{03} \\ F^{10} & F^{11} & F^{12} & F^{13} \\ F^{20} & F^{21} & F^{22} & F^{23} \\ F^{30} & F^{31} & F^{32} & F^{33} \end{pmatrix} = \begin{pmatrix} 0 & E_x/c & E_y/c & E_z/c \\ -E_x/c & 0 & B_z & -B_y \\ -E_y/c & -B_z & 0 & B_x \\ -E_z/c & B_y & -B_x & 0 \end{pmatrix},$$

and the components of $\Lambda^{\mu}{}_{\nu}$ are given in Eq. (18.55). The boosted electric field component E_x is given by

$$\begin{aligned} \frac{E'_x}{c} &= F'^{01} = \Lambda^0{}_{\alpha} \Lambda^1{}_{\beta} F^{\alpha\beta} \\ &= \Lambda^0{}_0 \Lambda^1{}_1 F^{01} + \Lambda^0{}_1 \Lambda^1{}_0 F^{10} \\ &= \gamma^2 \frac{E_x}{c} - \frac{\gamma^2 v^2}{c^2} \frac{E_x}{c} = \frac{E_x}{c} \end{aligned}$$

where $\gamma = (1 - v^2/c^2)^{1/2}$ was used. Thus, $E'_x = E_x$. Likewise, the boosted magnetic field component B'_z is given by

$$\begin{aligned} B_z = F'^{12} &= \Lambda^1{}_\alpha \Lambda^2{}_\beta F^{\alpha\beta} \\ &= \Lambda^1{}_0 \Lambda^2{}_2 F^{02} + \Lambda^1{}_1 \Lambda^2{}_2 F^{12} \\ &= -\frac{\gamma v}{c^2} E_y + \gamma B_z \\ &= \gamma \left(B_z - \frac{v}{c^2} E_y \right). \end{aligned}$$

By such evaluations one finds that the boosted electric and magnetic field components are

$$\begin{aligned} E'_x = E_x \qquad E'_y = \gamma(E_y - vB_z) \qquad E'_z = \gamma(E_z + vB_y) \\ B'_x = B_x \qquad B'_y = \gamma \left(B_y + \frac{v}{c^2} E_z \right) \qquad B'_z = \gamma \left(B_z - \frac{v}{c^2} E_y \right). \end{aligned}$$

Thus we see clearly that the Lorentz boost mixes electric and magnetic fields in a similar manner as it mixes space and time.

18.12 Covariance and the Lorentz Force Law

We have shown that the Maxwell equations can be written in a manifestly Lorentz covariant form, but we also need to check that the Lorentz force law is consistent with special relativity, since it separate and not implied by the Maxwell equations.

The remainder of this section is under construction.

Background and Further Reading

Portions of this chapter have adapted from Refs. [36, 38]. For an introduction to special relativity, see Kogut [45]. Special and general relativity are introduced at an accessible level in Guidry [36]. The use of linearized gravity in describing gravitational waves far from strong sources, and the similarity of the linearized Einstein equations to the Maxwell equations, is discussed in Ch. 22 of Ref. [36].

Problems

18.1 The primed axes (x', t') plotted in the coordinate system of the unprimed axes in Fig. 18.6 do not appear to be orthogonal, but they must be since the unprimed axes are orthogonal (their scalar product vanishes) and the scalar product is preserved under Lorentz transformations. Show generally that two vectors in a spacetime diagram are orthogonal if each makes the same angle with respect to the lightcone. Show that this proves that a lightlike vector is necessarily orthogonal to itself. ***

18.2 If a Lorentz transformation matrix is denoted by $\Lambda^{\mu}{}_{\nu}$, prove that the Lorentz transformation given by $\Lambda_{\mu}{}^{\nu} = \eta_{\mu\alpha}\eta^{\nu\beta}\Lambda^{\alpha}{}_{\beta}$ is its inverse.

18.3 (a) Prove that the Maxwell field tensor $F^{\mu\nu}$ is invariant under a gauge transformation of the 4-vector potential A^{μ}. (b) By appealing to the definitions (18.30), demonstrate that the Maxwell field tensor $F^{\mu\nu}$ has components given by Eqs. (18.46) and (18.48).

18.4 Show that the Maxwell equations written in the covariant form (18.52) and (18.53) are equivalent to the non-covariant form of the Maxwell equations given by Eqs. (18.29a)–(18.29d).

18.5 Two events in Minkowski space have a timelike separation. Use the invariance of the interval ds^2 to show that the time between the events as measured by any inertial observer is always greater than or equal to the proper time between the events. ***

18.6 Consider the system from Problem 10.2 in a laboratory frame $\mathcal{O}$, where the center of the spherical shell rests at the origin. An observer in frame $\mathcal{O}'$ moves with a constant relativistic velocity $\boldsymbol{v} = v\hat{\boldsymbol{x}}$ relative to the shell.

a. Construct the covariant Faraday tensor $F^{\mu\nu}$ of Eq. (18.48) for the region inside the shell in the laboratory frame $\mathcal{O}$.

b. Apply a Lorentz transformation to determine the Faraday tensor $F'^{\mu\nu}$ in the moving frame $\mathcal{O}'$.

c. Extract the physical electric and magnetic fields ($\boldsymbol{E}'$ and $\boldsymbol{B}'$) observed inside the shell by the moving observer. Express these entirely in terms of the spacetime coordinates (ct', x', y', z') for the moving observer.

Discuss briefly the physical origin of the spatial dependence in the phase of the transformed fields.

18.7 Notice that in Fig. 18.8 the electric field is compressed in the direction of motion by Lorentz length contraction, but the electric field lines remain straight with origin at the location of the charge for all values of $\beta = v/c$. Rationalize this behavior by examining how the components of $F^{\mu\nu}$ behave under a Lorentz boost. *Hint*: It is useful to decompose the $\boldsymbol{E}$ and $\boldsymbol{B}$ fields into components parallel to the x axis and transverse to the x axis for this discussion.

18.8 Imagine a lab frame $\mathcal{S}$ where an observer sees a static electric field pointing in the

y direction, and no magnetic field,

$$E = (E_x, E_y, E_z) = (0, E_0, 0) \qquad B = (B_x, B_y, B_z) = (0, 0, 0).$$

Now consider a moving frame $\mathcal{S}'$ traveling in the positive x direction relative to $\mathcal{S}$ with speed v. Find the electric and magnetic fields seen by an observer in $\mathcal{S}'$ and discuss the physical implications *Hint*: It is useful to decompose the $\boldsymbol{E}$ and $\boldsymbol{B}$ fields into components parallel to the x axis and transverse to the x axis (y and z directions) for this discussion.

Numerical and GenAI Problems

19 Geometry and Topology in Electromagnetism

This section is under construction.

19.1 A Brief Introduction to Topology

19.2 Differential Forms

19.3 Fiber Bundles

19.4 Topological Aspects of Electromagnetism

It is a profound conceptual journey from the intuitive geometry of "boundaries" in electromagnetic problems to the high-level abstraction of differential forms applied to the same physics, but there is considerable reward in the effort. Let's now consider some important geometrical and topological aspects of electromagnetism, expressed in the language of algebraic topology and differential geometry. This discussion will assume a familiarity with the concepts that are outlined in Appendix D.

19.4.1 The Boundary Operator

A k-dimensional geometrical object (like a line, surface, or volume) is termed a *k-chain* or just *chain* for brevity, with a chain being a combination of geometrical shapes that are called *simplices*.[1] The boundary operator, denoted by ∂, maps a k-dimensional object to its $(k-1)$-dimensional boundary. For example, a 3D closed manifold has a boundary that is a 2D manifold.

19.4.2 The Boundary of a Boundary

The concept that "the boundary of a boundary is zero" is a foundational principle of algebraic topology and differential geometry that provides the geometric scaffolding for much

[1] A simplex (plural: simplices) is a simple shape such as a point or a triangle.

of modern physics, particularly electromagnetism. The topological framework called *homology* is described in Box 19.1. The fundamental identity of *homology* is:

$$\partial^2 = \partial(\partial c) = 0, \tag{19.1}$$

for any chain c, which may be abbreviated as $\partial^2 = 0$ (where zero generally means the empty set $\emptyset$).

In words, *the boundary of any object has no boundary of its own.* Essentially, this is because it is impossible for an object to satisfy the requirements of boundryhood if it has a boundary itself.

Let us illustrate these ideas with a simple example.

Example 19.1 Consider a solid 3D ball (filled sphere) B^3, which is a *3-chain*. The boundary of the solid ball is the 2-sphere (the surface shell): $\partial B^3 = S^2$. Now, take the boundary of that surface shell S^2. A sphere is a closed surface, with no edges or endpoints. Therefore: $\partial S^2 = \partial(\partial B^3) = \emptyset$, demonstrating that the boundary of the boundary for a 3-ball is equal to the null set $\emptyset$.

Duals and Duality: Mathematically, a *duality* links two objects that "pair" according to some prescription to produce a scalar. For example, the scalar product of a dual vector with a vector yields a (scalar) number, and one says that dual vectors and vectors are dual to each other, or that they are related by a duality (see Section 17.3.6).

Let us now introduce an object that is dual to the boundary operator ∂.

19.4.3 The Exterior Derivative and Duality

The *exterior derivative* d is the "functional" version of the boundary operator ∂. While ∂ acts on regions of space, d acts on the differential forms (fields) living on those regions. In the language of differential forms, the geometric boundary operator ∂ has a *functional dual:* the exterior derivative d. While ∂ decreases dimensionality, d increases the "degree" of a form.[2] For any differential form ω the property $\partial^2 = 0$ translates directly to

$$d(d\omega) = d^2\omega = 0, \tag{19.2}$$

which is the formal expression of two fundamental vector calculus identities,

[2] In the present context this is termed a *functional duality* because the exterior derivative d is the functional version of the boundary operator: while ∂ operates on the regions of space that we integrate over (domains), d acts on the differential forms (functions, integrands) that live on those regions of space. Thus a functional maps a function to a number, with integration providing the linkage.

Box 19.1 Homology and Cohomology

Homology is a theoretical framework for assigning a sequence of algebraic objects to a topological space that provide a quantitative distinction between spaces by measuring their topological invariants, in particular their "holes". Homology can be abstract, but the underlying idea is simple.

The Basic Idea: Count the Holes

Homology classifies the topological structure of a space by counting its independent, non-deformable holes across different dimensions. The ranks of these homology groups are known as the *Betti numbers* (b_k). For example,

1. *0-dimensional homology* (H_0): Measures the number of connected components. The Betti number b_0 is the number of disconnected parts.
2. *1-dimensional homology* (H_1): Measures the number of 1D, cylindrical holes or "tunnels." *Example:* For a closed loop, $b_1 = 1$; for a figure-eight, $b_1 = 2$.
3. *2-dimensional homology* (H_2): Measures the number of 2D voids or spherical cavities. *Example:* For a hollow sphere, $b_2 = 1$.

Cycles, Boundaries, and Homology Groups

The algebraic concepts of *chains*, *cycles*, and *boundaries* are used to calculate the topological invariants, as described in the text. Briefly,

1. A k-chain C_k is a linear combination of k-dimensional simple shapes that make up the space.
2. The boundary operator ∂ is a linear map taking a k-chain to its $k-1$-dimensional boundary; fundamentally, *a boundary of a boundary is zero*.
3. A cycle Z_k is a k-chain that has no boundary.
4. A k-chain is a boundary B_k if it bounds a $(k-1)$-dimensional chain.

A homology group is the quotient group of cycles modulo boundaries: in group theory language, $H_k = Z_k/B_k$. This means that a homology class represents a closed loop (cycle) that isn't the boundary of any higher-dimensional surface.

The Deep Relationship to Modern Physics

Through *de Rham cohomology*,[a] these topological concepts map onto the exterior calculus. This accounts for why Maxwell's equations may be expressed concisely in terms of closed and exact forms, for the Dirac monopole, and for why the Aharonov–Bohm effect can be viewed as a topological hole in the underlying space of fields.

[a] *Cohomology* is algebraically dual to homology. If homology is the study of geometric spaces (curves, surfaces, ...), cohomology is the study of the things being integrated (forms and fields) on those spaces. Due this duality, cohomology is often more useful in physics than homology. Experiments can't measure a topological hole in a space (domain of homology) but they can measure the fields and potentials in that space (domain of cohomology).

Table 19.1 Summary of generalized Stokes' theorem relationships

Physical concept	Mathematical object	Generalized Stokes' Theorem role
Flux	Integral of form ω over $\partial\Omega$	"Boundary" side of equation
Conserved charge	Integral of $d\omega$ over Ω	"Volume" side of equation
Conservation law	$d\omega = 0$ (closed form)	Ensures charge is constant
Continuity	$dJ = -\dot{\rho}$	Relates change in charge to flux

- The *curl of a gradient is zero:* $\boldsymbol{\nabla} \times \boldsymbol{\nabla}\phi = 0$.
- The divergence of a curl is zero: $\boldsymbol{\nabla} \cdot (\boldsymbol{\nabla} \times \mathbf{A}) = 0$.

Thus the boundary operator and the exterior derivative are both *nilpotent*, meaning that they vanish when raised to some positive integer power. The *exterior derivative* is the differential geometry version of the boundary operator, acting on the *forms* (fields) rather than the manifolds (shapes). The relationship between the boundary operator and the exterior derivative is encapsulated succintly in the *Generalized Stokes' Theorem* (see Box D.1), which takes the compact form

$$\int_{\Omega} d\omega = \int_{\partial\Omega} \omega, \tag{19.3}$$

in the present abstract notation. In words, this identity states that the integral of a derivative over a domain Ω is equal to the integral of the form itself over the boundary $\partial\Omega$ of that domain. This equation shows that the derivative d shifting "up" in dimension on the integrand is perfectly balanced by the boundary operator ∂ shifting "down" in dimension on the domain. Because $\partial^2 = 0$, it follows by duality that the exterior derivative of a derivative is zero: $d^2 = d \circ d = 0$. Thus d and ∂ are adjoints: moving d from the integrand to the boundary transforms it into ∂. The relationships of quantities entering into the generalized Stokes' theorem are illustrated in Table 19.1. The duality of the boundary operator and the exterior derivative imply that just as "a boundary of a boundary is zero" ($\partial^2 = 0$), so too "a change of a change is zero" ($d^2 = 0$).

> If Eq. (19.3) is applied to a boundary (where $\Omega = \partial\Sigma$), the right side involves $\partial(\partial\Sigma)$, which is zero. Formally, it is this consistency that allows the definition of conserved charges and fluxes in physics.

With this as general background, let us now translate the four vacuum Maxwell's equations of Eq. (1.1) into the language of differential forms.

19.4.4 Maxwell's Equations Using Exterior Calculus

Differential forms and the exterior calculus allow us to express the Maxwell equations very concisely. The four Maxwell equations written in vector calculus notation contract into two rather elegant statements when expressed in differential forms notation. We

represent the electric and magnetic fields using a 2-form F called the *Faraday tensor* and a *source 3-form* J representing charge density and current.

Inhomogeneous Maxwell Equations: Gauss's Law for Magnetism ($\boldsymbol{\nabla} \cdot \boldsymbol{B} = 0$) and Faraday's Law ($\boldsymbol{\nabla} \times \boldsymbol{E} = -\partial \boldsymbol{B}/\partial t$) are combined into the single compact equation

$$dF = 0 \qquad \text{(Source-free Maxwell equations).} \tag{19.4}$$

This equation is sometimes called the *Bianchi identity*. Because $d^2 = 0$, Eq. (19.4) implies that F can be written locally as the derivative of a *potential 1-form* A; that is $F = dA$.

Homogeneous Maxwell Equations: To include charges and currents, we use the Hodge star operator ($\star$), which is essential because it accounts for the geometry of the vacuum (the metric). The Hodge star performs a duality transformation, roughly swapping "flux" for "circulation" by mapping a k-form to an $(n-k)$-form in n-dimensional space. In 4D Minkowski spacetime with metric signature $(-+++)$, the Hodge star exchanges spacetime components like so,

$$\star(dt \wedge dx) = dy \wedge dz \qquad \star(dx \wedge dy) = dt \wedge dz. \tag{19.5}$$

Then in the Maxwell equations,

1. the *Faraday tensor* F is a 2-form representing $\boldsymbol{E}$ and $\boldsymbol{B}$, and
2. $\star F$ is the "dual" 2-form, which essentially swaps the roles of **E** and **B** (with some sign changes) to allow the derivative d to act as a divergence-like operator.

The Gauss Law for Electricity ($\boldsymbol{\nabla} \cdot \boldsymbol{D} = \rho$) and the Ampère–Maxwell Law ($\boldsymbol{\nabla} \times \boldsymbol{H} - \partial \boldsymbol{D}/\partial t = \boldsymbol{J}$) then take the concise form

$$d\star F = J \qquad \text{(Sourced Maxwell equations),} \tag{19.6}$$

where J is the source 3-form and F is again the Faraday tensor. The Maxwell equations expressed as differential forms and the vector calculus equivalents are illustrated in Table 19.2.

By applying d to the with-sources equation $d\star F = J$, we get $d(d\star F) = dJ$. Since $d^2 = 0$, this yields immediately,

$$dJ = 0. \tag{19.7}$$

This is the continuity equation (1.3), expressed as the exterior derivative of a 3-form source J. Thus we have proved that local conservation of charge is a direct mathematical consequence of the principle that "a boundary of a boundary is zero".

Example 19.2 Defining the Faraday 2-form F in the $(-+++)$ Minkowski signature:

$$F = E_i dx^i \wedge dt + B_x dy \wedge dz + B_y dz \wedge dx + B_z dx \wedge dy. \tag{19.8}$$

Table 19.2 Maxwell equations in forms and in vector notation

Maxwell equations	Differential forms	Vector calculus equivalent
Source-free	$dF = 0$	$\boldsymbol{\nabla} \cdot \boldsymbol{B} = 0$ and $\boldsymbol{\nabla} \times \boldsymbol{E} = -\dfrac{\partial \boldsymbol{B}}{\partial t}$
With sources	$d\star F = J$	$\boldsymbol{\nabla} \cdot \boldsymbol{D} = \rho$ and $\boldsymbol{\nabla} \times \boldsymbol{H} - \dfrac{\partial \boldsymbol{D}}{\partial t} = \boldsymbol{J}$

The component of dF containing only spatial differentials (dx, dy, dz) is:

$$dF_{\text{spatial}} = \left(\frac{\partial B_x}{\partial x} + \frac{\partial B_y}{\partial y} + \frac{\partial B_z}{\partial z} \right) dx \wedge dy \wedge dz.$$

Since $dF = 0$, from Eq. (19.4) the coefficient must vanish, yielding $\boldsymbol{\nabla} \cdot \boldsymbol{B} = 0$, which is Gauss's magnetic law (6.50c) in vector calculus notation.

19.4.5 Conserved Charges and Fluxes

In physics, the Generalized Stokes' Theorem is the mathematical bridge that allows us to equate a local field property (like a charge density) with a global measurement (like the flux through a surface). It effectively states that the "stuff" inside a region is equal to the "flow" across the boundary of that region. Let us show how conservation laws arise by deriving the conservation of electrical current using the exterior calculus developed above.

Example 19.3 The inhomogeneous Maxwell equations in the language of differential forms are given by

$$d(\star F) = \mu_0 J,$$

where F is the Faraday 2-form and J is the source 3-form. By taking the exterior derivative of both sides and invoking the identity $d^2 \equiv 0$, we find:

$$d(d(*F)) = \mu_0 dJ \implies dJ = 0.$$

Applying the Generalized Stokes' Theorem over a four-dimensional manifold $\mathcal{M}$,

$$\int_{\mathcal{M}} dJ = \int_{\partial \mathcal{M}} J = 0,$$

which demonstrates that the conservation of the electromagnetic current is a direct consequence of the topological structure of the gauge fields.

19.4.6 The Exterior Calculus

Exterior calculus is the natural mathematical language for extending multivariable calculus to smooth manifolds.[3] It connects differential geometry, algebraic topology, and modern theoretical physics by subsuming concepts of vector calculus such as the divergence, gradient, and curl into a single, *coordinate-independent* framework. More mathematically, it provides a link between the continuous shape of a space (typically a smooth manifold, for our purposes) and the algebraic tools that may be used to analyze it.

Differential Forms: *Standard vector calculus* on the manifold $\mathbb{R}^3$ works primarily with scalar functions and vector fields. *Exterior calculus* replaces these with completely antisymmetric covariant tensors that are called *differential forms:*

1. *0-forms,* which are scalar functions like $f(x, y, z)$.
2. *1-forms,* which are dual vector fields that can be thought of geometrically as sets of parallel surfaces that a vector pierces.
3. *2-forms,* which are antisymmetric rank-2 tensors, corresponding geometrically to flux through a surface.
4. k*-forms,* which are fields designed to be integrated over k-dimensional submanifolds.

Algebraic Operations: Exterior calculus relies on operations that manipulate forms without the need of a specific coordinate system.

1. *The Wedge Product ($\wedge$):* The algebraic building block used to construct higher-degree forms from lower-degree ones. It is completely antisymmetric. For a k-form α and an l-form β, the wedge product satisfies $\alpha \wedge \beta = (-1)^{kl} \beta \wedge \alpha$. This implied antisymmetry encodes the geometric concept of oriented volumes and areas naturally.
2. *The Exterior Derivative (d):* The single differential operator of exterior calculus. It maps k-forms to $(k+1)$-forms, and has the fundamental property that applying the exterior derivative twice always yields zero: $d^2 = 0$ This simple nilpotency rule ($d(d\omega) = 0$) encapsulates the vector calculus facts that the curl of a gradient and the divergence of a curl are both zero.
3. *The Hodge Star ($\star$):* The wedge product and the exterior derivative are purely topological (they require no concept of distance), but the Hodge star operator introduces geometry because it requires a metric tensor to map k-forms to $(n-k)$-forms, which represent orthogonal complements.

Generalized Stokes' Theorem: The crowning achievement of exterior calculus is the

[3] The exterior calculus rests on the foundation of *Grassmann algebra*, developed by Hermann Grassmann (1809-1867). Basically, exterior calculus results from applying Grassmann algebra to every point of a smooth manifold, and then introducing the analytic concepts of differentiation and integration, which was largely associated with Élie Cartan (1869-1951). Grassmann introduced the wedge product (sometimes called the exterior product) of Eq. (D.1), and the addition of the exterior derivative, integration, and the Hodge star operator led to the present exterior calculus.

Generalized Stokes' Theorem, which subsumes the classical theorems of Green, Gauss, and Stokes into one elegant equation,

$$\int_{\partial M} \omega = \int_M d\omega,$$

where M is an oriented manifold, ∂M is its boundary, ω is a differential form, and $d\omega$ is its exterior derivative.

The Connection to Algebraic Topology: In algebraic topology, exterior calculus provides the foundation for *de Rham Cohomology*.

1. Because $d^2 = 0$, any form ω that is exact ($\omega = d\alpha$ for some α) must also be closed ($d\omega = 0$).
2. However, not all closed forms are exact; this depends on the global "holes" in the manifold.
3. De Rham cohomology measures exactly this discrepancy.

Therefore, De Rham cohomology provides a way to extract the global topological invariants of a manifold, purely by solving linear differential equations (finding closed forms modulo exact forms) locally.

> The mathematical statement $d^2 = 0$ is the direct dual to the geometric boundary operator property $\partial^2 = 0$ (the boundary of a boundary is zero).

The Connection to Differential Geometry and Physics: *Exterior calculus is coordinate-free,* making it an optimal framework for differential geometry. In classical electromagnetism, the traditional vector calculus approach is elegantly subsumed by the exterior calculus.

1. The rank-2 electromagnetic tensor is simply a 2-form F.
2. Maxwell's four equations shed their complex coordinate dependencies in vector calculus representation and reduce to two profoundly simple geometric statements under exterior calculus:

$$dF = 0 \qquad d\star F = \star J \tag{19.9}$$

   where J is the 1-form source current.

The first equation, $dF = 0$, is *purely topological* because the exterior derivative is independent of the metric; it encodes both Gauss's magnetic law (absence of magnetic monopoles) and Faraday's law of induction. The second equation, $d\star F = \star J$, *depends on the spacetime metric* because of the Hodge star operator and encodes Gauss's (electric) law and the Ampère–Maxwell law. Box 19.2 summarizes the exterior calculus for electromagnetism.

Although it is not our focus here, in modern general relativity and abelian and nonabelian gauge theories exterior derivatives and connection 1-forms are used to describe

curvature, symmetry, and broken symmetry in an elegant and concise manner. Thus the exterior calculus provides a unified mathematical framework for classical electromagnetism, gauge field theories, and general relativity.

Example 19.4 illustrates taking the exterior derivative of a product.

Example 19.4 Let's compute the exterior derivative of the 1-form $A = A_\mu dx^\mu$. Taking the exterior derivative of both sides yields

$$dA = d(A_\mu dx^\mu).$$

For a p-form ω and q-form η, the exterior derivative is given by

$$d(\omega \wedge \eta) = d\omega \wedge \eta + (-1)^p \, \omega \wedge d\eta.$$

From the expression $A = A_\mu dx^\mu$, we have that A is a 1-form and A_μ is a scalar (0-form), so $p = 0$ and dx^μ is a 1-form. Thus, setting $\omega = A_\mu$ and $\eta = dx^\mu$, the product is

$$\begin{aligned} dA = d(A_\mu dx^\mu) &= dA_\mu \wedge dx^\mu + (-1)^0 A_\mu \wedge d(dx^\mu) \\ &= dA_\mu \wedge dx^\mu + A_\mu d(dx^\mu), \end{aligned}$$

where we have used in the second step that A_μ is a 0-form so $A_\mu \wedge d(dx^\mu) = A_\mu d(dx^\mu)$. Now the exterior derivative obeys the fundamental rule that applying it twice gives zero: $d^2 = 0$, but dx^μ is the exterior derivative of the coordinate x^μ so $d(dx^\mu) = d(d(x^\mu)) = 0$ and we are left with

$$dA = dA_\mu \wedge dx^\mu.$$

Now dA_μ is the exterior derivative of a zero-form (scalar) function, which is just the gradient, so using the chain rule we can write

$$dA_\mu = \frac{\partial A_\mu}{\partial x^\nu} \, dx^\nu = \partial_\nu A_\mu dx^\nu,$$

and substituting this back in the expression for dA,

$$dA = (\partial_\nu A_\mu dx^\nu) \wedge dx^\mu = \partial_\nu A_\mu dx^\nu \wedge dx^\mu.$$

This is the correct answer, but it is standard practice in differential geometry and physics to express the answer using explicitly antisymmetric coefficients. Therefore, let us write the answer above as

$$\begin{aligned} dA &= \frac{1}{2}\partial_\nu A_\mu dx^\nu \wedge dx^\mu + \frac{1}{2}\partial_\nu A_\mu dx^\nu \wedge dx^\mu \\ &= \frac{1}{2}\partial_\nu A_\mu dx^\nu \wedge dx^\mu + \frac{1}{2}\partial_\mu A_\nu dx^\mu \wedge dx^\nu \\ &= \frac{1}{2}\partial_\nu A_\mu dx^\nu \wedge dx^\mu - \frac{1}{2}\partial_\mu A_\nu dx^\nu \wedge dx^\mu \\ &= \frac{1}{2}\left(\partial_\nu A_\mu - \partial_\mu A_\nu\right) dx^\nu \wedge dx^\mu, \end{aligned}$$

Box 19.2 **Exterior Calculus and Electromagnetism**

In algebraic topology and differential geometry, *exterior calculus* is a framework that provides a coordinate-free way to differentiate and integrate on manifolds. It is essentially the calculus of differential forms. While standard vector calculus (gradient, curl, divergence) is often tied to the specific Euclidean geometry of 3D space, exterior calculus generalizes these concepts to any dimension and any shape. Exterior calculus is often preferred over standard calculus for advanced topics because it simplifies complex relationships in a single, consistent language.

Fundamental Operators

- *Wedge Product ($\wedge$):* k-form $\wedge$ l-form $\to (k+l)$-form.

$$\alpha \wedge \beta = (-1)^{kl}(\beta \wedge \alpha)$$

- *Exterior Derivative (d):* k-form $\to (k+1)$-form.

$$d(\alpha \wedge \beta) = d\alpha \wedge \beta + (-1)^k(\alpha \wedge d\beta)$$

$$d^2 = d \circ d \equiv 0$$

- *Hodge Star ($*$):* k-form $\to (n-k)$-form (in n dimensions).

$$** \omega = (-1)^{k(n-k)} s\omega \quad \text{(where } s \text{ is the metric signature)}$$

Relationship to Vector Calculus (in $\mathbb{R}^3$)

If f is a 0-form and $\mathbf{V}$ a vector field associated with 1-form ω^1 and 2-form ω^2

- *Gradient:* df is the 1-form equivalent of ∇f.
- *Curl:* $d\omega^1$ is the 2-form equivalent of $\nabla \times \mathbf{V}$.
- *Divergence:* $d(*\omega^1)$ is the 3-form equivalent of $\nabla \cdot \mathbf{V}$.

Maxwell's Equations in Differential Forms

Using the Faraday 2-form F and the source 3-form J,

- *Homogeneous (Bianchi Identity):* $dF = 0$
- *Inhomogeneous (Source):* $d * F = \mu_0 J$
- *Vector Potential:* $F = dA$ (where A is the 1-form potential).

Integration and Topology

- *Generalized Stokes' Theorem:* $\int_\Omega d\omega = \int_{\partial\Omega} \omega$
- *De Rham Cohomology:*

$$H^k_{DR}(M) = \frac{\text{Ker}(d_k : \Omega^k \to \Omega^{k+1})}{\text{Im}(d_{k-1} : \Omega^{k-1} \to \Omega^k)} = \frac{\text{Closed Forms}}{\text{Exact Forms}}$$

where in the first line we have split dA into two equivalent terms, in the second line we have switched the dummy summation indices $\mu \leftrightarrow \nu$, and in the third line we have used the antisymmetric property of the wedge product, $dx^\nu \wedge dx^\mu = -dx^\mu \wedge dx^\nu$. Thus the exterior derivative of $A_\mu dx^\nu$ yields a 2-form

$$F = dA = \frac{1}{2} F_{\nu\mu} \qquad F_{\nu\mu} \equiv \partial_\nu A_\mu - \partial_\mu A_\nu, .$$

If A is the electromagnetic 4-potential, the 2-form $F_{\nu\mu}$ is precisely the electromagnetic field tensor given in Eq. (18.46) (but written here in terms of two lower indices).

19.4.7 Maxwell's Equations from the Exterior Calculus

To derive Maxwell's equations using exterior calculus, we must formulate electrodynamics geometrically on a 4-dimensional spacetime manifold. For this derivation, we will work in Minkowski spacetime $\mathbb{R}^{1,3}$ with the mostly-minus metric signature $(+,-,-,-)$ and natural units where $c = \mu_0 = \epsilon_0 = 1$.

Geometrical Setup: We define our spacetime coordinates as $x^\mu = (t, x, y, z)$. The foundational object is the four-potential 1-form, A, which unifies the scalar potential Φ and the vector potential $\boldsymbol{A}$,

$$A = A_\mu dx^\mu = \Phi dt - A_x dx - A_y dy - A_z dz. \tag{19.10}$$

From this we construct the 2-form *Faraday tensor* as the exterior derivative of A. From Example 19.4,

$$F = dA = (A_\mu dx^\mu) = \frac{1}{2}(\partial_\mu A_\nu - \partial_\nu A_\mu) dx^\mu \wedge dx^\nu, \tag{19.11}$$

which encodes both the electric field $\boldsymbol{E}$ and the magnetic field $\boldsymbol{B}$, with $F_0 i = E_i$ and $F_{ij} = -\epsilon_{ijk} B_k$. Explicitly using wedge products,

$$\begin{aligned} F = {} & E_x dx \wedge dt + E_y dy \wedge dt + E_z dz \wedge dt \\ & + B_x dy \wedge dz + B_y dz \wedge dx + B_z dx \wedge dy. \end{aligned} \tag{19.12}$$

The Homogeneous Maxwell Equations: The two homogeneous Maxwell's equations arise purely from the topology of differential forms, requiring no metric. Because $F = dA$, taking the exterior derivative of F must yield zero ($d^2 = 0$),

$$dF = d(dA) = 0. \tag{19.13}$$

The Inhomogeneous Maxwell Equations: To see how $d\star F = J$ becomes the familiar inhomogeneous Maxwell equations, let's work in Minkowski coordinates (t, x, y, z) with the alternative metric $\eta = \text{diag}(-1, 1, 1, 1)$. The Faraday 2-form is again

$$\begin{aligned} F = {} & E_x dx \wedge dt + E_y dy \wedge dt + E_z dz \wedge dt \\ & + B_x dy \wedge dz + B_y dz \wedge dx + B_z dx \wedge dy \end{aligned} \tag{19.14}$$

The Hodge star operator maps components such that $dt \wedge dx \to dy \wedge dz$ and $dy \wedge dz \to -dt \wedge dx$, so

$$\begin{aligned} \star F = &-B_x dx \wedge dt - B_y dy \wedge dt - B_z dz \wedge dt \\ &+ E_x dy \wedge dz + E_y dz \wedge dx + E_z dx \wedge dy. \end{aligned} \tag{19.15}$$

When we apply $d = \dfrac{\partial}{\partial t} dt + \dfrac{\partial}{\partial x} dx + \ldots$, we get terms like

1. The *time-like component* ($dx \wedge dy \wedge dz$) yields

$$\left(\frac{\partial E_x}{\partial x} + \frac{\partial E_y}{\partial y} + \frac{\partial E_z}{\partial z} \right) = \nabla \cdot \boldsymbol{E}. \tag{19.16}$$

2. The *space-like components* such as $dt \wedge dx \wedge dy$), which yields the components of

$$\nabla \times \mathbf{B} - \frac{\partial \mathbf{E}}{\partial t}.$$

Setting this equal to the source current J (which contains charge density ρ and current density $\boldsymbol{J}$) recovers the inhomogeneous Maxwell equations exactly.

19.4.8 Topology and the Aharonov–Bohm Effect

In Section 21.5 we discussed the Aharonov–Bohm effect and in Section 21.5.4 we stated that the surprising results of this experiment follow from the setup of the apparatus corresponding to a multiply-connected space exhibiting non-trivial topology. In this section we elaborate on the topology associated with the Aharonov–Bohm effect.

In Fig. 21.1, the magnetic field is related to the vector potential by $\boldsymbol{B} = \boldsymbol{\nabla} \times \boldsymbol{A}$. Outside the solenoid there is an electromagnetic vacuum with $\boldsymbol{B} = 0$. This is satisfied by the obvious choice $\boldsymbol{A} = 0$, but by gauge invariance $\boldsymbol{B}$ is invariant under the transformation $A_\mu \to A_\mu + \partial_\mu \chi \equiv A'_\mu$, where χ is an arbitrary scalar function. Thus, a gauge transform of the trivial vacuum $A_\mu = 0$, which is given by $A_\mu = \partial_\mu \chi$, *also satisfies the boundary condition.* It follows that in the cylindrical coordinates of Fig. 21.1(b),

$$\boldsymbol{A} = (A_r, A_\phi, A_z) = \boldsymbol{\nabla} \chi \tag{19.17}$$

is the most general vector potential giving a vanishing electromagnetic field. The scalar function χ is then

$$\chi = \frac{1}{2} B R^2 \phi, \tag{19.18}$$

and χ increases by $\pi B R^2$ as ϕ increases by 2π and *isn't single-valued.* This is possible because *the vacuum configuration of the Aharonov–Bohm experiment isn't simply connected.*

From Fig. 21.1, the Aharonov–Bohm experiment corresponds to a plane pierced by a hole corresponding to the solenoid; topologically this is the product of the real numbers and a circle, $\mathbb{R} \times S^1$. As discussed in Box 21.2, the gauge group for electromagnetism is U(1), which has a manifold that is S^1 topologically. Thus, we must consider mappings between $\mathbb{R} \times S^1$ and S^1. But $\mathbb{R}$ is simply connected so $S^1 \to S^1$ is the only part of the mapping that matters topologically, and this mapping is characterized by an infinity

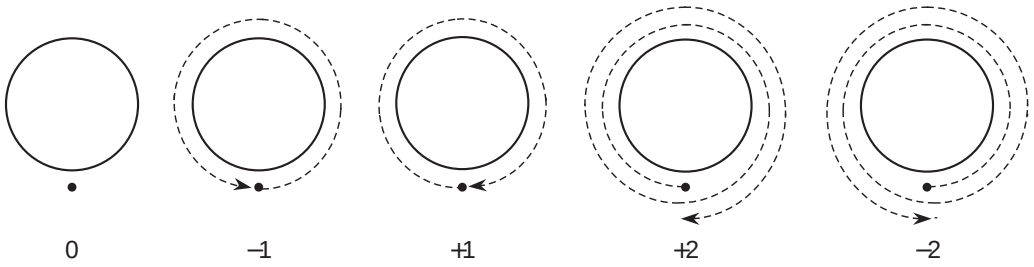

Fig. 19.1 Some winding numbers characterizing the topology of the U(1) manifold S^1. Intuitively the winding number is the number of times the dashed curve is wrapped around the solid circle, clockwise $(+)$ or counterclockwise $(-)$.

of integer winding numbers giving how many times one circle is wrapped around the other, as illustrated in Fig. 19.1. Therefore, *the gauge function χ is multivalued* because the mappings are not all deformable to the trivial mapping $\chi =$ constant, which would give $A_\mu = 0$ and no Aharonov–Bohm effect, by virtue of Eq. (19.17).

19.5 Covariant Derivatives

19.6 Differential Forms

Background and Further Reading

See Schutz[66], Misner, Thorne, and Wheeler [54]

Problems

19.1 Beginning from Eq. (19.6) expressed in differential forms, derive the vector calculus version of the Ampère–Maxwell Law (6.50d).

Numerical and GenAI Problems

20 Action Formulation of Classical Electromagnetism

In this chapter we will demonstrate that classical electromagnetism can be formulated in terms of a least-action principle such that the Lagrangian and Hamiltonian methods of classical mechanics can be applied to the electromagnetic field.

20.1 The Principle of Least Action

20.2 The Action Principle For Fields

20.3 A Lagrangian Formulation of Electromagnetism

Since the starting point for a field theory is typically a Lagrangian from which the fields can be derived through a variational principle, it is useful write down a *Lagrangian density* (a Lagrangian evaluated at a single spacetime point) appropriate for the electromagnetic field.

20.3.1 Principle of Extremal Proper Time

The motion of free particles in Minkowski spacetime is governed by a simple principle: the worldline for free particles between points separated by timelike intervals extremizes the proper time. This is called the *principle of extremal proper time* and is illustrated in Fig. 20.1. The proper time between the points A and B in Fig. 20.1 can be computed from Eq. (18.5) as,

$$\tau_{AB} = \int_A^B (dt^2 - dx^2 - dy^2 - dz^2)^{1/2}. \tag{20.1}$$

Parameterizing a path by a variable σ that varies continuously from 0 to 1 as the particle moves from A to B, the path is specified by $x^\mu = x^\mu(\sigma)$ and

$$\tau_{AB} = \int_0^1 \left[\left(\frac{dt}{d\sigma}\right)^2 - \left(\frac{dx}{d\sigma}\right)^2 - \left(\frac{dy}{d\sigma}\right)^2 - \left(\frac{dz}{d\sigma}\right)^2 \right]^{1/2} d\sigma. \tag{20.2}$$

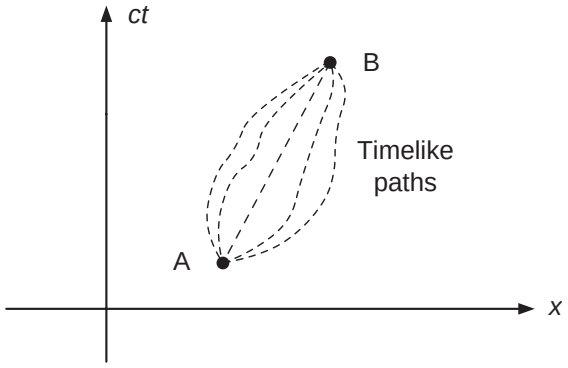

Fig. 20.1 *Principle of Extremal Proper Time:* of all the possible classical paths between two timelike-separated points A and B in spacetime, a free particle follows one that *extremizes the proper time*. Adapted from Ref. [36].

The solution to finding the path that extremizes the action is described in Box 20.1, where the condition for an extremum is found to be

$$\delta \int d\tau = 0. \tag{20.3}$$

Defining a *Lagrangian* L as

$$L = \left(-g_{\mu\nu} \frac{dx^\mu}{d\sigma} \frac{dx^\nu}{d\sigma} \right)^{1/2}, \tag{20.4}$$

where $g_{\mu\nu}$ is the metric tensor, so that

$$\tau_{AB} = \int_0^1 L \, d\sigma, \tag{20.5}$$

then results in the *Euler–Lagrange equation of motion*

$$-\frac{d}{d\sigma} \left(\frac{\partial L}{\partial (dx^\mu / d\sigma)} \right) + \frac{\partial L}{\partial x^\mu} = 0. \tag{20.6}$$

Requiring that the Lagrangian L obey the differential equation (20.6) satisfies the variational condition (20.3).

20.3.2 Construction of Classical Fields

The standard approach to classical field theory is to define fields that obey appropriate equations of (classical) motion. The classical action S is defined by

$$S = \int d^4x \, \mathcal{L} = \int_{t_1}^{t_2} L \, dt, \tag{20.7}$$

where $\mathcal{L} = \mathcal{L}(x)$ is the Lagrangian defined at a Minkowski spacetime point (the *Lagrangian density*). The total Lagrangian L is then given by

$$L = \int d^3x \, \mathcal{L}(x). \tag{20.8}$$

Box 20.1 The Euler–Lagrange Equations [36]

Consider the paths in spacetime between the fixed points labeled A and B in Fig. 20.1. For a function $L\left(x^\mu(\sigma), \dot{x}^\mu(\sigma)\right)$, where σ parameterizes the path and $\dot{x}^\mu \equiv dx^\mu/d\sigma$, define the path integral

$$S = \int_A^B L\left(x^\mu(\sigma), \dot{x}^\mu(\sigma)\right)\, d\sigma.$$

For an arbitrary small variation in the path $x^\mu(\sigma) \to x^\mu(\sigma) + \delta x^\mu(\sigma)$, the corresponding variation in the value of the integral is

$$\delta S \equiv \int_A^B \delta L\, d\sigma = \int_A^B \left(\frac{\partial L}{\partial \dot{x}^\mu(\sigma)}\, \delta \dot{x}^\mu(\sigma) + \frac{\partial L}{\partial x^\mu(\sigma)}\, \delta x^\mu(\sigma) \right) d\sigma.$$

The first term can be integrated by parts, giving

$$\delta S = \frac{\partial L}{\partial \dot{x}^\mu(\sigma)}\, \delta x^\mu(\sigma) \Bigg|_A^B + \int_A^B \left[-\frac{d}{d\sigma} \left(\frac{\partial L}{\partial \dot{x}^\mu(\sigma)} \right) + \frac{\partial L}{\partial x^\mu(\sigma)} \right] \delta x^\mu(\sigma) d\sigma,$$

but the variation $\delta x^\mu(\sigma)$ vanishes at the fixed endpoints so the first term is zero and

$$\delta S = \int_A^B \left[-\frac{d}{d\sigma} \left(\frac{\partial L}{\partial \dot{x}^\mu(\sigma)} \right) + \frac{\partial L}{\partial x^\mu(\sigma)} \right] \delta x^\mu(\sigma) d\sigma.$$

For paths that extremize the integral $\delta S = 0$ and for arbitrary variations $\delta x^\mu(\sigma)$ this will be true only if the expression inside the square brackets of the above integrand vanishes. Thus

$$-\frac{d}{d\sigma} \left(\frac{\partial L}{\partial \dot{x}^\mu(\sigma)} \right) + \frac{\partial L}{\partial x^\mu(\sigma)} = 0,$$

which is the *Euler–Lagrange equation* (20.6). Satisfying the variational condition $\delta S = 0$ characterizing an extremal path is equivalent to requiring that the function L satisfy the Euler–Lagrange equation.

We may view the action S as the central quantity for field quantization. It determines the equations of motion for the classical fields to be quantized in the canonical method, and enters even more obviously in the path integral method because each path in the functional integral is weighted by a factor $\exp(iS)$.

The formal starting point for developing a field theory is to construct the appropriate Lagrangian density, which then leads to the action through Eq. (20.7), and thus to the equations of motion for the field (20.6).

Thus, we need appropriate Lagrangian densities for the fields of interest.

20.3.3 Lagrangian Densities for Photons and Charged Fields

The Lagrangian densities that we require are constructed precisely to yield the appropriate fields when the variational principle (20.3) is applied. Let's summarize a few important wave equations entering into formulations of a field theory for electromagnetism and for charged particles coupled to electromagnetism.

1. The *Maxwell wave equation* for massless vector fields $A^\mu(x)$ is, in Lorentz gauge,
$$\Box A^\mu(x) = j^\mu \qquad \text{(Lorenz gauge)}, \tag{20.9}$$
which is quadratic in ∂^μ.
2. The *Klein–Gordon equation* for scalar (single-component) fields $\Phi(x)$
$$(\Box + m^2)\Phi(x) = 0 \qquad \Box \equiv \partial_\mu \partial^\mu, \tag{20.10}$$
which is quadratic in ∂_μ and carries no Lorentz index.
3. The *Dirac equation* for 4-component Lorentz spinor fields $\Psi(x)$
$$(-i\gamma^\mu \partial_\mu + m)\Psi(x) = 0, \tag{20.11}$$
which is linear in ∂^μ.
4. The *massive vector* or *Proca field* $A^\mu(x)$, with an equation
$$(\Box + m^2)A^\mu(x) = 0 \tag{20.12}$$
that is quadratic in ∂^μ.

The corresponding Lagrangian densities that yield the wave equations given above are summarized in the following.

Massless Vector Field: In terms of the rank-2 *electromagnetic field tensor* $F^{\mu\nu} = \partial^\mu A^\nu - \partial^\nu A^\mu$ introduced in Eq. (18.46) through the 4-vector potential A^μ defined in Eq. (18.41), the free-field Lagrangian density appropriate for the massless vector (photon) field is
$$\mathcal{L}_0 = -\frac{1}{4} F_{\mu\nu} F^{\mu\nu} \qquad \text{(Massless vector field)}. \tag{20.13}$$
This Lagrangian density describes massless vector particles like the photon and satisfies the wave equation (20.9) in Lorentz gauge.

Complex Scalar or Pseudoscalar Fields: A complex scalar (or pseudoscalar) field $\phi(x)$ may be expressed in terms of two real scalar fields $\phi_1(x)$ and $\phi_2(x)$ having the same mass ($m_1 = m_2 \equiv m$),
$$\phi = \frac{1}{\sqrt{2}}(\phi_1 + i\phi_2) \qquad \phi^\dagger = \frac{1}{\sqrt{2}}(\phi_1 - i\phi_2), \tag{20.14}$$
where the corresponding free Lagrangian density is
$$\mathcal{L}_0 = (\partial^\mu \phi)^\dagger (\partial_\mu \phi) - m^2 \phi^\dagger \phi \qquad \text{(Complex scalar field)}. \tag{20.15}$$

Separate variations of ϕ and $\phi^\dagger$ then lead to two independent Klein–Gordon equations (20.10),

$$(\Box + m^2)\phi(x) = 0 \qquad (\Box + m^2)\phi^\dagger(x) = 0. \tag{20.16}$$

Charged scalar or pseudoscalar particles are associated with complex scalar fields.

Dirac Spinor Field: For a Dirac field $\psi(x)$ and a conjugate (adjoint spinor) field $\overline{\psi}(x)$ defined by

$$\overline{\psi}(x) \equiv \psi^\dagger(x)\,\gamma^0, \tag{20.17}$$

where the matrix γ_0 is defined through the 4×4 matrices γ^μ satisfying the anticommutator

$$\{\,\gamma_\mu, \gamma_\nu\,\} \equiv \gamma_\mu\gamma_\nu + \gamma_\nu\gamma_\mu = 2\eta_{\mu\nu} \tag{20.18}$$

that are termed the (Dirac) γ*-matrices.* Explicit forms in different representations and general properties of the gamma-matrices are summarized in Table 20.1. The Lagrangian density for a free Dirac spinor field is

$$\mathcal{L}_0 = \overline{\psi}(i\partial\!\!\!/ - m)\psi \qquad \text{(Dirac spinor field)}, \tag{20.19}$$

where m is the mass and *Feynman slash notation* has been used: a slash through a quantity indicates a 4-vector contracted completely with the γ-matrices: $\partial\!\!\!/ \equiv \gamma^\mu\partial_\mu$. The Lagrangian density (20.19) then yields the Dirac equation (20.11),

$$(i\partial\!\!\!/ - m)\psi = 0, \tag{20.20}$$

as the equation of motion for a charged fermion spinor field.

Massive Vector Field: For a vector field of finite mass m, the appropriate free-field Lagrangian density is obtained from Eq. (20.13) by adding a Lorentz-invariant mass term,

$$\mathcal{L}_0 = -\frac{1}{4}F_{\mu\nu}F^{\mu\nu} + \frac{1}{2}m^2A^\mu A_\mu \qquad \text{(Massive vector field)}. \tag{20.21}$$

This implies an equation of motion $(\Box + m^2)A^\mu = 0$ corresponding to the wave equation (20.12) for a massive vector field.

Background and Further Reading

See Wald [74], Zangwill [77], and Garg [31].

Table 20.1 Properties of the Dirac γ-matrices [38]

$$\{\alpha_i, \alpha_j\} = 2\delta_{ij} \qquad \{\alpha_i, \beta\} = 0 \qquad \alpha_i^2 = \beta^2 = 1$$

$$\gamma_0 = \gamma^0 \equiv \beta \qquad \gamma_i \equiv \gamma^0\alpha_i \qquad \gamma_5 = \gamma^5 \equiv i\gamma^0\gamma^1\gamma^2\gamma^3 \qquad \sigma^{\mu\nu} \equiv \tfrac{i}{2}[\gamma^\mu, \gamma^\nu]$$

$$\{\gamma^\mu, \gamma^\nu\} = 2\eta^{\mu\nu} \qquad \gamma_0\gamma_\mu^\dagger\gamma_0 = \gamma_\mu \qquad \{\gamma_5, \gamma^\mu\} = 0 \qquad (\gamma^i)^2 = -1$$

$$(\gamma^0)^2 = 1 \qquad (\gamma^5)^2 = 1 \qquad (\gamma_0)^\dagger = \gamma_0 \qquad (\gamma^i)^\dagger = -\gamma^i \qquad (\gamma^5)^\dagger = \gamma^5$$

Pauli–Dirac representation (4×4 matrices):

$$\gamma^0 = \begin{pmatrix} 1 & 0 \\ 0 & -1 \end{pmatrix} \quad \gamma^i = \begin{pmatrix} 0 & \sigma_i \\ -\sigma_i & 0 \end{pmatrix} \quad \gamma^5 = \begin{pmatrix} 0 & 1 \\ 1 & 0 \end{pmatrix} \quad \alpha_i = \begin{pmatrix} 0 & \sigma_i \\ \sigma_i & 0 \end{pmatrix}$$

$$\beta = \begin{pmatrix} 1 & 0 \\ 0 & -1 \end{pmatrix} \qquad \sigma^{ij} = \epsilon_{ijk}\begin{pmatrix} \sigma_k & 0 \\ 0 & \sigma_k \end{pmatrix} \qquad \sigma^{0k} = i\begin{pmatrix} 0 & \sigma_k \\ \sigma_k & 0 \end{pmatrix}$$

Weyl (chiral) representation (4×4 matrices):

$$\gamma^0 = \begin{pmatrix} 0 & 1 \\ 1 & 0 \end{pmatrix} \qquad \gamma^i = \begin{pmatrix} 0 & -\sigma_i \\ \sigma_i & 0 \end{pmatrix} \qquad \gamma^5 = \begin{pmatrix} 1 & 0 \\ 0 & -1 \end{pmatrix}$$

Majorana representation (4×4 matrices):

$$\gamma^0 = \begin{pmatrix} 0 & \sigma_2 \\ \sigma_2 & 0 \end{pmatrix} \quad \gamma^1 = \begin{pmatrix} i\sigma_1 & 0 \\ 0 & i\sigma_1 \end{pmatrix} \quad \gamma^2 = \begin{pmatrix} 0 & \sigma_2 \\ -\sigma_2 & 0 \end{pmatrix}$$

$$\gamma^3 = \begin{pmatrix} -i\sigma_3 & 0 \\ 0 & i\sigma^3 \end{pmatrix} \qquad \gamma^5 = \begin{pmatrix} \sigma_2 & 0 \\ 0 & \sigma_2 \end{pmatrix}$$

Standard Pauli matrices (2×2 matrices):

$$\sigma_1 = \begin{pmatrix} 0 & 1 \\ 1 & 0 \end{pmatrix} \qquad \sigma_2 = \begin{pmatrix} 0 & -i \\ i & 0 \end{pmatrix} \qquad \sigma_3 = \begin{pmatrix} 1 & 0 \\ 0 & -1 \end{pmatrix}$$

No problems yet for this chapter.

21 Electromagnetism as an Abelian Gauge Field Theory

As we have alluded to in various places, modern relativistic quantum field theory, in particular the Standard Model of elementary particle physics, is a quantized generalization of the gauge invariance principle of classical electromagnetism. In this chapter we provide some remarks intended to outline the relationship of classical gauge invariance to the more complex gauge symmetries prominent in modern gauge field theories. These more complex gauge symmetries are typically implemented in (usually relativistic) quantum field theories, so our discussion will occasionally touch on a quantum description. Therefore, the reader will be assumed to have an understanding of basic concepts from quantum mechanics at an advanced undergraduate level.

21.1 Symmetry and Gauge Invariance

Symmetries and broken symmetries are of fundamental importance in the generalization of the classical gauge invariance exhibited by the Maxwell equations to the varied manifestation of gauge invariance in modern quantum field theory. The natural language for describing gauge symmetries in their most general form is the theory of Lie groups and Lie algebras. The rudiments are described in Box 21.1. The essential difference between the gauge symmetry of electromagnetism and the gauge symmetries associated with the electromagnetic, weak, and strong interactions in the Standard Model is that electromagnetism is governed by a symmetry called U(1) (described in Box 21.2) that is *abelian*, but the weak and strong interactions are governed by gauge symmetries that correspond to larger and more complex *nonabelian* gauge groups.

21.2 The Minimal Coupling Prescription

Gauge invariance is of fundamental importance in classical electromagnetism and becomes even more so in quantum field theory. In either case it is important to ask what coupling terms between fields in Lagrangians or Hamiltonians are permitted that preserve gauge invariance. Note first that a classical particle carrying charge q and moving with 3-velocity $\boldsymbol{v}$ in an electromagnetic field experiences the *Lorentz force* of classical electromagnetism,

$$\boldsymbol{F} = q(\boldsymbol{E} + \boldsymbol{v} \times \boldsymbol{B}), \tag{21.1}$$

Box 21.1 Symmetries and Groups [36]

A group is a set $G = \{x, y, ...\}$ for which a binary operation $a \cdot b = c$ called *group multiplication* is defined that has the following properties

(i) *Closure:* If x and y are elements of G, then $x \cdot y$ is an element of G also.
(ii) *Identity:* An identity element e exists such that $e \cdot x = x \cdot e = x$ for $x \in G$.
(iii) *Existence of an Inverse:* For every group element x there is an inverse x^{-1} in the set such that $xx^{-1} = e$.
(iv) *Associativity:* Multiplication is associative: $(x \cdot y) \cdot z = x \cdot (y \cdot z)$ for $x, y, z \in G$.

For groups of transformations multiplication corresponds to applying first one and then the other transformation. The group definition requires associativity but not commutivity. A group consisting of commutative elements only is *abelian*; otherwise, it is *nonabelian*.

Example: The Lorentz group
There are six independent Lorentz transformations: three rotations about the spatial axes parameterized by real angles, and three boosts along the spatial axes parameterized by boost velocities. Because rotation angles and boost velocities can take continuous real values, the set of Lorentz transformations is infinite. The Lorentz transformations form a group:

1. Two successive transformations are equivalent to some other transformation.
2. Every Lorentz transformation has an inverse that is the transformation in the opposite direction (for example, $v \to -v$ for boosts).
3. The identity corresponds to no transformation.
4. It doesn't matter how three successive transformations are grouped, so multiplication is associative, but the *order* matters, so the Lorentz group is nonabelian.

An important class of groups corresponds to transformations that are continuous (analytical) in their parameters. These are called *Lie groups.* The Lorentz group is a Lie group. Groups also can be classified according to whether their parameter spaces are closed and bounded (*compact groups*) or not (*noncompact groups*).[a] Because boost velocities can approach c asymptotically but never reach it, the Lorentz-group parameter space is bounded by $v < c$ but not closed (the limit $v = c$ is not part of the set since Lorentz transformations diverge for $v = c$) and the group is noncompact.

Example: The Poincaré group
The Poincaré group is formed by adding to the Lorentz transformations the uniform translations along the four spacetime axes. It is a non-abelian, noncompact Lie group, and contains the Lorentz group as a *subgroup* (a subset of group elements that satisfy the same group postulates as the parent group).

[a] A closed set contains all its limit points. In a bounded set all point lie within some maximum fixed distance from each other. Example: $[0, a)$ (where "[" denotes a closed interval and ")" an open interval) is not a closed subset of the real numbers $\mathbb{R}$ because it contains 0 but doesn't contain a.

Box 21.2 The Gauge Group U(1)

A gauge transformation in electromagnetism corresponds to simultaneous transformations on the scalar potential Φ and vector potential A_i,

$$\Phi \to \Phi' = e^{iq\chi}\Phi \qquad A_i \to A_i' = A_i + \partial_\mu \chi$$

(in $\hbar = 1$ units), where q is the electrical charge and $\chi = \chi(x)$ is an arbitrary scalar function depending on the spacetime coordinates x. Gauge symmetry then implies that classically (Φ, A_i) and (Φ', A_i') are *physically equivalent*.[a] Thus, the gauge transformation acts on the charged scalar field Φ by multiplying it by a spacetime dependent phase factor. Mathematically, multiplication by a phase factor corresponds to a unitary map $\mathrm{U}\colon \mathbb{C} \to \mathbb{C}$ on the complex numbers $z \in \mathbb{C}$ that is defined in this case by $Uz = e^{iq\chi}z$, where U implements a *unitary transformation*.[b] The set of all unitary maps on $\mathbb{C}$ constitute a group (see Box 21.1) with the "multiplication" operation defined by composition (successive application) of maps. This group is commonly labeled $\mathrm{U}(1)$ in physics, where U denotes "unitary" and 1 denotes a 1D complex vector space $\mathbb{C}$. Since the complex vector space is one-dimensional, the group elements $e^{iq\chi}$ of $\mathrm{U}(1)$ are parameterized by a single parameter χ and the group is abelian. The unitary maps $Uz = e^{iq\chi}z$ are in one-to-one correspondence with the real numbers χ modulo $2\pi/q$, so the manifold of $\mathrm{U}(1)$ (the space traced out by allowing the group parameter χ to vary over all possible values) is represented naturally by a circle S^1 of circumference $2\pi/q$.

[a] They lead to the same classical electric and magnetic fields, and thus to the same solutions of the Maxwell equations. Since $\chi(x)$ is a local function of the coordinates, this is termed a *local gauge transformation* (a *global gauge transformation* corresponds to a constant χ). As discussed in Section 11.3 and Box 11.2, gauges related by the same gauge transformation constitute an *equivalence class*.

[b] A unitary transformation Uz is a linear map with the property $|Uz^2| = |z^2|$), so it preserves the modulus $|z^2|$ for all $z \in \mathbb{C}$). Such transformations are said to be *unimodular*.

provided that the classical Hamiltonian function is given by

$$H = \frac{1}{2m}(\boldsymbol{p} - q\boldsymbol{A})^2 + q\phi, \tag{21.2}$$

where $\boldsymbol{E}$ is the electric field, $\boldsymbol{B}$ is the magnetic field, $\boldsymbol{p}$ is the 3-momentum, $\boldsymbol{A}$ is the 3-vector potential, and ϕ is the scalar potential. Quantizing this Hamiltonian assuming non-relativistic quantum mechanics gives the modified Schrödinger equation

$$\left[\frac{1}{2m}(-i\boldsymbol{\nabla} - q\boldsymbol{A})^2 + q\phi\right]\psi(\boldsymbol{x}, t) = i\,\frac{\partial\psi(\boldsymbol{x}, t)}{\partial t}. \tag{21.3}$$

Comparing this expression with the free-particle Schrödinger equation

$$-\frac{1}{2m}\boldsymbol{\nabla}^2\psi(\boldsymbol{x}, t) = i\,\frac{\partial\psi(\boldsymbol{x}, t)}{\partial t},$$

suggests that a Schrödinger equation accounting for gauge-invariant coupling of charged particles to an electromagnetic field can be constructed from the free-particle Schrödinger equation by making the operator substitutions

$$\boldsymbol{\nabla} \to \boldsymbol{D} \equiv \boldsymbol{\nabla} - iq\boldsymbol{A} \qquad \frac{\partial}{\partial t} \to D^0 \equiv \frac{\partial}{\partial t} + iq\phi. \tag{21.4}$$

In covariant 4-vector notation this becomes

$$\partial^\mu \to D^\mu \equiv \partial^\mu + iqA^\mu, \tag{21.5}$$

where we have defined the 4-vectors $A^\mu = (\phi, \boldsymbol{A})$ and $D^\mu = (D^0, \boldsymbol{D})$. The replacement (21.5) is just the replacement of the partial derivative by the covariant derivative as in Eq. (17.55), with the notational change $\boldsymbol{\nabla}_\mu \to D^\mu$. Equation (21.5) is termed the *minimal coupling prescription* or the *minimal substitution*. The Schrödinger equation (21.3) is invariant under the *local gauge transformation* (11.10),

$$\boldsymbol{A} \to \boldsymbol{A} + \boldsymbol{\nabla}\chi \qquad \Phi \to \Phi - \frac{\partial \chi}{\partial t}, \tag{21.6}$$

provided that the wavefunction is transformed simultaneously as

$$\psi(\boldsymbol{x}, t) \to e^{iq\chi(x)}\psi(\boldsymbol{x}, t), \tag{21.7}$$

where χ is a scalar function that is *completely arbitrary* and is a *local function of the spacetime coordinates*.

For completeness we note that for relativisitic wave equations, minimal substitution in the Klein–Gordon equation (20.10) (appropriate for charged scalar or pseudoscalar particles if Φ is complex) gives the wave equation

$$\left(D^\mu D_\mu + m^2\right)\psi(x) = 0, \tag{21.8}$$

while minimal substitution in the Dirac equation (20.11) (appropriate for charged fermions if Ψ is complex) gives

$$\left(i\gamma_\mu D^\mu - m\right)\psi(x) = 0. \tag{21.9}$$

Both Eqs. (21.8) and (21.9) are invariant under a gauge transformation

$$A^\mu \to A^\mu - \partial^\mu \chi(x) \qquad \psi \to e^{iq\chi(x)}\psi, \tag{21.10}$$

where we emphasize again that these are *local* gauge transformations, since χ is a local function of the spacetime coordinate x. Summarizing:

Minimal Substitution: In a free charged-particle wave equation, replace all derivatives with covariant derivatives

$$\partial^\mu \to D^\mu \equiv \partial^\mu + iqA^\mu.$$

The resulting wave equation couples the electromagnetic and charged-particle fields and is *invariant under a local gauge transformation*

$$A^\mu \to A^\mu - \partial^\mu \chi(x) \qquad \psi \to e^{iq\chi(x)}\psi,$$

where q is charge, A^μ is the 4-vector potential, and $\chi(x)$ is an arbitrary *local* scalar field.

This is called *minimal substitution* or the *minimal coupling prescription* because it, and not a more complicated coupling, is adequate for implementing gauge-invariant coupling of charged particles to the electromagnetic field.

21.3 Gauge Invariance and the Photon Mass

The Lagrangian density for a *massless* vector field is given by Eq. (20.13). Since $F^{\mu\nu}F_{\mu\nu}$ is gauge invariant, the massless vector field (photon field) is gauge invariant. A *massive* vector field has a Lagrangian density given by Eq. (20.21). The first term for (20.21) is gauge invariant but the second (mass) term is not, since under the gauge transformation $A^\mu \to A^\mu - \partial^\mu \chi$,

$$A^\mu A_\mu \to (A^\mu - \partial^\mu \chi)(A_\mu - \partial_\mu \chi) \neq A^\mu A_\mu.$$

We reach a conclusion that has far-reaching implications for gauge symmetry and its influence on modern physics:

Gauge invariance of the electromagnetic field is tied directly both to

1. *conservation of electrical charge* and to
2. *masslessness of the gauge vector boson* (the photon) that mediates the electromagnetic interaction.

If the photon had a finite restmass (implying an explicit mass term in the Lagrangian density), the corresponding vector field would violate gauge invariance. These properties carry over to the non-abelian gauge symmetries of the Standard Model: gauge symmetries imply conservation of generalized charges, and an explicit mass term in the Lagrangian density would break gauge symmetry.

That local gauge invariance implies massless gauge bosons, and how a gauge boson can

acquire an effective mass through spontaneous breaking of the gauge symmetry in the Higgs mode, are crucial in understanding abelian and non-abelian gauge theories in the Standard Model. However, would take us deep into quantum field theory and is beyond the scope of our discussion here.

21.4 Conserved Currents and Charges

Observables in quantum field theory are often formulated through generalizations of electromagnetic charges and currents. Field-theory symmetries may be expressed in terms of conservation of those charges and currents.

21.4.1 Noether's Theorem

Conservation laws for field theories formulated in terms of Lagrangian densities often are expressed in terms of *Noether's theorem:*

> ***Noether's Theorem:*** For each continuous symmetry of a field theory Lagrangian there is a corresponding conserved quantity.

Conserved quantities may involve spacetime or internal symmetries and are termed *conserved Noether tensors.* Let's illustrate by deriving conservation of 4-momentum from invariance under spacetime translations.

21.4.2 Conservation of Energy and Momentum

This solution follows a discussion in Quigg [63]. Poincaré invariance[1] requires that the action be unchanged by a spacetime transformation $x_\mu \to x'_\mu = x_\mu + a_\mu$, where the infinitesimal displacement a_μ is independent of x_μ. The corresponding change in a scalar field Lagrangian density is

$$\delta\mathcal{L} = \mathcal{L}(x') - \mathcal{L}(x) = a^\mu \partial_\mu \mathcal{L}. \tag{21.11}$$

Assuming the Lagrangian density to be translationally invariant in spacetime (independent of spacetime coordinates x), but to depend on the field ϕ and $\partial_\mu\phi$, we may also write

$$\begin{gathered}\delta\mathcal{L} = \frac{\partial\mathcal{L}}{\partial\phi}\delta\phi + \frac{\partial\mathcal{L}}{\partial(\partial_\mu\phi)}\delta(\partial_\mu\phi) \qquad \delta\phi \equiv \phi(x') - \phi(x) = a^\mu\partial_\mu\phi, \\ \delta(\partial_\mu\phi) \equiv \partial_\mu\phi(x') - \partial_\mu\phi(x) = a^\nu\partial_\nu(\partial_\mu\phi).\end{gathered} \tag{21.12}$$

[1] The Poincaré group appends the generators of spacetime translations to the Lorentz transformations; see Box 21.1. Thus Poincaré symmetry means that the system is invariant under Lorentz transformations (which preserve the invariant spacetime interval) and also under uniform translations in spacetime (which implies conservation of energy and momentum).

But from the Euler–Lagrange equations (20.6),

$$\frac{\partial \mathcal{L}}{\partial \phi} = \partial_\mu \left(\frac{\partial \mathcal{L}}{\partial(\partial_\mu \phi)} \right), \tag{21.13}$$

and from Eqs. (21.13) and (21.12),

$$\delta \mathcal{L} = \left(\partial_\nu \frac{\partial \mathcal{L}}{\partial(\partial_\nu \phi)} \right) a^\mu \partial_\mu \phi + \frac{\partial \mathcal{L}}{\partial(\partial_\nu \phi)} a^\mu \partial_\mu (\partial_\nu \phi) = \partial_\nu \frac{\partial \mathcal{L}}{\partial(\partial_\nu \phi)} a^\mu \partial_\mu \phi,$$

where the last step may be checked by taking the derivative of the product. Equating this expression with Eq. (21.11) and rearranging (remember that repeated indices are dummy indices that can be changed without affecting the validity of the equation) leads to

$$a_\nu \partial_\mu \left(\frac{\partial \mathcal{L}}{\partial(\partial_\mu \phi)} \partial^\nu \phi - \eta^{\mu\nu} \mathcal{L} \right) = 0,$$

where $\eta^{\mu\nu}$ is the metric tensor of flat spacetime. This relation must evaluate to zero for arbitrary displacements a_ν, which implies that

$$\partial_\mu \left(\frac{\partial \mathcal{L}}{\partial(\partial_\mu \phi)} \partial^\nu \phi - \eta^{\mu\nu} \mathcal{L} \right) = 0.$$

Let us define the *stress–energy–momentum tensor*

$$\Theta^{\mu\nu} \equiv \frac{\partial \mathcal{L}}{\partial(\partial_\mu \phi)} \partial^\nu \phi - \eta^{\mu\nu} \mathcal{L}, \tag{21.14}$$

for which it may be shown that Θ^{00} is the energy density and the Θ^{0k} are momentum densities. This leads to a local conservation law

$$\partial_\mu \Theta^{\mu\nu}(x) = 0,$$

for energy and momentum. The quantity $\Theta^{\mu\nu}$ is an example of a conserved Noether tensor that in this case links 4-momentum conservation with spacetime translational invariance. In this example the symmetry is a spacetime symmetry, but probably the most important applications of Noether's theorem are to conserved charges and currents associated with internal degrees of freedom for elementary particles, particularly the gauge degrees of freedom.

21.4.3 Internal Noether Currents and Charges

For an internal symmetry with a symmetry group described by a set of matrix generators T^a and a Lagrangian density $\mathcal{L}$, the *conserved Noether currents* J^a_μ are given by

$$J^a_\mu = -i \frac{\partial \mathcal{L}}{\partial(\partial^\mu \phi_i)} T^a_{ij} \phi_j, \tag{21.15}$$

where a labels an internal symmetry generator, μ is a spacetime index, and i and j label entries in the matrix T^a. Given a local 4-current

$$J^\mu = \left(J^0(x), J^1(x), J^2(x), J^3(x) \right),$$

as in Eq. (21.15), an associated charge $Q(t)$ may be defined by

$$Q(t) \equiv \int J^0(x)\, d^3x. \tag{21.16}$$

For example, the electromagnetic 4-current $j = (\rho, \mathbf{j})$ implies an electrical charge

$$Q_{\rm e} = \int \rho(x)\, d^3x \, = \int j^0(x)\, d^3x\,. \tag{21.17}$$

The charge operator satisfies the *Heisenberg equation of motion* for quantum operators,

$$\dot{Q} \equiv \frac{dQ(t)}{dt} = i\,[\,H, Q(t)\,], \tag{21.18}$$

where H is the Hamiltonian operator and the commutator of operators A and B is denoted by $[A, B] \equiv AB - BA$. If J^μ has vanishing 4-divergence,

$$\partial_\mu J^\mu \equiv \partial_0 J^0 + \boldsymbol{\nabla} \cdot \boldsymbol{J} = \partial_0 J^0 + \partial_k J^k = 0. \tag{21.19}$$

Then $[\,H, Q\,] = 0$ and Q is a constant of motion.

Conserved Charges: If a 4-current $J^\mu(x)$ satisfies $\partial_\mu J^\mu = 0$, the charge Q defined by the spatial integral of $J^0(x)$ is conserved.

This establishes a formal link between conserved Noether currents in a Lagrangian formulation of a problem (which have vanishing 4-divergence) and conserved charges that are constants of motion in a Hamiltonian formulation of the same problem (the charge operator commutes with the Hamiltonian).

Example 21.1 The electromagnetic 4-current $j^\mu = (\rho, \mathbf{j})$ has $\partial_\mu j^\mu = 0$, implying that the electrical charge $Q_{\rm e}$ of Eq. (21.17) is conserved.

Example 21.1 is well known for electrical charges and currents. However, the preceding derivation implies that *any charge* defined through Eq. (21.16) is conserved (it is a constant of motion) if the 4-divergence of the associated current J^μ vanishes. In the generalizations of the gauge symmetry of classical electromagnetism that underly the Standard Model of elementary particle physics, one encounters gauge charges and associated currents that generalize the electromagnetic charge and current. The U(1) symmetry of electromagnetism (see Box 21.2) has generators that can be represented as 1×1 matrices and the symmetry is abelian. For Standard Model gauge symmetries many of the symmetry groups are non-abelian and the matrices entering Eq. (21.15) are $n \times n$ matrices with $n > 1$.

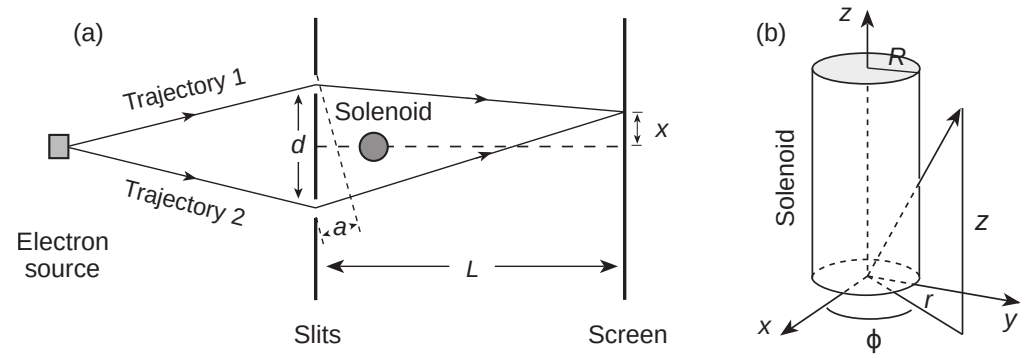

Fig. 21.1 (a) Aharonov–Bohm experiment. (b) Cylindrical coordinates for the Aharonov–Bohm effect.

21.5 The Aharonov–Bohm Effect

The Aharonov–Bohm effect [15] demonstrates that the electromagnetic 4-vector potential can have measurable consequences in a quantum theory, even for regions having no electric or magnetic fields. This contrasts with classical electromagnetism, where electric and magnetic fields are fundamental and vector potentials are only a mathematical convenience. Although the Aharonov–Bohm effect is usually discussed in the context of quantum mechanics, we shall see that it is relevant to our discussion of classical electromagnetism for two fundamental reasons:

1. It is a primary indication that the fundamental fields in electromagnetism are not the magnetic field $\boldsymbol{B}$ and the electric field $\boldsymbol{E}$, but rather the vector potential field $\boldsymbol{A}$ and the scalar potential field Φ.
2. Although the *detection* of the Aharonov–Bohm effect involves a quantum principle (the interference between wavefunctions for paths passing on either side of a solenoid, the *reason* for the surprising result is the *non-trivial topology of the experimental setup*, which can be understood in classical terms.

Let's now analyze the Aharonov–Bohm experiment and the implications of the observed experimental result. Our discussion will be patterned after that in Ref. [38].

21.5.1 Experimental Setup

An experimental setup to test the Aharonov–Bohm effect is illustrated in Fig. 21.1(a). It is a two-slit, electron-scattering interference experiment, with a long, thin solenoid is placed behind the screen and between the two classical paths that electrons passing through the slits would follow to reach the screen. The solenoid confines the magnetic field to regions that that classically the electrons cannot pass through, but experiments show that the solenoid alters the interference pattern for the electrons scattering through the two slits

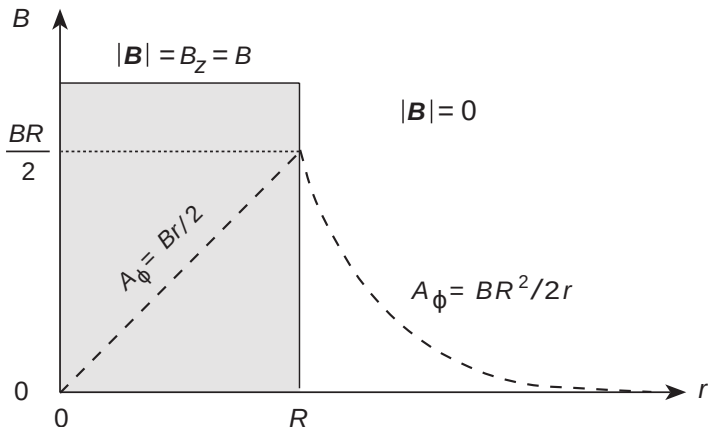

Fig. 21.2 Magnetic field B and vector potential A_ϕ for a solenoid of radius R in Fig. 21.1(a).

[24]. We now show that this results from the gauge symmetry of the electromagnetic field and the non-trivial topology of the scattering plane due to the solenoid [64].

21.5.2 Analysis of Magnetic Fields

From Fig. 21.1(a), the phase difference between waves of de Broglie wavelength λ associated with paths 1 and 2 is $\delta = 2\pi a/\lambda$, implying that $x \simeq L\lambda\delta/2\pi d$, where we've assumed $a \simeq (x/L)d$ for $x \ll L$. In the cylindrical coordinate system of Fig. 21.1(b) the vector potential takes the form

$$\begin{aligned} \text{Inside solenoid:} \quad & A_r = A_z = 0 \qquad A_\phi = \frac{Br}{2}, \\ \text{Outside solenoid:} \quad & A_r = A_z = 0 \qquad A_\phi = \frac{BR^2}{2r}, \end{aligned} \tag{21.20}$$

so that the components of the magnetic field $\boldsymbol{B} = \boldsymbol{\nabla} \times \boldsymbol{A}$ are

$$\begin{aligned} \text{Inside solenoid:} \quad & B_r = 0 \qquad B_\phi = 0 \qquad B_z = B, \\ \text{Outside solenoid:} \quad & B_r = 0 \qquad B_\phi = 0 \qquad B_z = 0. \end{aligned} \tag{21.21}$$

Outside the solenoid the magnetic field $\boldsymbol{B}$ vanishes but the vector potential A_ϕ remains finite, falling off as $1/r$ for $r > R$ (Fig. 21.2). Experimentally, one can use a very thin solenoid and shielding to ensure that the electrons never enter the solenoid and therefore never encounter a finite magnetic field. Classically, a particle of charge q in an electromagnetic field experiences a Lorentz force, $\boldsymbol{F} = q(\boldsymbol{E} + \boldsymbol{v} \times \boldsymbol{B})$, where $\boldsymbol{v}$ the velocity, $\boldsymbol{E}$ the electric field and $\boldsymbol{B}$ the magnetic field. Thus classically electrons experience no Lorentz force in the Aharonov–Bohm experiment. However, the electrons pass through regions where vector potential is finite, which has non-trivial implications in quantum theory.

21.5.3 Phase of the Electron Wavefunction

The free-electron wavefunction is $\psi = |\psi| e^{i\alpha}$, where $\alpha \equiv \boldsymbol{p} \cdot \boldsymbol{r}/\hbar$. Gauge invariance requires the minimal substitution $\boldsymbol{p} \to \boldsymbol{p} - e\boldsymbol{A}$, where $\boldsymbol{A}$ is the 3-vector potential, altering the electron phase to,

$$\alpha \to \frac{1}{\hbar}(\boldsymbol{p} \cdot \boldsymbol{r} - e\boldsymbol{A} \cdot \boldsymbol{r}) = \alpha - \frac{e}{\hbar}\, \boldsymbol{A} \cdot \boldsymbol{r}.$$

Then over a trajectory τ the change in phase is

$$\Delta\alpha = -\frac{e}{\hbar} \int_\tau \boldsymbol{A} \cdot d\boldsymbol{r}, \tag{21.22}$$

and the shift in phase between trajectories 1 and 2 is

$$\Delta\delta = \frac{e}{\hbar} \left(\int_1 \boldsymbol{A} \cdot d\boldsymbol{r} - \int_2 \boldsymbol{A} \cdot d\boldsymbol{r} \right) = \frac{e}{\hbar} \oint \boldsymbol{A} \cdot d\boldsymbol{r}. \tag{21.23}$$

Now apply Stokes' theorem:

$$\oint_C \boldsymbol{A} \cdot d\boldsymbol{r} = \int_S (\boldsymbol{\nabla} \times \boldsymbol{A}) \cdot \boldsymbol{n}\, dS \equiv \int_S (\boldsymbol{\nabla} \times \boldsymbol{A}) \cdot d\boldsymbol{S}, \tag{21.24}$$

where $\boldsymbol{S}$ is the surface enclosed by the contour C and $\boldsymbol{n}$ is an outward normal to the surface, giving

$$\Delta\delta = \frac{e}{\hbar}\, \Phi \qquad \Phi \equiv \pi R^2 B, \tag{21.25}$$

where Φ is the magnetic flux through the solenoid. Thus, the solenoid shifts the interference pattern of Fig. 21.1(a) by

$$\Delta x = \frac{L\lambda}{2\pi d}\, \Delta\delta = \frac{L\lambda}{2\pi d}\, \frac{e}{\hbar}\, \Phi, \tag{21.26}$$

even though the electrons never encounter the magnetic field $\boldsymbol{B}$. This predicted shift has been verified experimentally.

21.5.4 Topological Origin

As was discussed more extensively in Section 19.4.8, the origin of the Aharonov–Bohm effect is that the piercing of the 2D plane by the solenoid implies a non-trivial topology because the connectivity of the space is non-trivial. For example, a closed path that winds once clockwise around the the solenoid cannot be deformed continuously into a path that winds twice around it in a clockwise direction.

21.6 Primacy of the Potentials

Two pieces of evidence that become completely clear only in a full quantum treatment of electromagnetism demonstrate that it is the magnetic vector potential potential $\boldsymbol{A}$ and

the scalar potential Φ that are fundamental in electromagnetism, *not* the magnetic field $\boldsymbol{B}$ and the electric field $\boldsymbol{E}$:

1. The gauge invariant coupling of charged particles and the electromagnetic field can be implemented only through the *minimal coupling prescription* described in Section 21.2, which requires the 4-vector potential A_μ and cannot be formulated in terms of the electric and magnetic fields.
2. The *Aharonov–Bohm effect* described in Section 21.5 can be accounted for only through the influence of the magnetic vector potential $\boldsymbol{A}$, not through the magnetic field $\boldsymbol{B}$, which the test particle never encounters.

This primacy of the scalar and vector potentials is contrary to what one would infer from classical electromagnetism alone, where the Maxwell equations and Lorentz force implementing the full scope of classical electromagnetism are defined in terms of the electric and magnetic fields, and the vector and scalar potentials seem to be only optional mathematical conveniences.

Background and Further Reading

Chapter 9 of Wald [74] elaborates on some of the themes of this chapter. Gauge field theories in elementary particle physics are described in Guidry [34] and gauge fields in modern quantum field theory are discussed extensively from the perspective of symmetry and broken symmetry in Guidry and Sun [38].

Problems

21.1 The Euler–Lagrange equation (20.6) is used in a field-theory context in this chapter, but it is applicable to a broad range of problems. Show that inserting a Lagrangian $L(x, \dot{x}) = \frac{1}{2}\dot{m}^2 - V(x)$ in Eq. (20.6) leads to Newton's 2nd law of motion.

21.2 Show that if Eq. (21.19) is true, the charge Q defined in Eq. (21.16) is conserved. *Hint*: Use the Heisenberg equation of motion (21.18).

21.3 Show that the Lagrangian density of Eq. (20.13) leads to the field equation (18.52) for a free field in electromagnetism.

21.4 Use Eqs. (20.19) and (20.13) to write the Lagrangian density corresponding to non-interacting Dirac and electromagnetic fields. Introduce a gauge-invariant coupling between the fields by the minimal substitution, $\partial_\mu \to \partial_\mu + ieA_\mu$, where e is the charge of the particle described by the Dirac field and A_μ is the vector potential field associated with electromagnetism, to give a Lagrangian density

$$\mathcal{L} = \overline{\psi}(i\not{\partial} - m)\psi - \frac{1}{4}F_{\mu\nu}F^{\mu\nu} - e\overline{\psi}\not{A}\psi$$

(where $\not{A} \equiv \gamma_\mu A^\mu$ and $\not{\partial} \equiv \gamma_\mu \partial^\mu$), indicating that the minimal substitution has introduced an interaction term $\mathcal{L}_{\text{int}} = -e\overline{\psi}\not{A}\psi$ between the fields. Show that independent variation of this Lagrangian density with respect to the fields leads to the coupled equations of motion

$$(i\not{\partial} - m)\psi(x) = e\not{A}(x)\psi(x),$$
$$\partial_\nu F^{\mu\nu}(x) = e\overline{\psi}(x)\gamma^\mu\psi(x),$$

for the charged fermion and electromagnetic fields. ***

Numerical and GenAI Problems

A Appendix A Mathematics Review

This Appendix reviews mathematics required in this book. Readers are assumed to have prior acquaintance with this and mostly we list equations and concepts without proof. Books such as Griffiths [33] or Schey [67] may be consulted for proofs and more detail.

A.1 Vectors and other Tensors

Every physics student learns at her mother's knee that vectors have magnitude and direction, so they are specified by more than one number, and that this is indicated graphically by an arrow, with length indicating magnitude and orientation indicating direction. This view of vectors as directed line segments works in introductory physics but it can lead to erroneous views. For example, the directed line segment invites one to think of vectors as connecting two points in a manifold. This is wrong: a vector is *defined at a single point*; it does *not* connect two points. We can often get away with this sloppy thinking for flat manifolds, but how is one to interpret an extended straight line segment in a curved manifold? A more rigorous definition is required for advanced applications, particularly if the space is curved and/or described by non-cartesian coordinates.

At a somewhat more rigorous level, vectors are a special case of *tensors*, which we may think of (with the naive pragmatism of physicists unconstrained by rigorous mathematical training) as objects that obey particular transformation laws under a change of coordinate system, and that require n indices when expanded in a basis, with n termed the *rank* of the tensor. General transformation laws for 4D spacetime tensors with $n < 3$ are

$$\phi'(x') = \phi(x) \qquad \text{(Scalar)}, \tag{A.1a}$$

$$V'^{\mu}(x') = \frac{\partial x'^{\mu}}{\partial x^{\nu}} V^{\nu}(x) \qquad \text{(Vector)}, \tag{A.1b}$$

$$V'_{\mu}(x') = \frac{\partial x^{\nu}}{\partial x'^{\mu}} V_{\nu}(x) \qquad \text{(Dual vector)}, \tag{A.1c}$$

$$T'_{\mu\nu}(x') = \frac{\partial x^{\alpha}}{\partial x'^{\mu}} \frac{\partial x^{\beta}}{\partial x'^{\nu}} T_{\alpha\beta}(x) \qquad \text{(Covariant rank-2 tensor)}, \tag{A.1d}$$

$$T'^{\nu}{}_{\mu}(x') = \frac{\partial x^{\alpha}}{\partial x'^{\mu}} \frac{\partial x'^{\nu}}{\partial x^{\beta}} T^{\beta}{}_{\alpha}(x) \qquad \text{(Mixed rank-2 tensor)}, \tag{A.1e}$$

$$T'^{\mu\nu}(x') = \frac{\partial x'^{\mu}}{\partial x^{\alpha}} \frac{\partial x'^{\nu}}{\partial x^{\beta}} T^{\alpha\beta}(x) \qquad \text{(Contravariant rank-2 tensor)}. \tag{A.1f}$$

In these equations, unprimed coordinates refer to the original coordinate system, primed coordinates refer to the transformed coordinate system, and all partial derivatives in the general case depend on the spacetime coordinates and are understood to be evaluated at a specific spacetime point labeled by x in one coordinate system and by x' in the other coordinate system.[1] Note that we are using the usual conventions of special relativity, where the manifold is considered to be 4D spacetime [Minkowski space with coordinates ct, x, y, z)] and the use of greek indices signifies that the index can range over the time and all three spatial components.

Furthermore, in Eqs. (A.1) (and in various other places in these lectures) we employ the *Einstein summation convention*, where a repeated index, once in an upper position and once in a lower position signifies an implicit summation on that index. For example, from Eqs. (A.1) for vectors and contravariant rank-2 tensors, respectively,

$$V'^{\mu}(x') = \frac{\partial x'^{\mu}}{\partial x^{\nu}} V^{\nu}(x) \equiv \sum_{\nu} \frac{\partial x'^{\mu}}{\partial x^{\nu}} V^{\nu}(x),$$

$$T'^{\mu\nu}(x') = \frac{\partial x'^{\mu}}{\partial x^{\alpha}} \frac{\partial x'^{\nu}}{\partial x^{\beta}} T^{\alpha\beta}(x) \equiv \sum_{\alpha} \sum_{\beta} \frac{\partial x'^{\mu}}{\partial x^{\alpha}} \frac{\partial x'^{\nu}}{\partial x^{\beta}} T^{\alpha\beta}(x).$$

Note that a repeated index on the right side does not appear on the left side of the equation because it has been summed over, and indices that aren't repeated on the right side of the equation appear in the same positions (upper or lower) on the left side of the equation.

Before proceeding, let us concede that we are being rather sloppy mathematically by referring to objects carrying indices and obeying particular transformation laws as tensors. The indexed quantities appearing in Eqs. (A.1) are actually *tensor components* that have been expressed in a particular basis. Tensors are *geometrical objects,* meaning that their properties are *independent of expression in a particular basis*, as explained further in Box A.1. For example,

1. A *rank-0 tensor* or *scalar* transforms as $\phi'(x') = \phi(x)$ (it is unchanged by a coordinate transformation) and requires a single real number to specify it. "Ordinary numbers", such the age of your dog in years, are scalars.
2. There are two kinds of *rank-1 tensors*. Loosely in physics applications they are often both termed vectors, and the distinction is not of much practical importance for cartesian coordinates in non-curved spaces. However, in the general case of non-cartesian coordinate systems in possibly curved spaces, mathematical consistency requires that one must distinguish

[1] The partial derivatives in Eqs. (A.1) are generally functions of the spacetime coordinate but for the special case of flat Minkowski space and special relativity they are constants taking the same value at each spacetime point. A transformation where points in spacetime are merely relabeled in a new coordinate system is termed a *passive transformation.* A simple example is a plot displayed in cartesian coordinates (x, y, z) that is replotted in spherical polar coordinates (r, θ, ϕ). The physical content is unchanged but each point formerly labeled by values of the old coordinates (x, y, z) is now labeled by values of the new coordinates (r, θ, ϕ).

a. *vectors* (also called *contravariant vectors*), which transform as Eq. (A.1b),

$$V'^{\mu}(x') = \frac{\partial x'^{\mu}}{\partial x^{\nu}} V^{\nu}(x) \equiv \sum_{\nu} \frac{\partial x'^{\mu}}{\partial x^{\nu}} V^{\nu}(x),$$

and require a single index in an upper position, V^{α}, when expanding in a basis, from

b. *dual vectors* (also called *covariant vectors* or *1-forms*), which transform as Eq. (A.1c),

$$V'_{\mu}(x') = \frac{\partial x^{\nu}}{\partial x'^{\mu}} V_{\nu}(x),$$

and require a single index in a lower position, V_{α}, when expanded in a basis.

3. *Rank-2 tensors* require two indices, when expanding in a basis. Generalizing the distinction between vectors and dual vectors for rank-1 tensors when expanding in a basis, the two indices required for rank-2 tensor components can be in upper or lower positions, so there are three kinds of rank-2 tensors.

a. *Contravariant rank-2 tensors*, which transform as Eq. (A.1f),

$$T'^{\mu\nu} = \frac{\partial x'^{\mu}}{\partial x^{\alpha}} \frac{\partial x'^{\nu}}{\partial x^{\beta}} T^{\alpha\beta},$$

and require two indices in an upper position, $T^{\alpha\beta}$, when expanding in a basis.

b. *Covariant rank-2 tensors*, which transform as Eq. (A.1d),

$$T'_{\mu\nu} = \frac{\partial x^{\alpha}}{\partial x'^{\mu}} \frac{\partial x^{\beta}}{\partial x'^{\nu}} T_{\alpha\beta},$$

and require a two indices in a lower position, $T_{\alpha\beta}$, when expanding in a basis.

c. *Mixed rank-2 tensors*, which transform as Eq. (A.1e),

$$T'^{\nu}{}_{\mu} = \frac{\partial x^{\alpha}}{\partial x'^{\mu}} \frac{\partial x'^{\nu}}{\partial x^{\beta}} T^{\beta}{}_{\alpha},$$

and require a one index in a lower position and one in an upper position, $T^{\beta}{}_{\alpha}$, when expanding in a basis.

In a similar way, tensors of higher rank can be defined. For most physics applications tensors of rank 0, 1, and 2 are sufficient, but some applications require tensors of rank greater than two. For example, the curvature of 4D spacetime in general relativity is described by a rank-4 tensor called the *Riemann curvature tensor*, which may be viewed as the generalization of gaussian curvature from 2D space to 4D spacetime.

A.2 Vector Algebra

The *scalar product* of two vectors is

$$\boldsymbol{A} \cdot \boldsymbol{B} = AB\cos\theta \qquad \text{(Scalar product)}, \tag{A.2}$$

Box A.1 Geometrical Definition of Tensors

Tensors in Eqs. (A.1) were introduced in terms of the the transformation properties of their components when they are expressed a basis. For real physics or engineering problems it is often simplest to work with the components of tensors expressed in a basis rather than with the tensors themselves, so this is of practical utility. However, viewing tensors in terms of basis components obscures considerable mathematical beauty and elegance associated with tensor properties being independent of expression in any particular basis. Thus mathematicians prefer to define tensors *geometrically* (independent of expression in a particular basis), in terms of linear maps to the real numbers. For example,

1. a dual vector is mathematically an operator that accepts a vector as input and returns a real number, or
2. a dual vector is an object with components (when expanded in a basis) that transforms as Eq. (A.1c),

$$V'_\mu(x') = \frac{\partial x^\nu}{\partial x'^\mu} V_\nu(x),$$

at a point labeled by x in one coordinate system and by x' in a second coordinate system.

The two approaches embody different tradeoffs between utility and elegance, but lead to the same physical results if manipulated correctly. A more extensive discussion of these ideas and a general introduction to spacetime tensors in possibly curved spacetime as the basis for describing special and general relativity may be found in Ref. [36].

where θ is the angle between the vectors $\boldsymbol{A}$ and $\boldsymbol{B}$. The *vector product* or *cross product* of two vectors is

$$\boldsymbol{A} \times \boldsymbol{B} = AB \sin\theta \hat{\boldsymbol{n}} = \begin{vmatrix} \hat{\boldsymbol{x}} & \hat{\boldsymbol{y}} & \hat{\boldsymbol{z}} \\ B_x & B_y & B_z \\ C_x & C_y & C_z \end{vmatrix} \qquad \text{(Vector or cross product)}, \tag{A.3}$$

where $|\,|$ indicates the determinant, $\hat{\boldsymbol{n}}$ is a unit vector perpendicular to the plane containing $\boldsymbol{A}$ and $\boldsymbol{B}$ (with ambiguity of up and down resolved by the *right-hand rule*), θ is the angle between $\boldsymbol{A}$ and $\boldsymbol{B}$, and the cartesian unit vectors are denoted by $(\hat{\boldsymbol{x}}, \hat{\boldsymbol{y}}, \hat{\boldsymbol{z}})$. *Note*: The cross product doesn't commute: $\boldsymbol{A} \times \boldsymbol{B} \neq \boldsymbol{B} \times \boldsymbol{A}$, but the scalar product does: $\boldsymbol{A} \cdot \boldsymbol{B} = \boldsymbol{B} \cdot \boldsymbol{A}$.

The *scalar triple product* is

$$\boldsymbol{A} \cdot (\boldsymbol{B} \times \boldsymbol{C}) = \boldsymbol{B} \cdot (\boldsymbol{C} \times \boldsymbol{A}) = \boldsymbol{C} \cdot (\boldsymbol{A} \times \boldsymbol{B}) = \begin{vmatrix} A_x & A_y & A_z \\ B_x & B_y & B_z \\ C_x & C_y & C_z \end{vmatrix}. \tag{A.4}$$

The *vector triple product* is

$$\boldsymbol{A} \times (\boldsymbol{B} \times \boldsymbol{C}) = \boldsymbol{B}\,(\boldsymbol{A} \cdot \boldsymbol{C}) - \boldsymbol{C}\,(\boldsymbol{A} \cdot \boldsymbol{B}). \tag{A.5}$$

A.3 Useful Vector Identities

Some identities that are useful in manipulating vector equations are collected here, with $\boldsymbol{A}$ assumed to be an arbitrary vector and f assumed to be an arbitrary scalar.

$$\boldsymbol{\nabla} \cdot (\boldsymbol{\nabla} \times \boldsymbol{A}) = 0, \tag{A.6}$$

$$\boldsymbol{\nabla} \times (\boldsymbol{\nabla} f) = 0, \tag{A.7}$$

$$\boldsymbol{\nabla} \times (\boldsymbol{\nabla} \times \boldsymbol{A}) = \boldsymbol{\nabla}(\boldsymbol{\nabla} \cdot \boldsymbol{A}) - \nabla^2 \boldsymbol{A}. \tag{A.8}$$

Proofs may be found in standard books such as Griffiths [33].

A.4 Vector Calculus

Let's now consider the extension of the principles of calculus to vector equations, first for derivatives and then for integrals.

A.4.1 First Derivatives

The *gradient* $\boldsymbol{\nabla}$ of a scalar function F,

$$\boldsymbol{\nabla} F = \frac{\partial F}{\partial x}\,\hat{\boldsymbol{x}} + \frac{\partial F}{\partial y}\,\hat{\boldsymbol{y}} + \frac{\partial F}{\partial z}\,\hat{\boldsymbol{z}} \qquad \text{(Gradient)}, \tag{A.9}$$

is a vector quantity. The gradient can be viewed as a vector operator

$$\boldsymbol{\nabla} = \hat{\boldsymbol{x}}\,\frac{\partial}{\partial x} + \hat{\boldsymbol{y}}\,\frac{\partial}{\partial y} + \hat{\boldsymbol{z}}\,\frac{\partial}{\partial z} \qquad \text{(Gradient operator)} \tag{A.10}$$

that acts upon a scalar argument following it. The notation $\boldsymbol{\nabla}_x$ means explicitly that the gradient acts on the coordinate $\boldsymbol{x}$ while $\boldsymbol{\nabla}_{x'}$ means that the gradient acts on the coordinates $\boldsymbol{x}'$. (In the text we will often use the abbreviations $\boldsymbol{\nabla} \equiv \boldsymbol{\nabla}_x$ and $\boldsymbol{\nabla}' \equiv \boldsymbol{\nabla}_{x'}$.

Useful identities involving the gradient and Laplacian:

$$\boldsymbol{\nabla}_x\left(\frac{1}{|\boldsymbol{x}-\boldsymbol{x}'|}\right) = -\frac{\boldsymbol{x}-\boldsymbol{x}'}{|\boldsymbol{x}-\boldsymbol{x}'|^3}, \tag{A.11a}$$

$$\boldsymbol{\nabla}_{x'}\left(\frac{1}{|\boldsymbol{x}-\boldsymbol{x}'|}\right) = \frac{\boldsymbol{x}-\boldsymbol{x}'}{|\boldsymbol{x}-\boldsymbol{x}'|^3}, \tag{A.11b}$$

$$\boldsymbol{\nabla}_x\left(\frac{\boldsymbol{x}-\boldsymbol{x}'}{|\boldsymbol{x}-\boldsymbol{x}'|^3}\right) = 4\pi\delta(\boldsymbol{x}-\boldsymbol{x}'), \tag{A.11c}$$

$$\boldsymbol{\nabla}_{x'}\left(\frac{\boldsymbol{x}-\boldsymbol{x}'}{|\boldsymbol{x}-\boldsymbol{x}'|^3}\right) = -4\pi\delta(\boldsymbol{x}-\boldsymbol{x}'), \tag{A.11d}$$

$$\boldsymbol{\nabla}_x^2\left(\frac{1}{|\boldsymbol{x}-\boldsymbol{x}'|}\right) = \boldsymbol{\nabla}_{x'}^2\left(\frac{1}{|\boldsymbol{x}-\boldsymbol{x}'|}\right) = -4\pi\delta(\boldsymbol{x}-\boldsymbol{x}'), \tag{A.11e}$$

It will be useful to define the completely antisymmetric rank-3 tensor (Levi–Civita symbol) by

$$\epsilon_{ijk} = \begin{cases} 1 & (\text{If } i,j,k \text{ is cyclic permutation of } 1,2,3), \\ -1 & (\text{If } i,j,k \text{ is cyclic permutation of } 1,2,3), \\ 0 & (\text{Otherwise}), \end{cases} \tag{A.12}$$

The ϵ_{ijk} obey two important identities

$$\begin{aligned}\epsilon_{ijk}\epsilon_{lmn} = {} & \delta_{il}\delta_{jm}\delta_{kn} + \delta_{jl}\delta_{km}\delta_{in} + \delta_{kl}\delta_{im}\delta_{jn} \\ & - \delta_{jl}\delta_{im}\delta_{kn} - \delta_{kl}\delta_{jm}\delta_{in} - \delta_{il}\delta_{km}\delta_{jn},\end{aligned} \tag{A.13}$$

and

$$\sum_i \epsilon_{ijk}\epsilon_{imn} = \delta_{jm}\delta_{kn} - \delta_{km}\delta_{jn}. \tag{A.14}$$

The *divergence* of a vector $\boldsymbol{V}$ is

$$\boldsymbol{\nabla}\cdot V = \frac{\partial V_x}{\partial x} + \frac{\partial V_y}{\partial y} + \frac{\partial V_z}{\partial z} \qquad \text{(Divergence)}. \tag{A.15}$$

Note: The divergence of a vector is a scalar. The *curl* $(\boldsymbol{\nabla}\times)$ of a vector $\boldsymbol{V}$ is

$$\begin{aligned}\boldsymbol{\nabla}\times\boldsymbol{V} &= \begin{vmatrix} \hat{\boldsymbol{x}} & \hat{\boldsymbol{y}} & \hat{\boldsymbol{z}} \\ \frac{\partial}{\partial x} & \frac{\partial}{\partial y} & \frac{\partial}{\partial z} \\ V_x & V_y & V_z \end{vmatrix} \\ &= \left(\frac{\partial V_z}{\partial y} - \frac{\partial V_y}{\partial z}\right)\hat{\boldsymbol{x}} + \left(\frac{\partial V_x}{\partial z} - \frac{\partial V_z}{\partial x}\right)\hat{\boldsymbol{y}} + \left(\frac{\partial V_y}{\partial x} - \frac{\partial V_x}{\partial y}\right)\hat{\boldsymbol{z}} \quad \text{(Curl)},\end{aligned} \tag{A.16}$$

which can also be written as

$$(\boldsymbol{A}\times\boldsymbol{B})_i = \sum_{jk}\epsilon_{ijk}A_jB_k \tag{A.17}$$

Note: The curl of a vector is a vector.

Derivatives of products appear commonly in realistic problems and product rules for vector derivatives can be proved that are similar to product rules for ordinary derivatives. For example,

$$\boldsymbol{\nabla}(fg) = f\boldsymbol{\nabla}g + g\boldsymbol{\nabla}f, \tag{A.18a}$$

$$\boldsymbol{\nabla}(\boldsymbol{A}\cdot\boldsymbol{B}) = \boldsymbol{A}\times(\boldsymbol{\nabla}\times\boldsymbol{B}) + \boldsymbol{B}\times(\boldsymbol{\nabla}\times\boldsymbol{A}) + (\boldsymbol{A}\cdot\boldsymbol{\nabla})\,\boldsymbol{B} + (\boldsymbol{B}\cdot\boldsymbol{\nabla})\,\boldsymbol{A}, \tag{A.18b}$$

$$\boldsymbol{\nabla}\cdot(f\boldsymbol{A}) = f(\boldsymbol{\nabla}\cdot\boldsymbol{A}) + \boldsymbol{A}\cdot(\boldsymbol{\nabla}f), \tag{A.18c}$$

$$\boldsymbol{\nabla}\cdot(\boldsymbol{A}\times\boldsymbol{B}) = \boldsymbol{B}\cdot(\boldsymbol{\nabla}\times\boldsymbol{A}) - \boldsymbol{A}\cdot(\boldsymbol{\nabla}\times\boldsymbol{B}), \tag{A.18d}$$

$$\boldsymbol{\nabla}\times(f\boldsymbol{A}) = f(\boldsymbol{\nabla}\times\boldsymbol{A}) - \boldsymbol{A}\times(\boldsymbol{\nabla}f), \tag{A.18e}$$

$$\boldsymbol{\nabla}\times(\boldsymbol{A}\times\boldsymbol{B}) = (\boldsymbol{B}\cdot\boldsymbol{\nabla})\boldsymbol{A} - (\boldsymbol{A}\cdot\boldsymbol{\nabla})\boldsymbol{B} + \boldsymbol{A}(\boldsymbol{\nabla}\cdot\boldsymbol{B}) - \boldsymbol{B}(\boldsymbol{\nabla}\cdot\boldsymbol{A}), \tag{A.18f}$$

where $\boldsymbol{A}$ and $\boldsymbol{B}$ are arbitrary vectors and f and g are arbitrary scalar functions,

A.4.2 Directional Derivative and Normal Derivative

One often needs to know how a scalar field changes while moving in a specific direction, or how it behaves at a boundary between media. These concepts are captured by the *directional derivative* and its specific case, the *normal derivative*.

Directional Derivative: A directional derivative measures the rate of change of a scalar function $f(\boldsymbol{x})$ as you move along a unit vector $\boldsymbol{u}$. Given a gradient field of a field $\boldsymbol{\nabla}f$, the directional derivative in the direction $\boldsymbol{u}$ is the scalar projection of the gradient onto that direction; denoting the directional derivative in the direction $\boldsymbol{u}$ of a scalar function $f(\boldsymbol{x})$ by

$$D_{\boldsymbol{u}}f = \boldsymbol{\nabla}f\cdot\boldsymbol{u}. \tag{A.19}$$

Example: The component of the electric field $\boldsymbol{E} = -\boldsymbol{\nabla}\Phi$ in a direction $\boldsymbol{u}$ is

$$E_u = -\frac{\partial\Phi}{\partial u} = -(\boldsymbol{\nabla}\Phi\cdot\boldsymbol{u}).$$

Normal Derivative: A normal derivative is a specific type of directional derivative where the direction is chosen to be the unit normal vector $\hat{\boldsymbol{n}}$ perpendicular to a surface S. It is typically denoted as:

$$\frac{\partial f}{\partial n} = \boldsymbol{\nabla}f\cdot\hat{\boldsymbol{n}},$$

where $f(\boldsymbol{x})$ is a scalar function and $\boldsymbol{n}$ is the outward normal unit vector.

Example: On the surface of a conductor, the tangential electric field is zero and the entire electric field outside the surface is radial and proportional to the normal derivative of the potential $\Phi(\boldsymbol{x})$,

$$E_n = -\frac{\partial\Phi}{\partial n} = \frac{\sigma}{\epsilon_0},$$

where $\sigma(\boldsymbol{x})$ is the surface charge density. Properties and usage of directional and normal derivative are summarized in Table A.1.

Table A.1 Directional and normal derivatives

Derivative type	Direction	Mathematical form	Common E&M context
Directional	Any unit vector $\hat{\boldsymbol{u}}$	$\boldsymbol{\nabla}\Phi \cdot \hat{\boldsymbol{u}}$	Field components in arbitrary directions
Normal	Perpendicular to surface $\hat{\boldsymbol{n}}$	$\boldsymbol{\nabla}\Phi \cdot \hat{\boldsymbol{n}}$	Calculating surface charge; application of Neumann boundary conditions

A.4.3 Second Derivatives

As shown above in Section A.4.1, the first derivatives that can be constructed using the operator $\boldsymbol{\nabla}$ defined in Eq. (A.10) are

1. the *gradient* of a scalar, $\boldsymbol{\nabla} f$,
2. the *divergence* of a vector, $\boldsymbol{\nabla} \cdot \boldsymbol{A}$, and
3. the *curl* of a vector, $\boldsymbol{\nabla} \times \boldsymbol{A}$.

Second derivatives can be constructed by applying two first-derivative operators in succession. Lets consider the possibilities for second derivatives in vector equations.

1. The *divergence of a gradient*, $\boldsymbol{\nabla} \cdot (\boldsymbol{\nabla} f)$, gives in cartesian coordinates

$$\begin{aligned}\boldsymbol{\nabla} \cdot (\boldsymbol{\nabla} f) &= \left(\hat{\boldsymbol{x}}\,\frac{\partial}{\partial x} + \hat{\boldsymbol{y}}\,\frac{\partial}{\partial y} + \hat{\boldsymbol{z}}\,\frac{\partial}{\partial z}\right) \cdot \left(\hat{\boldsymbol{x}}\,\frac{\partial f}{\partial x} + \hat{\boldsymbol{y}}\,\frac{\partial f}{\partial y} + \hat{\boldsymbol{z}}\,\frac{\partial f}{\partial z}\right) \\ &= \frac{\partial^2 f}{\partial x^2} + \frac{\partial^2 f}{\partial y^2} + \frac{\partial^2 f}{\partial z^2}.\end{aligned}$$

This second derivative operator appears often and it is useful to define it as ∇^2; this is called the *Laplacian operator*, and we rewrite the preceding result as

$$\nabla^2 f = \frac{\partial^2 f}{\partial x^2} + \frac{\partial^2 f}{\partial y^2} + \frac{\partial^2 f}{\partial z^2}. \tag{A.20}$$

Notice that *the Laplacian applied to a scalar gives a scalar.*

2. The *curl of a gradient is always equal to zero*, $\boldsymbol{\nabla} \times (\boldsymbol{\nabla} f) = 0$, by the identity (A.7).

3. The *gradient of a divergence* $\boldsymbol{\nabla}(\boldsymbol{\nabla} \cdot \boldsymbol{A})$ is a valid mathematical operation but it is relatively uncommon in physical problems and has no special name.

4. The *divergence of a curl always vanishes*, $\boldsymbol{\nabla} \cdot (\boldsymbol{\nabla} \times \boldsymbol{A}) = 0$, by the identity (A.6).

5. The *curl of a curl* evaluates to

$$\boldsymbol{\nabla} \times (\boldsymbol{\nabla} \times \boldsymbol{A}) = \boldsymbol{\nabla}(\boldsymbol{\nabla} \cdot \boldsymbol{A}) - \nabla^2 \boldsymbol{A}$$

[see identity (A.8)], which gives nothing new since the first term on the right is just a number and the second is the Laplacian of a vector, which we considered in Eq. (A.20).

Thus we need consider only two kinds of second derivatives: (1) the Laplacian in Eq.

(A.20), which will play a fundamental role in electromagnetism, and the gradient of the divergence, which isn't very common. By similar procedures we could evaluate third derivatives in vector equations, but we will omit them since they seldom occur for the types of problems that we shall encounter.

A.4.4 Integrals

A *line integral* (or *path integral*) of a vector function $\boldsymbol{V}$ between points $\boldsymbol{A}$ and $\boldsymbol{B}$ is given by

$$\int_{\boldsymbol{A}}^{\boldsymbol{B}} \boldsymbol{V} \cdot d\boldsymbol{l} \qquad d\boldsymbol{l} \equiv \hat{\boldsymbol{x}}\, dx + \hat{\boldsymbol{y}}\, dy + \hat{\boldsymbol{z}}\, dz \qquad \text{(Line integral).} \tag{A.21}$$

The integral is carried out over a prescribed path from $\boldsymbol{A}$ to $\boldsymbol{B}$, with $d\boldsymbol{l}$ the infinitesimal displacement vector along the specified path (with magnitude equal to the length of the infinitesimal displacement and direction tangent to the path at that point). If the line integral is carried out over a closed loop ($\boldsymbol{B} = \boldsymbol{A}$), the line integral is called a *cyclic integral* and denoted

$$\oint \boldsymbol{V} \cdot d\boldsymbol{l} \qquad \text{(Closed line integral).} \tag{A.22}$$

A *surface integral* of a vector function $\boldsymbol{V}$ over a surface S is denoted by

$$\int_S \boldsymbol{V} \cdot d\boldsymbol{s} \qquad \text{(Surface integral),} \tag{A.23}$$

where $d\boldsymbol{s} \equiv \boldsymbol{n}\, ds$ is a vector associated with an infinitesimal patch of surface area having magnitude equal to the area of the patch and direction given by the normal $\boldsymbol{n}$ to the surface at the patch (implying that the sign is ambiguous since, there are two normals—"up" and "down"—at each point). If the surface is closed, the surface integral is denoted

$$\oint_S \boldsymbol{V} \cdot d\boldsymbol{s} \qquad \text{(Integral over closed surface),} \tag{A.24}$$

A *volume integral of a scalar function* over a volume V is indicated by

$$\int_V F\, d\tau \qquad \text{(Scalar volume integral),} \tag{A.25}$$

where F is a scalar function and $d\tau$ is an infinitesimal volume element. (For example, in cartesian coordinates $d\tau = dx\, dy\, dz$.) A *volume integral for a vector function* $\boldsymbol{F}$ is given by

$$\begin{aligned} \int \boldsymbol{F}\, d\tau &= \int_V (F_x \hat{\boldsymbol{x}} + F_y \hat{\boldsymbol{y}} + F_z \hat{\boldsymbol{z}}) \\ &= \hat{\boldsymbol{x}} \int_V F_x\, d\tau + \hat{\boldsymbol{y}} \int F_y\, d\tau + \hat{\boldsymbol{z}} \int F_z\, d\tau \qquad \text{(Vector volume integral),} \end{aligned} \tag{A.26}$$

where the unit vectors $(\hat{\boldsymbol{x}}, \hat{\boldsymbol{y}}, \hat{\boldsymbol{z}})$ have been pulled out of the integrals in the last step because they are constants.

A.5 Fundamental Theorems

Let us now list some fundamental theorems of calculus and of vector calculus that will be of use. The *fundamental theorem of (ordinary) calculus* is

$$\int_a^b \left(\frac{\partial f}{\partial x}\right) dx = \int_a^b F(x)\, dx = f(b) - f(a) \quad \text{(Fundamental theorem of calculus)}, \tag{A.27}$$

where $F(x) \equiv df/dx$. Thus the fundamental theorem of calculus tells us how to integrate $F(x)$: find a function $f(x)$ that has a derivative equal to $F(x)$, which implies that *integration and differentiation are inverse operations*. In vector calculus there are three fundamental types of derivatives:

1. the *gradient* of Eq. (A.9),
2. the *divergence* of Eq. (A.15), and
3. the *curl* of Eq. (A.16).

For each type of vector derivative one can formulate a "fundamental theorem" having the same general structure as the fundamental theorem of calculus given in Eq. (A.27):

> The integral of a derivative of a function over some region is determined by the values of the function on the boundaries of the region.

Let us consider the fundamental theorems of vector calculus for gradients, divergences, and curls.

A.5.1 Fundamental Theorem of Gradients

For *gradients*, the fundamental theorem takes the form

$$\int_{\boldsymbol{A}}^{\boldsymbol{B}} (\boldsymbol{\nabla} F) \cdot d\boldsymbol{l} = F(\boldsymbol{B}) - F(\boldsymbol{A}) \qquad \text{(Fundamental theorem of gradients)}, \tag{A.28}$$

for a scalar function $F(x, y, z)$ evaluated on a path from $\boldsymbol{A}$ to $\boldsymbol{B}$. Notice that Eq. (A.28) has the same structure as Eq. (A.27): the integral (a line integral here) of a derivative (a gradient here) is determined by the values of the function at the boundaries ($\boldsymbol{A}$ and $\boldsymbol{B}$ here).

A.5.2 Fundamental Theorem of Divergences

For *divergences*, the fundamental theorem takes the form [see Eqs. (A.24) and (A.25)],

$$\int_V (\boldsymbol{\nabla} \cdot \boldsymbol{A})\, d\tau = \oint_S \boldsymbol{A} \cdot d\boldsymbol{s} \qquad \text{(Divergence theorem)}, \tag{A.29}$$

where $\boldsymbol{A}$ is a vector field and $d\boldsymbol{s} = \boldsymbol{n}\, da$ with $\boldsymbol{n}$ the normal to the surface. This may be termed the *fundamental theorem for divergences*,[2] but it is commonly termed *the divergence theorem* in the literature and we will typically adopt that terminology.

A.5.3 Fundamental Theorem of Curls

The *fundamental theorem for curls* is given by

$$\int_S (\boldsymbol{\nabla} \times \boldsymbol{A}) \cdot d\boldsymbol{s} = \oint_P \boldsymbol{A} \cdot d\boldsymbol{l} \qquad \text{(Stokes' theorem)}, \tag{A.30}$$

where the left side is a surface integral over S and the right side is a line integral on the perimeter of the surface. This is the fundamental theorem for curls[3] but, as we have indicated, it is commonly called *Stokes' theorem* in the literature and we will typically use that terminology. Further discussion of Stokes' theorem is given in Box 2.3.

A.6 Laws, Theorems, and Definitions

Some important laws, theorems, and definitions of classical electromagnetism are listed here. In some cases both the integral and differential forms of the laws are given. Unless otherwise noted, SI units are assumed in all equations.

Coulomb's law (forces): The force between two charges is

$$\boldsymbol{F} = \frac{q_1 q_2}{4\pi\epsilon_0} \frac{\boldsymbol{x}_1 - \boldsymbol{x}_2}{|\boldsymbol{x}_1 - \boldsymbol{x}_2|^3} \tag{A.31}$$

where the charges q_1 and q_2 are located at the points $\boldsymbol{x}_1$ and $\boldsymbol{x}_2$, respectively.

Coulomb's law (electric fields): For a continuous charge distribution,

$$\boldsymbol{E}(\boldsymbol{x}) = \frac{1}{4\pi\epsilon_0} \int \rho(\boldsymbol{x}') \frac{\boldsymbol{x} - \boldsymbol{x}'}{|\boldsymbol{x} - \boldsymbol{x}'|^3}\, d^3x', \tag{A.32}$$

where $\rho(\boldsymbol{x})$ is the charge density.

Gauss's law: For a continuous charge distribution $\rho(\boldsymbol{x})$,

$$\boldsymbol{\nabla} \cdot \boldsymbol{E} = \frac{\rho}{\epsilon_0} \qquad \oint \boldsymbol{E} \cdot \boldsymbol{n}\, da = \frac{1}{\epsilon_0} \int_V \rho(\boldsymbol{x})\, d^3x, \tag{A.33}$$

where the integration is over the volume V contained within the surface S (see Fig. 2.5).

[2] Note that it has the same structure as Eq. (A.27): the integral of a derivative (here the divergence) over a region (here the volume V) is determined by the value of the function on the boundaries (the boundary of the volume V is the surface S). In this case the boundary term is a surface integral.

[3] Analogous to Eq. (A.27), the integral of a derivative (here the curl) over a region (here a patch of surface S) is determined by the value of the function on the boundary (the perimeter P of the surface patch). Notice that the boundary term in this case is itself an integral.

Divergence theorem: For a vector field defined within a volume V that is enclosed by a surface S,

$$\oint_S \boldsymbol{A} \cdot \boldsymbol{n}\, da = \int_V \boldsymbol{\nabla} \cdot \boldsymbol{A}\, d^3x, \tag{A.34}$$

where the left side is the surface integral of the outwardly directed normal component of the vector $\boldsymbol{A}$ and the right side is the volume integral of the divergence of $\boldsymbol{A}$ [equivalent to fundamental theorem for divergences given in Eq. (A.29)].

Stokes' theorem: For a 3D vector field $\boldsymbol{A}$ (see Box 2.3),

$$\oint_C \boldsymbol{A} \cdot d\boldsymbol{r} = \int_S (\boldsymbol{\nabla} \times \boldsymbol{A}) \cdot \boldsymbol{n}\, ds \equiv \int_S (\boldsymbol{\nabla} \times \boldsymbol{A}) \cdot d\boldsymbol{s}, \tag{A.35}$$

where S is the 2D surface enclosed by the 1D boundary C and the outward normal to the surface is $\mathbf{n}$ [equivalent to fundamental theorem for curls given in Eq. (A.30)].

Scalar potential: For an electric field $\boldsymbol{E}$ and scalar potential Φ,

$$\boldsymbol{E} = -\boldsymbol{\nabla}\Phi \qquad \Phi(\boldsymbol{x}) = -\int_{\mathcal{O}}^{\boldsymbol{x}} \boldsymbol{E}(\boldsymbol{x}) \cdot d\boldsymbol{l}, \tag{A.36}$$

where $\mathcal{O}$ is an arbitrary reference point.

Vector potential: The vector potential $\boldsymbol{A}$ is defined through

$$\boldsymbol{B} = \boldsymbol{\nabla} \times \boldsymbol{A}, \tag{A.37}$$

where $\boldsymbol{B}$ is the magnetic field. Eqs. (A.36) and (A.37) then allow the electric and magnetic fields to be eliminated in favor of vector and scalar potentials.

Poisson's equation: For a scalar field Φ,

$$\nabla^2\Phi = -\frac{\rho}{\epsilon_0}, \tag{A.38}$$

where the charge density is ρ.

Laplace's equation: For a scalar field Φ,

$$\nabla^2\Phi = 0. \tag{A.39}$$

This is Poisson's equation with zero charge density.

Lorentz force: For electric field $\boldsymbol{E}$ and magnetic field $\boldsymbol{B}$,

$$\boldsymbol{F} = q(\boldsymbol{E} + \boldsymbol{v} \times \boldsymbol{B}), \tag{A.40}$$

where q is the charge and $\boldsymbol{v}$ is the velocity of the particle.

A.7 Curvilinear Coordinate Systems

It is often advantageous to formulate electromagnetic problems in non-cartesian coordinates. We include some relevant equations in this Appendix for spherical coordinates and cylindrical coordinates.

A.7.1 Spherical Coordinates

The standard spherical coordinates (r, θ, ϕ) are related to cartesian coordinates (x, y, z) by

$$x = r\sin\theta\cos\phi \qquad y = r\sin\theta\sin\phi \qquad z = r\cos\theta. \tag{A.41}$$

Spherical unit vectors are related to cartesian unit vectors by

$$\begin{aligned}
\hat{\boldsymbol{r}} &= \sin\theta\cos\phi\,\hat{\boldsymbol{x}} + \sin\theta\sin\phi\,\hat{\boldsymbol{y}} + \cos\theta\,\hat{\boldsymbol{z}},\\
\hat{\boldsymbol{\theta}} &= \cos\theta\cos\phi\,\hat{\boldsymbol{x}} + \cos\theta\sin\phi\,\hat{\boldsymbol{y}} - \sin\theta\,\hat{\boldsymbol{z}},\\
\hat{\boldsymbol{\phi}} &= -\sin\phi\,\hat{\boldsymbol{x}} + \cos\phi\,\hat{\boldsymbol{y}},
\end{aligned} \tag{A.42}$$

or in matrix form, the transformation from cartesian to spherical coordinates is

$$\begin{pmatrix} \hat{\boldsymbol{r}} \\ \hat{\boldsymbol{\theta}} \\ \hat{\boldsymbol{\phi}} \end{pmatrix} = \begin{pmatrix} \sin\theta\cos\phi & \sin\theta\sin\phi & \cos\theta \\ \cos\theta\cos\phi & \cos\theta\sin\phi & -\sin\theta \\ -\sin\phi & \cos\phi & 0 \end{pmatrix} \begin{pmatrix} \hat{\boldsymbol{x}} \\ \hat{\boldsymbol{y}} \\ \hat{\boldsymbol{z}} \end{pmatrix}. \tag{A.43}$$

The transformation matrix is orthogonal so the inverse matrix is the transpose (interchange rows and columns) and the matrix transformation from spherical to cartesian coordinates is given by

$$\begin{pmatrix} \hat{\boldsymbol{x}} \\ \hat{\boldsymbol{y}} \\ \hat{\boldsymbol{z}} \end{pmatrix} = \begin{pmatrix} \sin\theta\cos\phi & \cos\theta\cos\phi & -\sin\phi \\ \sin\theta\sin\phi & \cos\theta\sin\phi & \cos\phi \\ \cos\theta & -\sin\theta & 0 \end{pmatrix} \begin{pmatrix} \hat{\boldsymbol{r}} \\ \hat{\boldsymbol{\theta}} \\ \hat{\boldsymbol{\phi}} \end{pmatrix}. \tag{A.44}$$

This means that an arbitrarary vector $\boldsymbol{V}$ can be decomposed as

$$\boldsymbol{V} = (\hat{\boldsymbol{r}}\cdot\boldsymbol{V})\hat{\boldsymbol{r}} + (\hat{\boldsymbol{\theta}}\cdot\boldsymbol{V})\hat{\boldsymbol{\theta}} + (\hat{\boldsymbol{\phi}}\cdot\boldsymbol{V})\hat{\boldsymbol{\phi}}. \tag{A.45}$$

The spherical line element is

$$d\boldsymbol{l} = dr\,\hat{\boldsymbol{r}} + r\,d\theta\hat{\boldsymbol{\theta}} + r\sin\theta d\phi\,\hat{\boldsymbol{\phi}}, \tag{A.46}$$

and the spherical volume element is

$$d\tau = r^2\sin\theta dr\,d\theta\,d\phi. \tag{A.47}$$

The vector derivatives are given by

$$\text{Gradient:} \quad \boldsymbol{\nabla} F = \frac{\partial F}{\partial r}\,\hat{\boldsymbol{r}} + \frac{1}{r}\frac{\partial F}{\partial \theta}\hat{\boldsymbol{\theta}} + \frac{1}{r\sin\theta}\frac{\partial F}{\partial \phi}\,\hat{\boldsymbol{\phi}}, \tag{A.48}$$

$$\text{Divergence:} \quad \boldsymbol{\nabla}\cdot\boldsymbol{V} = \frac{1}{r^2}\frac{\partial}{\partial r}(r^2 V_r) + \frac{1}{r\sin\theta}\frac{\partial}{\partial \theta}(\sin\theta V_\theta) + \frac{1}{r\sin\theta}\frac{\partial V_\phi}{\partial \phi}, \tag{A.49}$$

$$\begin{aligned}\text{Curl:} \quad \boldsymbol{\nabla}\times\boldsymbol{V} = {} & \frac{1}{r\sin\theta}\left[\frac{\partial}{\partial\theta}(\sin\theta V_\phi) - \frac{\partial V_\theta}{\partial\phi}\right]\hat{\boldsymbol{r}} \\ & + \frac{1}{r}\left[\frac{1}{\sin\theta}\frac{\partial V_r}{\partial\phi} - \frac{\partial}{\partial r}(rV_\phi)\right]\hat{\boldsymbol{\theta}} + \frac{1}{r}\left[\frac{\partial}{\partial r}(rV_\theta - \frac{\partial V_r}{\partial\theta}\right]\hat{\boldsymbol{\phi}},\end{aligned} \tag{A.50}$$

$$\begin{aligned}\text{Laplacian:} \quad \nabla^2 F = {} & \frac{1}{r^2}\frac{\partial}{\partial r}\left(r^2\frac{\partial F}{\partial r}\right) \\ & + \frac{1}{r^2\sin\theta}\frac{\partial}{\partial\theta}\left(\sin\theta\frac{\partial F}{\partial\theta}\right) + \frac{1}{r^2\sin^2\theta}\frac{\partial^2 F}{\partial\phi^2},\end{aligned} \tag{A.51}$$

when expressed in spherical coordinates.

A.7.2 Cylindrical Coordinates

Standard cylindrical coordinates (ρ, ϕ, z) are related to cartesian coordinates (x, y, z) by

$$x = \rho\cos\phi \qquad y = \rho\sin\phi \qquad z = z, \tag{A.52}$$

the line element is

$$d\boldsymbol{l} = d\rho\hat{\boldsymbol{\rho}} + \rho d\phi\,\hat{\boldsymbol{\phi}} + dz\,\hat{\boldsymbol{z}}, \tag{A.53}$$

and the volume element is

$$d\tau = \rho d\rho\, d\phi\, dz. \tag{A.54}$$

The vector derivatives are given by

$$\text{Gradient:} \quad \boldsymbol{\nabla} F = \frac{\partial F}{\partial \rho}\,\hat{\boldsymbol{\rho}} + \frac{1}{\rho}\frac{\partial F}{\partial \phi}\,\hat{\boldsymbol{\phi}} + \frac{\partial F}{\partial z}\,\hat{\boldsymbol{z}}, \tag{A.55}$$

$$\text{Divergence:} \quad \boldsymbol{\nabla}\cdot\boldsymbol{V} = \frac{1}{\rho}\frac{\partial}{\partial\rho}(\rho V_\rho) + \frac{1}{\rho}\frac{\partial V_\phi}{\partial\phi} + \frac{\partial V_z}{\partial z}, \tag{A.56}$$

$$\begin{aligned}\text{Curl:} \quad \boldsymbol{\nabla}\times\boldsymbol{V} = {} & \left(\frac{1}{\rho}\frac{\partial V_z}{\partial\phi} - \frac{\partial V_\phi}{\partial z}\right)\hat{\boldsymbol{\rho}} \\ & + \left(\frac{\partial V_\rho}{\partial z} - \frac{\partial V_z}{\partial\rho}\right)\hat{\boldsymbol{\phi}} + \frac{1}{\rho}\left[\frac{\partial}{\partial\rho}(\rho V_\phi - \frac{\partial V_\rho}{\partial\phi}\right]\hat{\boldsymbol{z}},\end{aligned} \tag{A.57}$$

$$\text{Laplacian:} \quad \nabla^2 F = \frac{1}{\rho}\frac{\partial}{\partial\rho}\left(\rho\frac{\partial F}{\partial\rho}\right) + \frac{1}{\rho^2}\frac{\partial^2 F}{\partial\phi^2} + \frac{\partial^2 F}{\partial z^2}, \tag{A.58}$$

when expressed in cylindrical coordinates.

A.8 Taylor Series Expansion

In one dimension a Taylor series expansion may be written for infinitesimal ϵ as

$$\begin{aligned} f(x+\epsilon) &= f(x) + \epsilon \frac{df}{dx} + \frac{1}{2!} e^2 \frac{d^2 f}{dx^2} + \cdots \\ &= \left[1 + \epsilon \frac{d}{dx} + \frac{1}{2!} \left(\epsilon \frac{d}{dx} \right)^2 + \cdots \right] f(x) = \exp\left(\epsilon \frac{d}{dx} \right) f(x). \end{aligned} \tag{A.59}$$

For a function of three variables this generalizes to

$$f(x+\epsilon_x, y+\epsilon_y, z+\epsilon_z) = \exp\left(\epsilon_x \frac{\partial}{\partial x} \right) \exp\left(\epsilon_y \frac{\partial}{\partial y} \right) \exp\left(\epsilon_z \frac{\partial}{\partial z} \right) f(x,y,z), \tag{A.60}$$

which may be written in vector notation as

$$f(\boldsymbol{r} + \boldsymbol{\epsilon}) = \exp(\boldsymbol{\epsilon} \cdot \boldsymbol{\nabla}) f(\boldsymbol{r}) = \left[1 + \boldsymbol{\epsilon} \cdot \boldsymbol{\nabla} + \frac{1}{2!} (\boldsymbol{\epsilon} \cdot \boldsymbol{\nabla})^2 + \cdots \right] f(\boldsymbol{r}). \tag{A.61}$$

A.9 Binomial Expansion

The binomial expansion is

$$(1+a)^n = 1 + na + \frac{n(n-1)}{2!} a^2 + \frac{n(n-1)(n-2)}{3!} a^3 + \cdots \tag{A.62}$$

It is particularly useful when $a \ll 1$, since then $(1+a)^n \simeq 1 + na$.

A.10 Miscellaneous Equations

LAW OF COSINES:

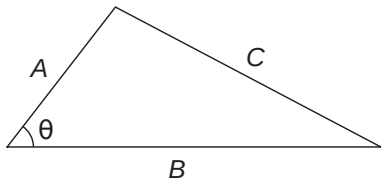

$$C^2 = A^2 + B^2 - 2AB\cos\theta \qquad \text{(Law of cosines).} \tag{A.63}$$

A.11 Integration by Parts

For scalar functions u and v, by basic calculus manipulations

$$\int_a^b \frac{d}{dx}(uv)dx = uv|_a^b = \int_a^b u\left(\frac{dv}{dx}\right)dx + \int_a^b v\left(\frac{du}{dx}\right)dx,$$

from which we may write

$$\int_a^b u\left(\frac{dv}{dx}\right)dx = uv|_a^b - \int_a^b v\left(\frac{du}{dx}\right)dx, \tag{A.64}$$

which is often expressed more compactly as

$$\int udv = uv - \int vdu. \tag{A.65}$$

This is called *integration by parts*, and is often useful when it is necessary to itegrate a function multiplied by a derivative of another function. The net effect of integration by parts is to transfer the derivative operation from one function to the other, at the expense of adding a boundary term $uv|_a^b$. For vector calculus this generalizes to equations of the form

$$\int_V \phi(\boldsymbol{\nabla}\cdot\boldsymbol{A})d\tau = -\int_V \boldsymbol{A}\cdot(\boldsymbol{\nabla}\phi)d\tau + \oint_S \phi\boldsymbol{A}\cdot d\boldsymbol{a}, \tag{A.66}$$

$$\int_S \phi(\boldsymbol{\nabla}\times\boldsymbol{A})\cdot d\boldsymbol{a} = \int_S [\boldsymbol{A}\times(\boldsymbol{\nabla}\phi)]\cdot d\boldsymbol{a} + \oint_P \phi\boldsymbol{A}\cdot d\boldsymbol{l}, \tag{A.67}$$

$$\int_V \boldsymbol{B}\cdot(\boldsymbol{\nabla}\times\boldsymbol{A})d\tau = \int_V \boldsymbol{A}\cdot(\boldsymbol{\nabla}\times\boldsymbol{B})d\tau + \oint_S (\boldsymbol{A}\times\boldsymbol{B})\cdot d\boldsymbol{a}, \tag{A.68}$$

where $\boldsymbol{A}$ and $\boldsymbol{B}$ are arbitrary vectors, ϕ is an arbitrary scalar function, a subscript V indicates a volume integral, a subscript S indicates a surface integral, and a subscript P indicates a line integral. Notice that in these expressions also one is integrating a function times a vector derivative (divergence or curl) of a function, and the operation transfers the derivative from one function to the other (as a gradient or curl), at the expense of an additional boundary term. Such equations can be derived by using the product rules and fundamental theorems of vector calculus.

A.12 The Dirac Delta Function

In one dimension the *Dirac delta function* is a (mathematically improper) function written $\delta(x-a)$ and having the properties that

$$\delta(x-a) = \begin{cases} 0 & (\text{if } x \neq a), \\ \infty & (\text{if } x = a), \end{cases} \tag{A.69}$$

with the normalization

$$\int_{-\infty}^{+\infty} \delta(x-a)dx = 1. \tag{A.70}$$

The Dirac delta function can be viewed intuitively (but non-rigorously) as the limit of a peaked curve that becomes higher and higher as it is made narrower and narrower, in such as way that the *area under the curve remains constant.*[4] For an arbitrary continuous function $f(x)$,

$$f(x)\delta(x-a) = f(a)\delta(x-a) \tag{A.71}$$

and insertion of a Dirac delta function in an integral over a function picks out the value of the integrand at $x = a$,

$$\int_{-\infty}^{+\infty} f(x)\delta(x-a)dx = f(a). \tag{A.72}$$

In n dimensions the Dirac delta function $\delta^n(\boldsymbol{x} - \boldsymbol{X})$ can be written as a product of n 1D delta functions; for example, in a 3D space parameterized by cartesian coordinates $\boldsymbol{x} = (x_1, x_2, x_3)$,

$$\delta^3(\boldsymbol{x} - \boldsymbol{X}) \equiv \delta(x_1 - X_1)\delta(x_2 - X_2)\delta(x_3 - X_3). \tag{A.73}$$

This vanishes everywhere except at $\boldsymbol{x} = \boldsymbol{X}$, and generalizing Eqs. (A.69) and (A.70) to 3D,

$$\int_{\Delta V} \delta^3(\boldsymbol{x} - \boldsymbol{X})\, d^3x = \begin{cases} 1 & (\text{If } \Delta V \text{ contains } \boldsymbol{x} = \boldsymbol{X}), \\ 0 & (\text{If } \Delta V \text{ doesn't contain } \boldsymbol{x} = \boldsymbol{X}), \end{cases} \tag{A.74}$$

where ΔV is the integration volume over d^3x, while Eq. (A.72) generalizes to

$$\int_{\Delta V} f(\boldsymbol{x})\, \delta^3(\boldsymbol{x} - \boldsymbol{a})\, d^3x = f(\boldsymbol{a}). \tag{A.75}$$

Thus, just as in 1D the 3D Dirac delta function $\delta^3(\boldsymbol{x} - \boldsymbol{a})$ picks out the point $\boldsymbol{x} = \boldsymbol{a}$ in the integration. Notice from the preceding definitions that a Dirac delta function in n dimensions has the dimensionality of inverse volume in n-dimensional space. Applying the Laplacian operator ∇^2 to $|\boldsymbol{x} - \boldsymbol{x}'|^{-1}$ gives a result proportional to a 3D δ-function,

$$\nabla^2 \left(\frac{1}{|\boldsymbol{x} - \boldsymbol{x}'|} \right) = -4\pi\delta^3(\boldsymbol{x} - \boldsymbol{x}'), \tag{A.76}$$

which can be of considerable utility in evaluating electrostatic integrals (see Example 2.10). By evaluating

$$\int_a^b \frac{d\delta(x)}{dx} f(x)\, dx$$

[4] The Dirac delta function was first introduced by Dirac to aid in normalization of probability integrals in quantum mechanics. It was met by considerable initial skepticism from mathematicians. However, contrary to what might be inferred from our loose discussion here, the Dirac delta function can be placed on a mathematically rigorous footing by viewing it as a *generalized function* or *distribution* (meaning a quantity that only makes sense when it is integrated over) over the real numbers, which has a value of zero everywhere except at zero, and has an integral over the entire real number line that is equal to one. See Lighthill [48] for a more complete exposition.

by "parts" for $f(x)$ an arbitrary function, one can show that the delta function *anticommutes with derivative operators such as* $\boldsymbol{\nabla}$ under an integral; schematically,

$$\frac{d}{dx}\delta = -\delta\frac{d}{dx}. \tag{A.77}$$

(One can show that this "parts" operation is legitimate, even though δ is not a true function.)

B Appendix B Electromagnetic Units

We have used SI units systematically throughout this book except for employing Heaviside–Lorentz units in discussing the Lorentz invariance of the Maxwell equations in Section 18.9. This Appendix gives the Maxwell equations and Lorentz force equations expressed in SI units, gaussian or CGS units, and Heaviside–Lorentz units.

B.1 Maxwell Equations in SI Units

In SI units the vacuum Maxwell equations are

$$\boldsymbol{\nabla} \cdot \boldsymbol{E} = \frac{\rho}{\epsilon_0} \qquad \text{(Gauss's law)}, \tag{B.1a}$$

$$\boldsymbol{\nabla} \times \boldsymbol{E} + \frac{\partial \boldsymbol{B}}{\partial t} = 0 \qquad \text{(Faraday's law)}, \tag{B.1b}$$

$$\boldsymbol{\nabla} \cdot \boldsymbol{B} = 0 \qquad \text{(No magnetic charges)}, \tag{B.1c}$$

$$\boldsymbol{\nabla} \times \boldsymbol{B} - \frac{1}{c^2}\frac{\partial \boldsymbol{E}}{\partial t} = \mu_0 \boldsymbol{J} \qquad \text{(Ampère–Maxwell law)}, \tag{B.1d}$$

where $\boldsymbol{E}$ is the electric field, $\boldsymbol{B}$ is the magnetic field, ρ is the charge density, $\boldsymbol{J}$ is the current vector, ϵ_0 is the permittivity of free space [defined in Eq. (2.3)], and μ_0 is the permeability of free space (related by $\epsilon_0 \mu_0 = 1/c^2$). The corresponding Lorentz force in SI units is

$$\boldsymbol{F} = q(\boldsymbol{E} + \boldsymbol{v} \times \boldsymbol{B}) \qquad \text{(Lorentz force)}, \tag{B.2}$$

where q is the charge and $\boldsymbol{b}$ the velocity of a test charge.

B.2 Maxwell Equations in Gaussian (CGS) Units

In gaussian (CGS) or electrostatic units the vacuum Maxwell equations are

$$\boldsymbol{\nabla} \cdot \boldsymbol{E} = 4\pi\rho \qquad \text{(Gauss's law)}, \tag{B.3a}$$

$$\boldsymbol{\nabla} \times \boldsymbol{E} + \frac{1}{c}\frac{\partial \boldsymbol{B}}{\partial t} = 0 \qquad \text{(Faraday's law)}, \tag{B.3b}$$

$$\boldsymbol{\nabla} \cdot \boldsymbol{B} = 0 \qquad \text{(No magnetic charges)}, \tag{B.3c}$$

$$\boldsymbol{\nabla} \times \boldsymbol{B} - \frac{1}{c}\frac{\partial \boldsymbol{E}}{\partial t} = \frac{4\pi}{c}\boldsymbol{J} \qquad \text{(Ampère–Maxwell law)}, \tag{B.3d}$$

where $\boldsymbol{E}$ is the electric field, $\boldsymbol{B}$ is the magnetic field, ρ is the charge density, and $\boldsymbol{J}$ is the current vector. The corresponding Lorentz force in CGS units is

$$\boldsymbol{F} = q\left(\boldsymbol{E} + \frac{1}{c}\boldsymbol{v} \times \boldsymbol{B}\right) \qquad \text{(Lorentz force)}, \tag{B.4}$$

where q is the charge and $\boldsymbol{v}$ the velocity of a test charge.

B.3 Maxwell Equations in Heaviside–Lorentz Units

In Heaviside–Lorentz units (common in high energy physics) the vacuum Maxwell equations are given by

$$\boldsymbol{\nabla} \cdot \boldsymbol{E} = \rho \qquad \text{(Gauss's law)}, \tag{B.5a}$$

$$\boldsymbol{\nabla} \times \boldsymbol{E} + \frac{\partial \boldsymbol{B}}{\partial t} = 0 \qquad \text{(Faraday's law)}, \tag{B.5b}$$

$$\boldsymbol{\nabla} \cdot \boldsymbol{B} = 0 \qquad \text{(No magnetic charges)}, \tag{B.5c}$$

$$\boldsymbol{\nabla} \times \boldsymbol{B} - \frac{\partial \boldsymbol{E}}{\partial t} = \boldsymbol{J} \qquad \text{(Ampère–Maxwell law)}, \tag{B.5d}$$

where $\boldsymbol{E}$ is the electric field, $\boldsymbol{B}$ is the magnetic field, ρ is the charge density, and $\boldsymbol{J}$ is the current vector. The corresponding Lorentz force in CGS units is

$$\boldsymbol{F} = q\left(\boldsymbol{E} + \frac{1}{c}\boldsymbol{v} \times \boldsymbol{B}\right) \qquad \text{(Lorentz force)}, \tag{B.6}$$

where q is the charge and $\boldsymbol{v}$ the velocity of a test charge.

C Appendix C The Faraday Tensor

The rank-2 electromagnetic or Faraday tensor F in Eq. (18.48), and the dual rank-2 tensor $\star F$ in Eq. (18.50), are the central quantities for a covariant formulation of classical electromagnetism. Unfortunately there are a variety of ways that the same quantities are expressed in the physics literature, primarily for two reasons:

1. The F and $\star F$ tensors change their sign structure depending on the metric signature you choose, with the most common choices being
   a. The "mostly plus" or "East Coast" metric with signature $(-+++)$, which tends to be favored in general relativity, and
   b. The "mostly minus" or "West Coast" metric with signature $(+---)$, which tends to be favored in quantum field theory.

   The differences arise because lowering or raising indices using the metric tensor $\eta_{\mu\nu}$ flips the signs of either the time or spatial components.
2. The F and $\star F$ tensors may be expressed in contravariant (indices up) or covariant (indices down) form.

These different conventions are internally self-consistent, but can lead to confusion in comparing sources using different conventions. In this brief Appendix, the forms for F and $\star F$ in different conventions are summarized.

C.1 The Faraday Tensor F

The electromagnetic tensor can be expressed with either the $\eta_{\mu\nu} = \text{diag}\,(-1,1,1,1)$ or the $\eta_{\mu\nu} = \text{diag}\,(1,-1,-1,-1)$ metric, and in contravariant or covariant form.

C.1.1 The "Mostly Plus" Signature

For the "Mostly Plus"or "East Coast" metric $\eta_{\mu\nu} = \text{diag}(-1,1,1,1)$,

$$\textit{Contravariant Faraday Tensor:} \quad F^{\mu\nu} = \begin{pmatrix} 0 & E_x/c & E_y/c & E_z/c \\ -E_x/c & 0 & B_z & -B_y \\ -E_y/c & -B_z & 0 & B_x \\ -E_z/c & B_y & -B_x & 0 \end{pmatrix}. \tag{C.1}$$

$$\textit{Covariant Faraday Tensor:} \quad F_{\mu\nu} = \begin{pmatrix} 0 & -E_x/c & -E_y/c & -E_z/c \\ E_x/c & 0 & B_z & -B_y \\ E_y/c & -B_z & 0 & B_x \\ E_z/c & B_y & -B_x & 0 \end{pmatrix}. \tag{C.2}$$

C.1.2 The "Mostly Minus" Signature

For the "Mostly Minus" or "West Coast" metric $\eta_{\mu\nu} = \text{diag}\,(1, -1, -1, -1)$,

$$\textit{Contravariant Faraday Tensor:} \quad F^{\mu\nu} = \begin{pmatrix} 0 & -E_x/c & -E_y/c & -E_z/c \\ E_x/c & 0 & -B_z & B_y \\ E_y/c & B_z & 0 & -B_x \\ E_z/c & -B_y & B_x & 0 \end{pmatrix}. \tag{C.3}$$

$$\textit{Covariant Faraday Tensor:} \quad F_{\mu\nu} = \begin{pmatrix} 0 & E_x/c & E_y/c & E_z/c \\ -E_x/c & 0 & -B_z & B_y \\ -E_y/c & B_z & 0 & -B_x \\ -E_z/c & -B_y & B_x & 0 \end{pmatrix}. \tag{C.4}$$

C.2 The Dual Electromagnetic Tensor $\star F$

The dual electromagnetic tensor (often denoted $\star F^{\mu\nu}$ or $\tilde{F}^{\mu\nu}$) is defined using the Levi-Civita tensor:

$$\star F^{\mu\nu} = \frac{1}{2}\epsilon^{\mu\nu\alpha\beta}F_{\alpha\beta}.$$

Physically, taking the dual effectively swaps the roles of the electric and magnetic fields (the duality transformation: $\mathbf{E}/c \to \mathbf{B}$ and $\mathbf{B} \to -\mathbf{E}/c$). Just like the standard Faraday tensor, the signs of the components depend on the chosen metric signature and whether the tensor is in contravariant or covariant form.

C.2.1 The "Mostly Plus" Signature

For the "Mostly Plus" or "East Coast" metric $\eta_{\mu\nu} = \text{diag}\,(-1, 1, 1, 1)$

$$\textit{Contravariant Dual Tensor:} \quad \star F^{\mu\nu} = \begin{pmatrix} 0 & B_x & B_y & B_z \\ -B_x & 0 & -E_z/c & E_y/c \\ -B_y & E_z/c & 0 & -E_x/c \\ -B_z & -E_y/c & E_x/c & 0 \end{pmatrix}. \tag{C.5}$$

$$\textit{Covariant Dual Tensor:} \quad \star F_{\mu\nu} = \begin{pmatrix} 0 & -B_x & -B_y & -B_z \\ B_x & 0 & -E_z/c & E_y/c \\ B_y & E_z/c & 0 & -E_x/c \\ B_z & -E_y/c & E_x/c & 0 \end{pmatrix}. \tag{C.6}$$

C.2.2 The "Mostly Minus" Signature

For the "Mostly Minus" or "West Coast" metric $\eta_{\mu\nu} = \text{diag}(1, -1, -1, -1)$,

$$\textit{Contravariant Dual Tensor:} \quad \star F^{\mu\nu} = \begin{pmatrix} 0 & -B_x & -B_y & -B_z \\ B_x & 0 & -E_z/c & E_y/c \\ B_y & E_z/c & 0 & -E_x/c \\ B_z & -E_y/c & E_x/c & 0 \end{pmatrix}. \tag{C.7}$$

$$\textit{Covariant Dual Tensor:} \quad \star F_{\mu\nu} = \begin{pmatrix} 0 & B_x & B_y & B_z \\ -B_x & 0 & -E_z/c & E_y/c \\ -B_y & E_z/c & 0 & -E_x/c \\ -B_z & -E_y/c & E_x/c & 0 \end{pmatrix}. \tag{C.8}$$

These equations are all expressed in SI units. It is also common to use $c = 1$ units for compactness. Then to restore SI units one has only to divide all E components by c.

D Appendix D The Exterior Calculus

We have seen in Section 17.3 that one can introduce spacetime tensors in a coordinate-independent way by defining them in terms of maps of vectors and dual vectors to the real numbers, which is independent of expansion in any particular basis.[1] Likewise, in the study of differential geometry and algebraic topology a coordinate-independent framework for integration and differentiation on a manifold $\mathcal{M}$ can be developed using *differential forms* and the *exterior derivative*. As shown in Chapter 19, this abstraction allows the equations and concepts associated with classical electromagnetism to be stated in an extremely concise manner. This Appendix gives a brief overview of that formalism.

D.1 Differential k-Forms

Mathematically, a *differential k-form* ω is a smooth (C^∞) section of the k-th exterior power of the cotangent bundle for a manifold $\mathcal{M}$ (see Section 17.3.2), denoted $\Lambda^k(T^*M)$.

1. *0-forms* are smooth scalar functions $f \in C^\infty(M)$.
2. *1-forms:* can be expressed locally as $\omega = \sum_i f_i dx^i$. They are linear functionals that "eat" a tangent vector at a point on the manifold and spit out a number).
3. *k-forms* act as a smoothly varying, antisymmetric, multilinear function on tangent vectors at each point of a manifold

The algebra of forms is governed by the *exterior or wedge product* $\wedge$, which anticommutes:

$$dx^i \wedge dx^j = -dx^j \wedge dx^i. \tag{D.1}$$

The antisymmetry of the wedge product captures the geometric notion of oriented volume for an oriented manifold.

D.2 The Wedge Product

While they both involve antisymmetry and "multiplying" two vectors to get an oriented area, the *wedge product* (also termed the *exterior product*) is a more powerful, higher-dimensional generalization of the 3D cross product.

[1] Though of course it is often convenient in practical applications to expand in a well-chosen basis and work in terms of tensor components labeled by indices.

D.2.1 Dimensionality and Results

The cross product ($\times$) is strictly a 3D operation. It takes two vectors in $\mathbb{R}^3$ and produces a third vector that is perpendicular to the first two. The wedge product ($\wedge$) works in any dimension n. It takes two vectors and produces a *bivector*–a flat, oriented plane segment. In 3D, we can "cheat" and represent a plane by its normal vector (the cross product). In 4D or higher, a plane cannot be uniquely identified by a single normal vector, so the cross product fails, but the wedge product remains perfectly defined.

D.2.2 Geometrical Interpretation

It can be useful to think of the difference between cross products and wedge products as the contrast between an arrow and a plane. The cross product ($\boldsymbol{a} \times \boldsymbol{b}$) produces a vector (an arrow). The direction of the arrow represents the orientation of the plane formed by $\boldsymbol{a}$ and $\boldsymbol{b}$ via the right-hand rule, and its length is the area. The wedge product ($v \wedge w$) produces the plane segment itself. It doesn't point "away" from the surface; *it is the surface*, which carries the magnitude (area) and the orientation (the sense of rotation from v to w in $v \wedge w$).

D.2.3 Algebraic Properties

Both the standard cross product of vector calculus and the wedge product of exterior calculus share the property of anticommutivity:

$$\vec{a} \times \vec{b} = -(\vec{b} \times \vec{a}) \qquad v \wedge w = -(w \wedge v). \tag{D.2}$$

However, the wedge product is associative,

$$(u \wedge v) \wedge w = u \wedge (v \wedge w), \tag{D.3}$$

which allows building higher-dimensional "volumes" (trivectors, 4-vectors, ...). Conversely, since

$$(\boldsymbol{a} \times \boldsymbol{b}) \times \boldsymbol{c} \neq \boldsymbol{a} \times (\boldsymbol{b} \times \boldsymbol{c}), \tag{D.4}$$

the cross product generally isn't associative.

D.2.4 The Formal Link: The Hodge Star

In 3D specifically, the cross product and wedge product are related by the Hodge Star operator ($\star$), which maps k-forms to $(n-k)$-forms. In $\mathbb{R}^3$ it maps a 2-form (a bivector) to a 1-form (a vector):

$$\boldsymbol{a} \times \boldsymbol{b} = \star(\boldsymbol{a} \wedge \boldsymbol{b}) \tag{D.5}$$

This relationship is why one can use the cross product for physics in 3D, but must switch to differential forms or tensors when working in 4D spacetime or higher-dimensional string theory. These comparisons between cross products and wedge products are summarized in Table D.1.

Table D.1 Comparison of cross product and wedge products

Feature	Cross product ($\times$)	Wedge product ($\wedge$)
Dimension	Only 3D	Any dimension n
Output type	Vector (1-form/pseudovector)	bivector (2-form)
Commutative	No	No
Associative	No	Yes
Geometric unit	Directed line	Oriented plane segment

D.3 Exterior Derivatives

The *exterior derivative* $d : \Omega^k(M) \to \Omega^{k+1}(M)$ is the unique linear operator that transforms a k-form into a $(k+1)$-form. It generalizes the concepts of gradient, curl, and divergence from vector calculus into a single framework. For a 0-form f, the exterior derivative is the total differential:

$$df = \sum_i \frac{\partial f}{\partial x^i} dx^i. \tag{D.6}$$

For a higher-order form, d is applied to the coefficients. A fundamental property of the exterior derivative is its *nilpotency*:

$$d^2 = d \circ d = 0. \tag{D.7}$$

This property is the foundation of *De Rham cohomology*, where a form ω is called *closed* if $d\omega = 0$ and *exact* if $\omega = d\eta$ for some form η. The relationship between a form and its derivative is most powerfully expressed by the *Generalized Stokes' Theorem*, as illustrated in Box D.1.

D.4 Cohomology

In algebraic topology, *cohomology* is a formalism used to count and classify "holes" of different dimensions in a geometric object like a manifold. While *homotopy* focuses on deforming loops to determine connectedness, *homology* focuses on the relationship between boundaries and cycles (where a *k-cycle* is a k-chain that has no boundary). The basic question asked by homology is whether a closed loop is the boundary of something, or whether it is a hole, with the key insight being that *a cycle that is not a boundary is a hole.*

Example D.1 The endpoints of a line segment are boundaries, so a line segment is a chain but it is not a cycle. However, if you connect those endpoints to form a circle, the boundary "cancels out" (the start is the end), making it a cycle.

Box D.1 The Generalized Stokes' Theorem

Let Ω be an oriented $(k+1)$-dimensional manifold with boundary $\partial\Omega$, and let ω be a smooth k-form with compact support (see Box D.2). Then:

$$\int_{\Omega} d\omega = \int_{\partial\Omega} \omega \qquad \text{(Generalized Stokes' theorem).}$$

This identity relates the "differential" behavior of a form within a volume to its "integral" behavior on the boundary, effectively linking the local geometry to the global topology. The key points are

1. Forms represent the "density" or "flux" to be measured, while d describes how that density or flux changes. These are *geometrical* but not topological objects.
2. That $d^2 = 0$ allows us to define *cohomology groups*, which detect "holes" in a space. A form that is closed ($d\omega = 0$) but not exact ($\omega \neq d\eta$) often indicates a *topological feature* of the manifold.

These provide the link between geometry and topology inherent in the generalized Stokes' theorem.

Box D.2 Compact Support

A function with compact support is "well-behaved", becoming zero everywhere outside of a bounded, closed region. Formally, for X a topological space, a continuous function $f : X \to R$ has compact support if the closure of the set of points where the function is non-zero is a compact set. The *Heine–Borel theorem* states that a set in $\mathbb{R}^n$ is compact if and only if it is closed and bounded. Thus a function $f(x)$ has compact support if (1) There is some finite distance R such that $f(x) = 0$ for all $|x| > R$. (2) It doesn't "leak" out to infinity or approach zero asymptotically (it is *strictly zero* outside a certain "box" or "ball".) Compact support is a powerful attribute because it allows us to ignore "boundary terms" at infinity. This is important for integration, the generalized Stokes' theorem, and for test functions in the theory of distributions like the Dirac delta function.

Example D.2 A single triangle has three edges as its boundary, so it is not a cycle. But the surface of a tetrahedron (four triangles joined together) has no boundary edges, so it is a cycle.

The relationship is defined by a series of nested sets:

1. *Chains (C_k):* Everything that can be built.
2. *Cycles (Z_k):* Chains that have no boundary ($\partial c = 0$).
3. *Boundaries (B_k):* Cycles that are themselves the boundary of something ($c = \partial d$).

This matters because the goal of homology is to find *cycles that are not boundaries*. If a cycle is a boundary (for example, a circle drawn on a flat sheet of paper), it surrounds a solid area and there is no hole. Conversely, if a cycle is not a boundary it surrounds a hole.

E Appendix E Solutions and Visualization with Computers

Because realistic applications often require computer-aided solutions, a graduate education in advanced classical electromagnetism isn't complete without at least a basic understanding of how to apply a computer to typical problems. Furthermore, an understanding of physics in general, and E&M problems in particular, is often facilitated by well-chosen graphics and animated graphics generated by modern computer graphics packages. Students often acquire such knowledge from separate computer science and computational science courses, but I have chosen to integrate it with the subject matter by providing a website (see [7]) with structure parallel to the chapters in the book that addresses computer solutions as an option in using this book.

E.1 Optional Computer Problems

Consequently, this book emphasizes the traditional analytical mathematical physics approach to E&M problems, but also contains various examples and problems that the student is required to solve numerically and to generate appropriate graphics to illustrate the solution. Students may use whatever computer languages and software that they wish to accomplish this, but the standard that I have adopted is to solve problems using the *Python* programming language, with associated graphics generated either by

1. *Python*'s built-in graphics capabilities, or
2. the graphics package *gnuplot*.[1]

This choice was made because both *Python* and *gnuplot* are cross-platform, open source, free of charge, and free of embedded advertising, and because both are capable of generating publication-quality vector or bitmap graphics output files.

As discussed in Appendix G, a similar approach proactive with respect to generative artifical intelligence (*GenAI*) has been developed for this book, through a website (see [8]) with structure parallel to the chapters in the book that addresses the use of generative AI in learning and understanding advanced classical electromagnetism. In the problems at the ends of chapters, the ones under the subheading "Numerical and *GenAI* Problems"

[1] The accepted convention is that the name *gnuplot* is always written with lower-case letters, even when it begins a sentence. If starting a sentence with a lower-case letter offends your sensibilities, you may wish to rewrite sentences to avoid the first word being *gnuplot*. The accepted pronunciation of *gnuplot* is "new-plot" with the leading "g" silent. The *gnuplot* package has nothing to do with the Free Software Foundation's *GNU project* (where the leading letter is pronounced as a hard "G": "guh-new'). Computer snobs may judge you a newby if you pronounce the "g" in *gnuplot* or fail to pronounce the hard "G" in *Gnu project*.

often emphasize a combination of *GenAI* alone, and numerical computing with code written, debugged, and verified with the assistance of *GenAI*.

E.2 Option of Numerical and Graphical Problems

As a consequence of this parallel structure developed on freely available but optional websites, the present book may be used as a traditional advanced E&M text by ignoring this appendix and Appendix G, the computational [7] and AI [8] websites, and all problems at the ends of chapters under the problem section heading "Numerical and *GenAI* Problems". If one instead includes those additional resources, this book and the websites allow varying levels of integrating a traditional textbook presentation with creative *GenAI* and numerical approaches to classical electromagnetism.

E.3 Programming with AI Prompts

If one chooses to use *GenAI* as a programming assistant, the starting point is ask the *GenAI* to produce initial code for debugging, testing, improvement, and enhancement. Here is a sample workflow.[2]

1. Compose an appropriate prompt for the *GenAI* to write code to accomplish this task in *Python*. For example, a *Gemini* prompt

   > "Write python code to plot a 2D vector field having components $(u = -y, v = x)$, where (x, y) are the cartesian coordinated for your 2D plot. Plot to the screen, and also output the plot to *.eps*, *.pdf*, and *.png* files."

   was used in solving Problem 1.5.[3]
2. Execute the code generated by the AI using your installation of *Python*.

[2] This workflow assumes that you have already installed and tested *Python* on your computer. Typing "python –version" at a command prompt in a terminal window should return the version number if *Python* is installed. For problems in this book it will be assumed that your version of *Python* is current, but is at least *Python* 3 or later (at the time of writing this *Python* 3.14 is current). If your computer does not have *Python* installed, step by step instructions for installing, verifying functionality, program execution, and troubleshooting it on Mac, Windows, or Linux systems may be found at the link [9]. If you get error messages indicating that your version isn't current enough for a particular problem, use the *GenAI* to fix it (paste the error message directly in the *GenAI* chat window and implement the fix that the AI suggests).

[3] *Gemini* speaks and comprehends LaTeX fluently, so the most foolproof way to communicate equations in a Gemini prompt is to express it in LaTeX. It goes the other way too: you can ask *Gemini* to translate a response into a LaTeX snippet or a full LaTeX document. Even if you save a *Gemini* response to *Google Docs*, equations will likely be written in LaTeX, since *Google Docs* understands basic LaTeX.

3. If the compile and execution indicates errors, use the GenAi to debug (copy error messages and paste into the *GenAI* prompt window, or type an explanation of the problem into the *GenAI* prompt window).
4. Once the code is executing without error, verify that it is working correctly:
   - *Qualitative:* Is the result plausible? (Is it obviously violating any laws of physics?)
   - *Quantitative:* check some specifics (calculate some points with a calculator).
5. Include in your solution of the question (a) the AI prompts that you used, (b) a brief description of what the code does, and (c) a brief discussion of how you verified that the results could be trusted.

Also include in your answer representative images from any graphics files generated in the solution. Note that if audio or video files of any significant duration are generated, they will likely be too large to send by email attachment (tens to hundreds of megabytes, even with efficient compression). Large media files can be made available to others by uploading to cloud storage like Google Docs and sharing the link, or by sharing a NotebookLM project.

E.4 Debugging with AI Prompts

In the author's experience, if you don't make a dumb error like failing to paste the code into the file that you execute, the code is likely to run correctly out of the box. But if it doesn't, the best help desk for debugging *Python* code is a *GenAI*. If your code fails to execute properly and generates an error message, copy the entire error message with the mouse and paste it into the *GenAI* prompt window (typically no further explanation is required). If it fails to execute but generates no clear error message (which is unusual), type a short description of what happened into the prompt window. The *GenAI* will likely diagnose the error almost immediately, tell you why it happened, tell you the fix, explain why the fix should work, and then generate a new code listing, or possibly just generate a short segment of code and tell you where to insert it in the old code. Execute the revised code. If the code works, proceed with checking whether the results make sense; if it still produces errors, iterate the procedure outlined above until the code runs successfully.

F Appendix F Iterative PDE Solvers

This Appendix contains some technical details of the solvers used for the Python-based numerical E&M problems in this book. Table 3.1 may be consulted for an overview, and further discussion may be found in Section 3.4.

F.1 Jacobi vs. Gauss–Seidel Iterative Solvers

In the context of solving the linear system $A\boldsymbol{x} = \boldsymbol{b}$ derived from finite difference discretizations, iterative methods are often preferred over direct solvers for large, sparse matrices. The two most fundamental methods are the *Jacobi algorithm* and the *Gauss–Seidel algorithm*.

F.1.1 The Jacobi Method

The *Jacobi algorithm* is a method of *simultaneous updates*. It updates every grid point using only values from the *previous* iteration (iteration k). For a 2D Laplacian, the value at iteration $k+1$ is:

$$\Phi_{i,j}^{(k+1)} = \frac{1}{4}\left(\Phi_{i+1,j}^{(k)} + \Phi_{i-1,j}^{(k)} + \Phi_{i,j+1}^{(k)} + \Phi_{i,j-1}^{(k)}\right). \tag{F.1}$$

1. *Memory:* Requires two separate arrays (one for state k, one for $k+1$) to prevent data contamination.
2. *Parallelization:* Highly parallelizable (vectorizable) since each point is independent of the others within the same step.
3. *Convergence:* Generally slow, as information propagates only one grid cell per iteration.

As a consequence of the slow convergence, the Jacobi algorithm is typically used only for simple problems.

F.1.2 The Gauss–Seidel Method

The *Gauss–Seidel algorithm* is a method of *sequential updates*. It updates grid points one by one, using the *most recently computed* values immediately. Assuming a lexicographic order (looping over i, then over j), the update rule is

$$\Phi_{i,j}^{(k+1)} = \frac{1}{4}\left(\Phi_{i+1,j}^{(k)} + \Phi_{i-1,j}^{(k+1)} + \Phi_{i,j+1}^{(k)} + \Phi_{i,j-1}^{(k+1)}\right). \tag{F.2}$$

Note that neighbors $(i-1,j)$ and $(i,j-1)$ have already been updated to state $k+1$.

1. *Memory:* efficient; requires only one array (updates happen "in-place").
2. *Parallelization:* Difficult due to data dependencies (calculating point i requires the result of $i-1$). This is often mitigated using Red–Black ordering, as discussed below.
3. *Convergence:* Typically converges twice as fast as Jacobi, since boundary information propagates across the domain more rapidly [47].

As will be discussed below, the *Successive Over-Relaxation (SOR) method* can accelerate the convergence of Gauss–Seidel iteration (see Section F.2), and Red–Black ordering permits effective parallelization of the SOR algorithm (see Section F.3).

F.2 Successive Over-Relaxation (SOR)

Successive Over-Relaxation (SOR) is an iterative technique designed to accelerate the convergence of the Gauss-Seidel method for solving linear systems of equations. It is particularly effective for systems arising from finite difference discretizations of elliptic partial differential equations, such as the Poisson equation.

F.2.1 The Core Concept: Extrapolation

The standard Gauss-Seidel method updates a grid point value Φ_{old} by moving it towards a calculated target value Φ_{GS}. SOR improves upon this by extrapolating the correction, effectively "overshooting" the target to anticipate future adjustments in the same direction.

F.2.2 The Algorithm

For a grid point (i,j), the new value Φ_{new} is computed as a weighted average of the old value and the Gauss-Seidel prediction:

$$\Phi_{i,j}^{(k+1)} = (1-\omega)\Phi_{i,j}^{(k)} + \omega\Phi_{GS}^{(k+1)} \tag{F.3}$$

where $\Phi_{\text{GS}}^{(k+1)}$ is the value that would be obtained using the standard Gauss-Seidel formula (using the most recent neighbor values):

$$\Phi_{\text{GS}}^{(k+1)} = \frac{1}{4}\left(\Phi_{i+1,j}^{(k)} + \Phi_{i-1,j}^{(k+1)} + \Phi_{i,j+1}^{(k)} + \Phi_{i,j-1}^{(k+1)}\right) \tag{F.4}$$

Substituting the expression for Φ_{GS}, the full update equation becomes:

$$\Phi_{i,j}^{(k+1)} = (1-\omega)\Phi_{i,j}^{(k)} + \frac{\omega}{4}\left(\Phi_{i+1,j}^{(k)} + \Phi_{i-1,j}^{(k+1)} + \Phi_{i,j+1}^{(k)} + \Phi_{i,j-1}^{(k+1)}\right) \tag{F.5}$$

F.2.3 The Relaxation Parameter (ω)

The choice of the relaxation parameter ω determines the behavior and stability of the method:

- $0 < \omega < 1$ *(Under-Relaxation):* Used to stabilize the iteration if the system is diverging or oscillating. It slows down the update by taking a smaller step than Gauss-Seidel.
- $\omega = 1$ *(Gauss-Seidel):* The method reduces exactly to the standard Gauss-Seidel iteration.
- $1 < \omega < 2$ *(Over-Relaxation):* The standard range for SOR. It accelerates convergence by pushing the solution further in the direction of the calculated update.

Note: If $\omega \geq 2$, the method becomes unstable and the solution will diverge. For simple problems like the Laplace equation on a square grid of size $N \times N$, the optimal relaxation parameter ω_{opt} can be calculated analytically:

$$\omega_{\text{opt}} = \frac{2}{1 + \sin(\pi/N)} \approx 2 - \frac{2\pi}{N} \quad \text{for large } N. \tag{F.6}$$

F.3 Parallel Gauss–Seidel

A standard Gauss–Seidel algorithm updates grid points in *lexicographic order* (row by row).[1] For the 5-point stencil of Eq. (3.24), the update at the point (i, j) requires the *new* values at $(i-1, j)$ and $(i, j-1)$. This creates a *sequential data dependency*, which prevents parallelization or vectorization within a single sweep of the grid.

F.3.1 Checkerboard Ordering

To break this dependency, the domain Ω may be partitioned into two disjoint sub-grids, "Red" (Ω_{R}) and "Black" (Ω_{B}),

$$\Omega_{\text{R}} = \{(i, j) \mid i + j \text{ is even}\}, \tag{F.7}$$

$$\Omega_{\text{B}} = \{(i, j) \mid i + j \text{ is odd}\}, \tag{F.8}$$

which is analogous to the red/black pattern on a typical checkerboard. The reason that this helps is that for a 5-point stencil of a Laplacian [see Eq. (3.24)], a point (i, j) depends *only* on its immediate neighbors. If (i, j) is Red, all its neighbors are Black. If (i, j) is Black, all its neighbors are Red. This decoupling allows defining a highly parallel algorithm.

The Parallel Algorithm: The Gauss–Seidel sweep of the lattice can now be executed in two independent half-steps, with all points in a color set (Red or Black) updated simultaneously.

[1] Lexicographical ("dictionary") order arranges sequences (like words or lists) based on the order of their component elements. It compares items index-by-index from left to right; if the first elements differ, that determines the order, otherwise, it proceeds to the next element, and so on.

1. *Update Red Nodes:* Update all $\Phi_{i,j}$ where $(i,j) \in \Omega_{\text{R}}$. Since all neighbors are Black (hence fixed from the previous step), this step is fully parallelizable.

$$\forall (i,j) \in \Omega_{\text{R}}: \quad \Phi_{i,j}^{(k+1)} = \frac{1}{4}\left(\Phi_{i+1,j}^{(k)} + \Phi_{i-1,j}^{(k)} + \Phi_{i,j+1}^{(k)} + \Phi_{i,j-1}^{(k)}\right) \tag{F.9}$$

2. *Update Black Nodes:* Update all $\Phi_{i,j}$ where $(i,j) \in \Omega_{\text{B}}$, which uses the *newly computed* Red values.

$$\forall (i,j) \in \Omega_{\text{B}}: \quad \Phi_{i,j}^{(k+1)} = \frac{1}{4}\left(\Phi_{i+1,j}^{(k+1)} + \Phi_{i-1,j}^{(k+1)} + \Phi_{i,j+1}^{(k+1)} + \Phi_{i,j-1}^{(k+1)}\right) \tag{F.10}$$

This approach maintains the convergence rate of Gauss-Seidel while allowing for massive parallelism on GPUs and vector processors.

F.4 Finite Difference for 2D Laplace's Equation

A standard Laplace solution method that we will often use is a vectorized implementation of the Finite Difference Method (FDM) for solving Laplace's equation in two dimensions. Specifically, it executes a Jacobi relaxation step across the entire interior grid simultaneously.

F.4.1 Mathematical Derivation

In two dimensions, Laplace's equation for the electrostatic potential $\Phi(x,z)$ is

$$\nabla^2 \Phi = \frac{\partial^2 \Phi}{\partial x^2} + \frac{\partial^2 \Phi}{\partial z^2} = 0. \tag{F.11}$$

To solve this numerically on a 2D grid, we approximate the continuous second derivatives using the central finite difference method. Assuming a uniform Cartesian grid where the step size in both directions is equal ($\Delta x = \Delta z = h$), the second derivative with respect to x at a grid point (i,j) is approximated as

$$\frac{\partial^2 \Phi}{\partial x^2} \approx \frac{\Phi_{i+1,j} - 2\Phi_{i,j} + \Phi_{i-1,j}}{h^2}, \tag{F.12}$$

and similarly, for z,

$$\frac{\partial^2 \Phi}{\partial z^2} \approx \frac{\Phi_{i,j+1} - 2\Phi_{i,j} + \Phi_{i,j-1}}{h^2}. \tag{F.13}$$

Substituting these approximations back into Laplace's equation (F.11) yields the discrete form

$$\frac{\Phi_{i+1,j} - 2\Phi_{i,j} + \Phi_{i-1,j}}{h^2} + \frac{\Phi_{i,j+1} - 2\Phi_{i,j} + \Phi_{i,j-1}}{h^2} = 0. \tag{F.14}$$

Since the h^2 terms cancel out, we can solve for the potential at the central point $\Phi_{i,j}$,

$$\Phi_{i,j} = \frac{1}{4}\left(\Phi_{i+1,j} + \Phi_{i-1,j} + \Phi_{i,j+1} + \Phi_{i,j-1}\right), \tag{F.15}$$

which reveals a fundamental property of solutions to Laplace's equation (which are called *harmonic functions*):

> The value of the potential at any empty point in space is exactly equal to the average of the potential of its surrounding neighbors. This is the discrete equivalent of the mean value theorem for harmonic functions (see Section 3.2.1 and Problem 4.2).

Equation F.15 demonstrates that the potential at any given empty point in the grid is exactly equal to the arithmetic average of the potentials of its four immediate neighbors, which is the basis for Jacobi relaxation algorithms.

F.4.2 Computational Implementation

In a naive programming approach, you would use nested for loops to iterate over every i and j index to apply this averaging. However, looping over arrays element-by-element is computationally slow in *Python*. `NumPy` provides array slicing to perform this operation on the entire grid in a single compiled, C-level step. A typical *Python* statement in this loop looks like

```
phi[1:-1, 1:-1]= 0.25 * (phi[2:, 1:-1] + phi[:-2, 1:-1]
                         + phi[1:-1, 2:] + phi[1:-1, :-2]).
```

Here is how the array slices in this expression map to the physical grid points:

1. `phi[1:-1, 1:-1]` represents $\Phi_{i,j}$, targeting all interior points (excluding the boundaries 0 and -1).
2. `phi[2:, 1:-1]` represents $\Phi_{i+1,j}$, shifting the target area one step "down" (or "right", depending on axis orientation) to grab the neighbor on one side.
3. `phi[:-2, 1:-1]` represents $\Phi_{i-1,j}$, shifting the target area one step in the opposite direction.
4. `phi[1:-1, 2:]` represents $\Phi_{i,j+1}$.
5. `phi[1:-1, :-2]` represents $\Phi_{i,j-1}$.

By adding the last four shifted arrays together and multiplying by 0.25, the code simultaneously calculates the new average for every interior point on the grid.

F.4.3 The Relaxation Process

Because the potential at any given point depends on its neighbors, and its neighbors depend on their neighbors, the equation cannot be solved in a single pass. A loop applies this averaging process continuously. With each iteration the boundary conditions propagate their influence further into the interior grid. Eventually, the changes between iterations become negligibly small, and the grid "relaxes" into the unique, steady-state solution that satisfies the physical boundary constraints.

F.5 The Weak (Variational) Form of a PDE

The *weak form* (or *variational form*) is a reformulation of a differential equation that relaxes the continuity requirements of the solution. It is the mathematical foundation of the *finite element method (FEM)* described in Section 4.3.2.

F.5.1 Strong Form versus Weak Form

A PDE expressed in the standard way is known as the *strong form*. For the 1D Poisson equation,

$$-u''(x) = f(x) \quad \text{for } x \in (0,1), \quad u(0) = u(1) = 0, \tag{F.16}$$

where the double prime indicates the second partial derivative. This requires the solution u to be twice differentiable (C^2 continuity). This is problematic for discontinuous sources, material interfaces, or sharp corners where derivatives may be undefined. The *weak form* relaxes this by requiring the equation to hold in an integral sense rather than pointwise, allowing for solutions with lower continuity (C^1 or even C^0).

F.5.2 Derivation of Weak Form

The weak form of a PDE can be derived from the strong form through a three-step procedure [68]:

1. *Multiply by a test function:* Multiply the strong form by an arbitrary smooth *test function* $v(x)$ that satisfies the homogeneous boundary conditions,
$$-u''(x)v(x) = f(x)v(x). \tag{F.17}$$
2. *Integrate over the domain:*
$$-\int_0^1 u''(x)v(x)\,dx = \int_0^1 f(x)v(x)\,dx. \tag{F.18}$$
3. *Integrate by parts:* Apply integration by parts (or Green's Identity in higher dimensions) to transfer one derivative from u to v on the left side of Eq. (F.18),
$$\int_0^1 u'(x)v'(x)\,dx - [u'(x)v(x)]_0^1 = \int_0^1 f(x)v(x)\,dx. \tag{F.19}$$
Since $v(0) = v(1) = 0$, the boundary term vanishes and the problem has been reduced to finding u such that ,
$$\int_0^1 u'(x)v'(x)\,dx = \int_0^1 f(x)v(x)\,dx \tag{F.20}$$
for all valid test functions v.

This weak formulation requires only first derivatives to exist and to be square-integrable; thus it can accommodate "kinked" solutions that would fail the *strong form* test.

G Appendix G GenAI: Tutor, Assistant, and Problem Solver

This book offers the option of using *Generative Artificial Intelligence (GenAI)* to provide a variety of custom learning aids specific to material covered in the text, and contains optional examples and problems that require *generative AI* (*GenAI*) for solution. In particular, this often entails the use of *GenAI* to explore a topic in depth interactively with the *GenAI*, or to write, debug, and verify computer code for solving and generating graphics for E&M problems.

G.1 AI Content is Optional

These *GenAI* resources have been integrated with the book subject matter through optional access to a free website (see [8]) with structure parallel to the chapters in the book. If one opts to include these *GenAI* resources in a course using this book, students may choose to use other implementations but the standard approach adopted for the book uses the Google AI *Gemini* (the version current as of this writing is *Gemini 3*), leveraged by the Google AI notebook organizer and content generator *NotebookLM*, both of which are easy to access and free in their entry-tier implementations.[1] As a consequence of this parallel structure developed on freely available but optional websites, the present book may be used as a traditional advanced E&M text by ignoring this appendix and Appendix E, the computational [7] and AI [8] websites, and all problems at the ends of chapters under the problem section heading "Numerical and *GenAI* Problems". If one instead includes those additional resources, this book and the websites allow varying levels of integrating a traditional textbook presentation with creative *GenAI* and numerical approaches to classical electromagnetism.

G.2 GenAI and Computer Solutions of Problems

Generative AI (*GenAI*) is presented in this text as a transformative tool for solving electromagnetism problems, functioning primarily as an intelligent assistant for coding, visualization, and analytical reasoning. The text emphasizes a workflow that integrates *GenAI*

[1] The free tier should be adequate for student users. However, as discussed in the Preface, the subscription Pro tiers offer expanded productivity (particularly with respect to more generous size, volume, and daily time limits on AI use), and may be available free or at a discount to qualified students.

with the *Python* programming language and specific management and production tools like Google *NotebookLM* to enhance understanding and efficiency.

G.2.1 Writing and Debugging Computational Code

A primary application of *GenAI* in modern electromagnetism is assisting with the creation of computer code to solve problems numerically that are difficult to solve analytically and/or would benefit from corresponding computer graphics.

1. *Code Generation: GenAI* can be prompted to write Python scripts that calculate electromagnetic quantities, such as the electric potential or field for arbitrary charge distributions. For example, using AI to write code for specific numerical methods, such as the *Successive Over-Relaxation (SOR)* algorithm, to solve partial differential equations like the Laplace equation on a grid, and to measure performance for alternative implementation of the algorithm (for example, Jacobi versus Gauss–Siedel iteration, or serial versus vector/parallel versions of a code).
2. *Debugging:* It is remarkable how often *Gemini*-generated code runs correctly straight out of the box, but if the code fails to run initially, *GenAI* serves as an extremely effective debugging tool. Error messages or descriptions of the problem when the code is run on your computer can be pasted directly into the AI prompt window to receive (usually within a few seconds) corrections and explanations for why the error occurred, and how the proposed solution fixes those errors. Students are expected to describe the debugging process as part of their numerical solution of a problem.
3. *Verification:* The text emphasizes a systematic "Question and Verify" approach to using *GenAI* to solve problems. Students are required to discuss how they checked the validity of AI-generated code and its results to ensure they are not "hallucinations" (plausible but false or misleading information generated by an AI).

The author has found *Gemini* to be remarkably good at implementing *Python* code for a broad variety of simple and not so simple E&M (and other kinds of) problems, both in the classroom, and in research. Furthermore, if debugging is required, the process is extremely instructive because *Gemini* explains clearly at each step why the error occurred, what the proposed fix is, *why* the fix should work, and then generates immediately a new version incorporating the proposed fixes. Example G.1 illustrates a typical session for solving a realistic problem in the manner described above.

Example G.1 The following transcript illustrates the author's solution of Problem 2.15 from Chapter 2 of the text through interaction with Gemini 3.

PROBLEM STATEMENT: Use *GenAI* to implement and debug *Python* code using *successive over-relaxation (SOR)* to speed up convergence for a solution of the 2D Laplace equation on a 100×100 grid. (See Appendix F for an overview of these methods.)

a. Use the *GenAI* to set up timing and compare speed both with normal loops and with vectorization [*Red–Black (Checkerboard) ordering*; see Section F.3], so that timing can be compared among these methods with and without vectorization.
b. Use `matplotlib` to plot the resulting solution as a 2D heatmap and as a 3D wireframe plot.

Describe briefly the *GenAI* prompts that you used to obtain the desired results, any debugging steps that were required, and the methods that you used to verify that the code produced by the *GenAI* is giving legitimate answers and not hallucinations.

We begin by prompting the *GenAI* to write the code according to our specifications:

***Gemini prompt**: Use GenAI to implement and debug Python code using Successive Over-Relaxation (SOR) to speed up convergence for a solution of the 2D Laplace equation on a 100 × 100 2D grid. Set up timing and compare speed both with normal loops and with vectorization [Red–Black (Checkerboard) ordering], so that timing can be compared among these methods with and without vectorization. Use* `matplotlib` *to plot the resulting solution as a 2D heatmap and as a 3D wireframe plot.*

Gemini response: This is a fantastic exercise in numerical methods and high-performance Python. Solving the 2D Laplace equation ($\nabla^2 u = 0$) using successive over-relaxation (SOR) is a classic way to demonstrate why vectorization is often necessary when working with interpreted (and thus slow) languages like *Python*. Because standard SOR uses immediately updated values (a Gauss–Seidel approach), you can't simply vectorize it with a standard array operation.

Vectorization

Instead, we use *Red-Black (Checkerboard) ordering*. By dividing the grid into "red" and "black" cells, we guarantee that red cells only depend on black neighbors and vice versa. This uncouples the dependencies, allowing us to update all red cells at once, and then all black cells at once, utilizing `NumPy`'s optimized C backend.

Python Code

Here is the complete, ready-to-run Python script. It implements both methods, times them, calculates the theoretical optimal relaxation factor (ω), and plots the results.

```
# pythonTimingTests.py

import numpy as np
import time
import matplotlib.pyplot as plt
```

```
6
7  def setup_grid(N):
8      """Initializes an NxN grid with boundary conditions."""
9      u = np.zeros((N, N))
10     # Boundary Condition: Let's make the top wall 100 degrees, others 0
11     u[-1, :] = 100.0
12     return u
13
14 def solve_sor_loops(N, omega, tol=1e-4, max_iter=20000):
15     """Solves Laplace equation using standard nested Python loops."""
16     u = setup_grid(N)
17
18     start_time = time.time()
19     for it in range(max_iter):
20         max_diff = 0.0
21         # Iterate over internal grid points
22         for i in range(1, N-1):
23             for j in range(1, N-1):
24                 old_val = u[i, j]
25                 # Standard SOR update formula
26                 u[i, j] = (1 - omega) * old_val + (omega / 4.0) * (
27                     u[i+1, j] + u[i-1, j] + u[i, j+1] + u[i, j-1]
28                 )
29
30                 diff = abs(u[i, j] - old_val)
31                 if diff > max_diff:
32                     max_diff = diff
33
34         # Check convergence
35         if max_diff < tol:
36             break
37
38     elapsed_time = time.time() - start_time
39     return u, elapsed_time, it + 1
40
41 def solve_sor_vectorized(N, omega, tol=1e-4, max_iter=20000):
42     """Solves Laplace equation using Red-Black ordering for NumPy vectorization."""
43     u = setup_grid(N)
44
45     # We use slicing to grab the red and black sub-grids.
46     # R1: odd rows, odd cols | R2: even rows, even cols
47     # B1: odd rows, even cols | B2: even rows, odd cols
48
49     start_time = time.time()
50     for it in range(max_iter):
51         u_old = u.copy()
52
53         # --- Update RED cells ---
54         # R1 (Odd, Odd)
55         u[1:-1:2, 1:-1:2] = (1 - omega) * u[1:-1:2, 1:-1:2] + (omega / 4.0) * (
56             u[2::2, 1:-1:2] + u[:-2:2, 1:-1:2] + u[1:-1:2, 2::2] + u[1:-1:2, :-2:2]
57         )
58         # R2 (Even, Even)
59         u[2:-1:2, 2:-1:2] = (1 - omega) * u[2:-1:2, 2:-1:2] + (omega / 4.0) * (
60             u[3::2, 2:-1:2] + u[1:-2:2, 2:-1:2] + u[2:-1:2, 3::2] + u[2:-1:2, 1:-
    2:2]
```

```
        )

        # --- Update BLACK cells ---
        # B1 (Odd, Even)
        u[1:-1:2, 2:-1:2] = (1 - omega) * u[1:-1:2, 2:-1:2] + (omega / 4.0) * (
            u[2::2, 2:-1:2] + u[:-2:2, 2:-1:2] + u[1:-1:2, 3::2] + u[1:-1:2, 1:-2:2]
        )
        # B2 (Even, Odd)
        u[2:-1:2, 1:-1:2] = (1 - omega) * u[2:-1:2, 1:-1:2] + (omega / 4.0) * (
            u[3::2, 1:-1:2] + u[1:-2:2, 1:-1:2] + u[2:-1:2, 2::2] + u[2:-1:2, :-2:2]
        )

        # Check convergence (using NumPy's highly optimized max and abs)
        max_diff = np.max(np.abs(u - u_old))
        if max_diff < tol:
            break

    elapsed_time = time.time() - start_time
    return u, elapsed_time, it + 1

def main():
    N = 100
    # Calculate optimal relaxation factor omega for an NxN grid
    omega_opt = 2.0 / (1.0 + np.sin(np.pi / (N - 1)))
    print(f"Grid Size: {N}x{N}")
    print(f"Optimal Omega: {omega_opt:.4f}\n")

    # 1. Run Standard Loops
    print("Running standard Python loops...")
    u_loops, time_loops, iter_loops = solve_sor_loops(N, omega_opt)
    print(f"Loops finished in {time_loops:.4f} seconds ({iter_loops} iterations).")

    # 2. Run Vectorized Red-Black
    print("\nRunning vectorized Red-Black SOR...")
    u_vec, time_vec, iter_vec = solve_sor_vectorized(N, omega_opt)
    print(f"Vectorized finished in {time_vec:.4f} seconds ({iter_vec} iterations).")

    # 3. Calculate Speedup
    speedup = time_loops / time_vec
    print(f"\nSpeedup achieved: {speedup:.2f}x faster!")

    # 4. Visualization
    fig = plt.figure(figsize=(14, 6))

    # 2D Heatmap
    ax1 = fig.add_subplot(1, 2, 1)
    im = ax1.imshow(u_vec, cmap='inferno', origin='lower', extent=[0, 1, 0, 1])
    ax1.set_title('2D Heatmap of Solution')
    ax1.set_xlabel('X')
    ax1.set_ylabel('Y')
    fig.colorbar(im, ax=ax1, fraction=0.046, pad=0.04)

    # 3D Wireframe
```

```
    ax2 = fig.add_subplot(1, 2, 2, projection='3d')
    x = np.linspace(0, 1, N)
    y = np.linspace(0, 1, N)
    X, Y = np.meshgrid(x, y)

    # Using stride to thin out the wireframe for a cleaner look
    ax2.plot_wireframe(X, Y, u_vec, rstride=3, cstride=3, color='teal', linewidth
     =0.8)
    ax2.set_title('3D Wireframe of Solution')
    ax2.set_xlabel('X')
    ax2.set_ylabel('Y')
    ax2.set_zlabel('Temperature')

    plt.tight_layout()
    plt.show()

if __name__ == "__main__":
    main()
```

Here is the output from executing this *Python* script. The timing results:

```
[guidry@m1 Downloads]$ python pythonTimingTests.py

Grid Size: 100x100
Optimal Omega: 1.9385

Running standard Python loops...
Loops finished in 1.3695 seconds (241 iterations)

Running vectorized Red-Black SOR...
Vectorized finished in 0.0134 seconds (210 iterations)

Speedup achieved: 102.50x faster!
```

Debugging

No substantial debugging was required except for minor issues associated with aesthetics in the graphics.

Summary

Thus by using the checkerboard trick to break dependencies on the mesh, we have run the code more than 100 times faster than it would run without vectorization. That doesn't make much difference for this simple demonstration, but it would be huge if we were running a real-world code that takes much longer to execute. The plotted output of the calculation is displayed in Fig. G.1.

Testing Validity

The solutions have the reasonable behavior of a Laplace solution, with smooth behavior and no local minima or maxima in the interior, and we expected a substantial speedup because of the checkerboard trick. To test this timing result quantitatively requires comparison with other methods of solving the same problem, which we will leave for another

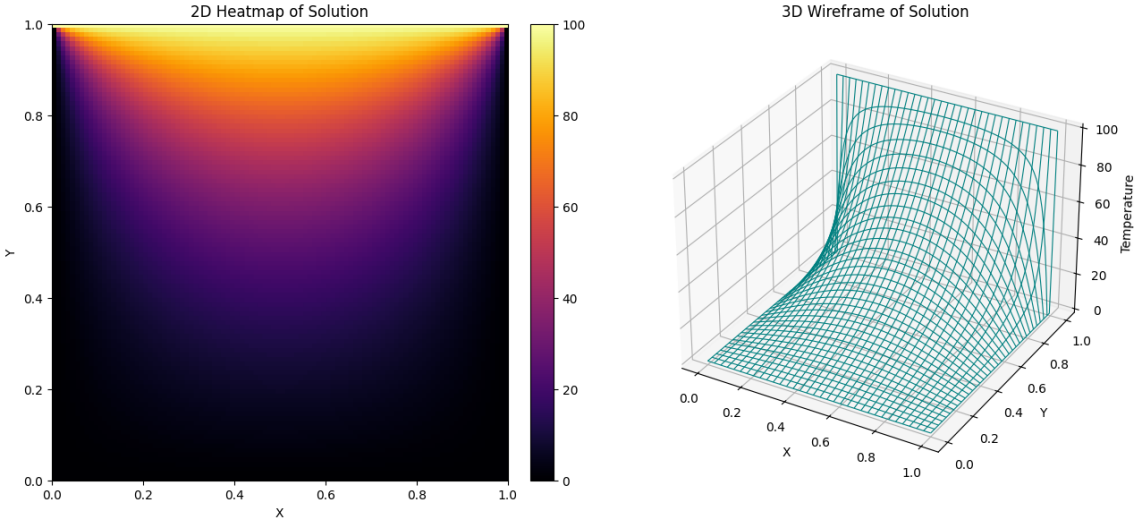

Fig. G.1 A heatmap and wireframe plot of the timed integration in Problem 2.15, as described in Example G.1. Notice the characteristic behavior of a Laplace solution: the surfaces are smooth and any local maxima or minima can occur only on the boundaries.

time since this is just a demonstration of approach.

G.2.2 Visualization of Abstract Concepts

GenAI can be used to generate scripts for visualizing complex electromagnetic fields, helping to relate mathematical equations to physical intuition.

1. *Plotting*: The sources describe using *GenAI* to write code (using libraries like *matplotlib* or software like *gnuplot*) that produces a broad variety of 2D vector field plots, streamline plots, and 3D surface plots of electric potentials.
2. *Publication-quality graphics:* The AI can be directed to format these graphics for high-quality output, such as high-resolution bitmap (*PNG*), or editable vector graphics (*EPS* or *PDF*) files.
3. *Easy graphical animation:* a *Python* script to produce high quality graphical animation can often be generated with just a 1-sentence prompt to the *GenAI*.

Needless to say, in the study of a scientific discipline like E&M, easily generated and immediately produced high-quality graphics and animation of solutions represents an extremely powerful learning aid.

G.2.3 Reasoning in Problem Solving

Beyond coding, GenAI models (specifically Large Language Models) demonstrate the capability to solve traditional mathematical physics problems directly.

1. *Problem solving:* The author notes that GenAI (specifically Google Gemini) was able to solve an advanced undergraduate-level midterm exam (Astronomy 411: Stars and Stellar Processes) with near 100% accuracy, providing both correct final answers and valid intermediate reasoning.
2. *Tutor role:* The AI acts as a "smarter than average" assistant or tutor, allowing users to ask questions about the material or request clarifications on complex topics.

In the author's experience, working interactively with a well-trained *GenAI* in solving problems is much like having Albert Einstein, Richard Feynman, and Mr. Spock from Star Trek at your beck and call.

G.2.4 Synthesis and Study Tools

This text highlights the use of tools like *NotebookLM*, which utilizes Retrieval-Augmented Generation (RAG) to ground AI responses in specific, user-selected source materials.

1. *Custom knowledge base:* Users can create projects by uploading specific textbooks or papers. The AI then answers questions based strictly on those sources, significantly reducing the risk of hallucination.
2. *Multimodal output generation:* This approach allows for the generation of summaries, study guides, infographics, slide decks, quizzes, audio overviews (podcasts and debates), and audiovisual overviews (YouTube-like MP4 files) where AI hosts discuss the complex material provided in the sources.

The use of *NotebookLM* will be discussed in more depth in Appendix H.

In summary, this text advocates for a modern approach where *GenAI* is not just a reference, but an active collaborator that writes the software needed to calculate fields, collaborates proactively in the debugging of the code, visualizes the results, and explains the underlying physics, provided that the user constructs appropriate prompts,[2] and proactively verifies the validity of the output.

[2] Much is made currently about how to construct just the right prompt to get a *GenAI* to produce desired output. In the author's experience, for the types of applications envisioned here the prompts need only be clear and in the right ballpark; the *GenAI* is usually quite capable of understanding what you mean to say and the context in which it is being said.

H Appendix H Using NotebookLM

This Appendix gives a concise overview of how to create and use projects in *NotebookLM*. More extensive discussion may be found at the website [10].

H.1 Creating a NotebookLM Project

First use *NotebookLM* [11] to create a project. Use a Web search (regular or AI-enhanced, like *Gemini* in the Chrome browser [12]) to add more sources to your project (the left **Sources** pane). Use "Search the web for new sources" with an appropriate prompt indicating the subject matter to add additional sources, if you choose. Note that *NotebookLM* is capable of handling many different kinds of sources: PDF files, text files, sound files, Web pages, YouTube content,[1] hand-written notes, ...

H.2 Chatting with NotebookLM

Once *NotebookLM* has processed all added sources, use the central **Chat panel** to learn more about how *Python* can be used to solve complex E&M problems (*NotebookLM* will suggest some possible queries, and you can make up your own). If a chat response seems particularly useful, you can save it by clicking "Save to note" at the bottom left of the **Chat panel**. This will add the note to the right **Studio panel**. If you choose, this note can be added to the sources (click the 3 vertical dots on the right and select "Convert to source"), which will add it as a source in the left **Source panel**).

H.3 Generative Content

Once you have explored some with Chat, try creating some output based on your project using the buttons at the top of the right **Studio panel**. You should explore on your own, but some initial ones to try are

[1] You can download each Web page manually using the *NotebookLM* interface, but there are browser extensions (for example, *Web Clipper for NotebookLM* on Chrome) that make this process easier, allowing a webpage or even an entire YouTube playlist to be downloaded with one click. See the link [13].

1. *Infographic*, which will generate an infographic summarizing the material in your project; customize it by clicking the pencil icon first.
2. *Slide Deck*, which will generate a slide deck suitable for presentation or summary; customize by clicking the pencil icon first.
3. *Audio Overview*, which will generate a podcast style or debate style audio overview that is surprisingly good; customize it by clicking the pencil icon first. If you choose "interactive" when you listen to the audio file, you can interrupt the podcast and ask a question, which the AI "participants" will try to answer in real time.
4. *Video Overview*, which will generate an audio-visual overview of the project.
5. *Reports*, which generates various kinds of reports depending on your choices and prompts.
6. *Quizzes*, which allows you to generate a multiple choice quiz of chosen difficulty over subject matter specified by your prompt. Perhaps the most useful feature of *NotebookLM* quizzes is that for each question, after answering you have the option of clicking an *Explain* button, which will open (after a short think by the AI) a multi-paragraph explanation in the chat window that goes into depth about the answer, and offers the option of follow-up prompts to expand on the information associated with the question and answer.

Some of these *NotebookLM*-generated products may take several minutes to process, so be patient, and you can run more than one type of output at the same time, and be doing other things with the *NotebookLM* interface while waiting. As noted above, if there is a pencil symbol on the button, clicking it will allow you to customize exactly what will be done, but you must click it before clicking the button itself to start the processing; otherwise you will get the default prompt associated with the button.

H.4 Editing Generative Output

The default *NotebookLM* output for sound files is M4A and for audiovisuals it is MP4. These will be large files (tens to hundreds of megabytes, typically), so handle accordingly.

1. Standard sound software can be used to convert M4A to MP3, which can lead to considerably smaller sound files.
2. Standard video editing software can be used to edit and manipulate MP4 files.
3. *NotebookLM*-generated quizzes can be output as `Excel` files, *.tsv* files for the flashcard program `Anki`, or JSON files.
4. Saving any images generated by these Studio options produces bitmapped files (PNG), which have limited post-processing editing options.[2]

[2] For the record, on my Linux systems I use free and open-source software that works cross-platform to process this output: *FFmpeg* to convert sound file formats, *Audacity* to mix and edit sound tracks, *Kdenlive* for video and audio editing and compositing, and *GIMP* for editing bitmapped files. All of these programs should work on Windows or Mac systems too, but consult your *GenAI* for the best options on your particular system.

However, as of early 2026, Google has begun to roll out prompt-generated editing for this generative content within *NotebookLM* itself.

> *Example:* "Increase all font sizes by 2 points, change the colormap to grayscale, and correct the misspelling 'coww' to 'cow'.

This is a rapidly developing subject, so a prompt to your *GenAI* is the most reliable way to determine what current native editing is possible for *NotebookLM*-produced content.

Example H.1 Let us illustrate using *NotebookLM* to make a custom study guide for the first chapter of this book. Following the instructions in this Appendix, create a *NotebookLM* project and give it a name like "Ch. 1 Study". A PDF of Ch. 1 from this book may be downloaded from Ref. [14], so add that link as your first source (click **+ Add sources** in the left **Source pane**, in the resulting popup window click the **Websites** button, and paste in the url from Ref. [14]) . Then add at least 10 additional references to your sources that are relevant to the material in Ch. 1. One simple way to do this is to use the left **Sources pane** in the *NotebookLM* interface, type in a prompt where it says "Search the web for new sources" (for example, from the Table of Contents for Ch. 1, the search string "Maxwell equations, charge conservation") relevant to the material of Ch. 1, select the **Fast Research** option and click the **Right-Arrow**. After a short search this should present a list of potential sources available from the Web. Select all, or uncheck any sources that you don't want to include, and click the **Import** button to import the sources to the project in the left pane (any sources that are shaded light red could not be imported; you can delete those using the three vertical dots on the left side of each source listing). I you want more sources, repeat the search process with an additional search string (for example "charge quantization, gauge symmetry").

Once processing of the new sources is complete, explore using the central **Chat pane**, asking your own questions or ones suggested by *NotebookLM*, saving relevant notes as described in this Appendix. After exploring your project in the **Chat pane**, try exporting some study resources using the right **Studio pane** (see Appendix H.3 for suggestions). You can add further sources if you choose, but you now have a customized and AI-smart study partner for Chapter 1 of this book.

References

[1] http://eagle.phys.utk.edu/guidry/541/AI/ch/ch0/Famous_AI_hallucinations.pdf.

[2] https://ethw.org/Maxwell%27s_Equations.

[3] http://eagle.phys.utk.edu/guidry/541/book/EM.pdf.

[4] https://youtube.com/playlist?list=PL7pvpBCXA-U8rV92XRjsmY5dc0XAVJCGr.

[5] http://eagle.phys.utk.edu/guidry/541/SS/BashShellScripts.pdf.

[6] https://www.youtube.com/watch?v=7HQdpApuuIU.

[7] http://eagle.phys.utk.edu/guidry/541/cs/cs.html.

[8] http://eagle.phys.utk.edu/guidry/541/AI/as.html.

[9] http://eagle.phys.utk.edu/guidry/541/cs/ch/ch0/Python_Installation_and_Execution_Guide.pdf.

[10] http://eagle.phys.utk.edu/guidry/541/AI/ch/ch0/ch0.html.

[11] https://notebooklm.google.com/.

[12] https://gemini.google.com/.

[13] http://eagle.phys.utk.edu/guidry/541/AI/ch/ch0/browserImportNLM.pdf.

[14] http://eagle.phys.utk.edu/guidry/541/SS/ch1.pdf.

[15] Aharonov, Y., and Bohm, D. 1959. *Phys. Rev.*, **115**, 484.

[16] Aitchison, I. J. R., and Hey, A. J. G. 1982. *Gauge Theories in Particle Physics.* Adam Hilger Ltd.

[17] Arfken, G. B., and Weber, H. J. 2005. *Mathematical Methods for Physicists, 6th ed.* Cambridge: Elsevier.

[18] Arianrhod, R. 2024. *Vector: A Surprising Story of Space, Time, and Mathematical Transformation.* Chicago: University of Chicago Press.

[19] Ashcroft, N. W., and Mermin, N. D. 1976. *Solid State Physics.* Toronto: Cengage.

[20] Barrera, R. G., Estevez, G. A., and Giraldo, J. 1985. *European J. Physics*, **6**, 287.

[21] Bhattacharya, K. 2016. *Physica Scripta*, **91**, 1 (arXiv:1509.09252 [physics.class–ph]).

[22] Carroll, S. M. 2004. *An Introduction to General Relativity, Spacetime, and Geometry.* San Francisco: Addison–Wesley.

[23] Chaichian, M., Merches, I., Radu, D., and Tureanu, A. 2016. *Electrodynamics: An Intensive Course.* Berlin: Springer.

[24] Chambers, R. G. 1960. *Phys. Rev. Lett.*, **5**, 3.

[25] Corson, D., and Lorrain, P. 1962. *Introduction to Electromagnetic Fields and Waves.* San Francisco: W. H. Freeman and Company.

[26] Drude, P. 1900a. *Ann. Physik*, **306**, 566.

[27] Drude, P. 1900b. *Ann. Physik*, **308**, 369.

[28] Eschrig, H. 2011. *Topology and Geometry for Physics.* Berlin–Heidelberg: Springer.

[29] Evans, L. C. 2010. *Partial Differential Equations. 2nd ed.* American Mathematical Society.
[30] Foster, J., and Nightingale, J. D. 2006. *A Short Course in General Relativity*. New York: Springer.
[31] Garg, A. 2012. *Classical Electromagnetism in a Nutshell.* Princeton: Princeton University Press.
[32] Goldhaber, A. S., and Nieto, M. M. 1971. *Rev. Mod. Phys.*, **43**, 277.
[33] Griffiths, D. J. 2024. *Introduction to Electrodynamics.* Cambridge: Cambridge University Press.
[34] Guidry, M. W. 1999. *Gauge Field Theories: An Introduction with Application.* New York: Wiley Interscience.
[35] Guidry, M. W. 2018. *Sci. Bull.*, **63**, 2 (DOI: 10.1016/j.scib.2017.11.021).
[36] Guidry, M. W. 2019a. *Modern General Relativity: Black Holes, Gravitational Waves, and Cosmology*. Cambridge: Cambridge University Press.
[37] Guidry, M. W. 2019b. *Stars and Stellar Processes.* Cambridge: Cambridge University Press.
[38] Guidry, M. W., and Sun, Y. 2022. *Symmetry, Broken Symmetry, and Topology in Modern Physics: A First Course.* Cambridge: Cambridge University Press.
[39] Hunt, B. J. 2003. *The Maxwellians.* Ithaca: Cornell University Press.
[40] Hunt, B. J. 2012 (11). *Phys. Today.*, **65**, 48.
[41] Jackson, J. D. 1999. *Classical Electrodynamics, 3rd ed.* New York: Wiley.
[42] Jackson, J. D., and Okun, L. B. 2001. *Phys. Rev. Mod. Phys.*, **75**, 663.
[43] Kamberaj, H. 2022. *Electromagnetism.* Springer.
[44] Kobzarev, I. Yu., and Okun, L. B. 1968. *Sov. Phys. Usp.*, **11**, 338.
[45] Kogut, John B. 2001. *Introduction to Relativity.* San Diego: Academic Press.
[46] Kragh, H. 1991. *Applied Optics*, **30**, 4688.
[47] Leveque, R. J. 2007. *Finite Difference Methods for Ordinary and Partial Differential Equations.* Philadelphia: SIAM.
[48] Lighthill, M. J. 1958. *Introduction to Fourier Analysis and Generalised Functions.* Cambridge: Cambridge University Press.
[49] Lorrain, P., and Corson, D. R. 1978. *Electromagnetism: Principles and Applications.* New York: W. H. Freeman and Company.
[50] Maxwell, J. C. 1865. A Dynamical Theory of the Electromagnetic Field. *Philosophical Transactions of the Royal Society of London*, **155**, 459 (DOI: 10.1098/rstl.1865.0008).
[51] Maxwell, J. C. 1890a. https://archive.org/details/scientificpapers01maxwuoft/page/498/mode/2up.
[52] Maxwell, J. C. 1890b. https://archive.org/details/scientificpapers01maxwuoft/page/500/mode/2up.
[53] Maxwell, James Clerk. 2005. *A Treatise on Electricity and Magnetism.* Oxford: Oxford University Press.
[54] Misner, C. W., Thorne, K. S., and Wheeler, J. A. 1973. *Gravitation.* W. H. Freeman.
[55] Morse, P. M., and Feshbach, H. 1953. *Methods of Theoretical Physics (Vol. I and II).* New York: McGraw–Hill.
[56] Nakahara, M. 2003. *Geometry, Topology and Physics.* Boca Raton: Taylor and Francis.
[57] Nash, C., and Sen, S. 1983. *Topology and Geometry for Physicists.* New York: Academic Press.

[58] Nolte, D. D. 2025. *Maxwellian Steampunk and the Origins of Maxwell's Equations.* https://galileo-unbound.blog/2025/03/05/maxwellian-steampunk-and-the-origins-of-maxwells-equations/.
[59] Peskin, M. E., and Schroeder, D. V. 1995. *An Introduction to Quantum field Theory.* Boston: Addison–Wesley.
[60] Pires, Antonio Sergio Teixera. 2019. *A Brief Introduction to Topology and Differential Geometry in Condensed Matter Physics.* Bristol: IOP Press.
[61] Press, W. H., Teukolsky, S. A., Vetterling, W. T., and Flannery, B. P. 2007. *Numerical Recipes: The Art of Scientific Computing.* Cambridge: Cambridge University Press.
[62] Purcell, E. M., and Morin, D. J. 2013. *Electricity and Magnetism.* Cambridge: Cambridge University Press.
[63] Quigg, C. 1983. *Gauge Theories of the Strong, Weak, and Electromagnetic Interactions.* Reading, Massachusetts: Benjamin/Cummings.
[64] Ryder, L. H. 1996. *Quantum Field Theory.* Cambridge: Cambridge University Press.
[65] Schneider, C. S, and Ertel, J. P. 1998. *Am. J. Phys.*, **66**, 686.
[66] Schutz, Bernard. 1980. *Geometrical Methods of Mathematical Physics.* Cambridge: Cambridge University Press.
[67] Sommerfield, A. 1952. *Electrodynamics.* New York: Academic.
[68] Strang, G., and Fix, G. J. 2008. *An Analysis of the Finite Element Method.* Wellesley–Cambridge Press.
[69] Strauss, W. A. 2007. *Partial Differential Equations: An Introduction.* Wiley.
[70] Tjossem, P. J. H., and Brost, E. C. 2011. *Am. J. Phys.*, **79**, 353.
[71] Tong, D. 2025a. *Electromagnetism (Volume 2): Lectures on Theoretical Physics.* Cambridge: Cambridge University Press.
[72] Tong, D. 2025b. *Fluid Mechanics (Volume 4): Lectures on Theoretical Physics.* Cambridge: Cambridge University Press.
[73] Tromp, J. 2025. *A Geometrical Introduction to Tensor Calculus.* Princeton: Princeton University Press.
[74] Wald, R. M. 2022. *Advanced Classical Electromagnetism.* Princeton: Princeton University Press.
[75] Weinberg, S. 2005. *Quantum Theory of Fields.* Cambridge: Cambridge University Press.
[76] Williams, E. R, Faller, J. E, and Hill, H. A. 1971. *Phys. Rev. Lett.*, **26**, 721.
[77] Zangwill, A. 2013. *Modern Electrodynamics.* Cambridge: Cambridge University Press.

Index

k-chains, *see* chains
Ørsted, H. C., 1, 226

absolute derivatives, 343
action, 395
action at a distance, 24
adaptive mesh, *see* numerical E&M problems
adaptive quadrature, *see* numerical E&M problems
advanced time, 253
aether, 232, 238, 257, 317–319
Aharonov–Bohm effect
  and 4-vector potential, 209, 408
  and de Rham cohomology, 381
  and gauge invariance, 390, 410
  experimental setup, 408, 409
  magnetic fields, 409
  phase of electron wavefunction, 410
  topological origin, 390, 391
amber, 1
Ampère's law, *see also* Ampère–Maxwell law
  and magnetic field of solenoid, 192
  compared with Ampére–Maxwell law, 236
  derived from Biot–Savart law, 191, 192
  in magnetized matter, 207
  modified by Maxwell, 5, 236, 240
Ampère, A.–M., 1, 226
Ampère–Maxwell law
  consistency with continuity equation, 240
  far-reaching implications, 5, 236, 240
  in medium, 150
  in vacuum, 2
  integral form, 152
  integral form in medium, 152
  Maxwell's modification, 5, 236, 240
Ampèrian loops, 193
ampere (amp) unit, 189
anholonomic basis, *see* non-coordinate basis
anomalies
  and charge quantization, 9, 11
  cancellation, 9, 11
  definition, 11
artificial intelligence (AI), *see also* generative AI (GenAI)
  generative (GenAI), xv, xvii
  hallucinations, xvii, xviii
  large language models (LLM), xv, xvii
  retrieval augmented generation (RAG), xviii
associated Legendre polynomials
  and derivative of Legendre polynomial, 157
  orthogonality, 157
  relation to spherical harmonics, 87
atlas, 323
atomic polarization, *see* polarization

ball
  closed, 30
  open, 30
baryon (definition), 11
basis
  and directional derivatives, 325–327
  anholonomic, 325–327
  coordinate, 325–327
  for a vector space, 330
  holonomic, 325–327
  non-coordinate, 325–327
  orthonormal, 324
binomial expansion, 88, 427
Biot, J.-B., 186
Biot–Savart law
  differential form, 189
  discovery, 186
  for line currents, 186
  for surface currents, 194
  for volume currents, 194
  integral form, 186, 189
  magnetic field of circular current loop, 187
  magnetic field of sheet of current, 194
  starting point for magnetostatics, 187
boost transformations, 357
bound charge, *see also* free charge
  definition for dielectrics, 133
  surface, 146
  volume, 146
boundary conditions
  Cauchy, 66, 67
  Dirichlet, 62, 66–68
  discontinuities at charge layers, 57, 58
  matching at interfaces, 146, 152–154
  matching tangential and normal components, 157
  mixed, 66–68
  naturalness of Dirichlet vs. Neumann, 62
  Neumann, 62, 63, 66–68, 291
  overdetermined, 66, 67
  physically acceptable, 6

boundary of a boundary is zero, 51
boundary of a boundary operator ∂^2, 51
boundary of closed volume: $S = \partial V$, 5, 51
boundary operator, 5, 51, 379
boundary value problems, 17–19, 50, 51
boundary-of operator, 379
Brewster's angle, 281, 289
Brewster's law, 281, 289

capacitance
  capacitor, 126
  and fringing fields, 145
  definition, 124
  effect of dielectrics, 126, 131–133
  energy stored in capacitor, 126
  parallel plate capacitor, 124, 171
  vacuum diode, 171
  work done in charging a capacitor, 126
capacitive effect, 230
capacitor, *see* capacitance
Cauchy theorem, 250
causal structure of spacetime, 361, 362
Cavendish, H., 1
chains, 379, 438
charge
  accelerated, 6–8
  and gauge invariance, 4
  bound, 133, 146
  conservation of, 4, 5, 238
  free, 133
  induced, 120
  is conserved locally, 238
  of neutron, 13
  of proton, 13
  quantization of, 9
  space, 173
  surface, 147
  volume, 147
charge conservation, 236, 240
Child–Langmuir law, 173
chiral molecules, 286
chirality, 286
Christoffel symbols
  are not tensors, 343
  definition, 343
  transformation law, 343
circular birefringence, 283, 285
circular polarization, *see* polarization
classical linear regime, 25
closure, 330
cohomology, *see* homology
color confinement, *see* quantum chromodynamics
commutator, 327
compact support, 439
composition
  as a machine, 313
  definition, 311, 313
  of maps, 311, 313
Compton scattering, 301
Compton wavelength, 8
conduction
  conduction electrons, 175
  Drude model, 175
conductivity
  and Ohm's law, 174
  and resistivity, 175
  conductivity tensor, 175, 178
conductors
  also termed metals, 120
  are equipotentials, 120, 122
  definition, 120
  Drude model, 175
  excess charge resides on surface, 120, 122
  external electric field normal to surface, 120, 122
  high mobility of charge carriers, 120
  lightning rods, 123, 125
  no electric charge inside, 120–122
  no electric fields inside, 120–122
  surface charge and curvature, 120, 123
  versus dielectrics (insulators), 120, 130
conformal mapping, 70
conservation laws
  in classical electromagnetism, 255
  symmetries of the Maxwell equations, 4
conservative field, 38
conservative force, 37
constituitive relationship
  in electrostatics, 143, 144
  in magnetostatics, 209
  non-linear for ferromagnets, 210
continuity C^n, 449
continuity equation, 3, 170, 236, 238, 240, 383
contravariant vectors, *see* vectors
convective derivative, *see* derivative
coordinate basis, 325–327
coordinate curve, 325–327
coordinate patches, 323
coordinate systems
  spacelike components, 322
  timelike components, 322
coordinates
  cylindrical, 15, 110, 426
  spherical, 425
cosine law, *see* law of cosines
cotangent bundle, 436
cotangent bundles, 324
Coulomb excitation, 94
Coulomb gauge, 197, 231, 244, 262
Coulomb potential
  acts instantaneously, 245
  and causality, 245
  solution in Coulomb gauge, 244, 245
Coulomb's law

continuous charge distributions, 423
definition, 20–22, 423
deviations from, 23
starting point for electrostatics, 187
Coulomb, C.-A., 1
covariance
and invariance, 368
and Maxwell equations, 322
and spacetime tensors, 321
manifest, 371, 373, 374
of Maxwell equations, 371, 373, 374
covariant derivative, 340, 343
and Christoffel symbols, 343
and minimal substitution, 403
and parallel transport, 345
implications, 345
is non-commuting operation, 344, 346
Leibniz rule for derivative of product, 345
of metric tensor vanishes, 345
rules for, 344
covariant vectors, *see* dual vectors (one-forms)
covectors, *see* dual vectors (one-forms)
Curie temperature, *see* ferromagnetism
curl
and the Helmholtz theorem, 69
definition, 419
fundamental theorem of (Stokes' theorem), 423
of long straight wire, 15
currents
and conservation of charge, 170
continuity equation, 170
convection current density, 171
field lines of steady current density, 171
in matter, 174
steady-current condition, 170
vacuum, 171
curvature
and radius of curvature, 123, 124
and surface charge density, 120, 123, 124
and tangent spaces, 324
vectors in curved space, 324
cycles, 438
cyclotron motion, 184, 185, 204

d'Alembertian operator
definition, 247, 370
for electromagnetic waves, 370
in Green function, 247
in wave equations, 396
Lorentz invariance, 371
demagnetizing field, 219
derivative
convective, 228
directional, 58
normal, 58
product rules, 419
second derivatives, 420
diamagnetic material, *see* diamagnets
diamagnets
definition, 206
magnetic field lines, 211
physical explanation, 209, 211
dielectric constant, 144, 163
dielectrics
definition, 120
dielectric constant, 144
polarization in capacitor, 131
properties, 130
shielding factor, 162
differential form, 436
differential forms, 379, 380, 382, 436, 439
differentiation
absolute, 343
covariant, 343
of tensors, 336, 340
partial, 336, 342
diple radiation, 301
dipole moment
definition, 88
in multipole expansion, 85, 86, 88
intrinsic, 130
magnetic, 207
sources in matter, 130
vector, 136
Dirac delta function
anticommutes with derivative operator, 429
as a distribution or generalized function, 428, 429
definition in 1D, 428, 429
definition in 3D, 428, 429
dimensionality, 429
Dirac equation, 396
Dirac matrices, 397
Pauli–Dirac representation, 397
Weyl representation, 397
Dirac topological monopoles, *see* magnetic monopoles
directional derivatives, 325–327, 419
Dirichlet boundary condition, *see* boundary conditions
discontinuity equations, 154
displacement, 143, 144, 209
displacement current, 5, 6, 236, 240
divergence
and Helmholtz theorem, 69
definition, 418
fundamental theorem of (divergence theorem), 422
of long straight wire, 15
divergence theorem, 29, 150, 424
Drude model
and Hall experiment, 202
and modern atomic theory, 176
and Ohm's law, 177
description, 175, 176

enabled by discovery of electron, 2
relaxation time (mean collision time), 177
dual (electromagnetic) field tensor, 373
dual vectors (one-forms)
and row vectors, 331
as maps to real numbers, 329
defining in curved space, 324
duality with vectors, 329, 336
transformation law, 335
duality
definition, 380
of boundary operator and exterior derivative, 380
of vectors and dual vectors, 380

Earnshaw's theorem, 59, 118
eddy currents, 231
Einstein summation convention, 324, 414
Einstein, A., 2
electric field
and the scalar potential, 36
curl of, 35
definition, 22, 25
discontinuous at charge layer, 57, 58
energy, 6–8
for conducting and dielectric spherical balls, 161
for discrete set of charges, 26
intrinsic strength relative to magnetic field, 182
is conservative, 37
of a point charge, 23
of continuous charge distribution, 26
of line charge, 26
of long straight wire, 26
of solid spherical ball, 30
time variation produces a magnetic field, 226
electric flux
and field lines, 43
definition, 43
electric permittivity, 144
electric potential, *see* scalar potential
electric susceptibility, 130, 144
electromagnetic induction
and unification of electricity and magnetism, 1, 226
discovery by Faraday, 1, 226
mutual inductance, 233
overview, 233
self-inductance, 233
electromagnetic waves
absorption, 303
and Maxwell equations, 5
and the displacement current, 236
circular polarization, 269
diffraction, 301
dispersion, 277, 303
dispersive, 276
elliptical polarization, 269
energy density, 264
energy flux density, 265
evanescent wave, 282
Fresnel equations, 279, 280
helicity, 270
in simple matter, 276
in terms of fields, 260
in terms of potentials, 262
in vacuum, 257, 260, 265, 276
index of refraction, 277
interpreted as light, 240
left circularly polarized (LCP), 269
momentum density, 265
non-dispersive, 276
p-polarization, 279, 280
plane polarization, 269
Poynting vector, 265
radiation pressure, 283
reflectance, 283
reflection, 277, 279
refraction (transmission), 277, 279
right circularly polarized (RCP), 269
s-polarization, 279, 280
scattering, 301
transmittance, 283
transverse polarization, 2, 260, 265, 267, 269
wave equation, 260
electromotive force (EMF)
and special relativity, 232
definition, 226, 227
motional, 232
proportional to time derivative of flux, 228
transformer, 232
electron
classical radius, 7
discovery of, 176
free electron approximation, 177
independent electron approximation, 177
self energy, 7
electrostatic induction, 19
electrostatic polarization, 19
electrostatics
Coulomb's law, 17
definition, 17
electric field, 22
Gauss's law, 27
Poisson and Laplace equations, 46
relationship of electric field and scalar potential, 35
scalar potential, 32
superposition principle, 23, 44
work and energy in electric fields, 37
elliptical PDEs
and equilibrium, 50
boundary value problems (BVP), 50
instantaneous propagation, 50
key properties, 50
no local extrema, 50
emergent states, 219

EMF, *see* electromotive force (EMF)
enantiomers, 286
energy, *see also* work
  of charge distribution in external field, 94
  stored in capacitor, 126
equipotential surfaces, *see* scalar potential
equivalence classes
  definition, 242
  of gauge transformations, 242, 402
Euclidean space
  geometry, 321
  metric signature, 321
Euler formula, 259
Euler–Lagrange equation, 394, 395
exterior calculus, 382, 436
  and electromagnetism, 388
  summary, 388
exterior derivative, 380, 436, 437, 439

farad (unit), 124
Faraday effect, 283, 285
Faraday flux rule, 227
Faraday Tensor, 371, 373, 374
Faraday's law
  and unified principle of induction, 227
  differential form, 229
  Faraday's experiments, 226
  generalized as a relationship between fields, 228
  in medium, 150
  in vacuum, 2
  integral form, 152, 228
  integral form in medium, 152
  production of transient current, 226
Faraday, M., 1, 226
ferroelectricity, 163, 181
ferromagnetism
  and permanent magnetism, 206
  Curie temperature, 210
  definition, 206
  depends on magnetic history, 206, 210
  hard ferromagnets, 214
  hysteresis, 210
  microscopic alignment of spins, 181
  non-linear constituitive relationship, 210
  spontaneously broken symmetry, 181
ferromagnets, *see* ferromagnetism
fiber bundle
  cotangent bundle, 324, 329
  definition, 379
  tangent bundle, 324, 329
field theory
  and action at a distance, 24
  classical electromagnetism as prototype, xv
  conserved currents and charges, 407
  Lagrangian densities, 396, 397
  Noether's theorem, 405, 407
  origination in Faraday's intuitive ideas, 227
  quantization of classical fields, 394, 396
  the classical action, 394, 396
finite difference, *see* numerical E&M problems
finite element method, *see* numerical E&M problems
Fourier series, 258
Fourier transforms
  connecting time and frequency domains, 297, 298
  conversion of PDE to algebraic equation, 248
  definition, 248
  inverse transform, 248
  normalization convention, 248
  of distributions, 248
  of functions, 248
  to obtain Green functions, 248, 249
free charge, *see also* bound charge
  and macroscopic current density in medium, 208
  definition for dielectrics, 133
  not bound in dielectrics, 133
frequency domain
  characteristics, 299
  definition, 297, 298
  examples, 299
  relationship to time domain, 297, 298
Fresnel equations, *see* electromagnetic waves
fringing fields, 145
fundamental theorem
  of calculus, 422
  of curls (Stokes' theorem), 423
  of divergences (divergence theorem), 422
  of gradients, 422

Galilean invariance
  and Maxwell equations, 4, 228
  in Faraday's law at low velocity, 229
  superceded by special relativity, 319
gauge bosons, 11
  mediators of force, 24
  quanta of gauge fields, 24
gauge fields, 24
gauge invariance, *see also* gauge symmetry
  Aharonov–Bohm effect, 390, 410
  and photon mass, 270, 404, 405
  in quantum mechanics, 403, 404
  minimal substitution, 403, 404
gauge symmetry, 270
  abelian, 9
  and charge conservation, 4, 5, 236, 240
  and decoupling of Maxwell equations, 242, 244
  and quantum electrodynamics, 5, 236, 240
  and the Standard Model, 5, 236, 240
  and unification of fundamental interactions, 8
  definition (classical, non-relativistic), 196
  gauge transformations, 196
  gauge-fixing condition, 242, 244
  in quantum mechanics, 403
  local, 402
  Lorenz gauge, 242, 244

minimal substitution, 403, 410
non-abelian, 9
gauge transformations, *see also* gauge symmetry
covariant formulation, 370
definition (classical, non-relativistic), 196
gauge-fixing constraint, 370
in electromagnetism, 370
invariance of electromagnetism under, 196, 369
on Maxwell equations, 369
to Coulomb gauge, 197, 370
to Lorenz gauge, 244, 370
gauss G (unit), 186
Gauss's law
definition, 27, 29, 30, 423
in medium, 150
in vacuum, 2
integral form, 152
integral form in medium, 152
Gauss–Seidel method, *see* numerical E&M problems
Gaussian surface, 30
general relativity
and action at a distance, 24
gravitational waves, 245
replaces Newtonian gravity, 245
the speed of gravity, 245
generative AI (GenAI)
and NotebookLM, 450
and numerical E&M problems, xiv, xviii, 450
as assistant, 450
as problem solver, xv, xviii, 450
as tutor, xiv, 450
Gemini, 450
integration with textbook, 450
Question and Verify mantra, xvi
generative AI(GenAI)
hallucinations, xvii, xviii
large language models (LLM), xvii
geometrical object, 332
Gibbs, J. Willard, 3
gradient
definition, 417
fundamental theorem of, 422
identities, 418
with respect to x, 190, 418
with respect to x', 190, 418
grand unified theories (GUTs), 10, 11
Graphical Processing Units (GPUs), 117
Green functions
and lightwaves, 242
and the image method, 80
as propagators in quantum field theory, 73
boundary-value problems, 73, 77
causal, 252
causality constraints in quantum field theory, 73
correlation functions in quantum field theory, 73
definition, 73, 75
difficulty of determining, 76
for conducting sphere, 80
for driven oscillator, 74
in quantum field theory, 73
of free space, 75
or "Green's functions"?, 73
retarded, 247, 249–252
solution of electrostatics problems, 73
solution of Poisson equation, 77
solution with Fourier transforms, 249
symmetry of, 81, 82
Green's first identity, 65
Green's second identity, *see* Green's theorem
Green's theorem (Green's second identity), 65
groups, *see also* symmetries
abelian, 401
definition, 401
Lorentz group, 401
nonabelian, 401
Poincaré group, 401
representations, 88
U(1) gauge group, 402
Gupta–Bleuler mechanism, 247

hadron (definition), 11
Hall effect
and tensor resistivity, 175
classical, 185
consequence of Lorentz force, 184
Hall field, 185
Hall resistance, 185
quantum, 185
harmonic functions
and the mean value theorem, 448
solutions of the Laplace equation, 448
Heaviside, O., 2, 3
Heine–Borel theorem, 436
Helmholtz decomposition, *see* Helmholtz theorem
Helmholtz equation, 49, 50
Helmholtz theorem, 69, 197, 246
hermitian conjugation, 287
hermitian matrix, 287
Herz, H., 2
Higgs mechanism, 211
Hodge star operator, 373, 437
holonomic basis, *see* coordinate basis
homogeneous differential equation, 73
homology
and de Rham cohomology, 381
Betti numbers, 381
cohomology, 438
De Rham cohomology, 438
de Rham cohomology, 386, 438
defined, 381
fundamental theorem of, 381
homology groups, 381
homotopy, 438

hypersurface, 323
hysteresis, *see* ferromagnetism

image charges, 78, 79
image method
  and a charge above a conducting plane, 78, 79
  and boundary conditions, 79
  and uniqueness, 78
  overview, 76
  relation to Green functions, 80
indefinite metric, 350
index of refraction, 277, 279
index position, *see* Einstein summation convention
induced charge, 120
induction, *see* electromagnetic induction
inertial frames
  no preferred ones in special relativity, 319
  preferred aether frame hypothesis, 257
inflationary cosmology, 10
inhomogeneous differential equation, 73
initial value problem, 51
insulators, *see* dielectrics
integration
  area of 2-sphere by invariant integration, 341
  by parts, 428
  covariant volume element, 341
  invariant, 341
  of tensors, 340
invariance
  and covariance, 368
ionization
  an stellar opacity, 301
  pressure, 301
  thermal, 301
irrotational current, 246

Jacobi method, *see* numerical E&M problems
Jacobian determinant, 341
Jacobian matrix, 336
Jones matrix, 274
jumping ring demonstration, 228, 234, 235

Klein–Gordon equation, 396
Kronecker delta, 328, 329, 337

Lagrangian, 395
Lagrangian density
  and the classical action, 394
  and the Lagrangian, 394
  for complex scalar or pseudoscalar field, 396
  for Dirac field, 397
  for massive vector field, 397
  for massless vector field, 396
Laplace's equation
  definition, 424
  in cartesian coordinates, 46
  linearity of, 48, 99, 103
  methods of solving, 70, 100
  numerical solution, 111
  with mixed boundary conditions, 68
Laplacian operator
  applied to $1/r$, 47, 429
  in cartesian coordinates, 47
  in cylindrical coordinates, 47, 426
  in spherical coordinates, 47, 426
large language models (LLM), *see* generative AI (GenAI)
lattice gauge theory, 12
law of cosines, 134, 427
Legendre polynomial
  (table), 108
  definition, 107
  multipole expansions, 84
  orthogonality relation, 109
  Rodrique's formula, 108
  spherical harmonic addition theorem, 85
legendre polynomial
  and rotational invariance, 108
  connection to spherical harmonics, 108
Legendre's equation, 107
Lenz's law, 211, 228
lepton (definition), 11
Levi–Civita symbol, 373, 418
lexicographic order, 446
Lie bracket, 327
Lie derivative
  and covariant differentiation, 343
  contrasted with covariant derivative, 343
lightcone, 359
  and causality, 251, 252, 361, 362
  and simultaneity, 360
  and the constant speed of light, 361
  lightlike intervals, 364
  null intervals, 364
  spacelike intervals, 364
lightlike intervals, *see* lightcone, null intervals
lightning rod, *see* conductors
line integral, 421
Linear polarization, *see* polarization
lodestone, 1
London penetration depth, *see* superconductors
longitudinal current, 246
Lorentz covariance
  of Maxwell equations, 4, 366
Lorentz factor
  in special relativity, 359
Lorentz force, 6, 182, 185, 239, 409, 424
Lorentz invariance, *see also* special relativity
  and electromagnetism, 4, 182, 365, 366
  conserves the spacetime interval, 351, 352
  in Lorenz gauge, 242
  superceded Galilean invariance, 319
Lorentz transformations, 353
  and causality, 352, 360, 362
  and Maxwell equations, 228

and simultaneity, 352, 360, 362, 363
and spacetime diagrams, 362
and special relativity, 319
as rotations in Minkowski space, 354
boosts between inertial systems, 355, 357, 359, 362
Lorentz group, 356, 401
spatial rotations, 355
Lorentzian manifold, 351
Lorenz gauge, 242, 244, 262, 371
luminiferous aether, *see* aether

macroscopic (averaged) quantities
for electric fields, 143
for magnetic fields, 208
preserves $\boldsymbol{B} = \boldsymbol{\nabla} \times \boldsymbol{A}$ for magnetic fields, 208
preserves $\boldsymbol{E} = -\boldsymbol{\nabla}\Phi$ for electric fields, 143
magnetars, 186
magnetic charges
absence of, 2, 150, 152, 190, 199
magnetic diffusion, 231
magnetic dipole
alignment in magnetic field, 207
and quantum nature of spin, 200
averaged over small volume, 207
classical relation to orbital angular momentum, 200
definition, 199
equivalence to current loops, 207
in matter, 206
in multipole expansion, 199
torque exerted by magnetic field, 207
magnetic field
alignment of magnetic dipoles, 206, 207
Ampèrian model, 206
at surface of Earth, 186
auxilliary $\boldsymbol{H}$ field, 209
Biot–Savart law, 186
Gilbert model, 206
in matter, 206
intrinsic strength relative to electric field, 182
irrotational, 219
is it $\boldsymbol{B}$ or $\boldsymbol{H}$?, 209
lines of, 188
magnetic flux, 187, 188, 228
of localized current distribution, 197
of long straight wire, 188, 365
produced by circular current loop, 187
solenoidal, 219
strongest known in Universe, 186
terminology, 209
time variation produces an electric field, 226
units, 186
when is it conservative?, 214, 215, 219
magnetic flux, *see* magnetic field, 227
magnetic force, *see* Lorentz force
magnetic Gauss's law, 3
magnetic moment, *see* magnetic dipole
magnetic moment density, *see* magnetization
magnetic monopoles
absence in Maxwell equations, 4
absence of experimental evidence, 9
and asymmetry between $\boldsymbol{E}$ and $\boldsymbol{B}$ fields, 4
and magnetic charge, 10
as emergent condensed matter states, 219
common in theories beyond the Standard Model, 10
diluted by inflationary cosmology, 10
Dirac monopole, 10, 381
magnetic permeability, 209
magnetic scalar potential, 195, 214, 215
magnetic shielding, 223
magnetic susceptibility, 209, 211
magnetization
approximately constant for hard ferromagnets, 214
definition, 199, 207
in diamagnetic media, 211
in ferromagnets, 210
in paramagnetic media, 211
linear for paramagnets and diamagnets, 211
magnetic moment, 199
magnetic moment density, 199
magnetization currents, 181
magnetized matter, 206
magneto-optic material
definition, 287
gyroelectric response, 287
gyromagnetic response, 287
magnetohydrodynamics, 231
magnetostatics
and special relativity, 181
definition, 180, 181
first law, 190
second law, 190
manifold, *see also* space
atlas, 323
charts, 323
coordinate patches, 323
definition, 323
differential, 323
Riemannian, 323
spacetime, 322
Maxwell equations, **366**
and aether, 317
and causality, 245
and exterior derivatives, 382
and Galilean invariance, 317
and linear superposition, 25
covariance, 371, 373, 374
differential forms notation, 382, 383
Faraday tensor, 382, 383
gauge transformations, 369
in gaussian units, 431
in Heaviside–Lorentz units, 366, 432

in medium, 150, 151
in SI units, 2, 431
in simple matter, 276
in vacuum, 2, 151, 431, 432
in vacuum and in medium, 151
integral form, 152
integral form in polarizable media, 152
Lorentz covariance, 4, 366, 368
Maxwell's original form, 3
original 20-equation form, 3
potential 1-form, 383
scalar and vector potentials, 369
source 3-form, 383
source-free in vacuum, 260
symmetries, 4
vector calculus and differential forms notation, 384
vector calculus notation, 3
Maxwell wave equation, 396
Maxwell, J. C., 236
Maxwell, J. C. , 1
mean value theorem, *see* Earnshaw's theorem, 59
Meissner effect, *see* superconductors
Mercator projection, 363
metric
indefinite, 351, 358
metric tensor, 338
signature, 320, 373
metric space, *see* metric
metric tensor
and line element, 338
and scalar products, 350
covariant derivative vanishes, 345
in Minkowski space, 350
indefinite metric, 350
signature, 351, 372, 433–435
used to raise and lower indices, 338, 339, 351
Michelson–Morley experiment, 257, 319
microscopic quantities, 143
Mie scattering, 302
minimal coupling prescription, 209, 400, 403, 410, 411
minimal substitution, *see* minimal coupling prescription
Minkowski space
and causality, 361
definition, 349
event, 351
indefinite metric, 350
invariance of spacetime interval, 351
lightcone structure, 359
lightlike intervals, 364
line element, 320, 328, 350
Lorentz transformations, 353
metric signature, 320, 351
metric tensor, 320, 328, 350
null (lightlike) intervals, 359, 364
rotations, 358
scalar product, 350
spacelike intervals, 359, 364
spacetime, 319
tensors, 353
timelike intervals, 359
worldline, 351
Minkowski, Hermann, 319
monopole (electric)
in multipole expansion, 85, 88
Mueller matrix, 273, 274
multipole expansion, *see also* multipole moments
binomial expansion, 134
cartesian coordinates, 88
electric field components, 93
in Legendre polynomials, 84
in spherical harmonics, 84, 85
molecular charge distribution, 135
of potential, 134
spherical coordinates, 87
Taylor series, 84
multipole moments, *see also* multipole expansion
cartesian vs. spherical definition, 88
definition may depend on coordinate system, 88
dipole potential, 86
in atomic nuclei, 94
quadrupole potential, 86
reducible and irreducible representations, 88

n-tuples
definition, 311
Neumann condition, *see* boundary conditions
neutrinos
flavors in Standard Model, 11
neutron stars, 186
Newtonian gravity
and causailty, 245
gravitational potential, 245
nilpotency, 438
Noether's theorem, 4, 407
4-momentum conservation, 406
and conserved charges and currents, 405
definition, 405
for internal symmetries, 406
Noether charges, 406
Noether currents, 406
Noether tensors, 405, 406
non-coordinate basis, 325–327
normal derivative, 62
normal derivatives, 419
NotebookLM
chatting, 458
creating projects, 458
generative output, 458
retrieval augmented generation (RAG), xviii
with Gemini and Nano Banana, xvi
with GenAI, 450
numerical E&M problems

adaptive mesh refinement, 117
adaptive quadrature, 117
and graphics, 442
array-slicing techniques, 115
boundary element method (BEM), 113
domain decomposition, 115
finite difference method, 111, 447
finite element method (FEM), 112, 113, 448
finite-difference time-domain (FDTD, 298
frequency domain, 298
Gauss–Seidel method, 444
gnuplot, 441
GPU acceleration, 115, 117
Jacobi method, 112, 444
Jacobi relaxation, 447
leap-frog algorithm, 299, 300
method of moments (MOM), 113
necessary part of graduate education, xviii, 441
parallel Gauss–Seidel, 446
parallelization, 115
programming using GenAI prompts, 442
Python, xviii, 441
relaxation methods, 445, 447, 448
SIMD, 115, 116
solving 2D Laplace equation numerically, 447
successive over-relaxation (SOR), 112, 445
time and frequency domains, 297
time domain, 298
vectorization, 114, 116
verifying solutions, 443
numerical methods, *see* numerical E&M problems

Ohm's law, 62, 174, 175, 177, 226
ohmic conductors, 62, 174
ohms Ω (unit), 174
one-forms, *see also* dual vectors (one-forms)
definition, 436
Optically active matter, 285
optically active matter, 286
ordinary differential equation (ODE), 59
overdetermined system, 66

p-polarization, *see* electromagnetic waves
paraelectricity, 163
parallel computing
checkerboard ordering, 446
sequential dependency, 446
paramagnetic material, *see* paramagnets
paramagnets
definition, 206
magnetic field lines, 211
physical explanation, 209, 211
partial differential equation (PDE), 59
passive transformation, *see* transformations
path integral, *see* line integral
PDE solvers
finite difference method (FSM), 72
finite element method (FEM), 72
for Poisson and Laplace equations (table), 70
Gauss–Seidel method, 444
Jacobi method, 444
overview, 444
red-black (checkerboard) ordering, 446, 447
relaxation methods, 72
spectral methods, 72
successive over-relaxation (SOR), 445
PDEs
classification, 48–50
elliptical, 48–50
hyperbolic, 48–50
linearity, 48, 50
parabolic, 48–50
strong form, 448, 449
weak form, 448, 449
permeability of free space, 21, 186
permittivity of free space, 21
photon
mass of, 23, 270
mass through the Higgs mechanism, 211
spin states, 270
Poincaré symmetry, 270
Poincaré transformations, 356, 401, 405
Poisson's equation
definition, 46, 424
for continuous 3D charge distribution, 47
for vector potential in Coulomb gauge, 197
in cartesian coordinates, 46
linearity of, 48
magnetic, 214
methods of solving, 70, 101
numerical solution, 111
solution at retarded time, 252
polar molecules, 137
polarization (charge)
amount of charge displacement in dielectric, 131
and induced dipole moment, 160
asymmetric, 137, 138
atomic polarizability, 130, 137
atomic polarizability (table), 138
definition, 139, 140, 160
density of dipole moments, 139, 143, 160
non-uniform, 144, 147
of dielectric, 131
of noble gas elements, 137
polarization density, 140
polarization tensor, 137, 138
polarization-charge density, 140, 144
uniformly polarized ball, 147, 160
polarization (light)
by reflection, 288, 289
circular polarization, 268, 269, 273, 285
converting linear to circular, 283
elliptical polarization, 269, 273
linear (plane) polarization, 267, 268, 273

of cosmic microwave background radiation, 266
Poincaré sphere, 272, 273
polarization ellipse, 266, 273
Stokes parameters, 271, 273
transverse electric (TE), 279, 280
transverse magnetic (TM), 279, 280
potential, *see* scalar potential
Poynting vector, 265, 283
principle of extremal proper time, 393
principle of relativity, 321
Proca (massive vector) field, 396
proper time, 350
pseudo-euclidean manifold, *see* Lorentzian manifold
Python, *see* numerical E&M problems

QCD, *see* quantum chromodynamics
QED, *see* quantum electrodynamics
QFT, *see* quantum field theory
quadrupole moment
as rank-2 tensor, 88
in multipole expansion, 85, 88
traceless, 88
quantum chromodynamics (QCD)
color confinement, 12
gauge symmetry, 9
quantum electrodynamics (QED), 5, 9, 236, 240, 246
quarks
color confinement, 12
electrical charge, 12
flavors in Standard Model, 11
quantum numbers, 12
quasistatic approximation, 111, 229–231

racemic mixture, 286
radiation gauge, *see* Coulomb gauge
radiation pressure, 283
Raleigh scattering
special case of Mie scattering, 302
Rayleigh scattering
angular distribution and polarization, 302
cross section, 302
dipole approximation, 302
overview, 302
reflection
kinematic laws of, 277, 279
law of reflection, 277, 279
Snell's law, 277, 279
total internal, 282
regularizations of integrals, 249
relativity principle, *see* principle of relativity
renormalization
and the renormalization group, 7
in quantum field theory, 7
repeated indices, *see* Einstein summation convention
resistance, 174
resistivity
and Ohm's law, 174, 175, 177
and resistance in Hall experiment, 175
resistivity tensor, 175, 177
retardance, 274
retardation effects, 230
retarded time, 230, 251, 252
Rodrique's formula, *see* Legendre polynomial

s-polarization, *see* electromagnetic waves
Savart, F., 186
scalar potential
and the vector potential, 195
definition, 35, 240, 424
displaying graphically, 40
equipotential surfaces, 40
for point charge, 84
magnetic scalar potential, 195
solving Maxwell equations, 240
self energy of point particles, 6–8, 39
separation of variables, 104
cartesian coordinates, 99
cylindrical coordinates, 110
spherical coordinates, 106
sets
cardinality, 307
closed, 306
definition of, 306, 307
equivalence classes of, 306
equivalence of, 307
intersection of, 307
membership in, 307
null set, 307
open, 306
set-builder notation, 307
subsets, 307
union of, 307
Venn diagrams, 307
simplices, 379
solenoidal current, 246
space, *see also* manifold
Minkowski, 320, 349
space charge, 173
spacelike surface, 360
spacetime, *see also* space
causal structure, 361
indefinite Minkowski metric, 350
invariance of interval, 351, 352
Minkowski space, 349
sparse matrix, 112
special relativity, *see also* Lorentz invariance
and causality, 245
and electric and magnetic fields, 182, 232, 365, 366
and electromagnetism, 182
constant speed of light, 319
event, 351
limiting speed for signals, 24, 238, 245
Lorentz invariance, 4
Lorentz transformations, 353
no preferred inertial systems, 232, 319

proper time, 350
relativity of simultaneity, 360, 363
removes need for aether in electromagnetism, 257
space contraction, 363
time dilation, 352, 363
twin paradox, 363
worldline, 351
speed of gravity, 245
spherical harmonic
addition theorem, 85
and rotational invariance, 108
completeness relation, 87
connection to Legendre polynomials, 108
multipole expansion, 85, 88
orthogonality condition, 87
relation to associated Legendre polynomials, 87
spontaneous symmetry breaking, 210, 211
Standard Electroweak Model, *see* Standard Model
Standard Model (of elementary particle physics)
and gauge symmetry, 5, 8, 9, 236, 240, 407
anomaly cancellation and charge quantization, 11
conserved charges and currents, 407
generations, 11
Higgs mechanism, 211
particles of, 10–12
renormalizability, 11
steampunk, 238
Stokes parameters, 271
Stokes vector, 272, 274
Stokes' theorem
and integral Maxwell equations, 151
and the Berry phase, 410
and the scalar potential, 33
definition, 33, 34, 424
generalized, 385, 439
physical interpretation, 34
right-hand rule for, 34
stress–energy–momentum tensor, 406
String Theory, 10
successive over-relaxation (SOR), *see* numerical E&M problems
summation convention, *see* Einstein summation convention
summation problems, 17, 18
superconductors
and diamagnetism, 211
London penetration depth, 211
Meissner effect, 211
superposition principle, 23, 25, 73, 248
surface charge, *see also* charge
discontinuity of displacement field, 153
discontinuity of electric field, 57, 58, 153
polarization charge on boundary of a dielectric, 140
surface integral, 421
surface-charge density, 146
symmetries, *see also* groups
and gauge invariance, 400
group theory, 356, 401
Lorentz group, 356, 401
Poincaré group, 356, 401
U(1) gauge group, 402
tangent bundles, 324
tangent space
and parallel transport, 324
and vectors in curved space, 324
Taylor series, 88, 427
tensors
and covariance, 321
and form invariance of equations, 346
antisymmetric (skew symmetric), 339
antisymmetrizing operation, 340
as geometrical objects, 414, 416
as linear maps, 328, 329
as operators, 328
calculus, 340
contravariant, 328
covariant, 328
defined by their transformation law, 328, 334, 338
differentiation, 340
dual vectors (one-forms), 335
Einstein summation convention, 324
Faraday tensor, 383
horizontal placement of indices, 339
in linear algebra, 331
in Minkowski space, 353
in quantum mechanics, 331
index-free formalism, 328, 329
integration, 340, 341
Kronecker delta, 328
Lorentz, 416
metric tensor, 338, 339
mixed, 328
rank, 328
rank of, 413
rank-2, 337
scalars, 334
spacetime, 416
symmetric, 339
symmetrizing operation, 340
tensor fields, 416
transformation laws, 413
transformation laws (table), 338
type, 328
vectors, 334, 336
vertical placement of indices, 322, 324
tesla T (unit), 186
thermionic emission, 171
Thomson scattering
and opacities in stellar plasmas, 301
cross section, 301
relationship to Compton scattering, 301

Thomson, J. J., 2
time domain
  characteristics, 299
  definition, 297, 298
  examples, 299
  relationship to frequency domain, 297, 298
time machines, *see* time travel
topological matter, 185
topology
  and electromagnetism, xv, xx, 379
  definition, 379
total internal reflection, 283
total time derivative, 228
transformations
  boosts, 357
  Galilean, 228
  gauge, 196
  gauge in electromagnetism, 369
  linear, 310
  Lorentz, 228, 319
  of derivatives, 328
  of fields, 328
  of integrals, 328
  of scalars, 335
  of vectors, 335
  passive, 322, 414
  Poincaré, 356, 401
  rotations in euclidean space, 354
  rotations in Minkowski space, 354
  spacetime, 322
  symmetry under, 321
  unitary, 402
  vectors, 335
transverse current, 246
transverse gauge, *see* Coulomb gauge
twin paradox, 363

uniqueness theorems
  and boundary conditions, 20, 66–68
  by Green's methods, 64
  definition, 61
  even if initial charge distributions not known, 20
  method of images, 76, 79
  Uniqueness Theorem I, 64, 76
  Uniqueness Theorem II, 64
units
  esu (CGS or Gaussian), 21
  Heaviside–Lorentz, 21
  SI, 21

vacuum diodes, 171
vacuum polarization, 25
vector area, 207
vector field
  longitudinal, 69
  transverse, 69
vector identities, 417
vector potential
  and minimal coupling prescription, 209
  definition, 195, 240, 424
  hard ferromagnets, 216
  in Coulomb gauge, 197
  multipole expansion, 197, 198
  Poisson equation for, 197
  solving Maxwell equations, 240
vector space, 309
  definition, 330
vector spherical harmonics, 198
vectors
  and column vectors, 331
  and tangent spaces, 324
  as maps to real numbers, 329
  defining in curved space, 324
  dual vector spaces, 329
  dual vectors, 335
  duality with dual vectors, 329, 336
  scalar product, 337
  transformation law, 336
  vector space, 329, 330
volume charge, *see* charge
volume integral, 421

wave equation
  in Lorenz gauge, 371
  linearity, 258
  scalar field, 258
  sinusoidal solution, 258
waveguides
  and Neumann boundary conditions, 62
  and the Helmholtz equation, 290
  cutoff frequency, 291
  decomposing into transverse fields, 290
  dominant mode, 292
  eigenvalue of transverse wave number, 291
  frequency cutoff, 291
  group velocity, 292
  intermodal dispersion, 292
  introduction, 289
  longitudinal propagation constant, 291
  phase velocity, 292
  rectangular metallic, 291
  transverse electric modes (TE), 290
  transverse magnetic modes (TM), 290
  transverse wavenumber, 290
waveplate, 274
waves
  electromagnetic, 257, 276
  monochromatic, 263
  phase velocity, 257, 258
  phaseshift, 258
  plane waves, 263
  speed, 257, 258
  wave equation, 257
wedge product, 436–438
work, *see also* energy

and the Lorentz force, 184
done in charging a capacitor, 126
done in electrical field, 38
energy of charge distribution in external field, 94
independent of path in electric field, 38
no work done by magnetic field, 184, 186
Yukawa potential, 23